

## **General Disclaimer**

### **One or more of the Following Statements may affect this Document**

- This document has been reproduced from the best copy furnished by the organizational source. It is being released in the interest of making available as much information as possible.
- This document may contain data, which exceeds the sheet parameters. It was furnished in this condition by the organizational source and is the best copy available.
- This document may contain tone-on-tone or color graphs, charts and/or pictures, which have been reproduced in black and white.
- This document is paginated as submitted by the original source.
- Portions of this document are not fully legible due to the historical nature of some of the material. However, it is the best reproduction available from the original submission.

{NASA-TM-76933} CONSTRUCTION, TESTING AND  
DEVELOPMENT OF LARGE WIND ENERGY FACILITIES  
(National Aeronautics and Space  
Administration) 412 p HC A18/MF A01

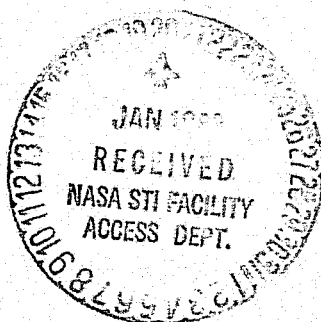
N83-16855

CSCL 10A G3/44 Unclass  
02456

CONSTRUCTION, TESTING AND DEVELOPMENT  
OF LARGE WIND ENERGY FACILITIES

R. Windheim and R. Cuntze, Editors

Translation of "Bau, Test und Entwicklung grosser Windenergie-  
anlagen" (Seminar on Efforts within the Framework of Programs on  
Energy Research and Technology of the Bundesminister fuer Forschung  
und Technologie, March 23/24, 1981), Juelich Nuclear Research  
Center, Juelich, West Germany, Report Juel-Spez-138, December  
1981, p 1-415.



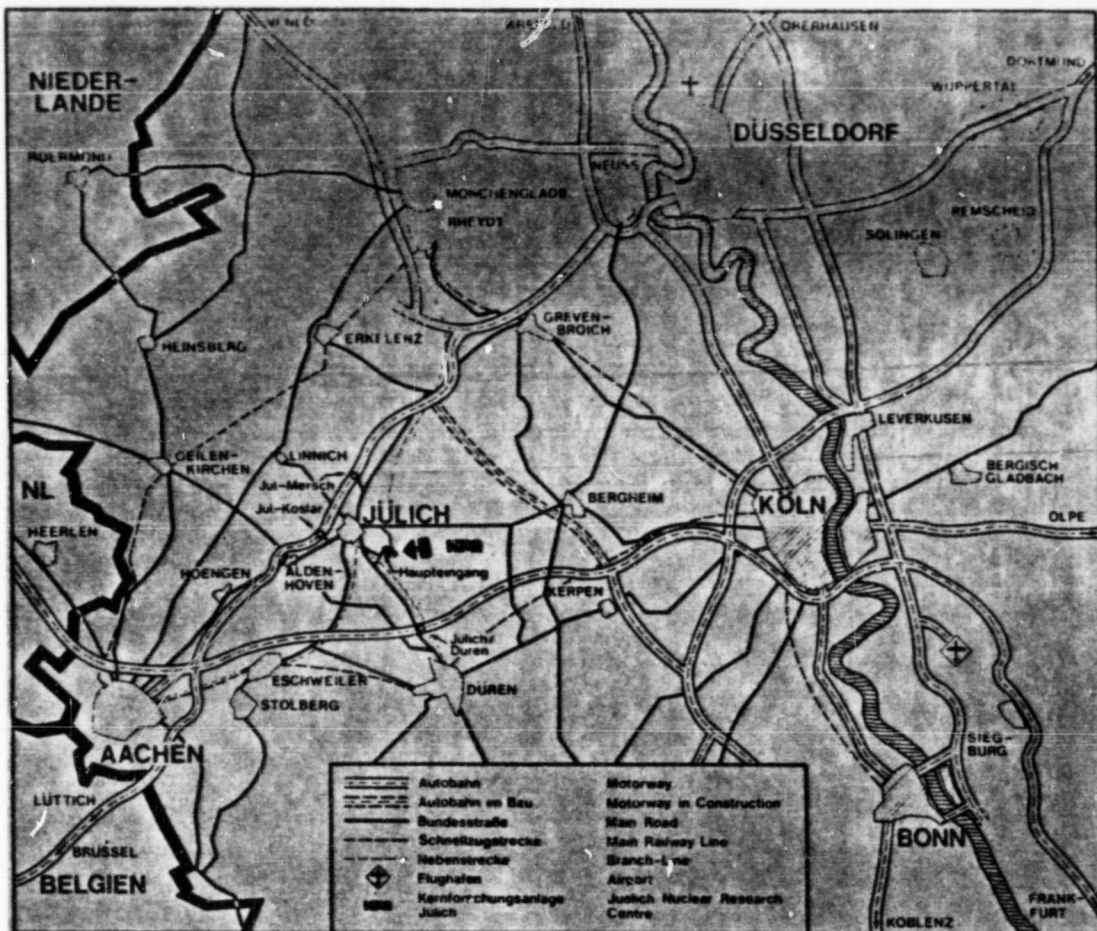
NATIONAL AERONAUTICS AND SPACE ADMINISTRATION  
WASHINGTON, D.C. 20546 SEPTEMBER 1982



ORIGINAL PAGE IS  
OF POOR QUALITY

STANDARD TITLE PAGE

1. Report No. NASA TM-76933	2. Government Accession No.	3. Recipient's Catalog No.	
4. Title and Subtitle CONSTRUCTION, TESTING AND DEVELOPMENT OF LARGE WIND ENERGY FACILITIES		5. Report Date September 1982	6. Performing Organization Code
		8. Performing Organization Report No.	10. Work Unit No.
7. Author(s)  R. Windheim and R. Cuntze, Editors		11. Contract or Grant No. NASA- 3542	
		12. Type of Report and Period Covered Translation	
9. Performing Organization Name and Address SCITRAN Box 5456 Santa Barbara, CA 93108		14. Sponsoring Agency Code	
12. Sponsoring Agency Name and Address National Aeronautics and Space Administration Washington, D.C. 20546			
15. Supplementary Notes  Translation of "Bau, Test und Entwicklung grosser Windenergieanlagen" (Seminar on Efforts within the Framework of Programs on Energy Research and Technology of the Bundesminister fuer Forschung und Technology, March 23/24, 1981), Juelich Nuclear Research Center, Juelich, West Germany, Report Juel-Spez-138, December 1981, p. 1-415			
16. Abstract  Reports given at a seminar on energy research held on 23-24 March 1981 are presented. Two special problems are discussed: building of large rotor blades and control of oscillations in large facilities. Based on data given in the seminar, it is concluded that the technical problems in the design of large rotor blades and control of oscillations can be solved.			
17. Key Words (Selected by Author(s))		18. Distribution Statement  Unclassified - Unlimited	
19. Security Classif. (of this report) Unclassified	20. Security Classif. (of this page) Unclassified	21. No. of Pages 1-41	22. Price



\*  
11

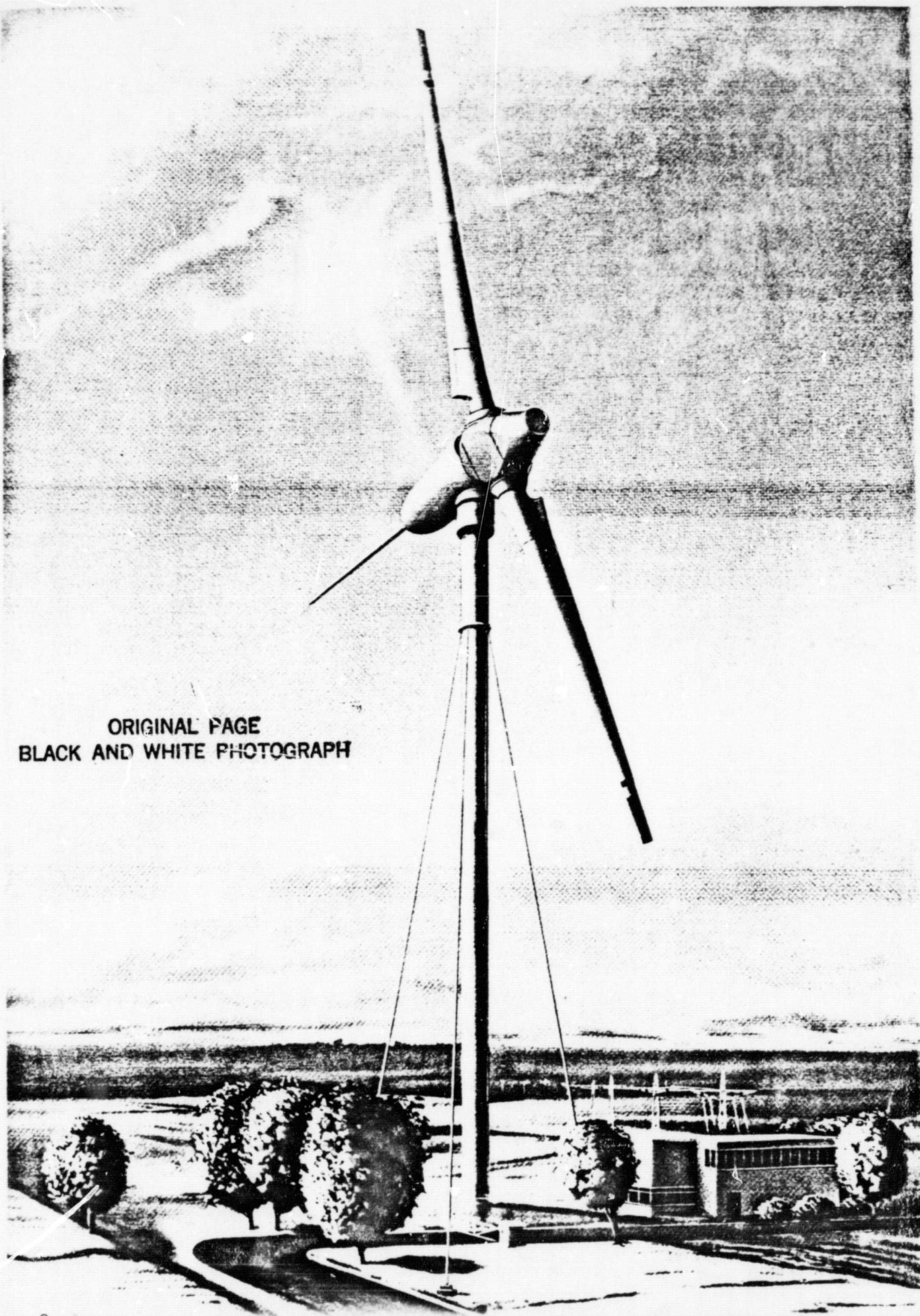
Map of area around Juelich, West Germany

Printed as a manuscript. Special report of the Research Facility Juelich no. 138. Energy Research Project Directorate Juel Spez 138. Can be obtained from

**ZENTRALBIBLIOTHEK der Kernforschungsanlage Jülich GmbH**  
Postfach 1913 · D-5170 Jülich (Bundesrepublik Deutschland)  
Telefon: 02461/610 · Telex: 833 556 kfa d

\* Numbers in margin indicate pagination of foreign text.

ORIGINAL PAGE  
BLACK AND WHITE PHOTOGRAPH



**ORIGINAL PAGE IS  
OF POOR QUALITY**

TITLE FIGURE: (page 2)

Large wind tunnel facility GROWIAN at Kaiser Wilhelm-Koog, Elbe Peninsula. Power: 3000 kW above 12 m/sec Wind speed.

Rotor diameter: 100.4 m

Tower height: 100 m

First operation: Fall 1982, see report on page 167.



## PREFACE

VI

At the present time within the energy research program of the Federal Minister for Research and Technology, about 50 projects for obtaining energy are being supported. Most funds are being expended on the development, building and testing of large facilities in the MW range. Long term projects include the introduction of wind energy to the power network.

The seminar was carried out on March 23-24, 1981. The purpose of this seminar was to exchange information among project leaders in the area of wind exploitation. In addition, based on this experience, future possible projects and directives were discussed within the framework of the energy research and technology project.

During the seminar, first of all, reports were presented about the status of large wind facility projects. After this, two special problems were addressed:

- building of large rotor blades
- control of oscillation in large facilities

Work on the development, building and testing of large wind energy facilities are at present stressing these two tests. According to our present knowledge, which was again confirmed in the seminar, the technical problems in the design of large rotor blades and the control of oscillations in large facilities are certainly solvable.

Testing of these large facilities is being performed in foreign countries in addition to West Germany. The purpose of this is to provide operational safety, especially with regard to optimum rotor blades and benign oscillation behavior. In addition, initial data is being selected about the economics of such facilities. The seminar of March 23-24, 1981 showed clearly that the program on energy research and technology of the BMFT for mastering wind energy by large facilities will result in the addition of a small percentage to our energy production.

The present reports are derived from ongoing research and devel- VII  
opment work and some of the reports will be of a preliminary nature. .  
The BMFT has agreed that this information should be published as a  
special Jul-Spez report of the nuclear research facility Juelich,  
accessible to the general public. At the same time, we are making a  
small contribution to the present energy controversy. We should like  
to mention that in the meantime an additional seminar on the exploita-  
tion of wind energy was carried out by the energy research PLE project  
office at KFA. The topic of the seminar which was carried out on May  
18-19, 1981 was "meteorological assumptions for the use of wind energy"  
(will also be published as Jul-Spez report no. 132). In addition, the  
results of the projects of the BMFT is being presented during regular  
seminar and status report wind seminars which will take place every  
two years.

We would like to thank all participants of the seminar for the  
interesting contributions and discussions about tasks during the exploi-  
tation of wind energy. We would like to thank the firm MAN-Neue Techno-  
logie, Muenchen, which made a substantial contribution to the first  
large wind facility in West Germany. We thank them for their hospital-  
ity. We would also like to thank Herr Dr. R. Cuntze, MAN-Neue Techno-  
logie. We thank Mrs. M. Abt, energy research project manager for  
excellent work in the processing of the manuscripts for the Juel-Spez  
report.

# TABLE OF CONTENTS, ACCORDING TO SEQUENCE OF SEMINAR PAPERS

## 50 m rotor blades for Growian

Pages

"Manufacturing development, building and testing of the GROWIAN rotor blade", MAN-Neue Technologie NT, project no. ET 4323 A: Visiting of the test stand for the GROWIAN test blade at the industrial facilities of Betriebsgesellschaft mbH, IABG, Muenchen. Status of the project: H. M. Thiele, MAN-NT (expanded by the results of the structural tests summer 1981, R. Windheim) ..... 10

## 265 kW wind energy facility VOITH GETRIEBE KG

Wind facility: "Development, manufacturing and testing of the prototype with 52 m rotor diameter and 265 kW terminal power", Voith-Getriebe KG, status of the project complex and especially ET 4104 A: Hofmann ..... 26

\*

Oscillation measurements: "Oscillation measurements of 26 m rotor blades with a 16 channel telemetry facility", Voith-Getriebe KG, project no. ET 4344 A, status of project: W. Spitteler ..... 73

Rotor blade development: "Development and building of rotor blades for the 265 kW Voith-wind energy facility", Voith-Getriebe KG with subcontractor Messerschmitt-Boelkow-Blohm MBB, status of project: R. Krautwald ..... 87

Building site Sept. 1981: R. Windheim, according to photographs of Voith ..... 133

## Projects for the building and development of Growian

Testing of rotor blades project: "Extensive project discussion of the "manufacturing development, building and testing of the Growian rotor blade (ET4323 A)", German Lloyd, project no. ET 4323 B, status of project: R. Lehmbus (collected by R. Windheim) ..... 140

\*See page 9.

	Pages
<u>Measurement program for Growian:</u> "Building of a measurement program and test program Growian", MAN-Neue Technologie, project no. 4364 A, status of project: F. Koerber .....	143
<u>Wind technology program:</u> "Wind technology program for large wind energy facilities", MAN-Neue Technologie, Project no. ET 4375 A, status of project: D. Muser .....	160
 <u>Building and operation of Growian</u>	
"Building and operation of large energy facilities Growian", large wind facility building and operating association mbH, project no. ET 4342 A, status of project: H. Witt (two contributions by R. Windheim) .....	167
 <u>Single wing wind facility</u>	
"Investigation of modern concepts for large wind energy facilities in the class of up to 135 m rotor blade diameter (according to 5 mW <sub>electr.</sub> at 11 m/sec wind speed). Building and testing of a demonstration installation on a model scale 1:3. Development of construction papers for a prototype large facility", Messerschmitt-Boelkow-Blohm, project no. ET 4240 A, status of project: R. Meggle (slight contribution: R. Windheim) .....	173
 <u>Fundamental research and development work for large facilities with a horizontal axis</u>	
<u>Optiwa:</u> "Optimization of large wind facilities", Institute for Statics and Dynamics of Aviation and Space Flight Designs of the University of Stuttgart and Statics and Dynamics Research Association mbA, Stuttgart, project no. ET 4406 A and B, status of project: I. H. Argyras and K. A. Braun. ....	196
<u>Gust generator:</u> "Development of a gust generator for a wind turbine" Institute for Aerodynamics and Gas Dynamics of the University of Stuttgart, project no. ET 4372 A, status of project: G. A. Walter and F. X. Wortmann .....	217



Operating behavior of wind energy facilities: "Investigation of operating behavior of wind energy facilities with horizontal axis by using adapted control methods and by using suitable mechanical-electrical energy converters", High School class Kassel/TU Braunschweig, project no. ET 4362 A, status of project: W Kleinkauf, W. Leonard (collected by: R. Windheim) ..... 235

Wind energy concentration: "Concentration of wind energy in vortex fields and their exploitation for purposes of energy generation (phase 1)", RWTH Aachen, project no. ET 4252 A, H. Staufenbiel and H. Oery (collected by: R. Windheim) ..... 315

Contributions on the problem of the building of large rotor blades

Rotor blade development Voith-facility, see page 61 ff for the projects on the Voith facility

Rotor blade Growian, see page 1 ff

Rotor blade for single wing wind facility, see page 169 ff

Project OPTIWA (see page 189): "Calculation of large rotor blades from the view of a computation engineer", Institute for Statics and Dynamics of Aviation and Space Flight Construction of the University of Stuttgart and Statics and Dynamic Research Association mbH, project no. ET 4406 A and B, I. A. Argyris, K. A. Braun and W. Lang ..... 321

Wing technology program: "Problem within the framework of the projects for fast and exact optimization of large rotor blades", MAN-Neue Technologie, project no. ET 4375 A, D. Muser ..... 332

Contributions on the problem of the control of oscillations of large facilities

Overall Growian dianamics: "Analysis of the overall dynamics of Growian", MAN-Neue Technologien with subcontractor Growian Construction and Operating Association mbH, project No. ET 4342 A, K. Kehl ..... 343

<u>Dynamics of large single blade facilities: "Control of oscillations of large facilities--Growian II: Single blade units. Dynamic design of the 350 kW demonstration facility", Messerschmitt-Boelkow-Blohm, project no. ET 4240 A, H. Strehlow and G. Seitz .....</u>	368
<u>Project OPTIWA (see page 189): "Investigation of the the dynamic behavior of wind energy facilities", Institute for Statics and Dynamics of Aviation and Space Flight Constructions", project no. ET 4406, A, I. A. Argyris and B. Kirchgaessner .....</u>	393
<u>The Conceptual Design of the High Speed Ratio Wind Rotor for the 52 M Diameter Horizontal Axis Voith Wind Energy Converter, W. Weber.....</u>	60

ORIGINAL PAGE  
BLACK AND WHITE PHOTOGRAPH

GROWIAN ROTOR BLADE  
MANUFACTURING, DEVELOPMENT, BUILDING AND TESTING

/1

H. M. Thiele



In January 1981, the Growian test rotor blade was finished after about 1-1/2 years development and construction time. This report discusses the manufacturing technologies and gives the experience made during the building and testing of this component.

## BOUNDARY CONDITIONS

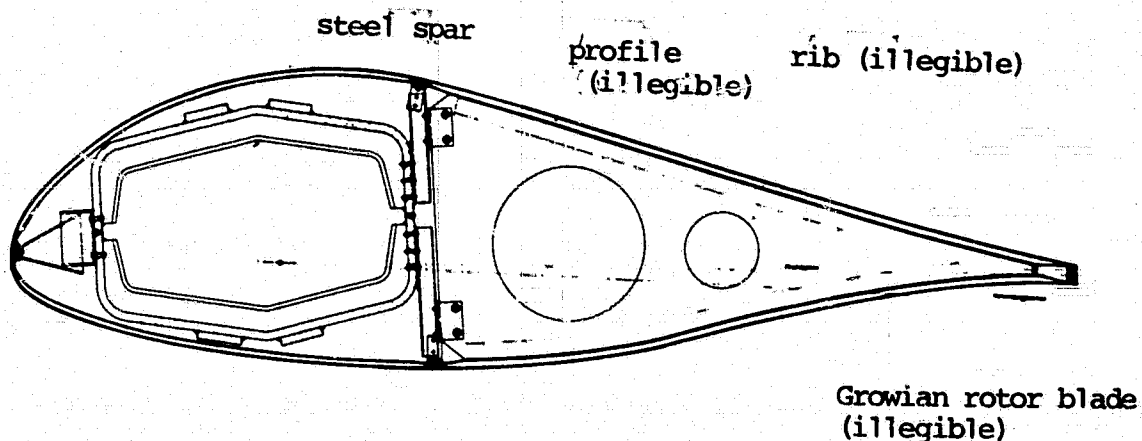
The following boundary conditions were adapted for the Growian two-blade rotor, a tower with simple support and the use of laminar profiles, assuming a design lifetime of 20 years.

- |                                     |   |
|-------------------------------------|---|
| specific facilities requirements    | - load assumptions<br>- blade geometry<br>- lifetime<br>- permissible blade tip deformations<br>- permissible eigen frequencies   |
| specific profile requirements       | - good shape maintenance<br>- low surface roughness<br>- close tolerance surface waviness   |
| specific manufacturing requirements | - use of tested and cheap manufacturing technologies<br>- extensive quality control<br>- maintenance of close manufacturing tolerances<br>- high requirements for welding seams<br>- maintenance of the same mass distribution for the two rotor blades<br>- resistant corrosion protection |

## DESIGN CONCEPT

A mixed construction method was selected as the design concept, /3 which has an untwisted steel box spar as the load supporting element. The external blade geometry is fixed by a GFK (glass fiber reinforced

carbon) sandwich design, which is connected to the spar with fittings. This shell design method comes from glider construction and makes it possible to satisfy the requirements for the small surface roughness and waviness of the laminar profiles.



blade cross-section

#### MANUFACTURING CONCEPT

Within this project, it is intended to build three rotor blades. /4 Therefore, manufacturing technologies were selected which would require the minimum amount of special equipment such as molds, pressing machines, etc. This measure, however, requires special skills by the workers in order to maintain the close construction tolerances.

With these assumptions, the following manufacturing concept was developed:

spar

- welded construction
- low tooling complexity
- reduction of the welding seam to a minimum

**ORIGINAL PAGE IS  
OF POOR QUALITY**

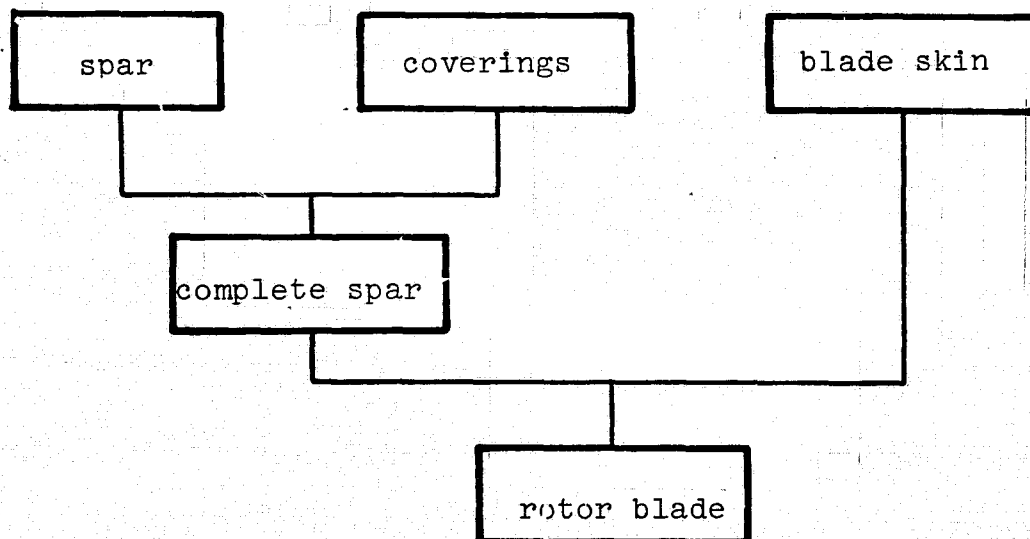
blade skin

- GFK (classified with reinforced carbon) sandwich design
- manual lamination method for the mold cavities
- production of the largest possible shell section
- simple installation

fittings

- simple welding designs
- variable design in order to equalize tolerances between the spar and the skin

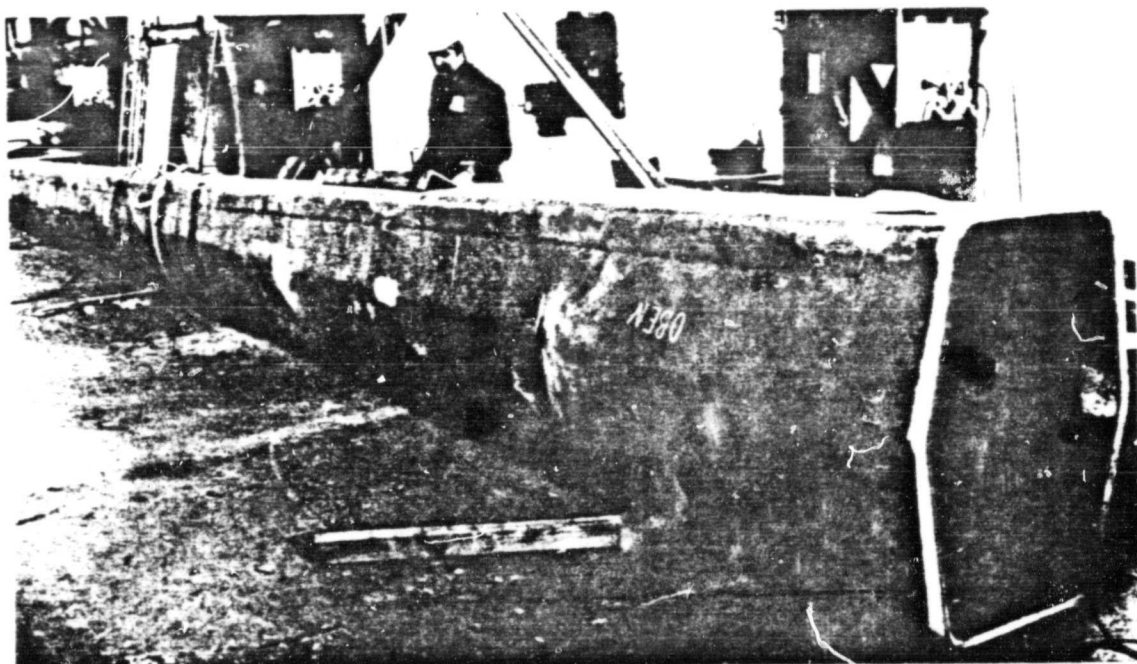
By dividing this into the three component groups, it was possible to have parallel manufacturing of individual components according to the following manufacturing plan.



15

MANUFACTURING

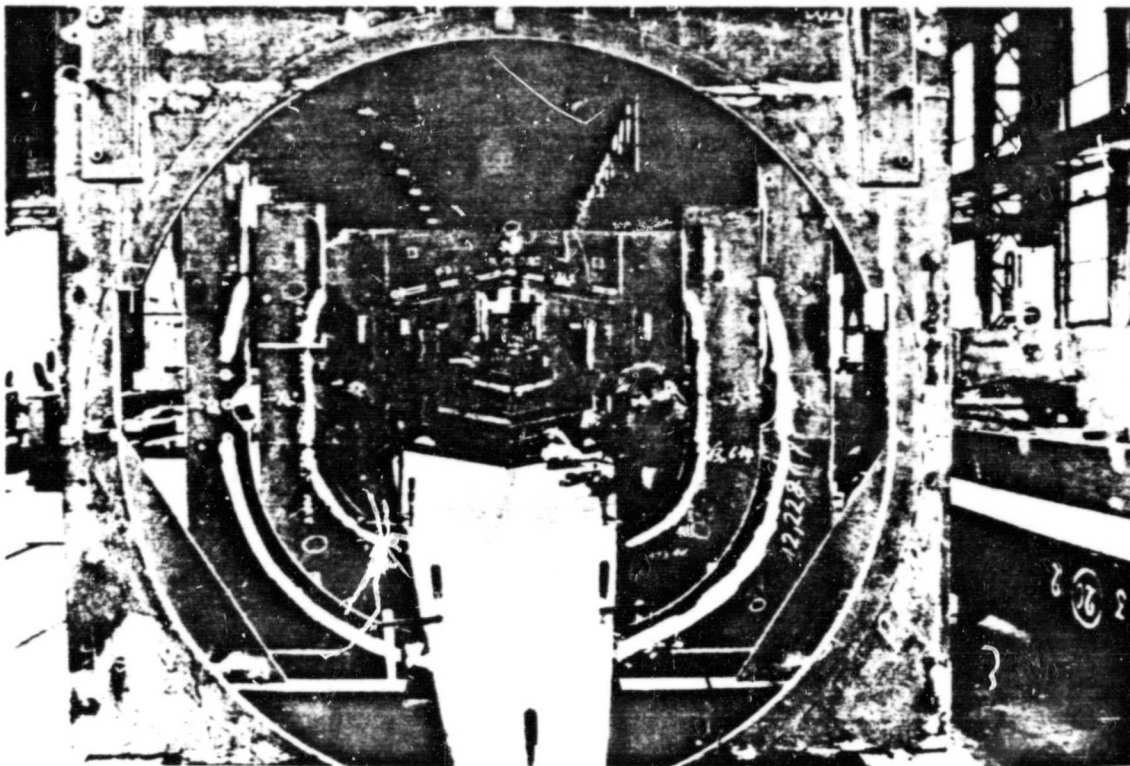
The spar box was a welded design which represents a reliable and tested manufacturing technique with appropriate quality control. The welds have to be done very carefully because the continuous strength of the basic material is greatly influenced by them. The welding instruction of the spar was adjusted to the manufacturing requirements and was divided into several spar segments. By making the steel sheets in the form of half shells with a length of up to 7.5 m, it is possible to greatly reduce the number of welded seams. In this way, it is possible to control the distortions of the components which occurred during welding.



spar section

A 40 m long berth was used for assembly where the individual spar sections were attached and measured. The spar was welded outside of the berth in order to make accessible the connection points from all three sides. The construction tolerances and the welding qualities were, therefore, maintained using this production method.

It was difficult to bend the steel sheets into half shells without special pressing tools. Deviations can easily occur which are made more difficult by the difficult handling of the sheets. The fittings



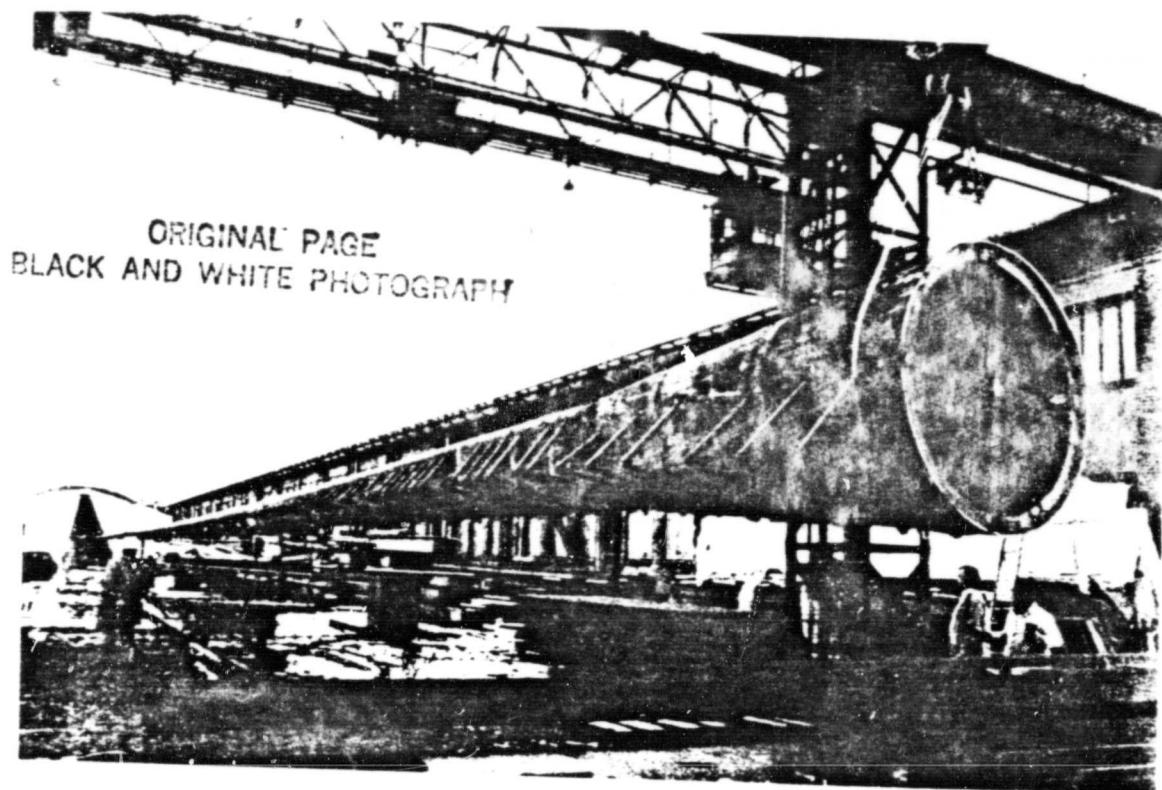
Assembly jig

for accepting the external skin on the ribs in the end box were also made as welding construction and then bolted to the spar. The connection surfaces to the external skin are adjustable so that it is possible to equalize tolerances between the spar and the skin. The fittings are 17 assembled in the berth. The external skin is measured later on at six measurement points.

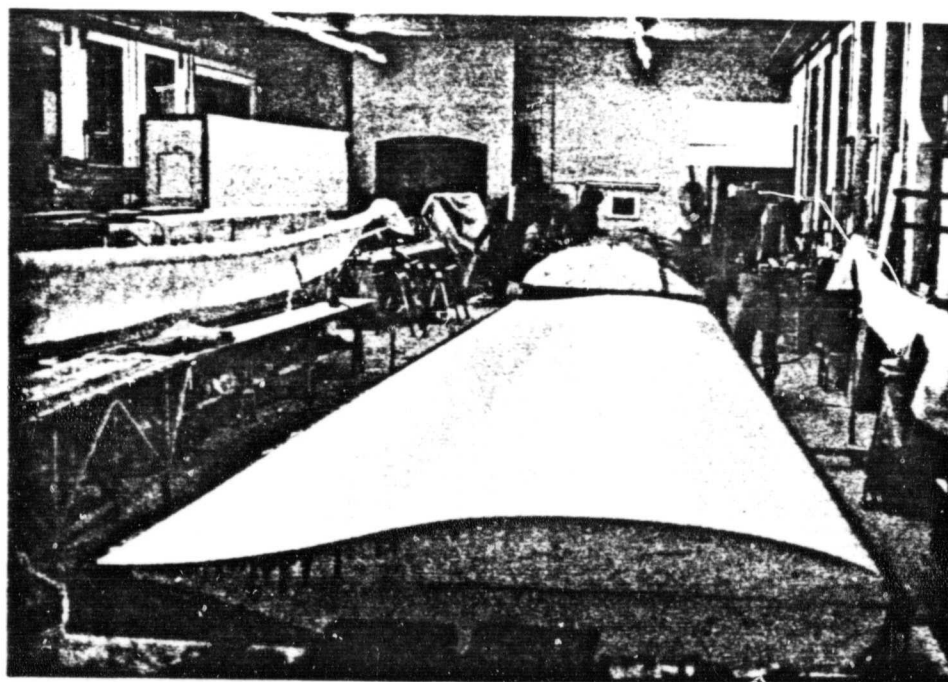
The shells of the blade external skin are made according to the proven plastic manufacturing technique. All of the shell components are laminated in negative molds. The separation plane of the shells are the profile chords and in the internal region after R 27.5, these are also at the spar trailing edge. In this way one obtains approximately equal shell sections which make sure that the hardening time of the resin system is not exceeded during lamination with the appropriate use of personnel. In addition, the center of the mold has to be accessible in the depth direction from the edge of the mold which is another boundary condition for the dimensions of the mold.

After an appropriate training time, it was possible to manufacturer 18 the individual shells without many problems. About 10 workers had to





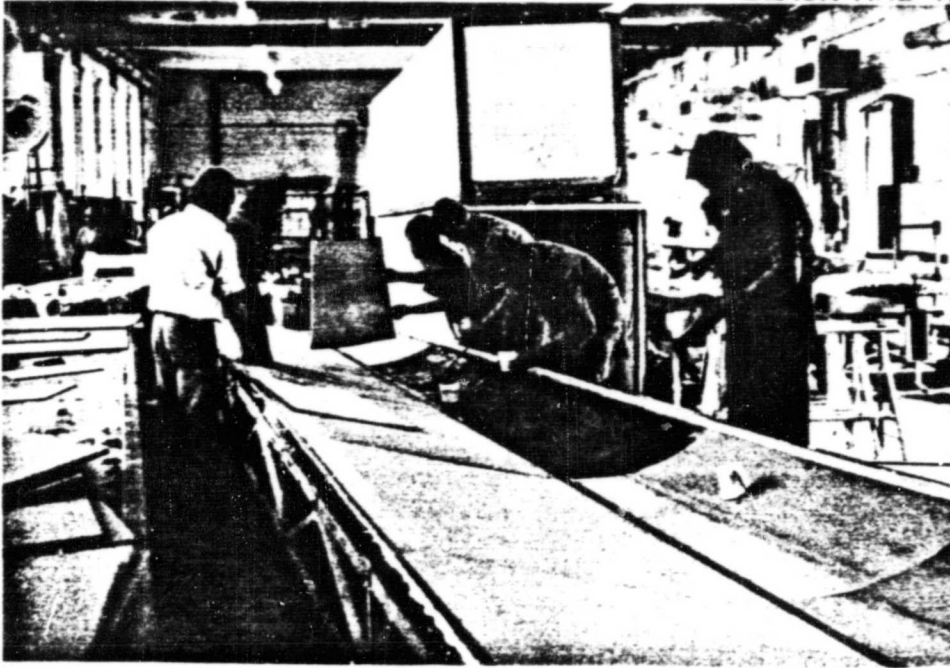
spar R-50, R10,85



form cavities with original model

ORIGINAL PAGE  
BLACK AND WHITE PHOTOGRAPH

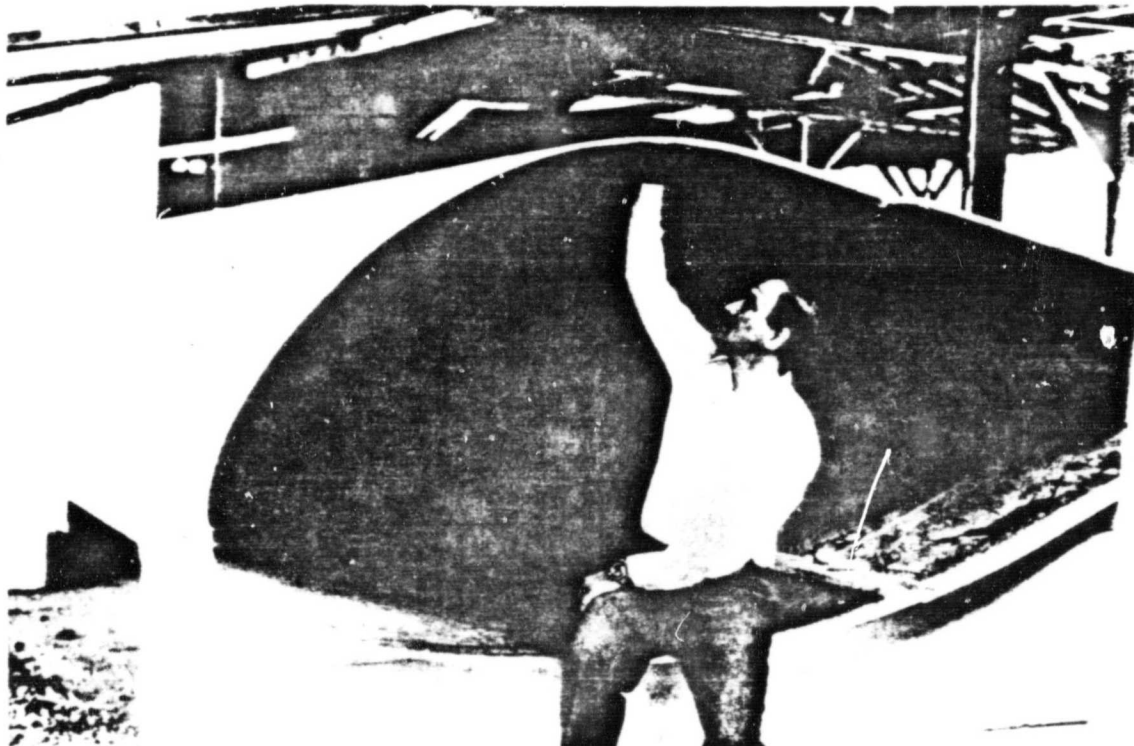
ORIGINAL PAGE  
BLACK AND WHITE PHOTOGRAPH



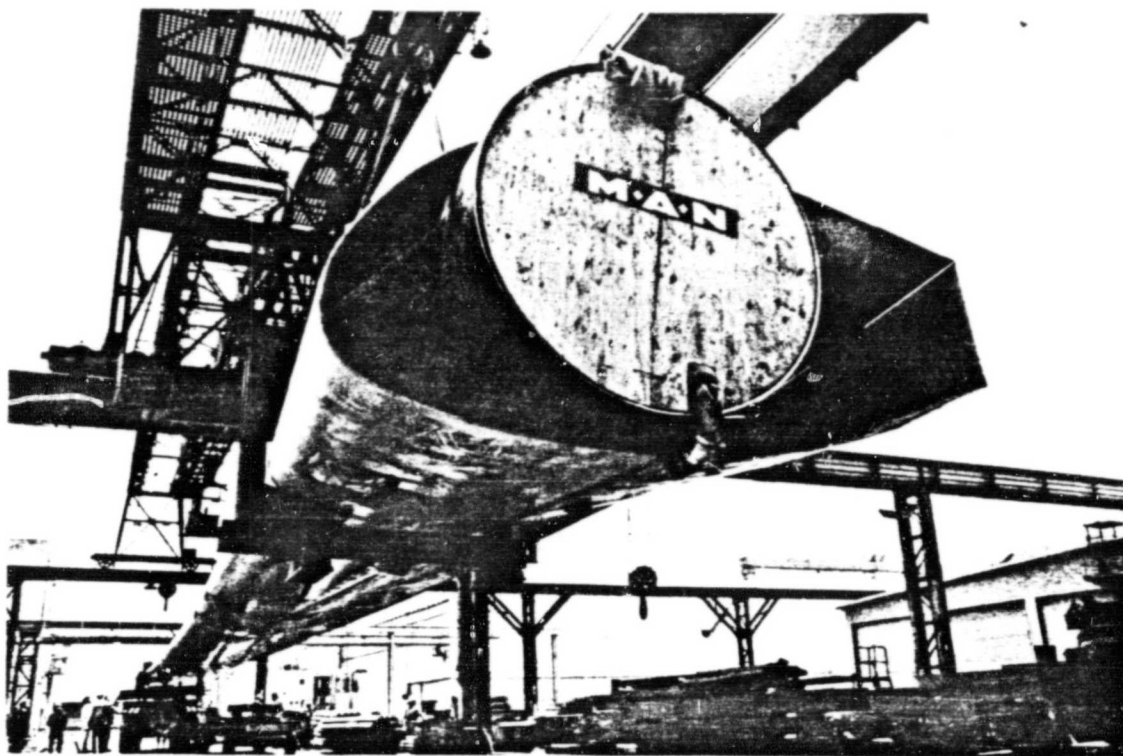
lamination of the shells

simultaneously handle the matrix of each half shell in order to not exceed the hardening time. After taking the shell parts out of the molds, examinations showed that the permissible surface roughness and waviness had to be maintained and was even less than required in the external blade region. The required accuracy of the shell weights of 2% could not be achieved, there were excesses of up to 5%.

19



shell set at the blade station R15.7



rotor blade R50, R10.85

The assembly procedure of the external skin to the spar has proven itself. Matching difficulties between the skin and the fittings did not occur. The examined profile sections and blade twist were within the permissible tolerances.

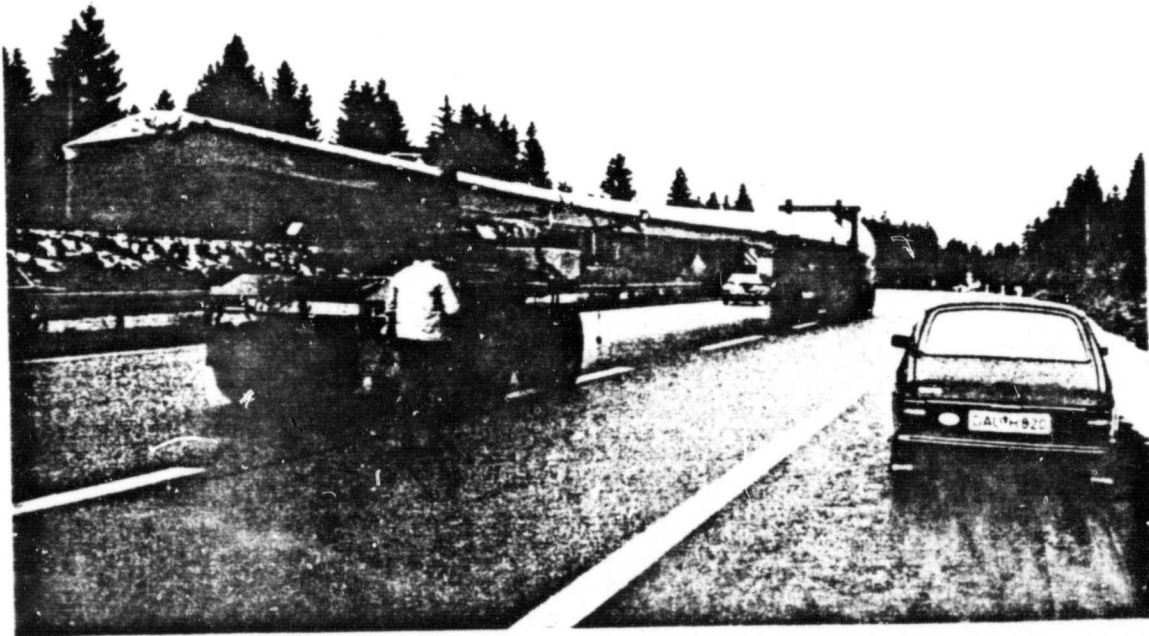
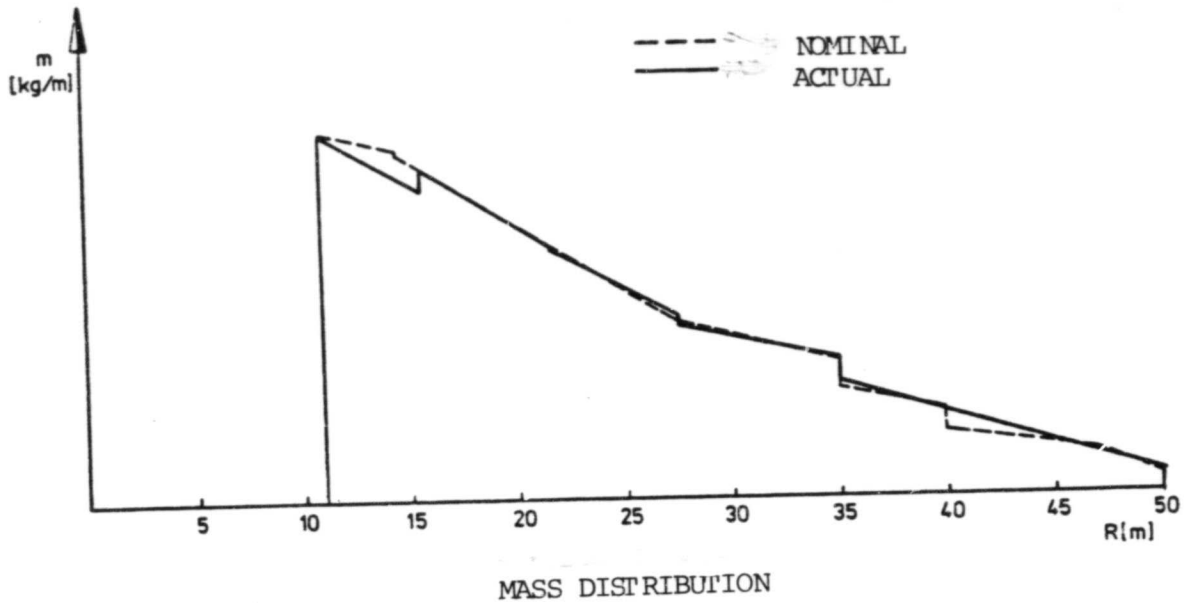
After manufacturing, the rotor blade was transported from Mainz to Munich on trucks. During the transport, the blade was supported at stations R15 and R45 on self-controlling trailer vehicles and was transported on the Autobahn at a speed of about 40 km/hr. The accelerations during transport were below 1g for the blade.

## RESULTS

Comparison between the calculated mass distribution and the measured ones showed that there was good agreement in the region between R10.85 and R40. At the blade tip the measured mass distribution deviates from the nominal values. This results in excessive shell weight and weighed weights of the spar section between R45-R50. This is because it was not possible to finally divide the spar section after each wall thickness jump because of the manufacturing process. After the installation of the blade on the test stand, we measured the bending under

ORIGINAL PAGE  
BLACK AND WHITE PHOTOGRAPH

/11



TRANSPORT OF THE ROTOR ELADES

eigen weight in the flapping direction at the blade tip. We also measured the eigen frequencies and eigen modes during test oscillation measurements. The deformation at the blade tip is 3% larger and the first flapping eigen frequency is 3.25% lower than calculated. The first deflection eigen frequency agrees well with the calculated one.

### STRUCTURAL TEST GROWIAN ROTOR BLADE

Four static load tests, one test band oscillation test and a dynamic load test at 50 LW were performed with the Growian rotor blade prototype.

A preliminary evaluation of the measured results shows good agreement between calculated and measured values. Deviations from the theoretical data occurred at blade station R27.5 which can be attributed to a deviation already found during the manufacturing. At the lower shell R27.5-R15.7 of the profile end box, delaminations were found during the tests which can be attributed to manufacturing errors.

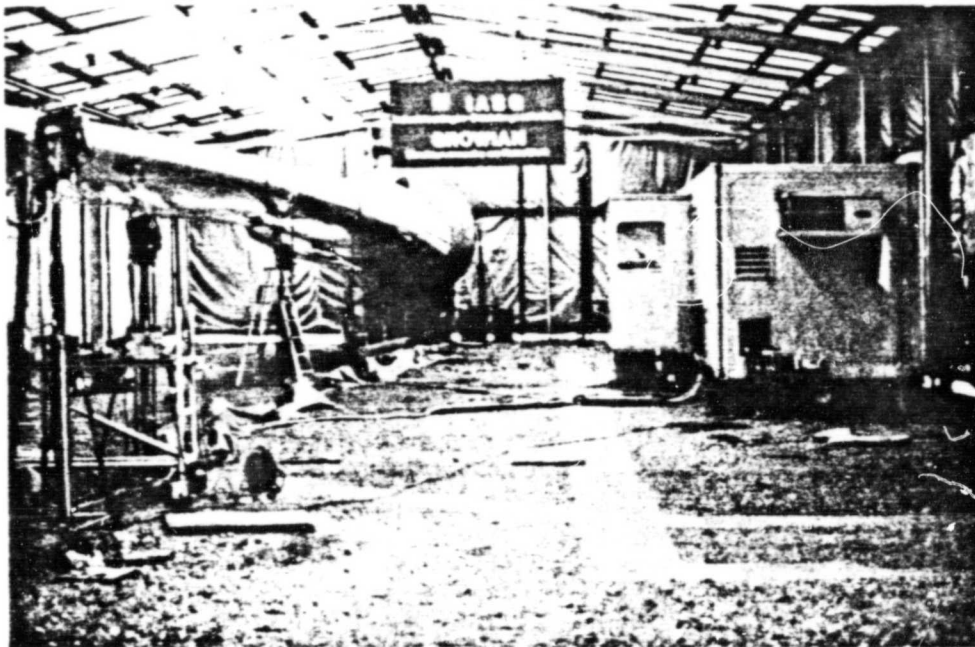
The tests were concluded with a fracture test which was performed with up to 170% of the safe load. We did not increase the load further because local failure of the structure was established at several points of the test specimen.

### TEST RESULTS

#### Test stand oscillation test

The test stand oscillation test was used for determining the eigen frequencies and eigen modes of the rotor blade. 16 eigen modes were determined using the phase resonance method. The rotor blade was excited to perform oscillations using 2 electrical-dynamic exciters and the oscillations were measured using 80 accelerometers distributed over the blade. Figure 1 shows the test configuration with the measurement container of the DFVLR-Goettingen.

ORIGINAL PAGE  
BLACK AND WHITE PHOTOGRAPH



/13

test setup for test stand oscillation test

Measurement results

The measured mass distribution of the blade including the force introduction fittings for load test as well as the DMS (strain gauge) cabling were considered over the spar in the determination of the theoretical values.

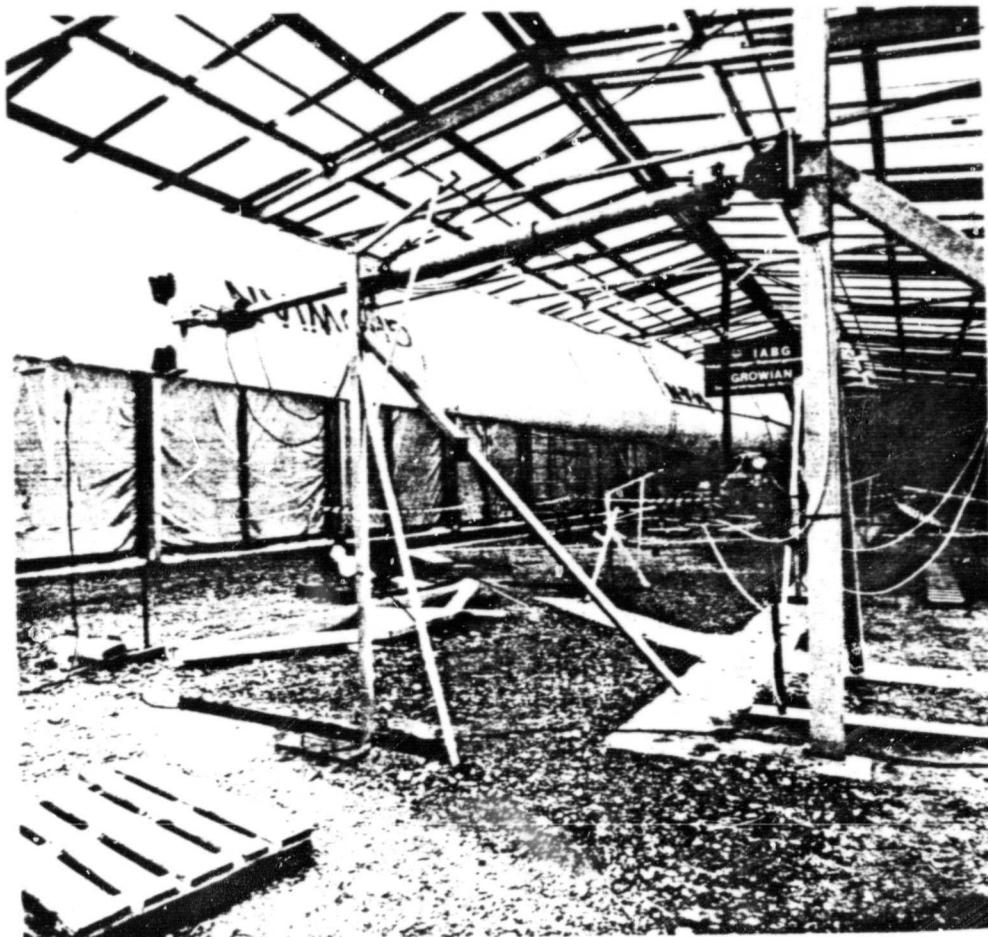
Mode	measured value	calculated value
1st flapping eigen frequency	0.923	0.956
1st deflection eigen frequency	1.27	1.27
2nd flapping eigen frequency	2.39	2.64
2nd deflection eigen frequency	3.55	3.64
1st torsion eigen frequency	21.67	26.19

/14

Load tests

The load of the test specimen was done using load equipment with hydraulic cylinders. The configuration of the cylinders was designed so that at blade stations R35 and R27.5 the bending moments were





test configuration load case 1.3

simulated as closely as possible. The intersection forces deviated by as much as 10% from the theoretical values at the other blade station. During tests, the additional strains due to the loading equipment and the cylinder loads were measured at 500 measurement points. Strains due to the eigen weight of the blade were measured only in load case 2.5 by rotating the test specimen by 180°.

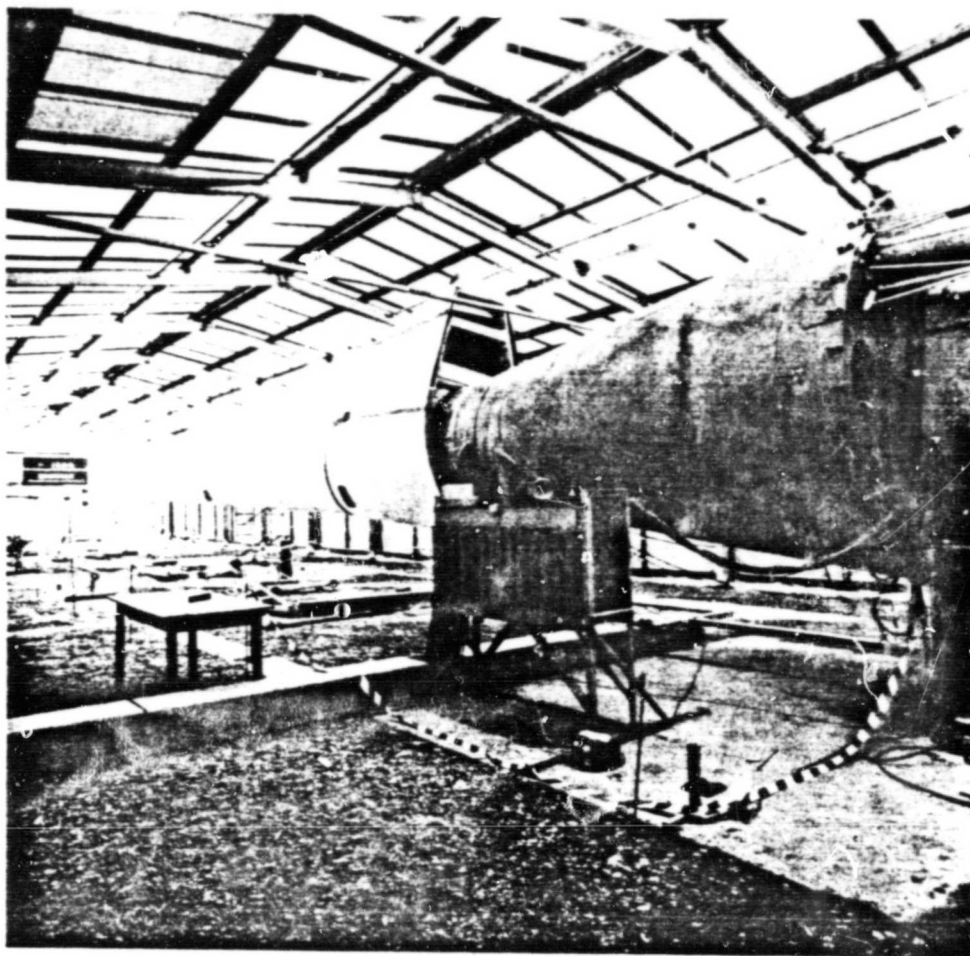
---

The loading of the test specimen is done using two cylinders at R41 (80 kN) and R13.6 (41 kN).

#### Measurement results:

/15

The measured strains for blade cross section R 27.4 (undisturbed cross section) have somewhat smaller values than the theoretical ones. For cross section R 27.5, the measured values are higher compared with theoretical ones by a factor of 1.56. This can be attributed to a



turning experiment

collapse of the welding seam and excessive edge displacement, which is not permissible for the two other rotor blades. The strains measured at the outer skin are also below the theoretically determined ones.

The blade deformation at the tip was  
 in the flapping direction      1.174 m  
 in the deflection direction      0.063 m

For determining the bearing friction moments, in the load case 16 1.3 of the test configuration, at 100% nominal load the rotor blade was rotated with a hydraulic cylinder by  $\pm 2.5^\circ$  at the blade control connection, around the blade longitudinal axis. 100 alternating loads with a frequency of 0.15 Hz were applied. The measurements at the



beginning and end of the tests showed a slight reduction in the friction moment. The blade displacement moments were

$M_D = 26.9$  kNm in the initial position and

$M_D = 44.92$  kNm in the final position

This data is within the theoretically predicted range.

#### Load case 2.5

Figure 4 shows the test configuration for load case 2.5. The load is applied to the test specimen by three hydraulic cylinders at stations R39 (133 kN) R24.6 (107 kN) and R15.6 (126 kN).

#### Measurement results:

The statements for load case 1.3 apply for this case. Here again the stresses were increased due to structural deviations at R27.5 by a factor of 1.56.

The blade deformation at the tip was:

in the flapping direction      0.792 m

in the deflection direction    1.929 m

#### Load case 2.5

After load case 2.5, a dynamic loading test with 50 alternating loads was performed. As a lower load, we selected 20% and as an upper load we selected 100% of the nominal load of load case 2.5. The measurement at the beginning and at the end of the test did not show any differences in the strains and deformations. The delamination points around the end box along the under side of the outer skin between R27.5-R15.7, however, increased; otherwise, no damage was found.

#### Fracture test

The fracture test was carried out using the test configuration of load case 2.5. When 170% of the case load was reached, the test was

terminated. At this time, at station R27.5, we found local instabilities in the structure, that is, the strains measured in the steel spar were no longer linear. In addition, there was a local buckling of the blade skin at R27.5 along the blade underside. A 150 mm hole in the skin was the reason for this, which had to be drilled in order to examine measurement points over the spar at the beginning of the test. Additional damage in the skin was not found (photograph page 18).

#### Measurement results:

The stresses in the spar and in the outer skin achieved for 170% of the safe load are shown in Figures 10-12.

The following was measured at the blade tip

flapping direction      3.235 m

deflection direction    0.888 m    measured

After unloading of the specimen, a residual deformation of about 0.400 m was found at the blade tip.

#### CONCLUSIONS

A rough evaluation of test results shows good agreement with calculated results. Since the rotor blade will be subjected up to 108 load alterations during operation, it was dimensioned for continuous strength. However, we can thereby explain the large separation between the safe load and the static fracture load ( $j^2$ ). In addition, tests have shown that the blade skin made of glass fiber plastic will follow the spar deformations without tearing and the strain of the skin are by a factor of 10 smaller than the measured fracture strain of the laminate.

## STATUS OF THE THREE PROJECTS OF THE VOITH FACILITY

Hofmann and associates

/19

### General remarks:

The Voith-Getriebe KG Heidenheim, West Germany, Division for Aviation Technology already in 1976 planned the development, manufacturing and testing of a wind energy converter of medium power and size for use as a fuel saver for island operation and network operation. It was primarily planned for regions with low infrastructure in the third world.

We consider an axial flow equal pressure turbine with a gondola rotor in the leeward side. It had 2 FVW rotor blades with the shell design which are positioned over a wind flag (no side wheel gondola deflection device). Also, we considered a steel tube mast supported with guy wires.

The star-shaped reinforced concrete foundation was not anchored to the ground.

As a location for the test, we used the terrain at (Huetter) in Stoetten in the Swabian Alps, in the Goeppingen district.

Professor Ulrich Huetter Stuttgart/Kirchheim (FWE) advised us about the aerodynamic design and the basic concept.

The firm MBB Munich was considered for the development and supplying of the high performance rotor blades after a long search.

The main data of the WEC is as follows and was maintained over the years:

rotor blade diameter 52  
nominal speed 8.5 m/s  
mast height 30 m

rotor rpm 37 1/min  
rotor performance 316 kW  
synchronous generator 350 KVA

1. Goal of ET 4104 A (facility):

/20

According to the 52 m diameter size and the assumed DFVLR load assumption (see Figure 1) and a century gust of 60 m/sec, we consider the following:

- completely automatic facility, including startup and shutdown
- self-saving (fail-safe) machine installation
- a synchronous generator which switches in and out of a three-phase current network automatically (20 KV, 50 Hz)

The following was expected:

- long lifetime
- high availability
- operational safety
- easy assembly (if possible without excessively large cranes)
- easy maintenance with long intervals
- small weight with high strength
- competitive price
- national manufacturing components for the third world
- environmentally sound with regard to appearance and noise
- movability of the entire installation (other test field)
- safe against unauthorized removal

/21

2. Goal of ET 4343A (rotor blade development):

- the recommendations of Prof. Huetter included the following for the Voith facility with a fast running coefficient of

$$\lambda = \frac{\text{tip speed for a wind}}{\text{nominal speed}} = \frac{100.74}{8.5} = 11.85 \text{ (see Figure 1a)}$$

or for  $c_p$ -optimum = 0.45 according to an extremely high fast running number of  $\lambda_{\text{opt}} = \frac{100.74}{6.3} = 16$

(see Figure 2) and very slender rotor blades resulted with an area loading of

$$\frac{316000}{52^2} \times \tau = 149 \text{ W/m}^2$$

- we consider the fact that the masses of the completed gondola should be made as small as possible in order to not exceed the total eigen frequency of the WEC with an operating frequency of  $\frac{37}{60} \times 2 = 1.24$  Hz
- the rotor blade mass was limited to about 1000 kg per blade, and the slender profile family of the blade cross sections were specified by Prof. Huetter.

These parameters led to an extremely light hollow blade design with support foam inserts and transverse bolt attachment.

The initial plan to divide the blade into two lengths and to flange them together as required had to be given up because of oscillation problems.

/22

### 3. Goal of the ET 4344 A (telemetry):

The behavior of the two slender rotor blades has to be monitored especially when penetrating the wake of the mast and excessively high blade deflections have to be controlled by turning off the facility.

The transfer of the measured current of strain gauge strips and accelerometers cannot be done using slip rings.

### 4. Solution of the problems of ET 4104A (facility):

Reference Hoffman

#### 4.1 Structure

From a number of possibilities (see Figure 3) we finally decided for the prototype shown in Figure 4:

- pendulum hub according to Prof. Huetter (semi-cardan suspension), steel sheet welded construction with the possibility for self-controlled blade angle adjustment (in order to equalize shear

flow) and to block it (see Figure 5).

- pendulums bearing pair from prestressed double conical roller bearings (over dimensioned because of the fact that the periodic rotational motions were only small) using continuous grease lubrications
- rotor blade bearings, one prestressed and commercial crossed roller bearing each with a measured friction value under full load of about 0.003 with continuous grease lubrication and double seals against water entry
- adjustable control rods with commercial spherical joint head and continuous grease lubrication
- hub covering with trim disks as well as solar shells for measurement transducers mounted on the outer surface (ET 4344A, telemetry)
- the completed pendulum hub is connected to the rotor hollow shaft using a Hirth gear (see Figure 6). The shaft is supported at two places with a throat bearing which is developed as a cylinder full roller bearing which can be displaced in the axial direction and a prestressed conical roller bearing for the operational axis movements which occur during operation. Both bearings have oiled lubrication
- the conical wheel set 70/17 teeth or  $i = 4.12$  has a reducing effect on the aerodynamic thrust because of its axial thrust, that is, the conical roller bearings are unloaded in this way.
- the hollow rotor shaft accepts the rotor blade adjustment inside (see Figure 7).
- a differential system for rotor blade adjustment is also provided by a hydrostatic locking or damping of the piston rod. This could be important if blade angle deflections occur caused by pulsating

aerodynamic forces.

- a screw spring also provides blade adjustment in the "flag" direction which is integrated with the adjustment mechanics, that is, the blades then have no lift, the WEC facility will turn off itself in emergencies.
- the position information of the control rod or rotor blades which is important for the controller is done with a potentiometer (see Figure 8).
- the gondola hydraulics (see Figure 9) is supplied by a wing cell pump with 0 stroke control. The electrical motor obtains it current with slip rings (see Figure 9).
- the oil supply and removal for the differential system inside the rotor shaft is done with an electrical hydraulic control slide of our own design (see Figure 10).

the heatable oil container is installed in the gondola housing. All of the hydraulic lines are, therefore, short. The pump supply is done with a natural slope.

the hydraulic unit is attached outside on the housing and is easily accessible (see Figure 11).

- the gondola housing is flanged to a rotatable bearing (see Figure 12). The worm gear wheel is connected with a fixed mast, the gondola housing is centered using a conventional crossed roller bearing using the mast.

A three stage unlimited worm gear supported in the gondola housing gives a gear reduction ratio of  $i = \frac{50}{3} = 16.67$

After the worm gear shaft there is a combined commercial spur wheel worm gear which has  $i = 214.8$ . The drive motor has 1440 rpm. For a total  $i_{ges} = 214.8 \times 16.67 = 3.581$ , in other words,

the gondola would have a theoretical rpm of 0.4 rpm. Between the worm gear shaft and the spur gear worm gear there is an electrically controlled lamella coupling which is closed when power is available. This provides absolute self-control for the entire gondola operating range.

/24

When there is power failure, erroneous gondola positions, etc., or oblique loads for the unfavorable case of rotor blades in the flag position, a gondola torque could be created for very high wind speeds which would rotate the gondola out of the oblique incident wind position. This is possible because the electromagnetic coupling would not be switched in in this case.

- three electrically controlled hydraulic pistons are distributed along the circumference of the gondola and mast flange for operating the plier breaks. The brakes are turned on when the facility is operated and are only opened during a positioning command or in the event of power failure.
- in order to introduce current for the two gondola motors for the control voltages, receptacles, etc., a slip ring transmission is required (see Figure 13) which is below the gondola rotating gear and housing, and which belongs to the fixed mast.

The measured currents are not run through slip rings but are directed directly to the controller, recording devices, etc., with a 20 conductor flat cable. This winding sleeve makes it possible to have  $\pm 5$  gondola rotations before the connector connection would be opened. This means that already after about three gondola rotations a restoration command will be given and this would result in a turning back under favorable conditions.

- two pedestal planes are provided for assembly and maintenance work in gondola 2 (see Figure 14). A safety conductor goes from level 5m to the gondola plane.



- a wing wheel anemometer and a combined wind flag are located above the gondola housing as well as the required lightning protection.
- additional lightning slip rings are provided for protecting the main bearings between the rotor blades and the rotor shaft, between the rotor shaft and the gondola housing and between the gondola housing and the mast.

The mast is connected several times with iron reinforcement of the concrete foundation and the conventional grounding wires are used.

- The long tube shaft which goes downward (see Figure 15) between the conical shaft and the spur wheel shaft is supported with two V-belt connections and can be displaced in the longitudinal direction. In the central region (see Figure 15) it is supported with a pendulum ball bearing with respect to the mast in order to hold the critical bending rotation rate above the operating rate of 152.7 rpm.

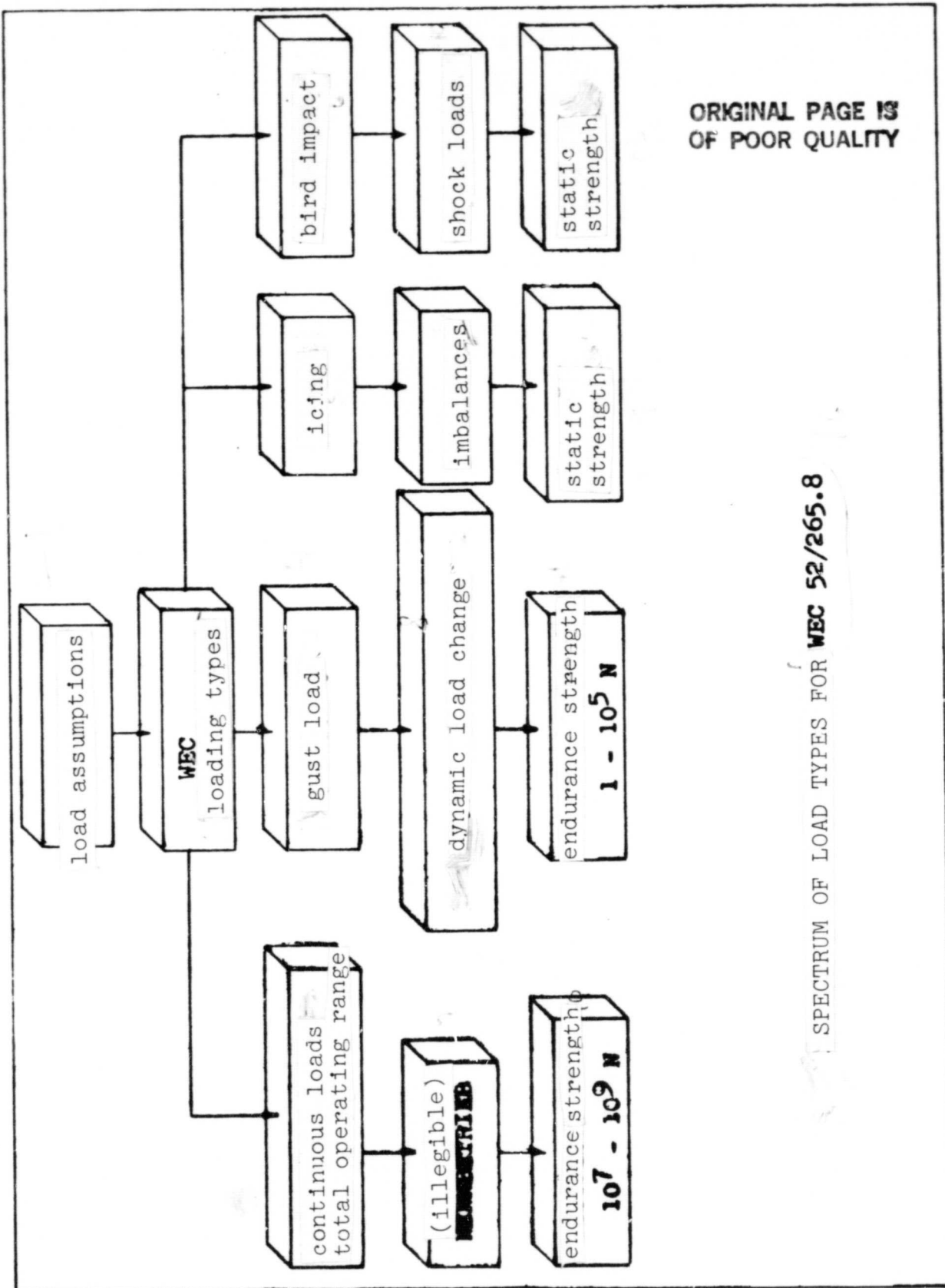
125

The spur wheel gear, the normal Voith design  $i = 9.82$ , is coupled through a jointed shaft (see Figure 16) with the 350 KVA synchronous generator.

2 ring tensioning rings between the generator shaft end and the coupling flange transmit the maximum torque =  $2.5 \times$  operating torque at about 300 kW and  $n = 1500$  rpm. In this way, possible short impacts from the WEC transmission are blocked.

- A fail-safe plier brake below the spur wheel gear output shaft (see Figure 16) provides for fixing of the entire shaft assembly including the rotor and the generator in the event of danger or during repairs.
- the generator has a tachomachine for monitoring rpm; two additional toothed disks with electrical transducers measure the





ORIGINAL PAGE IS  
OF POOR QUALITY

SPECTRUM OF LOAD TYPES FOR WEC 52/265.8

FIGURE 1

ORIGINAL PAGE IS  
OF POOR QUALITY

Gesamtleistungsbewert  $c_p = f(\lambda)$

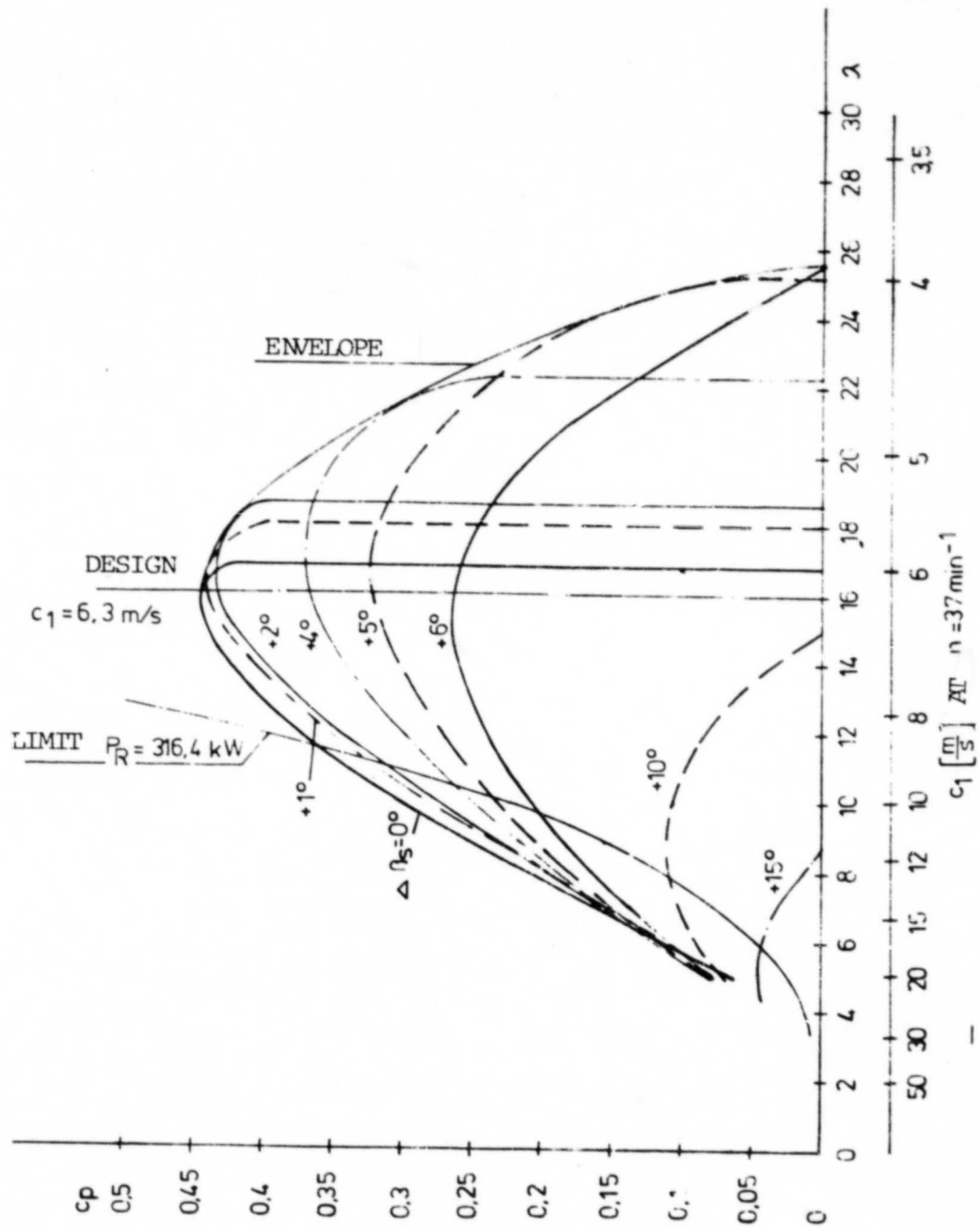
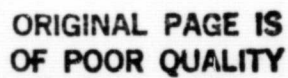


FIGURE 1a

00752



ORIGINAL PAGE IS  
OF POOR QUALITY

FIGURE 2 (CONTINUED)

KEY: 1--closed after (illegible); 2--tungsten granulate; 3--section;  
4--detail; 5--cross-section of blade; 6--Voith axes; 7--profile chord;  
8--sandwich region; 9--mode separation plane; 10--Voith axes: axis  
system for installation of blade to rotor head; 11--manufactured  
according to FV; 12--(illegible); 13--all laminates laminated with  
mixture of (illegible); 14--glued with mixtures from (illegible);  
15--left (illegible)...(others illegible)...

ORIGINAL PAGE IS  
OF POOR QUALITY

Status 1977: 14 component group combinations were investigated:  
(see drawing M 1:100 no. 3.73-201 sheets 1-3)

		1	2	3	4	5	6	7	8	9	10	11	12	13	14
1	2-blade rotor rpm 1/min	36 50	36 50	36 50	36 50	36 50	36 50	38 45	52 45	52 45	52 45	52 45	52 43	52 43	52 43
2	Rotor position	Lee	Lee	Lee	Lee	Lee	luff	luff	luff	Lee	Lee	Lee	Lee	Lee	Lee
3	Rotor suspension	rigid	semi card	semi card	semi card	semi card	full card	full card	full card	full card	full card	full card	full card	full card	full card
4	gear ratio about 1 =	2,15	-	3	3	3	2,75	3,24	3,24	3,24	3,24	3,24	3,55	3,55	3,55
5	gear type	crossed rope	jointed shaft	cone	cone	cone	crsd. rope	chain drive	chn. drv.	chn. drv.	con. drv.	con. drv.	con. drv.	con. drv.	plane drive
6	Transmission	crsd. rope	drive tube	drive tube	drive tube	drive tube	drive tube	drive tube	drive tube	drive tube	drive tube	drive tube	drive tube	drive tube	drive tube
7	gear degree about 1 =	2,15	15	10	10	10	10,9	4,5 2,2	4,5 2,2	10,29	10,29	10,29	9,82	9,82	--
8	gear type	1-3 belt	2stage drive	2stg drv.	2stg drv.	2stg drv.	2stg drv.	chn+ belt	chn+ belt	2stg drv.	2stg drv.	2stg drv.	2stg drv.	2stg drv.	2stg drv.
9	Generator 1/min	below 750	below 750	below 1500	below 1500	below 1500	below 1500	below 1500	below 1500	9 1500	11,5 1500	11 1500	7 1500	below 1500	below 1500
10	turntable ca.	top	below	below	below	below	below	below	below	7,5	12	11	27,5	27,13	26,5
11	mast position	1	teles	1	1	1	1	1	1	1	1	1	1	1	1
12	mast design	tube	copic tube	tels. tube	adjb tube	adj. tube	ellip tube	ellip tube	ellip tube	cyl. tube	cyl. tube	cyl. tube	tube	tube	tube
13	mast support	rods	-	-	-	-	-	-	-	pedestal	guy	same	same	same	same
14	chipping hinge	below	below	top+ bot.	top+ bot.	top+ bot.	top+ bot.	top+ bot.	top+ bot.	3ft top+ bot.	11,5 top+ bot.	11 top+ bot.	8,5 top+ bot.	9 top+ bot.	below bot.
15	pulling device	Wind	Wind	outside	inside	inside	inside	inside	inside	ins.	ins.	ins.	Wind	Hydr. cyl.	Hydr. cyl.
16	sidewheel 2,5 ø m ht. ca.	-	5,6	7	7	7	10	10	17	13,5	11,5	27,5	27,44	27	28,5
17	max. terminal performance kW	150	150	150	150	150	150	150	200	200	265	265	265	265	265
18	remarks	continuous rope strength?	large collar	aerodynamic cylinder. Wake too large	heavy tipping mast	high cg. fold- able mast	mast stability?	chain lifetime, mast stability?	high total weight	mast stability?	mast stability?	mast stability?	mast stability?	stable mast for critical condit	mast freq low excited freq
19	selected	-	-	-	-	-	-	-	-	-	-	-	-	-	-

Total cost: DM 2.814.100

support of: DM 1.324.400

government:

FIGURE 3

Abk. ungen: (6/1) geschrankter Seiltrieb  
(6/7) Gelenkwelle  
(8/2) zweistufig  
(12/2) Teleskop-Rohr  
(12/4) verstärkt  
(12/5) elliptisches/zylindrisches Rohr  
(13/12) Pardunen/Stangen  
(15/10)-(15/12) Hydraulikzylinder  
(16/12) stabiler Mast/unterkritischer Betrieb  
(18/17) Mastfrequenz unter Anregungsfrequenz

Patentmeldungen: (1/1)-(1/14) Schlaufentlastung  
(4/6)-(4/14) wellkard. Anhängung  
(6/1) Seiltrieb  
(14/3)-(14/12) Knickmast  
(15/3)-(15/10) Zugvorrichtung  
(15/12)-(15/13) Zugvorrichtung



FIGURE 3 (continued)

ABBREVIATIONS: ( 6/1 ) crossed rope operation  
( 6/2 ) jointed shaft  
( 8/2 ) two stage  
(12/2 ) telescopic tube  
(12/4 ) reinforced  
(12/5 ) elliptical/cylindrical tube  
(13/12) guy ropes/rods  
(15/10)+(15/12) hydraulic cylinder  
(18/12) stable mast/subcritical operation  
(18/13) mast frequency below excitation frequency

PATENT APPLICATIONS: ( 1/1 )-( 1/14) blade flange  
( 4/6 )-( 4/14) complete card. suspension  
( 6/1 ) rope operation  
(14/3 )-(14/12) buckled mast  
(15/3 )-(15/10) pulling device  
(15/12)-(15/13) pulling device



ORIGINAL PAGE IS  
OF POOR QUALITY.

▼ VOITH GETRIEBE KG

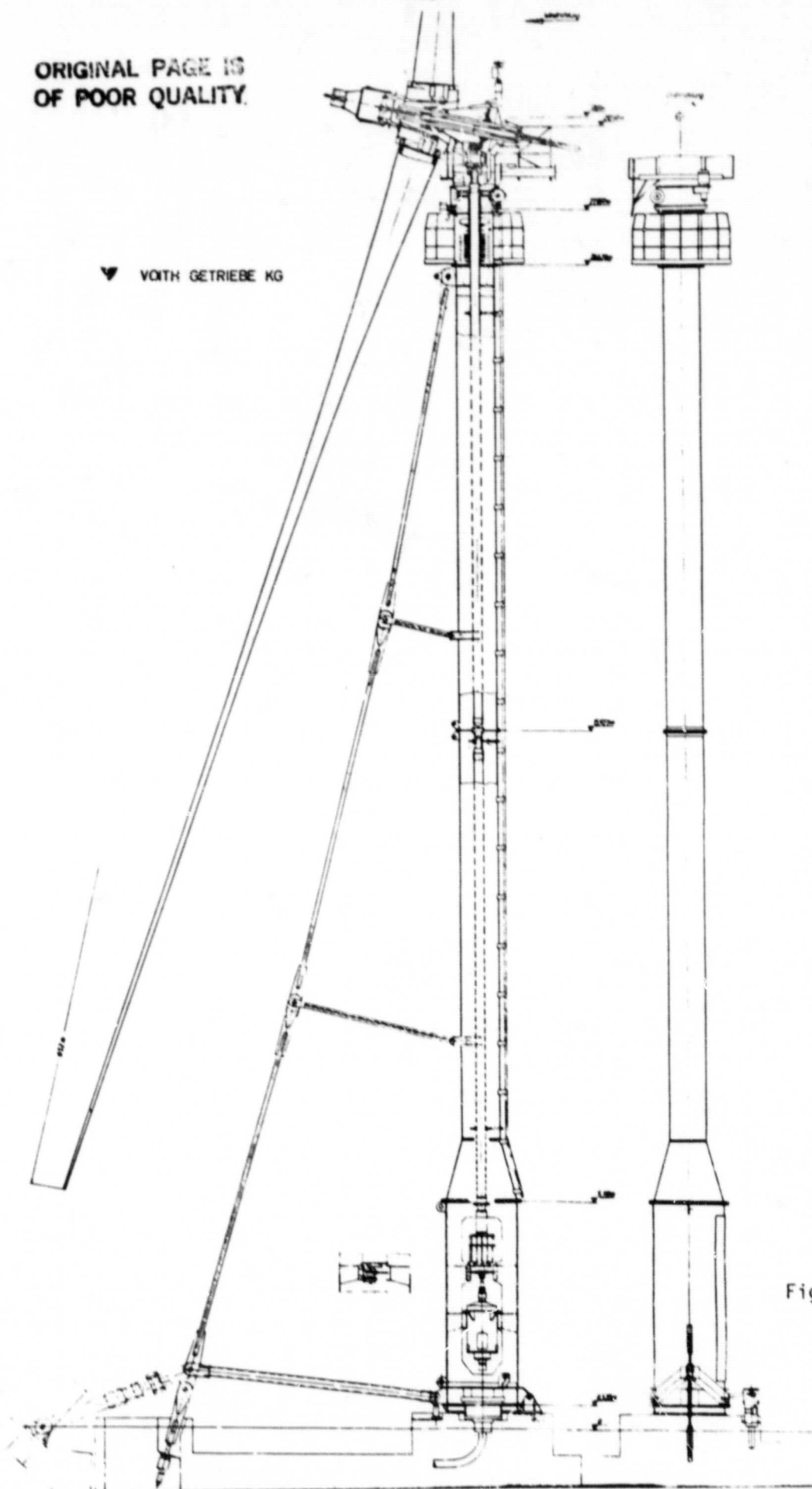
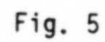
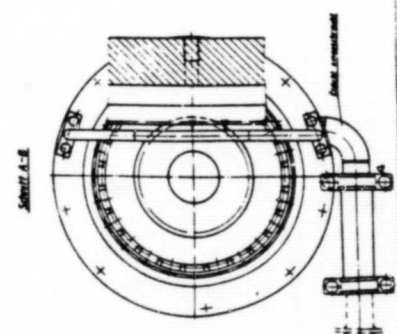


Fig. 4

(illegible)

WEC	Stellen 40 707
52 265 8	
	Mein Name ist
	Meine Adresse ist
	Meine Telefonnummer ist



[illegible]

(all illegible)







ORIGINAL PAGE IS  
OF POOR QUALITY

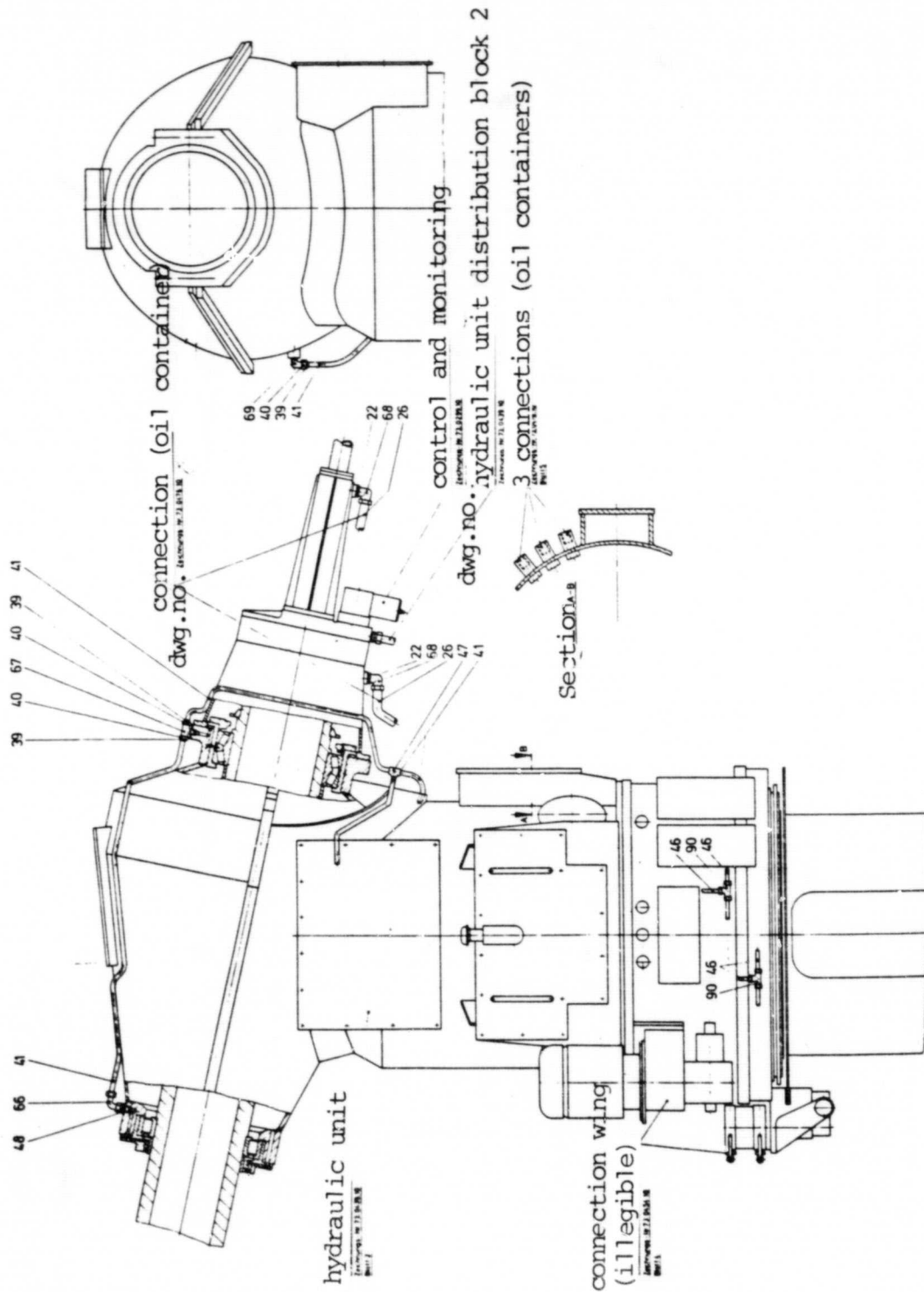
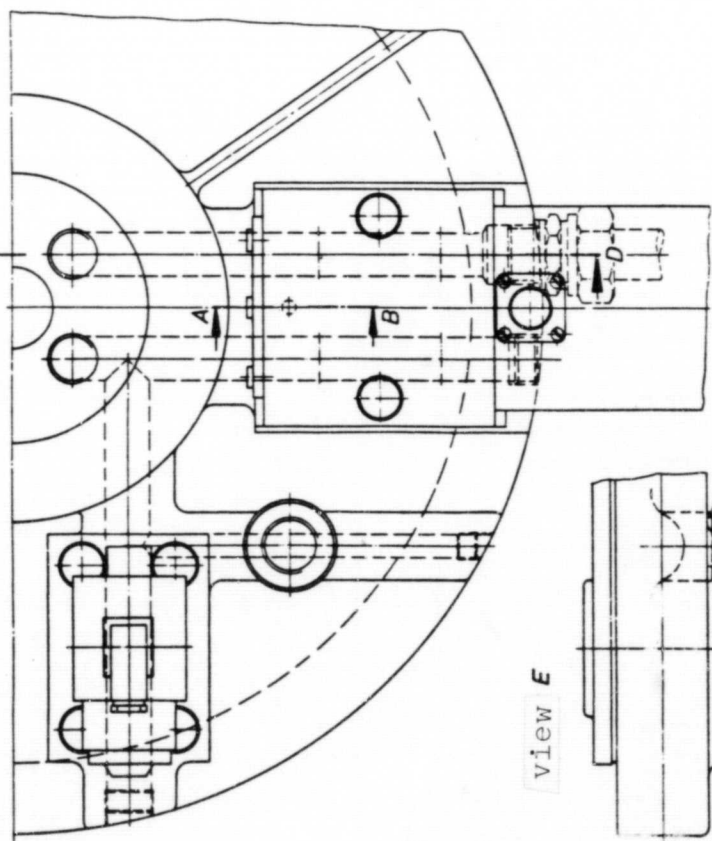
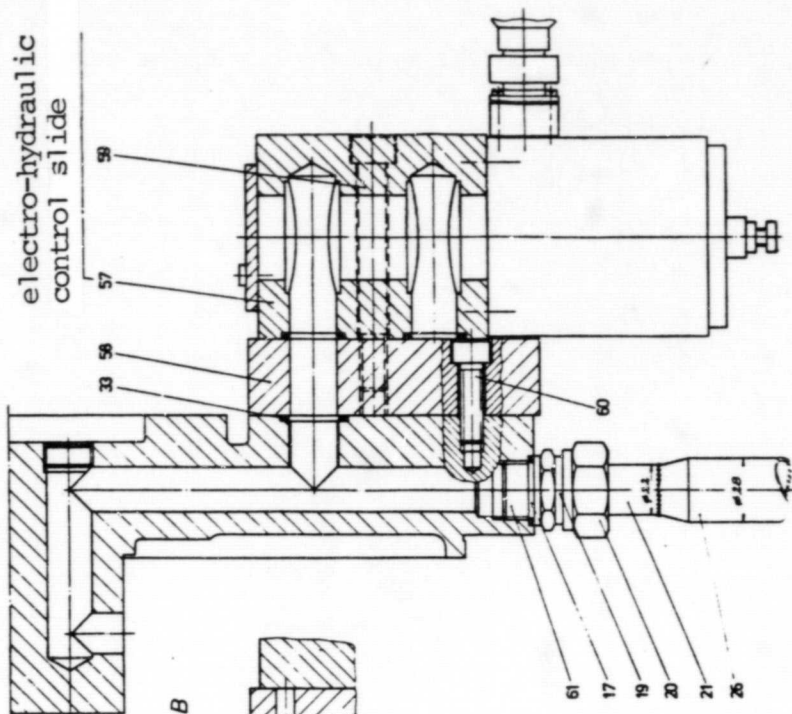


Fig. 9

Section C-D



view E

dwg. no. 73 0299 10  
from hydraulic unit distribution block no.

Hydraulik 8.3

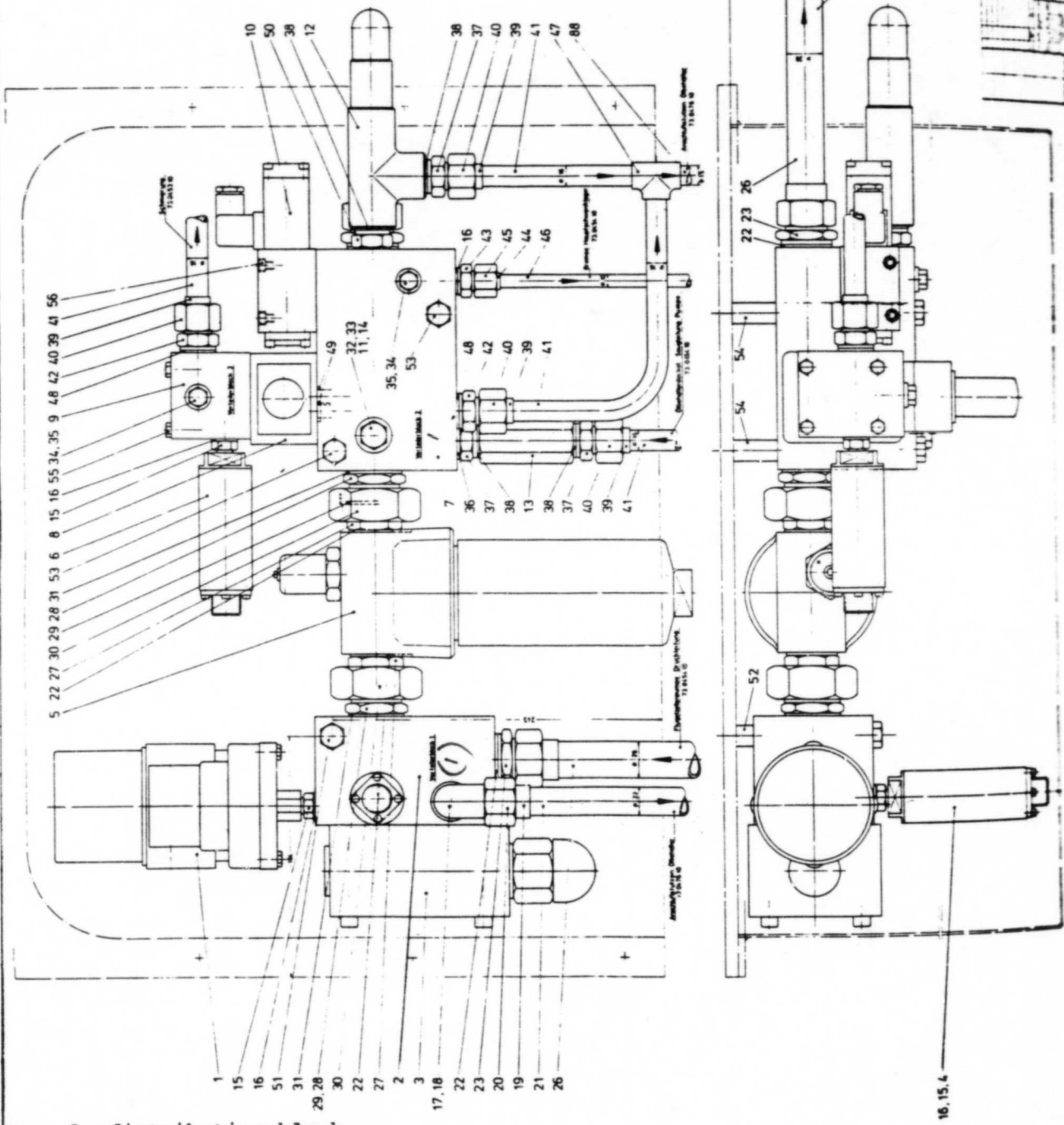
ORIGINAL PAGE IS  
OF POOR QUALITY

Zeichnung	73 0299 10
Titel	Steuerung u. Überwachung
Größe	1:1
Blatt	1 von 1
Gezeichnet	
Geprüft	
Freigegeben	
Technische Zeichnung	
Druck	

Fig. 10



ORIGINAL PAGE IS  
OF POOR QUALITY



Key: 1--distribution block  
others illegible

Fig. 11

without braking  
facility

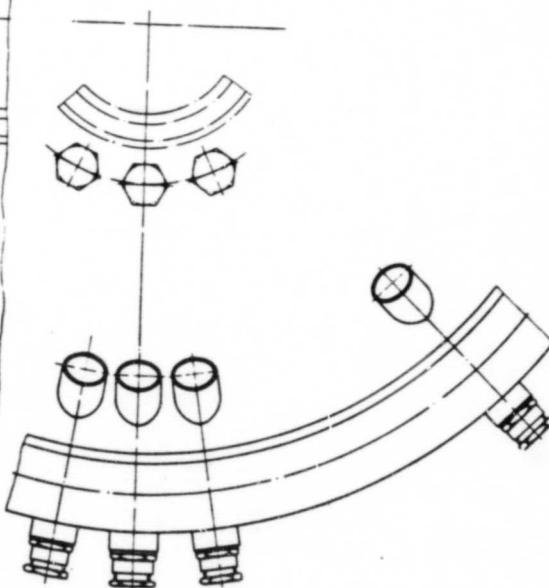


Fig. 12

[illegible]

ORIGINAL PAGE IS  
OF POOR QUALITY

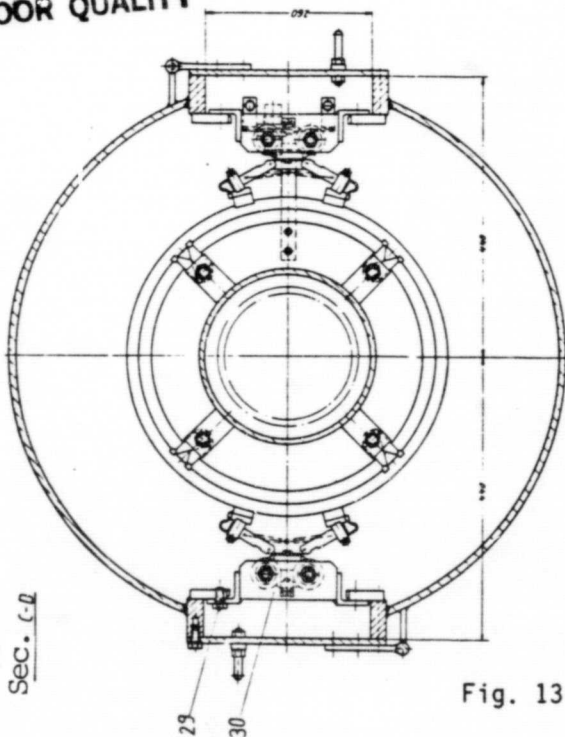
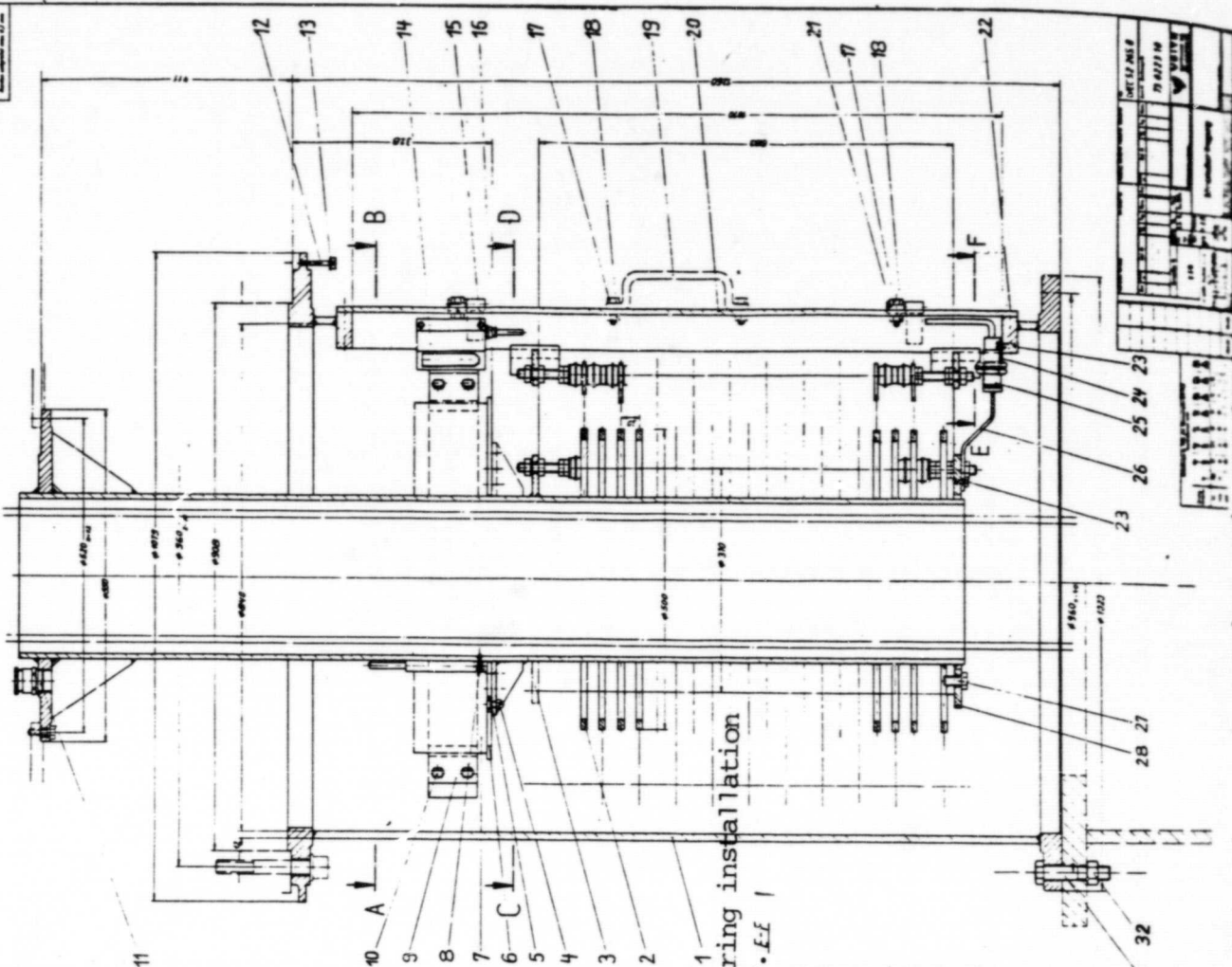
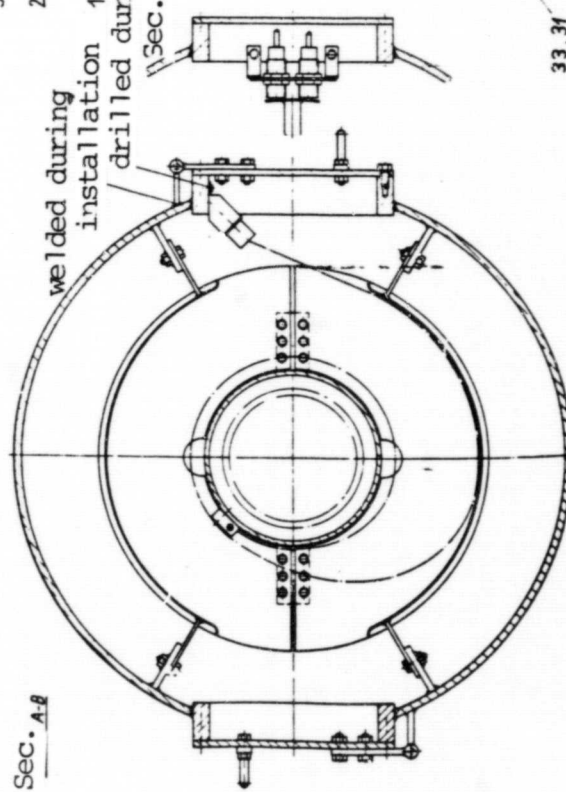


Fig. 13



1	2	3	4	5	6	7	8	9	10	11	12	13	14	15	16	17	18	19	20	21	22	23	24	25	26	27	28	29	30	31	32
---	---	---	---	---	---	---	---	---	----	----	----	----	----	----	----	----	----	----	----	----	----	----	----	----	----	----	----	----	----	----	----



**ORIGINAL PAGE IS  
OF POOR QUALITY**

FIGURE 14 (continued)

Key: 1--device for attaching transducers (for wind direction and wind speed); 2--platform not shown on this drawing; 2--grid support only at the indicated points; after this configuration of grid support rods; 3--view Z; 4--section; 5--view; 6--rail complete; 7--grid complete; 8--grid configuration; 9--design of upper pedestal with rail...(others illegible)...



ORIGINAL PAGE IS  
OF POOR QUALITY

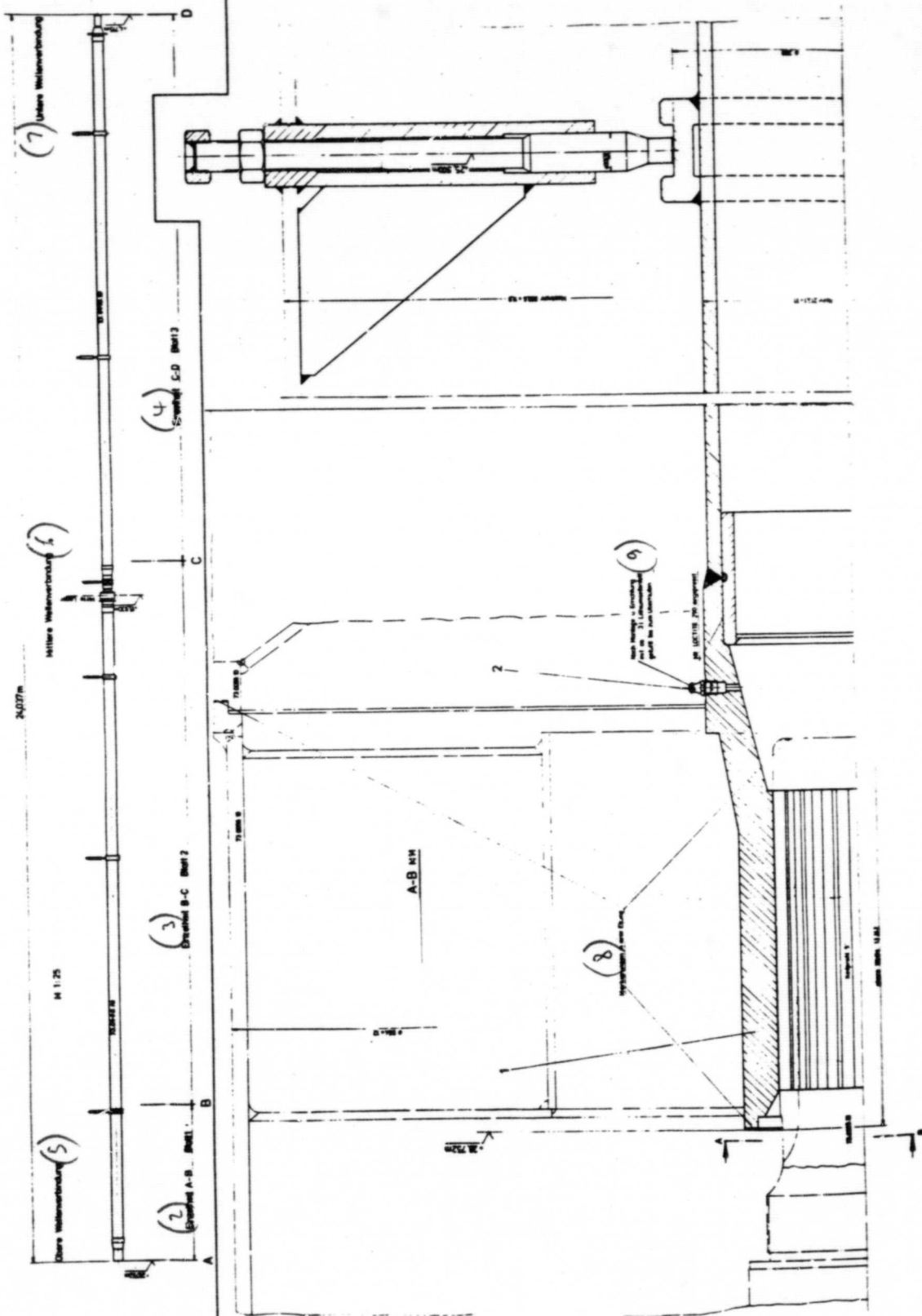


Fig. 15

ORIGINAL PAGE IS  
OF POOR QUALITY

FIGURE 15 (continued)

Key: 1--detail; 2--detail; 3--detail; 4--detail; 5--upper shaft connection; 6--middle shaft connection; 7--lower shaft connection; 8--markings in the plane; 9--after installation (illegible)



NO. 1000	REV. 1	DATE	BY	CHKD.
1000	1	10/10/50	J. H. H.	J. H. H.
1000	1	10/10/50	J. H. H.	J. H. H.
1000	1	10/10/50	J. H. H.	J. H. H.
1000	1	10/10/50	J. H. H.	J. H. H.
1000	1	10/10/50	J. H. H.	J. H. H.
1000	1	10/10/50	J. H. H.	J. H. H.
1000	1	10/10/50	J. H. H.	J. H. H.
1000	1	10/10/50	J. H. H.	J. H. H.
1000	1	10/10/50	J. H. H.	J. H. H.

ORIGINAL PAGE IS  
OF POOR QUALITY

Detail B-C

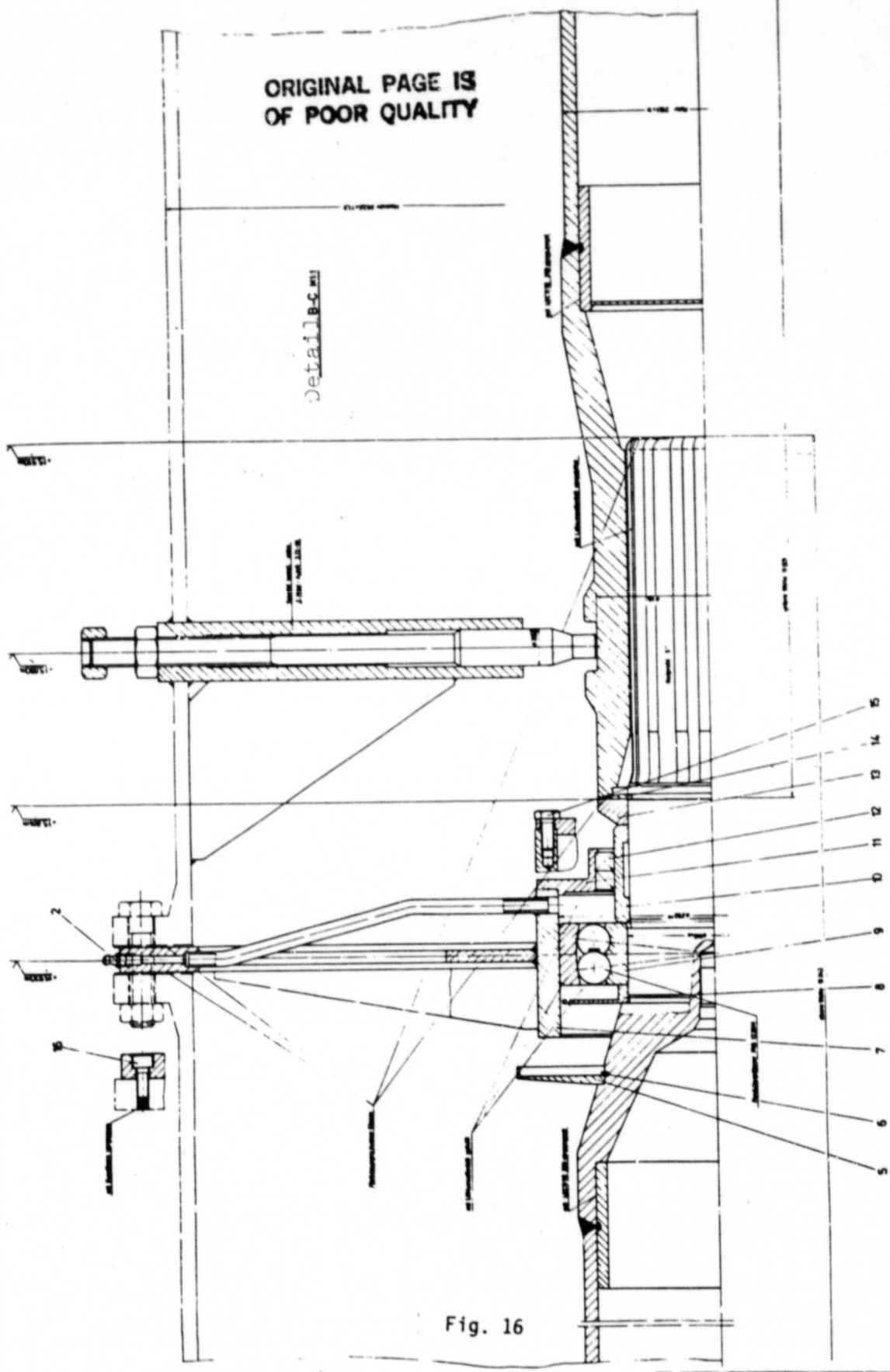
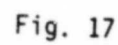
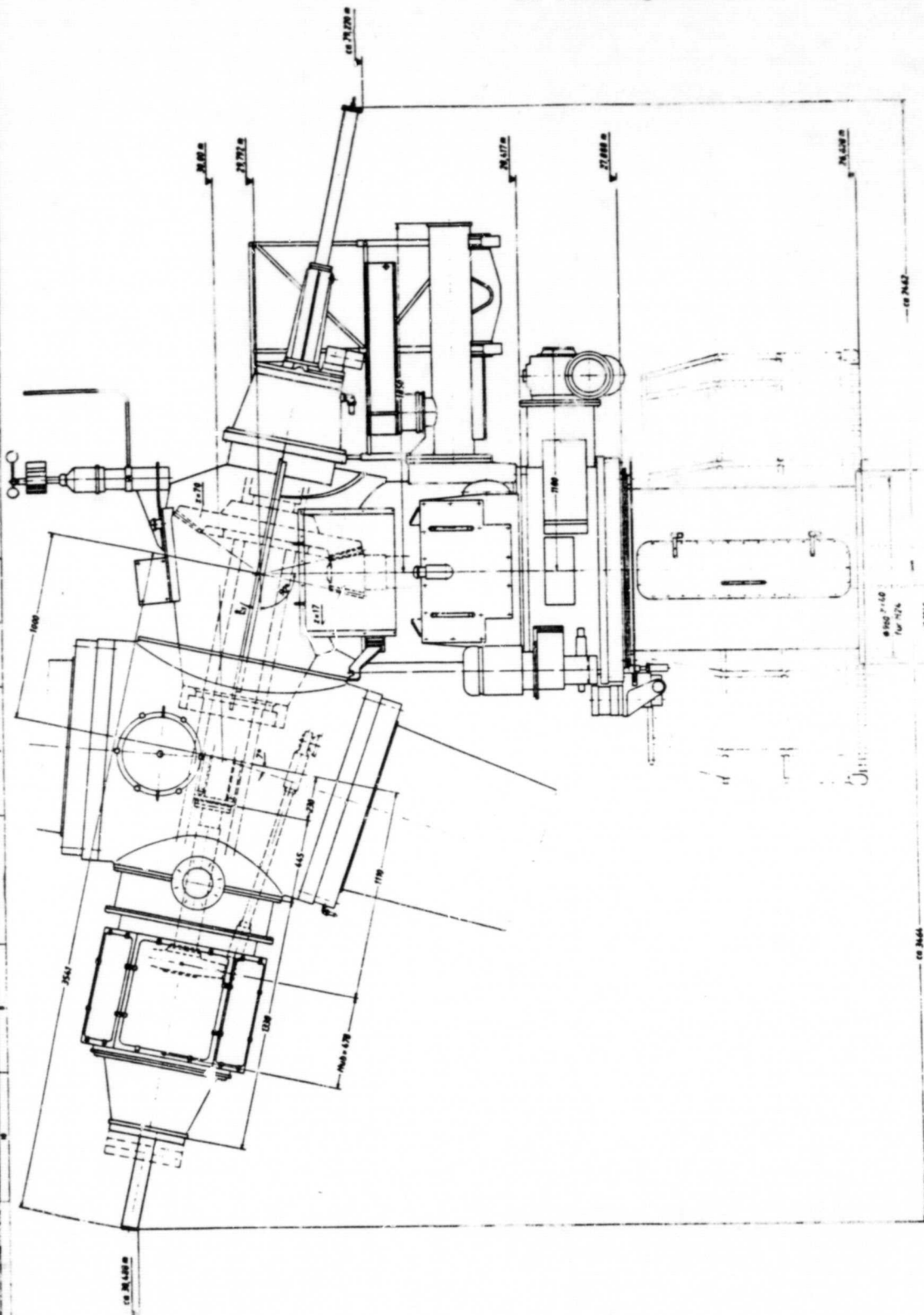


Fig. 16

(illegible)



[illegible]

Key: 1--turbine head with installation dimensions

Fig. 18

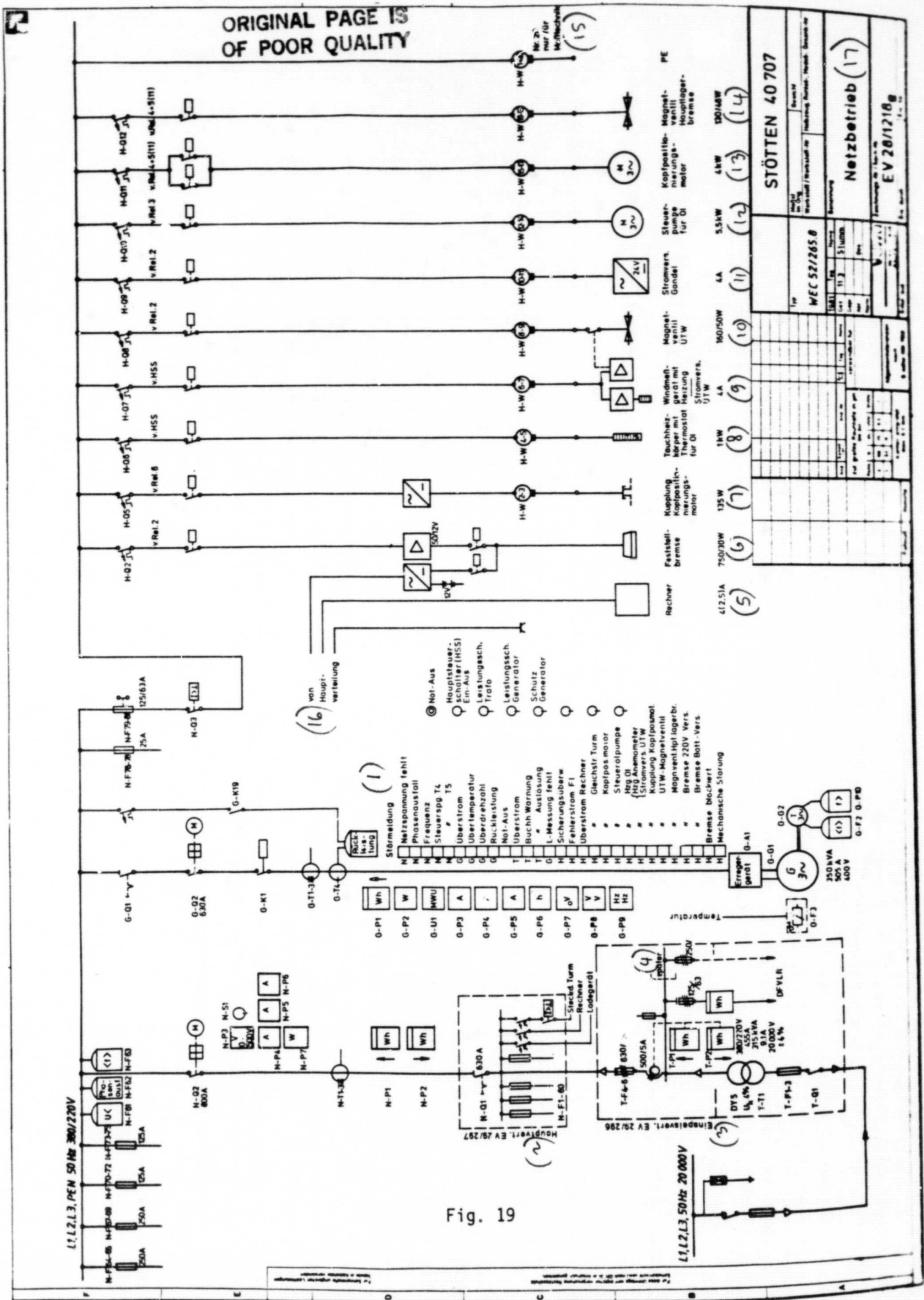


FIGURE 19 (continued)

Key: 1--alarm indication:

power out  
phase out  
frequency  
control voltage T4  
control voltage T5  
excess current  
excess temperature  
excess RPM  
reverse power  
emergency shut down  
excess current  
fracture warning  
fracture triggering  
L measurement absent  
safety monitoring  
erroneous current Fl  
excess current  
computer excess current  
DC tower head position motor  
excess current control oil pump  
excess current heating oil  
excess current heating anemometer  
excess current power supply  
UTW  
excess current coupling head position motor  
UTW magnetic valve  
excess current magnetic ventilation main bearing  
excess current brake 220V fuse  
excess current brake battery supply  
brake block  
mechanical disturbance

2--main distribution; 3--input distribution; 4--later; 5--computer;  
6--fixing brake; 7--coupling head position motor; 8--immersion body  
with thermostat for oil; 9--wind measurement device with heater  
power supply; 10--magnetic valve UTW; 11--power supply gondola;  
12--control pump for oil; 13--head positioning motor; 14--magnetic  
valve main bearing brake; 15--no. 24 measurement; 16--from main distri-  
bution; 17--power operation

ORIGINAL PAGE IS  
OF POOR QUALITY

/47

**THE CONCEPTUAL DESIGN OF THE  
HIGH SPEED RATIO WIND ROTOR FOR THE  
52 M DIAMETER HORIZONTAL AXIS VOITH WIND ENERGY CONVERTER**

W. Weber

Voith Getriebe KG, Federal Republic of Germany

**Summary**

The Voith wind turbine is a development of a horizontal axis turbine with two blades fully constructed in composite materials. It is designed either to supply electric power with a 265 kW generator to an electric grid or to be an independent electricity source for specific tasks in highly developed countries and in remote areas. For this reason the conceptual philosophy of this wind turbine goes in a slightly different direction to other developments of wind energy converters actually designed and in operation, a situation, which may be explained in the first chapter.



# 1. Specific power installation

According to the measurements of mean wind velocity distribution in Germany in /1/ as shown in Fig. 1, there is an evident difference between the coastal region with high mean wind velocity and inland areas with lower wind areas. The Voith wind turbine is designed specially for inland areas with a mean wind velocity of 4-5 m/sec. This wind distribution profile is not restricted to Germany. It is essentially also found in other countries. Therefore the Voith wind turbine is usable worldwide mainly in inland areas of most continental countries. For this region the right specific power installation should be analyzed.

The major distribution to the solution of this problem and the resulting conception of the wind rotor shape we obtained from U. Hütter.

According to his studies and the calculation based on different wind power measurements on several weather stations in Germany it is possible to describe the variation of the yearly wind power output from a specific power installation factor

$$\pi = \frac{P_R}{A}$$

with  $P_R$  = rated power

and  $A$  = rotor disk area

The results of calculations in /2/ demonstrate that a clear dependence exists of the zero operation time/year on this specific power installation factor  $\pi$ .

Fig. 2 gives a relative feature of this dependence on the mean wind velocity  $V_{10}$  measured at a height of 10 m. This figure shows that there is a need of low power installation factor  $\pi$ , if the wind turbine installation point lies in low wind regions of a country in order to get a fairly continuous delivery of wind energy. The Voith WEC 52/265.8, therefore with a factor of  $\pi = 125 \text{ W/m}^2$  has about the same operation time/year as the German Project GROWIAN with  $\pi = 380 \text{ W/m}^2$  on an installation point in the costal area of the North Sea. The ge-



neral trend in many wind power developments is towards high factors and installation points with high mean wind velocities.

ORIGINAL PAGE IS  
OF POOR QUALITY

/49

## 2. The choice of the speed ratio

The idea of the designed concept is to test a high-speed wind turbine with an efficient blade performance. According to the extensive studies of U. Hütter for the Voith wind turbine at the testfield in Stötten - the same place where the former W 34 were in operation from 1956 till 1964 - the maximum extractable wind power in Stötten and on comparable sites in central Germany is possible at a representative mean wind velocity of  $V_{10} = 6,3$  m/s at 10 m height as seen in Fig. 3.

For this wind speed the portion of the total energy output reaches a maximum, if the frequency distribution of the wind velocity after /1/ represented by different mean wind velocities is taken into account. Even though the low wind velocities reach the highest frequency distribution for the two stations selected as representative for the general - in Fig. 3, they do not get the most position of the possible energy output/year, the same situation as with the low frequency distribution of the high wind velocity of  $V_{10} = 9$  m/s and of  $V_{10} = 11$  m/s.

Based on the wind velocity of  $V_{10} = 6,3$  m/s and a constant angular velocity of  $\omega = 3,9$  1/sec ( $n = 37$  rev/min) the Voith wind energy converter has a designed tip speed ratio of

$$\lambda_T = \frac{\omega \cdot R}{V_{10}} = 16$$

with the rotor tip radius  $R = 26$  m  
and reaches the rated power at

$$\lambda_{TR} = 12 \quad (V_{10} = 8,7 \text{ m/s})$$

a ratio, which is an upper limit in respect to other wind turbines as mentioned in Fig. 4.

The consequence of this layout for the construction of the whole rotor gives some advantages and on the other hand some problems, which are outlined in the following context.

/50

### 3. The effects of the high tip speed ratio

#### a) The blade shape

Following the classical way of determining the optimum performance of wind turbines as published in /3/ and /4/, the designed speed ratio requires a certain contour form of the blade. The result for the Voith rotor is a wing blade which is extremely slender compared to other blade configurations as shown in Fig. 5.

The main geometric parameters are

$$\text{the aspect ratio of one blade } AR = \frac{R^2}{A_B} = 39$$

$$\text{the taper ratio } \tau = \frac{t_T}{t_{\max}} = 0,27$$

$$\text{and the solidity factor of the rotor } \sigma = \frac{A_B}{A} = 0,016$$

with  $A_B$  = blade area  
 $t_{\max}$  = maximum chord length  
 $t_T$  = chord length at blade tip

The blade twist has a range of

$$\Delta \beta_s = 7^\circ$$

in the relevant blade section from 6 m up to 26 m radius.

One designed goal for this rotor is to operate the wind turbine in a 1 p-upper-critical working range. In order to realize the required stiffness and mass distribution for these frequency and response calculations, the construction of the blades is only possible with the use of advanced composite technology. This

construction technique was solved in close collaboration with the helicopter division of the German aircraft manufacturers MBB, of whom we shall hear more in this meeting.

/51

b) The power coefficient

Going back to the definition of the power coefficient

ORIGINAL PAGE IS  
OF POOR QUALITY

$$C_P = \frac{P}{\frac{1}{2} \rho V_{10}^3 A}$$

with  $\rho$  = air density and the former definition of  $V_{10}$  and  $A$ , the power  $P$  can have under constant conditions of the other terms, different definitions:

In idealized conditions, which means without drag, the power coefficient is independent of the lift/drag ratio ( $L/D$ ) of the profiles:

$$C_{pid} \neq f(L/D)$$

In Fig. 6 this idealized power coefficient  $c_{pid}$  for the Voith rotor reaches its best values at a mean wind speed

$$5,5 \text{ m/s} \leq V_{10} \leq 6,5 \text{ m/s}$$

But, in general there is a strong influence of the profile drag on the power coefficient as it is published in /5/ and seen in Fig. 7.

With the increasing tip speed ratio a increasing  $L/D$  ratio is required to get a good performance of the rotor. The influence of  $L/D$  ratio is usually expressed by an efficiency factor  $\eta_{L/D}$ .

$$\eta_{L/D} = f(L/D)$$

For structural reasons with increasing bending and torsional moments and therefore necessary growing inertia moments towards the blade root it is not possible to have a constant L/D ratio over the rotorblade at all radii. Thus, the Voith <sup>152</sup> rotor blade with the given thickness distribution has a profile variation going from the thick profile GÖE 642 in the inner parts to the thin profile WH 301 in the outer parts of the blades, as is demonstrated in Fig. 8.

The L/D-ratio distribution is similar to the measured values of the Wortmann FX-W profile family going from about L/D = 30 in the 6 m section up to L/D = 150 at the blade tip. The calculation of L/D efficiency factor is given in Fig. 9.

For the representative radius of  $r = 0,75 R$  the L/D efficiency decrease not very much in the case of optimum pitch angle with  $\Delta \beta_s = 0^\circ$ , between  $\lambda = \lambda_T = 18$  which indicates a good utilisation of the profiles by the designed tip speed ratio of  $\lambda_T = 16$ .

From Fig. 7 it can also be seen that the influence of the number  $z$  of blades to the power coefficient  $c_p$  of the rotor decreases with increasing tip speed ratio and therefore does not tremendously effect the Voith rotor with a designed tip speed ratio of  $\lambda_T = 16$ .

The effect of the number of blades  $z$  can be expressed in an analogous matter to the L/D influence, which means, to calculate an efficiency factor  $\eta_z$ . The factor is consequently a function of the tip speed ratio  $\lambda_T$

$$\eta_z = f(\lambda_T)$$

Including all effects, the integrated mean power coefficient of the whole rotor becomes finally

$$c_{pg} = \eta_z \frac{1}{R} \int_0^R c_p \cdot \eta_{L/D} dr$$

ORIGINAL PAGE IS  
OF POOR QUALITY

The results are given in Fig. 10. The Voith rotor will have a range of operation between a cut-in wind velocity of  $V_{10} = 4,5$  m/s and a cut-out wind velocity of  $V_{10} = 25$  m/s.

/53

The rated power will be reached at  $V_{10} = 8,7$  m/s mean wind velocity. An impression of the rotor loading conditions give the mean lift coefficient  $c_a$  of the rotor blades. It can be seen that with decreasing tip speed ratio the lift coefficient  $c_a$  of the blades increases up to the rated power. At the rated power and with further increasing wind velocity the mean lift coefficient goes back again, while there is no need to use the whole capable wind energy. The blade pitch angle should be turned toward the lower angle of attack.

#### 4. The consequences of the high performance blades on the construction and the aeroelastic behavior

To conclude the presentation of the designed Voith rotor concept in respect of power optimization it is necessary to give a survey of the consequences on structural and aeroelastic behavior of the blades. The rotor as presented here, has in some aspects considerable advantages.

a) The slender blades with low blade area give a considerable mass reduction compared to bigger blades with low designed tip speed ratio as shown in Fig. 5. Therefore the alternating in-plane bending moments and forces due to the gravitational loads, the gyroscopic moments and other mass related characteristics are reduced.

b) In the loading cases of high wind speed with no rotating blades the blade root moments are in the same order as the moments at rated speed and have no greater problems than the moments at rated speed.

c) The high rotation speed of the rotor shaft reduces the needed gear ratio to the generator and reduces consequently the loss of efficiency due to this gear ratio.

ORIGINAL PAGE IS  
OF POOR QUALITY

d) The torsional natural frequency of these slender blades are high, which has a positive effect on the aeroelastic stability behavior.

154

On the other hand the chosen rotor concept has also realisation difficulties, which are to be solved.

a) The L/D ratio requires an aerodynamic performance which results in a necessity for composite materials with surface conditions of the blades comparable to the wing configurations of modern plastic competition gliders.

b) The required stiffness and mass distribution for this slender blade is only possible to realize through the extensive use of carbon fibre composite material. Both the components and the handling process are relatively expensive. But on the other hand, a mass production of rotor blades in this configuration will bring the cost to a lower level.

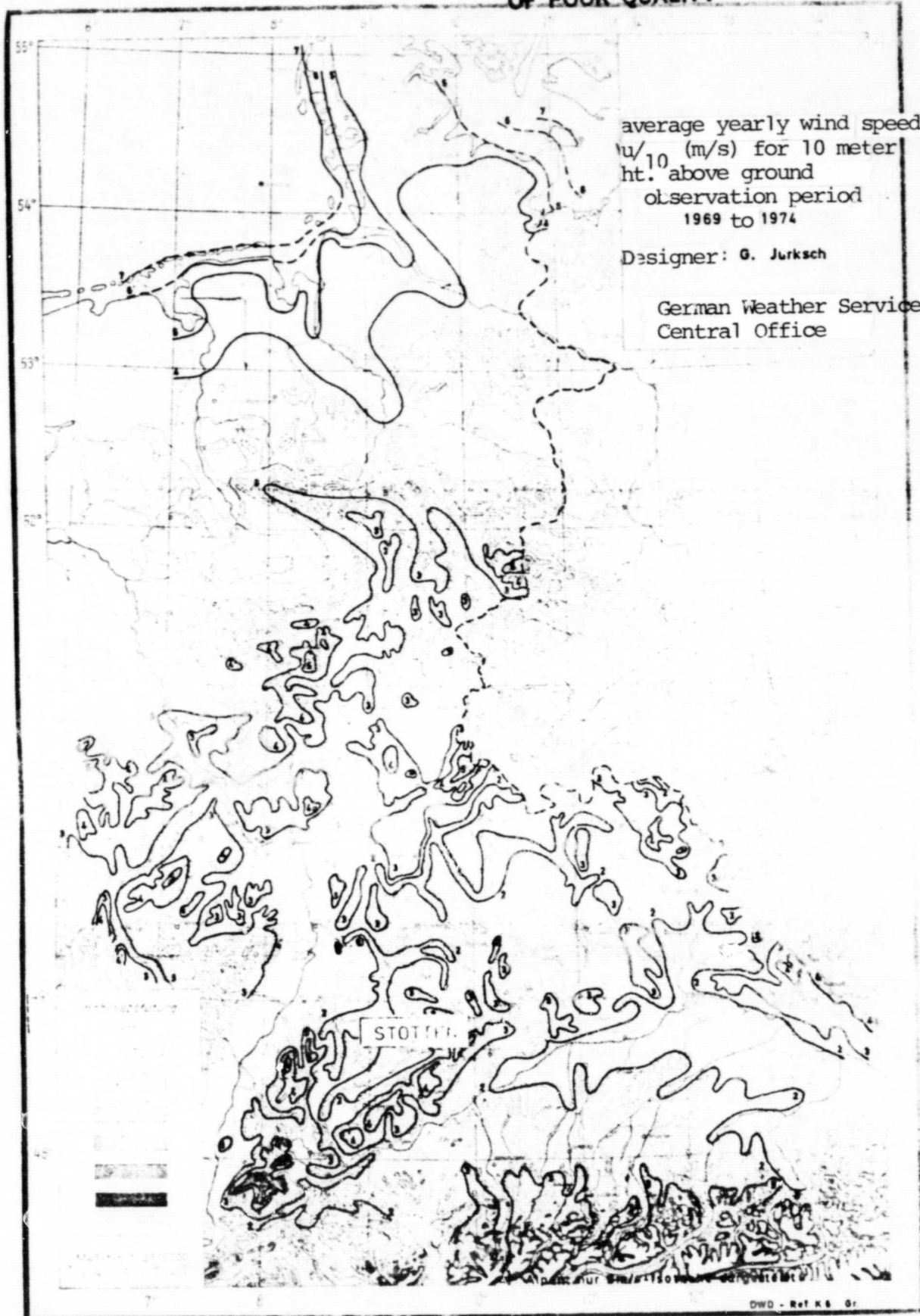
The presented development of the Voith rotor will expect some improvements for wind power utilisation. A final evaluation will give the operation of the wind turbine and the related study of the cost effectiveness of the concept.

#### References

1. Benesch, W. et al.: "Wind conditions in the Federal Republic of Germany with reference to wind energy utilisation". Bericht des Deutschen Wetterdienstes Nr. 147 (Report 147 of the German Meteorological Service) Selbstverlag Offenbach/Main, 1978. (In German).
2. Armbrust, S. et al.: "Wind energy utilisation. Part 3 of the study Energy sources for tomorrow". Programmstudie des BMFT, Umschau Verlag, Breidenstein KG, Frankfurt/Main, 1976, p. 104. (In German).
3. Hütter, U.: "The aerodynamic layout of wing blades of wind turbines with high tip speed ratio". Bericht E/Conf. 35/W/31 zur Konferenz der Vereinten Nationen (United Nations Conference), Rome 1961.
4. Weber, W.: "Optimal rotary blade layout for horizontal wind energy converter". Zeitschrift für Flugwissenschaften, 23. 12, December, 1975. (In German).
5. Mally, U. P.: "Wind energy in theory and practice, fundamentals and application". Verlag C. F. Müller, Karlsruhe, 1978, p. 36. (In German).



ORIGINAL PAGE IS  
OF POOR QUALITY



155



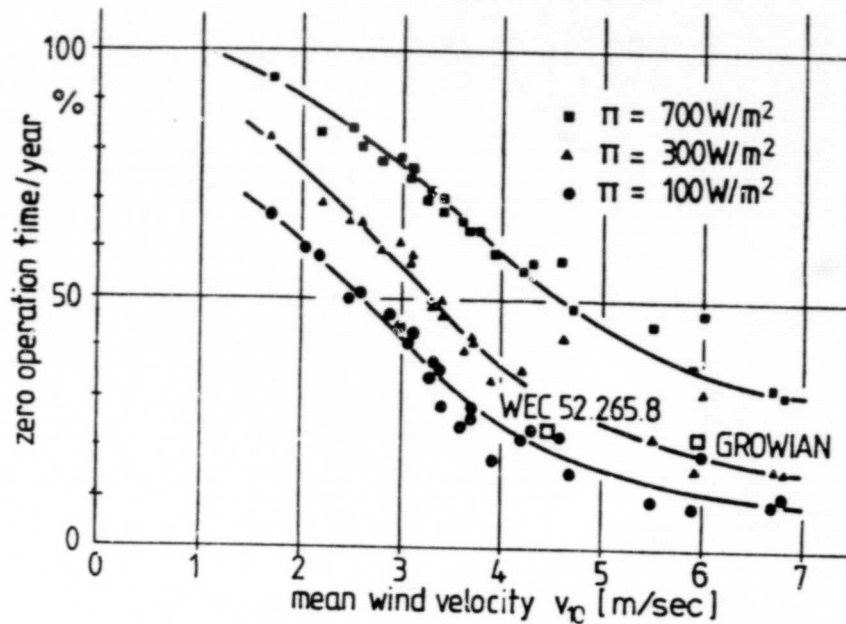


Fig. 2: Zero operation time/year for different power calculations  
on 25 weather stations throughout Germany

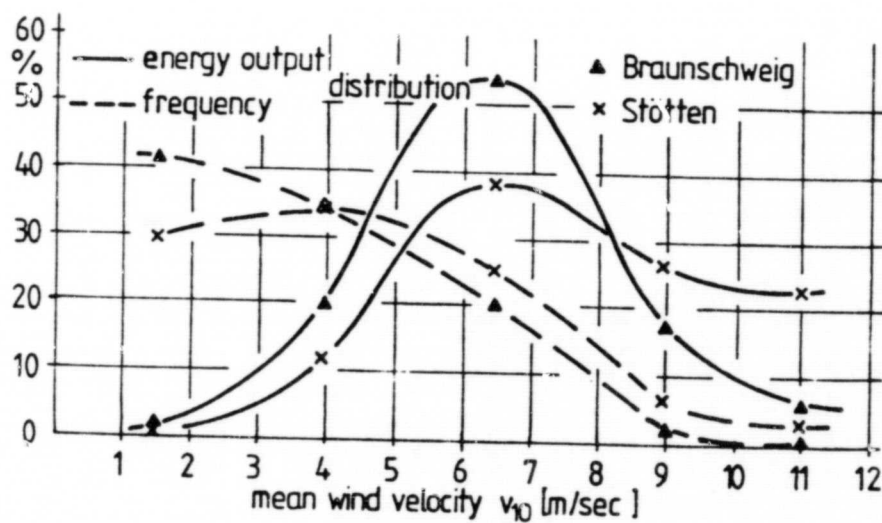


Fig. 3: Frequency distribution of mean wind velocity and annual  
energy output distribution per year of two selected  
weather stations in Germany

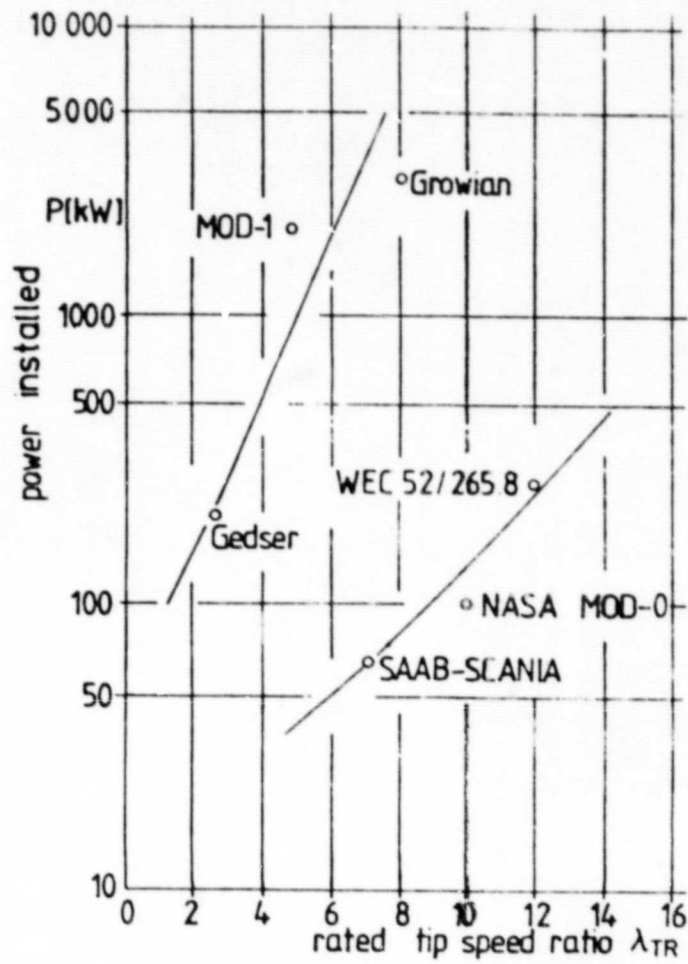
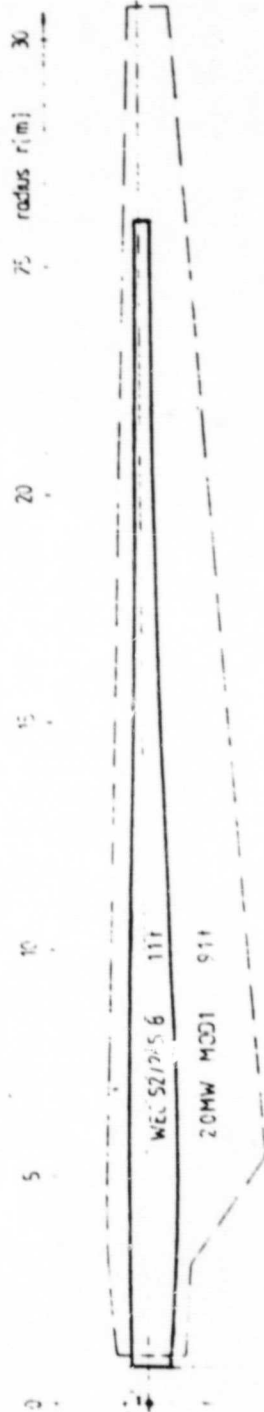


Fig. 4: Comparison of trends in the design of power installation on different wind turbines

Fig. 5: The blade geometry of the Voith WEC 52/265.8 wind turbine in relation to the GE MOD-1 rotor blade

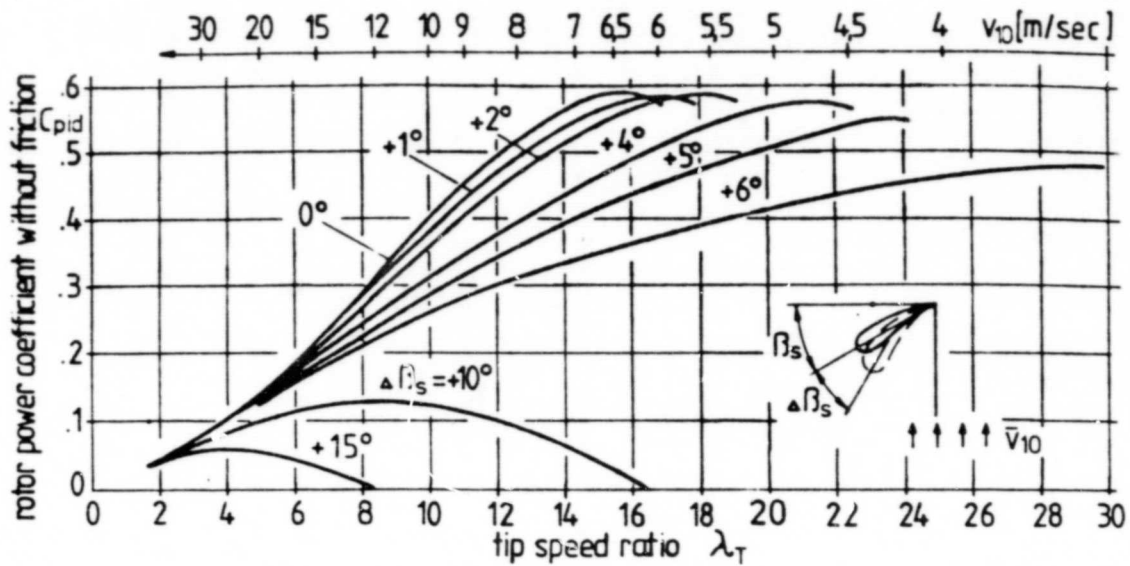


Fig. 6: The power coefficient of the WEC 52/265.8 rotor concept in idealized condition without friction

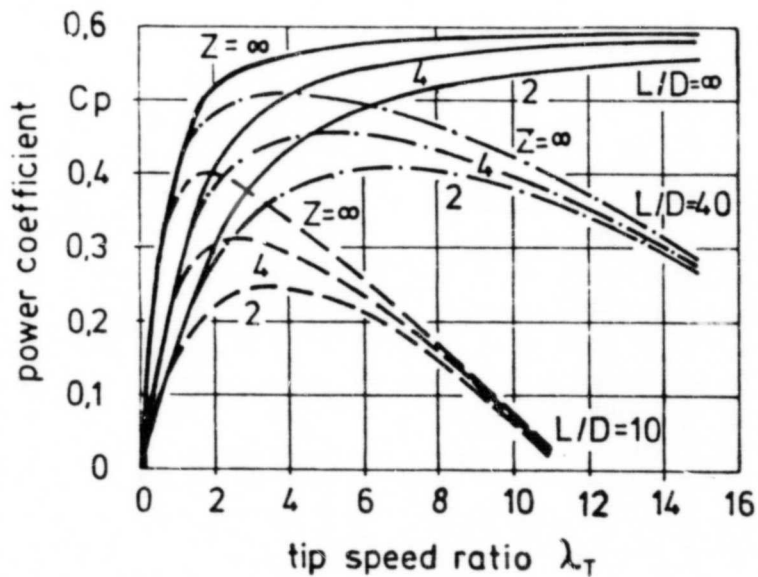


Fig. 7: The influence of the lift/drag ratio  $L/D$ , and the number of blades  $z$  on the power coefficient

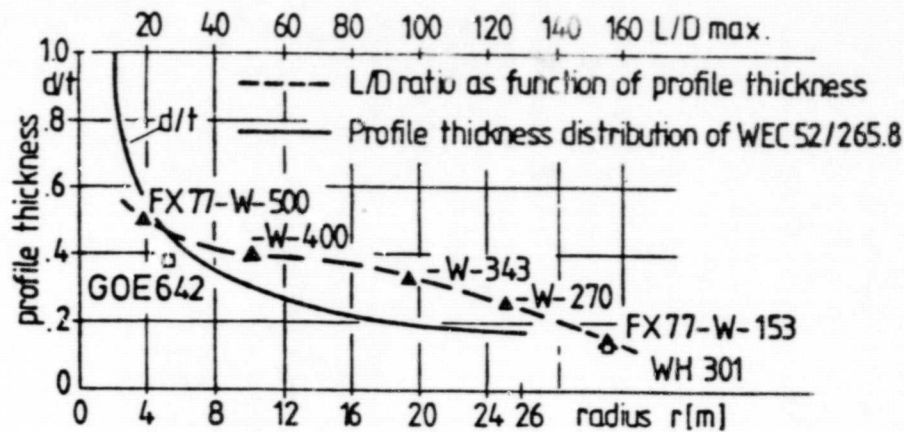


Fig. 8: The distribution of the thickness  $d/t$  over the rotor blade and the associated  $L/D$  ratio as a function of thickness ratio  $d/t$ .

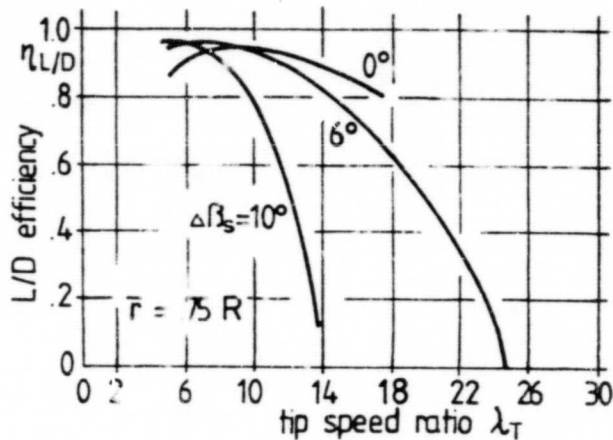


Fig. 9: The efficiency of the  $L/D$  ratio by different blade pitch angles  $\Delta\beta_s$  at the representative blade radius  $r = 75 \% R$ .

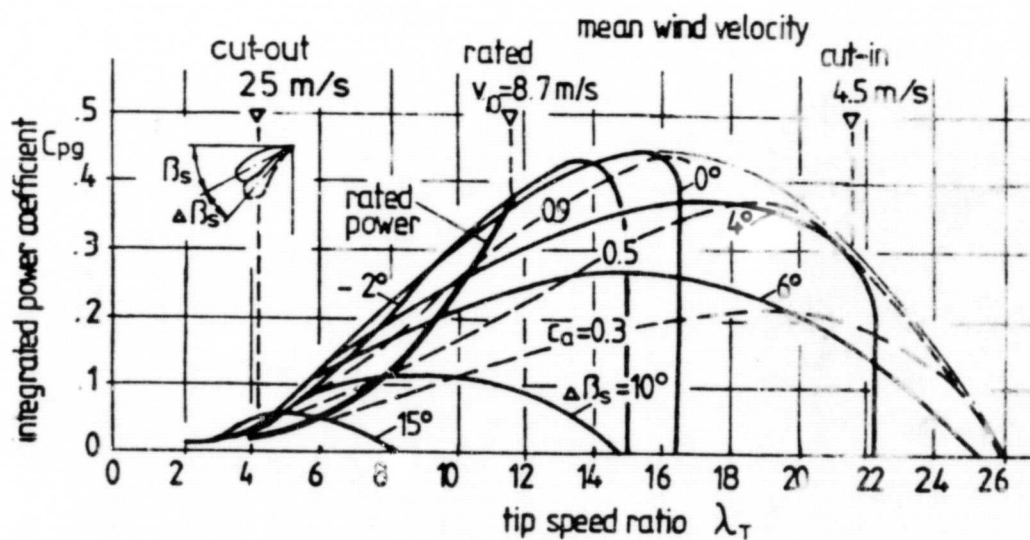


Fig. 10: The characteristics of specific power  $c_{pg}$  versus tip speed ratio for the Voith wind rotor

OSCILLATION MEASUREMENTS ON A TWO BLADE GFK/CFK  
(GLASS FIBER REINFORCED PLASTIC/CARBON FIBER RE-  
INFORCED PLASTIC) WIND TURBINE ROTOR OF THE  
WEC 52/265.8 USING A 16-CHANNEL TELEMETRY  
INSTALLATION \*

/61

Werner Spittler

Voith Getriebe KG, Heidenheim

TABLE OF CONTENTS

1. Introduction
2. Measurement task
3. Components of the telemetry measurement installation
4. Partial assembly of the telemetry components
5. Present assembly status
6. Outlook

---

\* Research Project ET 4344 A

## 1. Introduction

/62

Within our research project ET 4104 A with the title "Development, building and testing of a wind energy converter WEC 52/265.8", it very soon became clear that the design of the rotor and its blades was very important.

New technologies and design methods for building the rotor blades. Rotor blades with a composite fiber design were developed and CFK (carbon fiber reinforced plastic) with T 300 fibers were used for the primary structure.

Extensive calculations on strength, stiffness and structural damping gave good results using this method.

However, not all of the required input data were available for the calculations so that estimates and assumptions had to be made. Especially coupling influences of the rotor blades on the mast were difficult to establish for dynamic behavior.

For safety reasons, therefore, experiments were made with single rotor blades in test band experiments and also rotors were tested under loads in a complete assembly. In this way, one wishes to verify the assumed data or to make corrections for the design.

/63

Measurements of rotating rotor blades of WEC's are not very conventional because measured signals have to be transmitted for data recording to a ground station on three rotating planes, that is, the rotor blade plane, the rotor shaft plane and the gondola rotating plane.

Analysis shows that the dynamic behavior of the wind turbine rotor could be sufficiently covered using 16 measurement points so that the solution of the measurement task would best be satisfied by using a 16 channel telemetry facility.

## 2. Measurement task

For the oscillation measurements of the two blade wind turbine rotor, 16 transducers have to be installed on each rotor blade. In order to record measurement signals for deflection and flapping motions at the blade tips, one accelerometer transducer each is required. For the other measurement points, strain gauges have to be installed. Accordingly, 16 analog measurement points are to be measured at about the same time. Remote control for measurement point switching from one rotor blade to the other will allow on-off switching of the telemetry measurement installation from the power supply.

The measurement point distribution on both rotor blades was established after the conclusion of the EDP calculations of rotor blade optimizations and when plotter results were available for the rotor blade eigen oscillation modes. A measurement point distribution according to Figure 1 was used.

/64

Because of the geographically exposed location of the wind energy converter, and the fact that the rotor blade was partially made of CFK (carbon reinforced plastic) fiber material and, therefore, could conduct electricity. The telemetry installation has to be protected against lightning.

In order to provide a high degree of data transmission safety, the measurement signals have to be amplified in the rotor head, they have to be digitalized and a pulsed code is made for wireless measurement value transmission (PCM code). The measurement data which can be transmitted are to be transmitted to the ground reception station through a PCM link. There the measurement data are decoded again, first of all, using a line recorder they are optically recorded. In addition, they are stored in parallel using an analog tape machine for later evaluation with the EDP installation.

The measurement task was performed in two tests:



## 2.1 Test stand experiment

The calibration of the measurement transducers is an important part of the test. For this purpose, both rotor blades are statically loaded in a test device in the deflection and flapping direction. The load is introduced in steps to the rotor blade through a load device and the deflections which occur have to be determined.

/65

The entire telemetry installation in the original version has to be tested during measurement value calibration.

The research task ET 4343 A for the rotor blade development which was performed as a subcontract by MBB, also contains model analysis of the finished rotor blade.

Using the telemetry installation, data recorded in parallel and stored on tape are then evaluated later on as a test example by the oscillation analysis devices of the firm MBB.

This evaluation at the same time is used to test the adaption capacity of the various devices in order to later on be able to evaluate the measurement data of MBB recorded during free field tests by Voith.

## 2.2 Free field tests

The dynamic overall behavior of the two blade wind turbine rotor where the incident flow comes from the leeward direction has to be determined over the entire operating range.

## 3. Components of the telemetry measurement installation

The following description will give some information about the operation and structure of the components of the telemetry measurement installation shown in Figure 2. As already mentioned, the rotor blades are equipped with strain gauges and accelerometer transducers for recording measurements (see Figure 1).

Both measurement transducer types are switched in a full bridge /65 circuit and can be treated electrically in the same way. The measurement transducers are the main current users for the power supply and, therefore, their internal resistance is made small. The measurement transducers are connected with lightning protection units through simply twisted and shielded cables installed in the rotor head.

In the case of lightning impact in the rotor blades, induction of voltages in the shielded measurement and supply voltage cables cannot be avoided. The lightning protection unit is, therefore, dimensioned so that induced voltages of up to 40 kV can be removed through combined self-extinguishing spark gap and diode networks against the mast.

In order to switch all the measurement points including their power supplies from rotor blade A to B, a mechanical relay system protected against vibration is used.

Switching through a remote control radio device, which is planned for turning the circuits on and off of the telemetry measurement installation, is operated from the ground station.

The power supply of the measurement transducers, preamplifiers and telemetry units from the measurement station was selected from various possibilities. This is located in the rotor head. However, because of possible disturbing influences, slip rings had to be avoided. The installation of radial and axial inductibly coupled current transmitters was investigated. Both would have been possible but the /67 latter version was not possible due to the design. Therefore, we considered an autonomous current production using 5 silicon solar generator panels which are installed ahead of the rotor. Discharge protection diodes prevent influencing of the solar generators.

A voltage precontroller provides continuous charging of the nickel-cadmium buffer battery. For unfavorable weather conditions and a full battery, an operating time of at least 24 hours is achieved.

The central part of the telemetry measurement installation contains the current supply unit, conversion of the battery voltage and this supplies the measurement transducers, preamplifiers, PCM encoder and HF transmitter.

The individual bridge voltages of the measurement transducers are amplified in the preamplifiers and are switched to a single channel using the time multiplex method and then directed to the PCM encoder. Here there is analog to digital conversion, the measured values are represented as digital words, parallel to serial conversion takes place and the code is converted. The produced data stream is then frequency modulated and is superimposed in the HF transmitter onto a carrier frequency of a radial link according to the requirements of the German post office. The reverse data conversion occurs in the reproduction of electronics within the ground reception station. The measurement /68 data obtained in this way are either directed to the line recorder for display or are stored on magnetic tape in parallel. In the EDP facility the PCM decoder also has an interface for the computer for further processing.

#### 4. Partial assembly of the telemetry components

The telemetry components can be seen in both order housing parts in Figures 3 and 4. The housing parts are arranged diagonally between the rotor blades. Although the connectors were designed according to MIL-SPEC because the high requirements against contact certainty and water tighteners are required. Figure 5 in the lower part shows the control console of the WEC with the telemetry encoder.

#### 5. Present state of assembly

The planning of the rotor blade oscillation measurement was designed originally for an early production schedule of the entire facility.

This means that partial assembly of the telemetry components was already complete during the first quarter of 1980.

At the present time the individual parts of the rotor head are manufactured and are being assembled.

/69

In this connection, we now are carrying out the calibration of the strain gauge measurement points 16 which can be seen in Figure 6 on a thrust yoke on the rotor shaft. This figure also shows the wiring work.

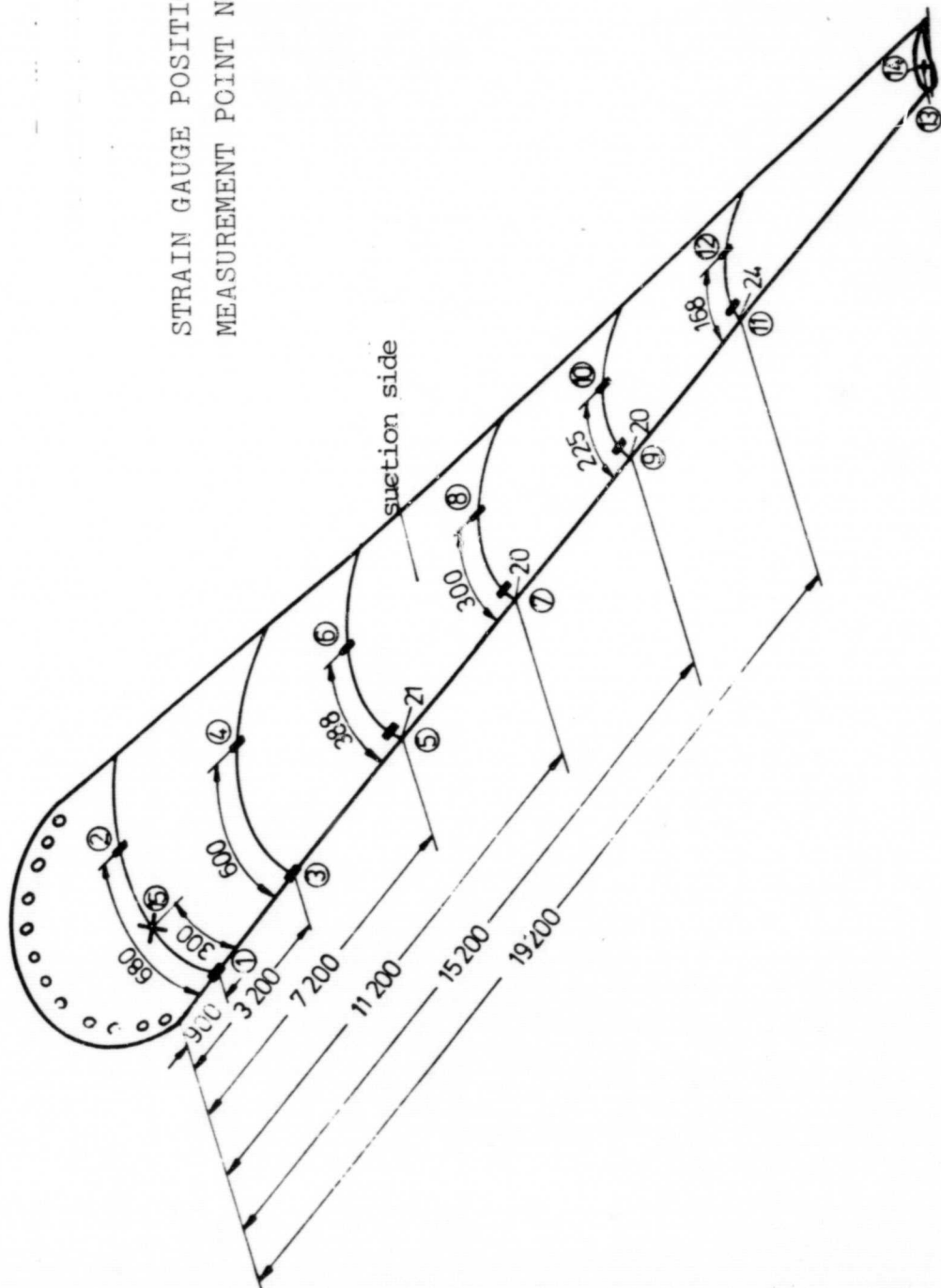
#### 6. Planned schedule

Test band experiment 2.1 will be carried out immediately after completion of the rotor blade. The firm MBB has indicated that this would occur at the beginning of the second quarter of 1981 and MBB according to 2.1 is responsible for the development of the rotor blades. The outdoors test will probably be able to start during the third quarter of 1981.

ORIGINAL PAGE IS  
OF POOR QUALITY

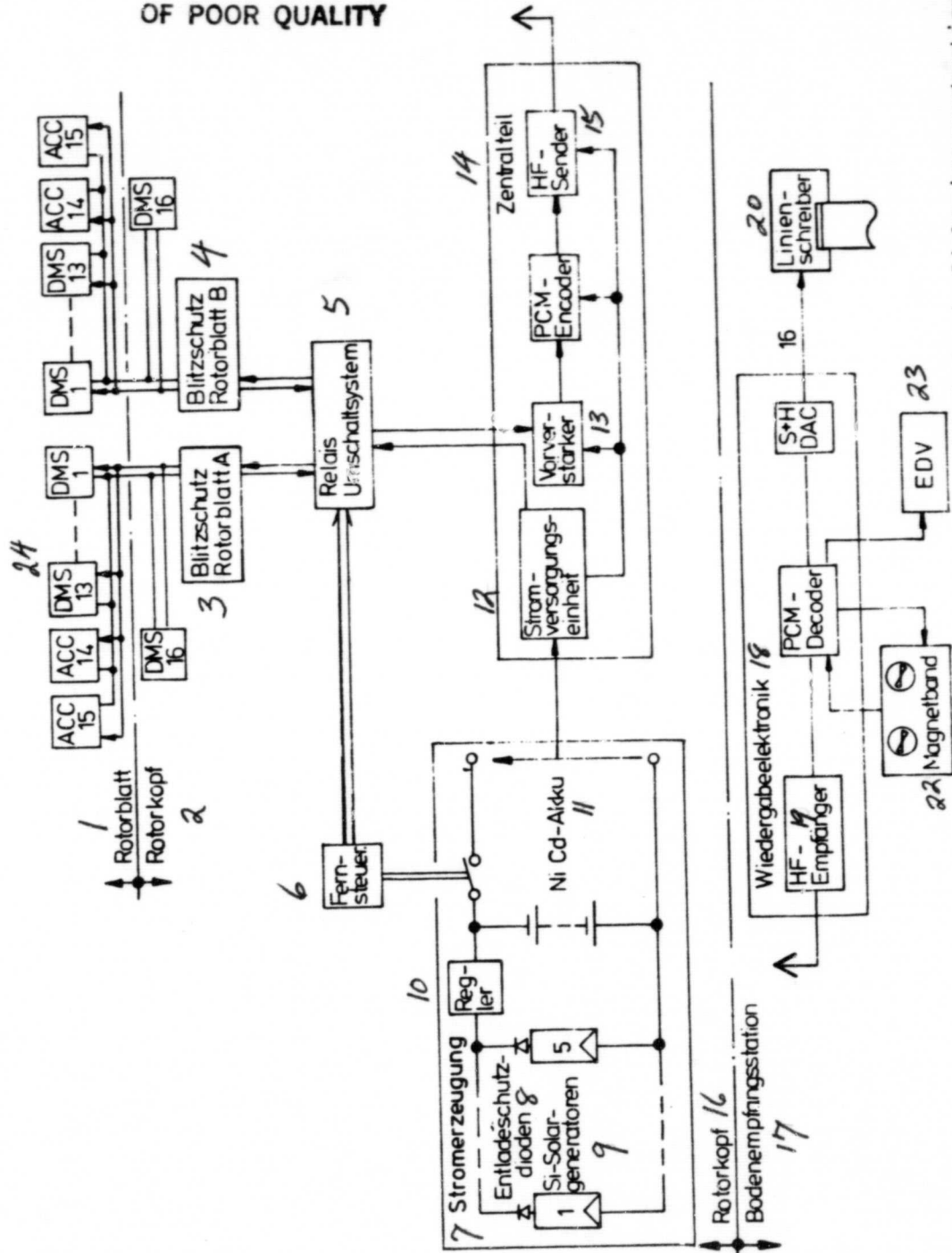
FIGURE 1

STRAIN GAUGE POSITIONING AND  
MEASUREMENT POINT NOTATION ON ROTOR BLADES



# COMPONENTS OF THE TELEMETRY INSTALLATION

ORIGINAL PAGE IS  
OF POOR QUALITY



KEY: 1--rotor blade; 2--rotor head; 3--lightning protection rotor blade A; 4--lightning protection rotor blade B; 5--relays switching system; 6--remote control; 7--power production; 8--discharge protection diodes; 9--Si solar generators; 10--controller; 11--accumulators; 12--power supply unit; 13--pre-amplifier; 14--central part; 15--high frequency transmitter; 16--rotor head; 17--ground reception station; 18--reproduction electronics; 19--HF receiver; 20--line printer; 21--magnetic tape; 22--EDP; 23--SG.

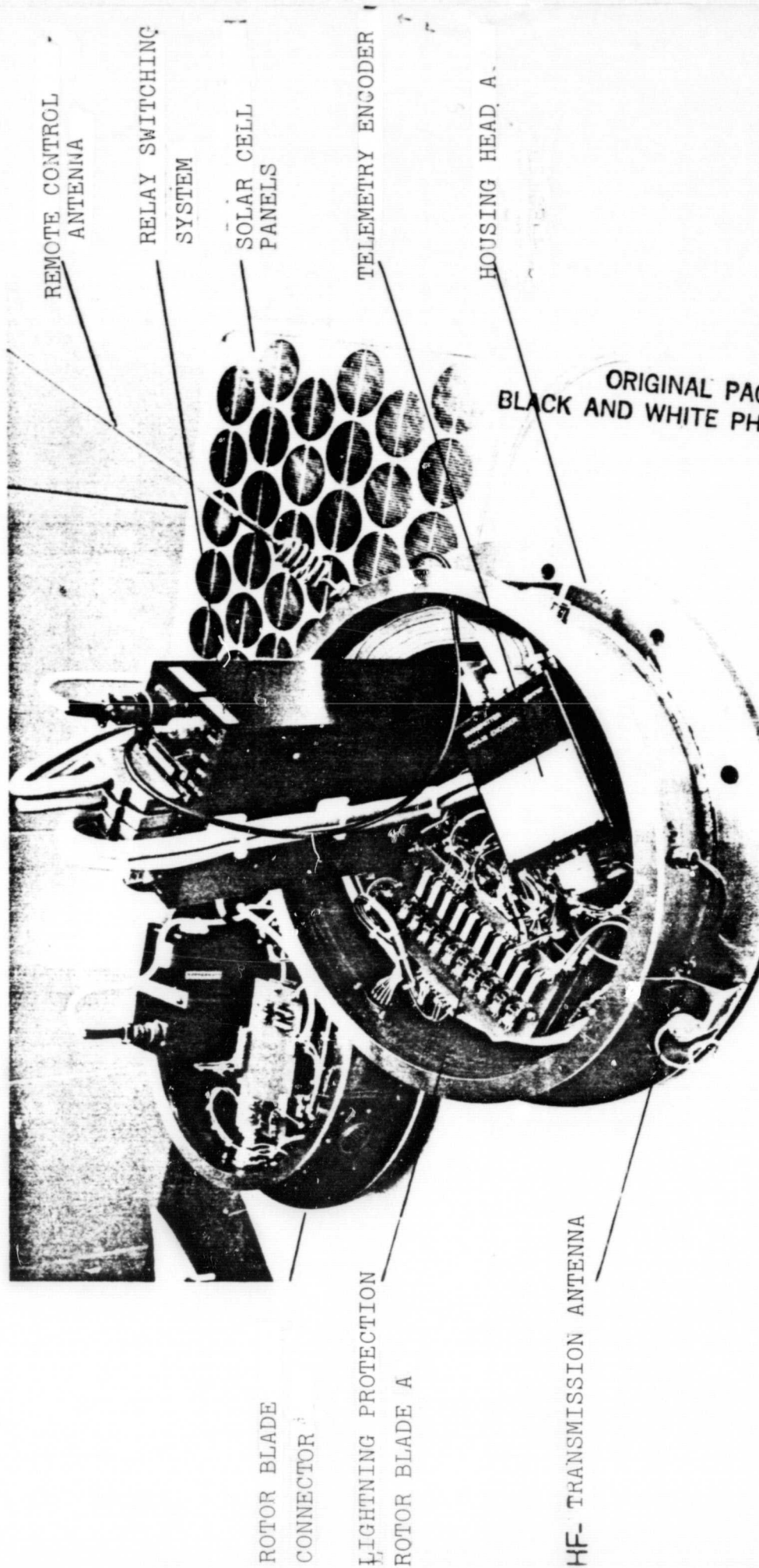
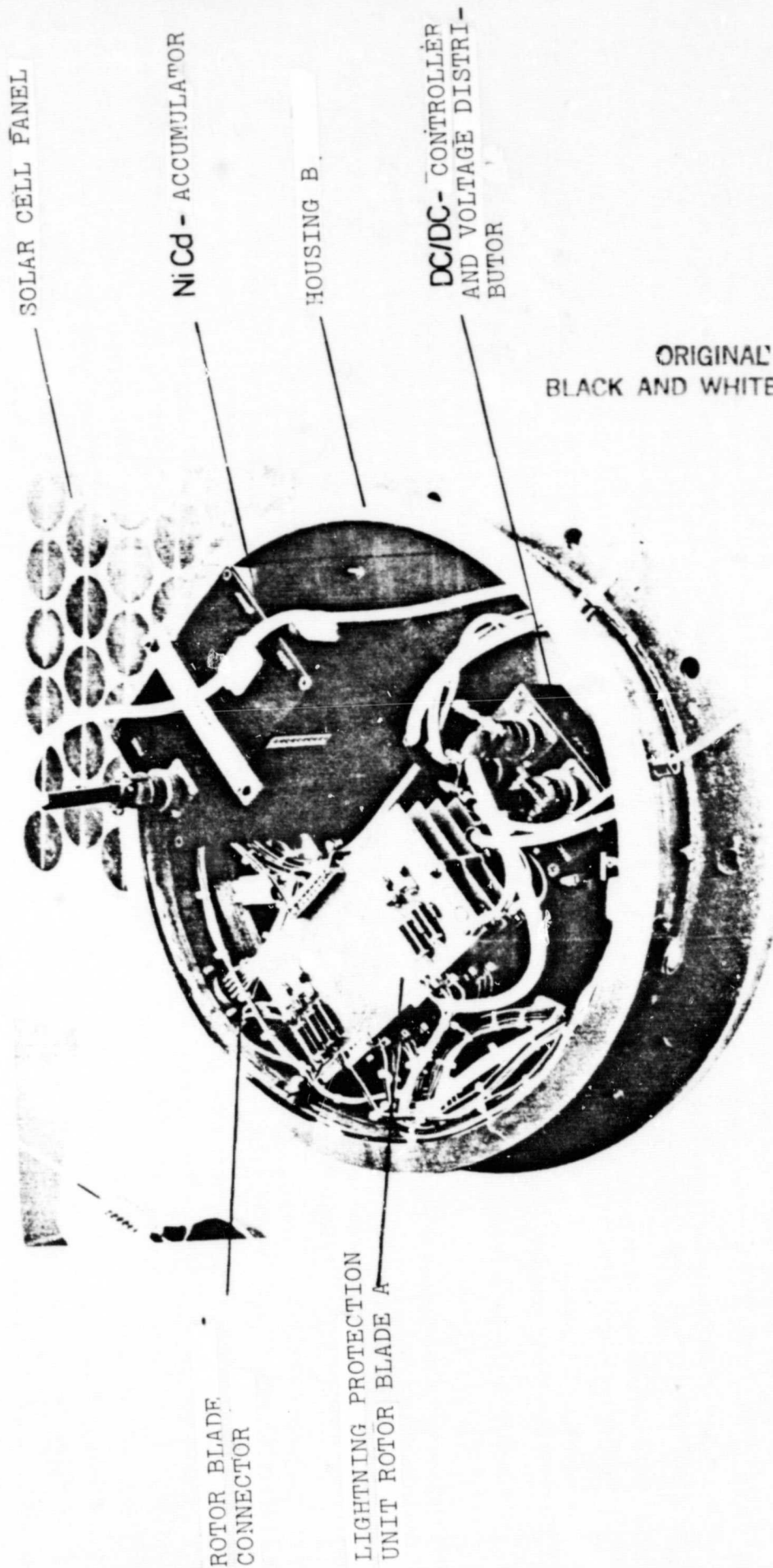


FIGURE 3





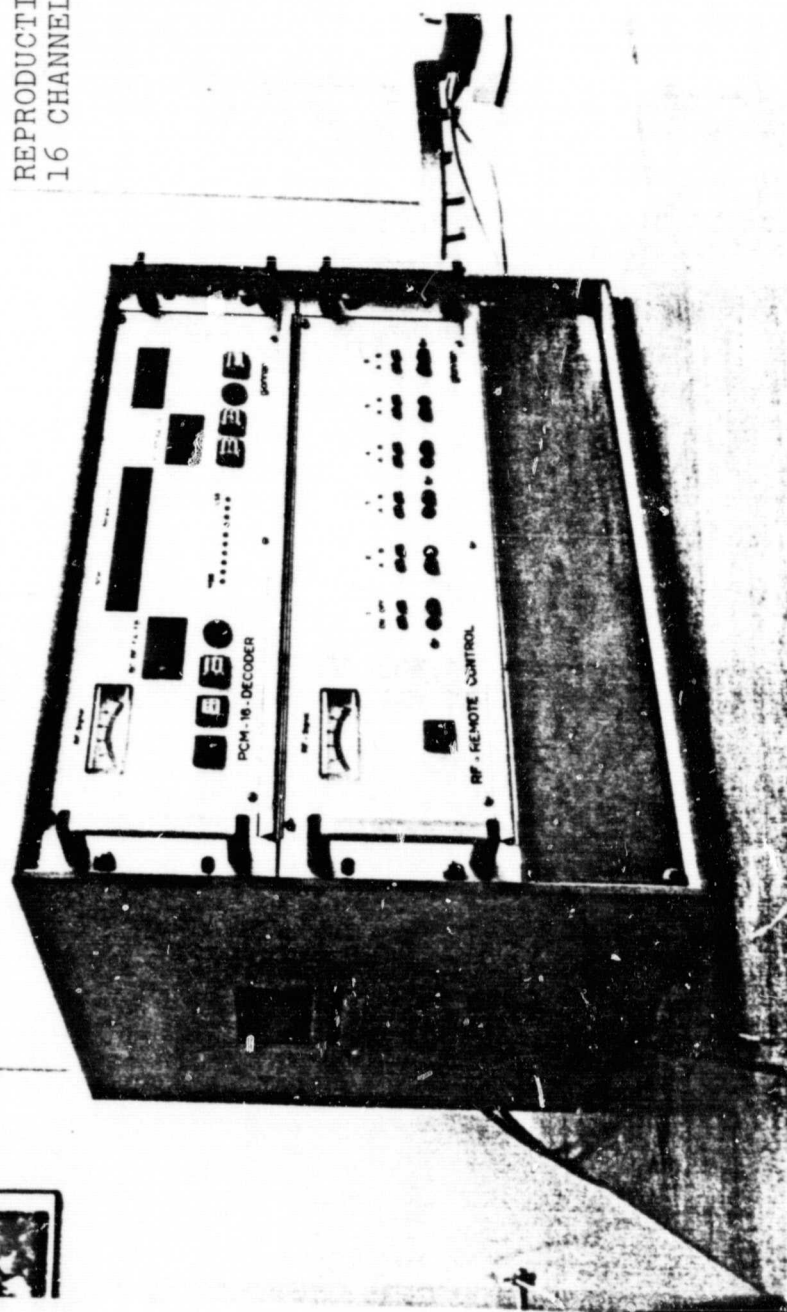
ORIGINAL PAGE  
BLACK AND WHITE PHOTOGRAPH

FIGURE 4

ORIGINAL PAGE  
BLACK AND WHITE PHOTOGRAPH

REPRODUCTION ELECTRONICS OF THE  
16 CHANNEL PCM TELEMETRY

FIGURE 5



# Telemetrie - Geräteanordnung

ORIGINAL PAGE IS  
OF POOR QUALITY

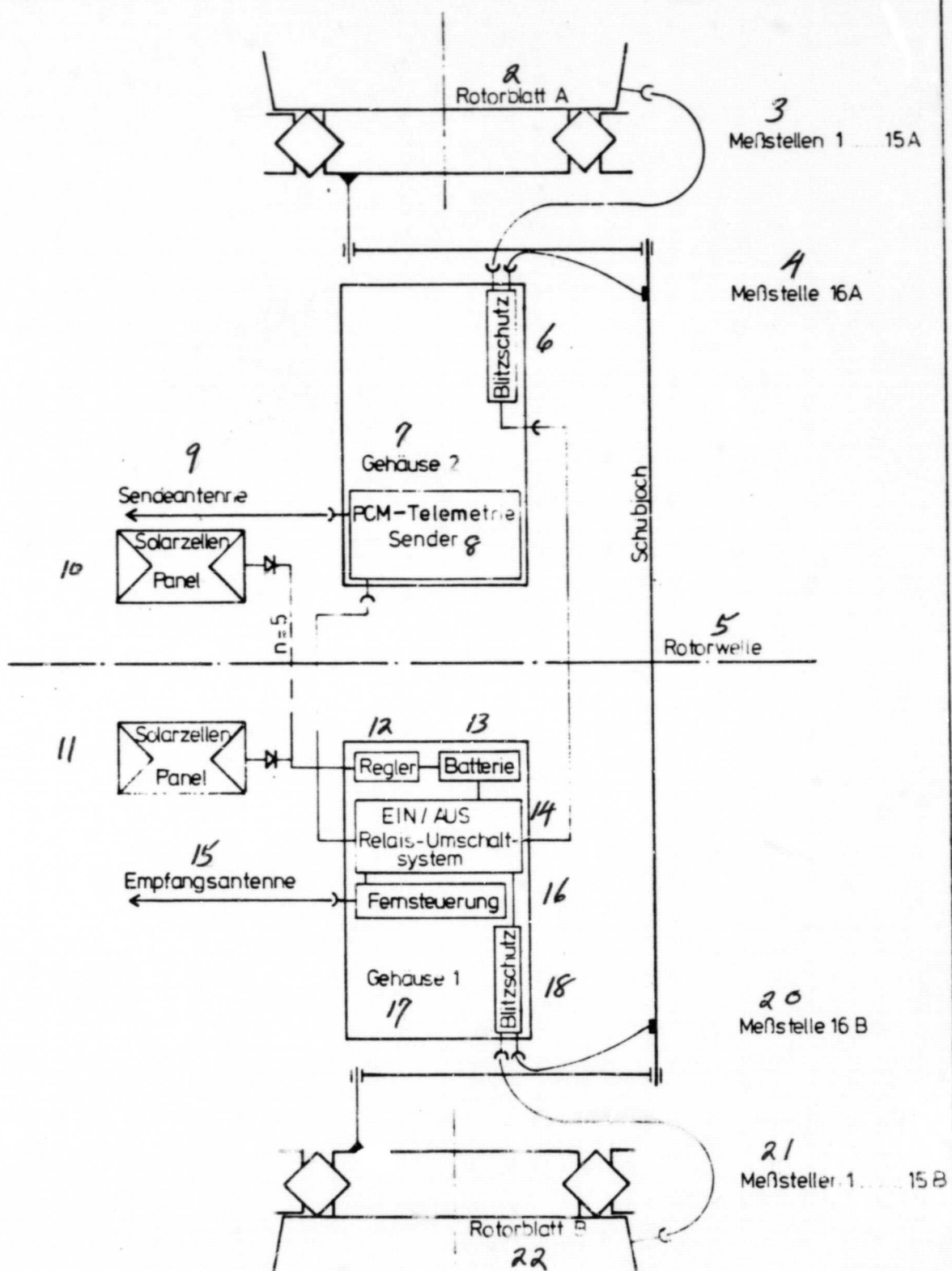


FIGURE 6

**ORIGINAL PAGE IS  
OF POOR QUALITY**

**FIGURE 6 (continued):**

**Key:** 1--telemetry configuration; 2--rotor blade A; 3--measurement point; 4--measurement point; 5--rotor shaft; 6--lightning protection; 7--housing 2; 8--PCM telemetry transmitter; 9--transmission antenna; 10--solar cell panel; 11--solar cell panel; 12--controller; 13--battery; 14--on/off relay switching system; 15--reception antenna; 16--remote control; 17--housing 1; 18--lightning protection; 20--measurement point 16B; 21--measurement point 1...15B; 22--rotor blade B

ROTOR BLADE DEVELOPMENT ET 4343 A \*

/77

Reinhard Krautwald

/78

SUMMARY

This report describes the development and manufacturing activity performed during the rotor blade development ET 4343 A for wind energy facility Stoetten 40707b task during the period between May 1, 1979 to February 28, 1981.

With consideration of the basic data of the overall design such as geometry, mass and stiffness distribution, a rotor blade using the fiber compound construction method was constructed. We demonstrated that the planned goals were achieved using static and dynamic tests on a 10.2 m prototype of the internal blade region.

In addition, a new kind of molding and working concept is described which makes it possible to manufacture components of this size and this is compared with conventional manufacturing technologies with a small manufacturing complexity.

The report ends with a discussion about the manufacture of the half wing shells of the first 26 m long blade.

---

\* Status: February 28, 1981  
Messerschmitt-Bolkow-Blohm GMBH  
Helicopters and Traffic, Munich  
Project director: Ralf-Thilo Schultz

# TABLE OF CONTENTS

	page
Summary	87
I. Goals	90
II. Construction	90
II.1 Blade design	90
II.2 Structure	90
II.3 Material	92
III. Manufacturing means	92
III.1 Lamination molds	92
III.1.1 Surface definition	92
III.1.2 Shell molds	92
III.1.3 Mold heating	93
III.1.4 Blade mold installation	93
III.1.5 Quality assurance measures for blade molding installation	95
III.2 Surfacing device	96
III.3 Cutting devices and drilling devices	96
III.3.1 Cutting device	96
III.3.2 Drilling template	96
III.3.3 Drilling device	97
IV. Full size component manufacture	97
IV.1 Manufacturing of the laminate shells	97
IV.1.1 Laying in work	97
IV.1.2 Vacuum structure	98
IV.1.3 Hardening of the laminate	98
IV.2 Manufacturing of the foam core	99
IV.2.1 Molding and gluing of the foam core	99
IV.2.2 Surfacing of the foam core	99
IV.3 Assembly	99
IV.4 Cutting of the connection cross section	99
IV.5 Drilling	100
V. Test and prototype testing	100
V.1 Sample testing and component test	100
V.2 Prototype testing	100
V.2.1 Dynamic test	100

**ORIGINAL PAGE IS  
OF POOR QUALITY**

	page
V.2.2 Static test	101
V.2.3 Fracture test	102
V.3 Final consideration	103
VI. Concept development	103
VI.1 Construction document reworking and release	103
VI.2 Development of the manufacturing concept	104
VI.2.1 Installation of foam core	104
VI.2.2 Surfacing of foam core	104
VI.2.3 Cutting concept development	105
VI.2.4 Drilling concept development	105
VII. Full scale wing manufacturing	105
VII.1 Manufacturing tool completion	105
VII.2 Laminate shell manufacture	106
VII.3 Foam core manufacture	106
VIII. Source list	106
IX. Figures	107-132

/81



## I. Goals

/82

With consideration of specified design parameters (essentially blade geometry and blade stiffness), two rotor blades for the wind energy facility "Stoetten 40707 b" are to be developed using the composite fiber construction method and these are to be manufactured.

## II. Construction

### II.1 Blade design

Since the blade mass, mass distribution and stiffness distribution are related directly, it is only possible to achieve an approximation to the final goal using blade cross section calculations and bar model calculations and several iterations. After achieving the required values, the blade data are compared with the requirements for the total facility and are then verified.

With consideration of the loads which occurred during operation, the connection elements (expanding bolts and transverse bolts) were dimensioned and the blade connection stiffnesses were tested. Thermally, the blade connection was designed so that the thermal expansion coefficient of the connection cross section agrees with that of the steel blade bearing so that there will be no friction between the components.

### II.2 Construction design

Based on the high stiffness requirements with the lowest possible blade mass, a "embedded" blade (foam core) was considered as the design principle because the spar construction method for large wings has a less favorable ratio of stiffness and mass. In addition, for a full foam blade, the fitting and control problems do not exist which would occur for spar fittings of small height in the external blade region.

The bending stiffness in the flapping deflection directions is provided for by unidirectional carbon fiber tissue paths (warp, weft ratio 9:1) in the blade longitudinal direction. The torsion stiffness is provided by glass fiber tissue paths in the  $\pm 45^\circ$  direction with respect to the blade longitudinal axis.

183

Because of the fact that the blade mold cannot be closed (III.1.2) in each case a half a wing is built up and then both blade halves are glued together. The torsion connection is provided by gluing on torsion shells to the nose edge and the end edge. The foam core acts as a local support structure (bulges) for the shells as well as for accepting shear forces. Force introduction into the rotor blade bearing is done by means of the blade connection already discussed during the DNW program (German Holland Wind Tunnel) using transverse bolts and expansion screws. Transverse forces are introduced into the bearing through a base plate glued to the blade connection using shear fittings.

The lightning protection system consists of a profile aluminum strand (cross section area  $50 \text{ mm}^2$ ) which is integrated with the blade structure. The trailing edge protection consists of a 1 mm thick and 50 mm wide aluminum foil glued on after manufacture to the trailing edge. The aluminum foil is inside the blade contour. Before the part is manufactured, a strip is inserted into the mold for the corresponding throughput. The leading edge and trailing edge conductors are connected at the blade tip by means of an aluminum cap. As an area protection, a thin aluminum tissue (Alu-mesh) is pasted on along the outer third of the blade which is then electrically connected with the main conductors by means of research screws.

When the design parameters were achieved, the blade was further detailed after freezing the design and a set of drawings was made.

The set of drawings include lamination plans which specify the laminate structure and the tissue deposition to be used as production room drawings.

## II.3 Material

High requirements are placed on the blade for large wind energy facilities. This involves lifetime, lightness and stiffness. Because of the high specific stiffness in strength CFI (carbon fiber reinforced plastic) was adapted as the primary structure with T 300 fibers in the form of tissue-prepegs.

As a matrix, we selected the M 10-resin system qualified for aviation in France. This resin system has a pot time of 60 days at room temperature and requires a minimum hardening pressure of only 0.5 bar. This extremely long pot time allows continuous manufacturing of the wing without intermediate hardening. The materials required for building the two rotor blades were for the most part already delivered by suppliers. Residual deliveries are expected up to April 1981.

/84

## III. Manufacturing means

### III.1 Lamination molds

#### III.1.1 Surface definition

By dividing the surface of the wings into areas, by accepting small errors the slightly spherically curved surface of a section can be transformed into a two-dimensional surface using the tangent condition (equal inclinations over the same profile points) and can, therefore, be developed. The developed surfaces were provided with the bending lines which depend on the profile contour and this represents the development drawings with two cross section drawings each per section, as the basis for manufacturing the blade mold shells.

#### III.1.2 Molding shells

The blade mold consists of two half shells which cannot be closed with 5 sections (sections). Each section is manufactured from 8 mm thick sheet metal which is bent, which is then attached to a frame

made of mero building block elements and which is anchored on the ground. Because of the thermal expansion which occurred during heating of the shell, the support points between the shell and the frame are designed so that thermal uncoupling of both components is provided for. The sheet metal shell has so little torsional strength that the blade turning angle (twist) can be considered when setting up.

According to discussions in III.1.1 and III.1.2, 11 shell molds made of 8 mm thick steel sheet were bent as well as 11 mold supports made of mero components and these were assembled. The 11th shell mold was required for geometric reasons as an additional shell in the connection region (circular connection cross section of the blade).

### III.1.3 Mold heating

The heating of the mold is done using a 1.5 mm thick CFK-GFK (carbon reinforced plastic-glass fiber glass reinforced plastic) mat.

After final acceptance of the assembly of the lamination mold, a thin GFK laminate was laminated down to the mold surface as an installation layer on to which carbon fiber tissue paths could be glued and to which a unit could be connected.

By applying electrical current, the carbon fiber tissue heats up due to its own resistance.

The heating unit is a transformer-like unit with installed control device which makes it possible to have heating at constant temperature during the various phases of the hardening cycle and to control it.

The described heating technology was developed and qualified by extensive tests during which the temperature distribution and its consistency over the test time was measured as a means for manufacturing wings.

### III.1.4 Blade mode installation

The blade mold as well as the mold installation and heating technology represent new technologies. Therefore, the first two mold segments for the internal blade region (radius points  $R = 0.8$  to  $R = 11$  m) were assembled for manufacturing a 10.2 m long blade segment.

### Set-up description

#### Assembly of the shell mold-frame

The shell molds were screwed together with the various bearing heads which could be adjusted in height. The holes were sealed.

#### Shell mold-shell mode connection

The shell molds were screwed together without any torque using a metal strip bent according to the profile contour so that the shock between the shell mold could be sealed with a round silicon sealing string.

#### Manufacturing of contour templates

Using the profile cross section drawings already made available for mold manufacturing, wood templates with the nominal profile contour were produced for the beginning and end of each shell mold. The positions of the profile threading axis was characterized by a hole in each case.

#### Alignment of the molds

First of all, the wood templates at the radius point 0.8m, 6m and 11m were positioned for the best fit. Using the bearing element of the frames which could be adjusted in height, the shell molds were positioned so that

a) the holes (threading axis) of the templates lay along one line (measurement with a theodolite).

b) reference lines marked on the templates were horizontal (measured with a level).

786

The profile threading axes of both shell molds have to run parallel to one another both to the side and in the elevation direction.

#### Adjustment of the molds for flatness

Since the shell molds are developed surfaces, that is, non-spherical surfaces, the bending lines have to be straight lines. Their straightness is tested using a ruler and may be corrected by adjusting the bearing element.

#### Fixing of the configuration

After again testing the configuration, the blade molds were fixed and the displacement elements were sealed.

#### Displacement of the rails

Driving rails for the alignment port were measured at a defined side and elevation separation and, therefore, reference to the floor of the plant.

### III.1.5 Quality assurance measures for the blade mold installation

Control measures were used for acceptance of the shell mold contour and for the blade mold installation. The control requirements specified the extent of controls, the time of controls and the type of controls used.

The corrected configuration state for manufacture of the mold is tested continuously by continuous presence of a controller during the set-up work and during a final acceptance of the molds according to the control specifications.

### III.2 Surfacing device

A surfacing device was constructed and designed for milling the blade separation plane. The surfacing device consists of a port made of mero building components which runs along two rails and covers both blade molds. The milling device is suspended in the port which essentially consists of a support with two drive units for two pot disks in the form of surfacing tools which runs in the blade chord direction. The twisting of the blade plane requires variable inclination of the milling device with respect to the horizontal which is provided for by a guy track to the side of the blade mold.

/87

### III.3 Cutting and drilling devices

The devices for working the blade connection described in the following were designed, constructed and used during manufacturing of the full scale part. Drive for the drilling and cutting tools is done through a central drive unit through a flexible shaft.

#### III.3.1 Cutting device

The cutting device essentially consists of a guide ring which goes around the blade root on which a cutting device is mounted which can move in the radial and circumferential direction. This means that manually it is possible to cut through the blade connection laminate which are about 90 mm thick. A diamond saw blade was used as the cutting tool.

The positioning of the guide ring over the component is provided for by marks in the mold and its impressions are again found in the unmolded part.

#### III.3.2 Drilling template

The drilling template defines the position of the holes in the blade longitudinal direction and the position of the passage holes in the



radial direction. The drilling template is designed so that the drilling device can be attached to it.

### III.3.3 Drilling device

The drilling device consists of a frame which can be flanged to the drilling template with a drilling device and an advance device. The advance is done through a tooth wheel and tooth rod using a manual wheel. With the drilling device, it is possible to drill both the pocket holes in the longitudinal blade direction as well as the passage holes in the radial direction by flipping over the advance unit by 90°.

## IV. Full scale part manufacture

In order to be able to compare the theoretical properties (especially mass and thickness distribution) with the actually realized component properties under manufacturing conditions, a 10.2 full scale component of the blade internal region was manufactured with the original laminate structure for testing purposes. Relevant parameters, such as workability of the prepeg, lamination time, heating rates and alignment accuracy of the fibers were examined and specified again.

788

### IV.1 Manufacturing of the laminate shells

#### IV.1.1 Laying in work

Before starting the laying in work, a separation agent was introduced into the lamination molds containing the heating unit. The GFK (glass fiber reinforced plastic) tissue prepegs were inserted with an orientation angle of  $\pm 45^\circ$  into the mold which were cut for the torsion skin and this was rolled on with teflon rollers. Without intermediate hardening and starting at the radius point  $R = 11 \text{ m}$ , the CFK (carbon fiber reinforced plastic) unidirectional layers were laid in in the same way but in a zero degree direction but spliced in the direction of the blade connection. The CFK layers provide for the flapping and deflection stiffness of the blade.

Additional CFK layers in the zero degree direction were applied directly to the blade connection in order to stiffen it and in the 90° direction for reasons of thermal expansion.

In order to thicken the belt laminate in the internal blade region and, therefore, to reduce the hole internal pressure and for better stress distribution, spliced GFK layers spliced into the CFK strip are used.

In order to have an even larger hollow area, an internal GFK wedge laminate is applied so that the internal and external belt position is separated and this makes it possible to connect a laminate about 90 mm thick using a transverse bolt. The sequences of the prepreg types to be used, the numbers of layers and the fiber orientation angles are specified in lamination plans.

#### IV.1.2 Vacuum structure

After ending the laying in work, the vacuum facility was installed which was used for large area pressing of the laminate and for sucking off part of the lamination resin.

The unit itself consists of a foil which covers the entire laminate and is sealed off everywhere and the air underneath it is evacuated.

#### IV.1.3 Hardening of the laminate

Hardening of the reaction resin is done exothermally. The characteristic of the temperature time variation was determined already before with sample laminates of the same thickness as the blade connection laminate.

Thermal elements were installed and laminated into the heating laminates which are connected to the control devices of the heating unit. This measure assures that at the beginning there will be a uniform heating of the laminate and after the exothermal reaction, there will be no additional energy supply by the heating system. The entire

heating cycle followed the determined characteristic of the temperature /89 time variation and was continuously monitored.

## IV.2 Manufacturing of the foam core

### IV.2.1 Molding and gluing in of the foam core

After removing the vacuum unit, the foam core was fitted into the completely hardened laminate shells. This consists of about 80 mm thick PVC foam plates which are cut according to the internal shell contour. From  $R = 6$  m to  $R = 11$  m, these were glued in staggered in the blade core direction. From  $R = 0.8$  m to  $R = 6$  m, they were inserted in the form of a spar. Gluing of the core to the laminate was done using an expandable cold foamable epoxy gluing system (XB 3054 A + hardener XB 3054 B + propellant XB 2972 C) which fills cavities caused by cutting inaccuracies. In addition, 1 GFK (glass fiber reinforced plastic) rib was laminated in for the static test.

### IV.2.2 Surfacing of the foam core

Milling of the blade separation planes was done using the surfacing device mentioned under III.2. Tool advance was done manually.

## IV.3 Assembly

The surface wing path shells were placed above one another, positioned along the blade leading edge and then glued with the cold foaming adhesive system already described under III.2.1. The third shell in the form of a "wedge" required for geometric reasons (see III.1.2) was matched by hand and was connected with cold hardening CFK wet laminates with the wing half shells. The torsion complex was also closed using wet laminates at the wing nose and trailing edge.

### IV.4 Cutting of the connection cross section

The cutting device discussed under III.3.1 was positioned on the wing and the 90 mm thick laminates were separated with a slight excess.

The separation surface obtained in this way was surfaced using an additional device with an accuracy of  $\pm 0.2$  mm to the final tolerance.

/90

#### IV.5 Drilling

The drilling template and drilling device (see III.3.2 and III.3.3) were assembled and positioned as a unit at the connection cross-section. Using a hard metal tool, there was a stepwise drilling of the hole for the force introduction elements up to a drilling diameter of 45 mm.

### V. Test and prototype testing

#### V.1 Sample testing and component test

Before the prototypes were used, all of the new kinds of materials (for example, foam system XB 3054) were subjected to technological tests and the mechanical properties were determined by tension, shear and torsion samples.

The basic properties of the blade connection method are already well known from the DNW program (German-Holland Wind Tunnel). We did not make any component tests.

#### V.2 Prototype testing

In order to test the extent to which the theoretical component properties agree with the ones found after manufacturing, static and dynamic tests were performed with the 10.2 m full size component. For this purpose, it was screwed horizontally to a 3.3 ton tube-like bearing block designed for this purpose which itself was mounted on two 8 mm high and 13 m long double T supports. The support block is designed so that the original connection elements could be used and, therefore, the original clamping conditions could be simulated.

##### V.2.1 Dynamic test

The measurement of the eigen frequencies of the component allows

one to determine the extent to which the mass and stiffness distribution (especially their coupling) can be maintained with a specified tolerance width.

The measurements were performed with a test band oscillation multiple position measurement installation.

Using electrodynamic exciters, the full scale component was excited over the range 0 - 200 Hz and all resonance frequencies up to 200 Hz and oscillation modes up to 100 Hz were identified with accelerometers and measured.

/91

Since completely rigid clamping of the blade cannot be realized in practice, the motions of the clamping points were also measured by their own measurement transducers (accelerometers) for all of the eigen modes. The measurements themselves were performed for two positions of the blade because the clamping for horizontal blade oscillations had a larger yield.

We had the following results:

1st flapping bending	9.84 Hz	calculated 8.6 Hz
1st deflection bending	9.99 Hz	calculated 8.9 Hz
2nd flapping bending	31.8 Hz	
2nd deflection bending	36.9 Hz	
1st torsion	45.5 Hz	

Further results are contained in MBB/FE173/Tr12.

The calculated values are taken from a frequency calculation of the firm Voith Getriebe KG.

The test results show that the goals of the contracting agency were exceeded and the mass and stiffness specifications are within tolerances.

#### V.2.2 Static tests

The theoretically determined bending stiffness safety factors are to be demonstrated in the static test with the full scale component.

The clamp component was loaded by a resulting force at the blade radius points  $R = 6\text{ m}$  and  $R = 10.8\text{ m}$  so that the flapping and deflection moments were simulated at the same time. In addition, a pure deflection test was carried out. The blade deformations which occurred were measured using strain gauges and path recorders. A single force was introduced by means of a wooden scissors in such a way that its line of action passed through the thrust center. The load was increased in steps up to a maximum of 130 kN at the radius point 10.8 m.

From the strains, the stiffnesses in the region  $2.5\text{ m} < R < 6\text{ m}$  were determined. In the other regions, they could not be accurately determined because there only small strains occurred outside due to the small bending moment and in the root region because of the high bending stiffnesses.

The determined stiffnesses are above the nominal values. Bending lines recorded in this region also show smaller bending compared with calculations and therefore higher stiffness.

### V.2.3 Fracture test

/92

The fracture test is intended to determine values for the most critical failure case considered to be crumpling of the belt laminate along the wing side subject to compression. In this failure mode, the belt separates locally at a critical pressure stress because the support by the foam is no longer sufficient. In the test the component failed at a load of 130 kN ahead of the rib installed at 6 m in the region of the area which was the least safe for the component according to theory (only is valid from moment loads by individual forces at the component tip).

## Safety Factors achieved

### a) Local pressure stability

For the strains which occurred at a failure load of  $F = 130$  kN, we find a safety factor against crumpling for the entire blade of  $j = 1.36$  for the maximum positive gust. This value, therefore, applies for the "century gust" load case.

### b) Transverse force

The smallest safety factor against transverse force thrust was found for the test component at the point  $R = 6.5$  m:  $j = 4.0$

### c) Safety against bending moments for the WEC entire blade

From the point  $R = 9.7$  m up to the root region, for the test component a higher bending moment was simulated as occurs during operation.

### d) Blade connection

With the test load of 130 kN, the 3.2 time root moment was demonstrated.

Further results are contained in TN DE 133-1/81

## V.3 Concluding remarks

With the test described in Chapter V.2, the eigen frequencies, the static component strength and stiffness and, therefore, the achievement of the goals has been demonstrated..

/93

## VI. Concept development

### VI.1 Component development and release

According to the prototype qualifications discussed in Chapter V,



the drawing sets were reworked and were released for manufacturing the first 25.2 m wings. Based on knowledge from the full scale manufacturing (Chapter IV) in the meantime detailed manufacturing and control specifications have been developed and released.:

## VI.2 Manufacturing concepts development--

### VI.2.1 Installation of foam core

In the manufacturing of the prototype (IV.2.1), it was found that it takes a lot of time to individually fit in the foam plates. In addition, the filling of the foam plates was not always perfect because the pressure required for gluing ( ) could only be applied in the direction of the laminate shells. Based on these problems, the foam core was glued in as follows in the full scale wings.

Approximately 3 mm thick foam strips were glued in in the blade longitudinal direction into the laminate shells. In this way, the foam core has a well defined distance from the laminate shell and only has to be roughly tailored. Because of the defined gap, one obtains a perfect gluing of the entire foam core surface and the shell with the cold expanding foam system XB 3054. In addition, about 10 roughly tailored foam plates were glued together into a block using screws. Gluing of the blocks among themselves is done in a different manner as during prototype manufacturing, also using XB 3054. Based on these improvements, possible erroneous gluing can almost be excluded.

### VI.2.2 Surfacing of foam core

During the surfacing work on the prototype (point IV.2.2), the surfacing tool (rasp-like pot disk) was found to be insufficient because of reduced chip performance due to chip size and the reduced possible advanced rates.

A tool was designed for milling work for the large wing and it was built. The tool consists of a flat aluminum plate where chisels

can be installed in four holes. With this tool, because of its good cutting performance, the milling time of the large wing could be reduced to about 1/4 of the milling time of the prototype. The GFK /94 (glass fiber reinforced plastic) rib at  $R = 6$  m which is a disturbing element for the foam milling (tool wear) is only installed after milling.

### VI.2.3 Cutting concept development

The separation of the connection cross section discussed under IV.4 led to steps in the connection plane due to guidance inaccuracies and discontinuous separations which had to be removed with a large amount of effort. A new device was constructed for cutting the large wing and it was manufactured which allows continuous separation of the approximately 90 mm safe blade connection laminates and uses a diamond blade which rotates in the blade circumferential direction. In this way, the required reworking can be reduced to a minimum.

### VI.2.4 Drilling concept development

During the drilling of the prototype (IV.5), it was necessary to predrill up to four different steps which required a great deal of time. Based on extensive research with special firms, a hard metal drilling tool was found which allows one to make the 30 mm and 40 mm diameter holes with suction removal of the dust in one step with the prescribed fitting quality. The drilling device was modified in order to use these tools.

## VII. Large wing manufacture

### VII.1 Manufacturing tool completion

Lamination molds in the same way as discussed in III.1.4 were installed from  $R = 11$  m to  $R = 26$  m for manufacturing the large wing, as were the driving tracks for the surfacing port which was extended to about 30 meters. After optical measurements and evaluation of the individual values, the lamination molds were released. After lamination

of the mold heating units, electrical connection and functional control by heating, the cooled molds were again optically measured in order to detect possible displacements of the mold. Only after it was found that the remaining displacements were within tolerances were the molds finally released for manufacture.

195

## VII.2 Manufacturing of the laminate shells

Manufacture of the 26 m long laminate shells was done according to the manufacturing of the prototype laminate shells discussed under IV.1 without any manufacturing changes.

## VII.3 Manufacturing of the foam core

Up to the time of this report (February 28, 1981), the gluing in work and surfacing of the foam cores discussed under VI.2.1 and 2.2 has occurred including manufacturing of the trim chambers.

## VIII. Source list

- |               |   |
|---------------|---|
| Gatter, W.    | Oscillation measurements in the internal section of the WEC blade MBB/FE173/STR12 of June 26, 1980                  |
| Pfeifer, K.   | TN-DE 133-1/81 of January 23, 1981  |
| Krautwald, R. | Status report on rotor blade development ET 4343A for wind energy facility "Stoetten 40707b" status: March 30, 1980 |

ORIGINAL PAGE IS  
OF POOR QUALITY

IX. FIGURES

WIND ENERGY TECHNOLOGY

TEST ROTOR BLADE OF A  
**VOITH-Wind-Energy  
Converter (WEC).**

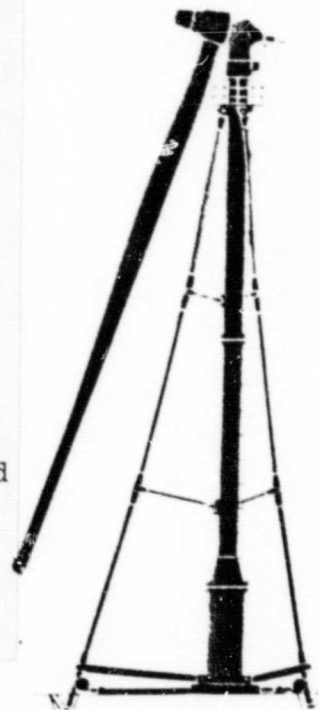
TECHNICAL DATA:

Rotor blade  
material CFK = carbon fiber plastic  
length of the object shown 11 m  
length of the rotor blade  
ready for operation 26 m  
largest CFK component in the  
world

Manufacturer MBB  
Hall 7  
Stand 201/301

Converter  
rotor type 2 blades  
rotor diameter 52 m  
rotor rpm 37 rpm  
rotor power 316 kW at 8.5 m/s wind  
purpose power generation

Manufacturer Voith Getriebe KG  
Aviation  
Hall 13  
Stand 603/703



WEC-Converter

light part of wing is the prototype

FIGURE 1.

SPAN 26,0m  
 LENGTH 25,2m  
 MAX CHORD 1,10m  
 MIN CHORD 0,28m  
 TWIST  $7,0^\circ$

ORIGINAL PAGE  
 BLACK AND WHITE PHOTOGRAPH

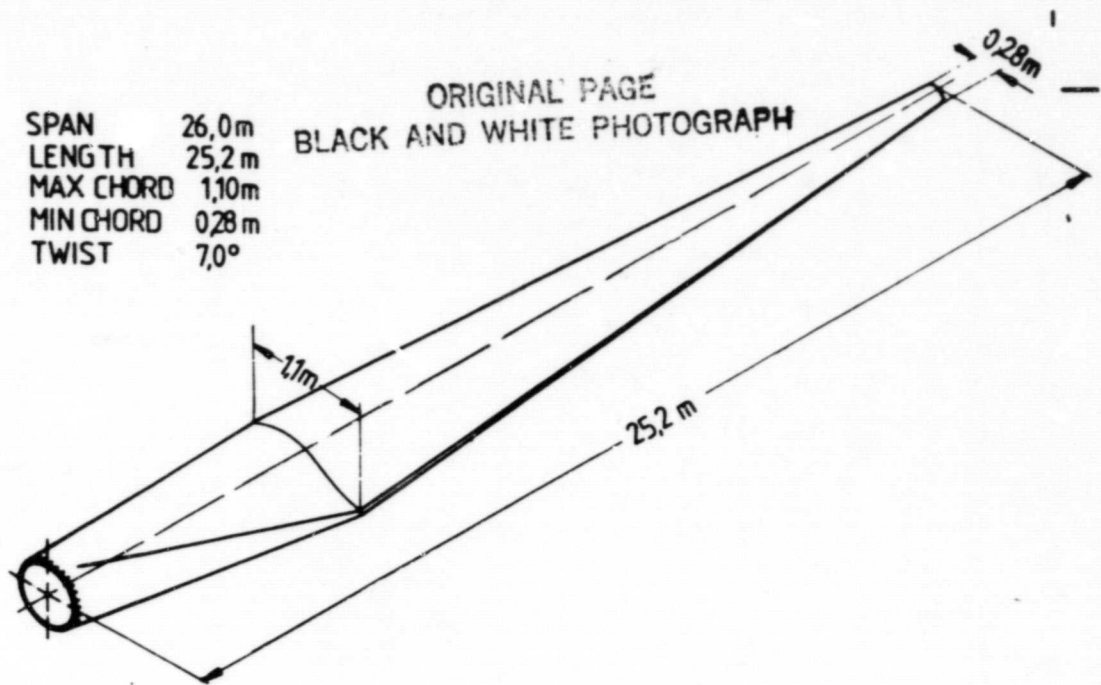


FIGURE 2. DIMENSIONS OF ROTOR BLADE

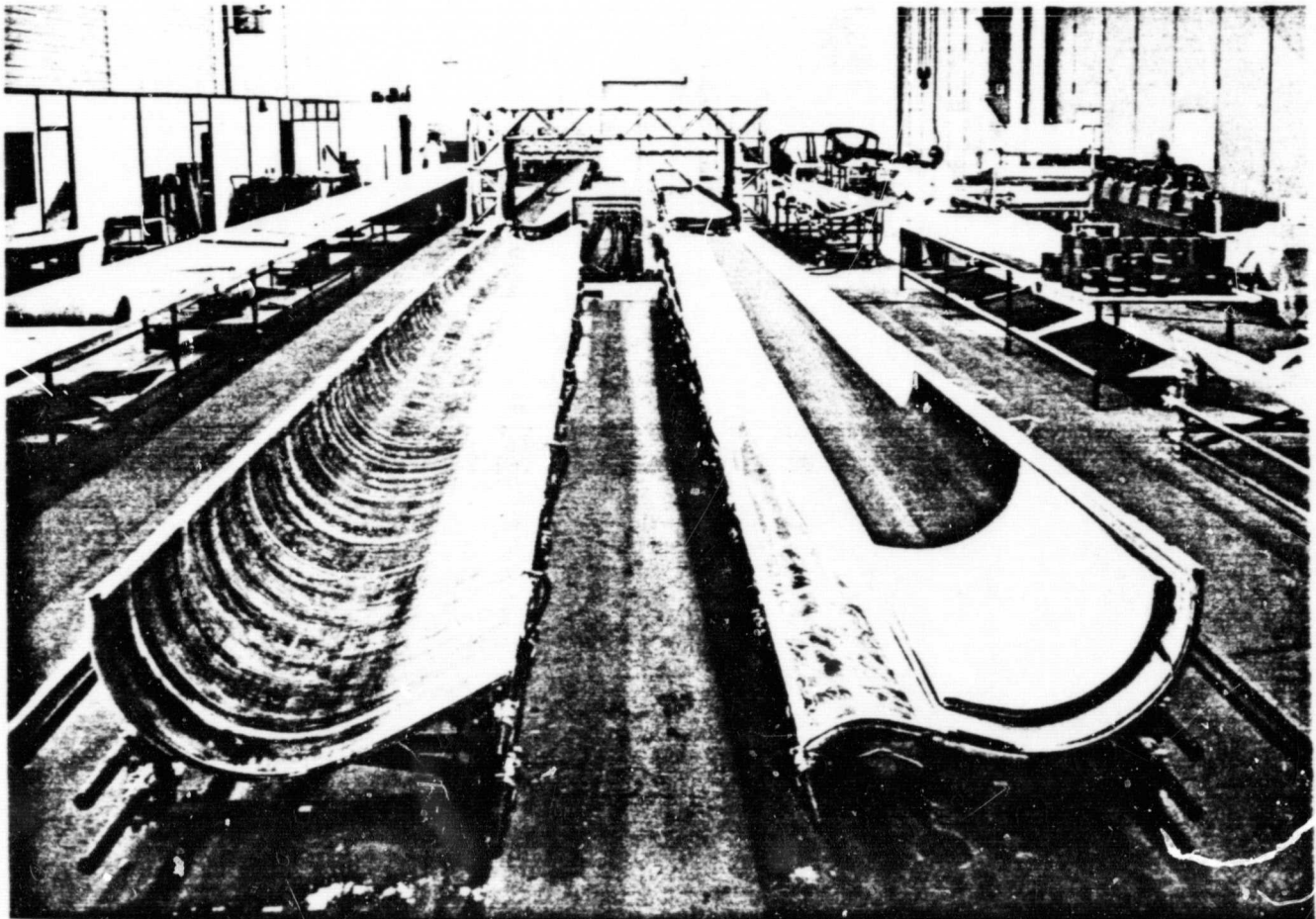
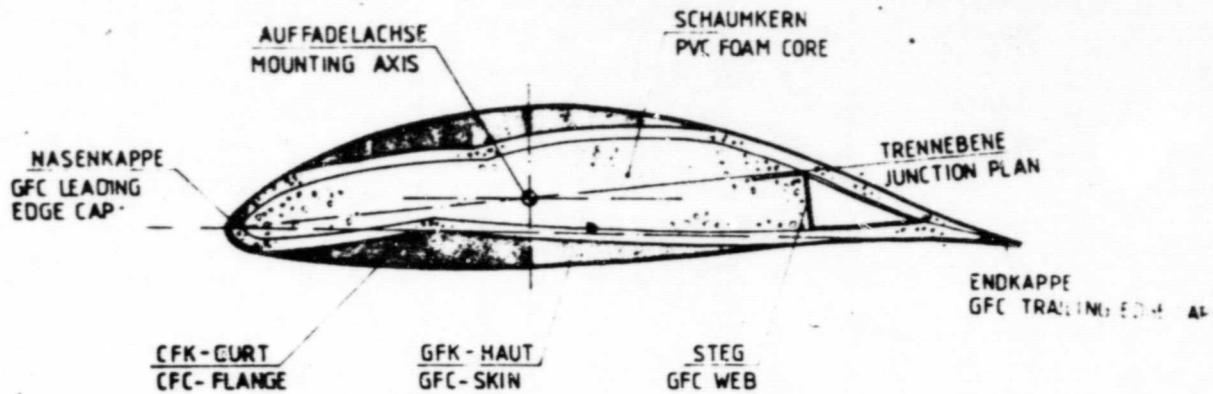


FIGURE 3. TOTAL VIEW OF THE WEC PROTOTYPE MANUFACTURER

ORIGINAL PAGE IS  
OF POOR QUALITY



ALL SECONDARY BONDINGS WITH USE OF LIQUICH (FOAMING) EPOXY ADHESIVE

FIGURE 4. BLADE CROSS SECTION

# KONSTRUKTIVER AUFBAU

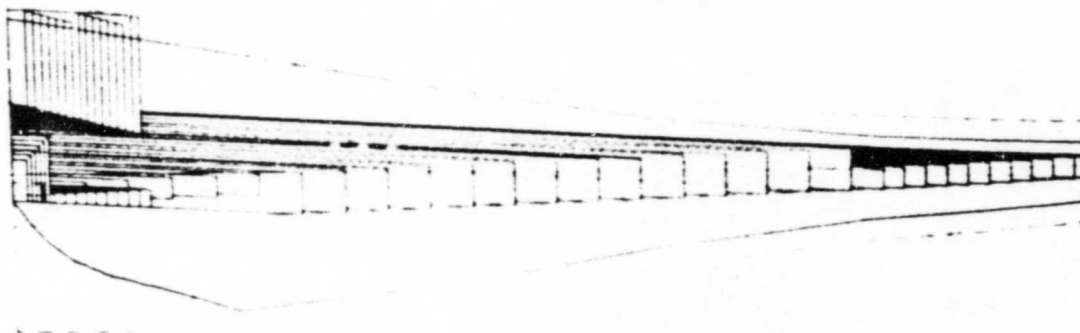


FIGURE 5. LAMINATE DESIGN



ORIGINAL PAGE IS  
OF POOR QUALITY

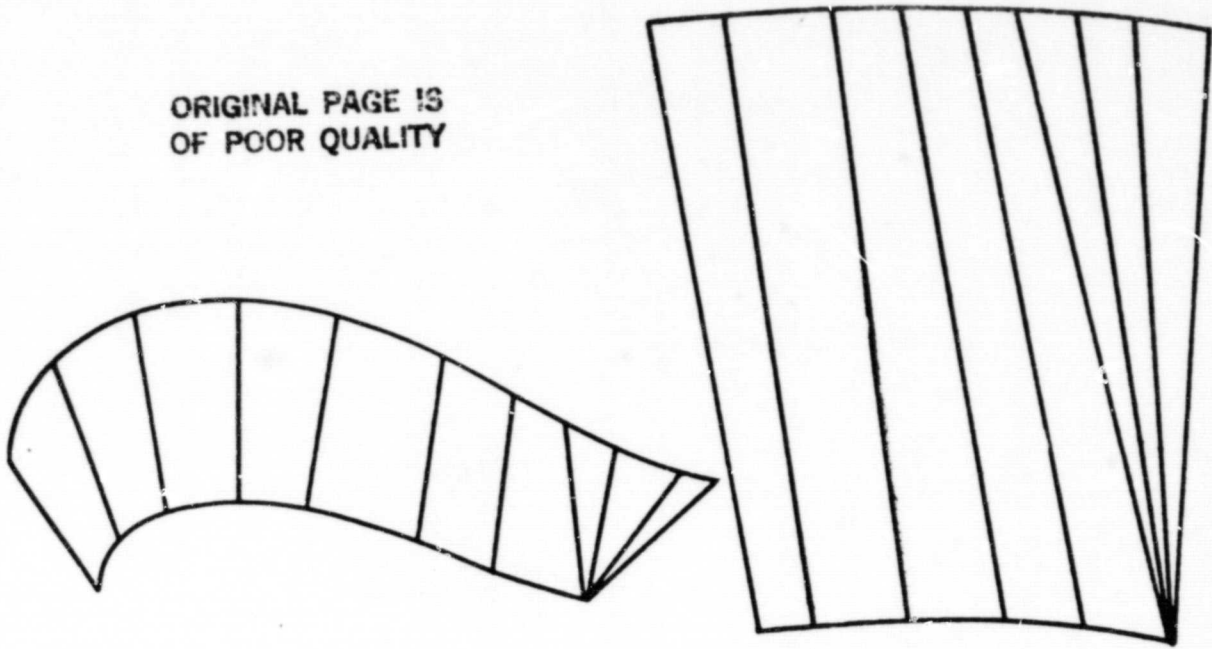


FIGURE 6. DEVELOPED SURFACE OF A MOLD SHELL

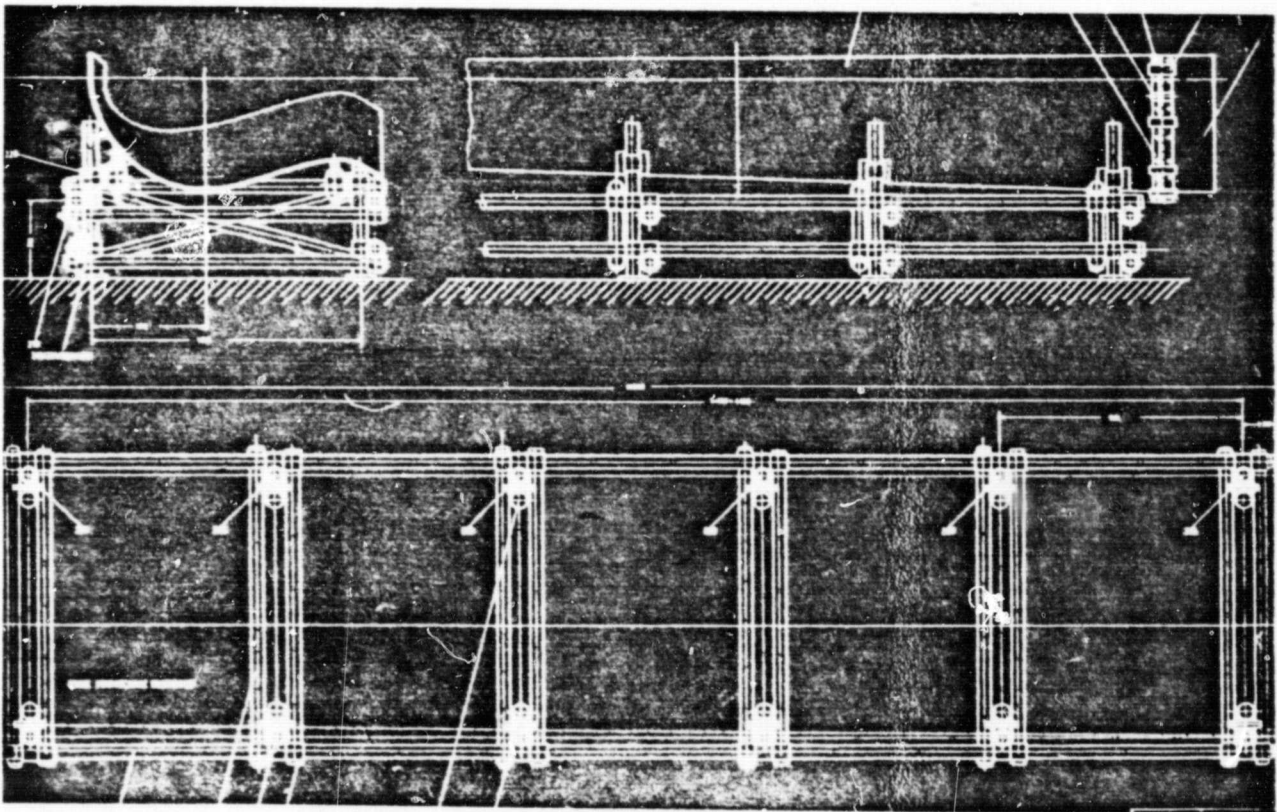


FIGURE 7. SKETCH OF THE LAMINATION MOLD (FIRST PASS)



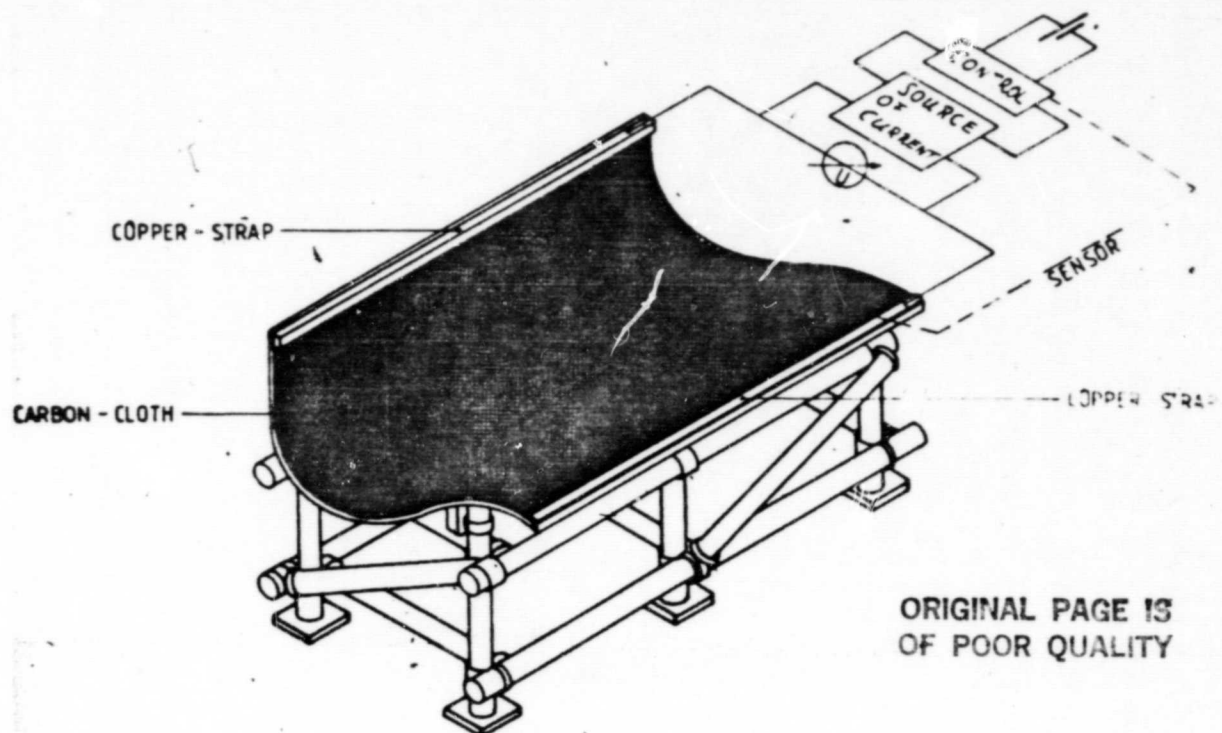


FIGURE 8. SKETCH OF MOLD HEATING

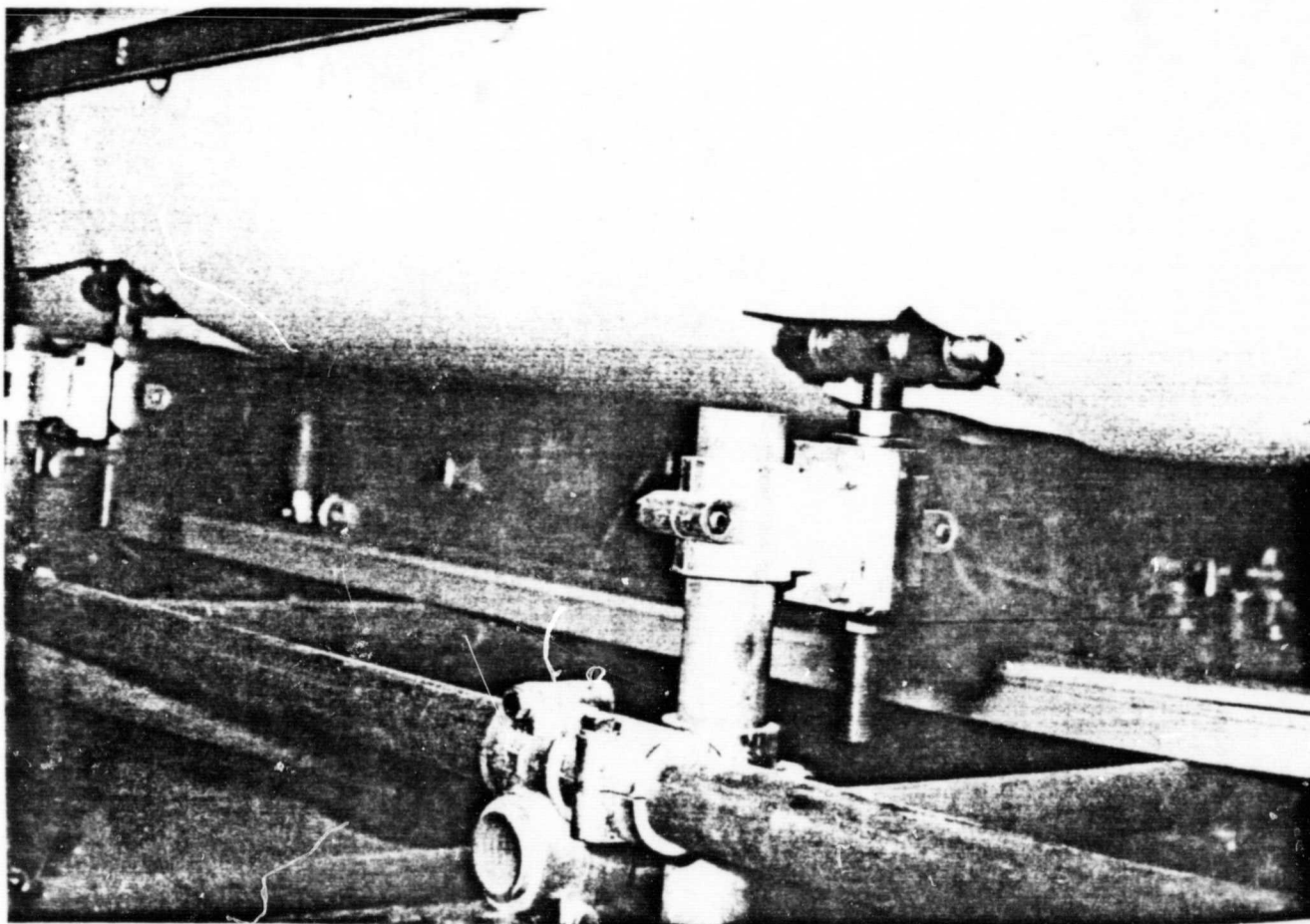


FIGURE 8. SUSPENSION POINT (ADJUSTABLE HEIGHT)  
OF THE MOLD SHELL UPPER LEFT:  
GUIDING TRACK

ORIGINAL PAGE  
BLACK AND WHITE PHOTOGRAPH



FIGURE 9. ROLLING THE TORSION LAYERS ONTO THE CONVEYER

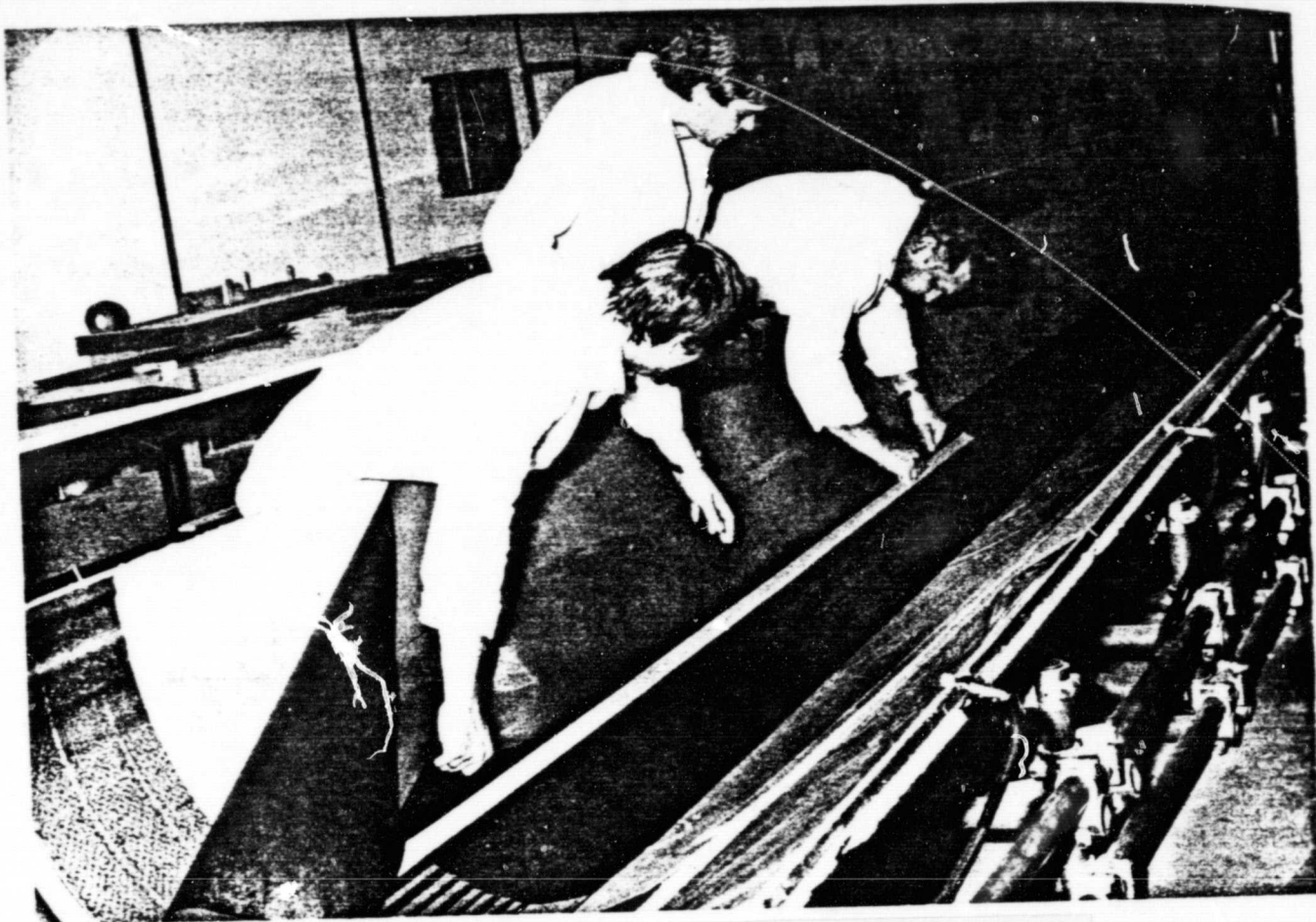


FIGURE 10. POSITIONING OF THE CARBON PREPEGS



FIGURE 11. TEARING OFF OF THE PROTECTIVE FOIL



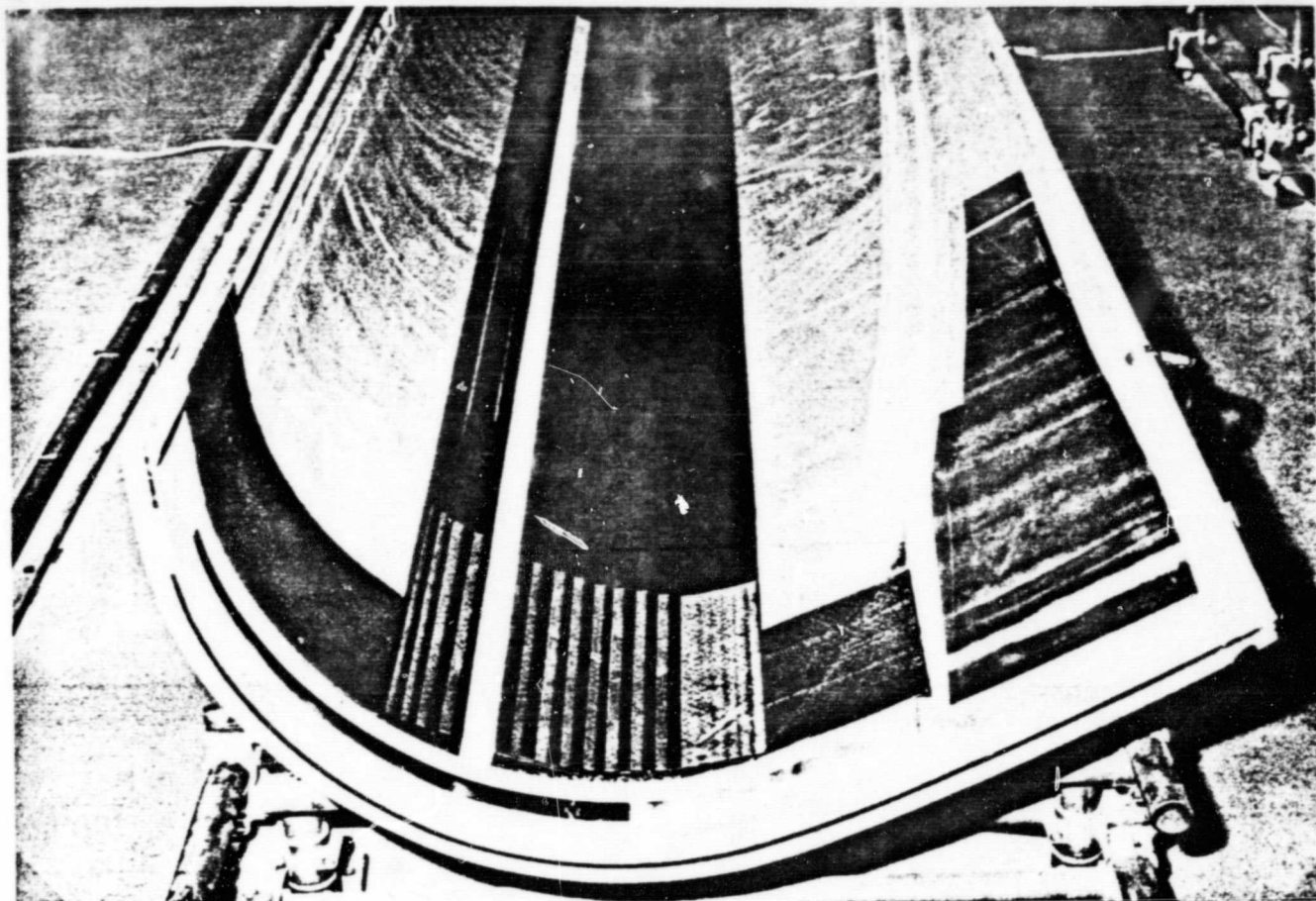
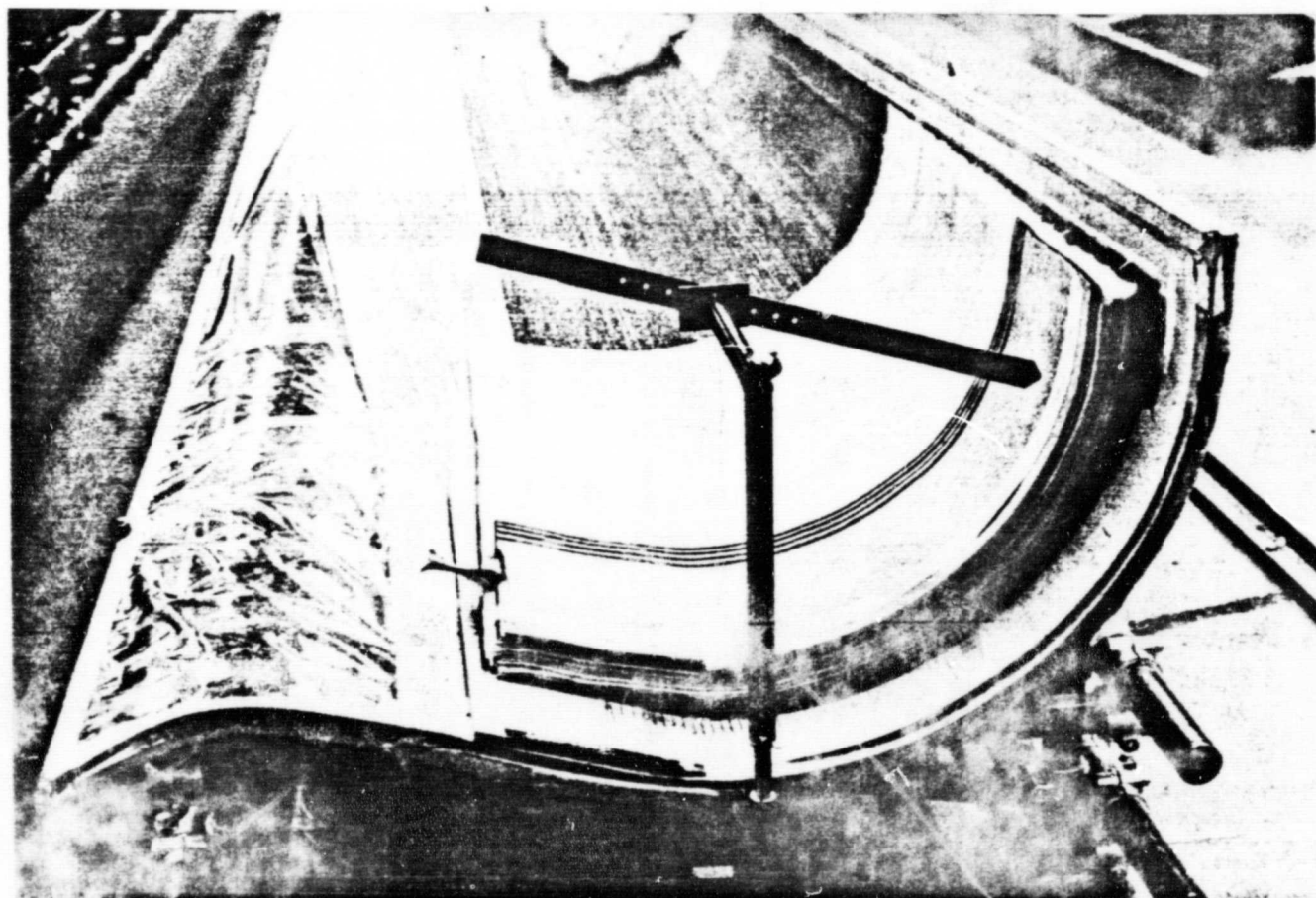


FIGURE 12. BELT LAYERS WITH GLASS FIBER PREPREG  
SHAFTS. WHITE:  $\pm 45^\circ$  TORSION LAMINATE



114 FIGURE 13. V BELT AT THE CONNECTION REGION

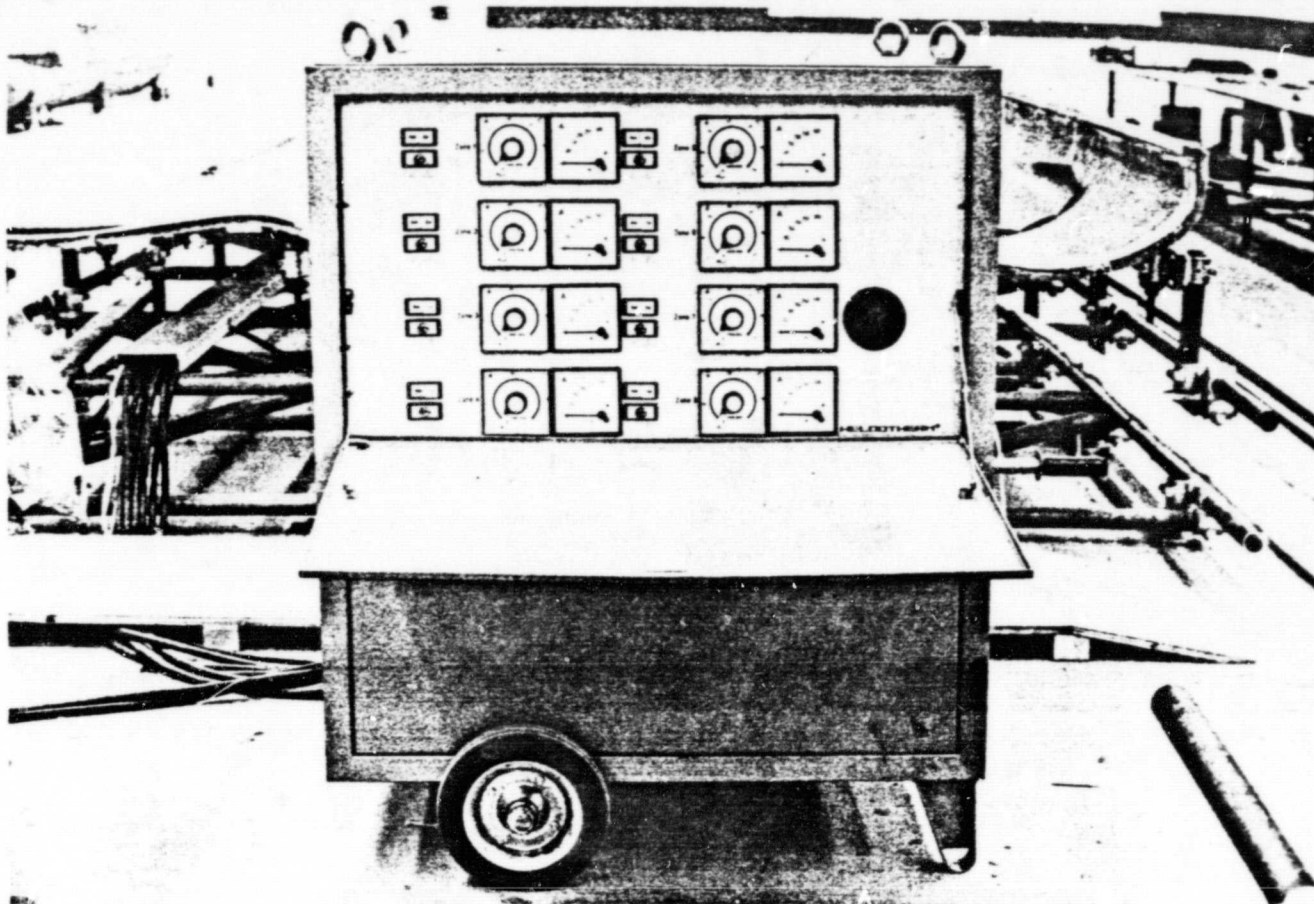


FIGURE 14. HEATING UNIT WITH 8 CONTROL CIRCUITS

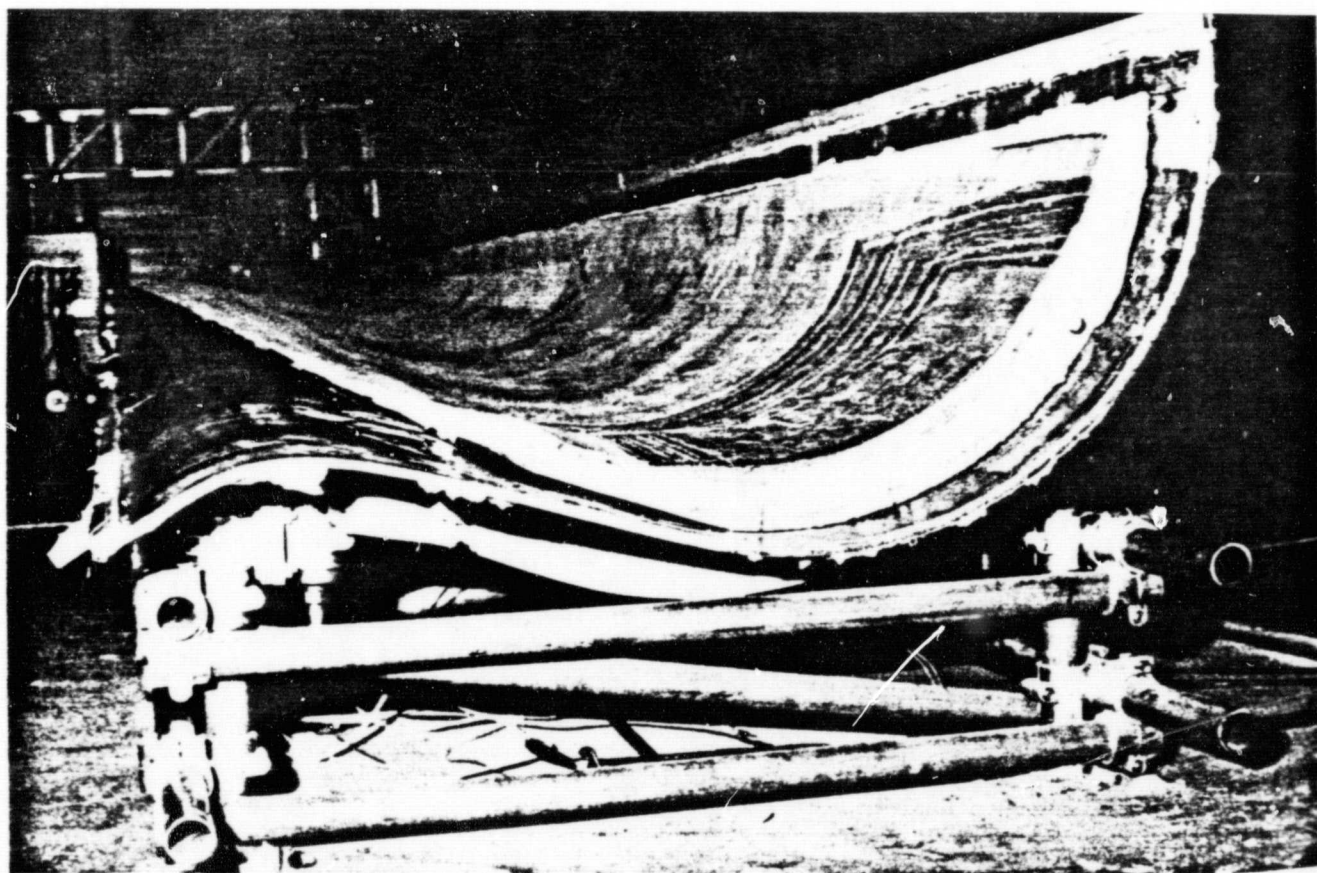


FIGURE 15. HARDENED LAMINATE SHELL



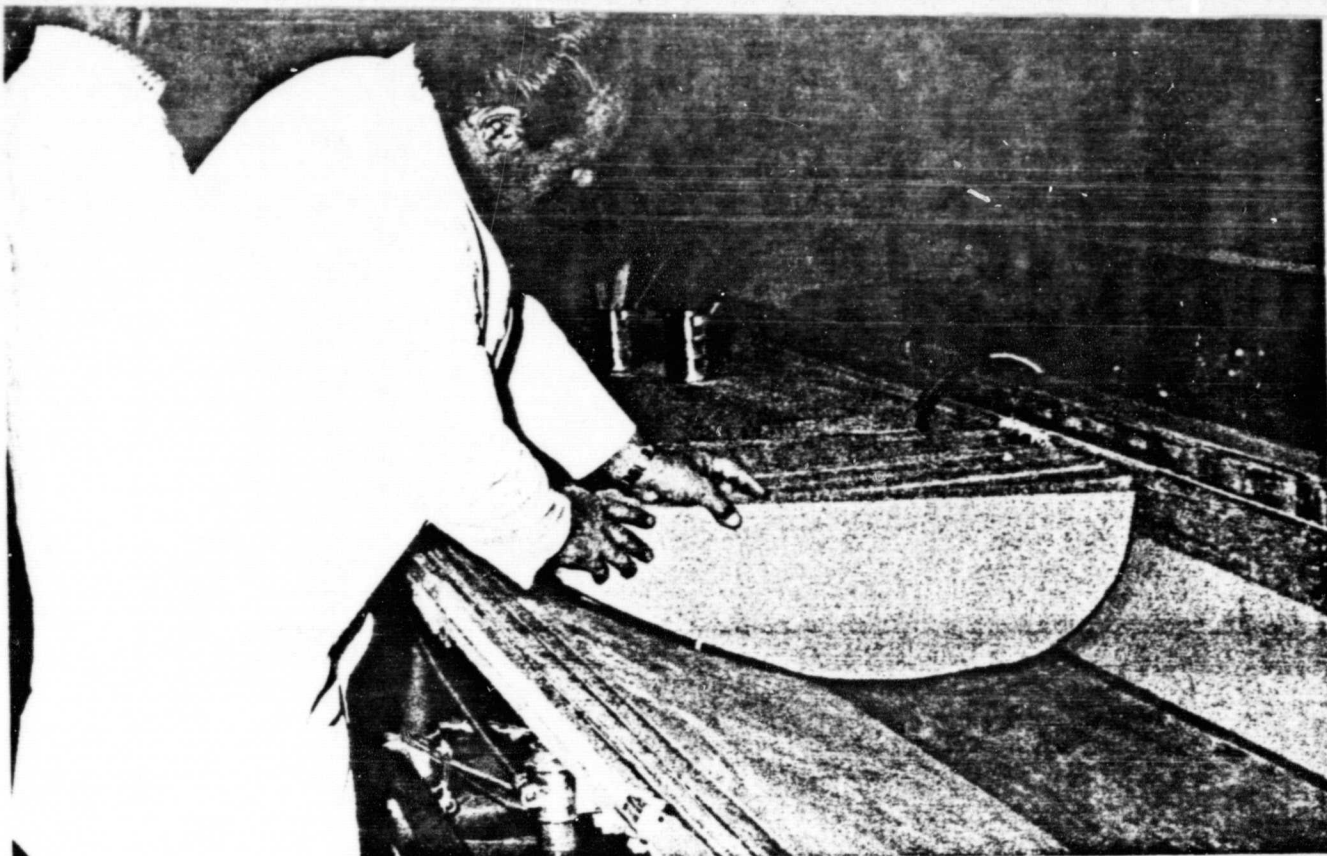


FIGURE 16. GLUING OF THE FOAM CORE

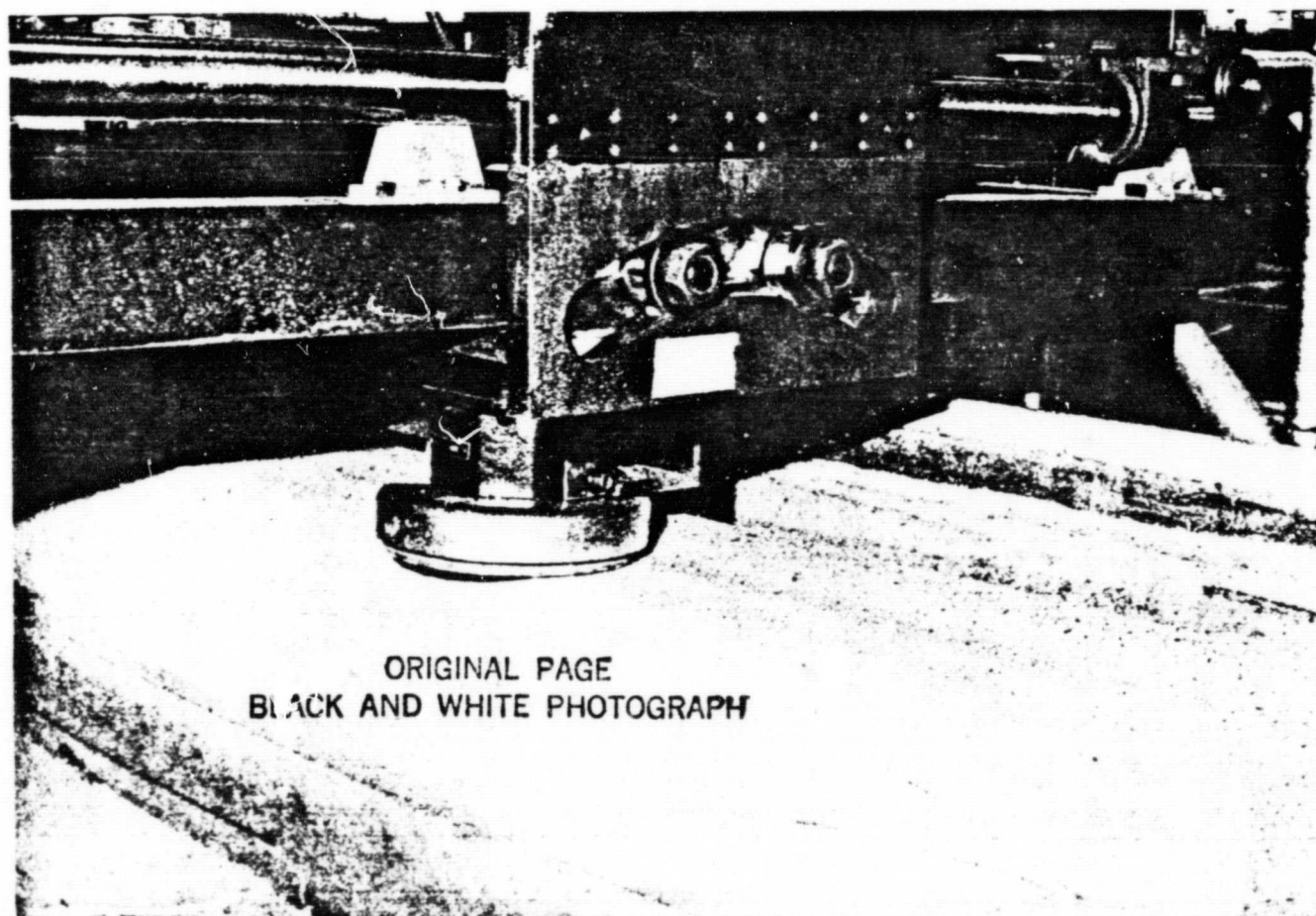
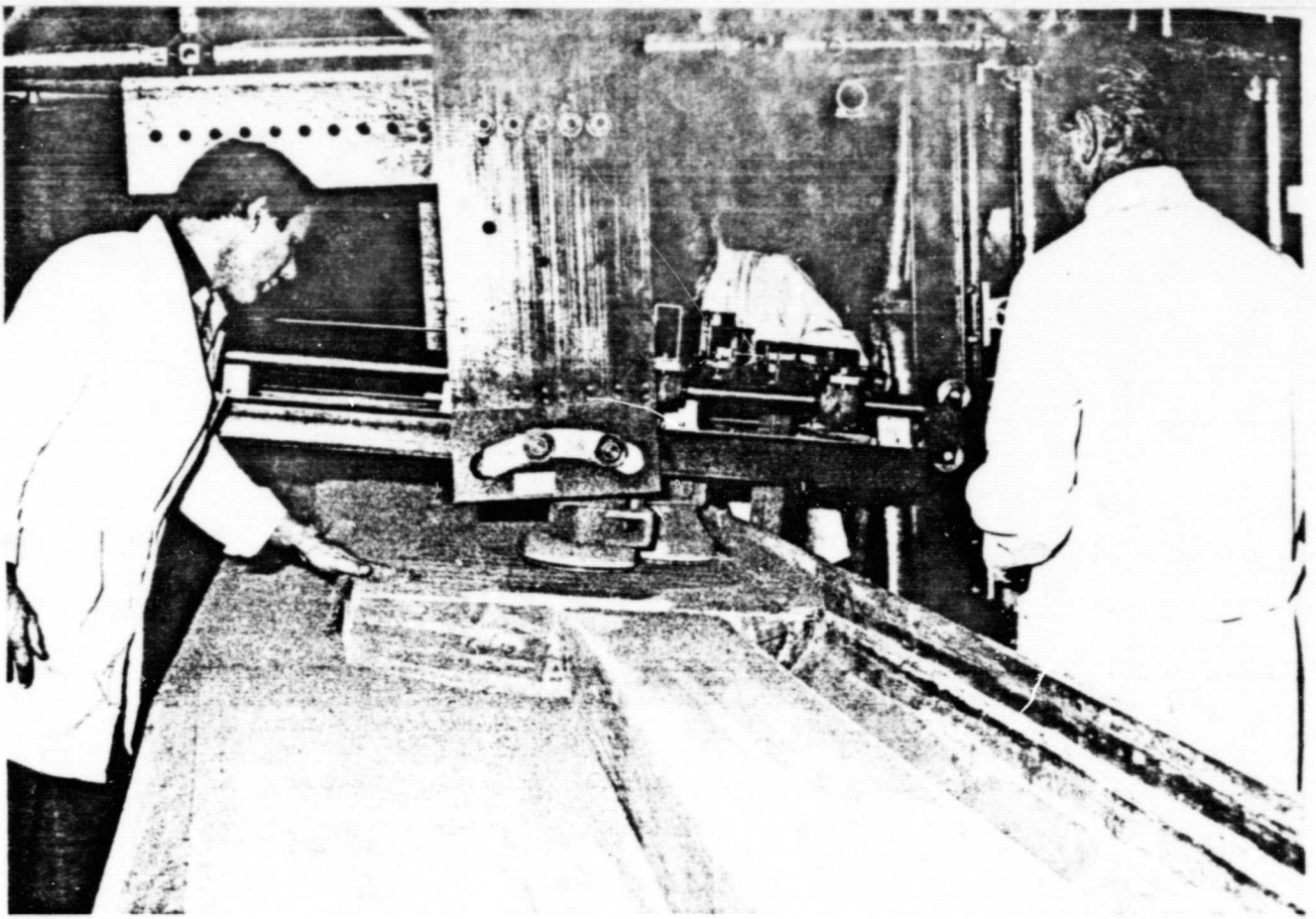
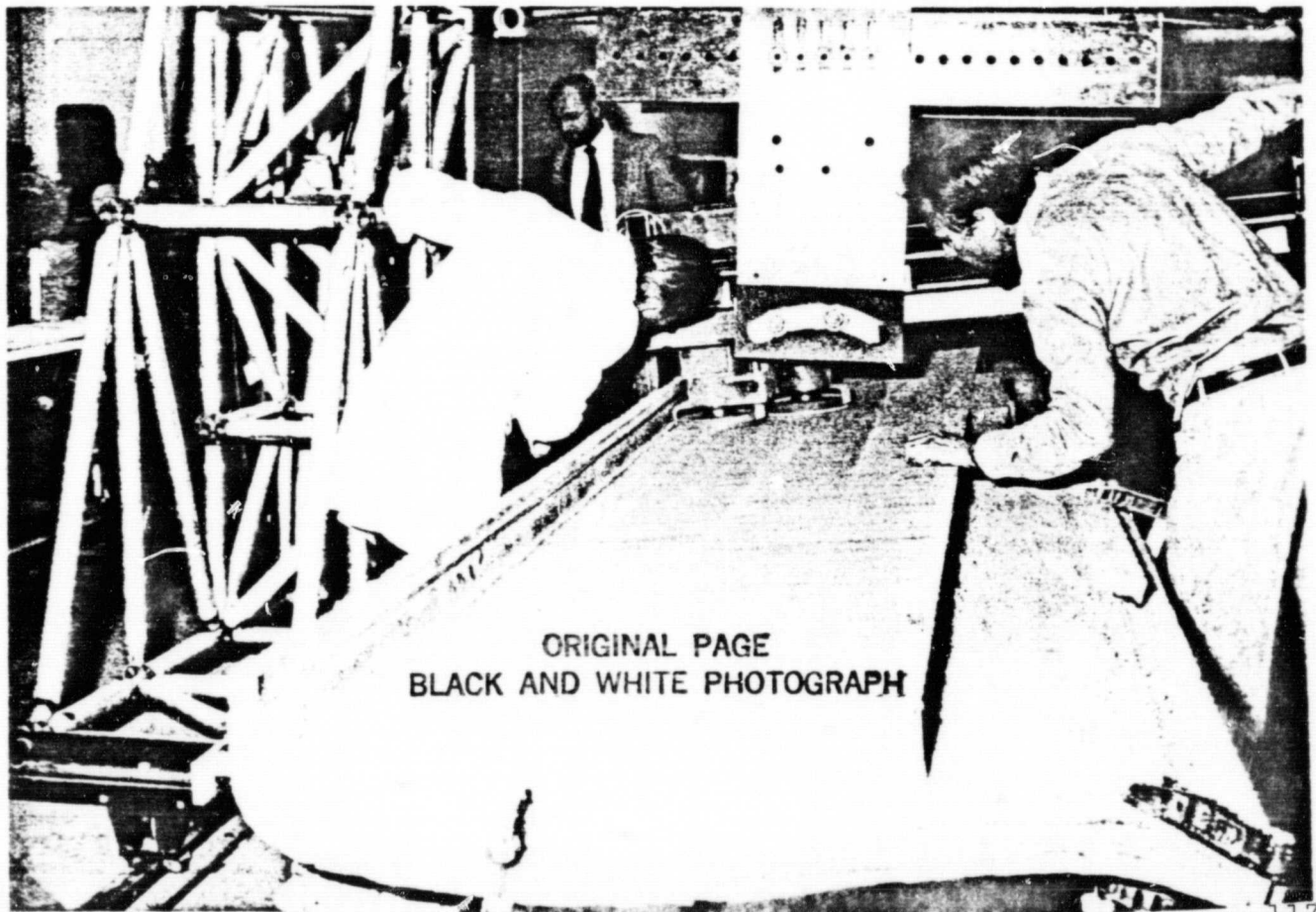


FIGURE 17. ALIGNMENT TOOL DURING MILLING OF THE FOAM SPAR



FIGURES 18 and 19. ALIGNMENT OF FOAM CORE





ORIGINAL PAGE  
BLACK AND WHITE PHOTOGRAPH

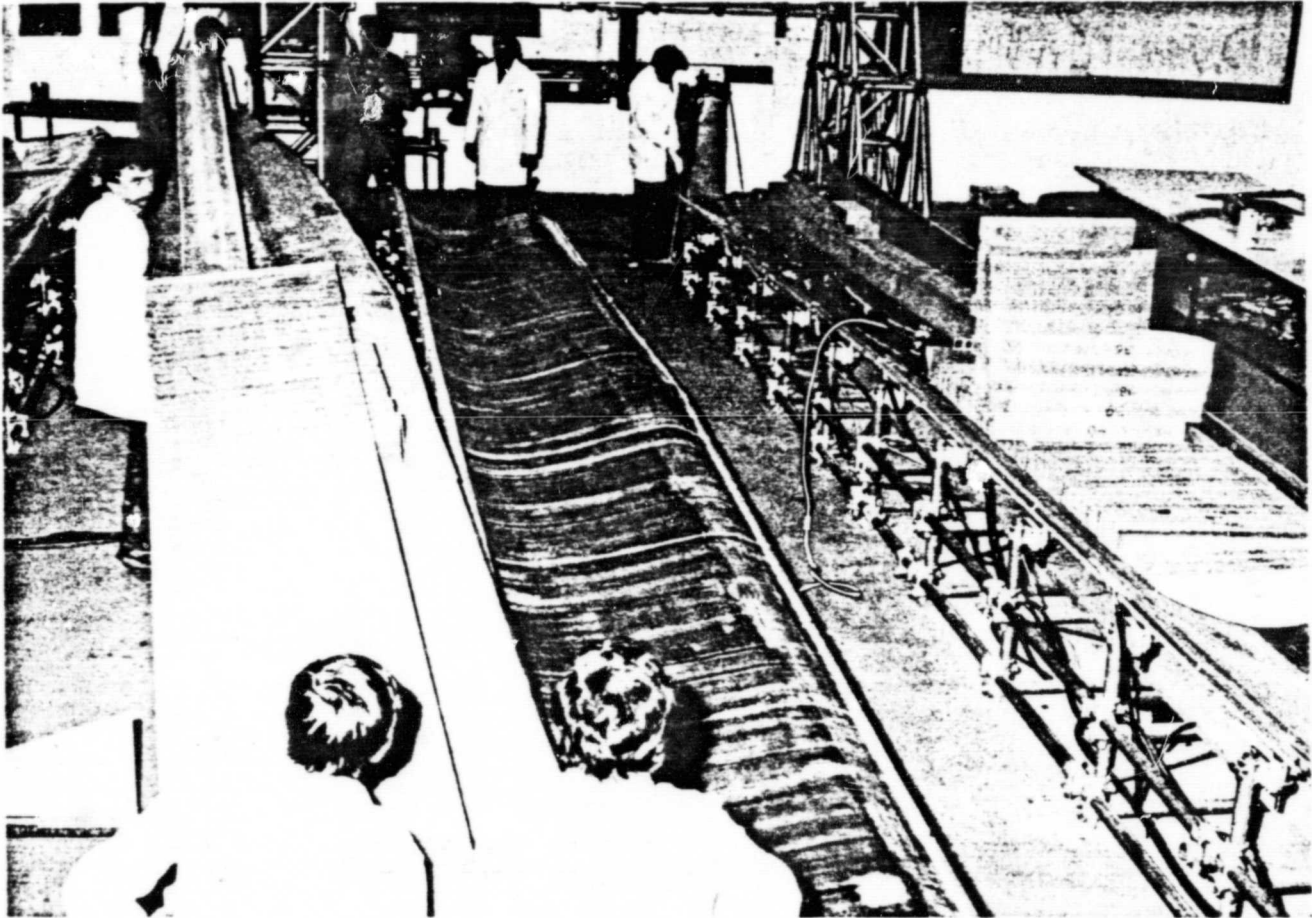
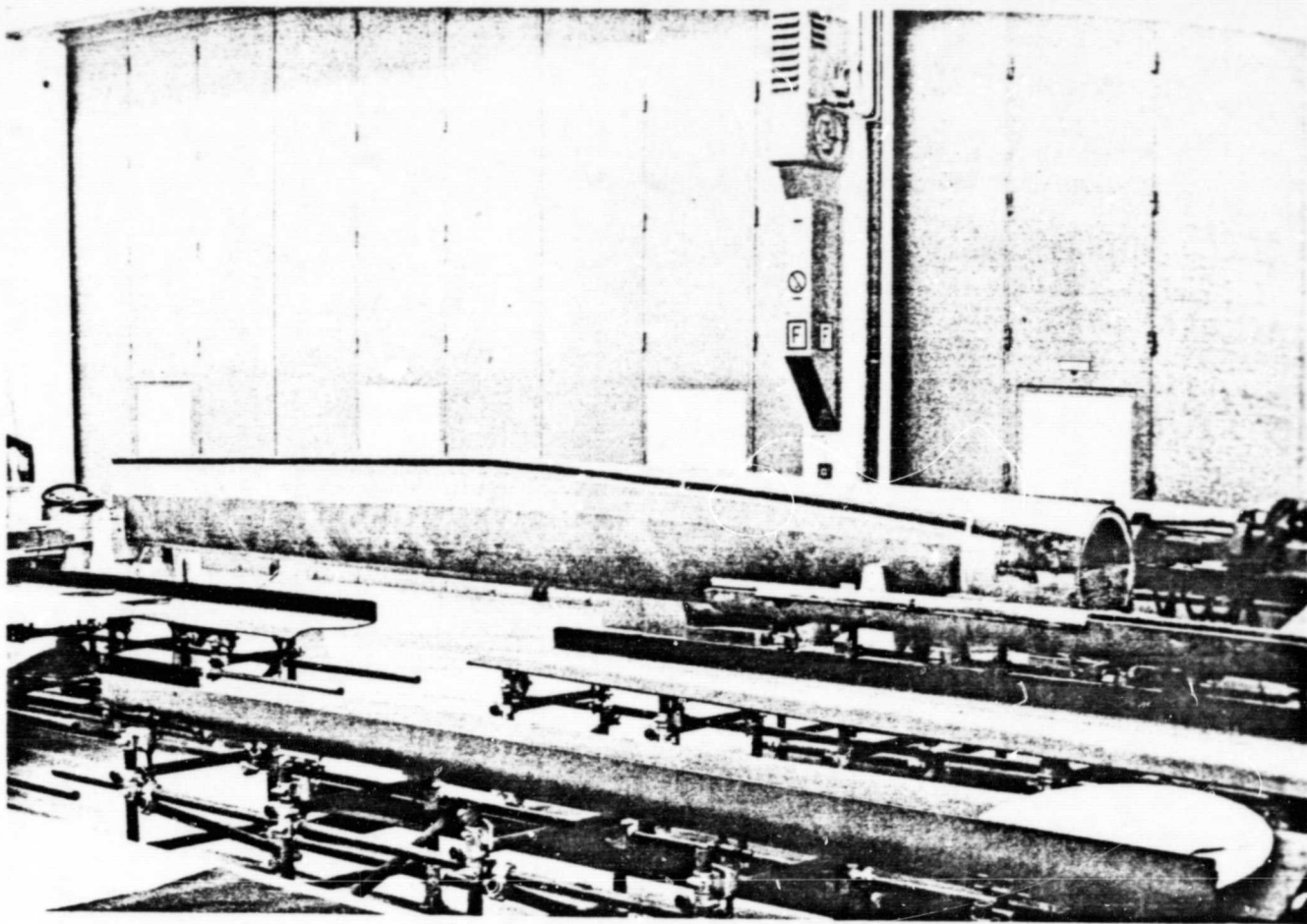
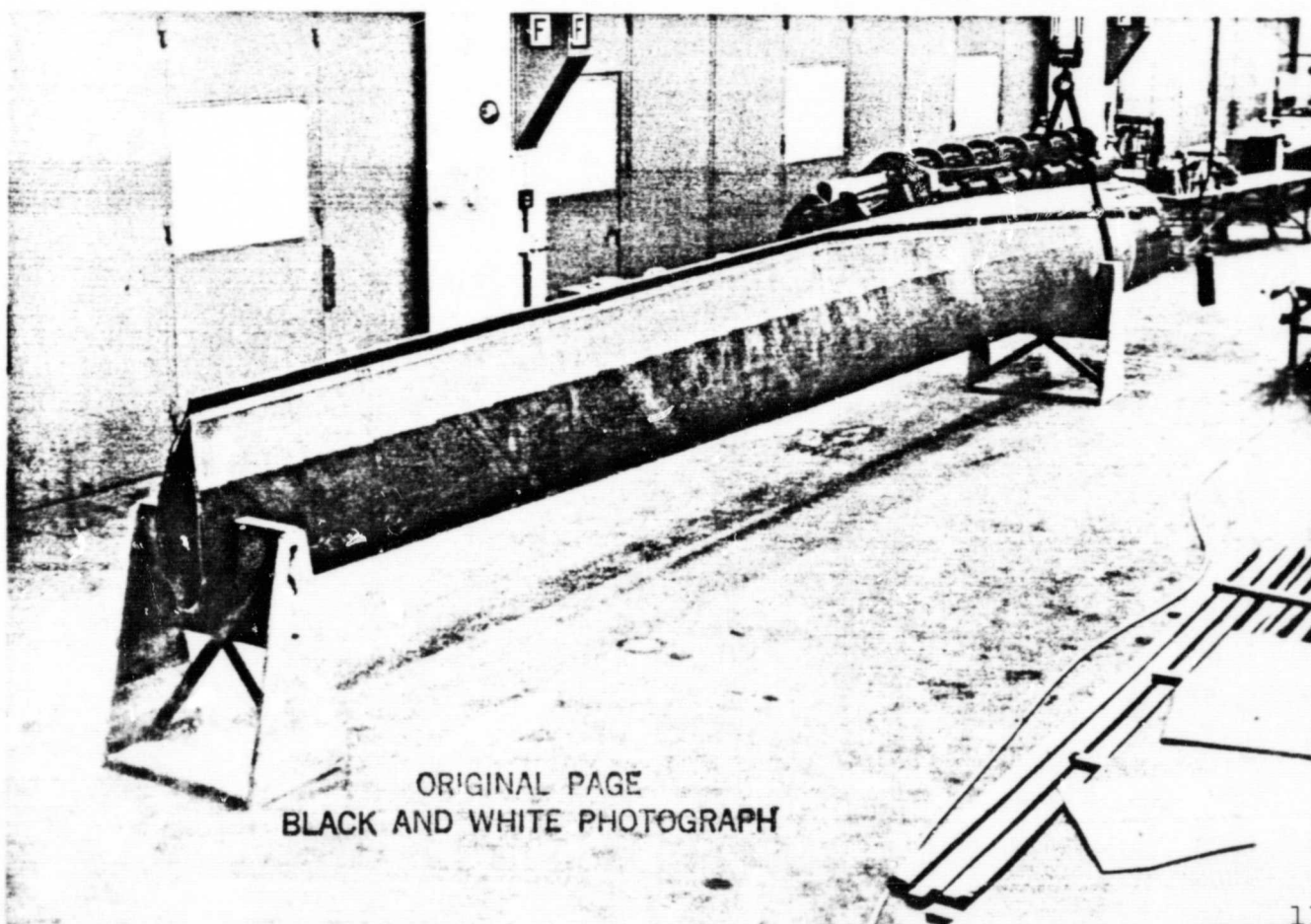


FIGURE 20. DEMOLDING OF A PROTOTYPE PATH SHELL



FIGURES 21 and 22. COMPLETELY GLUED PROTOTYPE



ORIGINAL PAGE  
BLACK AND WHITE PHOTOGRAPH

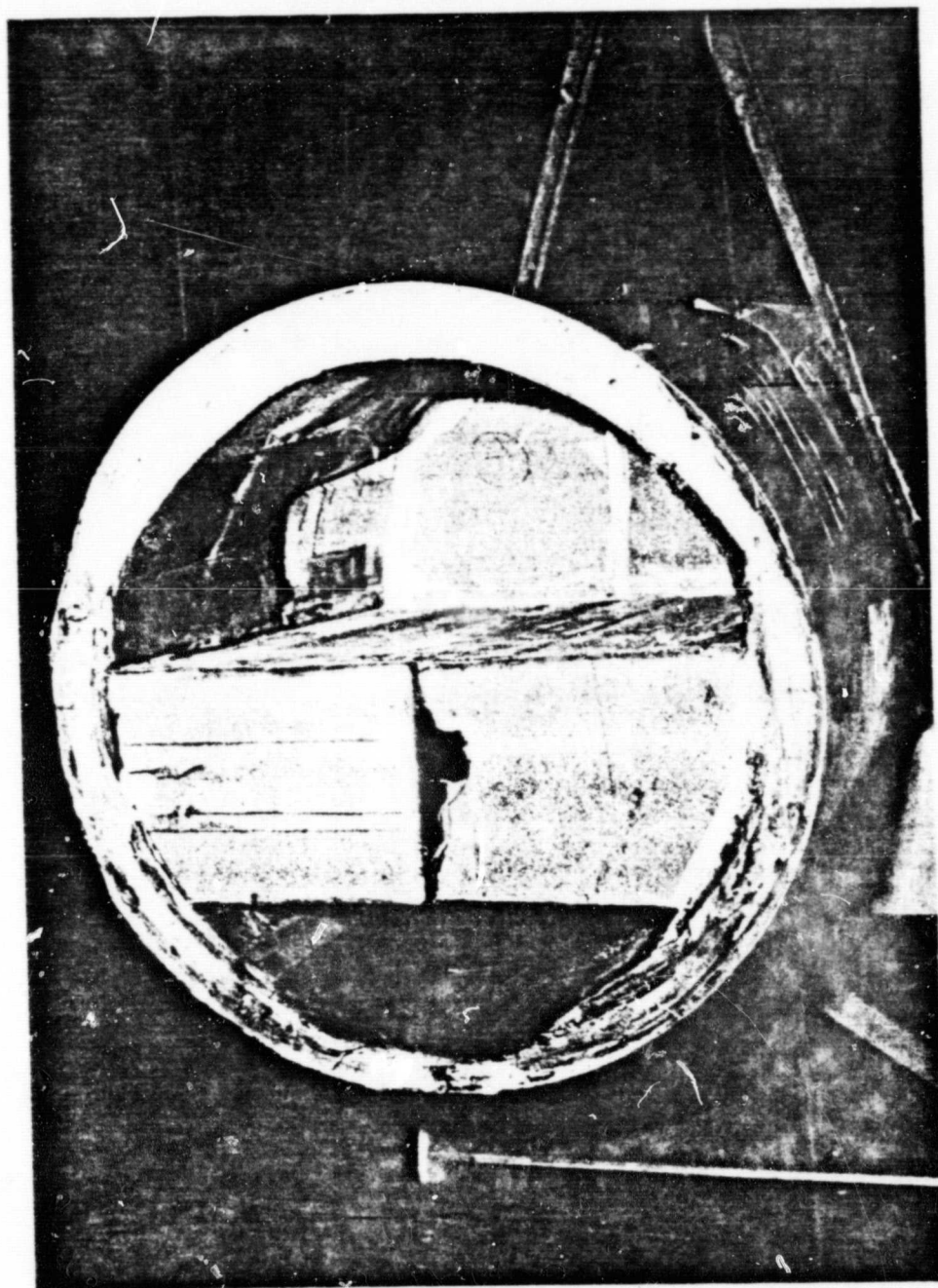


FIGURE 23. ROUGH STATE OF THE BLADE CONNECTION  
SURFACE FOR RADIUS POINT 0.8 m BEFORE CUTTING



ORIGINAL PAGE  
BLACK AND WHITE PHOTOGRAPH

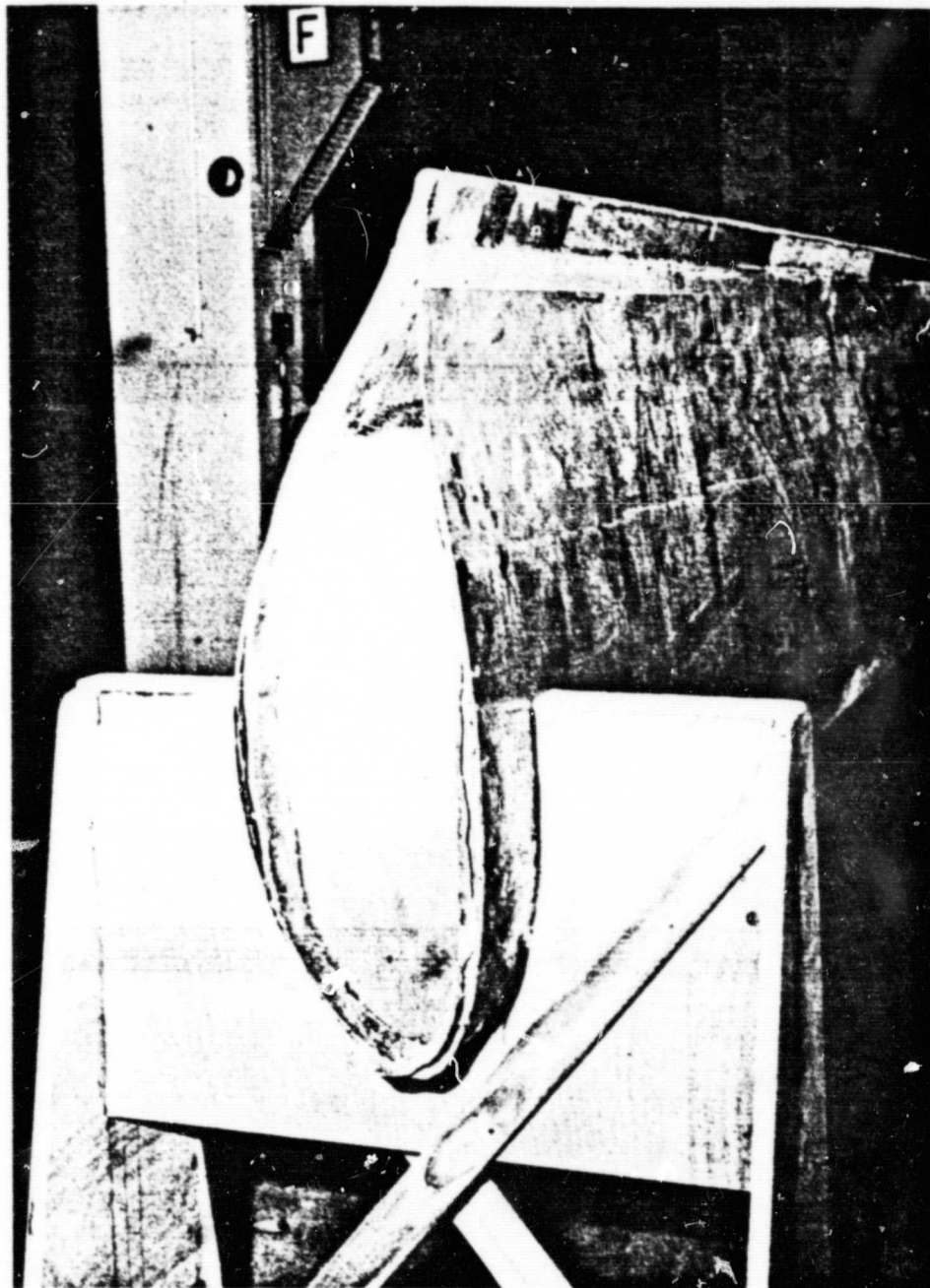


FIGURE 24. ROUGH STATE OF BLADE TIP AT RADIUS  
.11 m (BEFORE INSTALLATION OF THE RIB)

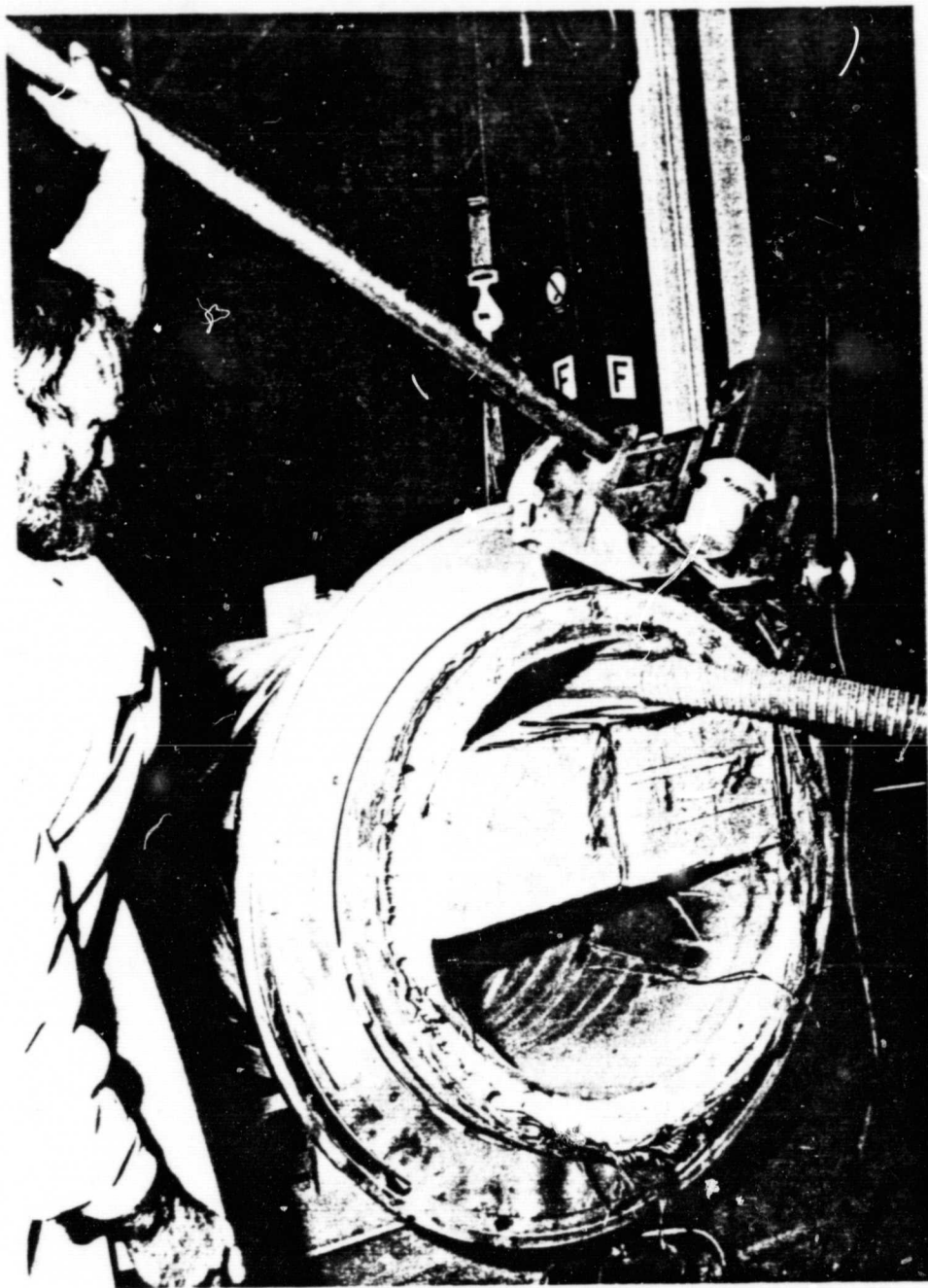


FIGURE 25. CUTTING OF THE CONNECTION CROSS SECTION

ORIGINAL PAGE  
BLACK AND WHITE PHOTOGRAPH

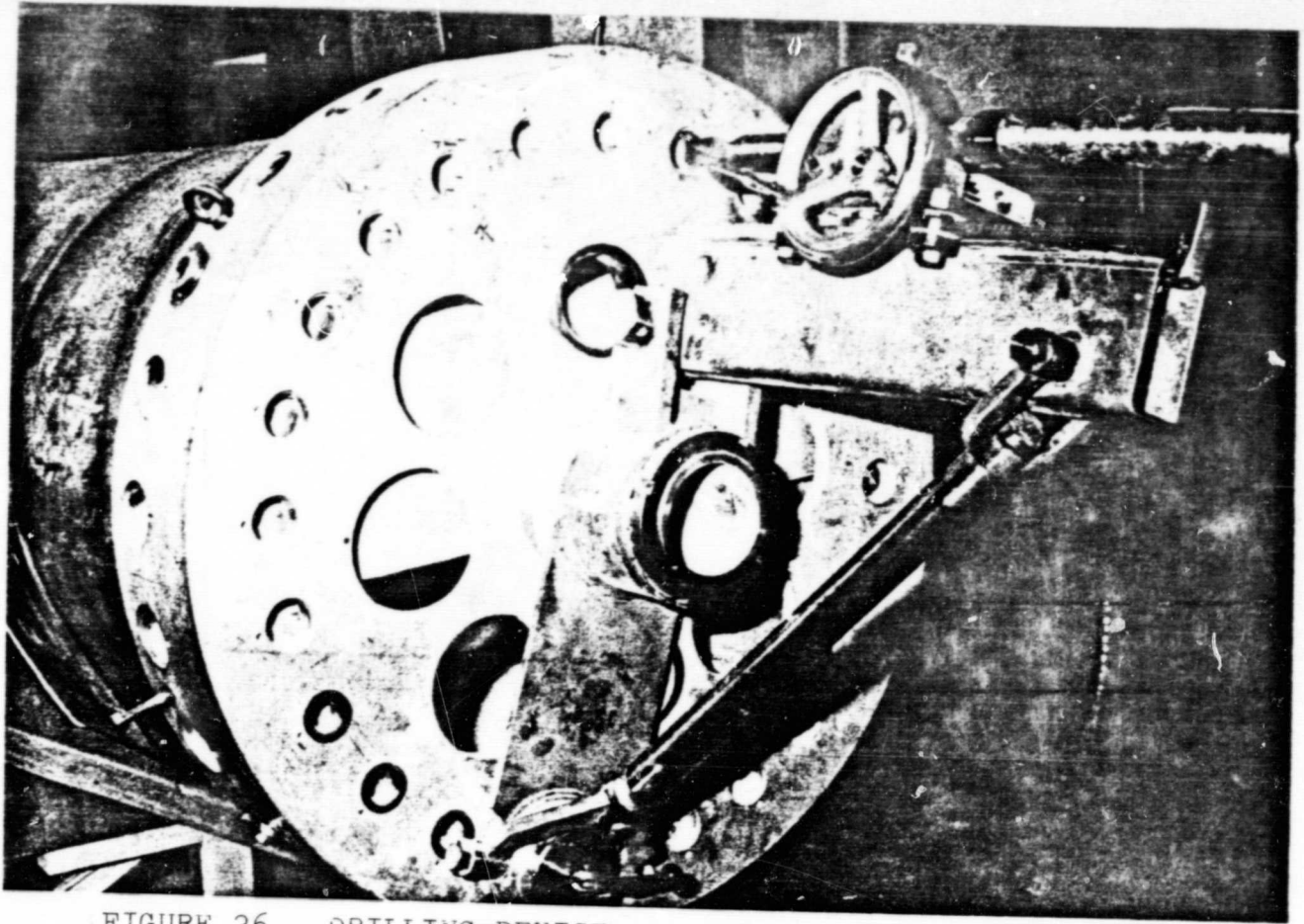


FIGURE 26. DRILLING DEVICE



ORIGINAL PAGE  
BLACK AND WHITE PHOTOGRAPH

FIGURE 27. BORING OF THE SACK HOLES DIAMETER 30

ORIGINAL PAGE  
BLACK AND WHITE PHOTOGRAPH

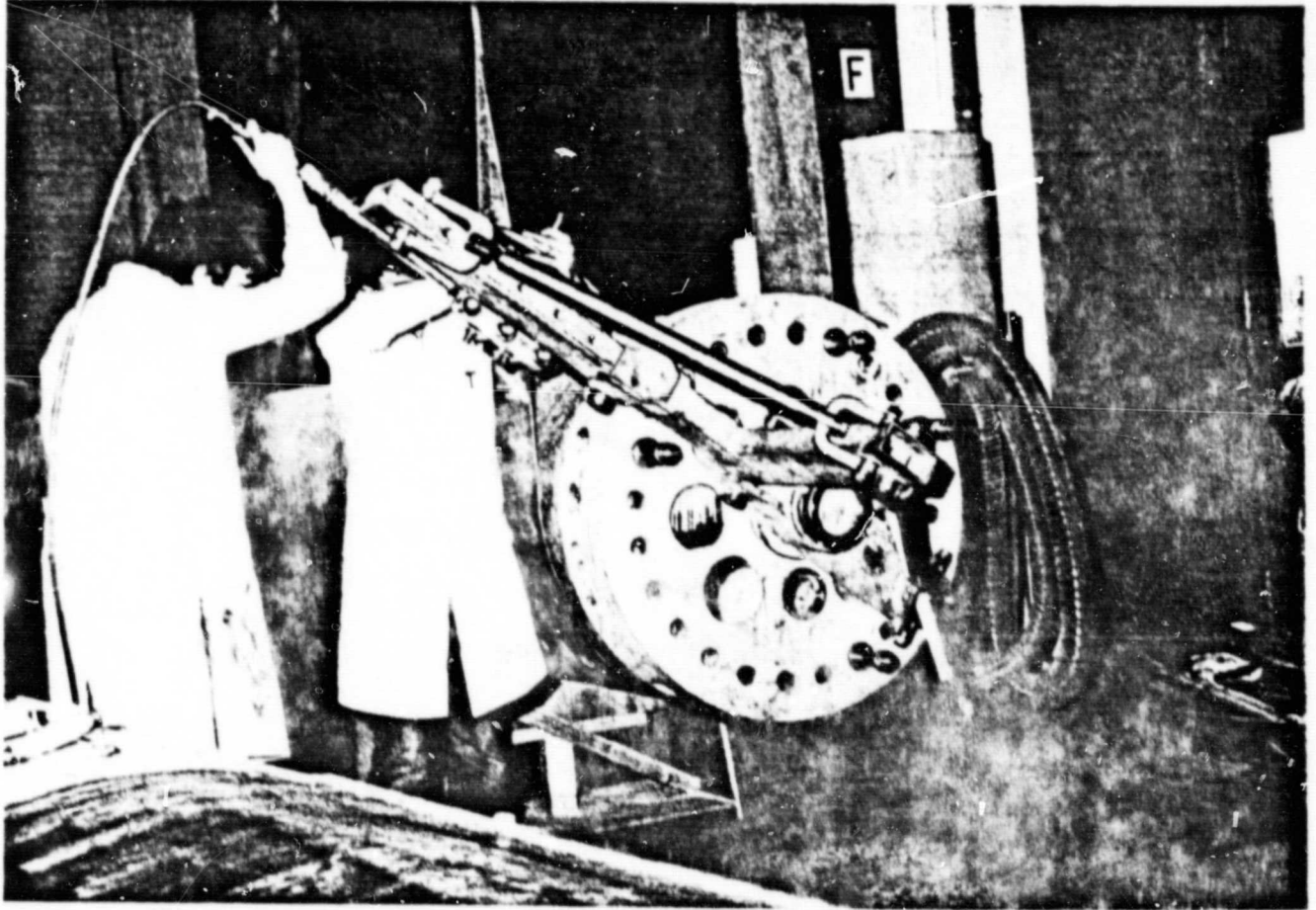


FIGURE 28. DRILLING OF THE TRANSVERSE BOLT HOLE DIAMETER 45



ORIGINAL PAGE  
BLACK AND WHITE PHOTOGRAPH

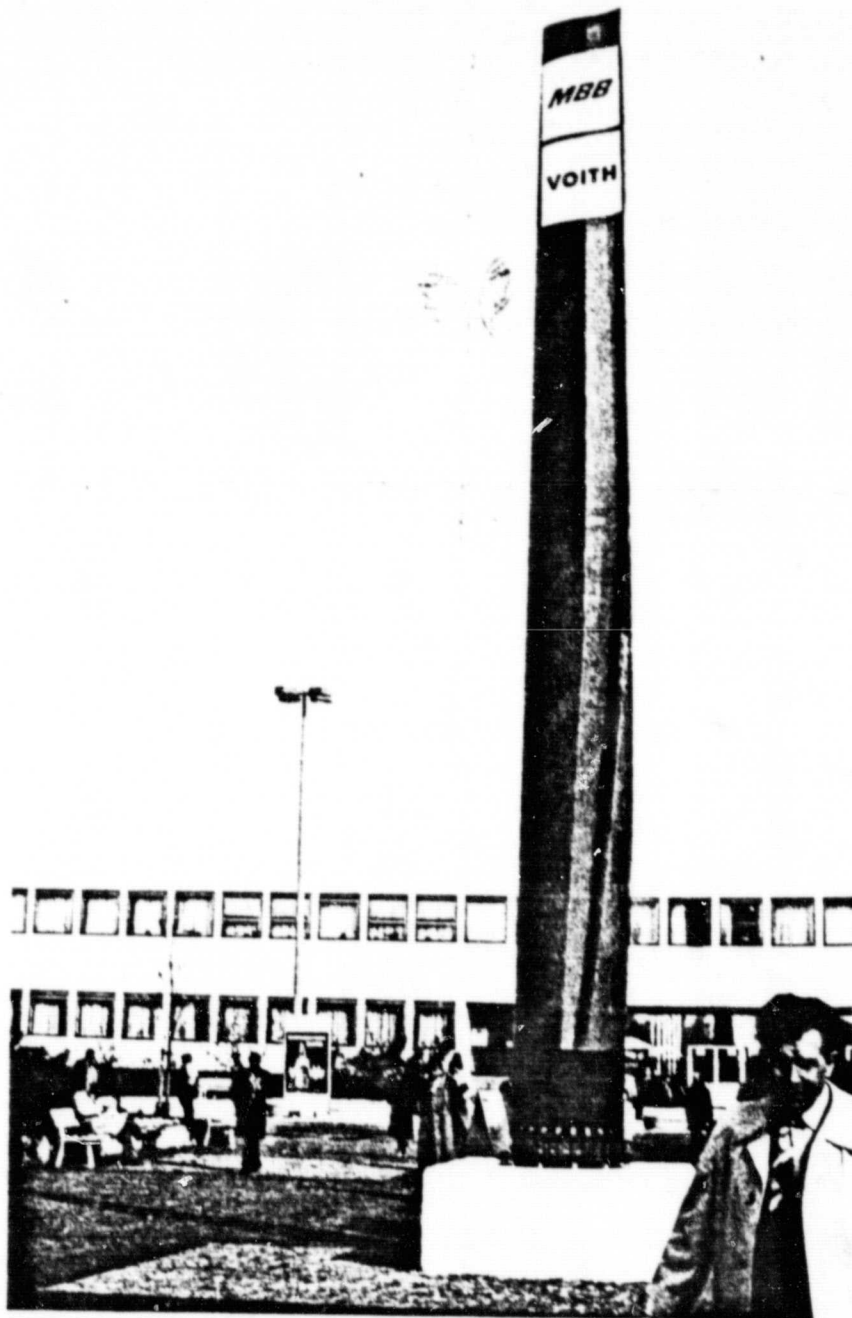


FIGURE 29. PRESENTATION OF PROTOTYPE AT THE  
HANNOVER FAIR 1980.

ORIGINAL PAGE  
BLACK AND WHITE PHOTOGRAPH

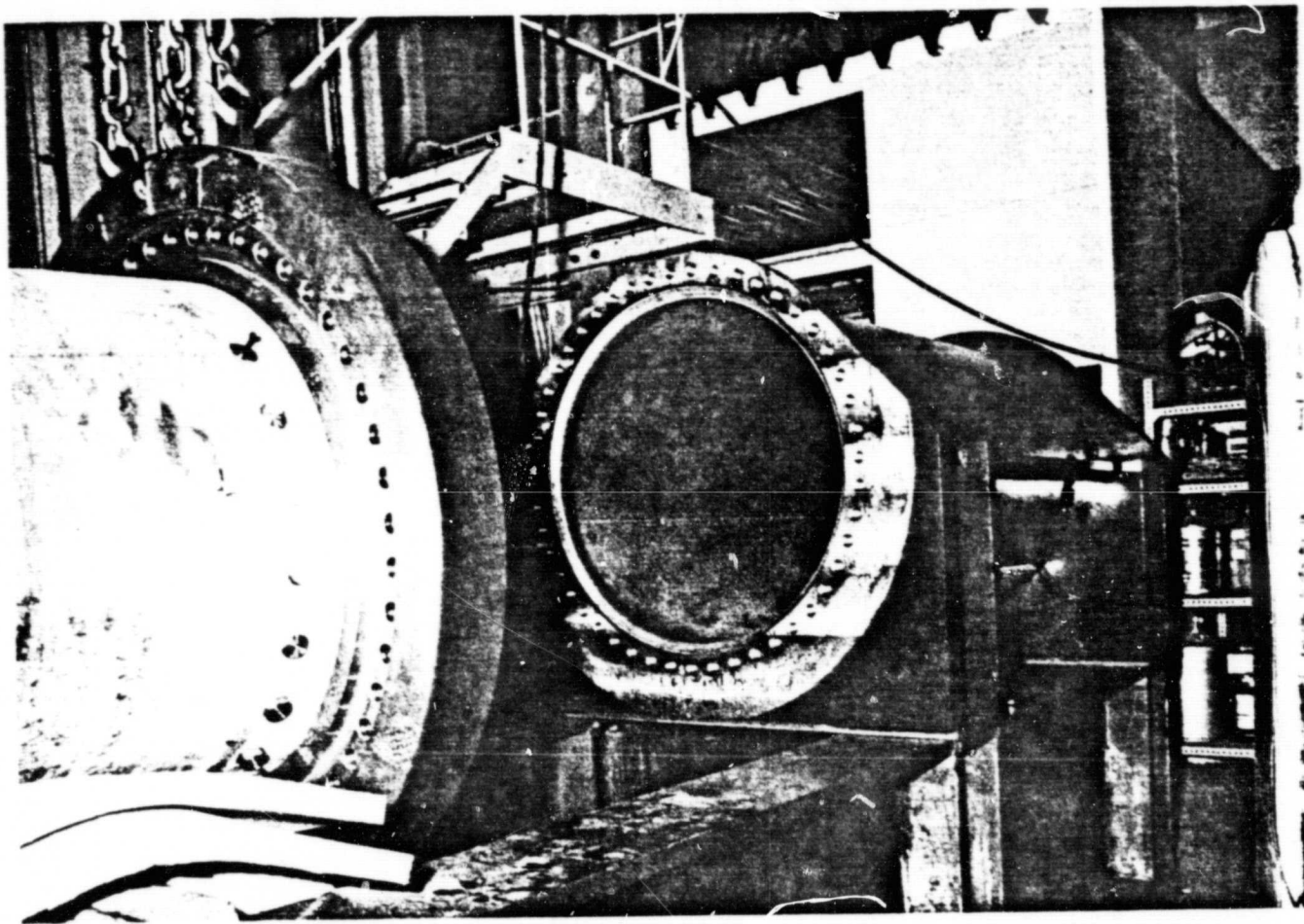
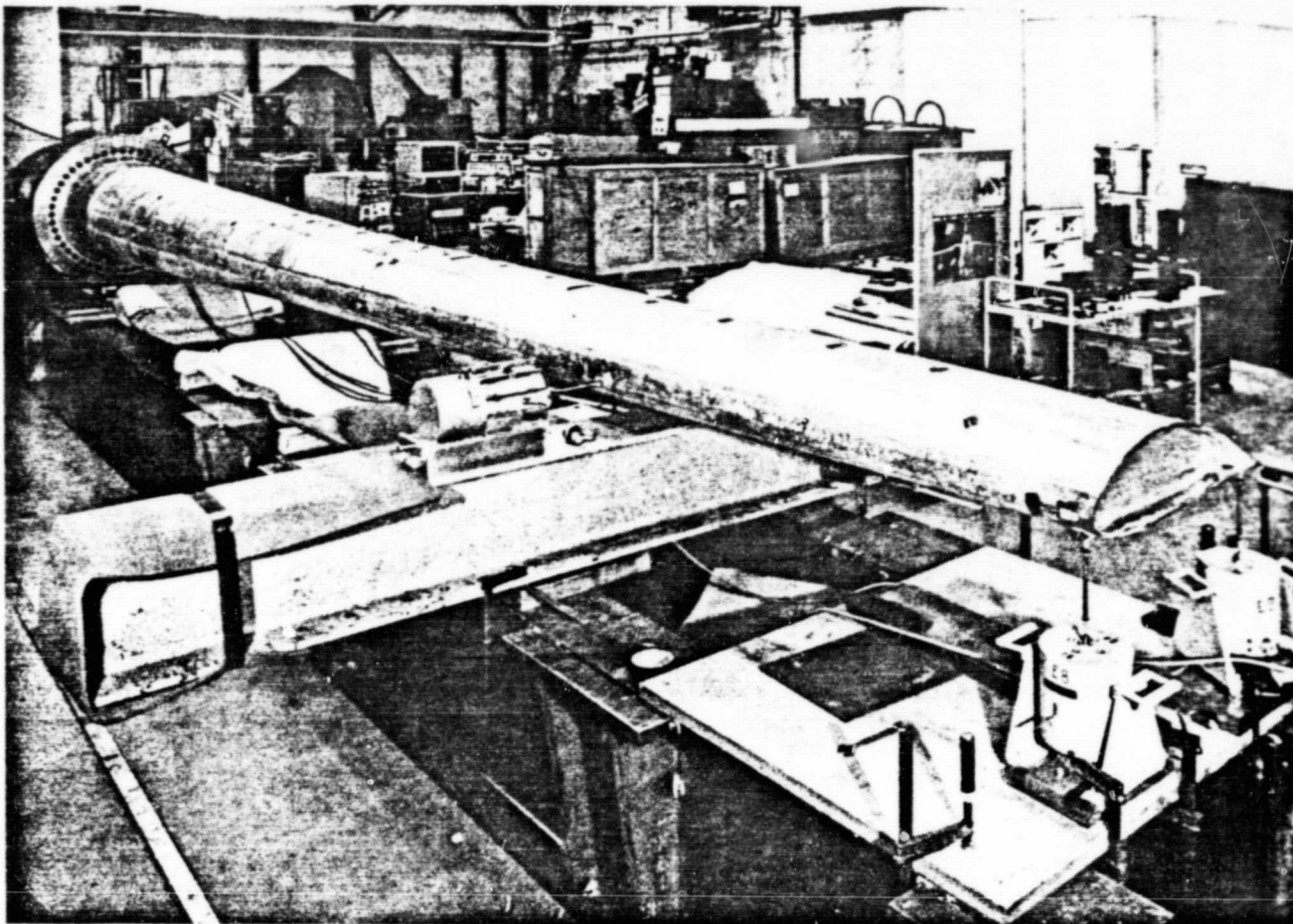
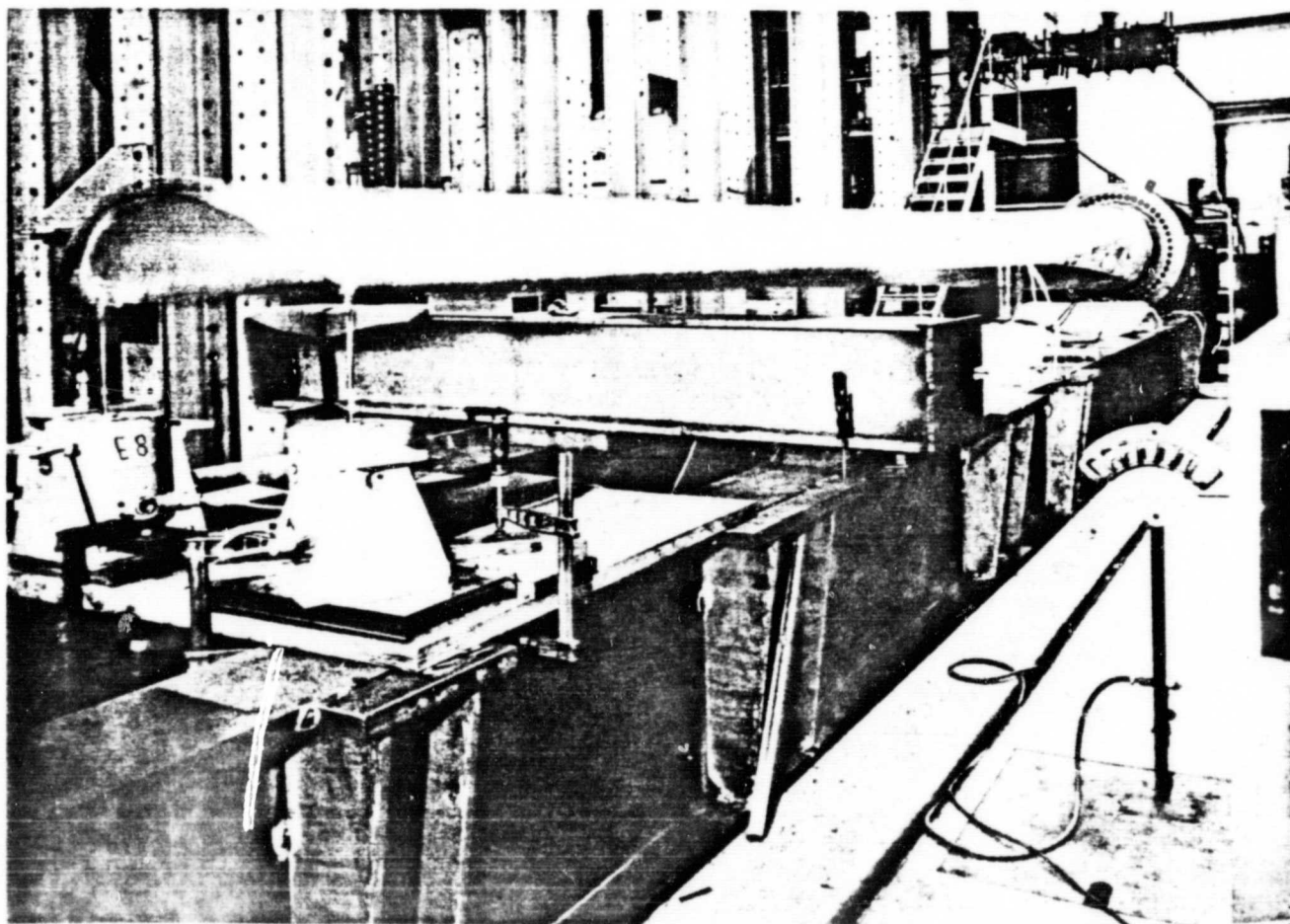


FIGURE 30. FLANGE CONNECTION OF COMPONENTS AND  
COMPONENT TESTING ON THE TEST DEVICE



FIGURES 31 and 32. DYNAMIC TEST

ORIGINAL PAGE  
BLACK AND WHITE PHOTOGRAPH



ORIGINAL PAGE  
BLACK AND WHITE PHOTOGRAPH

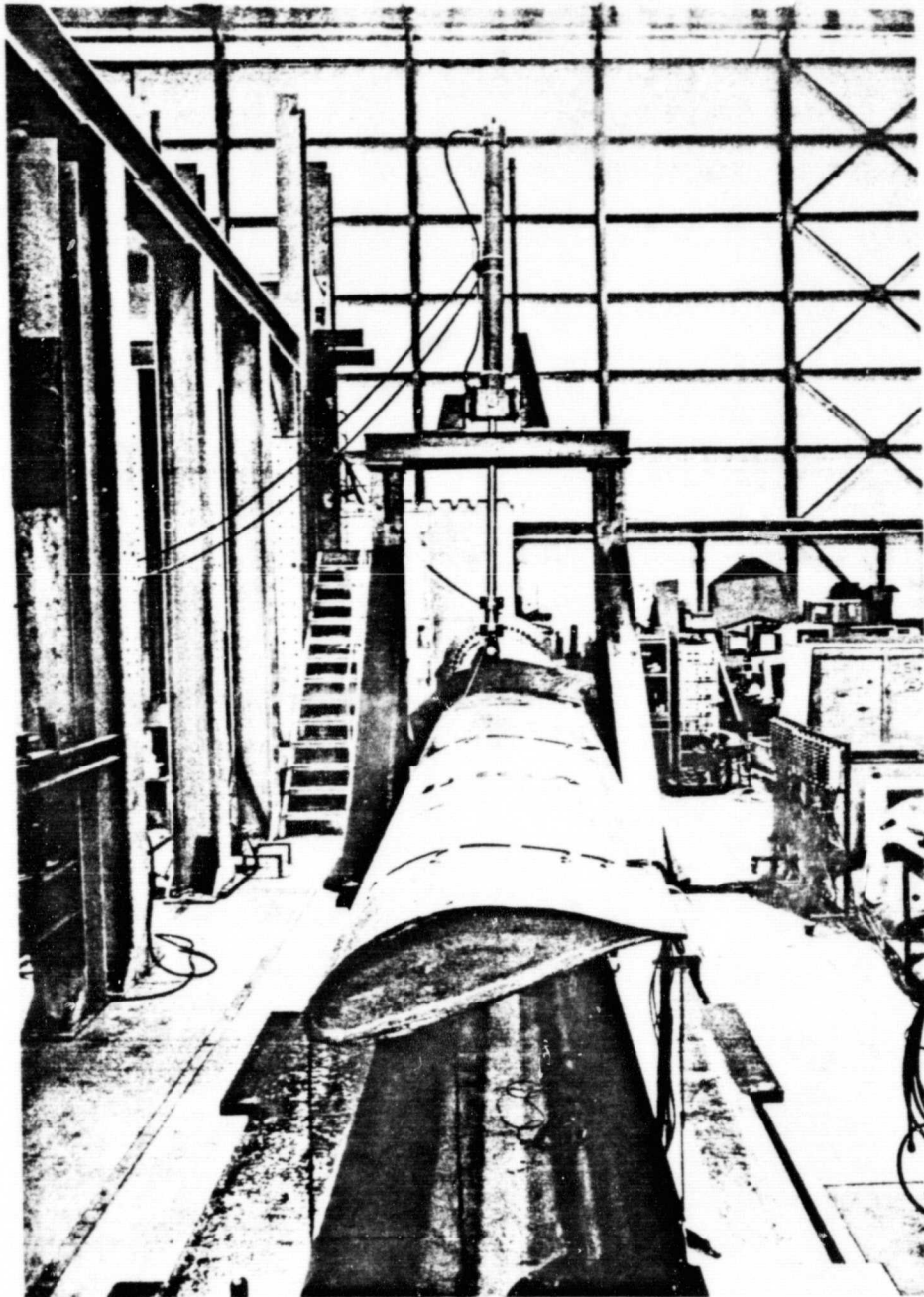


FIGURE 33. STATIC TEST AT  $R = 6\text{m}$





FIGURE 34. LOAD IN THE DEFLECTION DIRECTION  
AT  $R = 10,7 \text{ m}$

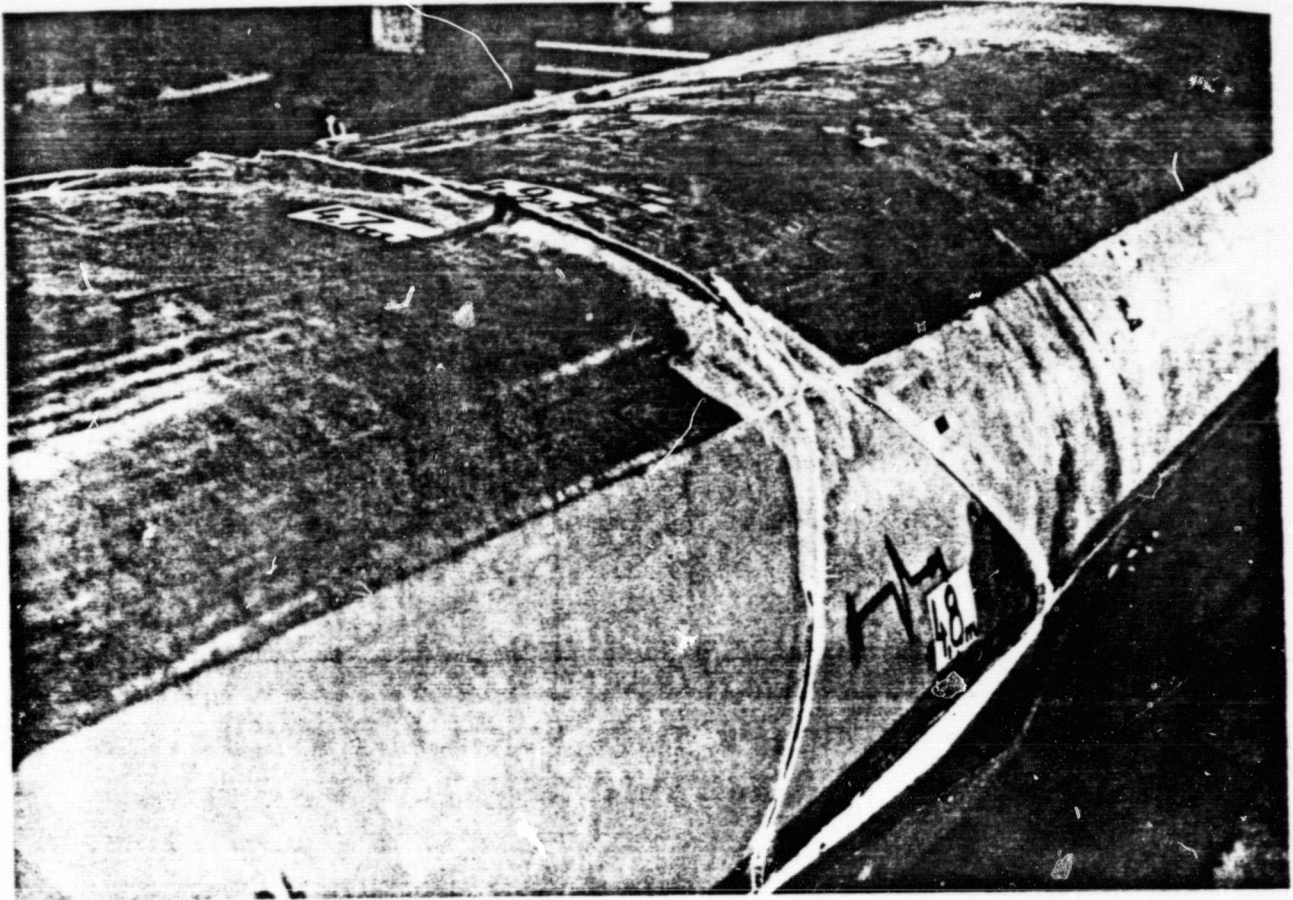
ORIGINAL PAGE  
BLACK AND WHITE PHOTOGRAPH

ORIGINAL PAGE  
BLACK AND WHITE PHOTOGRAPH



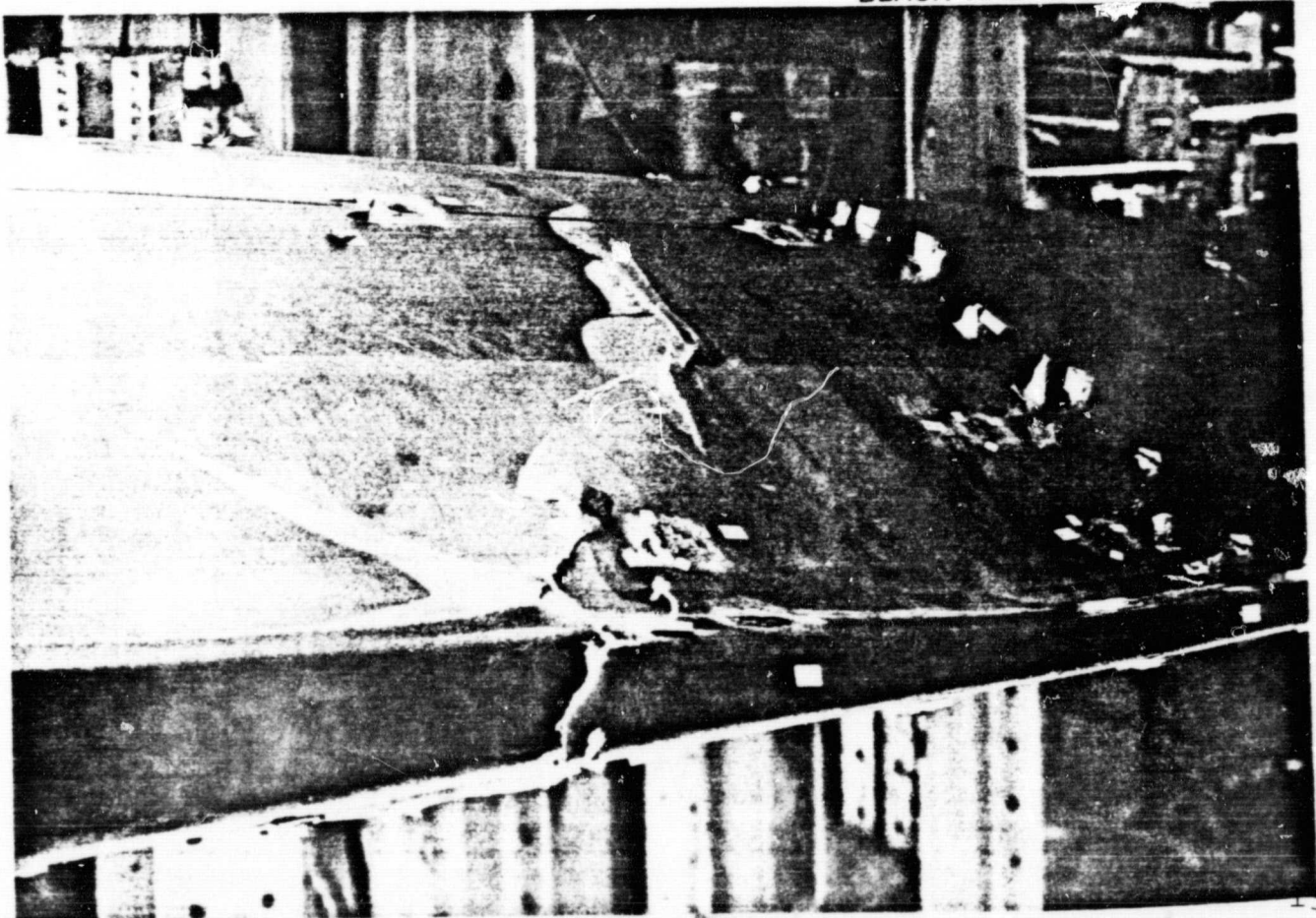
FIGURE 35. FRACTURE TEST





FIGURES 36 and 37. DETAILS OF THE FRACTURE POINT

ORIGINAL PAGE  
BLACK AND WHITE PHOTOGRAPH



ORIGINAL PAGE  
BLACK AND WHITE PHOTOGRAPH



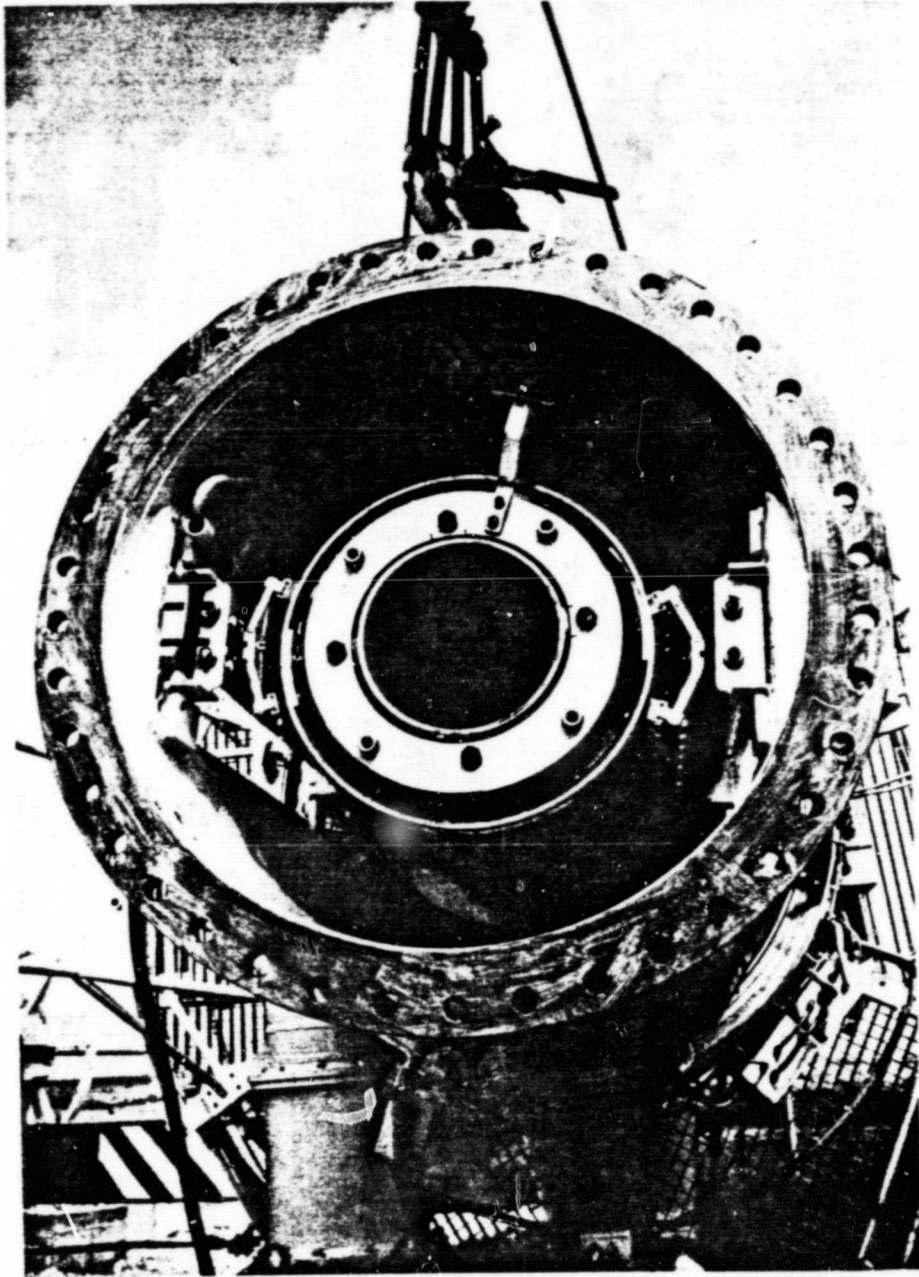
FIGURE 38. FABRICATION OF LAMINATE SHELLS FOR  
26 m BLADE.

Sept. 1981  
 BUILDING SITE OF THE VOITH  
 FACILITY AT STOETTEN  
 (WEST GERMANY)

ORIGINAL PAGE  
 BLACK AND WHITE PHOTOGRAPH



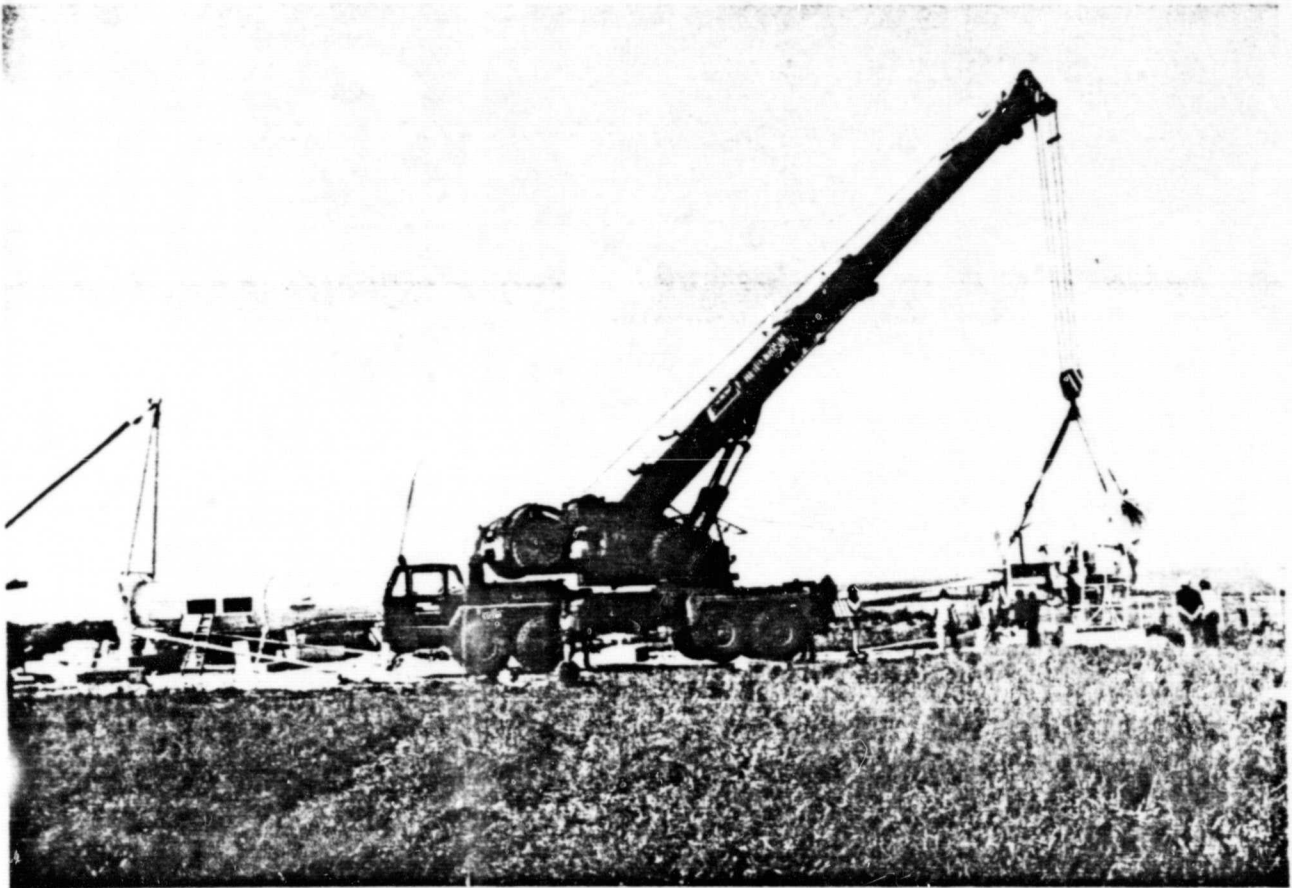
ORIGINAL PAGE  
BLACK AND WHITE PHOTOGRAPH



VIEW OF TOWER HEAD

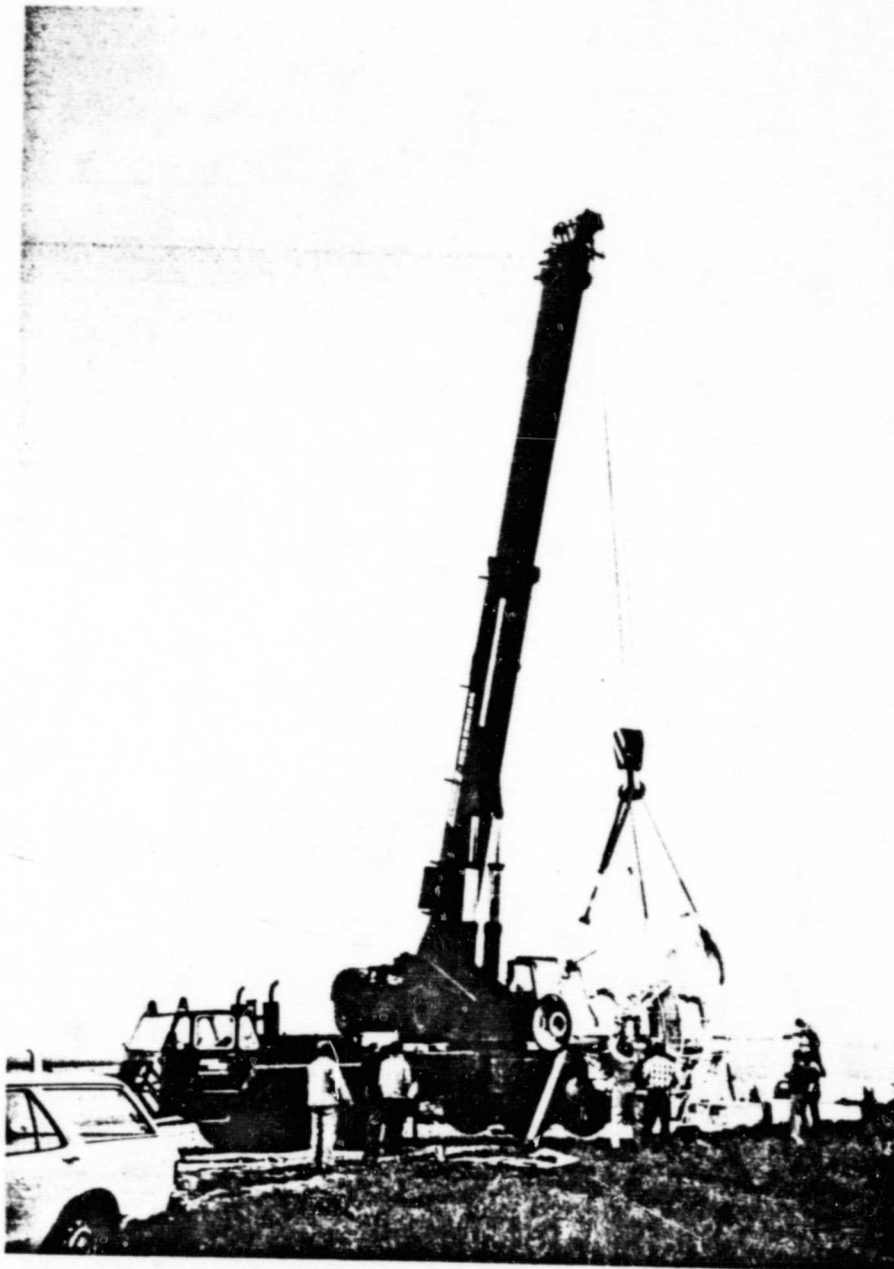


ORIGINAL PAGE  
BLACK AND WHITE PHOTOGRAPH



ROTOR HEAD IS LIFTED TO THE TOWER

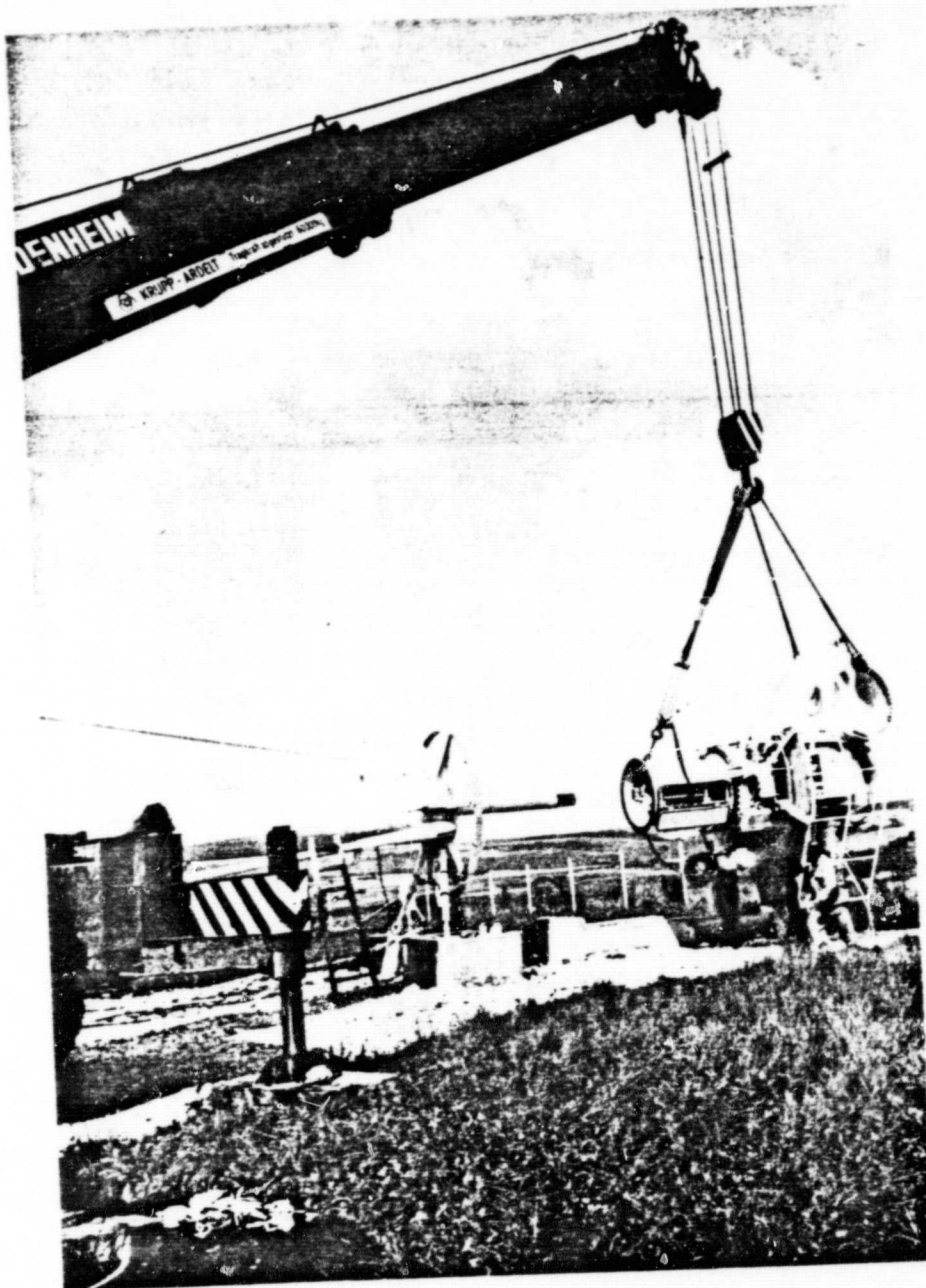
ORIGINAL PAGE  
BLACK AND WHITE PHOTOGRAPH



MOUNTING OF THE ROTOR HEAD TO THE TOWER

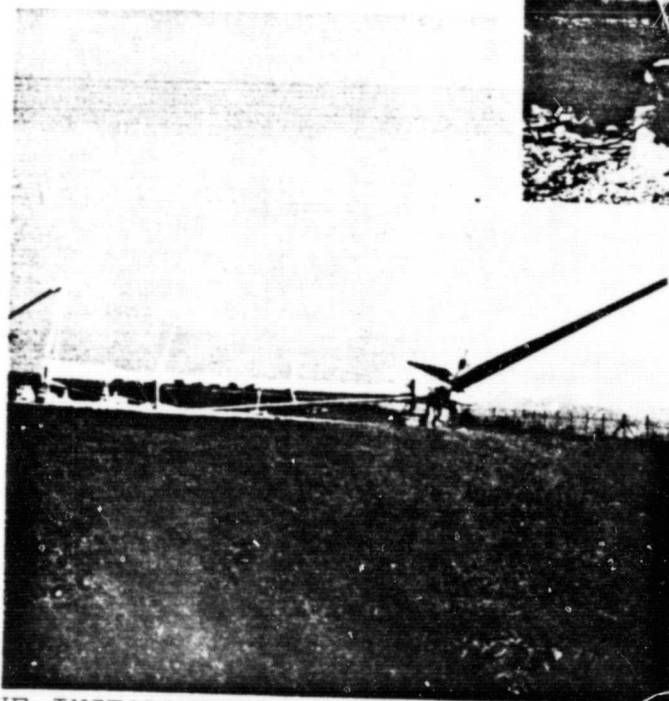
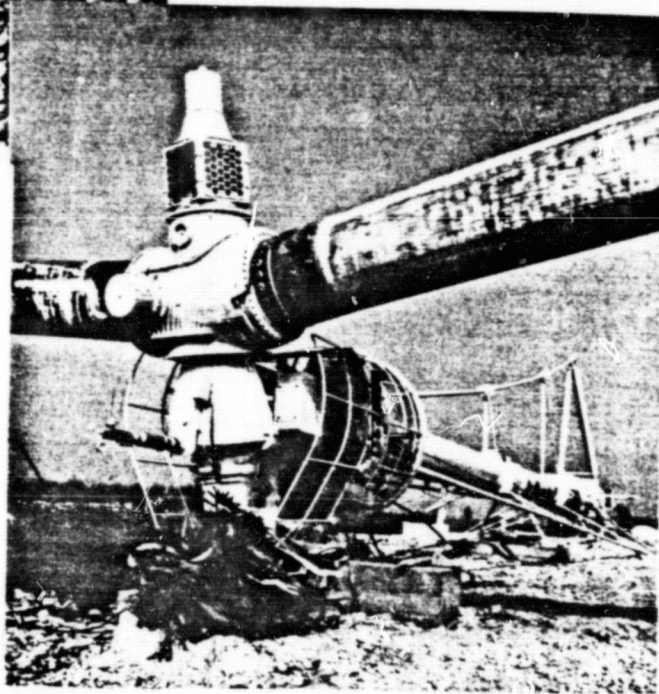
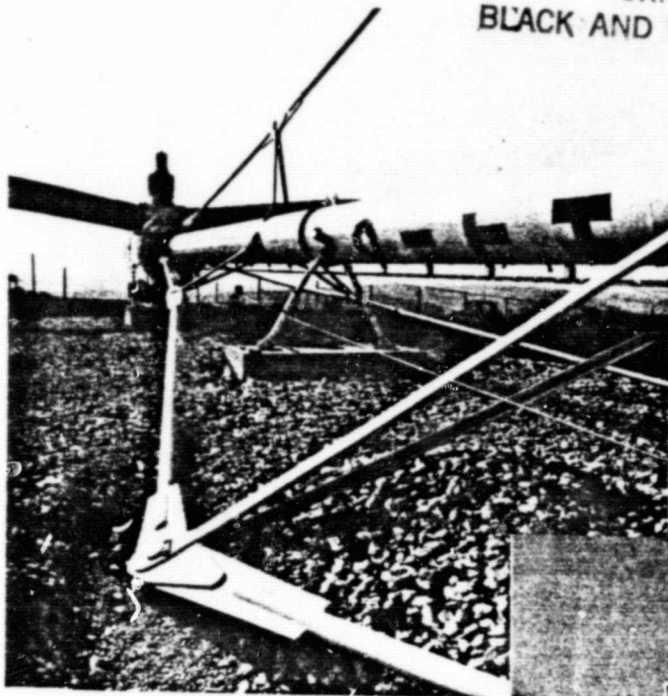


ORIGINAL PAGE  
BLACK AND WHITE PHOTOGRAPH



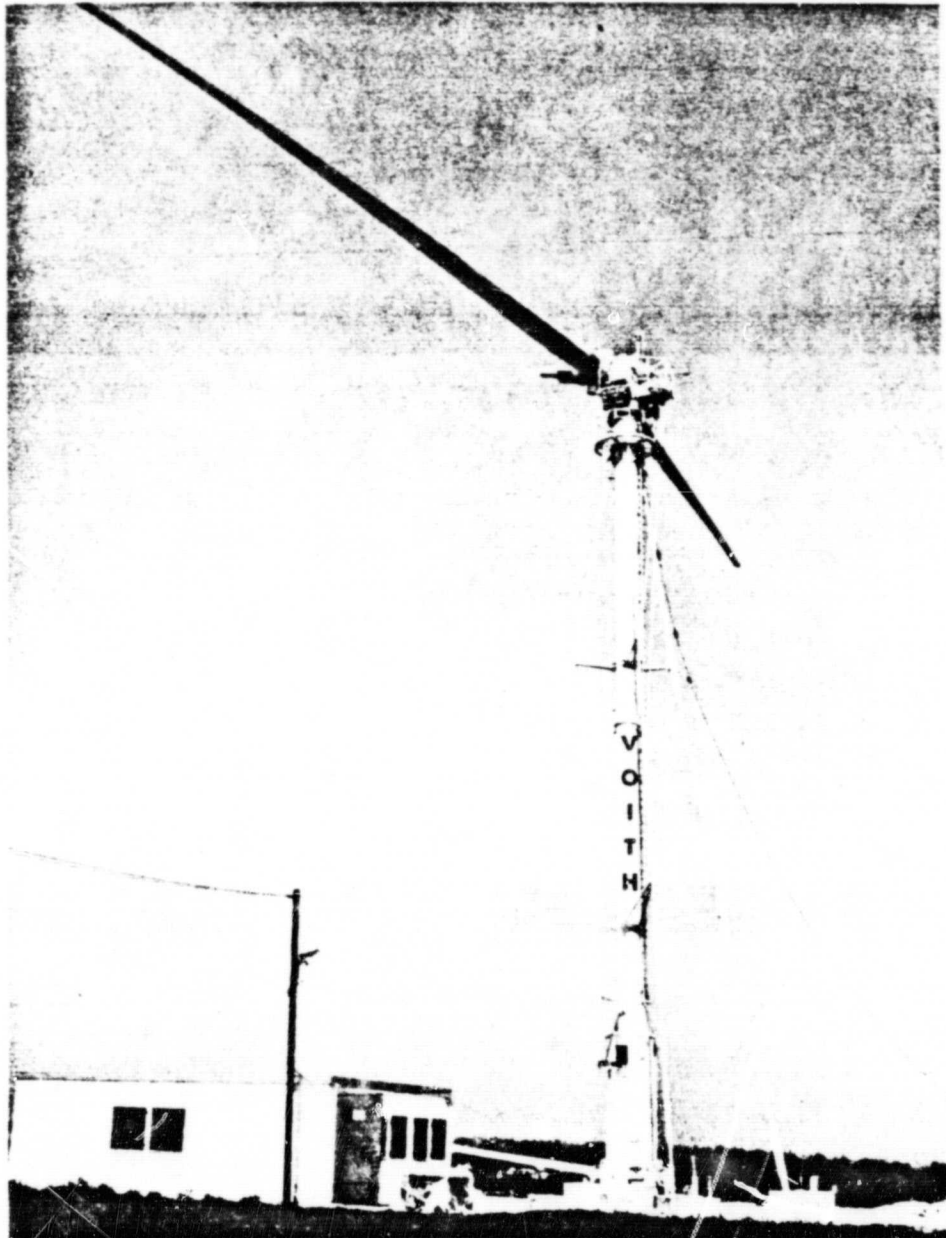
MOUNTING OF THE ROTOR HEAD TO THE TOWER

ORIGINAL PAGE  
BLACK AND WHITE PHOTOGRAPH



THE INSTALLATION IS ASSEMBLED AND CAN BE ERECTED HYDRAULICALLY.

ORIGINAL PAGE  
BLACK AND WHITE PHOTOGRAPH



THE FACILITY IS ERECTED.

**EXTENSIVE PROJECT CONTROL OF PROJECT ON THE MANUFACTURING  
DEVELOPMENT, BUILDING AND TESTING OF THE GROWIAN ROTOR  
BLADES ( ET 4223 A)**

/131

Project No. ET 4323 B

R. Lehmhus\*

1. Goal

The goal of the contract is to develop an ordered sequence for the work performed under the project "Production development, building and testing of the Growian rotor blade".

2. Work program

Examination of calculations, specification drawings of the rotor blades:

1. Evaluation and control of testing of design calculation drawings.
2. Production supervision of the rotor blades and testing during manufacturing.
3. Monitoring of the testing program for investigating a test blade.

3. Status

Item 1)

The building specifications, calculation data, construction data and production data for the steel spar of the rotor blade prototype presented by MAN were examined. An operational strength calculation (MAN) was not yet available. However, discussions were carried out about the way in which the operating strength demonstration would be implemented.

---

\* Project no. ET 4323 B

The data submitted up to the present by the MAN firm were primarily design data. MAN states that it can only present the final data during the first half year 1981 which will be the subject for evaluations.

The previously submitted strength demonstrations essentially agree with the results of our own FE investigations. Our calculations, however, show that in the range  $R = 35 \text{ m}$  (transition from transverse stiffening unit of the spar to longitudinal stiffening member) one would expect locally limited and impermissible stress excesses. At the present time it is assumed that these can be reduced to an unacceptable level by design changes.

Item 2)

/133

The production of the prototype steel spar at the Gustavsborg plant of MAN was examined by supervisors of the German Lloyd firm as regards material used, individual part manufacturing, assembling including welding work and evaluation of the results of the welding seam inspections, using random samples.

With one exception, the case of the welding weld at Hetebrueg, no important discrepancies in the steel spar were found as concerns the execution of the design.

/134

Item 3)

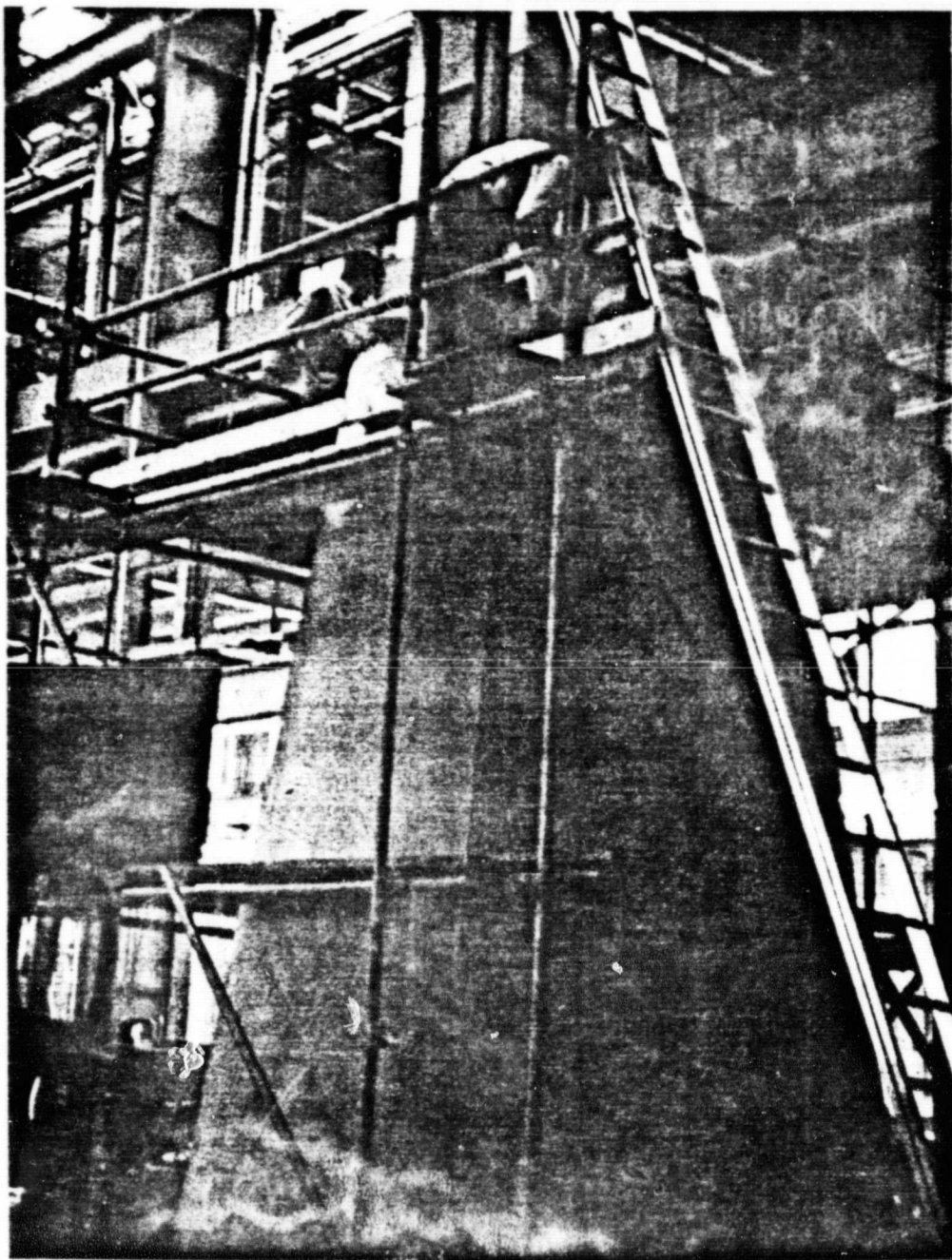
We expect the testing of the prototype blade at IABG Munich not before the second quarter 1981 according to the present plan of MAN. At the present time, we have reviewed the preliminary planning data for carrying out tests.

- Problems which occur

The development of data which can be used for examination by the MAN firm has involved substantial time delays in the advance of the

ORIGINAL PAGE  
BLACK AND WHITE PHOTOGRAPH

/133



Blade bearing tip for test blade at the MAN-Werk Nuernberg. Mr. Hetebrueg of Germanischen Lloyd is measuring the upper diameter of the several meters long bearing and its deviation from circular shape ( $2050 \pm 0.5$ ) mm. December 4, 1980

(Photograph: R. Windheim)



production of the prototype blade. The MAN firm was told that possible consequences of this may have to be borne by MAN.

- Deadline situation

According to our license, the project running time extends from November 13, 1979 to April 30, 1981. Since this project represents a task which accompanies FE work at the MAN firm (ET 4323 A), we can only perform our part of the project on time if the MAN firm holds to the schedule. At the end of 1980, it is clear that the MAN firm cannot maintain the planned schedule for their task.

/135

DEVELOPMENT OF A MEASUREMENT TEST  
PROGRAM FOR GROWIAN\*

Friedrich Koerber

CONTENT

/136

1. Summary
2. Classification of measurement program
3. Previous measurement programs
4. Purpose of GROWIAN measurement program
5. Tasks of the measurement program
6. Variables of interest
7. Measurement points
8. Measurement philosophy
9. Data recording and processing systems
10. Data evaluation

7 figures

---

\* ET 4364 A

## 1. SUMMARY

Under the title "Development of a measurement and test program for GROWIAN", at the end of 1979 a contract was awarded to the MAN-NEUE TECHNOLOGIE firm to develop a program for test operations for the GROWIAN wind energy facility in the planning stage.

The present report discusses the measurement program and shows solutions.

The main topics of the measurement program include the identification of the facility behavior, verification of the facility concept including models and the collection of operational experience with large wind energy facilities. Primarily, we are interested in the action of the environment and the reaction of the facility based on properties. The data selection and processing required for the work is suggested.

The purpose of the measurement program is to obtain knowledge with which technical problems of large wind force facilities and their economy can be better evaluated.

The ET 4364 A project includes a complete measurement program. The extent had to be restricted in order to save costs. The basic ideas of the program however remain unaffected.

/138

For simplicity, we will call the Growian measurement and test program simply the measurement program in the following.

## 2. CLASSIFICATION OF MEASUREMENT PROGRAM

Figure 1 shows the situation.

For the first phase of the overall project of the large Growian wind energy facility, there was included the development of "data ready for production".

ORIGINAL PAGE IS  
OF POOR QUALITY

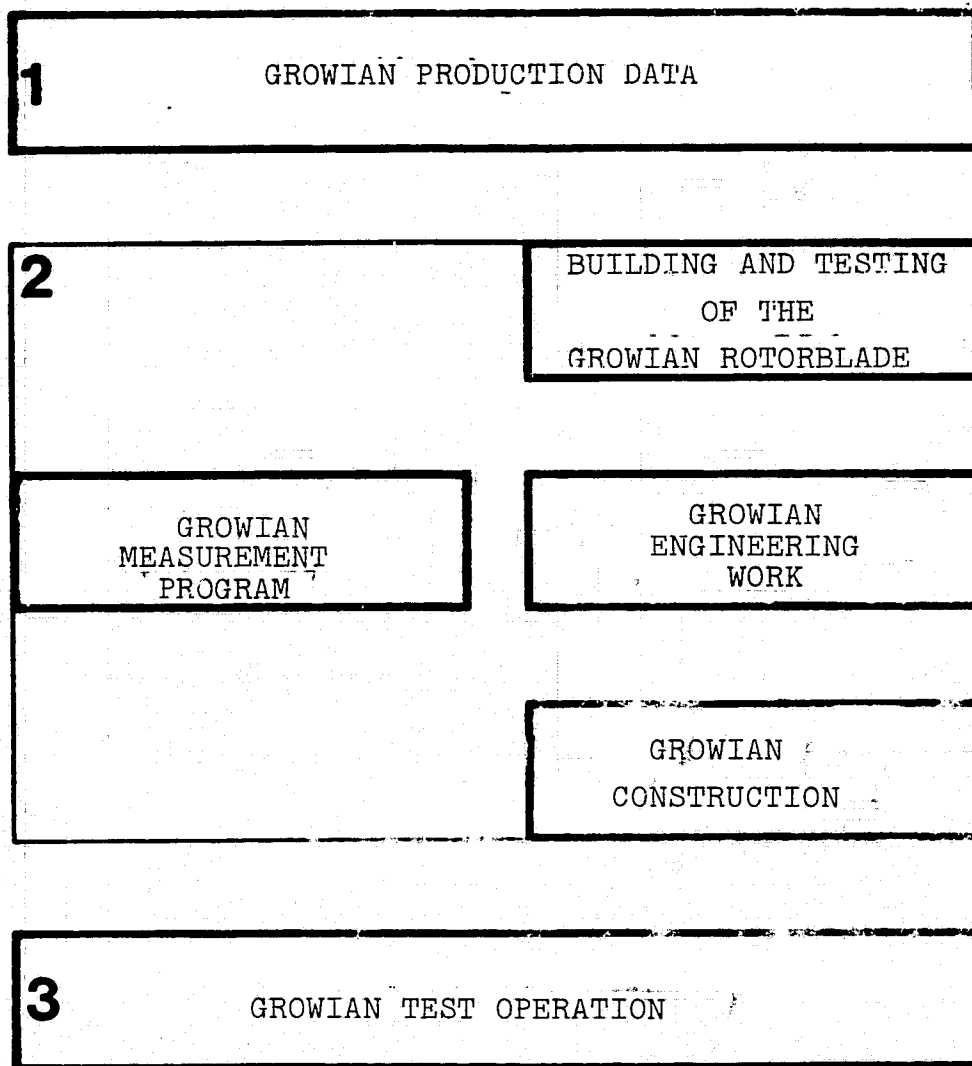


FIGURE 1. GROWIAN ACTIVITIES

At the present time the second phase is being implemented with the realization of the facility. In parallel with this, there is the development of a measurement and test program for Growian. In the next step, the measurement installation has to be integrated during construction. The measurement program specifies which measurement types are to be carried out and where certain measurements are to be performed at various points of the facility. We discuss the recording, processing and evaluation of the data.

In the third section we will discuss a multiyear measurement and test period, the purpose of which is to collect operational experience with a large wind energy facility. We will examine assumptions and will expand the state of the art in the calculation and design of large facilities.

### 3. PREVIOUS MEASUREMENT PROGRAMS AND WIND FORCE FACILITIES

The review of previous work must precede any new task.

Facilities with the size of the Growian project are only in their beginning stages. From the power level point of view, the American facility MOD-1 with 2 MW is the closest to the Growian. The first machine started in the summer of 1979 in Boone NC. At the present time the first measurement results are being published. For the most part they confirm the calculations of the design of the wind mill located there. Extensive data are available about the MOD-0 facilities (100/ 139 200 kW) in the USA which have been tested since 1975. However, their power level is less than 10% of that for Growian. Nevertheless, measurement procedures and results are a point of reference for the planned German project.

Extensive measurements exist for the 20 year old Gedser wind mill (200 kW). A measurement program started with two other new Danish wind mills (650 kW) and results are already available. Also measurement activity has started at the TVIND wind mill.

Finally, we should mention experience which was selected during the 60's on the 100 kW wind generation facility of the Wind Force Study Association as well as work in Sweden and Holland.

Summarizing, we have to point out that detailed investigation results are primarily available from smaller facilities and can only be transferred to a facility of the size of the Growian with reservation. This is especially true for determining the wind conditions, the component loads and the operational behavior of the wind generation facility. The state of the art cannot give any information about the long time quality of wind energy or the composite operation of wind generation facilities for producing electrical power.

#### 4. PURPOSE OF THE GROWIAN MEASUREMENT PROGRAM

It is the purpose of the measurement program to obtain information which will allow the understanding of the technical problems which then should lead to better solutions. This is both true for the selected Growian design as well as for basic boundary conditions of wind energy exploitation. For example, wind properties or facility types. Together with the operational experience with the prototype facility during test operation, we wish to obtain information about the economy of the wind flow from individual facilities and wind generation parks. /140

A number of steps will have to be followed in order to obtain these goals. Figure 2 shows some of them. In the design and construction of the Growian, assumptions and models have to be used. The first goal is therefore to verify the models. This means that the operational facility has to be identified so that its realistic properties become known. This then has to be compared with the assumptions and corrections have to be introduced. One would expect that, due to lack of information, several influences cannot or were not sufficiently modeled. As an example, we should mention the only approximately known damping property of the facility structure or its effect on loads. Also there is the influence of gust increase and decay times. They are important influences on the dynamics and would therefore have to be included in a load analysis

IDENTIFICATION OF GROWIAN PROPERTIES  
VERIFICATION OF MODELS  
CLARIFICATION OF ACTION OF THE ENVIRONMENT AND  
REACTION OF THE FACILITY  
TESTING OF THE DESIGN  
TESTING OF CONSTRUCTION DESIGNS  
COLLECTION OF OPERATIONAL DATA  
DEMONSTRATION OF LARGE SCALE USABILITY OF WIND ENERGY  
INFORMATION ON ECONOMY  
IMPROVEMENT OF FUTURE MACHINES  
OBTAINING ADDITIONAL DATA

FIGURE 2. PURPOSE OF THE MEASUREMENT PROGRAM



for the installation components.

Therefore, the model has to be refined so that effects not accurately represented in the model can be included. For example, this includes rotor instabilities or the realistic effect of the tower wind shadow. This influences the power yield and, therefore, occurs as an exciting element for oscillations of the overall systems.

The measurement program is tailored to offer generalization of models, a trend which is developing. Comparison of model calculations and measurement results is, therefore, supposed to lead to a non-refined model which then will be used to give rough estimates of future machines. This model will have to be free of unnecessary ballast and will have a low amount of input information.

#### 5. PURPOSES OF THE MEASUREMENT PROGRAM

The purpose of the measurement program defines the problems it will solve. During the Growian test operation, a number of test series will be performed. The measurement program plans and coordinates multiyear investigations by defining tasks and procedures.

/141

Growian was conceived as a standard unit of a wind energy facility. Its function as a measurement carrier during test operation means it is necessary to tailor the design to the requirements of measurement technology. This results in design changes which have to be traded off with the overall design.

The measurement plans for the individual parameters are the most extensive part of the measurement program:

- wind conditions
- facility power output
- facility kinematics and dynamics
- loads
- behavior of electrical system
- operational control
- emission and immission

A large number of data are obtained during the measurement programs. Therefore, it is also necessary to develop a concept of data recording, processing, storage and evaluation. Finally, a test and measurement catalog will be developed with which the test can be performed.

## 6. PARAMETERS OF INTEREST

The engineers are interested in the following three quantities of a wind energy facility:

- power - loads - emission

Once these are known, it is possible to develop the information required from the measurement program.

/142

Due to the action of the environment and system properties, one then can develop the parameters of the Growian reaction. Figure 3 shows this relationship and the arrows indicate the directions.

On the left column we show the contact points of Growian and the environment. For the most part we understand by this the action of the wind and the action of the network to which Growian supplies power.

The wind is most easily described by means of its velocity vector. Its absolute magnitude and direction change at a fixed point over time. In addition, the velocity vector at a fixed time changes greatly as a function of position. The wind field changes, therefore, in three space dimensions and in the time dimension. Work previously carried out under the Growian project again always showed that the wind field and its time change is a large and uncomfortable unknown which becomes very important considering the size of the facility. The measurement program, therefore, stresses this point.

The connection of the wind driven generator to the available medium voltage electrical network is another important point of contact of the facility. During normal operation, there are strict requirements for

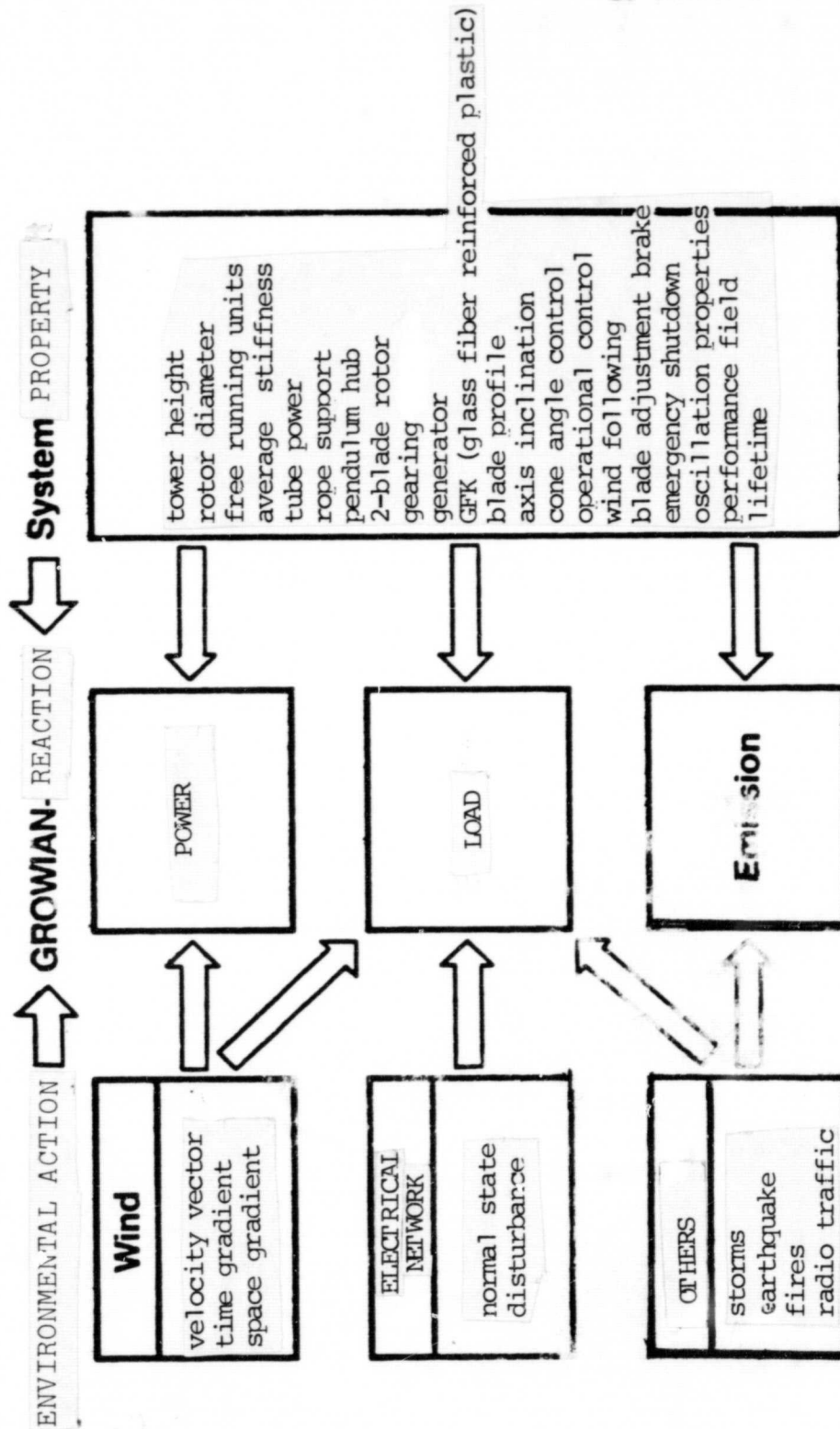


FIGURE 3. ACTION AND REACTION

the quality of the energy delivered: constant frequency, uniform power, low higher harmonic component. During disturbances in the net, a state is required from the facility which will allow resynchronization in an orderly manner. On the other hand, in the case of frequent net disturbances and, therefore, sudden removal of the load, which especially occurs during storms, must not be endangered. The network is very important because the usability of the large wind energy converters during joint operation depends greatly on the way in which it is connected to the network, especially during critical network states.

Influences of the environment have to be experienced and this will especially include natural influences.

Let us again refer to Figure 3 and consider the left side of the page. This shows a list of system properties of the wind generation facility. The absolute dimensions of Growian, the facility concept and the component types, the type of operational modes and the overall properties of the system influence the three quantities: power, loads, emission.

## 7. MEASUREMENT POINTS

According to the previous chapter, in order to determine the parameters of interest measurement points are selected over the entire wind generation facility. This includes transducers for mechanical, thermal and electrical measured values. Figure 4 gives a summary about the local correspondence of the measurement points and the observation points.

The measurement points include the following processes or states:

strain	force
acceleration	path
speed	temperature
voltage	current
frequency	pressure
torque	rpm
flow speed	flow direction

flow amount	global radiation
humidity	acoustic pressure (level)
switching state	surface state
FS signal	tremors
network state	operational measured values
optical	perception

## 8. MEASUREMENT PHILOSOPHY

/144

The measurement intervals during the measurement program vary widely. All of the data which are involved with the global energy supply and energy gain, lifetime and economy, have to be collected over long periods of time. The time scale can extend from one day (only for energy analysis) up to one or several years. These measurements are called long time measurements.

The study of the loads caused by the action of the environment will involve shorter time periods. The cyclical return of load, for example, due to rotor motion or gusts specifies a measurement duration of seconds and minutes. The analysis of the conversion of the flow energy of the air into the rotory energy of the rotor and the electrical energy delivered by the generator or transformers will involve this time scale. The influence of daily rhythms, such as air temperature and sound propagation, leads to a measurement duration on the order of one day. The prescribed order of measurements can be performed arbitrarily if one waits for the meteorological boundary conditions and if the corresponding state of the machines is implemented. These measurement sequences are, therefore, called measurement campaigns.

A wind generation facility is subjected to natural forces. Extreme cases of wind conditions have important influences. They occur stochastically and do not fit in with the previously discussed measurement processes. Also special operating states of the facility itself can occur, even in conjunction with meteorological special cases. These special operating states are controlled by the control system within the safety monitoring activity. The measurement program is intended to give information about the sequence and optimum possibilities of

controller involvement. In addition to long time measurements and measurement campaigns, we therefore introduce a third kind of measurement process. This is called event measurement and is continuously ready because of its task. This process begins when a limiting value of a number of exceptional measurement signals is exceeded. The recording duration of relevant measurement values then extends from several seconds up to 60 seconds. By the continuous buffering of all measured values, we then also have available the previous history of the event. This method of event-triggered initiation of measurement recording will make it possible to record the causes, the event itself and the consequences.

Figure 5 shows the correspondence between measurement topics and measurement modes. A solid dot indicates the emphasis of the activity, the smaller point shows processing of the topic. Figure 6 gives a summary of the measurement modes plan. We can read off the following characteristics:

long time measurement:	measurement during real operation.
measurement campaign:	measurement of selected states.
event measurement:	measurement of extreme states with automatic triggering.

## 9. DATA RECORDING AND PROCESSING SYSTEM

The design of the wind energy facility GROWIAN and the tasks of the measurement program with the measurement modes require a relatively close framework for the data acquisition system. Figure 7 gives a summary.

The data are distributed in space over the wind measurement tower 1, the wind measurement mast 2+3 (measurement grid), the facility itself and the operating building. In addition, there is a mobile outer station which is especially used for collecting emissions.

All of the measured values can be divided into groups. These groups correspond to the local positions of the measurement points. Most of the data involve the rotor blades, the hub and the rotating



units of the blade displacement device and the drive train. These data are collected in a data concentrator 1 and are merged into a data single stream. A data concentrator 2 is located in the machine house. /146 There it receives the incoming measured values and combines them to an additional data single stream. The same is done by data concentrator DK 3 in the tower, DK 4 in the operating building, DK 5 in the mobile outer station. In the data station the data individual streams are collected into a collective stream.

The number of measurement points (about 500) and their sampling rate (1-50Hz, in exceptional cases 160 Hz) suggests the use of a PCM facility. This makes it also possible to classify the individual data stream into a single total data stream. The subsequent distribution then leads the relevant measured values to the evaluation and recording units for long time measurements, measurement campaigns, event measurements and other tasks.

By dividing up the dedicated computer, we wish to achieve a greater operational safety and better handling capability. For a measurement and test project of this extent, it makes sense to select a flexible concept for data recording and processing because the operational experiences certainly will require modifications. This can be better satisfied by a building block scheme than with a complex large facility.

#### 10. DATA EVALUATION

In order to describe the data evaluation, we again have to distinguish by measurement modes.

The long time measured values are continuously evaluated by the program depending on the position. The status of the statistics must be callable in a short time.

The measurement campaigns are evaluated beforehand in the facility for orientation. The detailed analysis of the results with all scientific and technical aids will be done by specialists. The results of event measurements are treated in a similar way unless a valuation at the location is required.

ORIGINAL PAGE IS  
OF POOR QUALITY

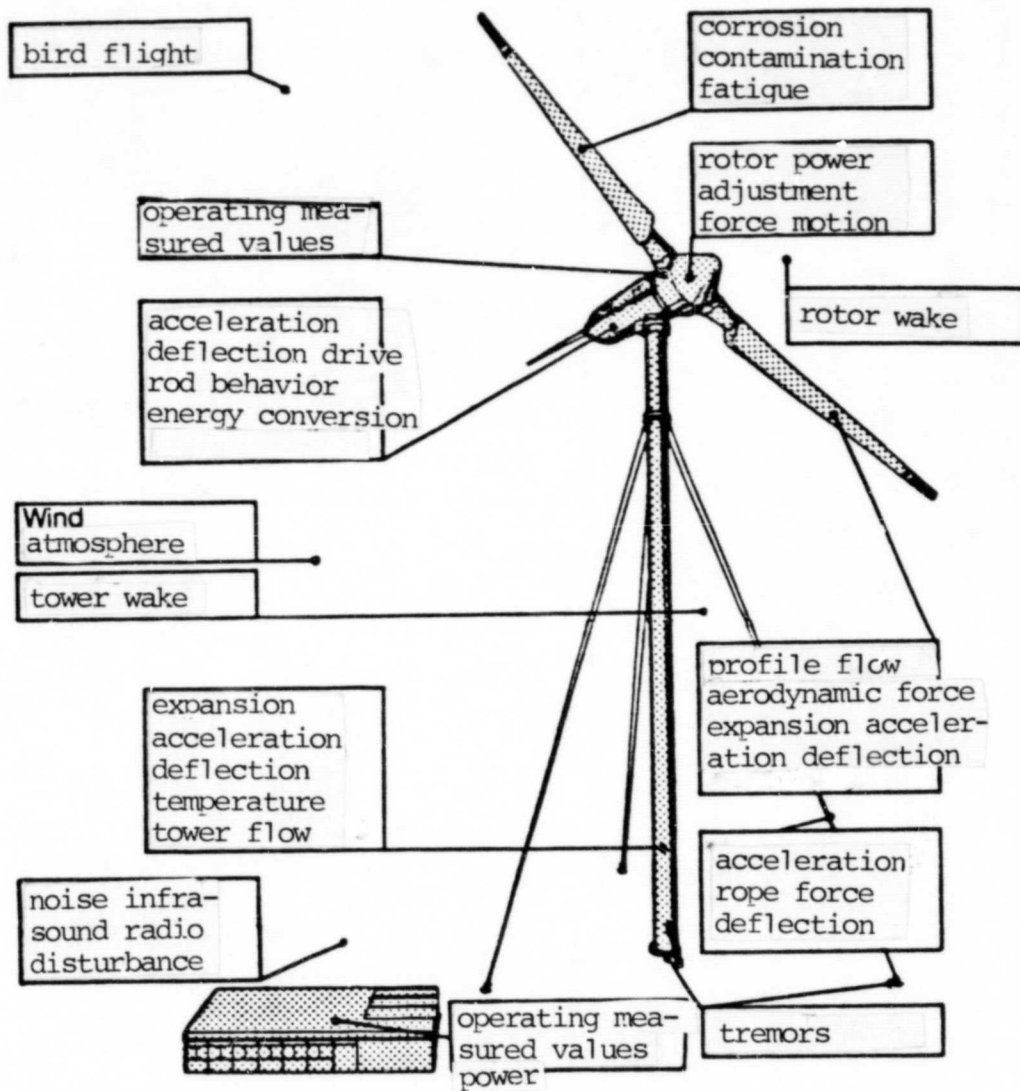


FIGURE 4. MEASUREMENT AND OBSERVATION POINTS ON THE GROWIAN

ORIGINAL PAGE IS  
OF POOR QUALITY

	long time measurement	measurement measurement campaign	event measurement
power	○	○	○
load	○	○	○
Emission	○	○	○

FIGURE 5. MEASUREMENT TOPICS AND MEASUREMENT MODES

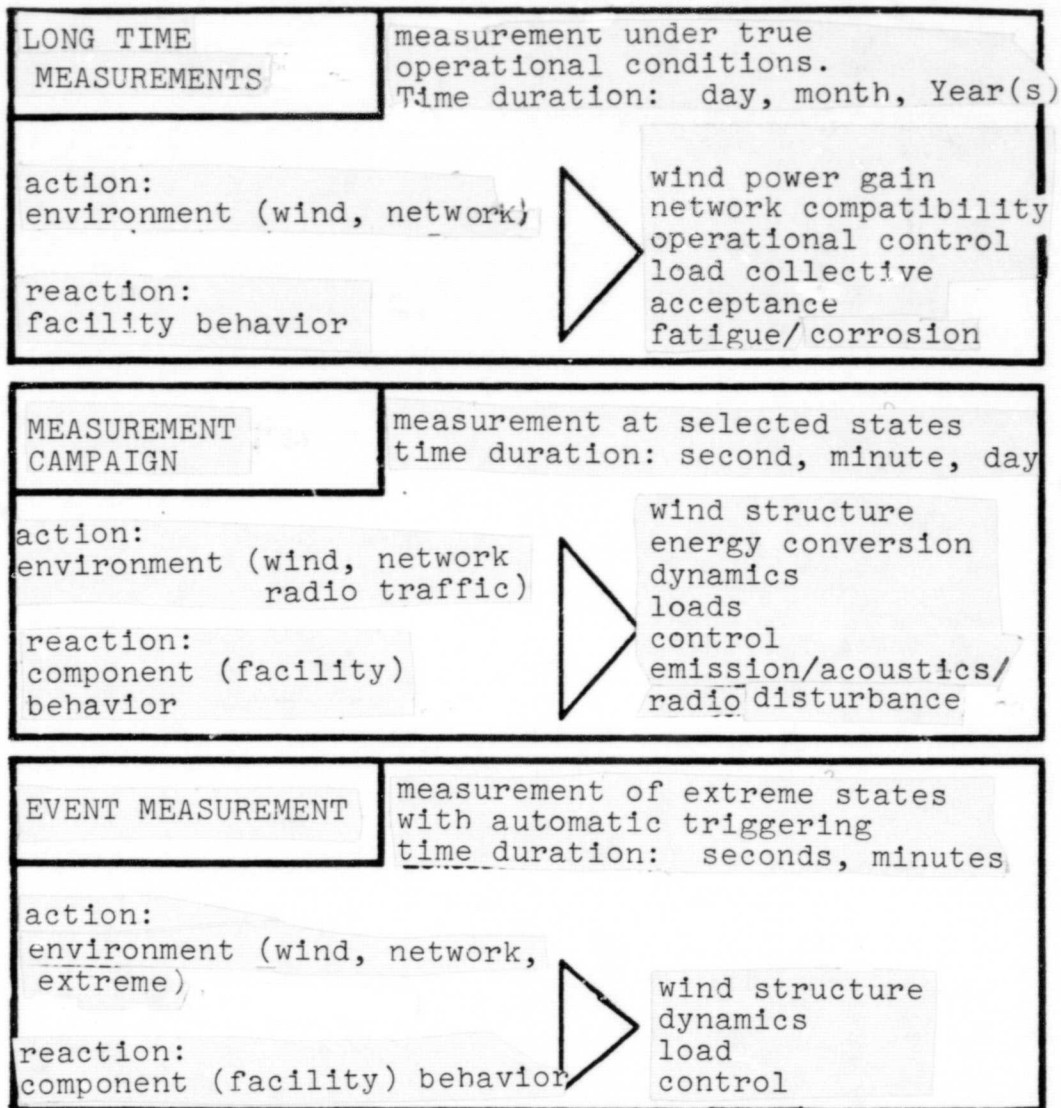


FIGURE 6. EXPLANATION OF MEASUREMENT MODES

ORIGINAL PAGE IS  
OF POOR QUALITY

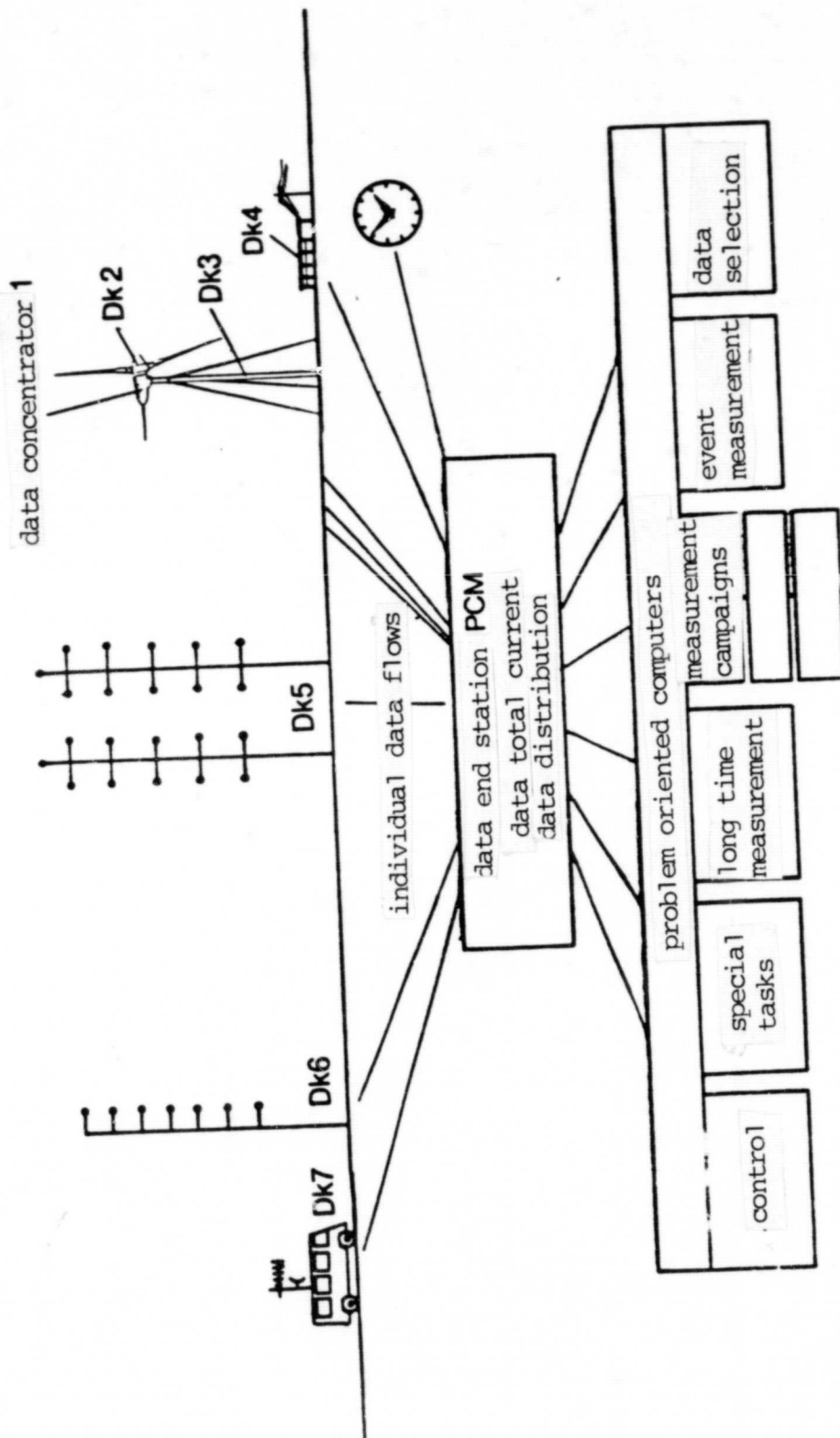
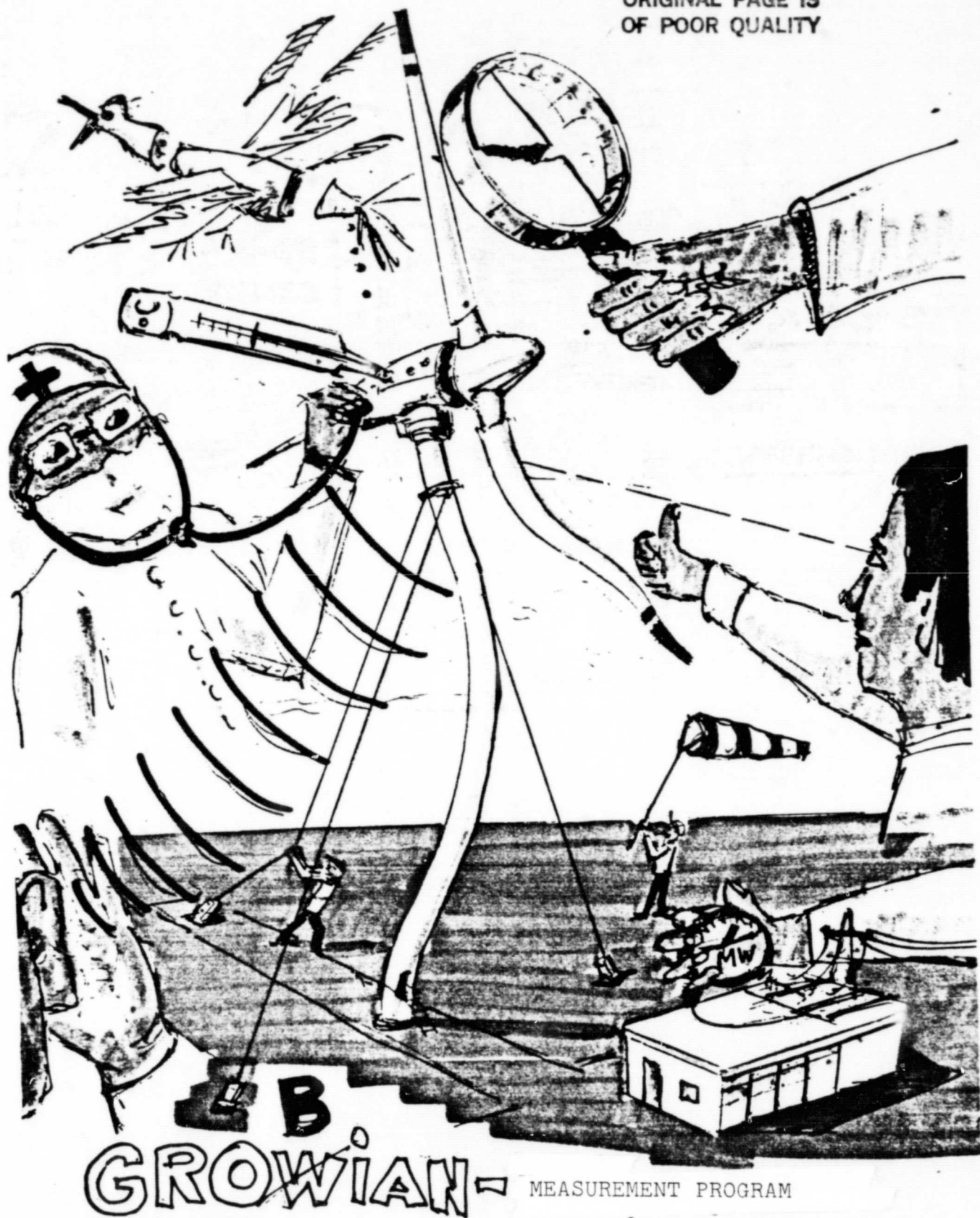


FIGURE 7. DATA ACQUISITION SYSTEM



We would like to show this cartoon (publisher's) about the measurement and test program for GROWIAN which the lecturer also showed.



BLADE TECHNOLOGY PROGRAM  
FOR LARGE WIND ENERGY FACILITIES\*

/155

Dieter Muser

Project goal

/156

Within the blade technology program for large wind energy facility tasks, optimum price rotor blades are to be developed. This means cost minimization of rotor blade structure as well as an optimization of the rotor blade aerodynamics. Interactions between the structure and the aerodynamics are to be considered in more detail than before.

Schedule situation

The project started at the beginning of the task in October 1979 and will run to the end of October 1982. According to schedule, at the end of 1980, the optimizations of the blade structure and the concept catalog will be developed. Part of the material investigations were done ahead in order to obtain better inputs for the structural calculations.

Program structure

The program was divided into four main tasks

- optimization
- concept catalog and concept collection
- concept design
- test program

During the optimization, statistical data are collected in order to obtain evaluation data. The aerodynamic optimization is still going on because no suitable computer models were available for displacing the blade sections and for the use of aerodynamic aids. In the

/157

---

\* ET 4375 A

ORIGINAL PAGE IS  
OF POOR QUALITY

WING TECHNOLOGY PROGRAM  
AND STRUCTURE

OPTIMIZATION

- POWER STRUCTURE
- STRUCTURE
- COST

CONCEPT CATALOG

- STEEL
- LIGHT METAL
- COMPOSITE FIBER
- OTHERS

CONCEPT SELECTION

TEST PROGRAM

- MATERIALS
- MANUFACTURING
- TESTING

OPTIMIZATION OF ROTOR BLADES

PERFORMANCE

- AERODYNAMICS
- GEOMETRY
- ADJUSTMENT

STRUCTURE

- MATERIALS
- CONSTRUCTION  
METHOD

COSTS

- BLADE
- FRACTION BLADE
- POWER $\leftrightarrow$ STRUCTURE

structural optimization, steel, light metals and composite materials were considered which were used with various structural concepts.

**ORIGINAL PAGE IS  
OF POOR QUALITY**

CONCEPT CATALOG INITIAL DATA

GROWIAN BLADE DESIGN	- GEOMETRY
	- PROFILING
	- LOAD CASES
GROWIAN	- MAX. BENDING 3 m (LF 2.5 NEGATIVE GUST)
	- EIGEN FREQUENCY > 0.8 Hz
TECHNOLOGY PROGRAM	- BLADE BEGINNING R = 10.85 m
	- SEPARATION POINT R = 27.50 m
	- SUITABILITY FOR THE SERIES

Cost determination based on single element costs was incorporated in the calculation program in order to obtain the influences of various structures.

/158

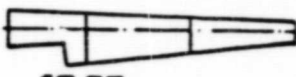
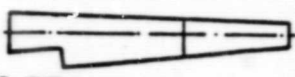







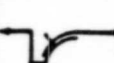
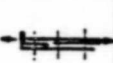




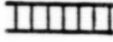


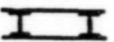
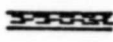
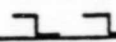




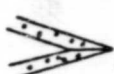
As initial values for the solution catalog and for predimensioning, values of Growian were taken over and our own data was added.

With these data the following were calculated for the various basic structural concepts

- mass
- bending
- eigen frequencies
- cost

/159

During the preliminary construction work, various details were produced at a scale of 1:1 in order to find the economical possibilities, for example, the spar--end box connection or the end beam. These points differ because of the strong profile changes over the blade length and are only conditionally suitable for rational design.

wing separation	 10,85		 4,85		 10,85		
basic structure							
Material	steel		alum.alloy		GFK *	CFK**	SFK***
force introduction							
connection	bolts		adhesives		mold closure		
shell	 web	 foam	 hose	 Pultrusion	 Coremat	 Pultrusion	
manufacturing	manually		Prepreg	injection	 winding	 winding	Pultrusion
Detail	 nose		 spark-shell		 terminal edge		

/158

\*fiber reinforced plastic  
 \*\*carbon reinforced plastic  
 \*\*\*silicon (?) reinforced plastic

The calculation of the blade masses results in clear advantages for the fiber composite rotor blades.

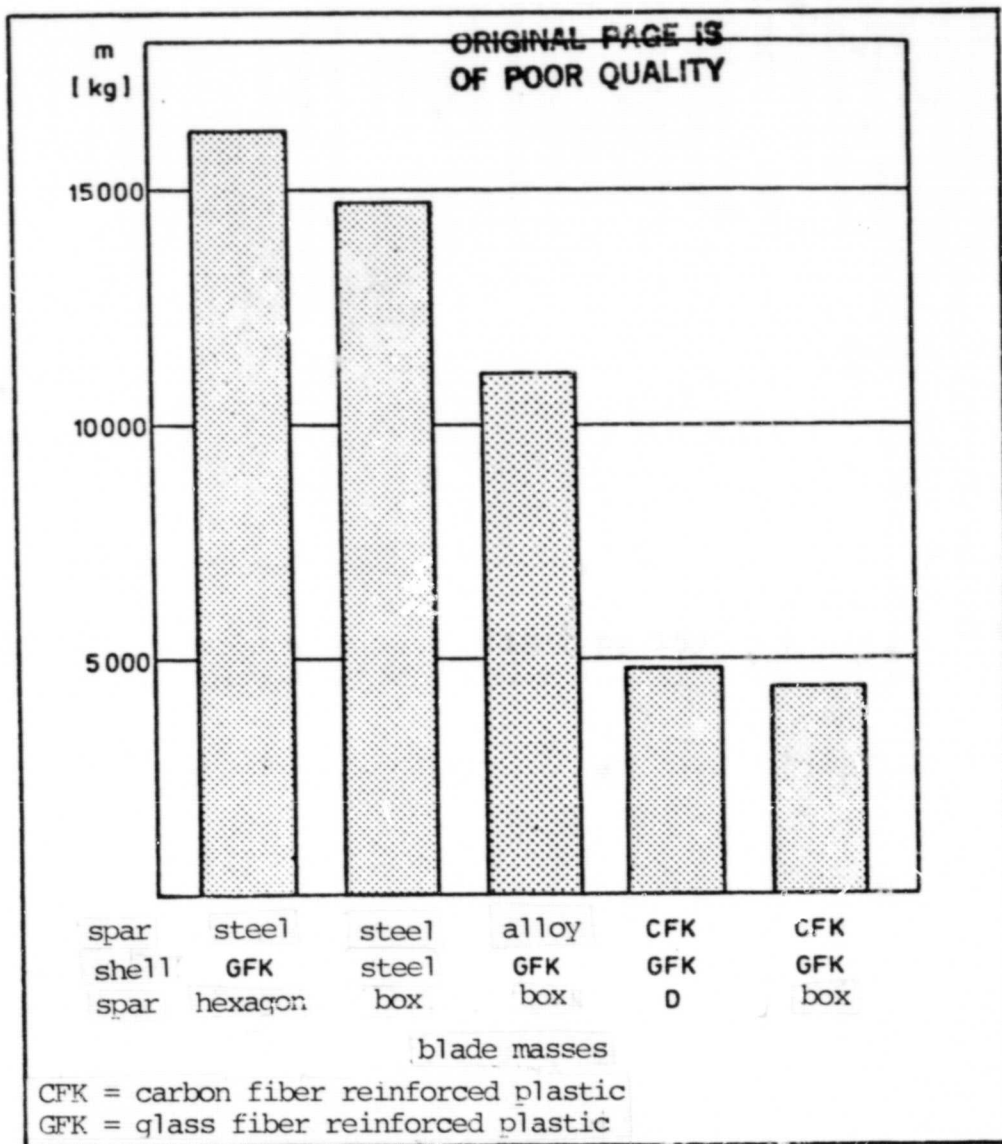
/160

This mass difference also seems to trickle down to the cost. Even though the composite fiber materials are much more expensive both for procurement and machining, drastic cost reductions can be expected by using machines in mass production. More exact data can only be obtained after conclusion of the first component test.

From all of the concept variations, according to the evaluation, two similar designs evolve for the further work.

The D spar up to 40% of the profile chord will use winding technology and is attached with the end box using hose winding building techniques and can be separated from the spar.

In the case of the box spar, between 5 and 40% of the profile chord will use prepreg technology for manufacturing with nonremovable and glued



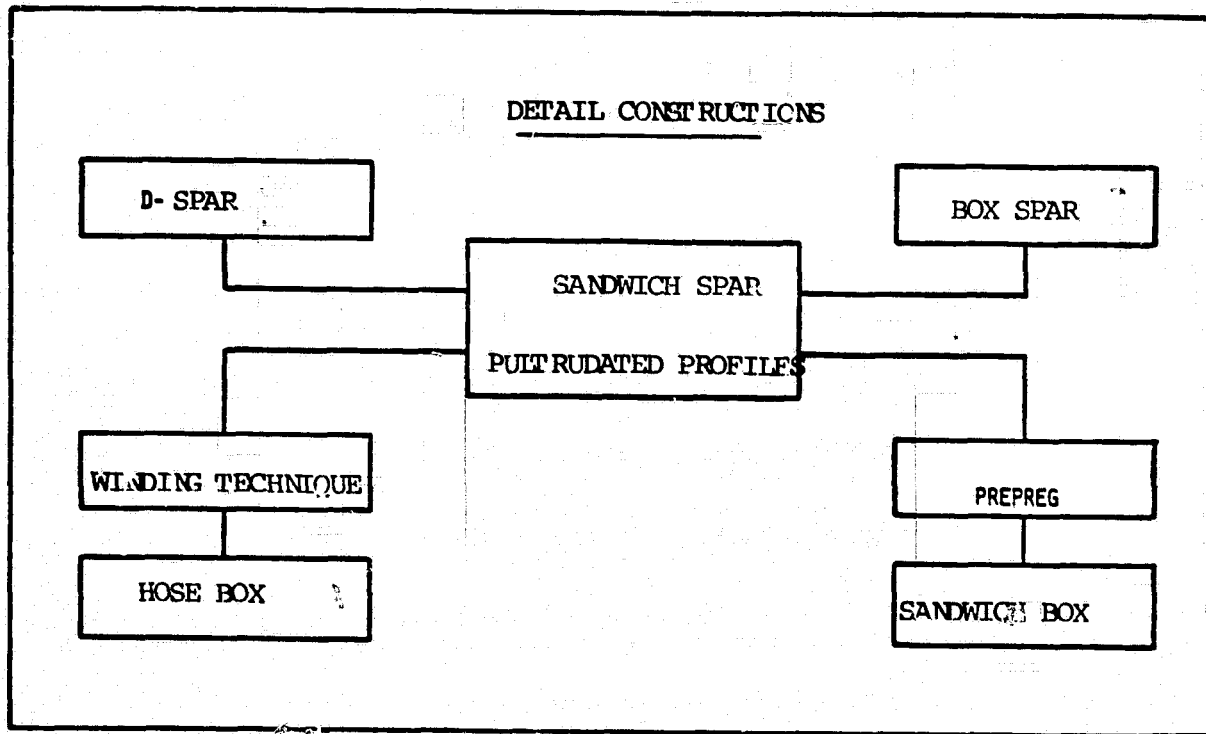
on sandwich end box.

Both concepts have a sandwich structure in order to stiffen it against bulges in the spar region. By using protruding profiles, it becomes possible to reduce manufacturing times and premanufacturing of the elements with machines will bring about a uniform high quality.

/161

By using these high value materials and by exact dimensioning, additional mass savings could be achieved. For the D spar we found a mass reduction of 4800 kg for the preliminary design without connection elements at the separation points.

ORIGINAL PAGE 13  
OF POOR QUALITY



	0	10.85m	27.5m
MASS [kg]	(4780) 3180	(2420) 1620	TOTAL (7200) 4800
SPAR [kg]	(4000) 2400	(1900) 1100	* CFK (5900) 3500
SHELL [kg]	780	520	** GFK 1300
AREA : [m <sup>2</sup> ]	63	44	
CHORD [m]	4.930	2.645	1300
SHELL CHORD	2.96	1.59	0.78
CONSTRUCTION METHOD	2 SHELLS SEPARABLE	2 SHELLS GLUED TOGETHER	WOUND SPAR HOSE BOX

\* CFK = fiber reinforced plastic; \*\* GFK = glass fiber reinforced plastic



Additional work includes detailed structural calculations for the separation points and the laminate structure as well as aerodynamic calculations of blade design. The manufacturing of the components in the form of partial shells will start in the second quarter of 1981. Apparently, the entire project will be carried out within the framework and scheduling constraints.

ORIGINAL PAGE IS  
OF POOR QUALITY

CONSTRUCTION AND OPERATION OF THE LARGE WIND ENERGY FACILITY GROWAN  
Project No. ET 4342 A

H. Witt

/163



## Status of project ET 4342 A, construction and operation of GROWIAN I

/164

Lecture during the seminar on building, testing and development of large wind energy facilities within the framework of projects supported by BMFT.

MAN Neue Technologie, Munich, March 23-24, 1981. Author: H. Witt.

<u>Contents</u>	1. Introduction
	2. Status of project tasks
	3. status of project
	4. Change methods
	5. Location
	6. Official permits
	7. Scheduling situation

### 1. Introduction

Based on the "production data", which were developed during the first development phase of the Growian I project, at the beginning of 1979 its realization was started. This second development phase was structured in several parallel research and development projects in order to reduce risks and because of the schedule. Among these we have the "construction and operation of Growian I" project.

The "Large Wind Energy Construction and Operating Association m b H" has taken on this task. The following are participating in this: The Hamburg Electrical Company AG, the SCHLESWAG AG and the Rhine Westphalia Electrical Company AG. The company was founded in January 1980.

### 2. Status of the project

In January 1980, the firm MAN in Nuermberg was given the contract about engineering work on the project based on the production data. In August of 1980 it was given the contract for delivery and assembly

of the system components. This includes: The rotor hub, the machine hubs, the control equipment and the electrical technology.

/165

The firm Maurer Sons, Munich, was given the contract for the steel tower delivery.

The operating buildings will be built using the space element construction method and are being delivered by the firm Kirschner, Duermen. These elements are being manufactured. The HS switching rooms, the transformer boxes and the emergency power diesel unit are now being awarded to contractors. These use conventional construction methods.

At the beginning of April 1981 we expect to let contracts for the foundation work for the tower and the guide wire foundations.

At the present time bids are being received for conventional electrical technology and the two 170 meter measurement masts, the building of which belongs to this project.

### 3. Status of project

#### 3.1 Rotor hub

- The pendulum frame and traverse construction group has been modified to correspond to the chain rotor blade bearing concept and the modified blade adjustment device. Manufacturing has started.
- The design data of the rotor bearing are available to the AG for examination. The manufacturing can be started shortly.
- The design detailed processing of the blade displacement device with hydraulic emergency shut down and the blade retraction device is almost concluded.

#### 3.2 Machine house

- The calculation and construction of the supporting elements has been concluded except for the final design of the connection to the tower head.

- The following are in process:

Concept and configuration of the oscillation damper/damping system in the front part of the machine house,  
concept for auxiliary construction for the assembly equalization ballast,  
concept of the wind direction following device,  
installation of the hydraulic lifting device

### 3.3 Control technology and electrical technical equipment

The concept and clarification of the automatic systems (operational control) of the measurement installation and the control for the emergency shut down system as well as the facility behavior during power shut down has been started according to the design stage.

/166

### 3.4 Tower construction

The detailed construction of the steel tower component elements has been started with consideration of the devices required for the lifting process and the support.

### 3.5 Operational buildings

The planning has been concluded. The building work at the construction site have started with the digging of the foundation.

## 4. Change methods

In order to be able to cover design changes, for example, based on technical developments or from calculations and to be able to determine their influences on the design of other components and their effects on schedules and costs, a special change procedure has been developed.

## 5. Location

The authorization for building the facility at the Kaiser Wilhelm

Koog was obtained formally in 1979 and is now concluded. Considering the large area for the support cables, approximately a 6 ha area had to be leased.

With consideration of the present ground conditions, it was found that a low foundation of the buildings was the most economical solution. The tower and its cable support have local concrete driven in posts with driven in base plates which are arranged vertically and obliquely. The ramming depth is about 18 m. The measurement mass foundations will have profile seal posts. The access road was started in the fall of 1980. The asphalt cover will be applied in March of this year.

#### 6. Official authorizations

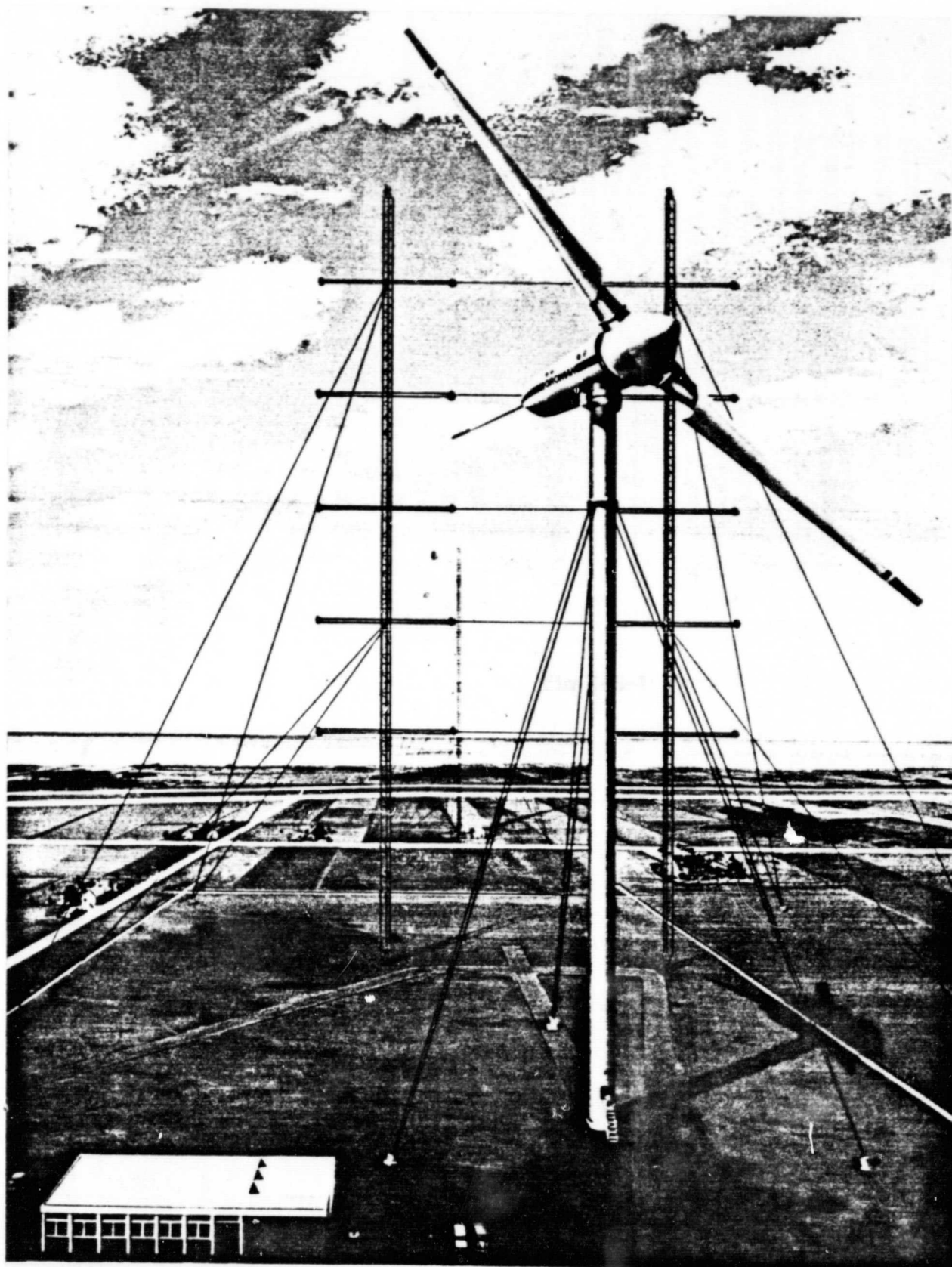
The permit to build the access road was given on October 21, 1980. /167

The permit for the entire installation was submitted on December 22, 1980 at the authorities. First partial authorizations are expected shortly. In agreement with the district building authority at Heide, the lowest authority, the German Lloyd firm will be used as an official authority for testing the safety aspects of components.

#### 7. Schedule situation

Today it looks as though no difficulties will occur with maintaining the schedule which plans for delivery on November 30, 1982. Delays in the projects for parts of the azimuth bearing can be equalized by measures for accelerating the production schedule.





Full scale GROWIAN wind facility at the Kaiser Wilhelm-Koog, Elbe Delta. View in the main wind direction towards the Elbe. The 3 wind measurement masts are to be built during the measurement and test program (see page 135). Performance of the facility 3000 kW after 12 m/sec. Wind speed, rotor diameter: 100.4 m, tower height: 100 m. Planned completion, fall of 1982.

/169

INVESTIGATION OF NEW CONCEPTS  
FOR LARGE WIND ENERGY FACILITIES IN THE CLASS  
OF UP TO 135 m ROTOR DIAMETER\*  
(ACCORDING TO 5 MW<sub>electr.</sub> AT A WIND SPEED OF 11 m/sec.)

Building and testing of a demonstration facility on a 1:3 scale  
Development of design data for a prototype full scale facility

R. Meggle

1. Purpose

The investigation of new concepts for large wind energy facilities in the class of 135 m rotordiameter (according to 5 MW delivered electrical power at a wind speed of about 11 m/sec). Testing and building of a demonstration facility on a model scale (about 1/3). Development of design data for a prototype full scale facility.

2. Working program

- a) Preliminary concept definition for a two- and a one-blade system. System design. Investigations of the oscillation and stability behavior. Determination of loads. Selection of preferred concepts.
- b) System optimization of full scale facility - definition of the demonstration facility and production of design data.
- c) Hardware definition of full scale facility - component manufacturing and partial integration of the demonstration facility.
- d) Hardware development (building and testing of selected test components) of full scale facility - assembly and operation of demonstration facility. Test operation.
- e) Preparation of design data for the full scale facility - disassembly of the demonstration facility and recultivation.

---

\* Project No. ET 4240 A

### 3. Status (end 1980)

- Work on the full scale facility: (5 MW<sub>el</sub>)  
Design studies for rotor blade and head
- Work on the demonstration facility (370 kW<sub>el</sub>)
- Generation of design data
- Advertisement of the main component groups. Contracts to the most important contractors
- Beginning of manufacturing for rotor blade, rotor head, gondola, generator system and measurement and data systems, inclusion of building interrogation for the Bremerhaven location.

/170

#### 1) GROWIAN II Program summary

##### - Goal

Investigations of new concepts for large wind energy facilities for the power class  $\geq 5$  MW<sub>el</sub> for the rotor class  $\geq 135$  MØ. Building and operation of a demonstration facility for a model scale of 1:3.

##### - Sequence

program beginning	7/78
concept selection	3/79
design data demonstration facility	12/80
production/assembly of demonstration facility	12/81
sample operation demonstration facility	after 12/81
design data for full scale facility	OPEN

##### - Design goals (for full scale facility)

specific investment costs according to  
power production

Design for wind conditions in the North German coast area.  
 $\geq 20$  years lifetime

completely automatic operation  
small operating and maintenance costs

- Location of demonstration facility: Bremerhaven-Weddewarden

171

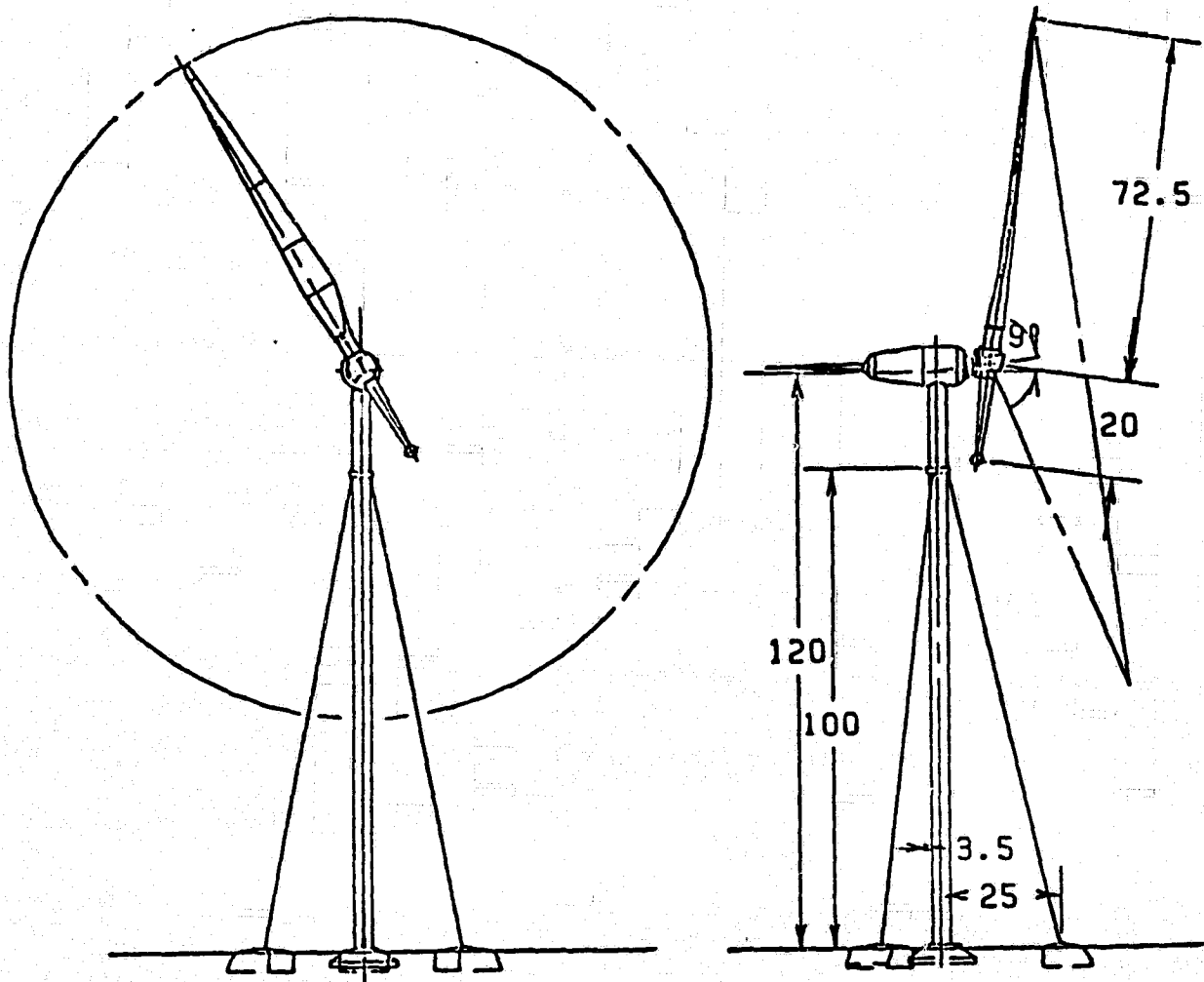
## 2) SELECTED CONCEPTS\*

- Single blade system, free wheeling with horizontal axis
- Static imbalance equalization by counterweight
- Rotor blade with composite fiber design: Shell design with support foam
- Pendulum hub
- Blade angle adjustment (redundant) of the entire blade including counterweight
- Azimuth following by redundant actuator units
- RPM yielding force transmission/generator concept
- Stiff shaft
- Transmission gear
- Slipping cup link, rotor brake, jointed shaft
- Synchronous generator
- Direct current intermediate circuit, static frequency rectifier
- Computer control operating control system with separate emergency off logic (fail safe)
- Soft (over critical) tower concepts: cylindrical steel tower with 3 guy ropes
- External lightning protection and protection for the electrical and electronic systems

---

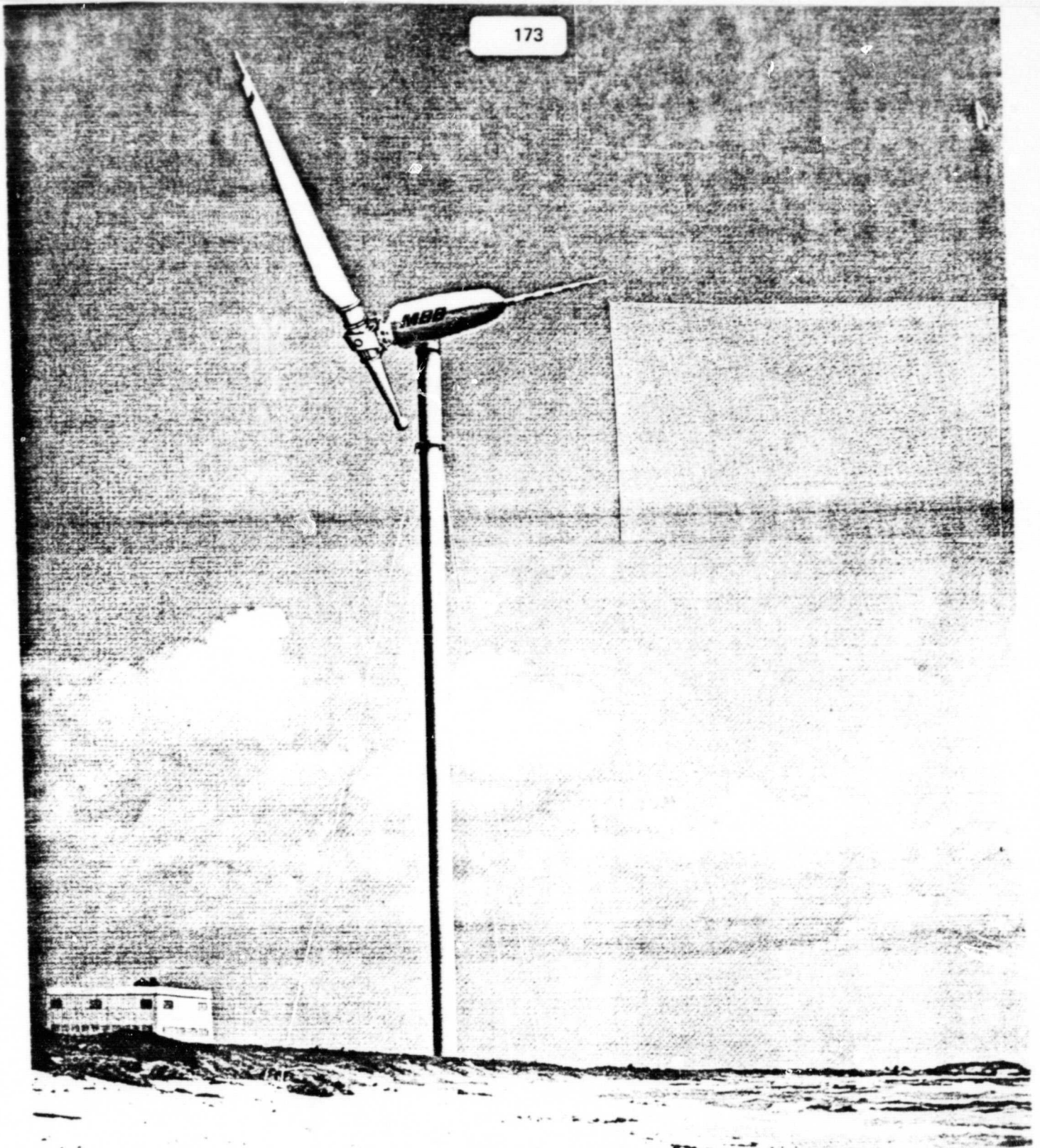
\* Detailed descriptions can be found in the status report on wind energy, VDI Publishing House, Duesseldorf 1980, publishers remarks.

ORIGINAL PAGE IS  
OF POOR QUALITY



WIND ENERGY FACILITY

WEA 5000

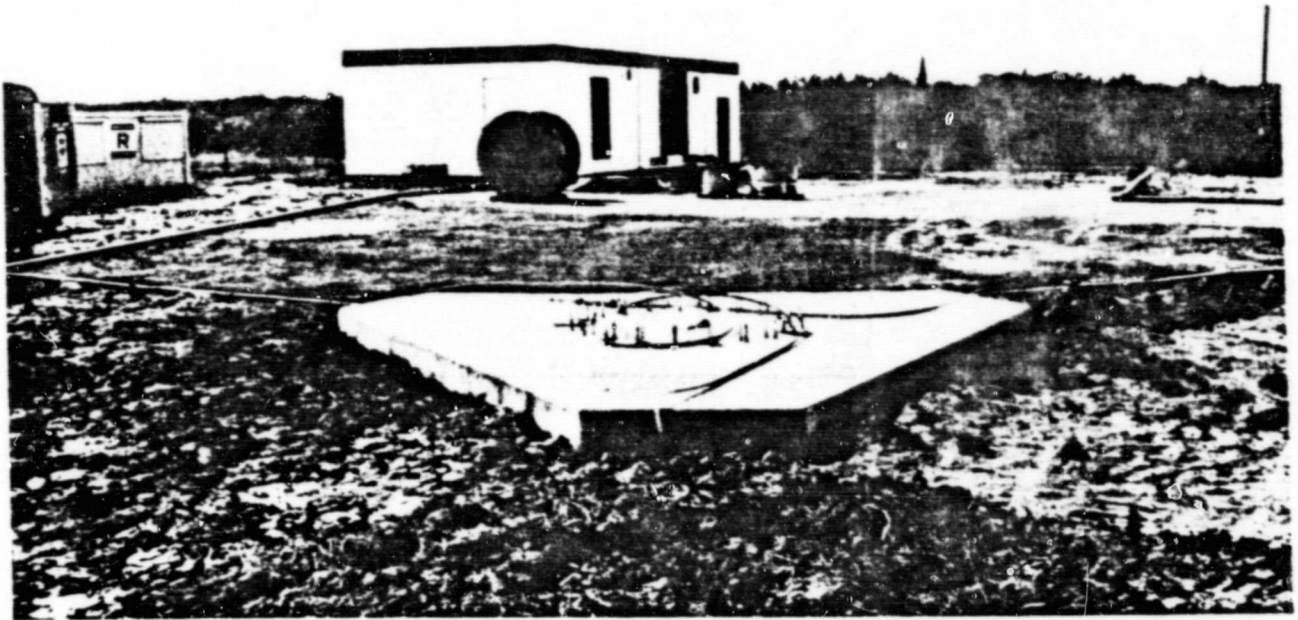


5MWel WIND ENERGY FACILITY

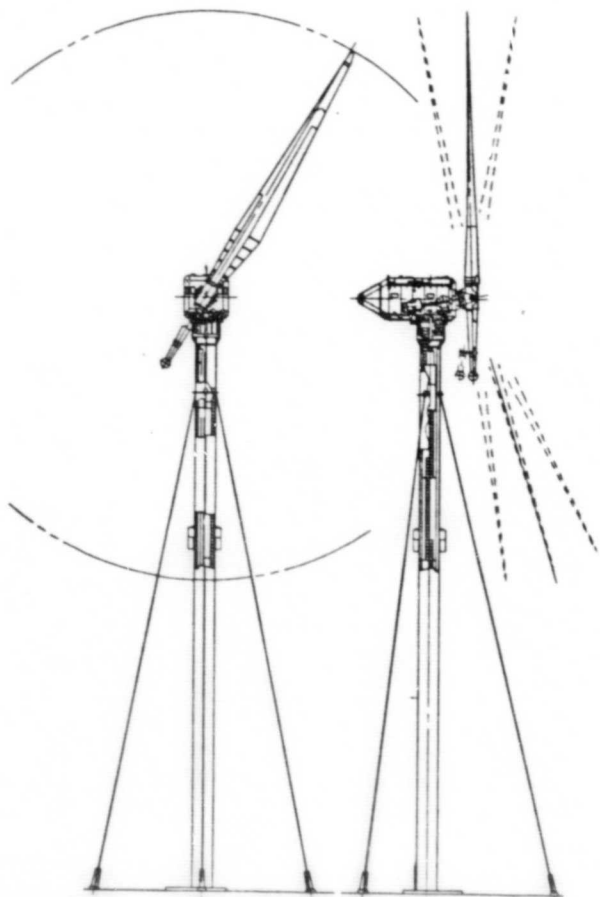
ORIGINAL PAGE IS  
OF POOR QUALITY



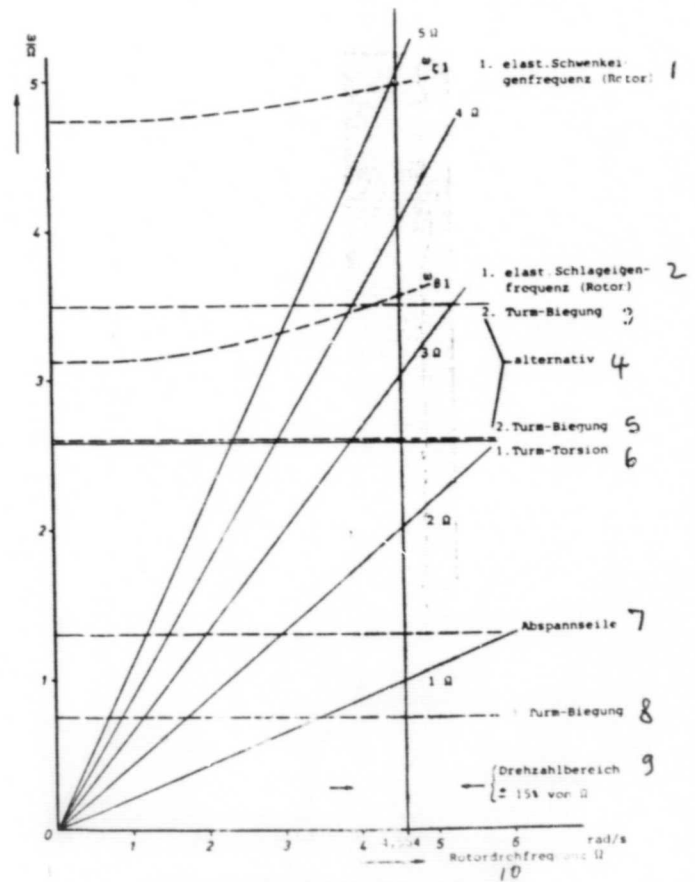
ORIGINAL PAGE IS  
OF POOR QUALITY



BUILDING SITE  
FOR TOWER FOUNDATION AND OPERATING BUILDING



Structure of the demonstration facility



eigen frequencies of the  
demonstration facility  $\Omega = 4,584 \text{ rad/s}$

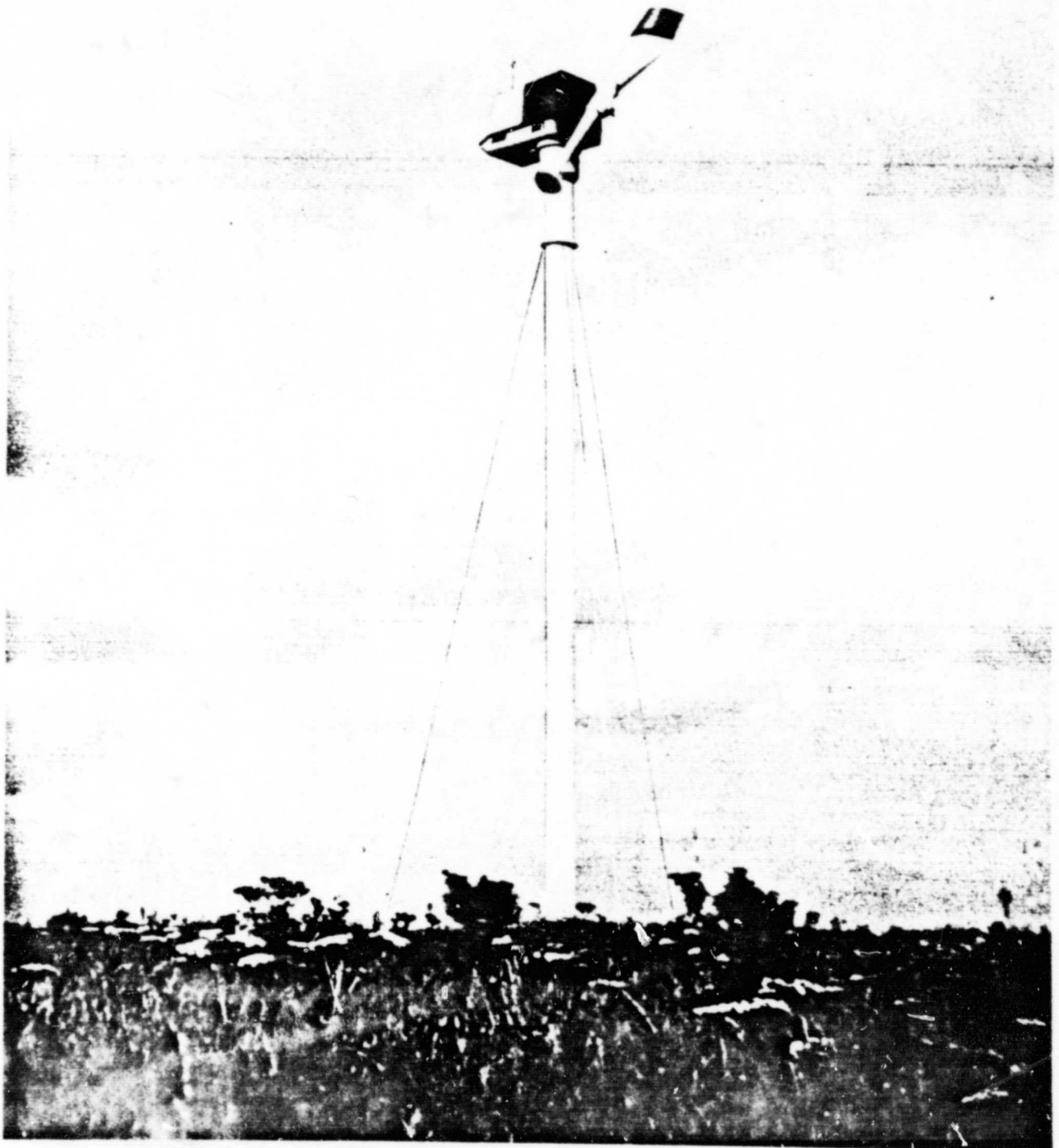


ORIGINAL PAGE 13  
OF POOR QUALITY

KEY TO DIAGRAM ON PRECEDING PAGE

Key: 1--1st elastic deflection eigen frequency (rotor); 2--1st elastic flapping eigen frequency (rotor); 3--2nd tower bending; 4--alternate; 5--2nd tower bending; 6--1st tower torsion; 7--support rope; 8--1st tower bending; 9--rpm range, 10--rotor rotating frequency

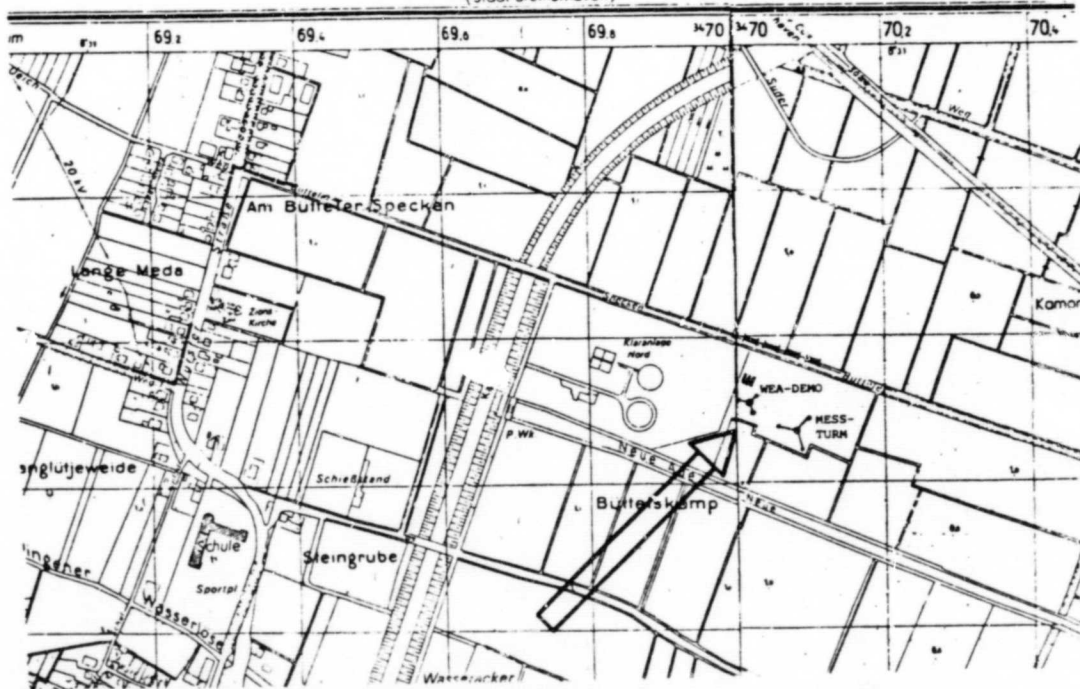
ORIGINAL PAGE  
BLACK AND WHITE PHOTOGRAPH





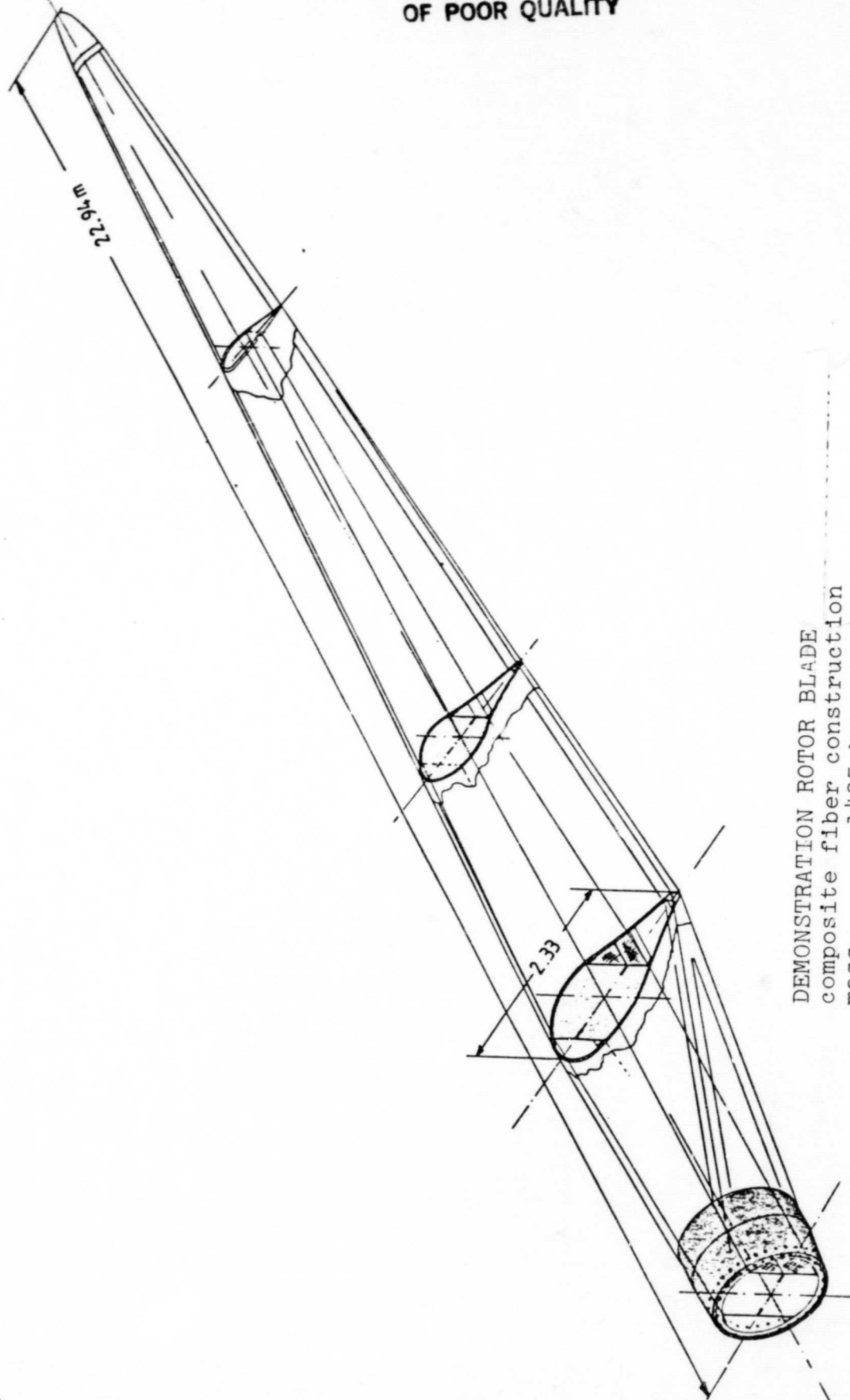
ORIGINAL PAGE IS  
OF POOR QUALITY

### Weddewarden (Stadt Bremerhaven)



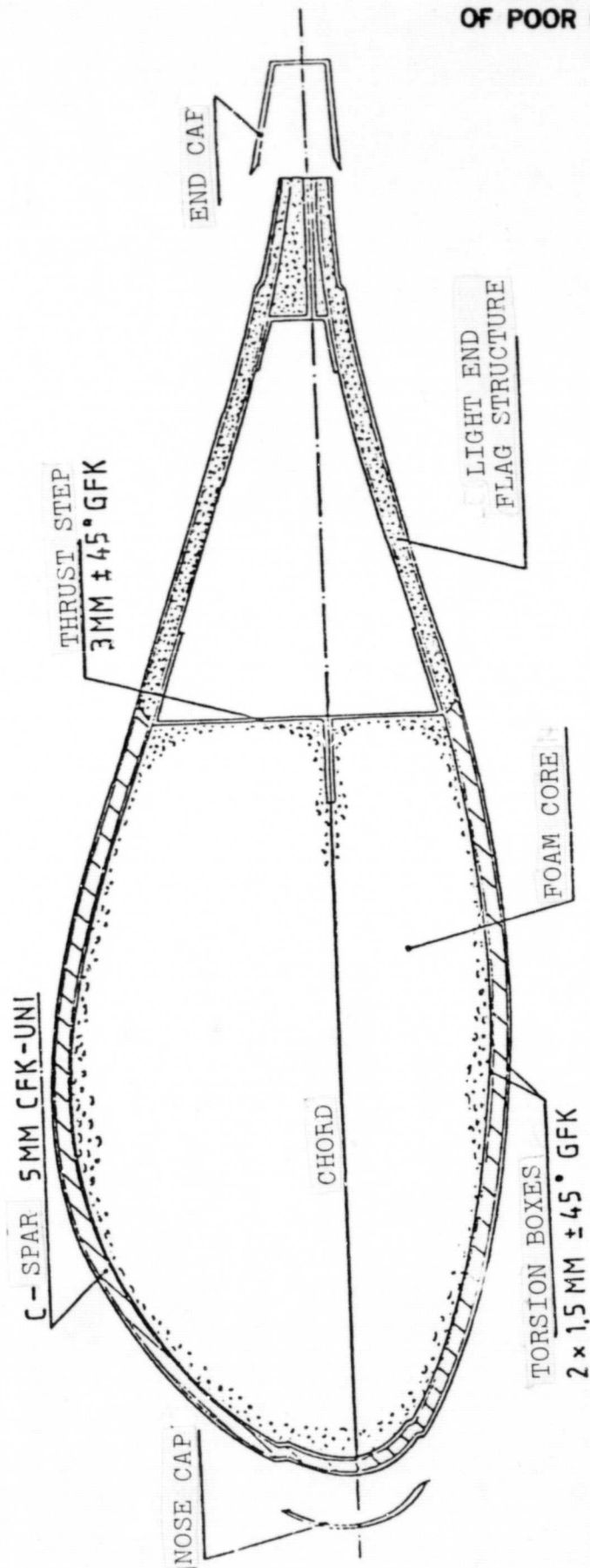
LOCATION OF THE 350 kW DEMONSTRATION FACILITY NEAR BREMERHAVEN,  
WEST GERMANY

ORIGINAL PAGE IS  
OF POOR QUALITY



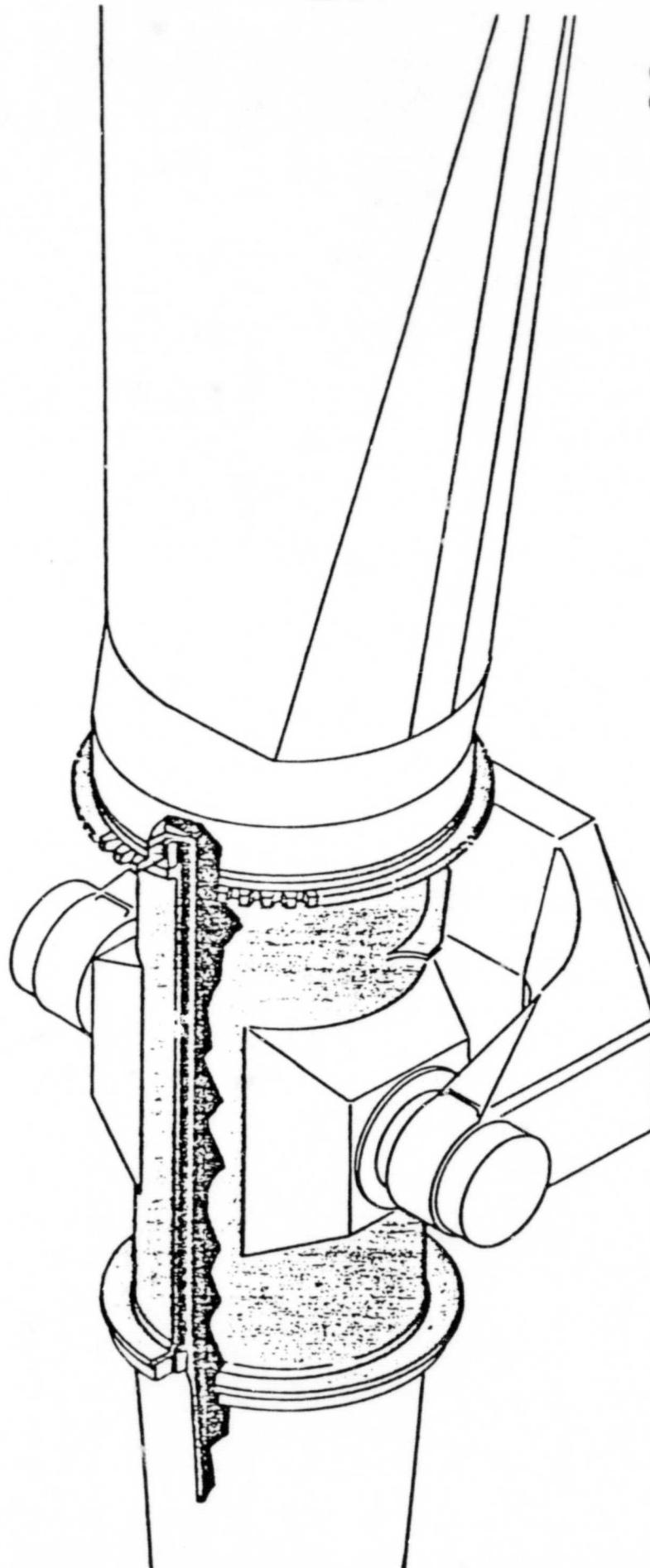
DEMONSTRATION ROTOR BLADE  
composite fiber construction  
mass 1425 kg  
WORTMANN FX-77-W  
ABOUT 15° TWIST

ORIGINAL PAGE IS  
OF POOR QUALITY



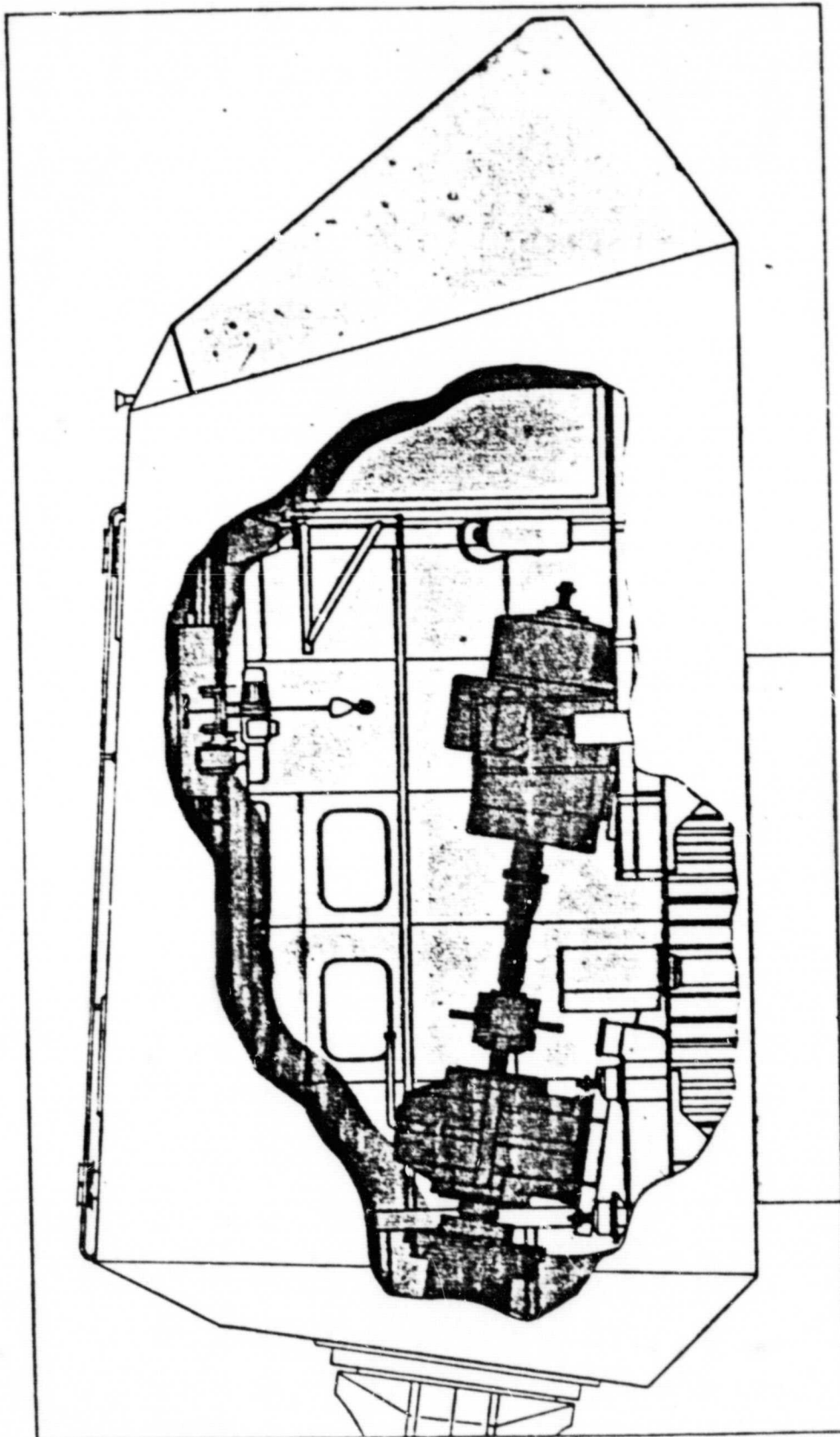
PROFILE CROSS SECTION OF DEMONSTRATION FACILITY ROTOR BLADE

ORIGINAL PAGE IS  
OF POOR QUALITY



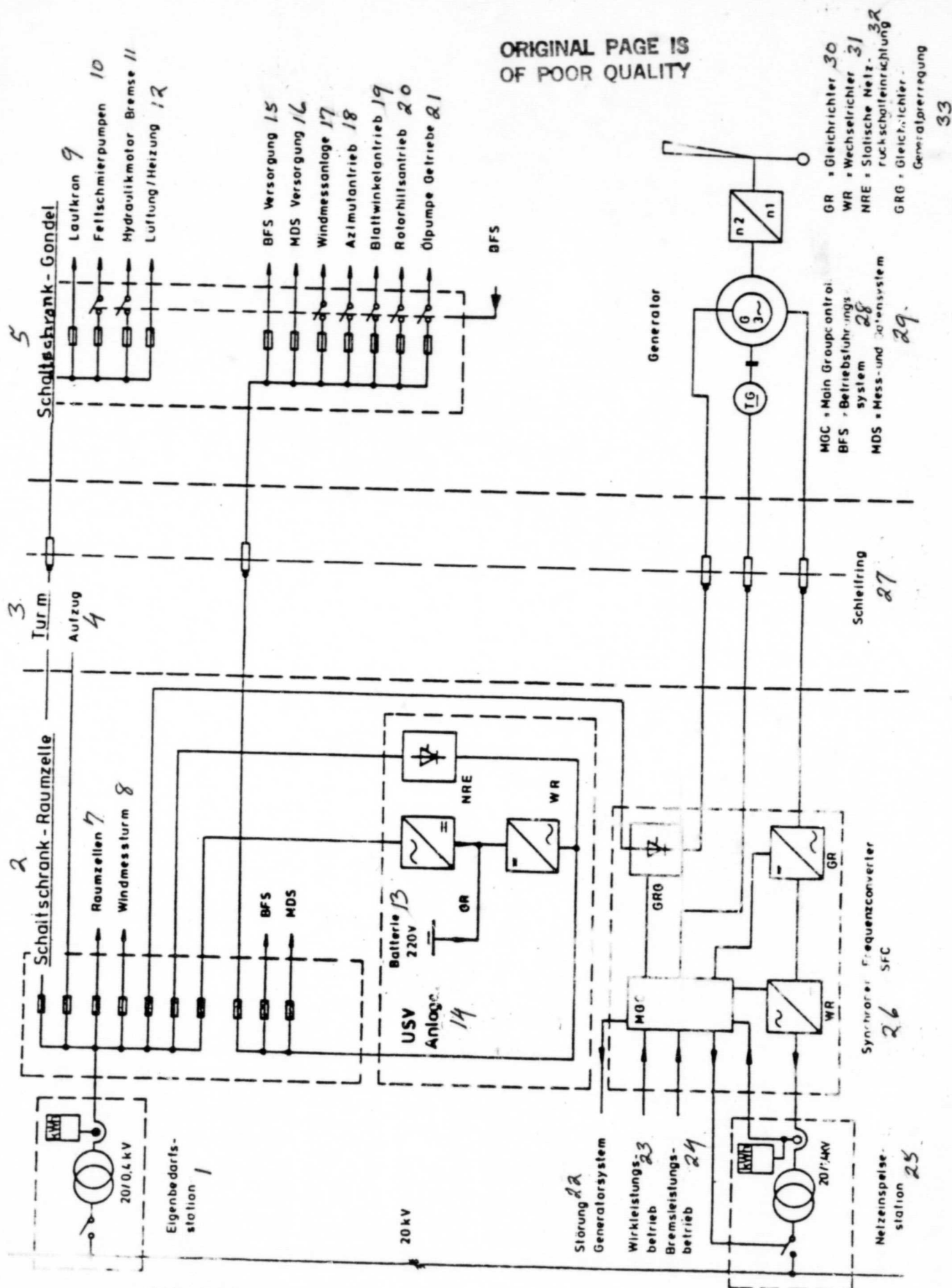
WEA ROTOR HEAD

ORIGINAL PAGE IS  
OF POOR QUALITY



DEMONSTRATION GONDOLA



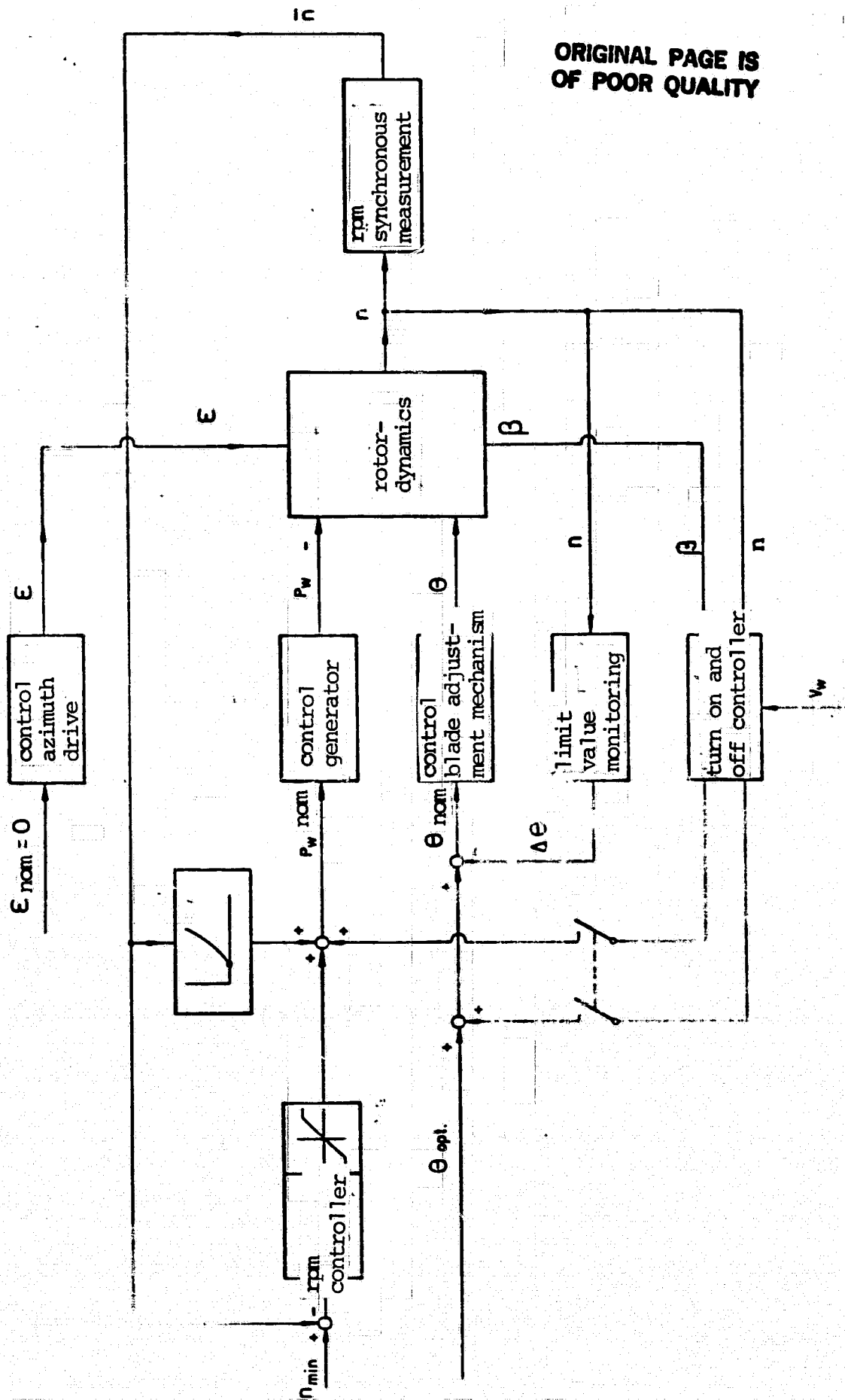


ELECTRICAL EQUIPMENT WEA DEMONSTRATION  
BLOCK DIAGRAM

ORIGINAL PAGE IS  
OF POOR QUALITY

KEY TO FIGURE PREVIOUS PAGE:

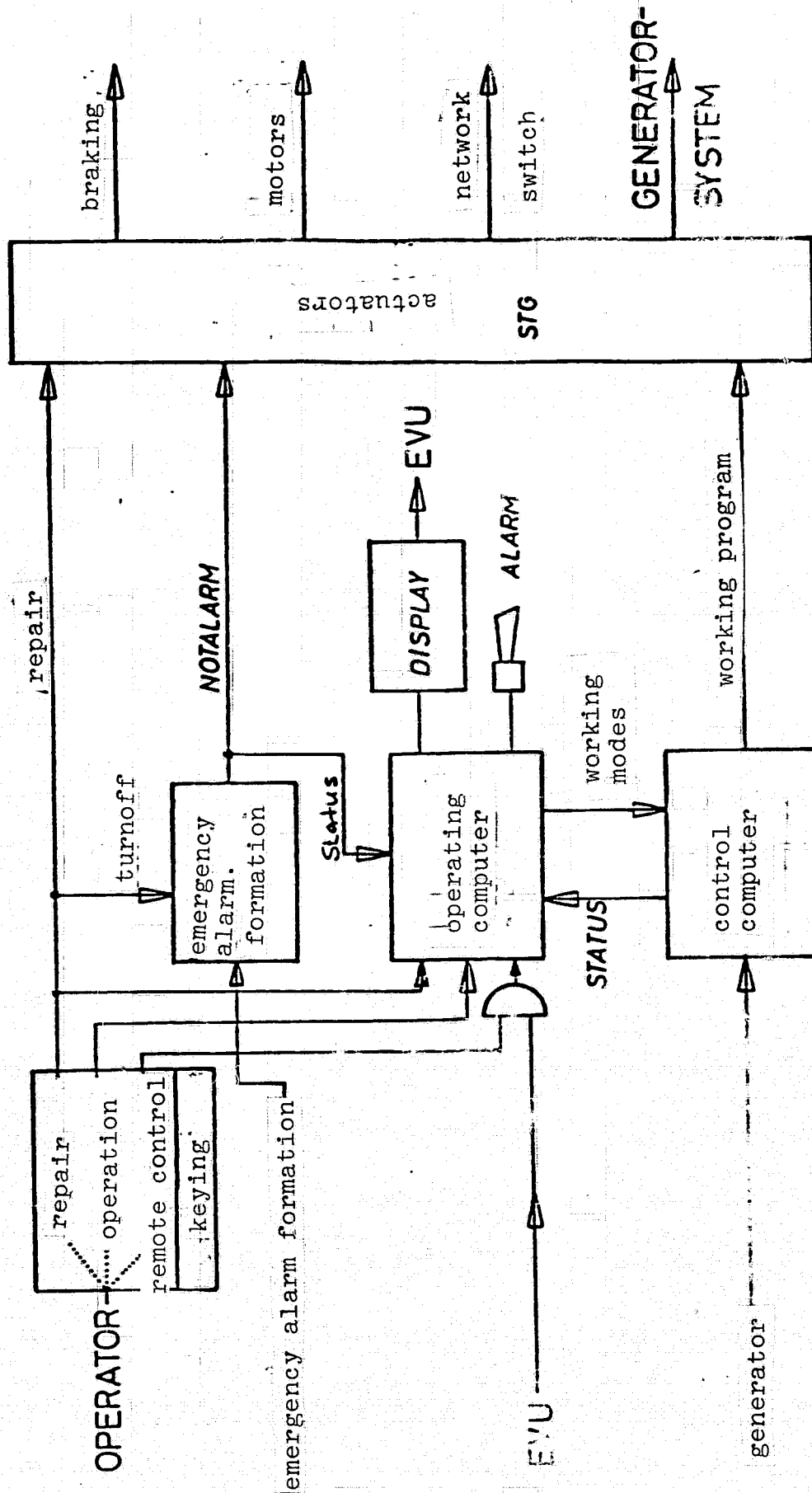
1--independent power source; 2--switching box space cell; 3--tower;  
4--elevator; 5--switching box gondola; 7--space cells; 8--wind measurement  
tower; 9--crane; 10--grease lubrication pump; 11--hydraulic brake;  
12--ventilation/heating; 13--battery; 14--facility; 15--supply;  
16--supply; 17--wind measurement installation; 18--azimuth drive;  
19--blade angle drive; 20--motor auxiliary drive; 21--oil pump gear;  
22--disturbance generator system; 23--power supply operation; 24--  
braking power operation; 25--network supply station; 26--synchronous  
frequency converter; 27--slip rings; 28--operating control system;  
29--measurement and data system; 30--rectifier; 31--alternating  
rectifier; 32--static net switching device; 33--rectifier generator  
control



ORIGINAL PAGE IS  
OF POOR QUALITY

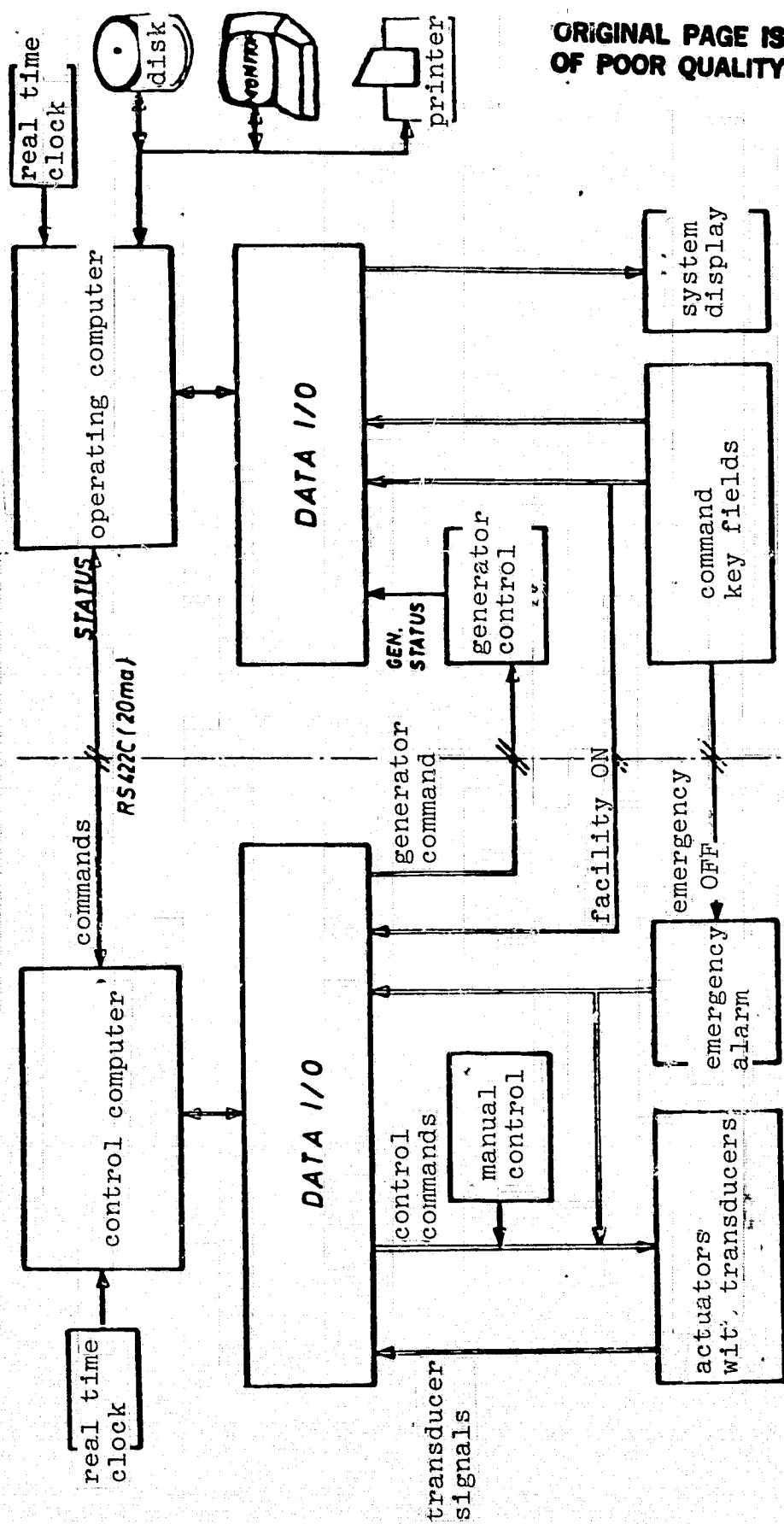
BLOCK DIAGRAM OF CONTROL

ORIGINAL PAGE IS  
OF POOR QUALITY



COMMAND HIERARCHY OF THE OPERATIONAL CONTROL SYSTEM

# INTERFACE OPERATING SYSTEM



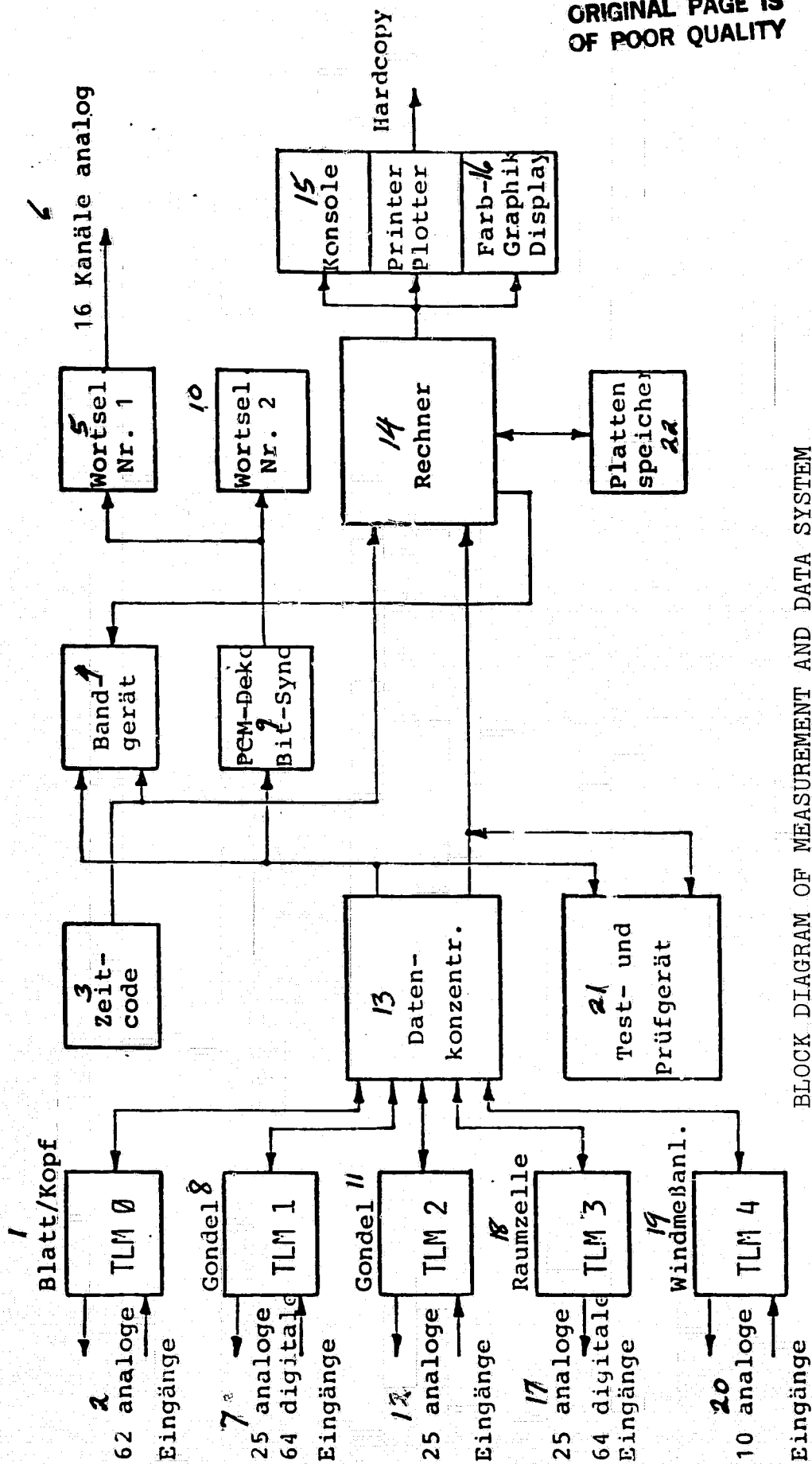
ORIGINAL PAGE IS  
OF POOR QUALITY

9.1.81  
Hb/gro

ground

gondola

# WIND ENERGY GROWIAN DEMONSTRATION FACILITY MEASUREMENT AND DATA SYSTEM



BLOCK DIAGRAM OF MEASUREMENT AND DATA SYSTEM

**ORIGINAL PAGE IS  
OF POOR QUALITY**

KEY TO DIAGRAM ON PRECEDING PAGE

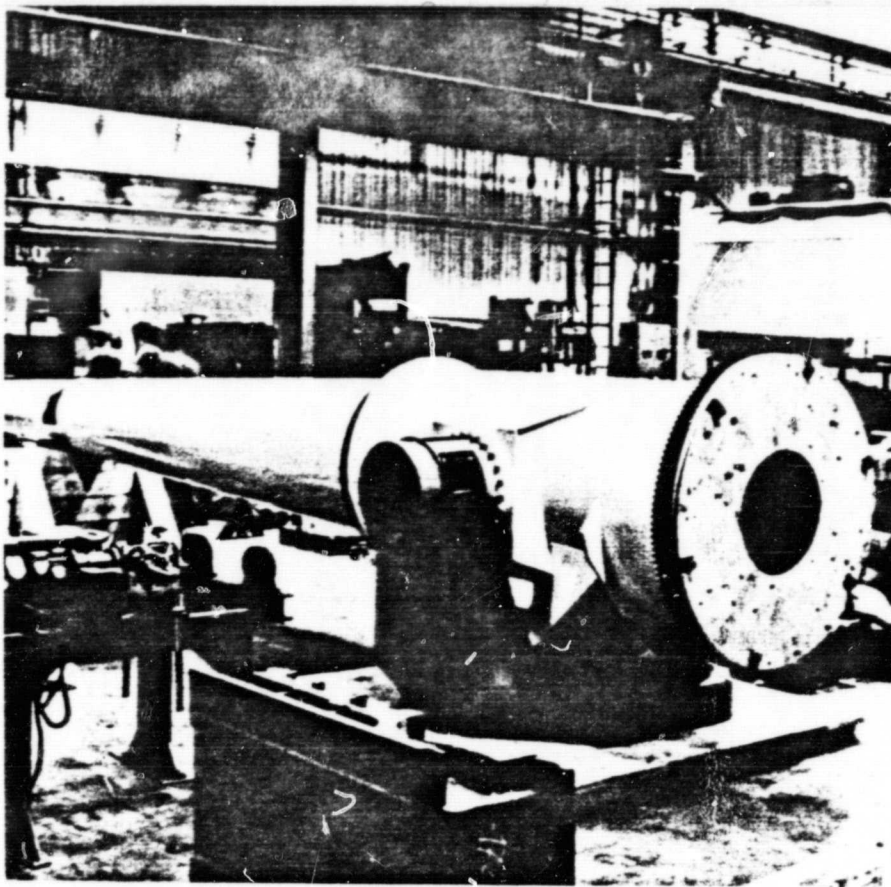
1--blade/head; 2--62 analog inputs; 3--time code; 4--tape machine;  
5--word selection no. 1; 6--16 channels analogs; 7--25 analog 64  
digital inputs; 8--gondola; 9--PCM decoding; 10--word selection no. 2;  
11--gondola; 12--25 analog inputs; 13--data concentration; 14--computer;  
15--console; 16--color graphic display; 17--25 analog 64 digital inputs;  
18--space cell; 19--wind measurement facility; 20--10 analog inputs;  
21--test and monitoring device; 22--disk storage



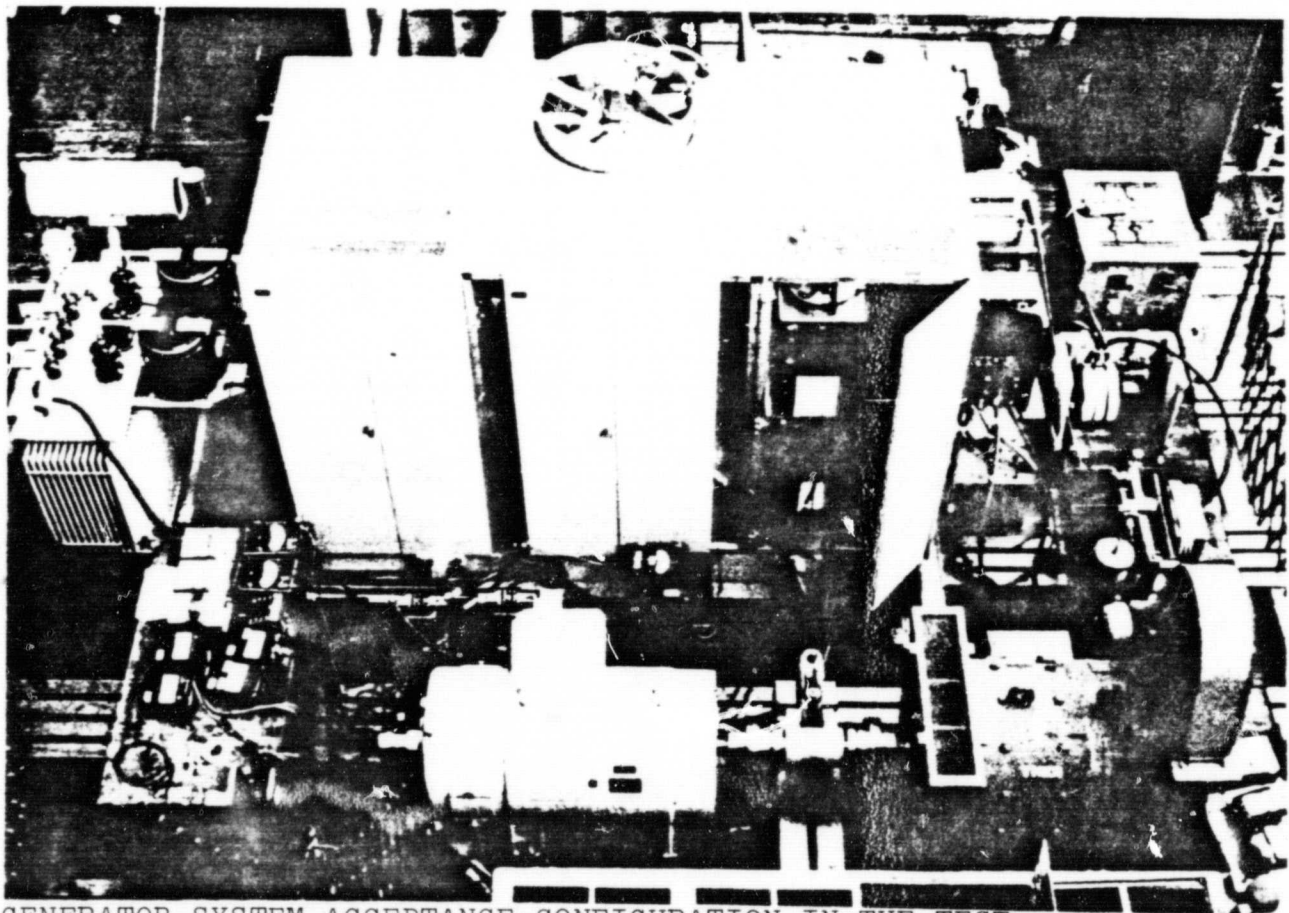
# GROWIAN II DATA

	demonstration facility	full scale facility
rotor diameter (m)	48,33	145
hub ht. (m)	50	120
delivered electrical power at the design point $n_o$ (kW)	370	5000
specific area power ( $W/m^2$ )	ca. 200	ca. 300
rotor hub power at design point (kW)	ca. 407	ca. 5490
design wind speed (m/s)	ca. 10	ca. 11,5
operating wind speed range (m/s)	ca. 5,7 bis 16	ca. 6,6 bis 18
yearly contribution (GW h/a)	> 1,3	> 17
static rpm range (Rad/s)	ca. 4,6 $\pm$ 0,46	ca. 1,8 $\pm$ 0,18
blade tip speed for design rpm (m/s)	ca. 120	ca. 138
fast running coefficients for design wind speed (-)	ca. 12	ca. 12
maximum power coefficient	ca. 0,39	ca. 0,40
blade profiles	Wortmann FX 77 - W-Serie	
blade beginning (circle) at $\frac{r}{R}$	0,05	0,05
largest/smallest blade chord (m) for $\frac{r}{R} = 0.25/\frac{r}{R} = 0.95$	2,33 / 0,56	7 / 1,68
twist, nonlinear (degrees)	ca. 15	ca. 15
rotor axis inclination to horizontal (degrees)	9	9
operational gearing ratio	34,5	ca. 89
Masses:		
total rotor (kg)	5910	ca. 100.000
rotor blade (kg)	1425	ca. 26.000
total gondola (kg)	27880	ca. 300.000

ORIGINAL PAGE IS  
OF POOR QUALITY

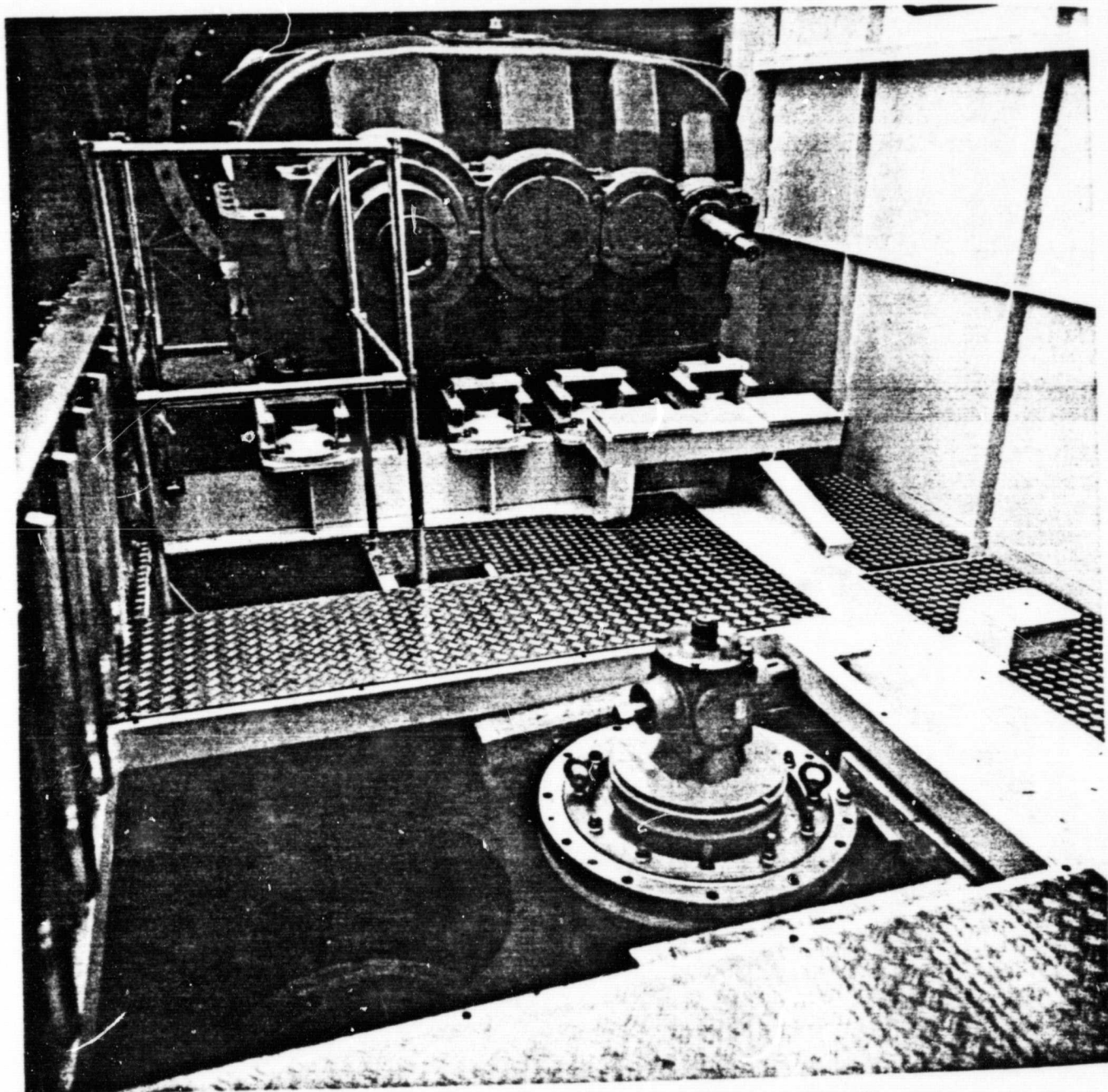


ROTORHEAD OVERALL (DEMONSTRATION)



GENERATOR SYSTEM ACCEPTANCE CONFIGURATION IN THE TEST FIELD AT BBC (DEMONSTRATION FACILITY)

ORIGINAL PAGE  
BLACK AND WHITE PHOTOGRAPH



GONDOLA WITH TRANSMISSION GEAR AND AZIMUTH  
DRIVE (DEMONSTRATION FACILITY)

## OPTIMIZATION OF LARGE WIND ENERGY FACILITIES

John H. Argyris and Kurt A. Braun

Summary

The project was carried out jointly by the University of Stuttgart and the Statics and Dynamics Research Association (m.b.H.) with the supervision of the Institute for Statics and Dynamics of the Aviation and Space Flight Design Department. The currently running phase I of the project started on November 11, 1979 and was extended by six months up to December 31, 1981 within the financial constraints.

During phase I, by developing new computer methods and by building the rotor hub including the data selection systems, conditions will be generated for optimization of large horizontal axis wind energy facilities.

During phase II which will not be discussed in the present report, various rotor concepts will be optimized and compared using the calculation and test tools developed. Figure 12 gives a sketch of the open air facility from the present day point of view.

/190Working points

The OPTIWA project can be structured along three lines:

1. Development of computer programs for the static and dynamics investigation of various rotor concepts.
2. Calculation methods for a new tower concept and design of a model tower.
3. Design and building of a computer control functional model with special rotor hub for simulation of various design and control concepts.

## 1. Development of computer programs

Here computer programs are developed by the computer engineer which allow static and dynamic investigation of various rotor concepts (rigid rotor, pendulum hub, individual flapping and/or deflecting with and without blade feedback, etc.). Precursors for these programs were already developed within the research project on "investigation of rotor stressing and smoothness of operation of large scale and wind energy conversion system" which was supported by BMFT and the IEA (International Energy Agency) (see [1-3]). The programs were tailored to the requirements of the design engineer in order to allow a fast and simple change of characteristic blade data on the monitor (see Figure 1). These are based on finite element packages ASKA [4,5]. Since we will discuss the calculation methods in [6,7], we will not discuss them here.

## 2. Calculation methods for a new tower concept

Under 2, calculation methods are developed and a model tower is calculated for a new kind of tower concept (Stuttgart tower) which is based on an idea of Professor Wortmann [8]. Based on the preliminary investigations in [9], the kinematics of the tower shown in Figure 2 are investigated and a static design is carried out using the nonlinear finite element package LARSTRAN [10]. The dynamic investigations, /191 resonance and responses are also carried out using LARSTRAN (see Figure 3).

The following disadvantages and advantages can be discerned compared with conventional tower concepts:

### Advantages:

- the ground resonance problem is made less important with the rotors under consideration because the thrust--dependent eigen frequency of the lateral oscillation (azimuth oscillation here) is far below the rotating rate and the eigen frequency of the vertical oscillation (pitch oscillation here) can be maintained far below the rotating rate.

- The tower orientation relative to the wind is always the same which allows a static, dynamic and aerodynamic matching of the tower cross sectional geometry.
- The tower will align itself in the direction of the wind without azimuth drive but may need a yaw damping.
- The rotor free wheeling condition is good and the rotor axis can probably be placed horizontally (tower inclination about  $8.3^\circ$ ).
- The tower-rotor blade distance is larger which is favorable for the tower shadow problem.

#### Disadvantages:

- The construction complexity is probably higher than for a conventional tower.

The mast length of the investigated model tower is 15 m and the radius of the base hexagon is 6.5 m. The tower was considered as a space gear with rigid connection rods between spherical joints for the kinematic investigation (see Figure 4). The actual joint at the tower base allows a rotation of the tower around the z axis (yaw) and pitch motions of the tower in the plane defined by it and the z axis. This means that the rotor axis will always be in the direction of the wind. A ring bearing is located at the tower tip which can rotate around the mast, to which ropes are attached. However, neither is important for the kinematic analysis. For a suitable selection of the rope geometry, the mast tip can carry out a circular trajectory around the z axis and the rope will remain tight. Since the tower should also adjust in the direction of the wind for low wind speed (shear forces), the trajectory of the mast tip must be as close as possible to a horizontal circle. With consideration of the required rotor free wheeling condition, the rope geometry was optimized so that the deviation from the circular trajectory with a radius of 2.18 m was only  $\pm 0.1\%$ , which corresponds to a waviness of the trajectory of  $\pm 0.32$  mm in the vertical direction. When installing the tower on terrain which is inclined by  $15^\circ$ , by slightly modifying the rope length, it is possible to maintain the deviation from the circular trajectory with a radius of 2.18 m to within  $\pm 0.12\%$ , which

/192



corresponds to a waviness of the trajectory of  $\pm 0.39$  mm in the vertical direction.

When the anchor point was set at 11 cm, the trajectory curve was again smoothed by extending the base rope by 7.5 cm so that the deviation from an average radius of 2.19 m was only  $\pm 0.55\%$  or  $\pm 1.77$  mm in the vertical direction.

All of the cases mentioned can be looked upon as uncritical, that is, the tower tip runs along a circular trajectory which is perfectly horizontal for practical applications.

However, this is different when a rope fails. For example, if a circumferential rope fails, then the tower has a preferred position provided that no other ropes are torn. The preferred position is opposite the position of the fractured rope.

We still have to investigate the dynamic properties of the tower.

### 3. Computer control functional model

Under 3 a computer control functional model of a horizontal model axis wind generation facility (first without a tower) is designed and built which later on will be used in open air tests. The hub will allow the simulation and testing of design concepts, control concepts and regulation concepts without construction changes because for the optimization task a large number of parameters have to be varied. This can be achieved by the fact that the blades can move arbitrarily and the force control can be achieved as an arbitrary function of measured deformation and load values.

/193

Deflection, flapping and angle of attack are varied independently using hydraulic cylinders. Measurement transducers for angle position, blade root moments and accelerations allow the valuation of the operational state and, therefore, optimum control with a minicomputer. The minicomputer integrated in the rotating system provides nominal values



for the analog hydraulic control system.

The supply of the minicomputer with programs and test parameters is done from the main computer using an optical transmission system without disturbances. Operational data of the rotor are transmitted to the same system to the main computer for processing.

In the laboratory the hub is driven by a controllable hydraulic motor which is also used for power removal as a generator considering phase II of the project.

The work on the computer control functional model can be divided into three points.

### 3.1 Mechanics and hydraulics

### 3.2 Process data processing

### 3.3 Communication between the stationary and rotating system

#### 3.1 Mechanics and hydraulics

Figure 5 gives the structure of the functional model, the individual components are shown in Figure 6, and the complete hub is given in Figure 10.

The rotor shaft is suspended with two ballbearings in a frame. The hydraulic disk brake, the mechanical drive for the gear and the flapping arms with the deflection arms are attached to it. The entire gondola is suspended with four rubber bearings to the test band. The rotor is driven by the hydraulic motor in the present phase I through the gear. During phase II, it can be used as a pump with a power uptake of up to 45 kW. The supply of the hydraulic flapping, the deflection and angle of attack variation in the rotating system is done with an axial hydraulic coupling.

#### 3.2 Process data processing

The diagram of the facility including connections to the external computer are shown in Figure 7. Figure 8 gives the data flow diagram for the rotor.

Two types of signals have to be distinguished. The measurement data are only transmitted from the rotating system to the stationary system. The control information is exchanged between the minicomputer LSI 11/23 and the main computer PDP 11/70. The transmission system is a further development of the system given in [11].

The analog measurement signals are partially amplified and given over to the data collection system. There they are digitalized and are transmitted bit-parallel through optical transmission systems to an XB terminal (see [12]). From here, using the X-bus system, they are transmitted to the main computer or an interactive graphic system. Here they can be stored on a disk or in the main computer, for example, for controlling the facility or for data reduction and they can be graphically represented.

The measurement data can be also transmitted to the minicomputer LSI 11/23 in digital form and can be used very rapidly using programs for controlling the hydraulic cylinder.

The minicomputer and the main computer can communicate through the optoring system when the facility is rotating and the test engineer can intervene into programs of the minicomputer through the graphic system.

### 3.3 Communication between the stationary and rotating system

The supply with hydraulic oil is done through an axial hydraulic coupling, the power supply occurs through sliprings and rotating transformers. The data transmission is done without contact through so-called optorings (see Figure 9). This is a set of plexiglass rings for transmission away from the rotating system and into the system. The individual values are transmitted using infrared diodes bit-parallel. The transmission rate is about 30,000 words/seconds.. The measurement data transmission is already operating satisfactorily on the test stand

because due to the high scanning rate, any errors can easily be detected with soft ware. However, the required reliability has not yet been /195 achieved for communications between the minicomputer and the main computer and the graphic system.

#### REFERENCES

- [ 1] J. H. Argyris, K. A. Braun, B. Kirchgassner: Static investigation of rotor blades with their own weight and for stationary operation. ISD report no. 243, Stuttgart 1979.
- [ 2] J. H. Argyris, B. Kirchgassner: Stability and gravity response of the flapping--deflection motion of a rigid rotor blade with blade angle feedback. ISD report No. 244, Stuttgart 1979.
- [ 3] J. H. Argyris, K. A. Braun, B. Kirchgassner: Dynamic analysis of a rotor blade with no flapping, no deflection and blade angle feedback. ISD report no. 258, Stuttgart 1979.
- [ 4] ASKA UM 202, ASKA Part I, Linear Static Analysis, User's Reference Manual, ISD report no. 73, Stuttgart 1971, Revision F, 1979.
- [ 5] ASKA UM 211, ASKA Part II, Linear Dynamic Analysis, User's Reference Manual, Stuttgart 1974, Revision B, 1979.
- [ 6] J. H. Argyris, B. Kirchgassner: Investigations on the dynamic behavior of wind energy facilities, contribution to the seminar "Building, testing and development of large wind energy facilities within the projects supported by BMFT", 23/24 March, 1981, Munich.
- [ 7] J. H. Argyris, K. A. Braun, W. Lang: Calculation of large rotor blades from the calculation engineer's point of view, contribution to the seminar on Building, Testing and Development of large Wind Energy Facilities with the BMFT projects", 23/24, March 1981, Munich.
- [ 8] F. X. Wortmann: Description of the concepts "Oscillating Wind turbine". Report of the Institute for Aerodynamics and Gas Dynamics, Stuttgart 1977.
- [ 9] J. H. Argyris, K. A. Braun: Static and dynamic investigations of various towers for wind turbines, ISD report no. 261, Stuttgart 1979.
- [10] T. Angelopoulos, F. Iguti, W. C. Knudson: LARSTRAN User's Manual, Large Strain Nonlinear Elastic Analysis, ISD report no. 231, Stuttgart 1978.
- [11] J. H. Argyris, W. Aicher, F. Karl, W. Kuemmerle, M. Mueller: Rotor model for verification of computer methods, ISD report 262, Stuttgart 1979.
- [12] J. H. Argyris, W. Aicher, M. Mueller: "XB experimental BUS system", development of a universal computer controlled multiuser test control system, ISD report 200, Stuttgart 1977.

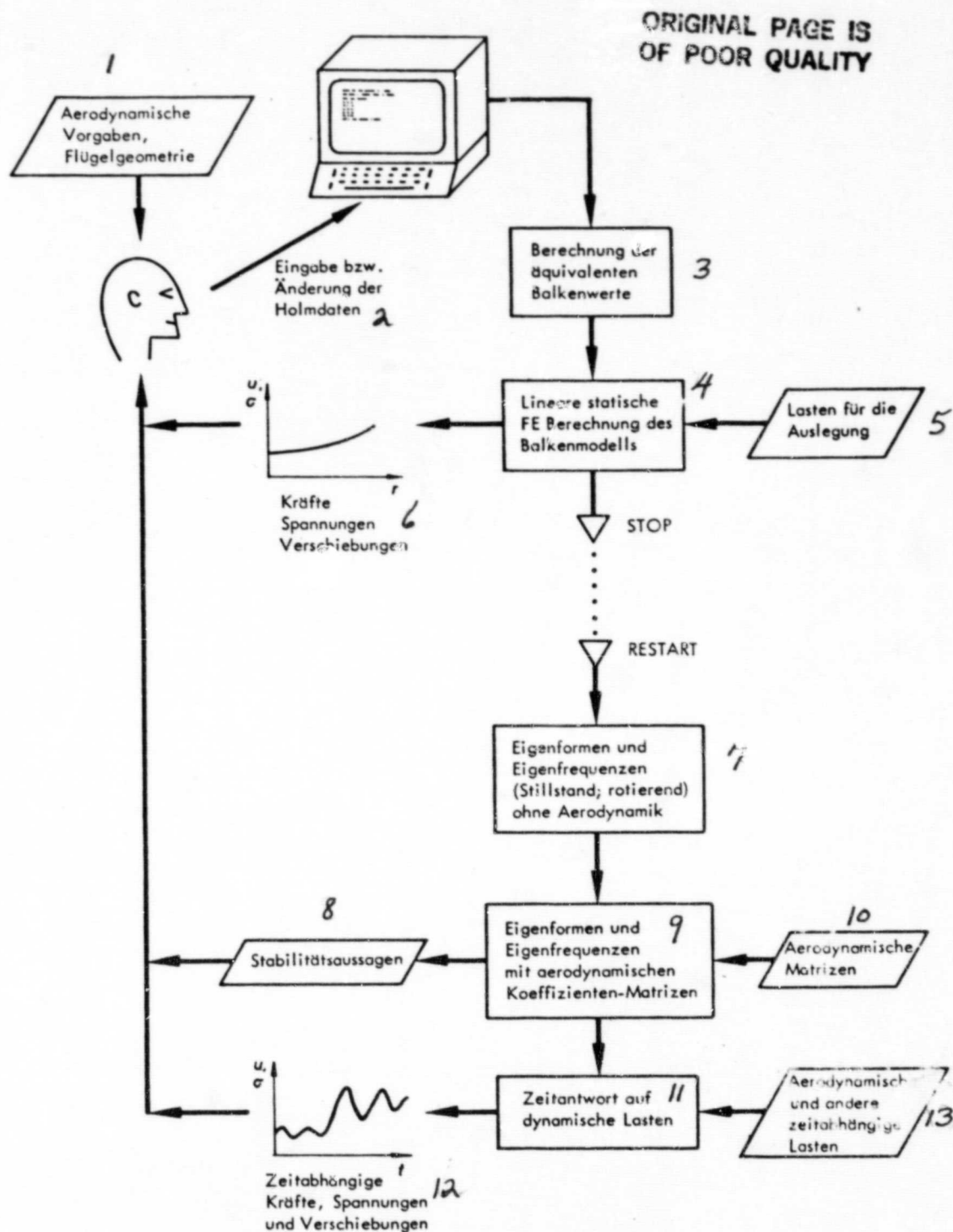


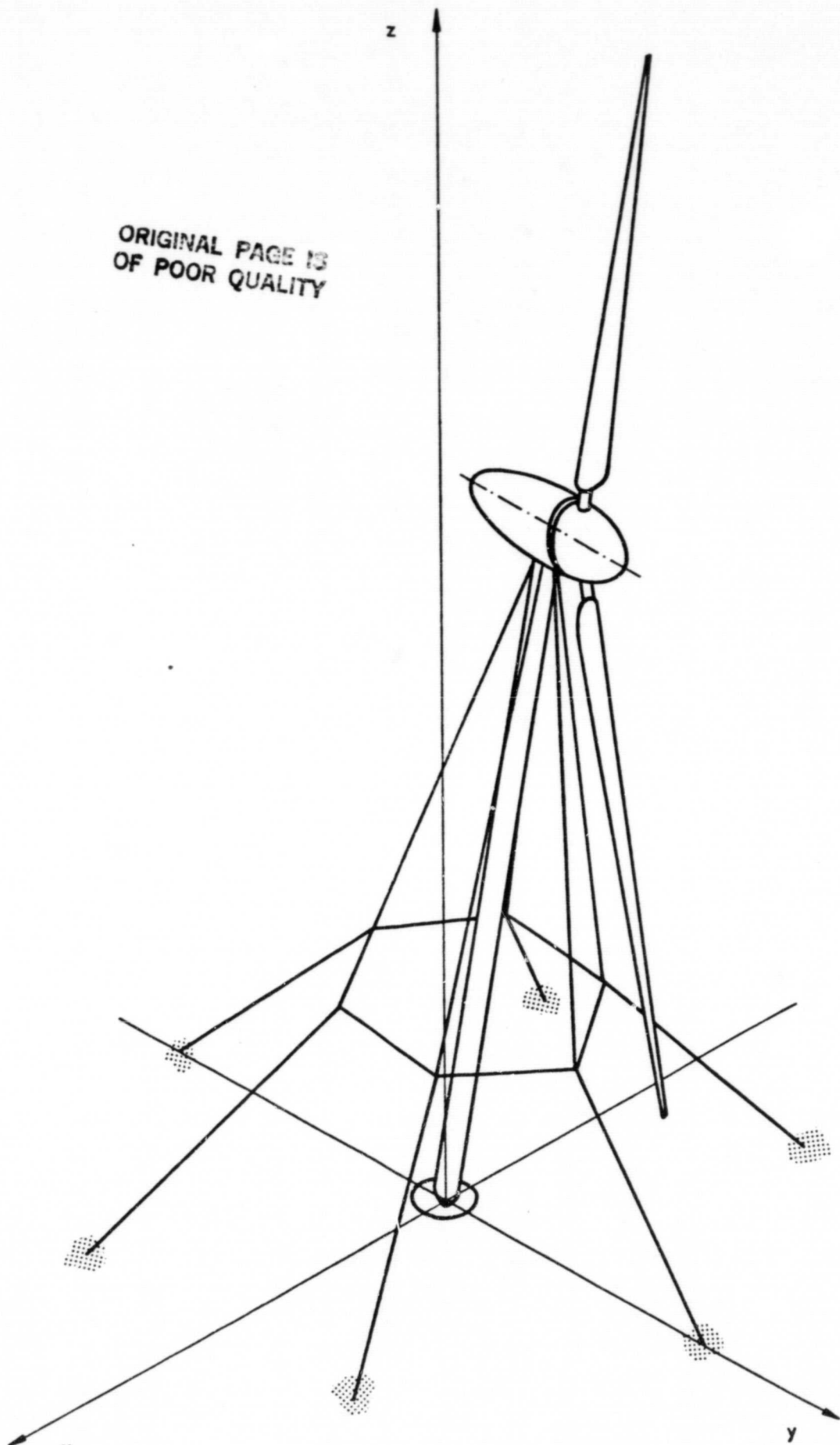
FIGURE 1. BLOCK DIAGRAM FOR LINEAR ROTOR BLADE CALCULATION

ORIGINAL PAGE IS  
OF POOR QUALITY

KEY TO FIGURE 1 ON PRECEDING PAGE:

1--aerodynamic data, wing geometry; 2--input and change of spar data;  
3--calculation of equivalent beam values; 4--linear static FE calculation of beam models; 5--loads for design; 6--forces, stresses, displacements; 7--eigen modes and eigen frequencies (at rest, rotating without aerodynamics); 8--stability data; 9--eigen modes and eigen frequencies with aerodynamic coefficient matrices; 10--aerodynamic matrices; 11--time response to dynamic loads; 12--time dependent forces, stresses and displacements; 13--aerodynamic and other time dependent loads.

ORIGINAL PAGE IS  
OF POOR QUALITY



x      y      z  
FIGURE 2. STUTTGART TOWER INCLUDING WIND TURBINE

Nonlinear static and dynamic test methods

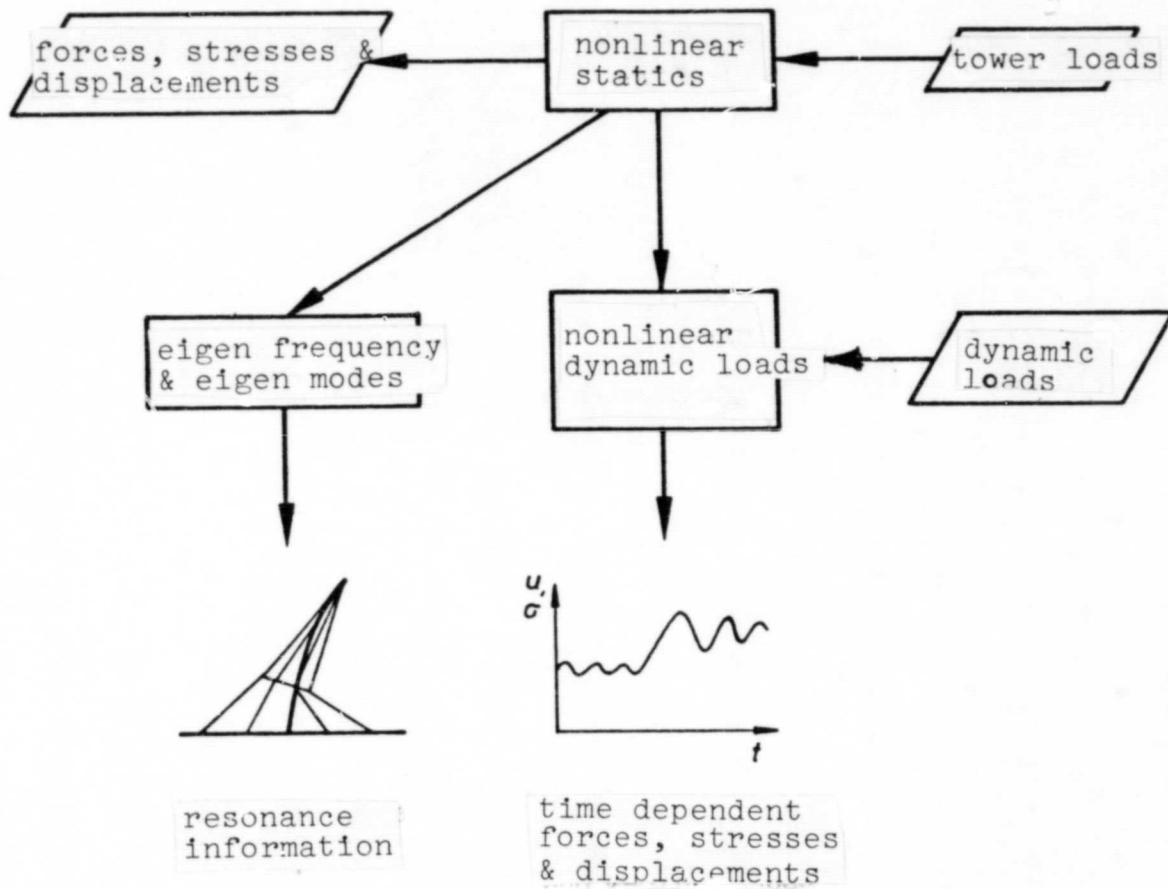


FIGURE 3. BLOCK DIAGRAM FOR CALCULATING THE STUTTGART TOWER



ORIGINAL PAGE IS  
OF POOR QUALITY

- o optimization of geometry
- o incorporation in inclined terrains
- o setting and the anchor
- o rope failure

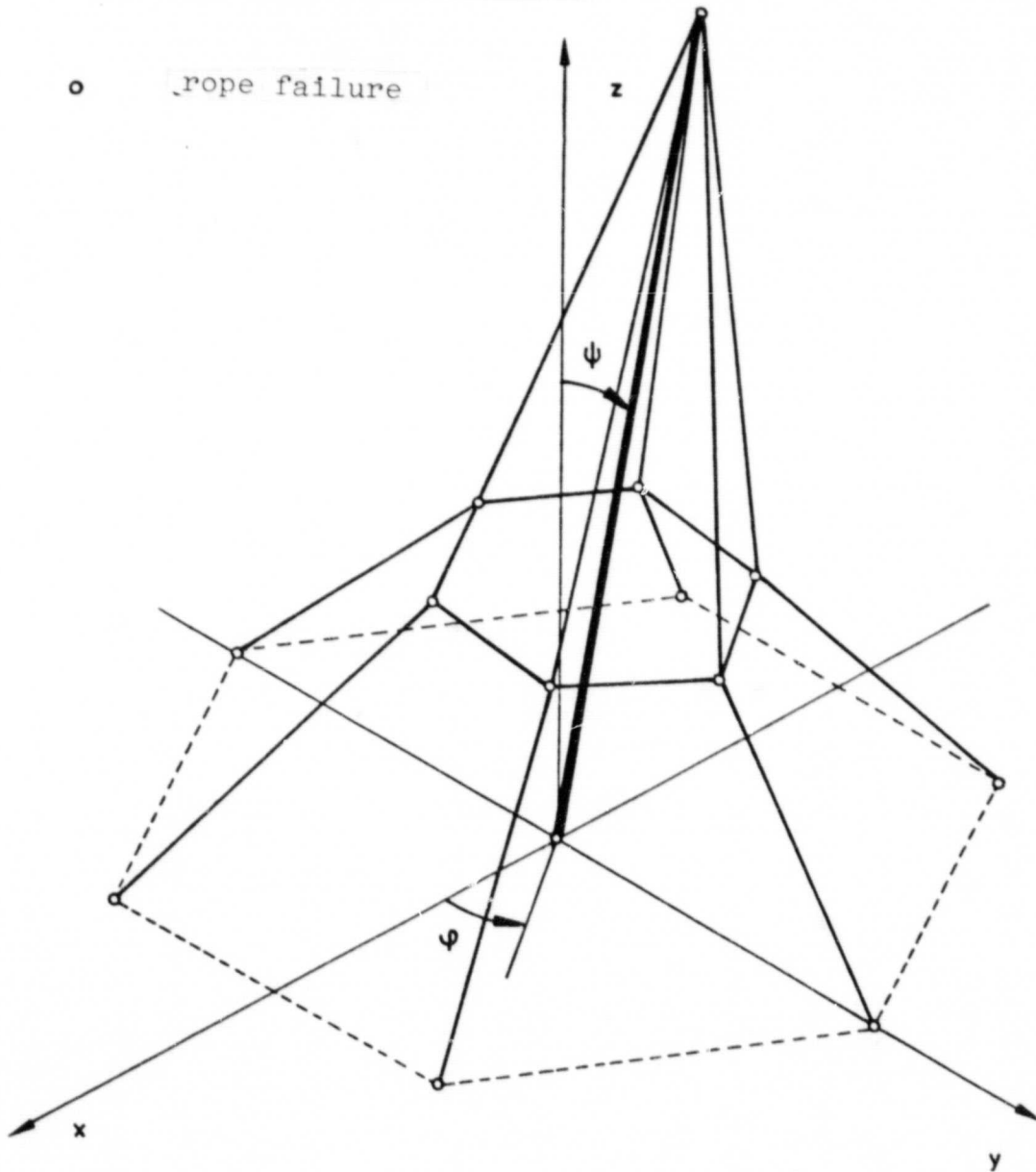
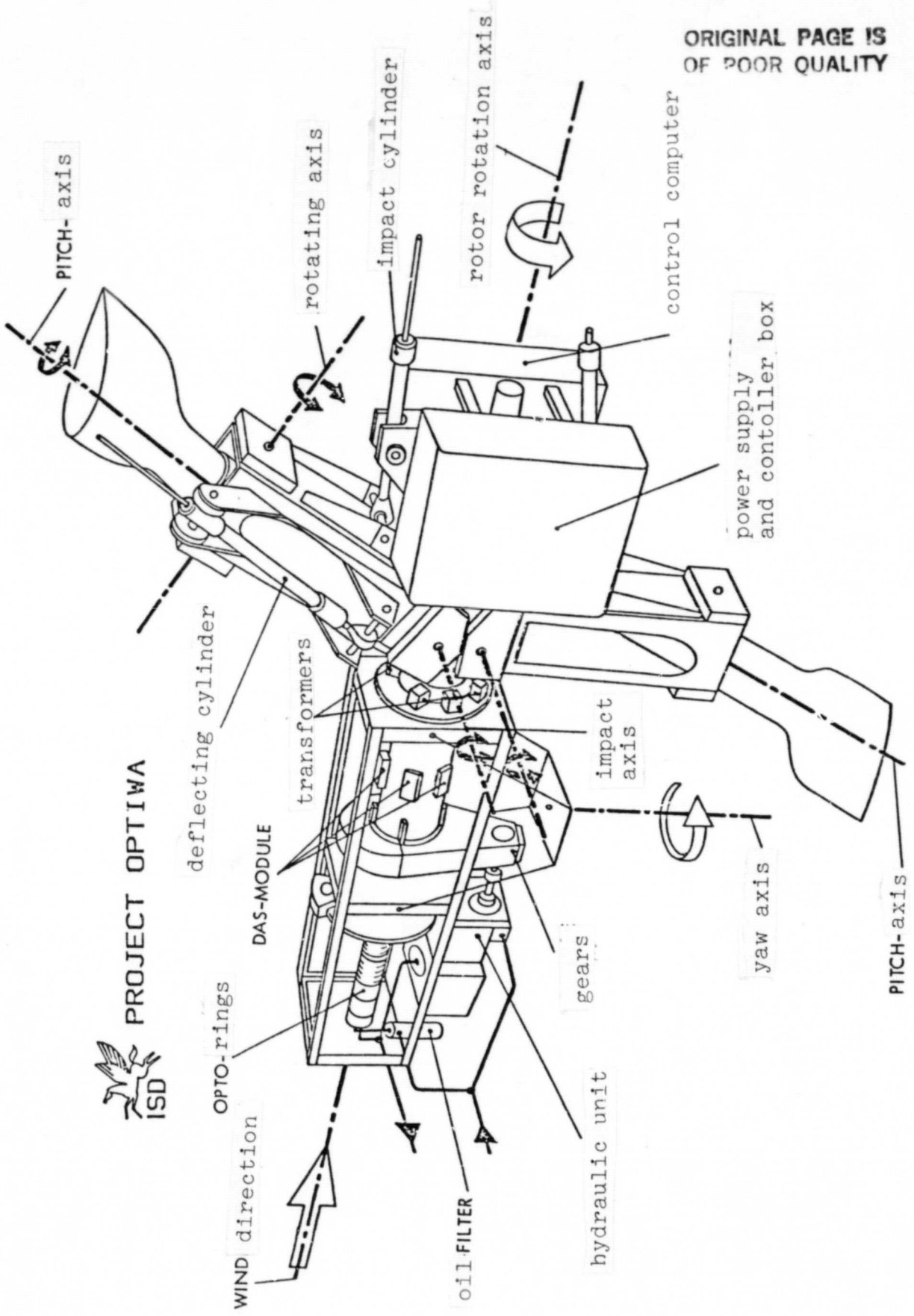


FIGURE 4. KINEMATIC INVESTIGATIONS ON THE STUTTGART TOWER  
(page 201)



ORIGINAL PAGE IS  
OF POOR QUALITY

FIGURE 5. STRUCTURAL OF FUNCTIONAL MODEL (1,FEWARD VIEW)

ORIGINAL PAGE IS  
OF POOR QUALITY

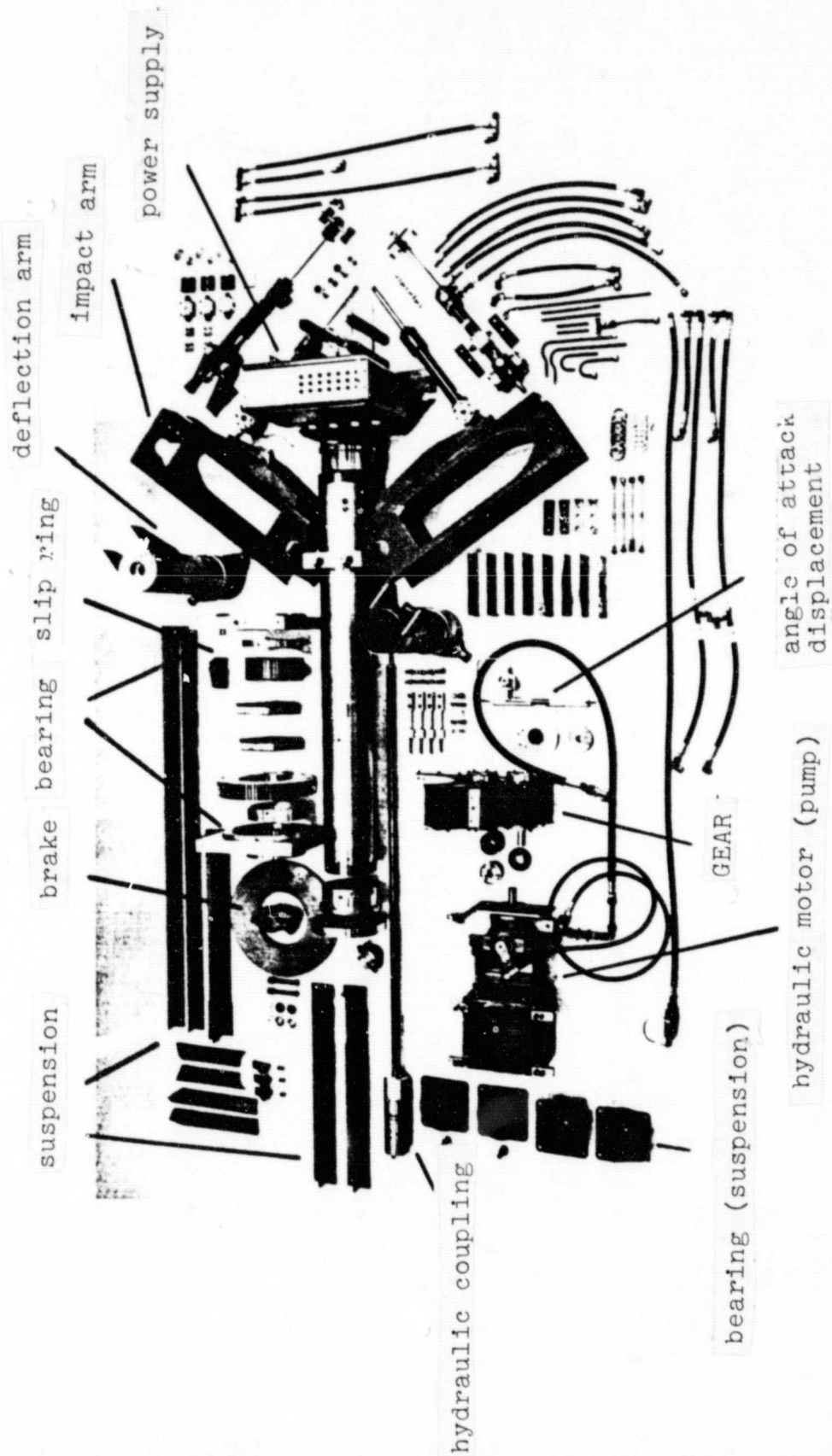


FIGURE 6. INDIVIDUAL COMPONENTS (HYDRAULICS, MECHANICS)

ORIGINAL PAGE IS  
OF POOR QUALITY

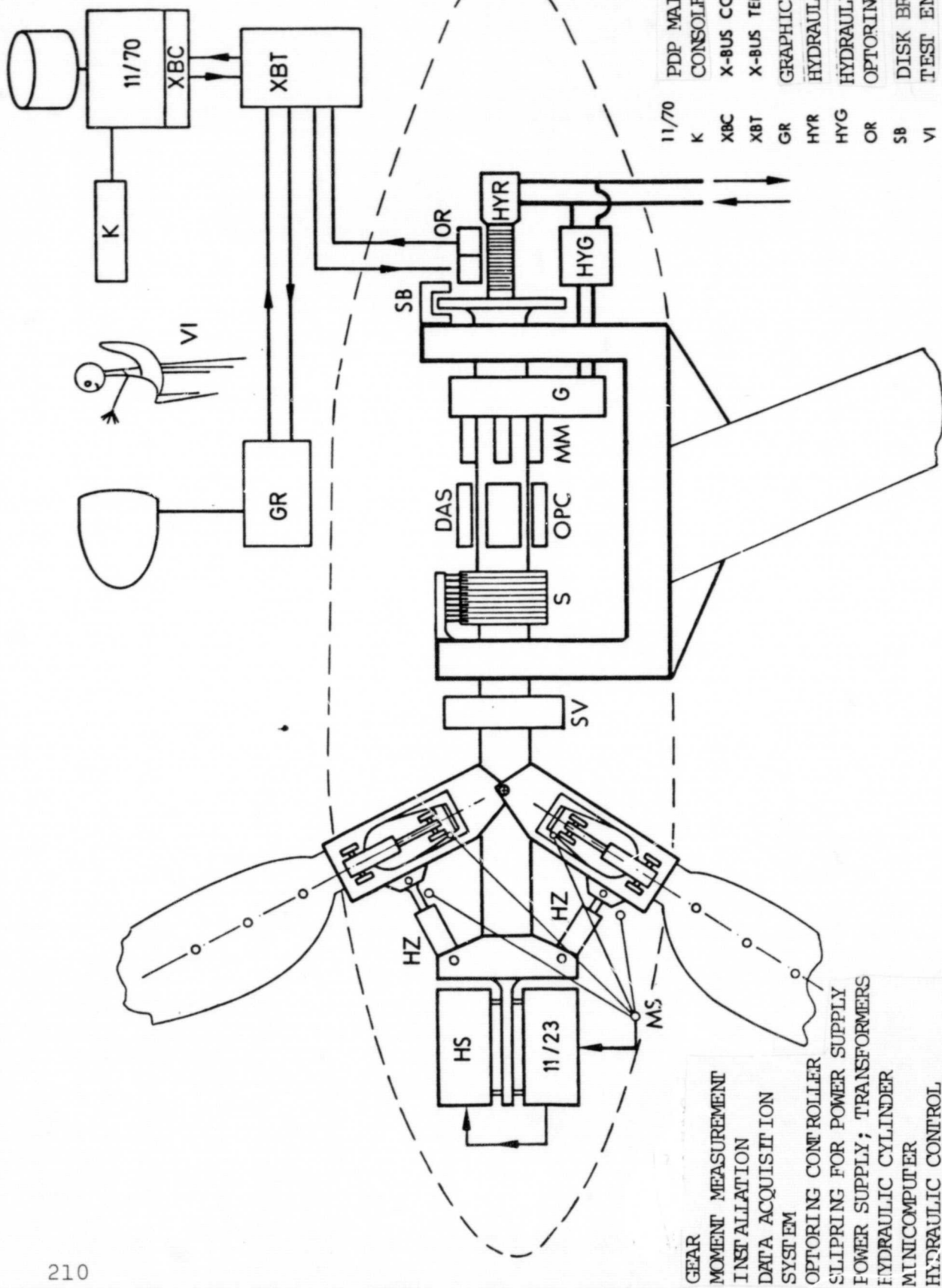


FIGURE 7. SCHEMATIC VIEW OF FACILITY

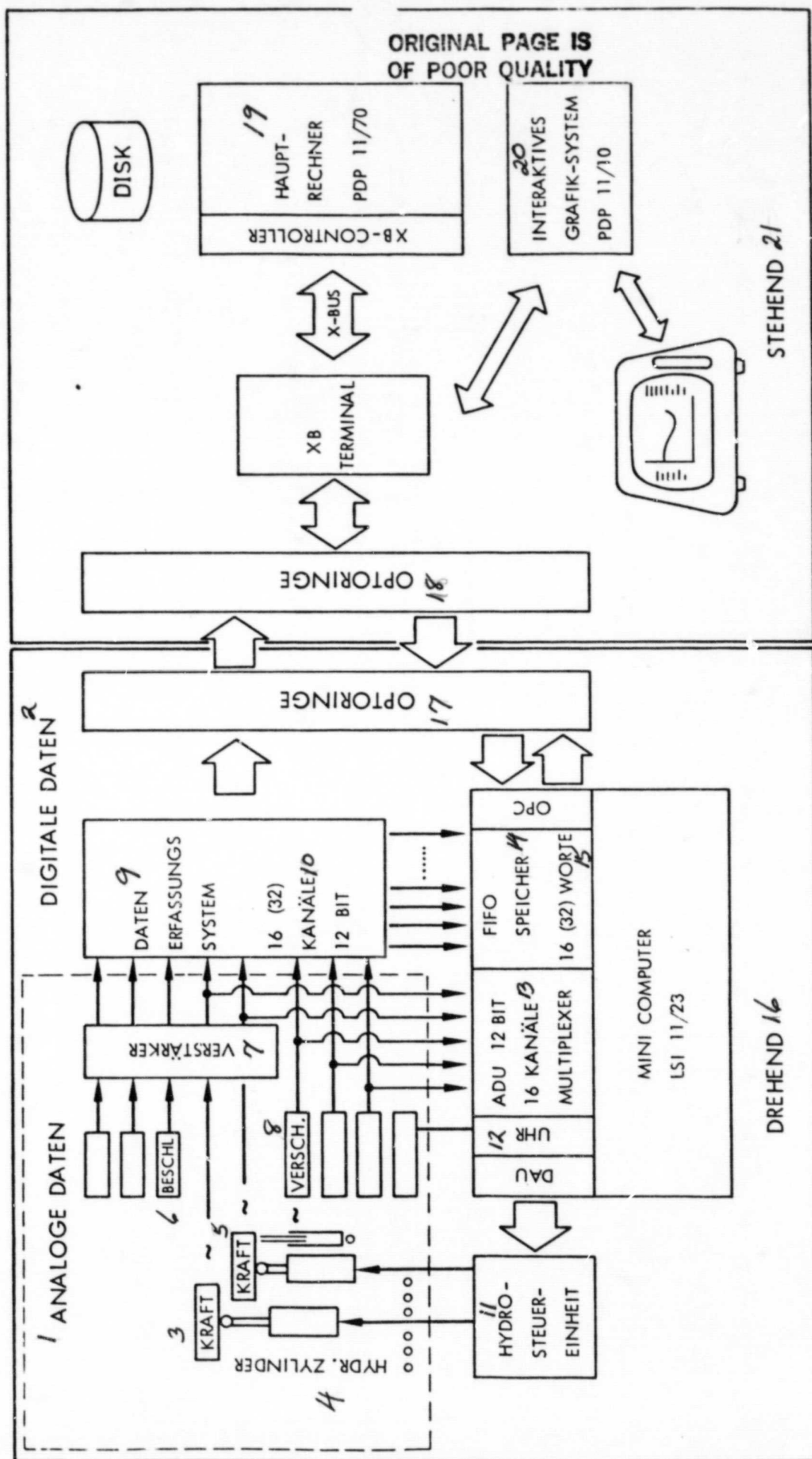


FIGURE 8. DATA FLOW DIAGRAM FOR THE ROTOR

ORIGINAL PAGE IS  
OF POOR QUALITY

KEY TO FIGURE 8 ON PRECEDING PAGE:

1--analog data; 2--digital data; 3--force; 4--hydraulic cylinders;  
5--force; 6--acceleration; 7--amplifier; 8--displacement; 9--data  
acquisition system; 10--channels; 11--hydraulic control unit;  
12--clock; 13--channels; 14--memory; 15--words; 16--rotating;  
17--optorings; 18--opt@rings; 19--main computer; 20--interactive  
graphic system; 21--at rest



ORIGINAL PAGE  
BLACK AND WHITE PHOTOGRAPH

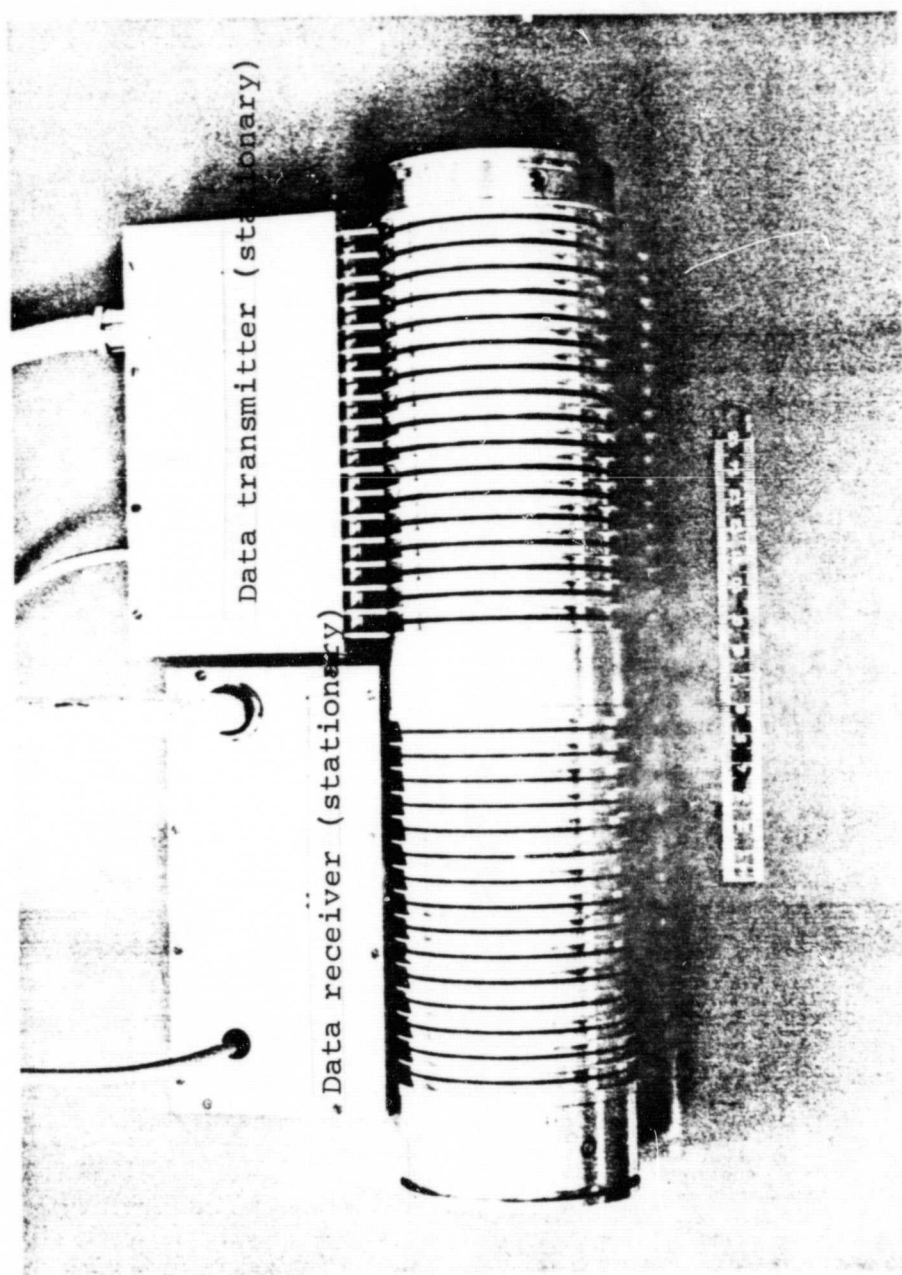


FIGURE 9. OPTORING TRANSMISSION UNIT



ORIGINAL PAGE  
BLACK AND WHITE PHOTOGRAPH

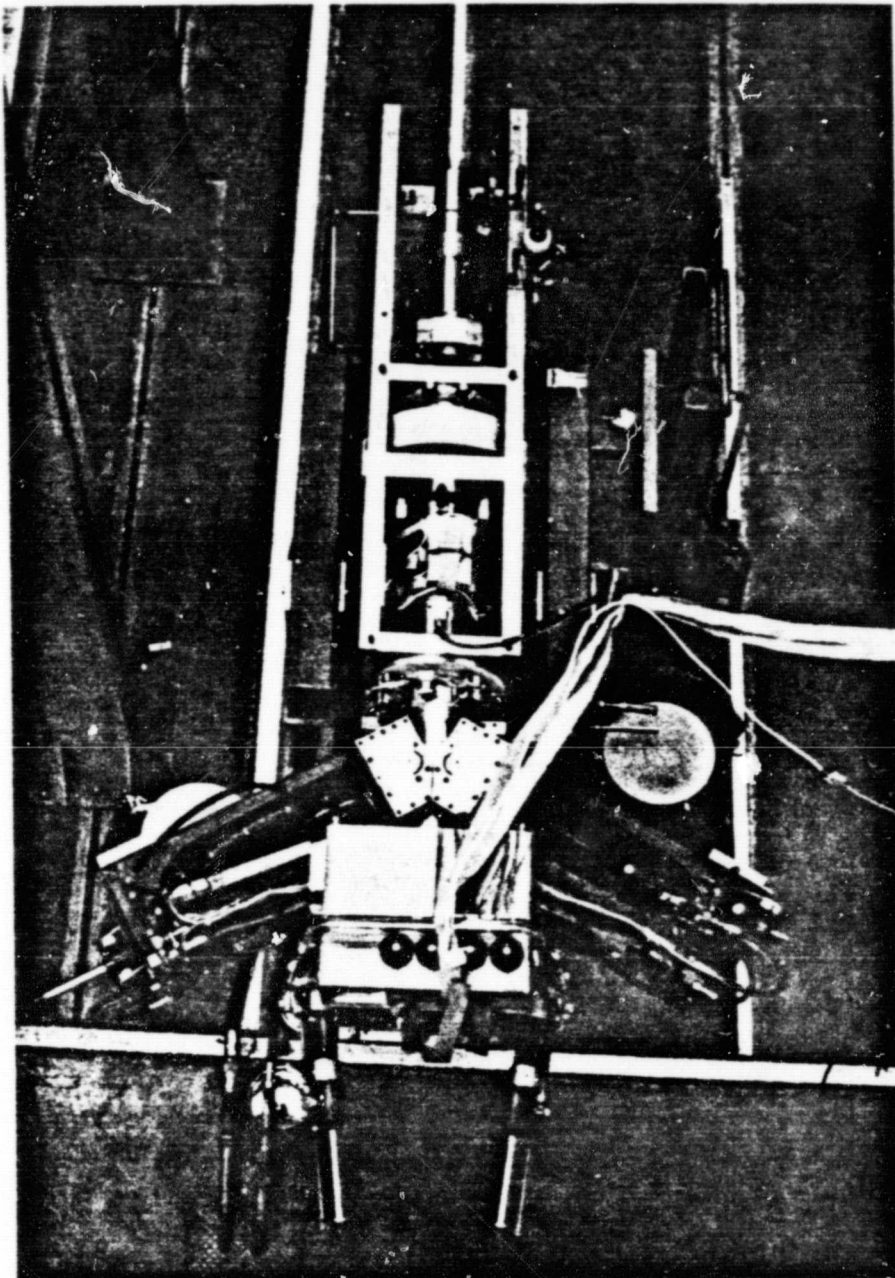


FIGURE 10. FACILITY WITHOUT BLADES ON ASSEMBLY DEVICE

ORIGINAL PAGE  
BLACK AND WHITE PHOTOGRAPH

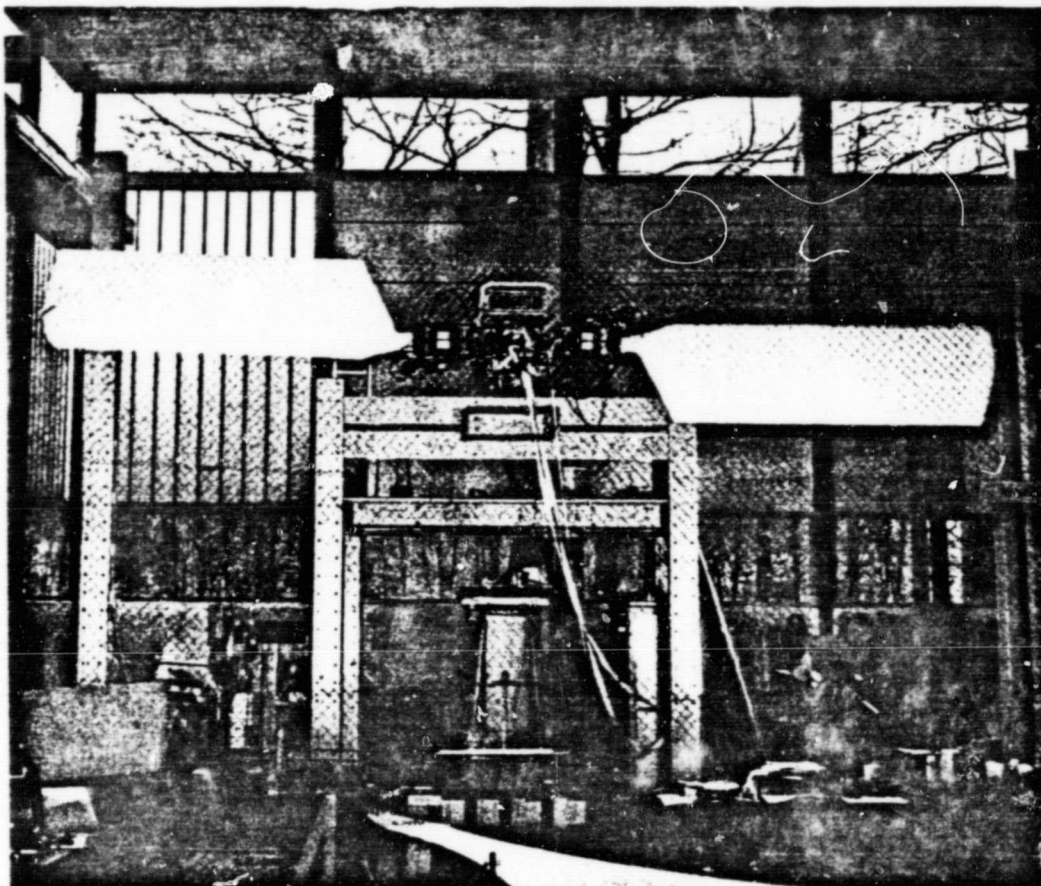


FIGURE 11. TEST STAND OF FACILITY (HALL MODEL)

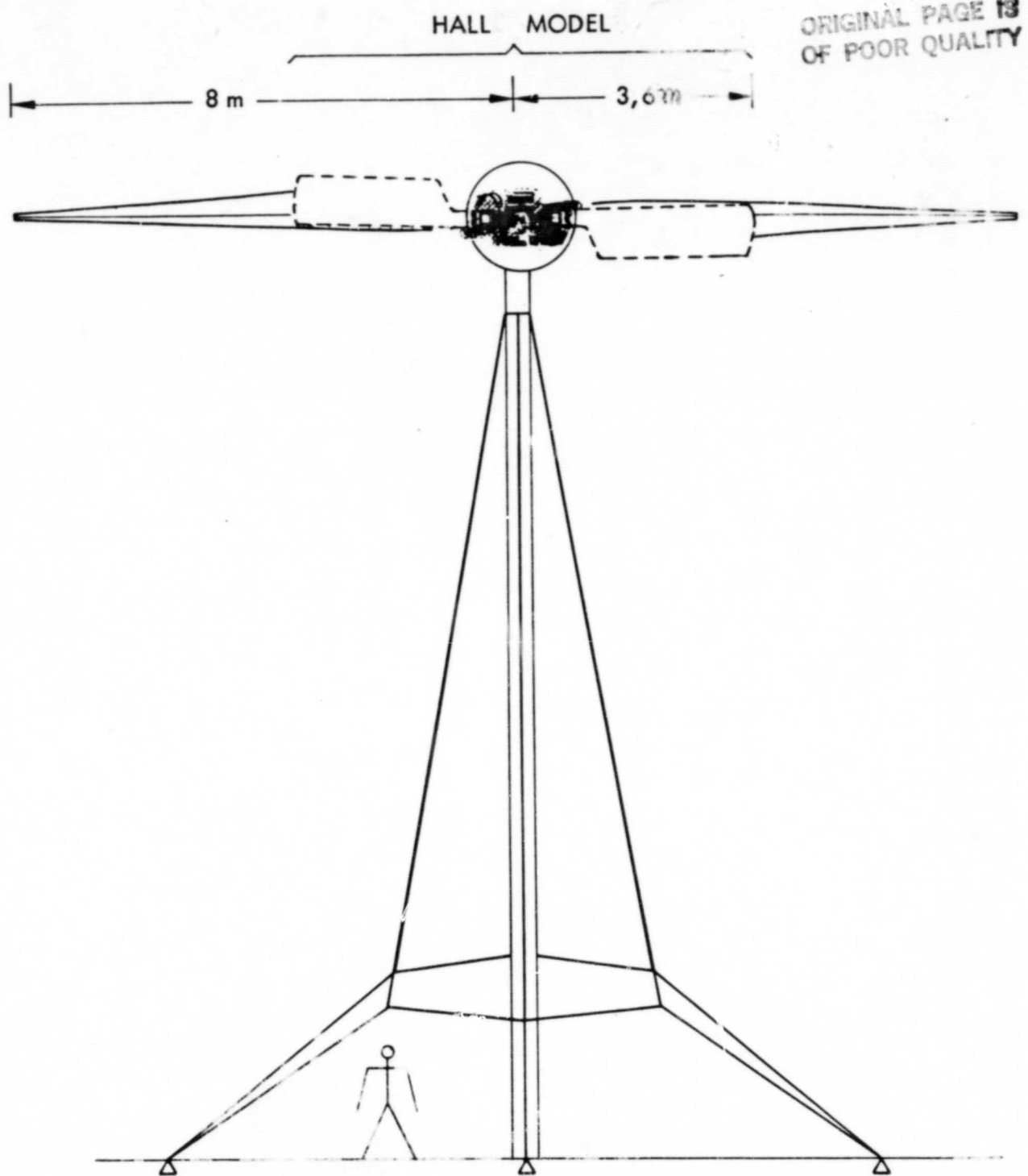


FIGURE 12. SIZE COMPARISON BETWEEN HALL MODEL AND  
PLANNED OPEN AIR DESIGN ON THE STUTTGART TOWER

Project No. ET 4372 A

G. A. Walter, F. X. Wortmann

1. Goals

A gust generator is used to produce reproducible gusts in time or in space with variable frequency, amplitude and spectral distribution in order to follow the responsive wind turbine models of suitable size.

2. Working program

First of all, experimental investigations were performed with a model tunnel in order to not excessively load the drive blower in spite of gust excitation. Special attention has to be given to the avoidance of possible tunnel resonances. The development of production data and contract awards occurs after the information has been collected. An investigation program in parallel with the manufacturing process is used to clarify the behavior of wind turbine models under gust loads and comparisons with theory are made.

3. Status (end 1980):

A model has been built with which experiments on the mechanism of gust production and the reduction of the unsteady additional loads for the blower can be performed. The knowledge obtained allows the development of planning and design data for defining the project. After tenuous and extensive discussions with competing firms, the contract was let for building the gust tunnel. At the present time the final documents, position documents, foundation documents and detail plans are being finished for guaranteeing the scheduled beginning of construction in the spring of 1981.

In parallel with this, computer programs are being developed for the numerical treatment of gust problems of wind turbines, in order to make comparisons with the subsequent investigation programs and their measurement data.

/210

#### Abstract:

The task definition for the gust generator now being built at the Institute for Aerodynamics and Gas Dynamics of the University of Stuttgart, consisting of the gust wind tunnel and the gust grid, includes the production of reproducible gusts with variable frequency, both in space and time with variable amplitude and spectral distribution. This is in order to determine the dynamic behavior of wind turbine models of suitable size.

A direct comparison between the measured values and results from the numerical treatment of gust problems then becomes possible. We then have an important instrument for testing computer programs, theories and assumptions and we can obtain direct information and functional control of various control concepts for the model rotor with consideration of all of the degrees of freedom.

The gust tunnel is designed as open Eiffel type and is determined by important model law requirements as far as dimensions are concerned. The gusts are produced by a gust grid attached to the beginning of the measurement chamber, using actuation wings which can be set at different settings according to gust type. An external cylinder ring chamber over the measurement chamber allows one to generate flow around obstacles with a large streamline extension.

/211

#### THE GUST GENERATOR AT THE INSTITUTE FOR AERODYNAMICS AND GAS DYNAMICS OF THE UNIVERSITY OF STUTTGART

##### 1. Introduction

Experience in the past has shown that at the present time it is not possible anywhere in the world to build large wind turbines which

are characterized by high operational safety and high lifetime as well as by simplicity and low investment costs.

If one follows the development of the research of these very complex machines, then one finds that often one proceeds directly to tests on full scale designs and this is related to the associated technical and financial risks. The results are not yet convincing because these machines are subjected not only to the enormous destruction potential of storms, but also to the continuously changing loads due to turbulence and gusts of a natural atmospheric wind. This requires detailed research under control and defined conditions in suitable wind tunnels.

For this project, it would seem that the use of low speed tunnels of conventional design would be suitable. Model rotors have very exact requirements in terms of design size and because of their high drag under loads they represent a large blockage to the tunnel.

In addition to the required measurement cross sections, substantial large changes are to be superimposed on the air stream in order to simulate typical gusts. At the present time, no such facility is available. /212

In the following we give a brief description of the gust generator.

## 2. Task and goals of the gust generator

In order to investigate the complex behavior of individual systems and the entire system of wind turbine models which allows transfer to full scale designs, a gust generator is being built at the Institute for Aerodynamics and Gas Dynamics of the University of Stuttgart.

The facility consists of a gust tunnel and a gust grid and is used to produce various kinds of reproducible gusts. These can be specified in terms of a space structure and a time structure with variable frequency, amplitude and spectral distribution.

Direct comparisons of various rotor concepts and their operational strategies and important comparisons between measured values and results from numerical analysis of gust problems become possible. This represents a high powered instrument for testing computer programs, theories and assumptions. In contrast to calculations, it is possible to consider all of the degrees of freedom of the dynamic system. Parameter investigations, functional controls and testing of different control concepts of the rotor model can be carried out with minimum risks.

/213

### 3. Design of the gust generator

The important data about the design of the gust tunnel, for example, measurement chamber diameter, speed and, therefore, power requirements, can be specified from the investigations of important model requirements. In order to have a meaningful transfer of measured results and experiences of the model motor to full scale designs, it is important to consider the characteristic coefficients. A detailed analysis is found in [1], [2]. An analysis of the special case of pure flapping motion of rotor blades is given in [3].

#### - Reynolds number

The Reynolds number is an important parameter for describing dynamic similarity of flows. If the same blade tip speed is maintained, the Re number referred to the profile chord should not be less than  $2 \cdot 10^5$ . A 4 m model rotor should achieve values which are about  $3 \cdot 10^5$ . This seems to be all right as far as the flow behavior is concerned.

#### - Mach number

The Mach number at the blade tip reaches values of about 0.3. Therefore, its importance is negligible.

#### - Froude number



This describes the influence of the gravity on the rotor. If other similarity laws are not to be violated, then equal Froude numbers of the model and the full scale version do not have to be maintained.

- Lock number

This parameter establishes the relationship between the moments applied to the rotor blade by the aerodynamic forces and centrifugal forces. This number in general can be maintained without great difficulty and does not give a minimum lower limit to the size of the model rotor.

/214

- Aeroelastic similarity

The aeroelastic similarity of the full scale version and the model rotor requires equal Strouhal and Cauchy numbers. Maintaining this requirement requires a great deal of complexity, but should be possible with model rotors with a diameter of 4 m.

- Free wheeling number

The ratio of blade tip speed and wind speed should be maintained for a true model gust excitation. This then leads to the derivation of relatively low speeds of about 15-20 m/s.

- Gust excitation

The controlling quantity here is the dimensionless time  $\tau = \Omega \cdot t$ . It should be maintained constantly. However, if the same blade tip speed of the model rotor and the full scale version is required, then for a decreasing size model this means an increase in the rotor rotation frequency  $\Omega$  and, therefore, a reduction in the gust-specific time  $t$  for example. For the gust grid, however, one very rapidly reaches the technical limit at the rotational frequency of the actuating fins. This implies a lower model rotor size.

#### 4. Technical description of the facility

##### - Location

The university area at the Institute for Aerodynamics and Gas Dynamics in the area of the laminar wind tunnel already in existence has been selected as the place to set up the gust generator. The position is protected against natural wind by buildings and forests.

##### - Facility components

The following main components characterize the gust generator and can be seen in Figure 1 with the most important dimension:

- measurement chamber with installations
- gust grid
- blower unit
- diffuser

The project is divided into two individual projects in terms of organization and execution. The gust tunnel consisting of the measurement chamber, blower unit and diffuser were let as a contract to a firm.

The construction of the gust grid is being carried out within the facilities of the Institute for Aerodynamics and Gas Dynamics.

##### 4.1 Measurement chamber with installations

Air is sucked in from the free atmosphere through a nozzle into the measurement chamber. In the measurement chamber the flow has the possibility of flowing around an obstacle with large streamline expansion, by evading into the ring space between the slotted measurement chamber inner wall and the external housing wall. The permeability of this internal wall can be varied widely by displacing U profiles on tracks. The cross sectional area of the outer cylinder ring space is almost of the same size as the cross sectional area of the internal measurement chamber space.

The flow is achieved which is as close as possible to reality. If one compares the relatively reduced power requirement, an average flow speed of 17 m/s is achieved.

Protection grids are planned at the nozzle inlet and at the head of the lower wheel.

The model rotor is supported on a separate foundation socket in order to uncouple the oscillations from the measurement chamber.

#### 4.2 Gust grid

The gusts are produced by a gust grid installed at the beginning of the measurement chamber and according to gust type, it has different configurations and controlled actuating wings. The flow behavior for the closed grid for unloaded wind turbines is shown schematically in Figure 1. How the flow enters the cylindrical ring space for open grid wing position and highly loaded model rotors is shown in Figure 2.

The conditions can be easily described with a measurement chamber cross section perpendicular to the channel axis as can be seen in Figure 3. The cross sectional area available to the flow is seen and the cross sectional area of the evasion ring space is about the same as the cross sectional area of an internal measurement chamber space. The area influenced by the gust grid is about  $1/4$  of the total cross sectional area.

It is natural to ask the question as to which goals of artificial gust production are to be achieved by a gust mechanism. For present problems in the case of wind turbines, there are close relationships between aerodynamics, structural dynamics and control. The exact simulation of the wide spectrum of the natural wind, its gustiness and the related stochastic properties are secondary for the most part. Instead, a reproducible and deterministic gust specification with defined energy density is very important, that is, with defined amplitude, frequency, structure, spectral density, etc.

The following grid configurations are suggested for the realization of characteristic gust shape in the gust tunnel:

- Longitudinal global and local gusts

Radially arranged actuating wings with symmetric circular arc cross section which are maintained by a wing structure can cause single or permanent longitudinal velocity fluctuations by changing the angle of attack (see Figure 4). The drive of the actuated wing is done within the wing ring.

- Lateral global and local gusts

Parallel arranged actuated wings with profile cross section which are also held by a ring wing structure produce single or permanent velocity fluctuations with one component perpendicular to the tunnel axis by changing the angle of attack. Compare Figure 5. The drive for the actuated wings is most simply installed in the middle stiffening rib.

Both configurations have an increase in the blocking degree of the gust grid with the possibility of flow in the wing ring. At the present time about 50% of the measurement chamber internal cross sectional area is used as the flow ring area in order to maintain the unsteady load due to pressure fluctuations as small as possible on the lower runner wheel. Also the required minimum model size must be maintained. The air mass to be accelerated and delayed for this gust generator design has to be held to about 25% of the air mass in the gust tunnel. /218

It is apparent that it is very important to have good flow around the ring wing structure. Therefore, tests with a grid model were made in a water tunnel in order to clarify questions such as profile selections, profile angle of attack, maximum permissible blockage and flow separation in the steady case.

In order to simulate the rotationally symmetric case for pure longitudinal global gusts, a NACA 0012 profile with 6 actuated wings

in the opposite direction were used in the model as the wing ring structure. The position angle of  $0^\circ$  corresponded to the open position. A position angle of  $90^\circ$  amounted to practically 100% blockage of the wing ring internal cross sectional area.

The incompressible flow processes are made visible using colored probes. The achievable Re numbers were in the range  $2 \cdot 10^4 - 6 \cdot 10^4$ .

Figures 6-9 give an impressive of the steady case for a ring wing position of  $\alpha_{RF} = 0^\circ$ , referred to the undisturbed flow. For angles of  $\alpha_{St} > 20^\circ$ , the flow separated.

#### 4.3 Blower unit-

The runner wheel supported on both sides is driven by a hydromotor without intermediate gear. The hydraulic units and the 315 kW 3-phase motor are installed underneath the blower unit in the foundation socket. The blower running wheel has a diameter of 5.6 m and consists of 8 individual running blades made of high quality spherical casting. They can be adjusted when standing still. It achieves a maximum circumferential speed of about 56 m/s. This means that the noise development can be looked upon as being minimum.

Both for reasons of costs and because of testing, we decided for rpm control of the runner wheel using hydraulics. This design has substantial hydraulic disadvantages. However, in addition to avoiding network feedback, for example, which occurs by operating with 3-phase current and a rectifier, hydraulic control has the important advantage for testing of a higher switching possibility and a faster braking of the runner wheel.

#### 4.4 Diffusor

Downstream of the blower there is pressure recovery in a diffusor. For cost reasons, the diffusor length had to be limited to 8.7 m for an area ratio of inlet/outlet area of 1:1.75. A rolling door is the shutoff at the end of the diffusor.

/219

## 5. Status of the work

The planning, position plan, foundation plan and detail plans of the gust tunnel are now ready.

The blower and the facility elements are already being manufactured.

At the present time, contract work on the foundations is being advertised. We count on the beginning of assembly in September 1981 and start up of the gust tunnel in the spring of 1982.

/220

## References

- [1] F. X. Wortmann: "A gust generator for wind turbines". University of Stuttgart, Institute for Aerodynamics and Gas Dynamics report no. 79-6, Stuttgart 1979.
- [2] F. X. Wortmann: A wind tunnel and gust generator for wind turbines". Report of the 6th Meeting of the Executive Committee of the IEA Implementing Agreement for Cooperation in the development of large scale Wind Energy Conversion Systems, London, Sept. 22, 1980.
- [3] S. Mickeler: "An analysis of the individual flapping freedom with coupled blade angle feedback of two blade rotors in synchronous operation". University of Stuttgart, Institute for Aerodynamics and Gas Dynamics report no. 79-24, Stuttgart 1979.

/221

## Appendix

- Summary about the most important technical data
- Figures

## Summary about the most important technical data

/222

- Data on the measurement chamber
  - internal diameter of the measurement chamber inner space 6300 mm
  - cross sectional area of measurement chamber inner space 31.2 m<sup>2</sup>
  - general diameter of measurement chamber housing 8700 mm
  - cross sectional area of measurement chamber housing about 59.5 m<sup>2</sup>

- measurement path length 6500 mm
  - inlet nozzle length 1500 mm
  - perforation of measurement chamber internal wall about 15-20%
  - external diameter of gust grid about 4200 mm
  - cross sectional area of gust grid 13.8 m<sup>2</sup>
  - frequency of gust grid up to about 10 Hz
  - average flow speed for empty measurement chamber 17 m/s
- Data on the blower and the motor
    - running wheel diameter 5600 mm
    - hub diameter 2660 mm
    - max. amount delivered 530 m<sup>3</sup>/s
    - max. total pressure  $p = 1.2 \text{ (kg/m}^3\text{)}$  about 300 Pa
    - total blower efficiency about 80%
    - power at blower shaft about 230 kW
    - rotation rate of blower about 190 rpm
    - power of 3-phase motor 315 kW
    - rpm of 3-phase motor about 1500 rpm
- Data on diffuser
    - inlet diameter 5600 mm
    - net cross sectional area at inlet about 19.0 m<sup>2</sup>
    - output diameter 6500 mm
    - cross sectional area at outlet about 33.2 m<sup>2</sup>
    - diffuser length 8700 mm
    - geometric opening angle about 6.4°



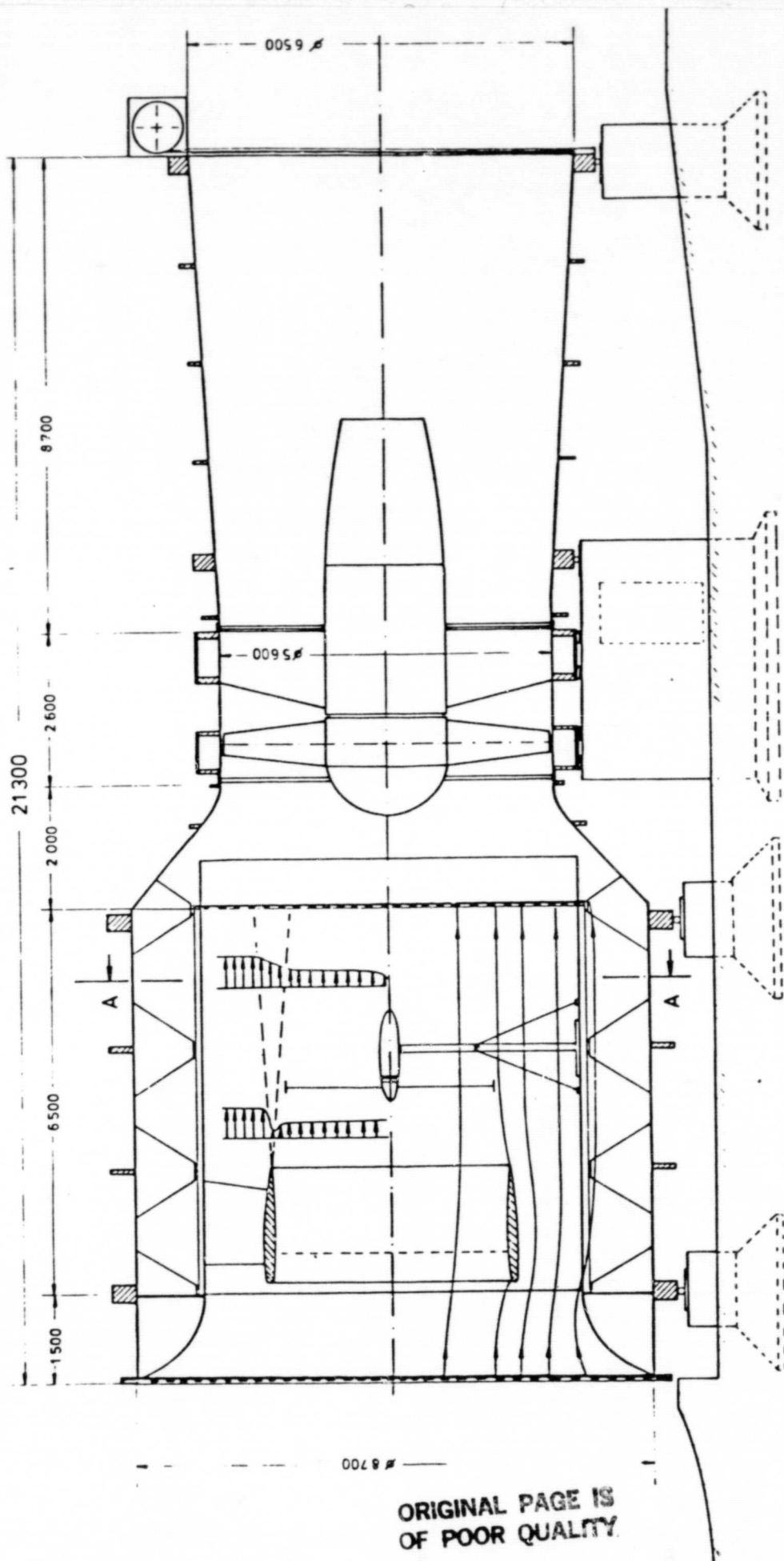
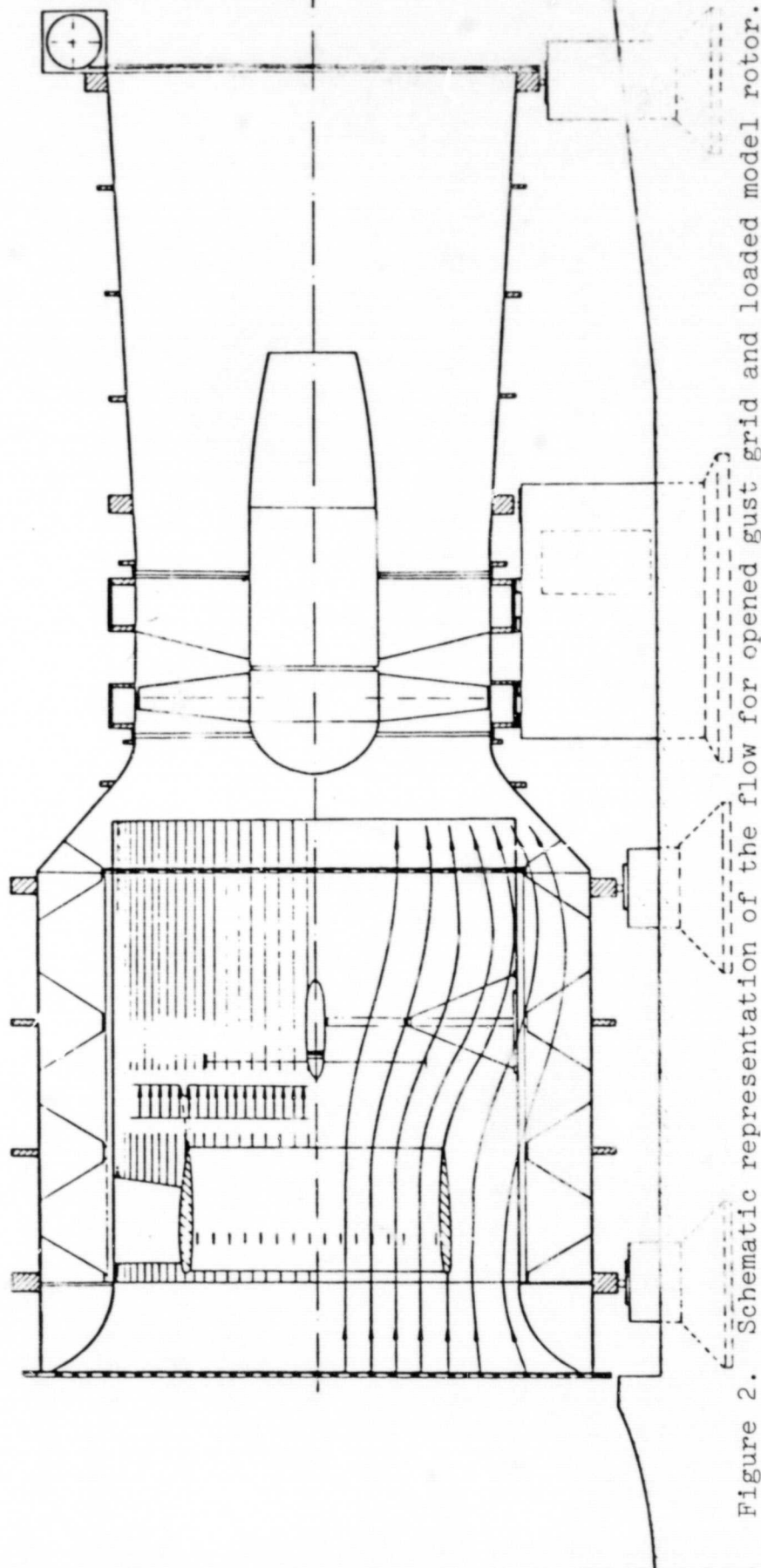


FIGURE 1. Intersection along the channel axis of the gust generator. The gust generator is in the closed position.

ORIGINAL PAGE IS  
OF POOR QUALITY



ORIGINAL PAGE IS  
OF POOR QUALITY

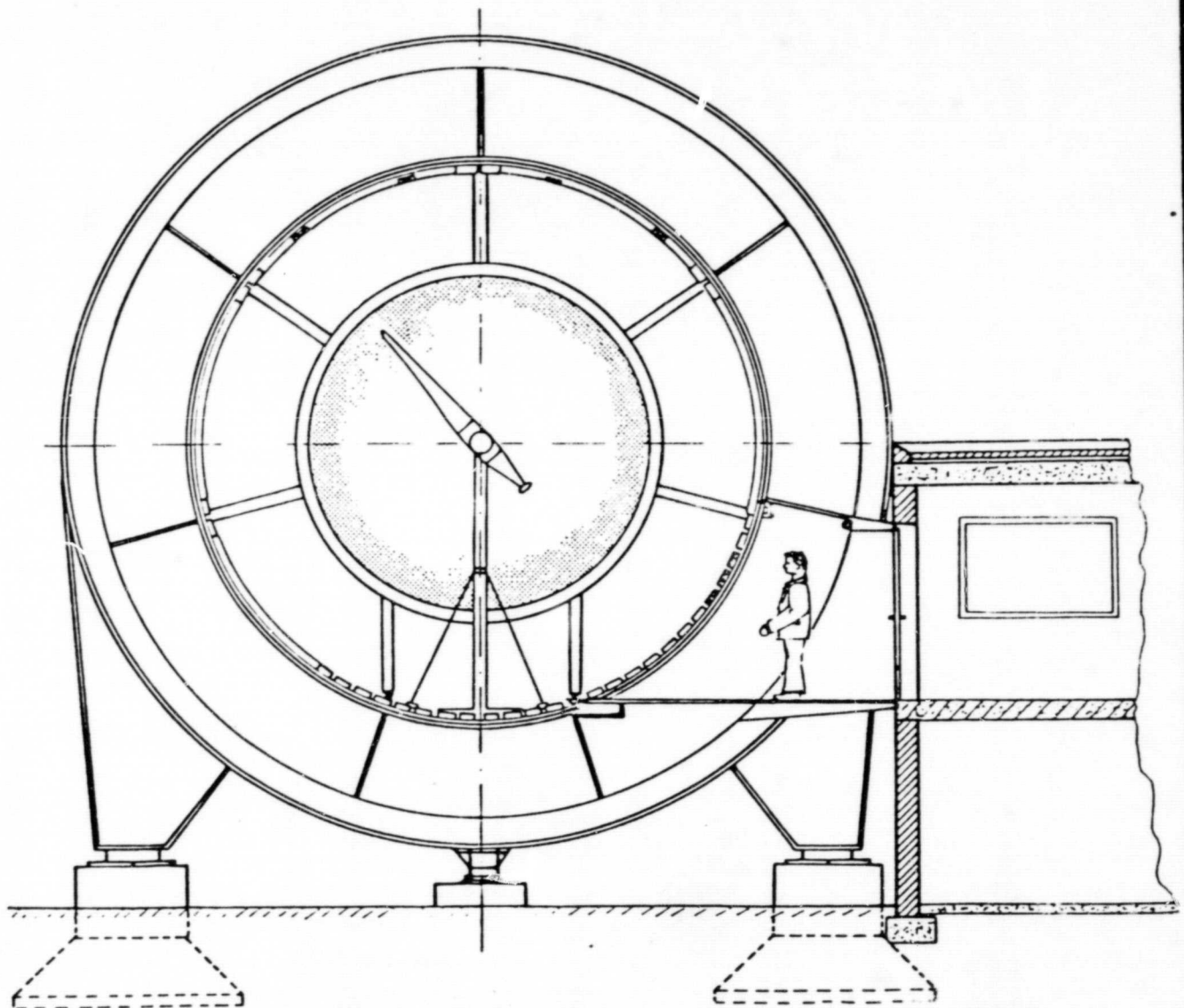


Figure 3. Measurement chamber cross section perpendicular to channel axis with viewing direction from blower to inlet. The following is represented in sequence: Model rotor, gust grid ring wing with support perforated measurement chamber in a wall, external measurement chamber wall

ORIGINAL PAGE IS  
OF POOR QUALITY

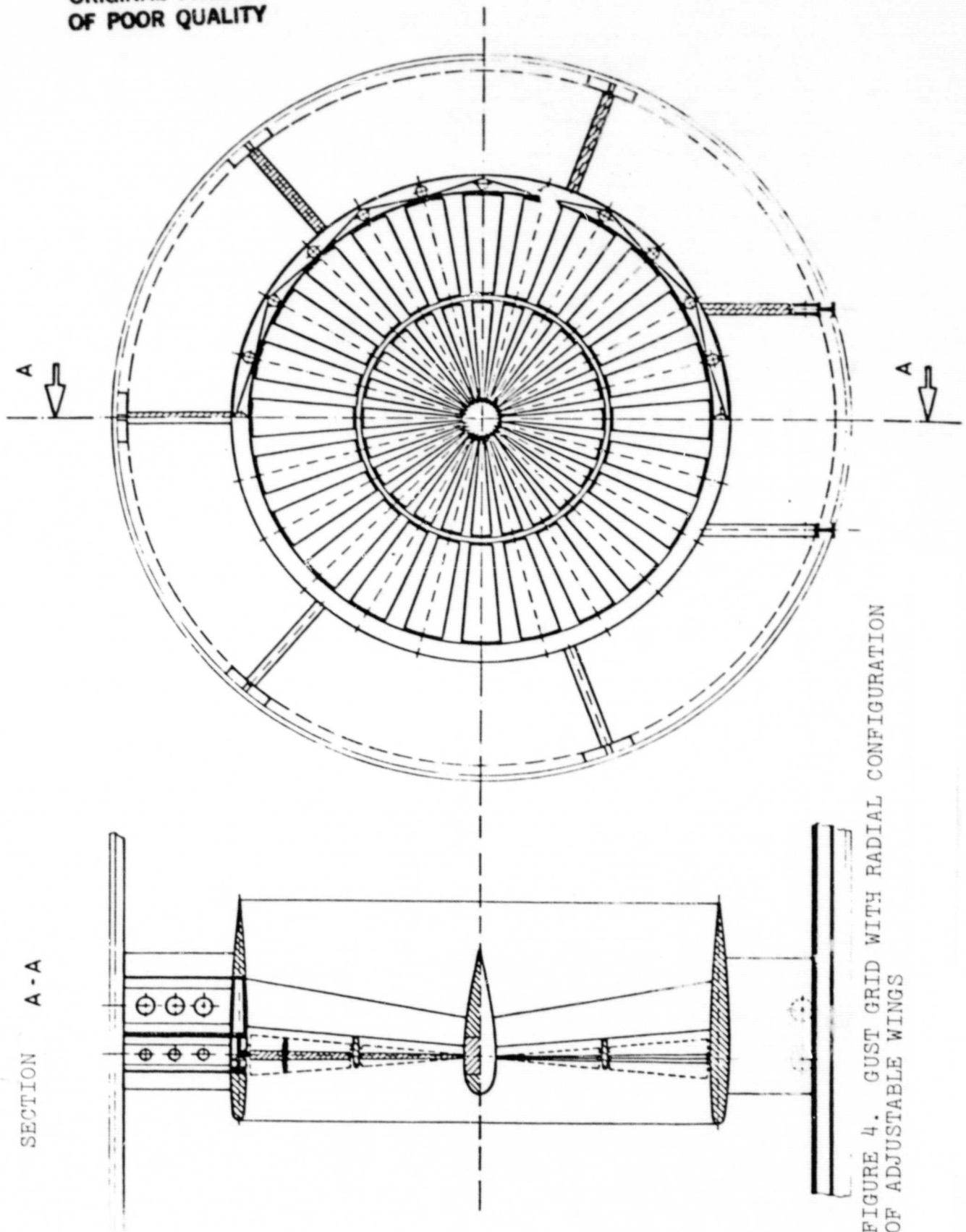
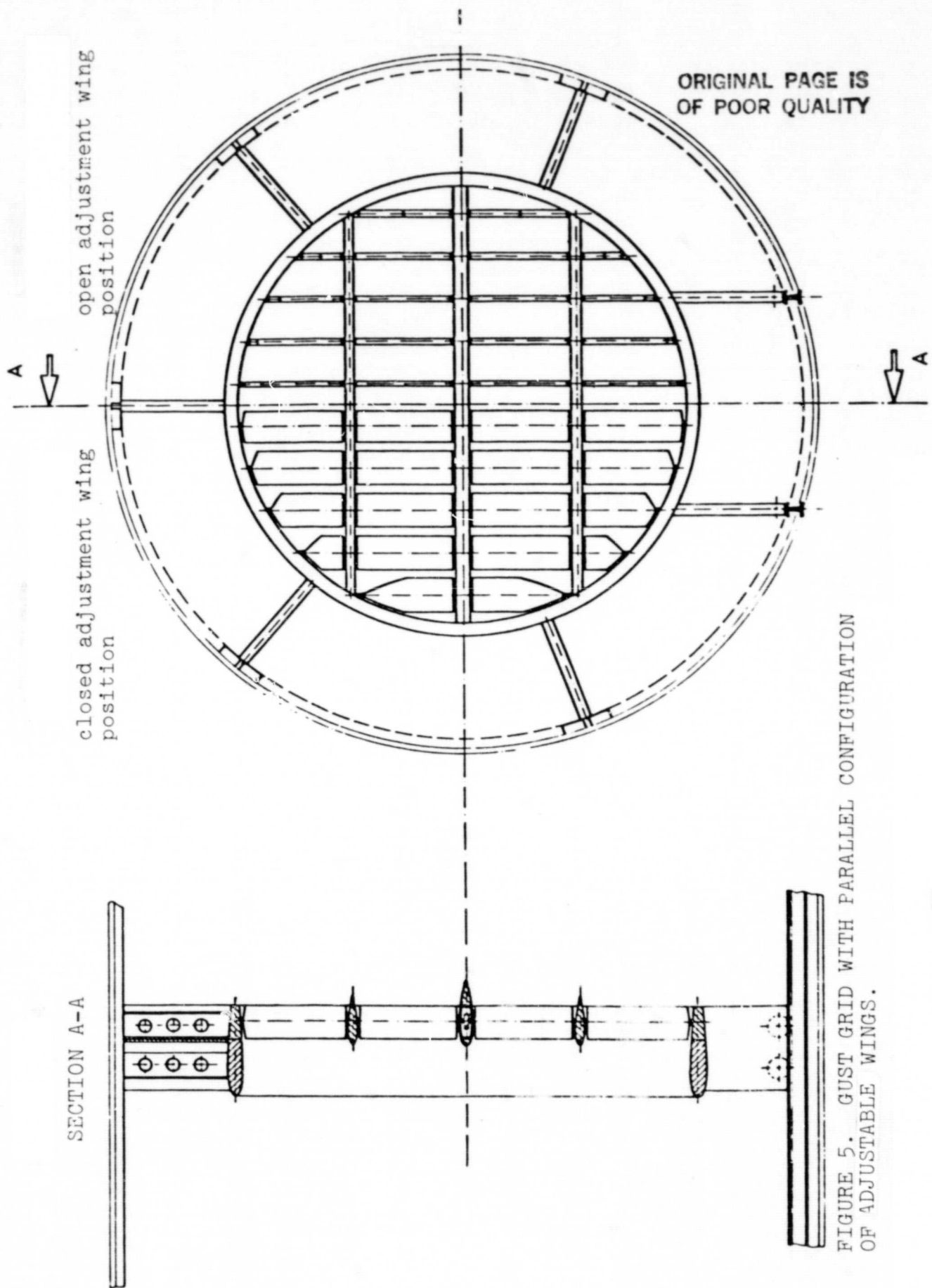


FIGURE 4. GUST GRID WITH RADIAL CONFIGURATION  
OF ADJUSTABLE WINGS





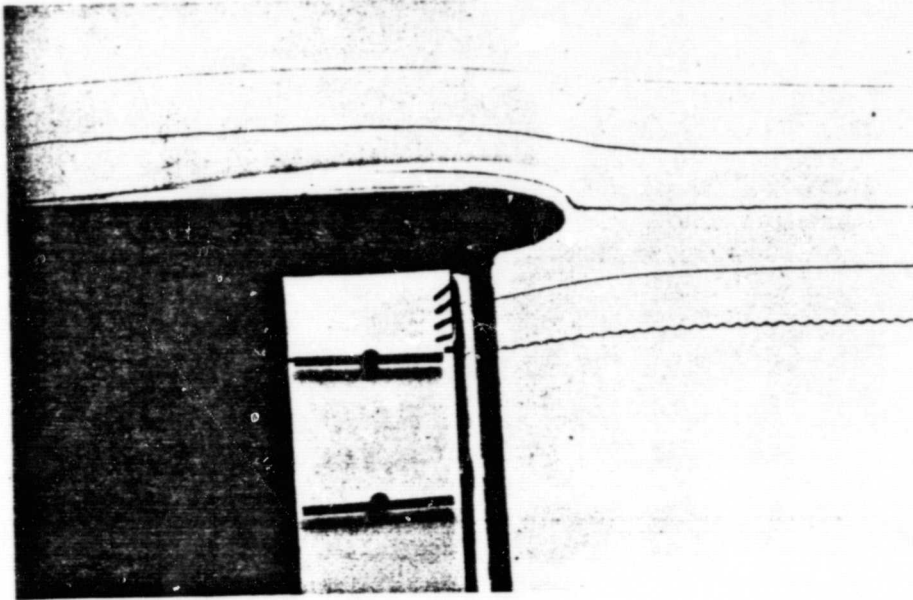


FIGURE 6. FLOW FOR OPEN GUST GRID. ANGLE OF ATTACK  
 $\alpha_{St} = 0^\circ$ .

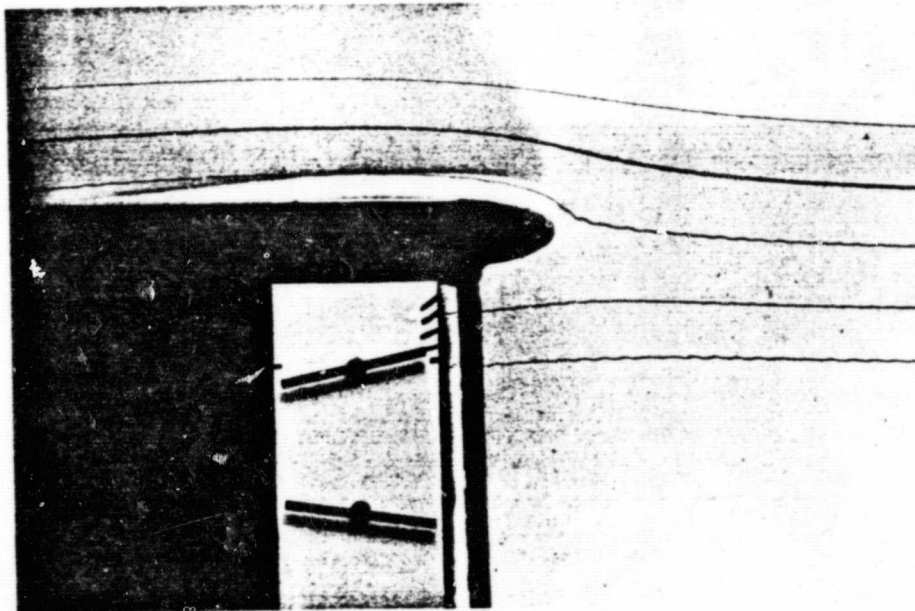


FIGURE 7. FLOW OVER GUST GRID RING WING WITH A  
SETTING ANGLE OF  $\alpha_{St} = 10^\circ$

ORIGINAL PAGE  
BLACK AND WHITE PHOTOGRAPH

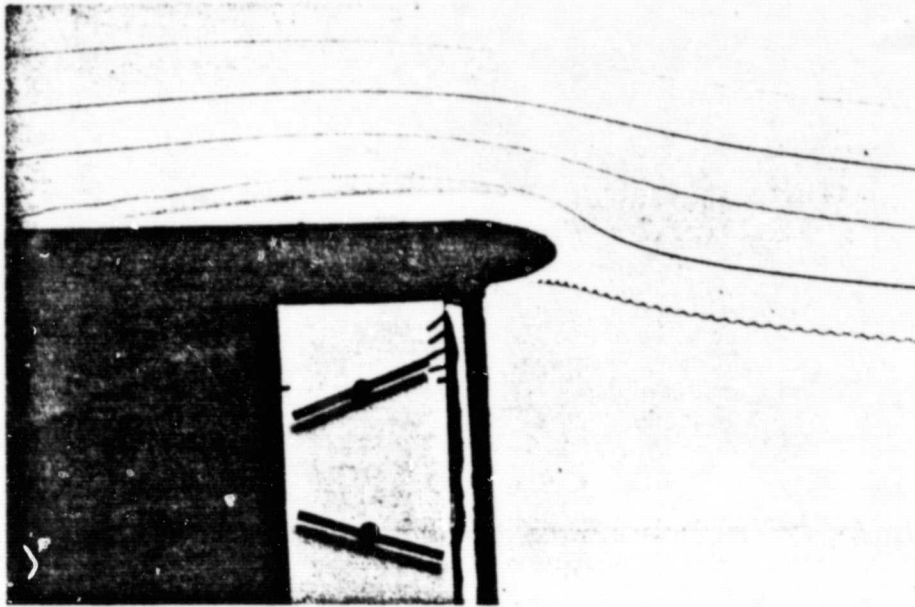


FIGURE 8. FLOW OVER GUST GRID RING WING FOR A  
SETTING ANGLE OF  $\alpha_{St} = 18^\circ$

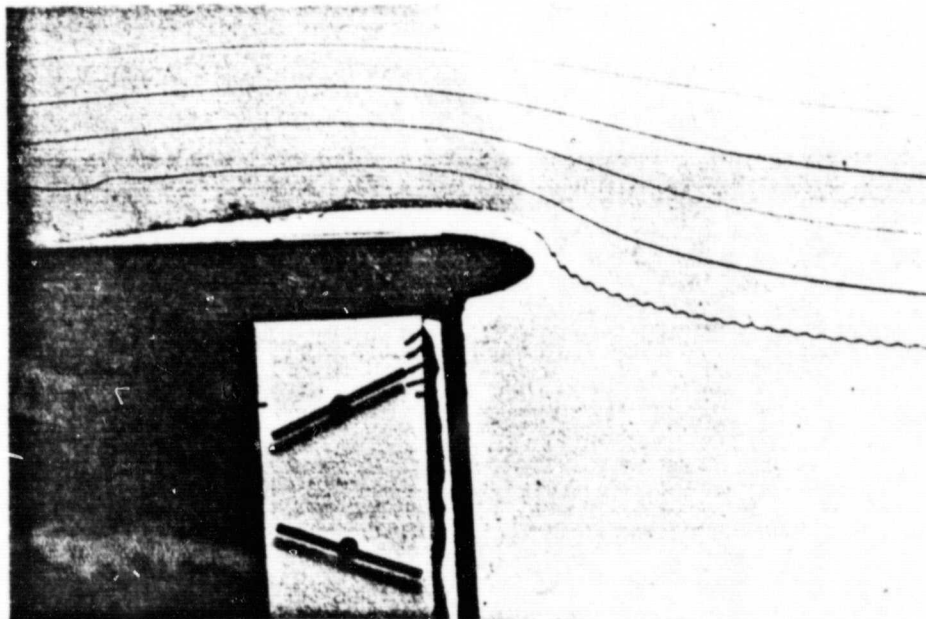


FIGURE 9. FLOW SEPARATION OVER RING WING FOR AN  
ADJUSTMENT ANGLE OF  $\alpha_{St} = 21^\circ$



W. Leonhard and W. Kleinkauf

1. Goals:

The operational behavior of wind energy facilities (horizontal axis machines) of various sizes is to be investigated by using suitable control methods and suitable mechanical-electrical energy converters.

2. Working program:

Determination of the dynamic behavior (transfer function) of the components of a wind energy facility--analysis of various electro-mechanical energy converters--development of control concept and investigation of the entire facility behavior (network and island operation)--verification of theoretical knowledge with practical investigations.

3. Status (end 1980):

The principal control structure of a wind energy facility was developed. For simple systems with blade adjustments equipped with asynchronous or synchronous generators and used in a network or individually, we designed control concepts. Using digital simulations, we obtained information about the dynamic behavior. We started with measurement technical work for covering the operational behavior of small facilities (10-20 kW).

As a first application, we investigated the use of a slipring asynchronous generator. The machine works in a stand within the three phase network of constant frequency. The rotor is applied by a direct converter so that subsynchronous and oversynchronous operation are possible. A simple variation to this is the oversynchronous current

circuit where the slip power is delivered to the network through a direct current intermediate circuit. The static and dynamic processes were analyzed theoretically using digital simulation and also with a 22-kW laboratory setup. The control used for field coordinates allows uncoupled specification of the effective power and the blind power. A 6-pulse circuit with 3-phase current output is used as direct converter. Control is done with a microcomputer.

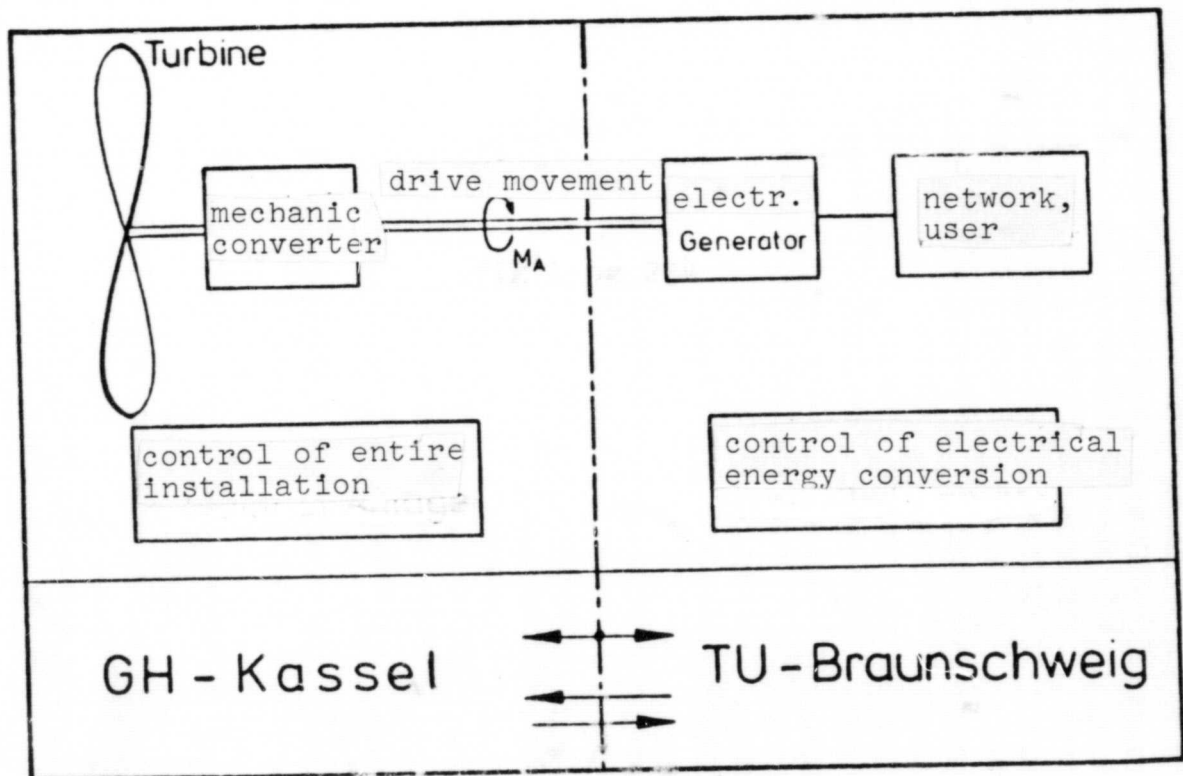
/234

General remarks

The project is being performed in conjunction with the Kassel Technical High School, Electrotechnical Division (Energy Technology office) and the Institute for Control Technology of the Braunschweig Technical University.

- Work division between Gh-Kassel and TU Braunschweig

The simplified structure of a wind energy facility in the figure shows the interface for the work.



The work division allows relatively great independence, especially for the practical investigations and the simulation calculations. However, a great deal of cooperation is required so that common evaluation and presentation of knowledge is assured.

/235

Gh Kassel:

## Control and dynamic behavior of wind energy facility I:

### Table of contents

1. Introduction
2. Control structure of a wind energy facility
  - 2.1 General remarks
  - 2.2 Mechanical control circuit components
  - 2.3 Simulation of facility behavior
3. Comments on the control of small wind energy facilities
4. Practical work
  - 4.1 Measurement investigations of components of wind energy facilities
  - 4.2 Control of wind energy facilities with joint operation
5. Other procedures

/236

### 1. Introduction

According to the detailed project descriptions of the contract, the investigations are concerned with wind energy facilities which have a horizontal axis design where the blade adjustment angle can be changed and which are intended to convert wind energy into electrical energy. With this restriction, we are assured that the investigations will concentrate on facilities now being developed and will, therefore, have a high degree of application.

The several basic considerations about the topic will now be presented for explanation.

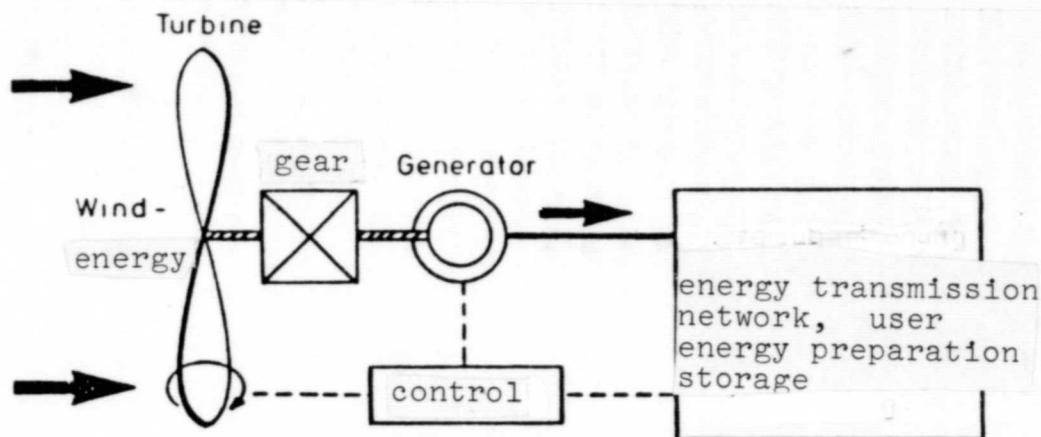


Figure 1. Wind energy facility, energy flow and control.

## 2. Control structure of a wind energy facility

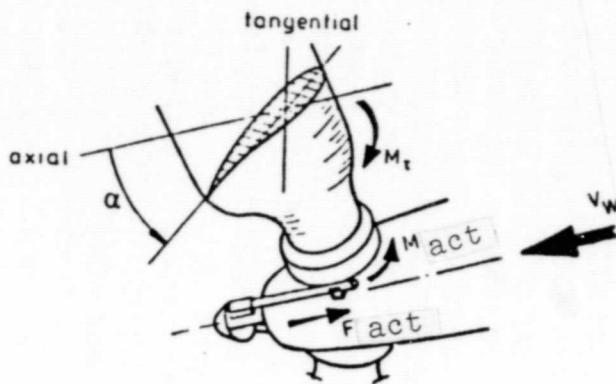
### 2.1 General remarks

When a wind energy facility is used for producing electrical power, the facility function has to be tuned to the user requirements. Detailed knowledge about the energy flow from wind energy up to electrical supply network for individual users is, therefore, very important. Figure 1 shows this chain.

The primary energy is specified by the fluctuating speed of the air flow. Control manipulations must, therefore, assure that excessive component loads, excessive power and rpm variations are avoided. The adjustment of the wind wheel blades around their longitudinal axis (see Figure 2) is the most often used possibility of influencing the energy absorption from the wind.

Control of energy absorption by operating the wind direction following system (turning of the towerhead) can only occur very slowly because of blade loads (gyroscopic forces) so that in the following they are not used for power limitations.

ORIGINAL PAGE IS  
OF POOR QUALITY



$\alpha$  ... blade adjustment angle  
( $\alpha = 0^\circ \hat{=}$  flag position)  
 $F_{act}$  ( $M_{act}$ ) ... force supplied  
by the actuator (or torque)  
 $M_t$  ... torsion moment applied  
by aerodynamic forces, etc.

Figure 2. Blade adjustment device

Figure 3 gives a simplified structure of the wind energy facility from the control point of view.

The entire installation is monitored by the operating control system. The control paths are characterized in their behavior by the bold face locks.

This includes the following:

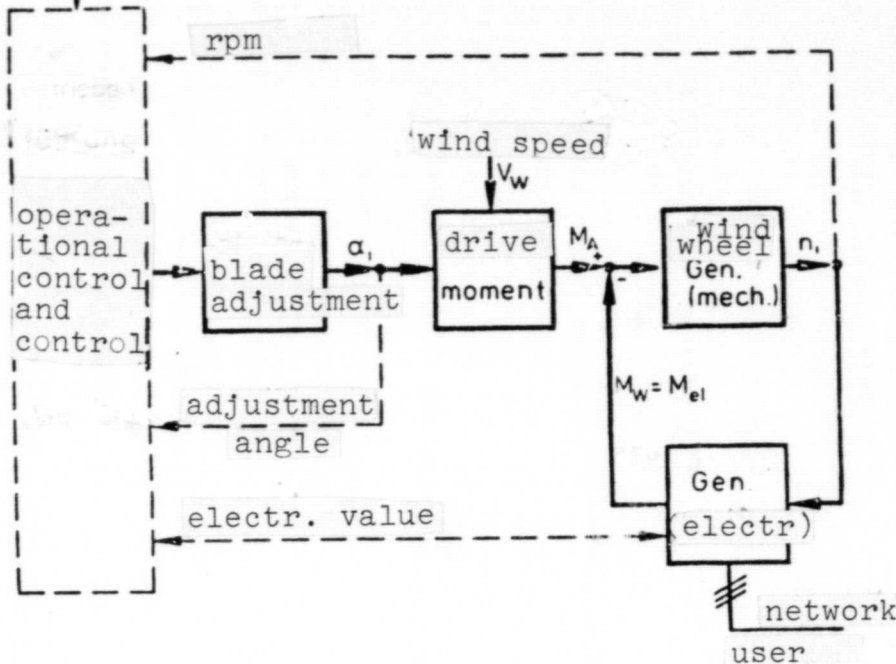
1. Behavior of the blade (or blades) for twisting around the longitudinal axis, blade adjustment path, where the actual value of the adjustment angle  $\alpha_i$  is the output.
2. Formation of the drive moment  $M_A$  from both of the main influencing parameters wind velocity  $v_w$  and adjustment angle  $\alpha$ .
3. Influence of the moments of inertia of rotating masses (essentially the wind wheel and the generator runner) on the actual rpm of the generator  $n_i$  and
4. conversion of mechanical energy into electrical energy by the electrical generator with formation of the electrical resistance moment  $M_W$  and the energy transportation to the network and users.

## 2.2 Mechanical control circuit members

Numerous additional influencing parameters which influence the control circuit of the facility have to be considered in a closer analysis. The behavior of the blade and its influencing by torsional moments is especially complicated. The following facts have to be considered.

external input

ORIGINAL PAGE IS  
OF POOR QUALITY



/238

Figure 3. Simplified structure of wind energy facility.

- moments due to lift forces over the blade
- moments due to bending of the blade and related mass displacements and lift displacements
- moments caused by the pendulum motion of the rotor
- propeller moments
- moments due to blade inertia, which for example, change with the blade bending (possibly additional consideration of the acceleration of air mass particles)
- moments by aerodynamic damping
- friction moments at the blade bearings
- moments due to spring and damping properties of the blade adjustment facility, etc.

/239

Depending on the type, these moments depend on changeable variables such as the rpm of the wind wheel  $n_w$ , blade adjustment angle  $\alpha$  as well as its derivatives, blade position during rotation  $\psi_{Bl}$  and wind speed  $v_w$ .

The calculation of the lift moments from the wind speed  $v_w$  with consideration of the adjustment angle  $\alpha$ , wind wheel rpm  $n_w$  and blade position  $\psi_{Bl}$  (for example, influence of tower shadow) requires exact knowledge about the power characteristic field of the wind turbine.

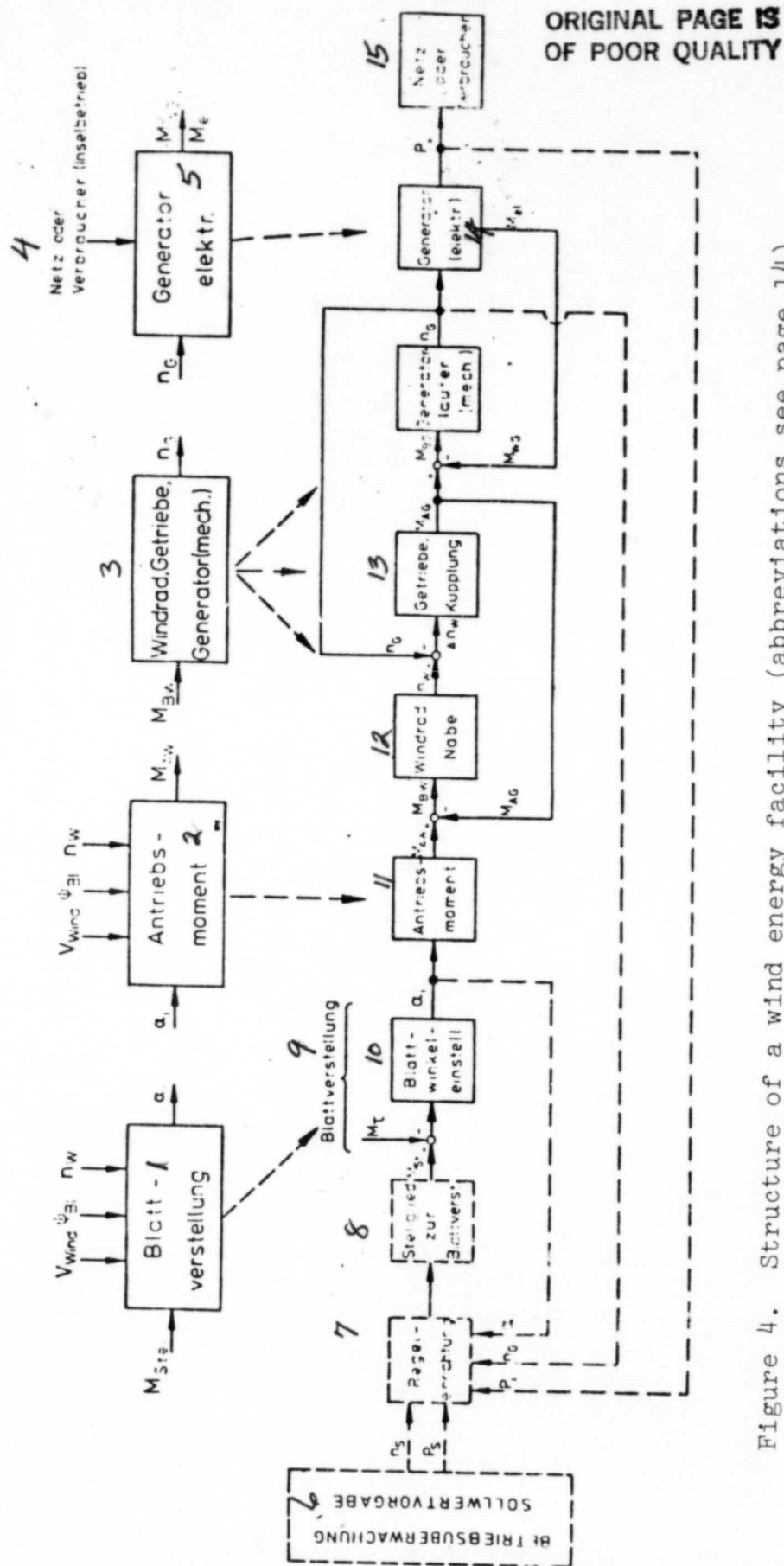


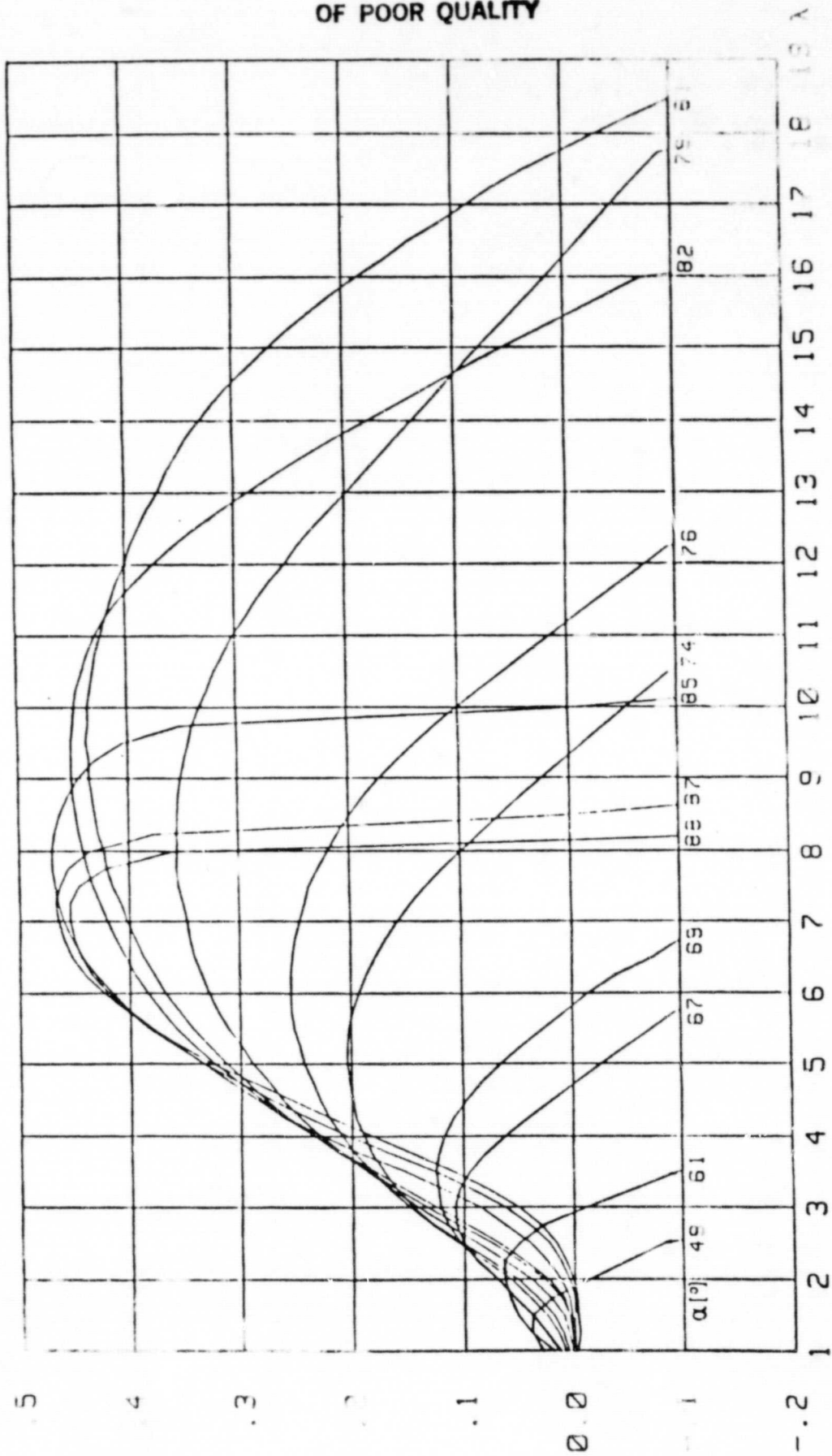
Figure 4. Structure of a wind energy facility (abbreviations see page 14).



KEY TO FIGURE 4 ON PRECEDING PAGE:

1--blade adjustment; 2--drive moment; 3--wind wheel gear generator (mechanic); 4--network or user (island operation); 5--electrical generator; 6--operational control nominal value specifications; 7--controller installation; 8--actuator for blade adjustment; 9--blade adjustment; 10--blade angle adjustment; 11--drive torque; 12--wind wheel hub; 13--gear coupling; 14--electr.; 15--network or user

$$C_p = f(\lambda, \alpha)$$



Among the additional dynamic influences due to mechanical components which participate in the energy transfer, we have the torsional stiffness and the damping behavior of the element as well as the inertia of the rotating masses.

Figure 4 gives a detail of Figure 3 and shows the structure of a wind energy facility which makes it possible to consider the influences mentioned. Starting with this structure, we can make simplifications depending on the investigation goal and the structure of the wind energy facility.

Exact analysis also requires the actuator for blade adjustment which is the power part of control. Special investigations at the present time are continuing for often used units with hydraulic oil and cog wheel pumps, control valves, adjustable pistons, etc.

### 2.3 Simulation of the facility behavior

/241

Wind speed variations have to be specified for the digital simulation of the facility behavior. The reactions of the coupled facility components are calculated and printed out for the wind speeds with inclusion of the time dependences. The basis of the facility control is a control system tailored to the properties of the components and the purpose of the facility. The important parts of the simulation program include:

- specification of the wind speed variation
- control and monitoring system
- facility structure (according to Figure 4) with subprograms for calculating the drive moment, blade behavior, etc.

In designing the program, we were especially interested in its general validity. We wanted to have the possibility of inputting the wind speed variations and to store extensive rotor characteristic line fields ( $c_m, c_p = f(\lambda)$ ).

With the software developed, it is possible to include their arbitrary wind speed conditions as well as directly measured conditions as excitation functions for the simulation of the facility behavior. Specification of the wind data can be done using a digital device using a satellite computer or directly from the wind measurement device through a telephone modem to the computer center (mass storage). In this way, we have the possibility of comparing the simulation results later with the actual behavior of the facility.

The most exact method at the present time for determining the drive moment is by using the characteristic line fields of the power coefficient ( $c_p$ ) or the rotation rate coefficient ( $c_m$ ) which is usually used by the blade designer for quasi-stationary states and requires a great deal of effort (it is usually represented as a function of the free wheeling coefficient  $\lambda$  with the blade angle  $\alpha$  as a parameter, see Figure 5). In addition to the high accuracy in the representation of the characteristic line fields, for a dynamic evaluation there has to be a good and rapid extrapolation in the intermediate range in order to avoid long computer calculation times. The evaluation of the stored characteristic lines was done for the simulation using a two-step method with interactive transfer from one spline function and was developed into a linear interpolation program which satisfies the requirements. In particular, critical and rapidly dropping characteristic field ranges /243 (see Figure 5) can be included for stability investigations.

At the present time, test runs of the previously designed simulation program are being made with a control system for island operation of small wind energy facilities (10 kW range).

### 3. Principal aspects of the control of small wind energy facilities

When using wind energy converters for generating electrical energy, three kinds of operations can be distinguished.

- island operation
- network operation
- island and network operations (selectable).

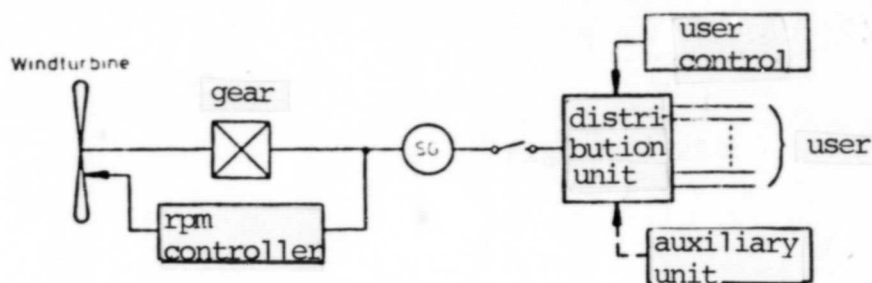


Figure 6. Configuration for island operation of wind energy converters

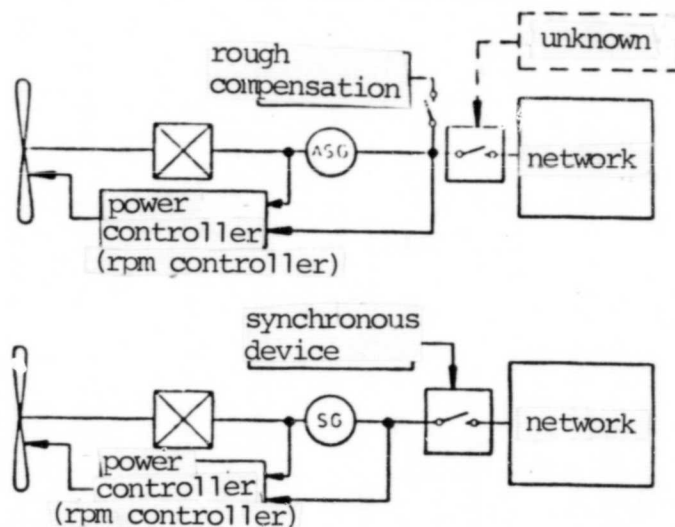


Figure 7. Configuration for network operation of wind energy converters with asynchronous and synchronous generator.

The following discussions refer to small wind energy facilities (up to 10 kW electrical power output) which are equipped with three-phase current generators. The use of special generators and current rectifier units which would allow variable rotor rpm would hardly be worthwhile because of the cost.

### 3.1 Island operation

The wind energy facility is not connected to the open public electrical supply network. For the mechanical-electrical energy conversion, a synchronous generator (SG) is suitable. The use of an asynchronous generator would mean that a controlled excitation blind power would have to be made available in order to achieve a constant voltage. The complexity for a controlled compensation device is improporportionately high in the normal case. In order to check the output frequency, the rpm of the wind energy facility has to be controlled (through the blade adjustment device). If the users require approximately a constant voltage, then when there is insufficient wind speed, in order to match power and rpm, less important energy users will have to be turned off through a user control system according to a priority method. In order to assure the supply to important users, depending on the user requirements, devices will have to be used which operate independent of the wind (Figure 6).

/244

### 3.2 Network operation

Now the wind energy facility will operate with the public supply network (see Figure 7) with approximately constant voltage and frequency. Asynchronous generators (ASG) or synchronous generators (SG) can be used as generators. Since the frequency is specified by the network (i.e., the rpm of the synchronous generator specified and the rpm of the asynchronous generator can be varied by slip values), then in order to avoid overload the power uptake of the facility has to be controlled (through the blade adjustment device). In order to switch these facilities equipped with an asynchronous or synchronous generator to the network, in addition a corresponding switching and synchronization device is required.

/245

In both facility types, the power control would have to be associated with an rpm control system so that during startup, shutdown and during synchronization network failure, etc., the control of the facility would be maintained by it.

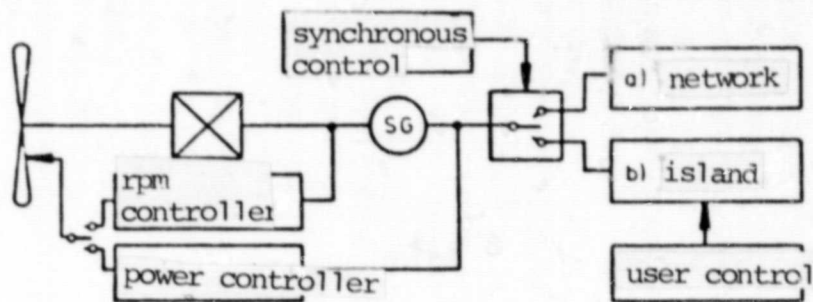


Figure 8. Configuration for network and island operation (selectable) of wind energy converters.

### 3.3 Network and island operation (selectable)

In the normal case the facility will operate on the network, but when the network fails, it is used also for electrical power supply. This operational condition requires the maintenance of the conditions given above for network and island operation. The use of a synchronous generator is probably more suitable for satisfying the requirements of an individual facility (see Figure 8).

## 4. Practical work

### 4.1 Measurement technical investigations of components of wind energy facilities

First of all, individual components of the wind energy converters such as the rotor blades and the transfer elements (for example, gears) are most important for the analysis. The examination of the operating behavior of the entire facility will be done later on.

When selecting measurement procedures, we are especially intent on using those which will not require extensive facility modifications.

The adjustable rotor blades represent the only actuator components in the power train of the wind energy facility. Its dynamic properties during the adjustment along the longitudinal axis are, therefore, very



important. The investigation of the torsional behavior of the rotating blades requires a high degree of complexity. /247

There with other methods the photogrammetric determination of the blade behavior can be done with relatively a small amount of effort without construction changes to the blades. Therefore, we planned to illuminate marks on the rotor blades stroboscopically and to then measure the images of two geometrically separated cameras. The optical evaluation gives the object coordinates in conjunction with a computer facility as well as the deformation of the rotor blades. The determination of the damping properties of the fins, etc., requires additional calculations. An estimation of the accuracy and information content of the measured values is only possible after measurements have been carried out. Since exact analysis has shown that in particular the image evaluation requires greater costs than expected, we are attempting to use another measurement method whose information content can be better estimated. For example, we are considering model analysis.

A structural dynamic analysis using accelerometers on the facility components to be investigated requires a high degree of complexity, but allows a simpler evaluation of measurements. The use of a structural dynamic analyzer also allows the investigation of other facility components such as the hub, gears, coupling, generator, machine house, tower and guy ropes, and foundations, etc. We can also obtain information about the dynamic behavior of the entire installation. At the present time we are investigating this possibility as an alternative for phototometry.

In addition to the behavior of the rotor blade, it is very important to know the time dependence of the drive moment in the gear and the generator for other investigations. Instantaneous fluctuations due to wind speed changes, tower shadow influences, etc., are especially important here. In collaboration with the DFVLR Stuttgart, measurements of the modulus facility in Schnittlingen are being performed on the Swabian Alp. For these measurements, the facility was equipped with a torque measurement shaft by the DFVLR on the wind wheel

side. Since this measurement method implies rather high equipment costs and is not easy to attach to already built and operating facilities, we are investigating a method which can also be used for other facilities.

/247

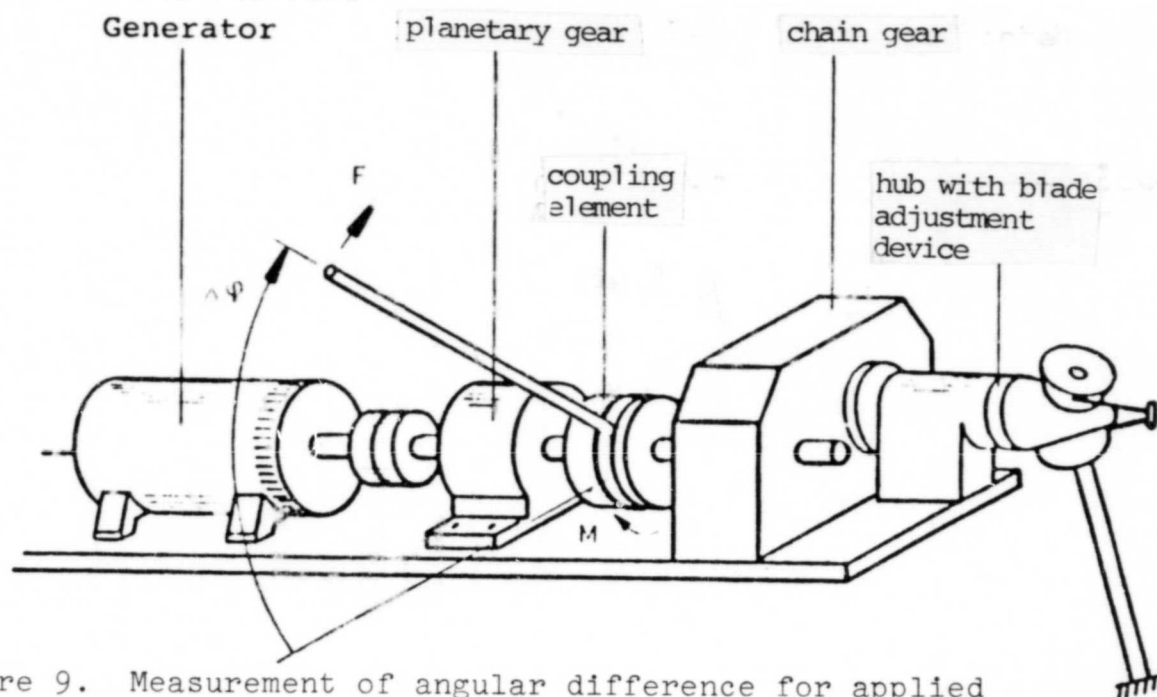


Figure 9. Measurement of angular difference for applied torque at the chain gear--modulus facility (10 kW) of the DFVLR.

We are investigating whether a rotation angle difference measurement between the input stage and the output stage on the gears would allow one to calculate the torques and the transmission ratio. Static preliminary investigations on the evaluation of dynamic measurements were already made on the installed transmission elements of the DFVLR modulus facility. As Figure 8 shows, the rotation angle on the chain gear was measured for static moment application. The same measurements were also carried out on the planetary gear and through both transmission stages. The measurements allow one to determine the gear stiffness and can be used for calibration.

Additional investigations of individual components and the examination of control concepts will probably be performed soon using the

Aeroman (10 kW power class) which is an internal MAN facility.

/248

#### 4.2 Control of wind energy facilities with joint operation

In addition to control concepts and the investigation of operational behavior of individual facilities, recently we have dealt with problems of the control of the wind energy joint facility. Since the funds for the practical investigation of a joint facility were not available from the project, using engineering excess funds we have started to build four controllable sets of machines using our own funds which are suitable for simulating joint operation (alternating current generator coupling). The generator power of the machines is between 5 to 15 kW.

The individual facilities will be controlled by a computer (in the form of fluctuating drive moments to the generator caused by variations in wind speed). The behavior of the facility and of the joint facility can later on be evaluated by a fast measurement collection system now being built (multiprogrammer for computer coupling, measurement value intermediate storage, control of processes, etc.).

#### 5. Further procedures

The important points of our procedure correspond to the work plan of the project and its steps.

We are especially interested in the measurement of the blade behavior and the final specification of the investigation method (photogrammetry or modal analysis method).

In addition to completing the program by including additional details (also the investigation results determined in Braunschweig) for the facility simulation, we are also pursuing another path which will lead to a great deal of program simplification. By comparison with the results of the extensive program, we are sure that there will be no important loss of information. Possibly we can use practical results obtained from the DFVLR and the MAN facility.

In addition, we have started with the building of a model controlled by microprocessors which will represent the properties of various wind energy facilities in a lucid way by using specified facility data.

/249

#### Abbreviations used

$c_p$	power coefficient of the wind wheel
$M_A$	drive moment
$M_{AG}$	drive moment of the generator
$M_{AW}$	drive moment of the wind wheel
$M_{BG}$	acceleration moment of the generator
$M_{BW}$	acceleration moment of the wind wheel
$M_{el}, M_{WG}$	electrical resistance moment of the generator
$M_{st}$	actuator moment on rotor blade
$M_T$	torsion moment on the blade
$n_G, n_1$	rpm of the generator (actual value)
$n_S$	nominal rpm
$n_W$	wind wheel rpm
$P_1$	power output of generator (actual value)
$P_S$	nominal power value
$v_w$	wind speed
$\alpha_1$	blade adjustment angle (nominal value)
$\psi_{Bl}$	blade position of wind wheel
$\lambda$	free wheeling coefficient

Gh Kassel:

CONTROL AND DYNAMIC BEHAVIOR OF WIND ENERGY FACILITIES II:

/250

Table of contents:

1. Introduction
2. Operating behavior of small wind energy facilities
  - 2.1 Network operation
    - 2.1.1 Control concept
    - 2.1.2 Facility behavior and measurement results
  - 2.2 Island operation
    - 2.2.1 Control concept
    - 2.2.2 rpm control and measurement results
3. Practical work
  - 3.1 Wind measurements
  - 3.2 Model of a wind energy facility
  - 3.3 Joint facility

/251

1. Introduction

Large wind energy facilities (MW range) where the dynamic influences on the operating behavior are especially interesting, in most cases, are now only in the design stage. This is also true for facilities which are being developed in West Germany.

In order to be able to examine calculation methods and theoretical results as early as possible, therefore, we have to apply them to existing facilities in the power range of about 10 kW electrical power output.

In the second report (I), in addition to general remarks and descriptions of the work performed during the project, we also present measurement results which for the first time allow a comparison with theoretical results.

2. Operational behavior of small wind energy facilities

## 2.1 Network operation

### 2.1.1 Control concept

As discussed in the first report (I) for wind energy facilities having asynchronous generators or synchronous generators, the power uptake from the wind has to be controlled or limited in order to avoid overloads. In order to allow startup and shutdown and switching of the generator to the network, additional controls are required which influence the rpm of the facility.

For the most often discussed cases of the use of 3-phase asynchronous generators with short circuit runners, we developed the control concept shown in Figure 1. We are considering a facility where by changing the blade adjustment angle, it is possible to vary the power uptake from the wind.

/253

The power controller and rpm controller are arranged in such a manner that the rpm controller has a limiting effect on the output of the power controller, that is, the nominal value of the blade adjustment angle  $\alpha_s$ . A reversal of the controller configuration would also be possible. For normal operation, that is, for network operation, the nominal rpm value  $n_s$  is set a few per cent higher than the corresponding value of the network frequency. Except for turnon and shutdown processes, the rpm control system will only intervene during disturbances, for example, network failure when  $n_i > n_s$ . For turning the system on or off and for providing network switching conditions, the nominal rpm value  $n_s$  can be changed (for example, turning on through a maximum value transducer and similar concepts).

The variable limitations at the output of the rpm controller (see figure) allow intervention in the rpm control without delay for  $P_{ws} > 0$  and I fractions as well as unencumbered operation of the power controller.

The dynamic behavior of a wind energy facility depends importantly on the type of operation. The selected configuration makes it possible

Key: 1--rpm controller; 2--comparator; 3--effective power controller; 4--island operation; 5--blade angle controller; 6--blade speed controller; 7--path blade adjustment device; 8--path blade long; 9--path drive torque; 10--path rotor generator (mech); 11--path generator (electr); 12--network

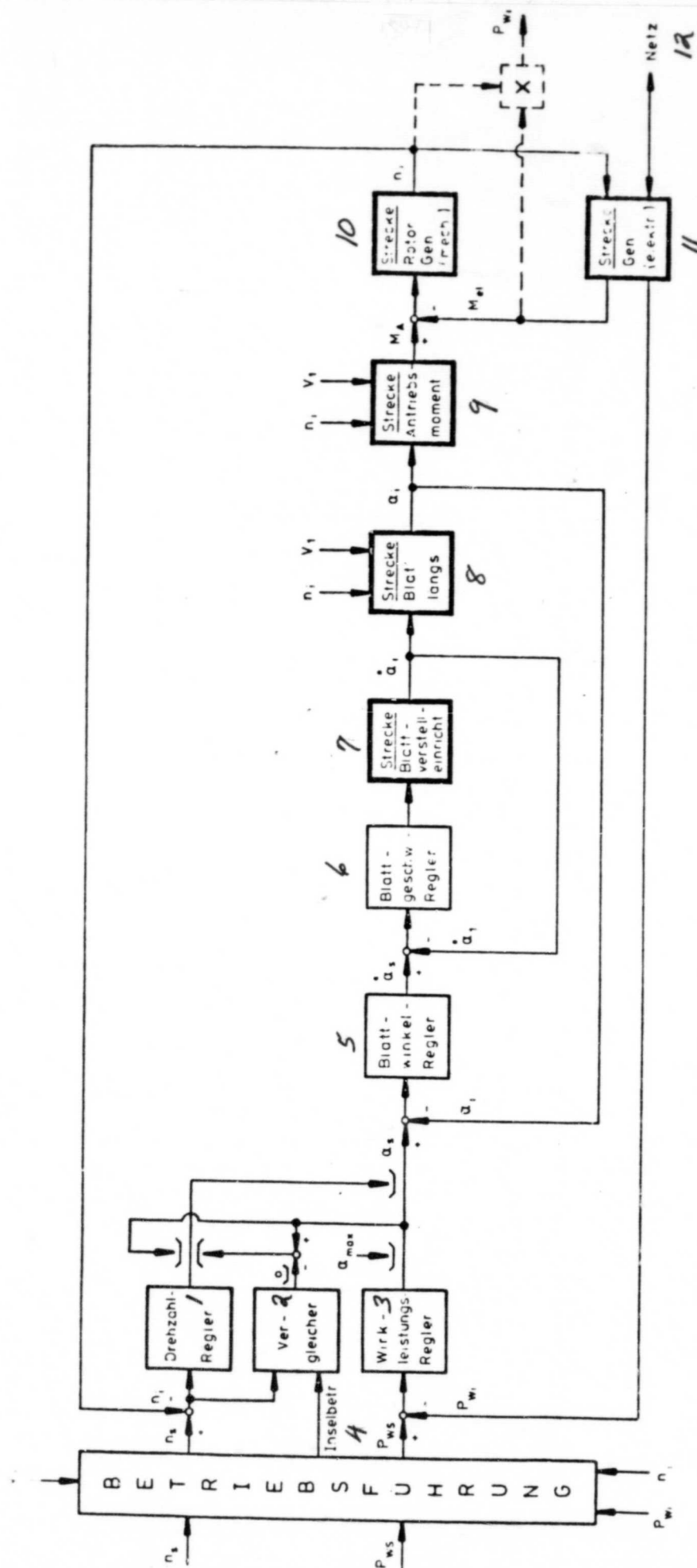


Figure 1. Control diagram for the facility with asynchronous generator. (Short circuit runner) at network.

ORIGINAL PAGE 13  
OF POOR QUALITY



to tune the rpm controller to free wheeling condition and the power controller to network operation.

The two control circuits mentioned have also a control of a blade adjustment angle  $\alpha$  and the blade adjustment angle rate ~~7~~ in order to improve stability and dynamics. We did not have an additional loop for controlling the blade angle acceleration ~~9~~ and, therefore, the actuating moments applied to the blade because of the fact that the frictional moments sometimes change discontinuously in the blade bearings.

For small facilities, the actual value determination (determination of the blade adjustment angle  $\alpha_1$  and the corresponding rate  $\dot{\alpha}_1$ ) will often be too complex. Using simulations, however, it was possible to show that when the two internal control loops were dropped (the power controller then directly affects the blade adjustment device) there will be stronger loads on the blades and the adjustment devices, but stable control behavior can be achieved nevertheless.

/254

#### 2.1.2 Installation behavior and measurement results

When calculating the facility reaction to various wind conditions, one has to determine the behavior of the blade in the longitudinal direction, its influence caused by the blade adjustment device, various moments applied to the blade as well as the formation of the drive power and the drive moment.

There are no extensive theoretical methods for determining the blade behavior. Numerous individual effects (aerodynamic torsion moments, moments due to blade bending, propeller moments, etc.) were incorporated in the simulation structure. At the present time we were not able to measure the blade dynamics because certain modifications to the converter are required. The preparation for carrying out a structural dynamic analysis was continued as mentioned in the first intermediate report. We plan to perform such measurements during the summer months at the DFVLR modulus facility in Schnittlingen.

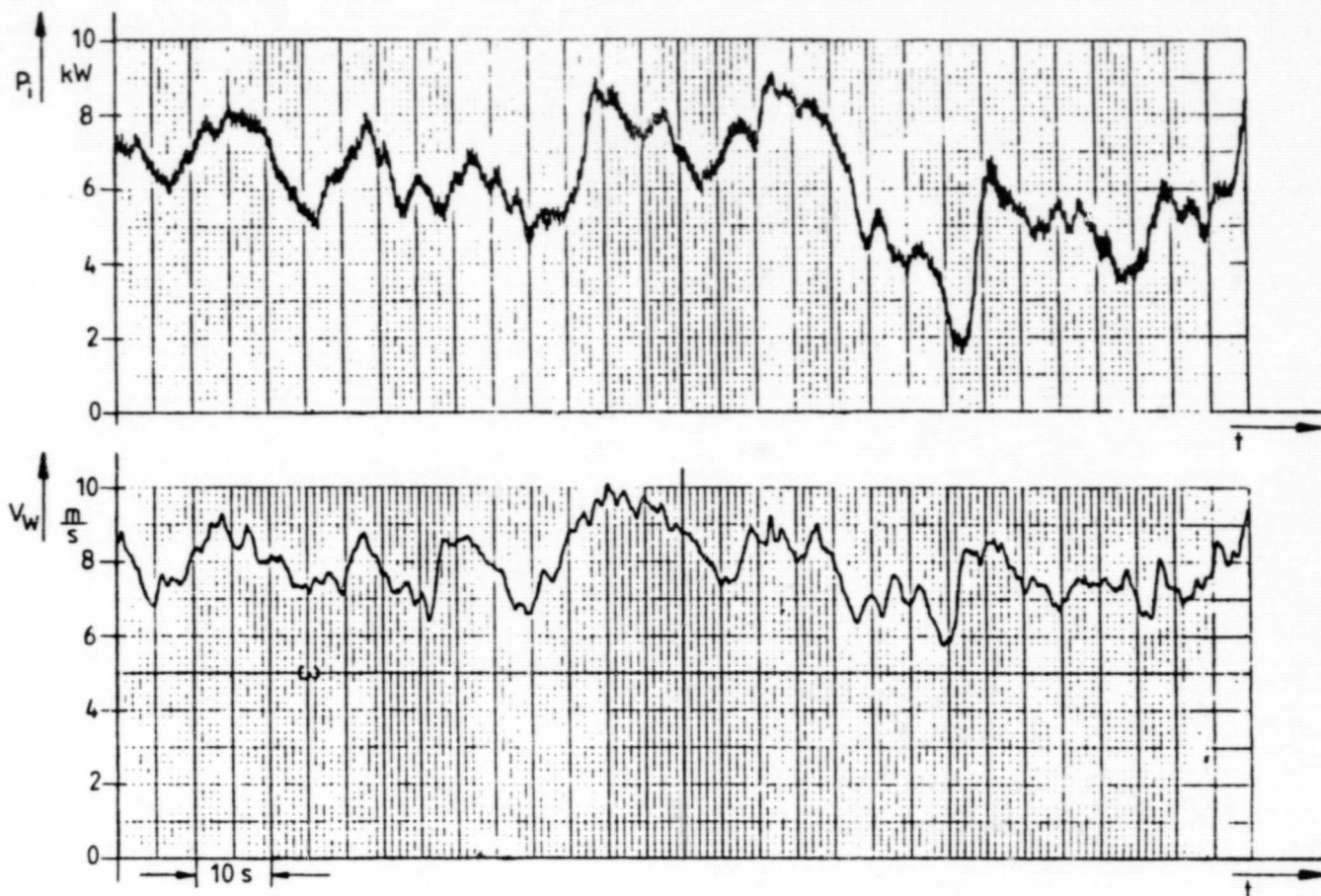


Figure 2a. Excerpt from a direct measurement value recording (multi-channel recorder)

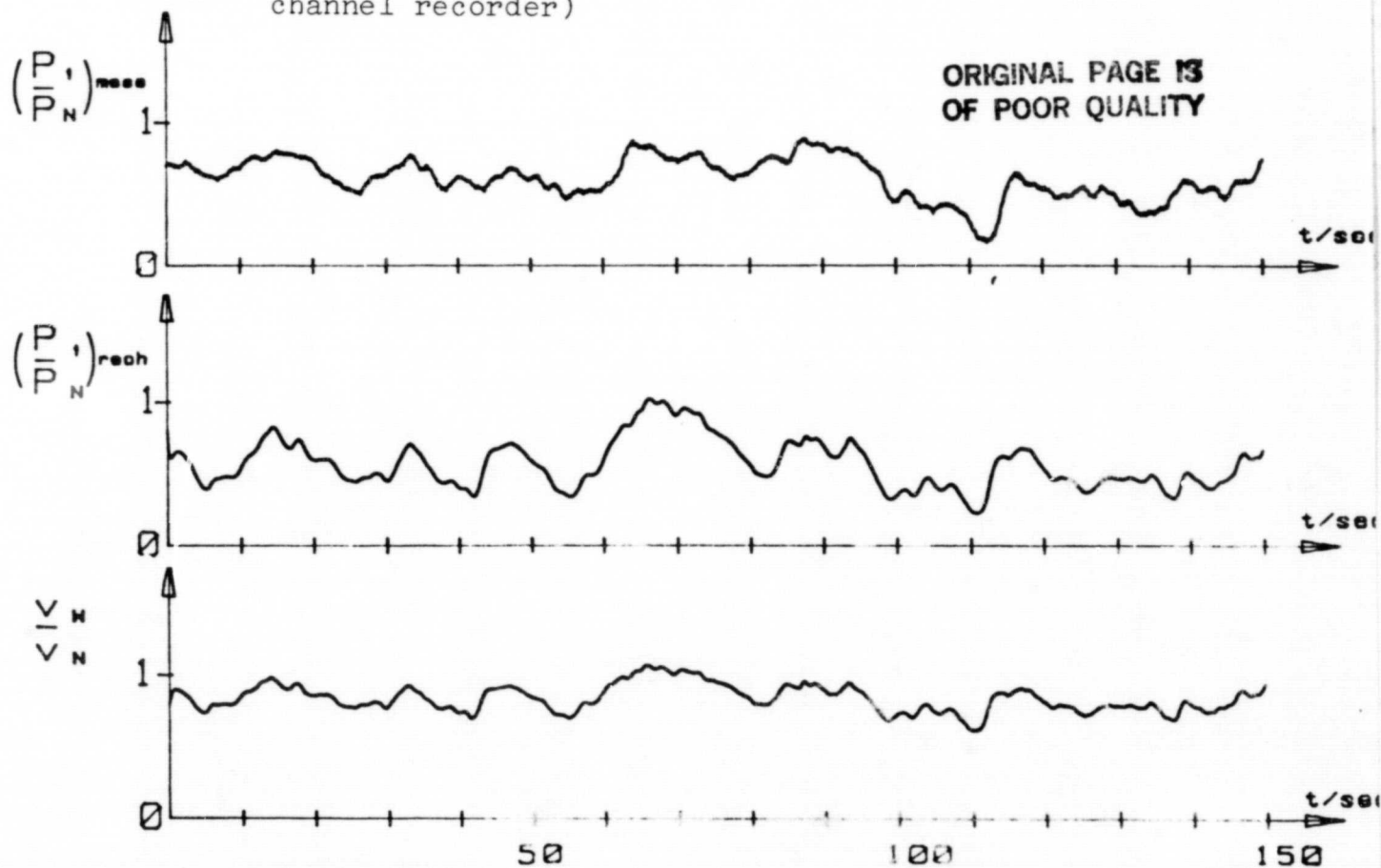


Figure 2b. Calculated variations compared with measured values

Figure 2. Electrical power  $P_e$  of a 10 kW wind energy facility with asynchronous generator for network operation (constant blade adjustment angle)  $V_w$  wind speed.

The calculation of the drive moment from the wind speed variation using the power coefficient/free wheeling coefficient characteristic fields was improved considering the fact that it could be evaluated on a digital computer. Figure 2 shows the critical determination of the output power of a 10 kW facility compared with actual measurement results (MAN facility AEROMAN). Since the wind speed was almost always below the nominal value, the power controller did not operate and the facility operated with a constant blade adjustment angle which was not completely optimum.

In the determination of the variations, we proceeded as follows: Using fast reacting measurement devices, we measured wind speed and electrical output power at the wind energy facility. This was recorded and stored on tape. The wind speed variation was later on specified through the input device to a digital computer. Using the simulation model, we were able to calculate the electrical output power in addition to other parameters. Complete agreement between measured and simulation results would mean that one had used the wind speed variation which determines the power uptake for calculating the facility behavior. /256

The calculated power variation is based on the wind results of one anemometer shown in Figure 2a. A wind speed variation of this type has only local applicability and can only be representative of the facility wind speed under certain conditions. As would be expected, details occur even though there is good agreement between the calculation and the measurement. One can see that the calculated power variation has a well defined contour and, therefore, confirms the expected trend that the measurement with an anemometer can only follow the different wind speeds of a rotor surface under certain conditions. There will be better agreement between theory and practice if several anemometers are used for determining the decisive wind speeds distributed over the rotor area (see Chapter 3.3).

Key: 1--operational control; 2--rpm controller; 3--blade angle controller; 4--blade speed controller;  
5--path blade adjustment device; 6--path blade length; 7--path drive moment; 8--path rotor generator (mech);  
9--path generator electr.; 10--constant load resistance or user control and user

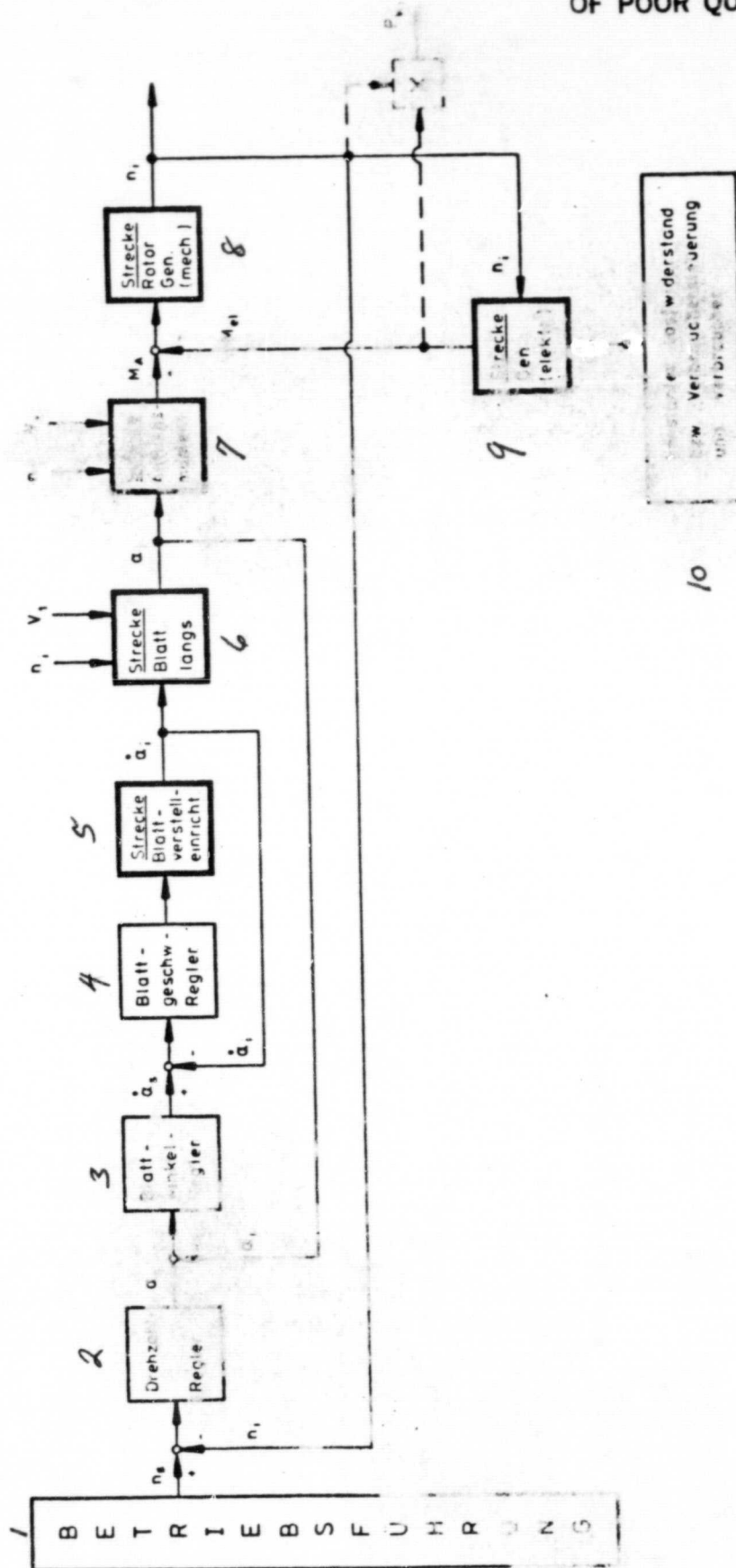


Figure 3. Control diagram of a wind energy facility with synchronous generator for island operation.

## 2.2 Island operation

### 2.2.1 Control concept

Based on the numerous applications, smaller facilities in the kW range are especially interesting for island operation. Two application regions have to be distinguished.

1. Supply of simple electrical users which have no great requirements for constant generator frequency and voltage, for example, heating resistances.
2. Supply of electrical users which require that the frequency and the voltage of the generator may only vary over a small fixed range.

The mechanical-electrical energy conversion is suitable for a 3-phase synchronous generator. Starting with the control requirements discussed in the first preliminary report, we developed the control scheme shown in Figure 3.

/258

An rpm controller influences the power drawn from the wind by the variation of the blade adjustment angle in such a manner that for sufficiently high wind speed, the rpm is maintained approximately constant. As already mentioned for the control of the facility with an asynchronous generator (Chapter 2.1.1), the two inner control circuits ( $\alpha$  and  $\delta$ ) are not needed if one disregards the influence of the dynamics during blade adjustment processes.

For the supply of less demanding users, it makes sense to use a self-excited synchronous generator whose output voltage is a function of the rpm so that below the nominal wind speed, there will be an equilibrium between the power offered by the wind and the power generated by the generator due to the fact that the voltage drops with rpm. The rpm controller can often be made in the simple form of a centrifugal force controller.

If frequency and voltage are only allowed to vary over a small range, then it is necessary to better tune the rpm controller to the behavior of the converter so that a mechanical controller usually does not satisfy the requirements. In order to prevent a dropping of the converter rpm over the partial load range, a user control which brings about turnoff of users of low priority has to provide for maintaining the delivered power below the maximum power which can be taken from the wind. A synchronous generator with electronically controlled voltage can be used as a generator.

### 2.2.2 RPM control and measurement results

For calculating the facility behavior, we proceeded just like in Chapter 2.1.2. The simulation calculations showed that when one uses rapidly operating blade adjustment devices (for example, hydraulic systems with electrically controllable valves), it is possible even for highly fluctuating wind speeds to maintain the rpm fluctuations to less than  $\pm 1\%$ . In order to test this information, we performed appropriate measurements on the MAN converter AEROMAN (10-kW facility). They are shown in Figures 4a and 4b. Figure 4a is based on a relatively slow working blade adjustment device with an electrical motor.

/260

Highly fluctuating and large wind speeds were present and the converter delivered the nominal load. From the measurement results, we find that the maximum rpm and frequency fluctuations are  $\pm 4\%$ .

In the measurements of Figure 4b on the other hand, we used a rapidly operating electromagnetically controlled hydraulic valve. The converter operates at wind speed below the nominal value under the free wheeling conditions which is a very difficult operating state for the control system. As a maximum rpm fluctuation, we find that  $\pm 1\%$ . This value was not exceeded even for higher wind speeds which fluctuated even more and for higher loads. If one considers that we did not use any optimized controllers and actuators in the facility, then as a result of the investigations we find that the rpm fluctuations can be maintained smaller than  $\pm 1\%$  even for smaller wind energy facilities. Therefore, it is

possible to satisfy the requirements of demanding electrical users with regard to voltage and frequency fluctuations.

### 3. Practical work

In addition to the measurements made, the activity also included a unit for determining wind data, building of a microprocessor--controlled operating control system and the building of laboratory devices for investigating a joint facility.

#### 3.1 Wind measurement

For testing calculations of the facility behavior, accurate measurements of the instantaneous wind speed are required. Almost no indications for this were found in the literature. We developed a shell cross anemometer which operates faster than commercial units and in addition to the wind speed and its average values, can also be used to measure the wind acceleration. The measured data can be used for processing and transferred directly to tape. In order to determine wind conditions typical for a wind energy facility, we started with measurement evaluations where the results were taken from several measurement points. Figure 5 shows the measured value  $v_1$  and  $v_2$  anemometers which were set up outside on a 10 meter high mast separated by 2 meters, and their connection line was perpendicular to the incoming wind. In spite of the small distances, there are wind speed fluctuations of more than 2 m/s as can be seen from the differences  $(v_1 - v_2)$  which were determined with the computer. For a larger separation of the measurement points (for example, for a distribution of the entire rotor area) correspondingly larger deviations should be expected. In order to obtain wind speed variations which determine the reaction of the wind converter, the values of several measurement points had to be processed. A simplified method without weighting of the wind speed effect ( $P \sim v^3$ ) would, for example, be forming the geometric average (see Figure,  $(v_1 + v_2)/2$ ).

/261



ORIGINAL PAGE IS  
OF POOR QUALITY

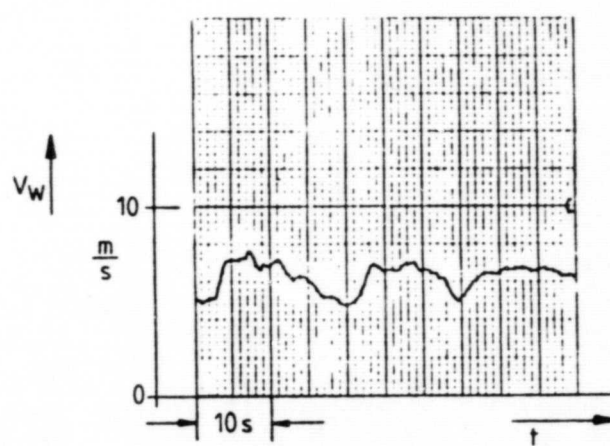
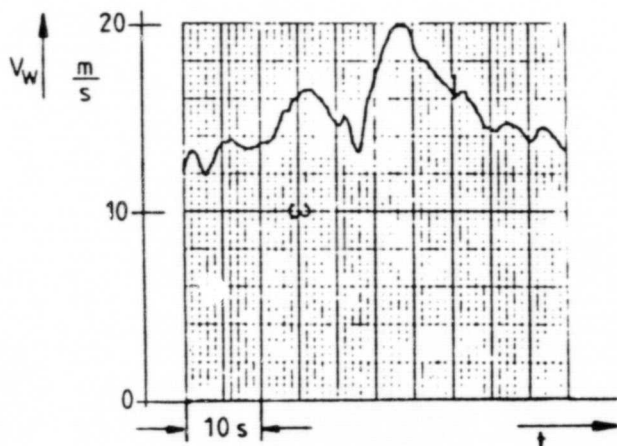
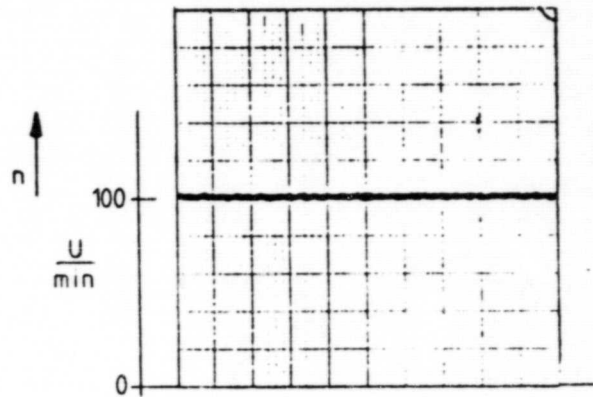
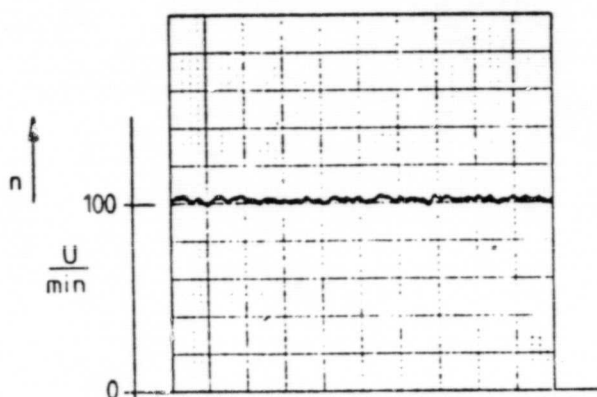
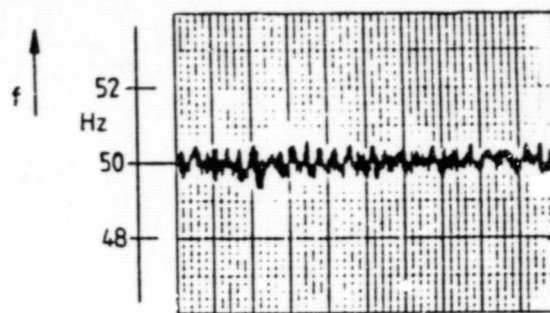
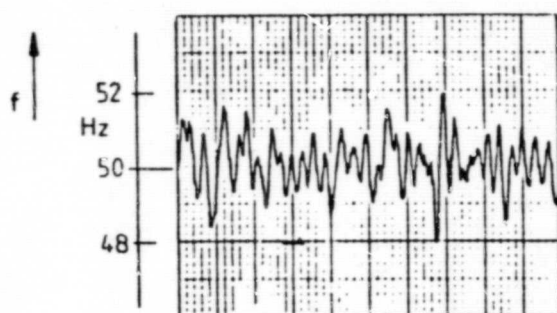


Figure 4a. Electrically driven  
blade adjustment nominal load

Figure 4b. Electrically con-  
trolled hydraulic valve in the  
blade adjustment direction.  
Free running

Figure 4. RPM control of a 10 kW wind energy facility with synchro-  
nous generator for island operation. Excerpt from direct measurement  
value recording (multichannel recorder).  $V_W$  wind speed,  $n$  converter  
rpm,  $f$  generator frequency.

ORIGINAL PAGE IS  
OF POOR QUALITY

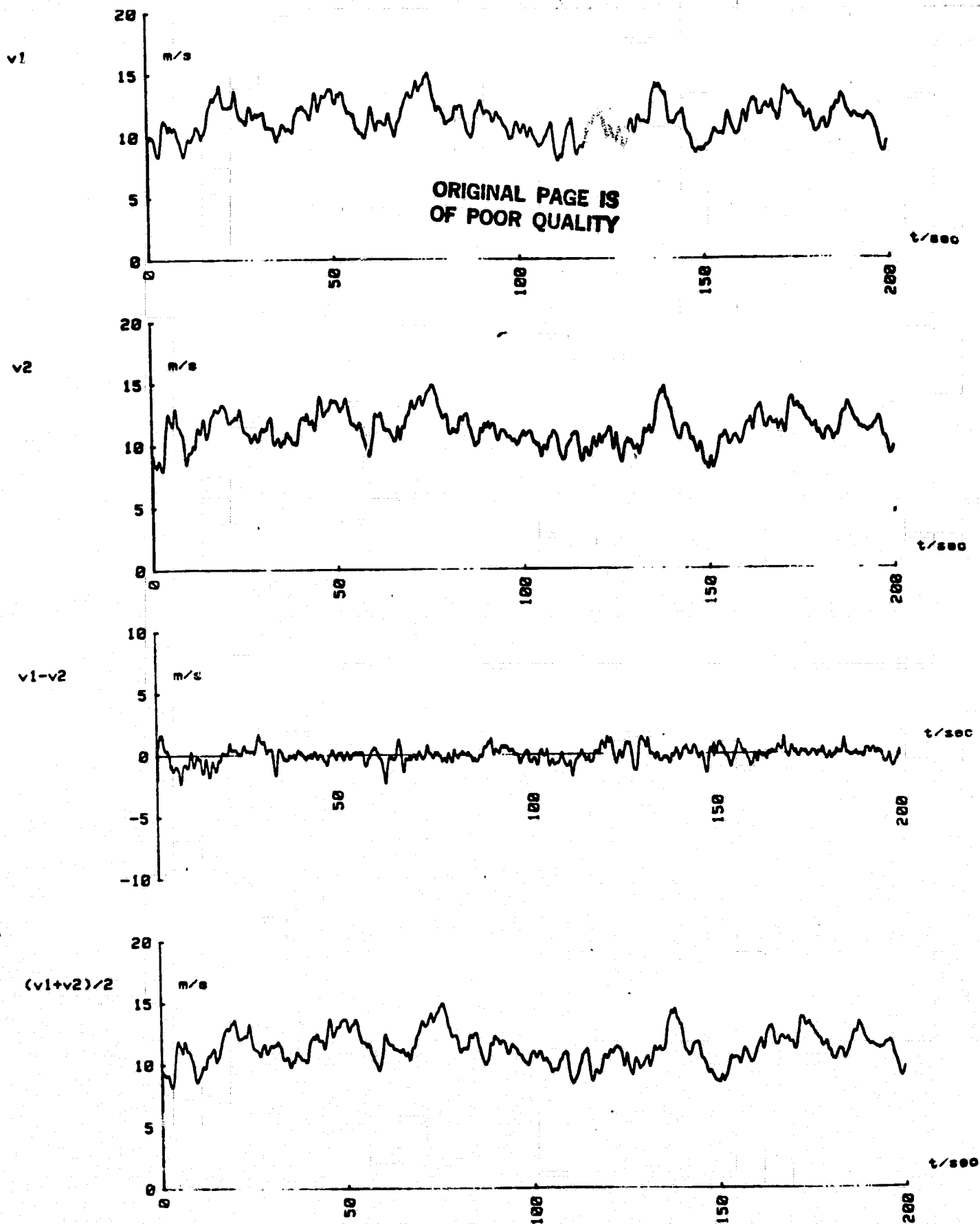


Figure 5. Wind speeds of 2 adjacent measurement points.

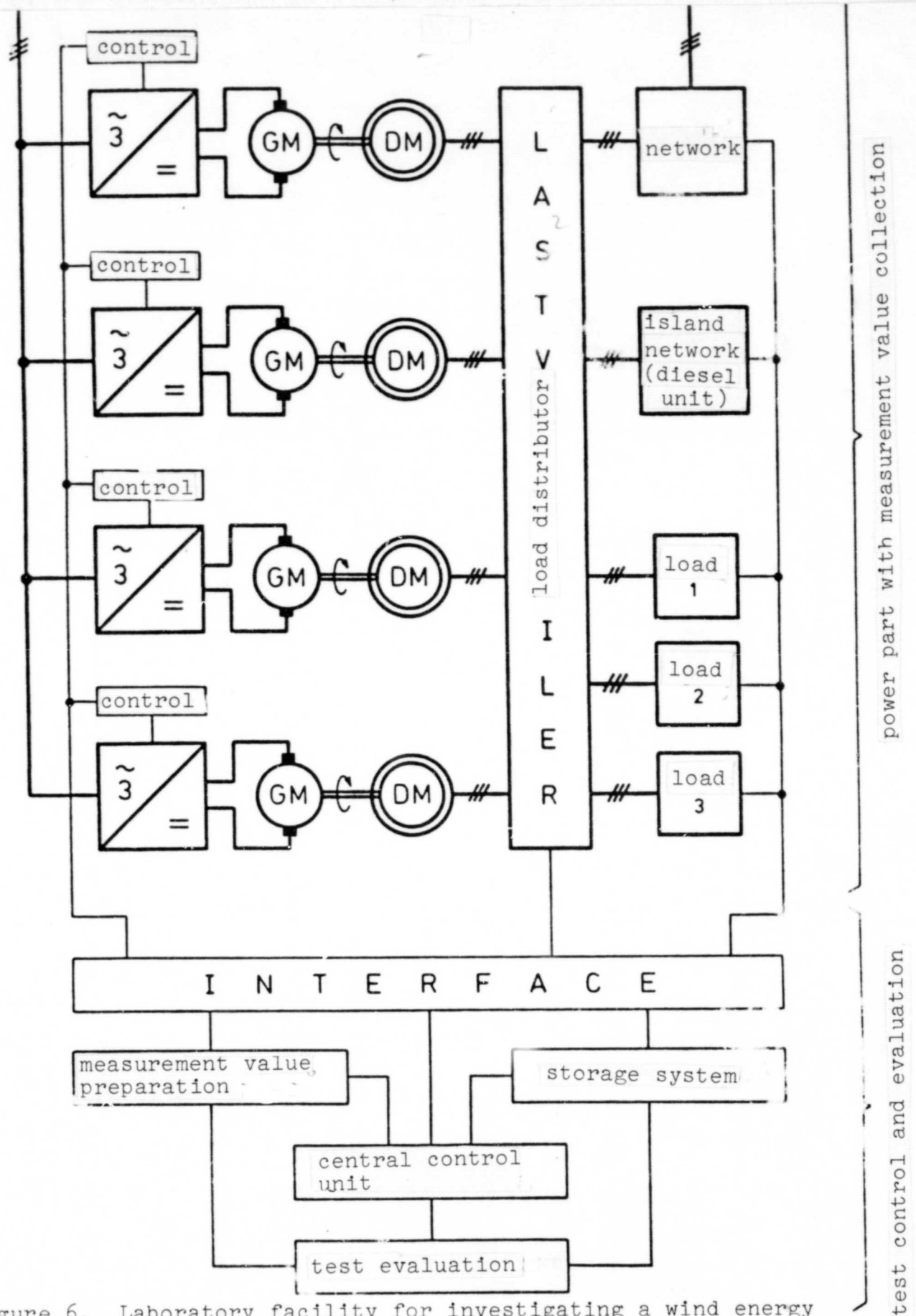


Figure 6. Laboratory facility for investigating a wind energy converter complex. GM DC current machine (15 kW drive)  
DM 3-phase machine (10 kW generator)

The wind speed determination will be very important in the other measurement investigations of dynamic processes in wind energy facilities.

### 3.2 Model of a wind energy facility

Within the development of a facility model for demonstration purposes, we started on an operational system which would have a wide validity (both in terms of facility size and operating range). At the present time, we are working on a microprocessor--controlled unit, which in particular satisfies the requirements of large facilities operating on a network. In the next step we plan to extend this to several operating conditions.

### 3.3 Joint operation of facilities

The further continuation of the joint operation system discussed in the first report (I), financed by university funds, was continued. Out of the block diagram of the planned overall structure shown in Figure 6, up to the present three motor generator sets were produced including the controlling regulation systems. Part of the measurement determination and measurement processing system are also available and at the present time are being complemented by interface units.

## ANALYSIS OF VARIOUS ENERGY CONVERTERS (I)\*

TABLE OF CONTENTS

1. Comparison of various generator types for a wind power plant.
2. Doubly supplied asynchronous machine as a wind power plant generator
  - 2.1 Principle of the doubly supplied ASM
  - 2.2 Theoretical treatment of the double supplied ASM
  - 2.3 Design of the power part of the rotor supply
  - 2.4 Realization of the control concept using microcomputers
    - 2.4.1 Hardware summary
    - 2.4.2 Software summary
3. Oversynchronous current rectification cascade
4. Present status and further procedure

ANALYSIS OF VARIOUS ENERGY CONVERTERS

/266

1. Comparison of various generator types for a wind power plant

For the selection of a suitable wind power plant generator, the following decision criteria have to be mentioned:

1. Operation for joint operation or island operation
2. Power range

This first report is restricted to high powered facilities ( $> 100 \text{ kW}$ ) which are to supply a joint network. The operator of the public power supply company (EVU) will require a supply with the constant effective power and idle power from a power generator source. In this case, it is necessary to store the fluctuating wind energy supply in a rotating mass. This is only possible when the rotor rpm of the generator  $f_2$  is not directly related to the network frequency  $f_3$  (see Figure 1.1).

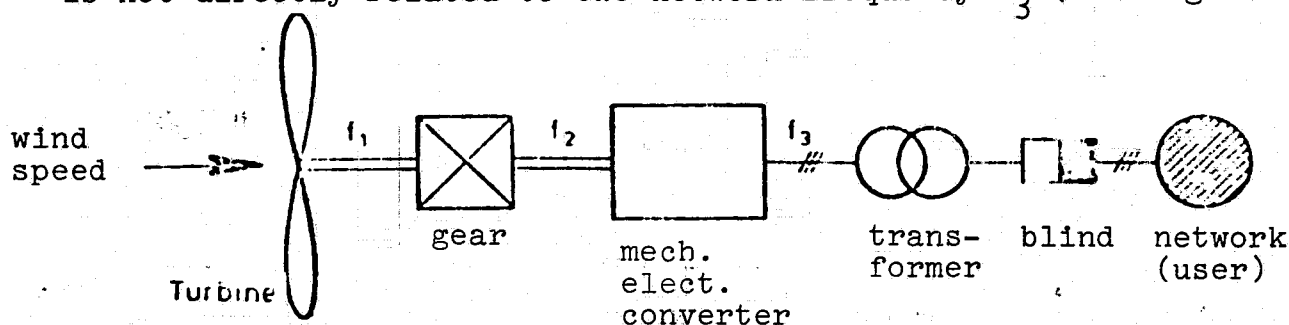


Figure 1.1 Power fraction of a wind energy facility

Synchronous power plants usually used for power production do not have this rpm flexibility. Therefore, either a variable gear or a dynamically high quality blade adjustment device is required in order to use this which will compensate for a variable wind energy supply. For constant power delivery to the network, primarily a synchronous generator should be considered, if the stator frequency  $f_2$  is uncoupled from the network frequency  $f_3$  to a direct current intermediate circuit. This concept has advantages for parallel operation of several wind turbines which together supply a direct current collection bus. By forming the sum, the local power fluctuations are smooth

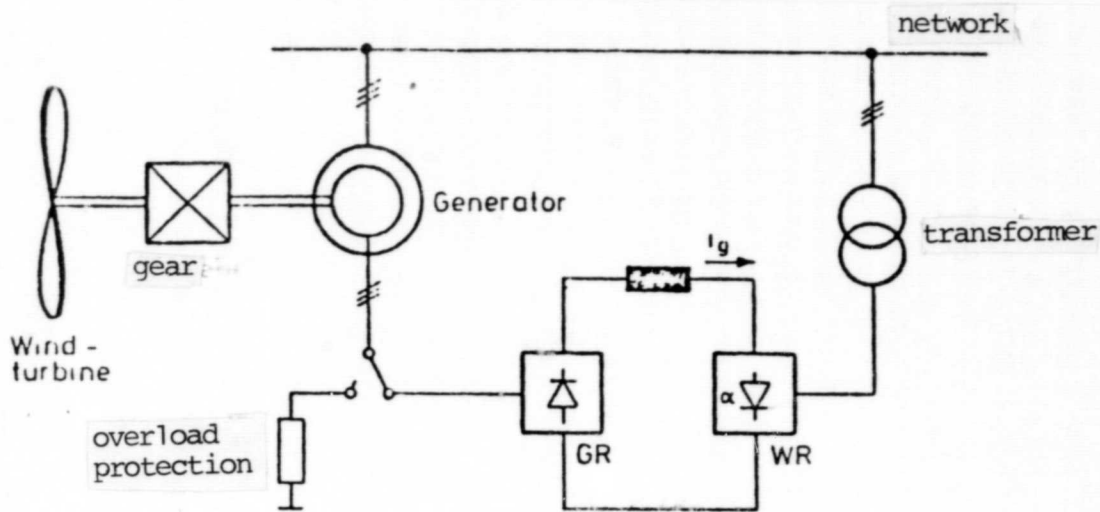


Figure 1.2 Wind energy facility with asynchronous generator and slip power recovery

in addition. However, this configuration does not allow the production of capacitive idle power for direct switching of the synchronous machine and the network. As an alternative to the method above, we can consider a slip ring runner asynchronous machine which is operated in an oversynchronous current rectification cascade circuit (Figure 1.2). For the oversynchronous operation, the rotor slip power is supplied through a direct current intermediate circuit to the network. Compared with the synchronous machine with the direct current intermediate circuit, this variation becomes more favorable the smaller the maximum rpm deflection is, because the rectifier only has to be designed for the slip power. The network feedbacks are also smaller because only the idle power is smooth through the current rectifier. This facility also requires condensers for producing idle current.

In order to eliminate this disadvantage, it is possible to use a direct converter in the rotor circuit instead of the direct current intermediate circuit (Figure 1.3) with which an independent rotory field is superimposed onto the rotor. In the case of load fluctuations, it then becomes possible to deviate into oversynchronous and under-synchronous operations and capacitive idle current can be produced.



These advantages, however, must be contrasted with the relatively great complexity for the direct converter and the more complicated control.

## 2. Double supply asynchronous machine as a wind power plant generator

### 2.1 Principle of the double supply ASM

Compared with the synchronous machine, the double supply ASM has the advantage that the flow direction in the rotor can be specified by means of a rotory field system which is imposed from the outside. For the synchronous condition, in spite of different load states, the machine is driven at a constant pole wheel angle using a control system. In addition, there is the possibility to influence the idle power requirement of the machine for a constant effective power delivery by means of rotation of the flow direction. Therefore, it is possible to have uncoupled effective power control and idle power control.

If the rotor is supplied with a low frequency rotory current, then the machine will operate in the oversynchronous or undersynchronous condition depending on the direction of the rotary field. Also an energy flow through the rotor in both directions is related to this (Figure 2.1). The rotor power is calculated to be  $P_R = s \cdot P_{\text{mech}}$ .

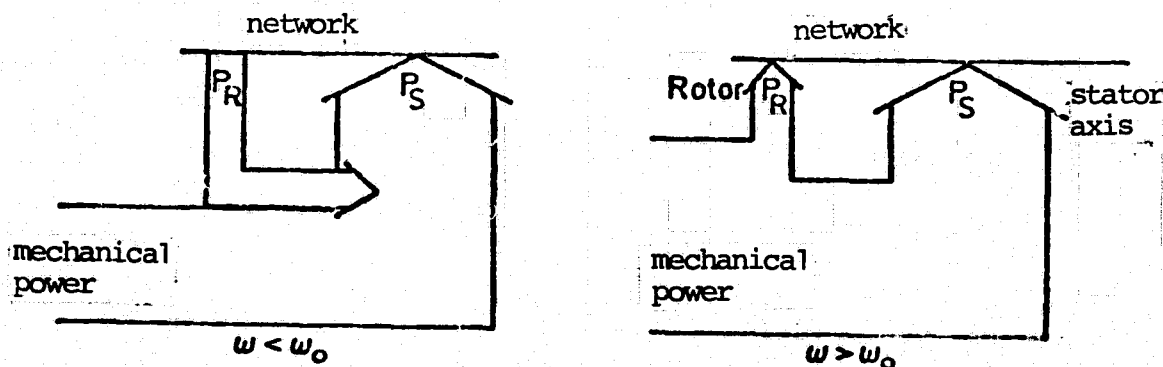


Figure 2.1

This means that in spite of a variable generator rpm, it is possible to maintain the delivered stator power constant. The runner flow has to be controlled in terms of frequency and phase by the rpm and angular position of the rotor so that the rotor and the stator rotary field are always synchronous. The machine has an operating behavior similar to an asynchronous machine.

## 2.2 Theoretical discussion of the double supply asynchronous machine

We will briefly outline a control method which will lead to a far reaching uncoupling of the magnetic processes along the longitudinal and transverse axis. The mathematical model of an asynchronous machine consists of two complex differential equations and two equations for the mechanical motion. A simplification of the relationships can be achieved if one assumes that the rotor currents controlled through the current rectifiers are assumed to be superimposed. This means that the voltage equation of the rotor circuit has no influence on the dynamics of the machine control. After conversion to the same winding number in the stator and the rotor, we have the following equations: /269

$$R_S \cdot \underline{i}_S + L_S \frac{d\underline{i}_S}{dt} + L_h \frac{d}{dt} (\underline{i}_R e^{j\epsilon}) = \underline{u}_N, \quad (1)$$

$$\Theta \frac{d\omega}{dt} = m_e + m_m = \frac{2}{3} L_h I_m \left[ \underline{i}_S \cdot \overline{\underline{i}_R e^{j\epsilon}} \right] + m_m, \quad (2)$$

$$\frac{d\epsilon}{dt} = \omega. \quad (3)$$

For the rotor current assumed to be superimposed, we assumed that

$$\underline{i}_R = i_{Ra}(t) + j i_{Rb}(t) = |\underline{i}_R| e^{j\epsilon}, \quad (4)$$

$$\frac{d\epsilon}{dt} = \omega_2. \quad (5)$$

In the following we will assume a two phase rotor winding. Using abbreviation

$$L_S = (1 + \sigma_S) \cdot L_h$$

equation (1) can be written in the following form:

$$R_S \cdot \underline{i}_S + L_h \frac{d}{dt} \left[ (1 + \sigma_s) \underline{i}_S + \underline{i}_R e^{j\epsilon} \right] = \underline{u}_N \quad (6)$$

The expression in the square brackets is defined as an extended magnetization vector

$$\underline{i}_{ms} = (1 + \sigma_s) \underline{i}_S + \underline{i}_R e^{j\epsilon} = |\underline{i}_{ms}| e^{j\mu} \quad (7)$$

$$\frac{d\mu}{dt} = \omega_{ms} \quad (8)$$

and this is used for eliminating the stator current. Using Equation /270 (2.6), we find that

$$\frac{L_S}{R_S} \frac{d\underline{i}_{ms}}{dt} + \underline{i}_{ms} = \frac{1 + \sigma_s}{R_S} \underline{u}_N + \underline{i}_R e^{j\epsilon} \quad (9)$$

$$m_{el} = \frac{2}{3} \frac{L_h}{(1 + \sigma_s)} \operatorname{Im} \left[ \underline{i}_{ms} \overline{\underline{i}_R} e^{-j\epsilon} \right] \quad (10)$$

By multiplication with  $e^{-j\mu}$  equation (9) is then transformed into a moving coordinate system which is defined by the magnetization current vector  $\underline{i}_{ms}$ . After introducing the polar coordinates for  $\underline{i}_{ms}$ ,  $\underline{i}_R$  and  $\underline{u}_N$ , we then find the following equations by splitting the above into real part and imaginary parts

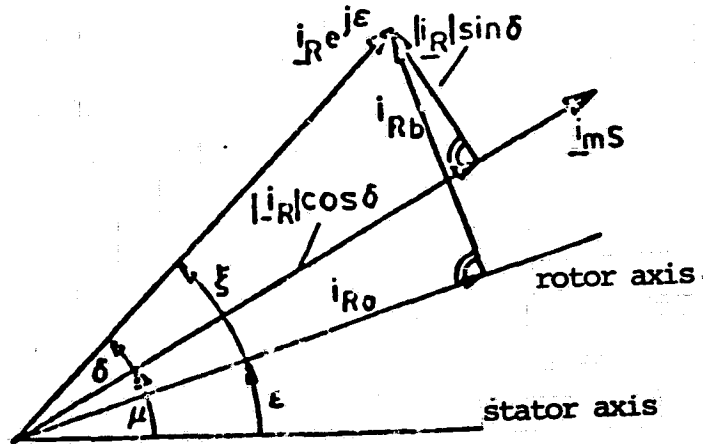
$$\begin{aligned} \frac{L_S}{R_S} \frac{d}{dt} |\underline{i}_{ms}| + |\underline{i}_{ms}| &= - \frac{1 + \sigma_s}{R_S} \frac{3\sqrt{2}}{2} U_N \sin(\omega_0 t - \mu) + \\ &+ |\underline{i}_R| \cos(\epsilon + \xi - \mu), \end{aligned} \quad (11)$$

$$\begin{aligned} \frac{L_S}{R_S} \omega_{ms} |\underline{i}_{ms}| &= \frac{1 + \sigma_s}{R_S} \frac{3\sqrt{2}}{2} U_N \sin(\omega_0 t - \mu) + \\ &+ |\underline{i}_R| \cos(\epsilon + \xi - \mu), \end{aligned} \quad (12)$$

$$m_{el} = - \frac{2}{3} \frac{L_h}{1 + \sigma_s} |\underline{i}_{ms}| |\underline{i}_R| \sin(\epsilon + \xi - \mu) \quad (13)$$

Figure 2.2 shows the various angular relationships.  $\epsilon + \xi - \mu = \delta$  corresponds to the load angle of the machine. The quantities  $|\underline{i}_R| \cos \delta$  and  $|\underline{i}_R| \sin \delta$  incorporate the longitudinal and transverse components of the rotor current vector referred to the expanded

ORIGINAL PAGE IS  
OF POOR QUALITY



magnetization current vector  $i_{ms}$ . The longitudinal component controls the magnitude of the magnetization current. The transverse component controls the angular speed  $\omega_{ms}$  of the magnetization current vector and the torque.

If these two rotor current components are changed independent of one another, then we have an independent uncoupled control for the idle power and the effective power of the stator or for the voltage and the torque of the machine.

After several transformations and normalization with the nominal values of the machine, we finally obtain the following equation system

$$T_S \frac{di_{ms}}{dt} + i_{ms} = (1 + \sigma_s) \left[ \frac{1}{r_s} u_{Nd} + \frac{2}{3} K_o i_{Rd} \right], \quad (14)$$

$$\frac{1}{\omega_o} \frac{d\mu}{dt} = \frac{\omega_{ms}}{\omega_o} = \frac{1 + \sigma_s}{x_d i_{ms}} \left[ u_{Nq} + \frac{2}{3} r_s \cdot K_o i_{Rq} \right]. \quad (15)$$

The stator time constant is

$$T_S = \frac{L_S}{R_S} = \frac{1}{r_s} x_d \frac{1}{\omega_o}. \quad (16)$$

In addition, we have  $\omega_o m_o = 3 U_{So} I_{So} \cos \varphi_o$

$$\frac{m_e}{m_o} = - \frac{2}{3} \frac{K_o x_d}{1 + \sigma_s} \frac{1}{\cos \varphi_o} i_{ms} i_{Rq}. \quad (17)$$

Here  $x_d$  is the normalized synchronous reactance

$$x_d = \omega_o L_s \frac{i_{s0}}{u_{s0}} = \frac{\omega_o \cdot L_s}{z_{s0}}$$

and  $K_o$  is the ratio of the stator short circuit current for nominal excitation divided by the nominal current.

These relationships are shown in Figure 2.3 in the form of a block circuit diagram. The normalized input quantities of this machine model are the two rotor currents, the network voltage and the drive torque. The nominal current values which vary sinusoidally for oversynchronous and undersynchronous operation have to be made available by the controlling control circuit. The quantities required for control are available by measurement for a doubly supplied machine ( $i_s, u_s, i_r, \omega, \epsilon$ ) or can be easily derived ( $i_{ms}, \mu, \sin(\epsilon - \mu), \cos(\epsilon - \mu)$ ).

A microcomputer can be used for this task.

Figure 2.3 gives an example how the field oriented control by a moment controller which affects  $i_{Rq}$  would be designed and a voltage controller which involves  $i_{Rd}$ .

The limiting dynamics and the restricted actuator path of the rectifier require that the rotor voltage induced for  $s \neq 0$  be switched in to improve the dynamics of current control which can be looked upon as a perturbation quantity. Figure 2.4 shows this and also we indicate how the residual delay of current control can be reduced by a linear delay unit in the nominal value input.

### 2.3 Design of the power part of the rotor supply

For supplying the rotor of the double supply asynchronous machine, we have selected a direct rectifier circuit according to Figure 2.5. This circuit consists of three antiparallel current rectifier bridges which are connected with a network through a transformer. The current rectifier bridges are switched in a star. The direct converter can allow power flow in both directions, depending on the phase sequence

(over or under synchronous operation). The star point of the rotor winding is not connected.

The transformer has the task of reducing the network voltage to the maximum required rotor voltage for control. It also prevents the formation of equalization currents between the three current rectifier bridges.

The three phases of the direct converter are commercial 4 quadrant current rectifier component groups which consist of a power part, a monitoring part and a nominal value determination device as well as a control logic system. The control of the individual current rectifier bridges in the present design is done with a microcomputer which from the actual and nominal values of the enter control circuit calculates three actuator signals which are displaced by  $120^\circ$ . The current rectifier bridges and the transformer are selected with power reserve in order to provide flexible testing. In this way, we wish to bring about that even in the most unfavorable operating case, we could examine how a moment shock of twice the nominal value could be controlled with a slip of 15%. In order to be able to investigate slip values of  $> 15\%$  and not to limit the controller dynamics by actuator limits, a transformer output voltage was designed for 21 times the rotor direct current for the synchronous condition (the factor of 21 was taken from a simulation). In order to determine the required limiting values, an actuator transformer is switched in ahead of the primary winding with which the maximum voltage can be continuously brought down.

/273

## 2.4 Realization of a controller concept using microcomputers

### 2.4.1 Hardware summary

At the institute we have developed a computer card with a microprocessor intel 8085 according to Figure 2.7 for controlling of the double supply ASM (Figure 2.7). This design allows simple operation in monitoring of all control circuits. In order to have a high scanning frequency, in the design of the computer system we have made sure

that time intensive operations will be carried out if possible through hardware. For example, the multiplications are performed by a fast 8x8 bit hardware multiplier and the phase deductions and phase divisions are realized by simple analog circuits.

The actual value determination of the rotor current and the stator current is done through Hall generators whose signals are amplified in order to obtain a larger perturbation voltage separation. For the position and rpm determination, an angle decoder was attached to the motor axis which allows a maximum resolution of  $0.1^\circ$ . These actual values are prepared according to the requirements of the control algorithm, filtered and are supplied to the computer through I/O ports. The interface between the analog part and the digital part is selected so that the minimum number of quantities have to be directed through the relatively time consuming AD/DA converter.

In order to allow extensive valuation of the dynamic behavior of the control circuit and its variables, the quantities of interest can be plotted if required. An analog output has been built for this.

/274

#### 2.4.2 Software summary

Shortly a program will have been finished which has the structure shown in Figure 2.8. The microprocessor takes over the calculation of the actual values for the electrical moment and the voltage. The calculation of the induced rotor voltage (perturbation voltage) and its switching as well as the transformation between the individual coordinate systems is also done in this way. The PI controller required for control can be performed by software with simple control algorithms. The entire programming sequence will be determined by the required minimum scanning rates of the individual partial control circuit and great calculation accuracy is required. The nominal rotor voltages in the a,b system are the output quantities which are directly given to the phase splitting device and the following direct converter.



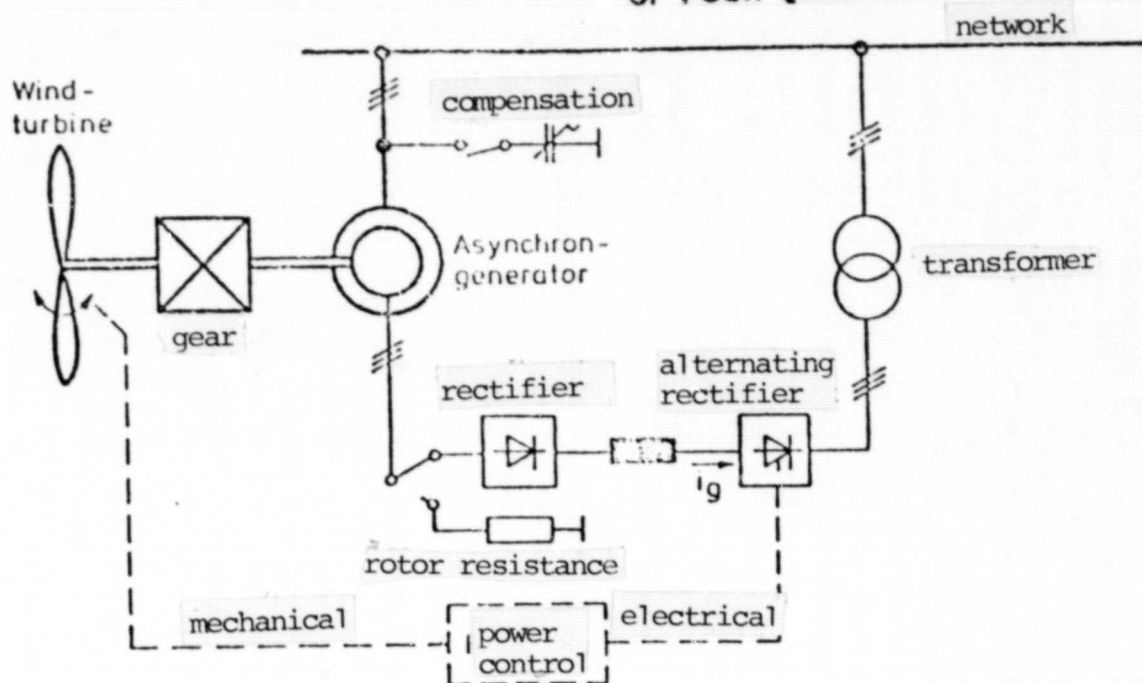


Figure 3.1 Wind energy facility with oversynchronous current rectifier cascade

### 3. Oversynchronous current rectification cascade

As a generator a slip ring runner ASM is used which operates only in the oversynchronous rpm range ( $\frac{n}{n_0} > 1$ ). The slip power  $s \cdot P_{\text{mech}}$  is supplied through a direct current intermediate circuit to the network, that is, in the rotor circuit it is possible to have only a single power direction in contrast to the facility discussed in section 2. The runner rotary field can be influenced in terms of current amplitude (by controlling the intermediate circuit current  $i_g$  through the rectifier). The phase and frequency, however, are determined by the stator rotary field and the rotor rpm, that is, only the effective power can be controlled. The machine as well as the rectifier take idle power from the network inductively which may be controllable by means of controllable condensers. The current rectifier complexity is small (6 diodes, 6 thyristors) and a circuit of the runner circuit to resistances is possible as overload and over rpm protection.

The rpm range is specified so that the rotating masses are capable for the maximum deviation from the nominal point to give off or take up

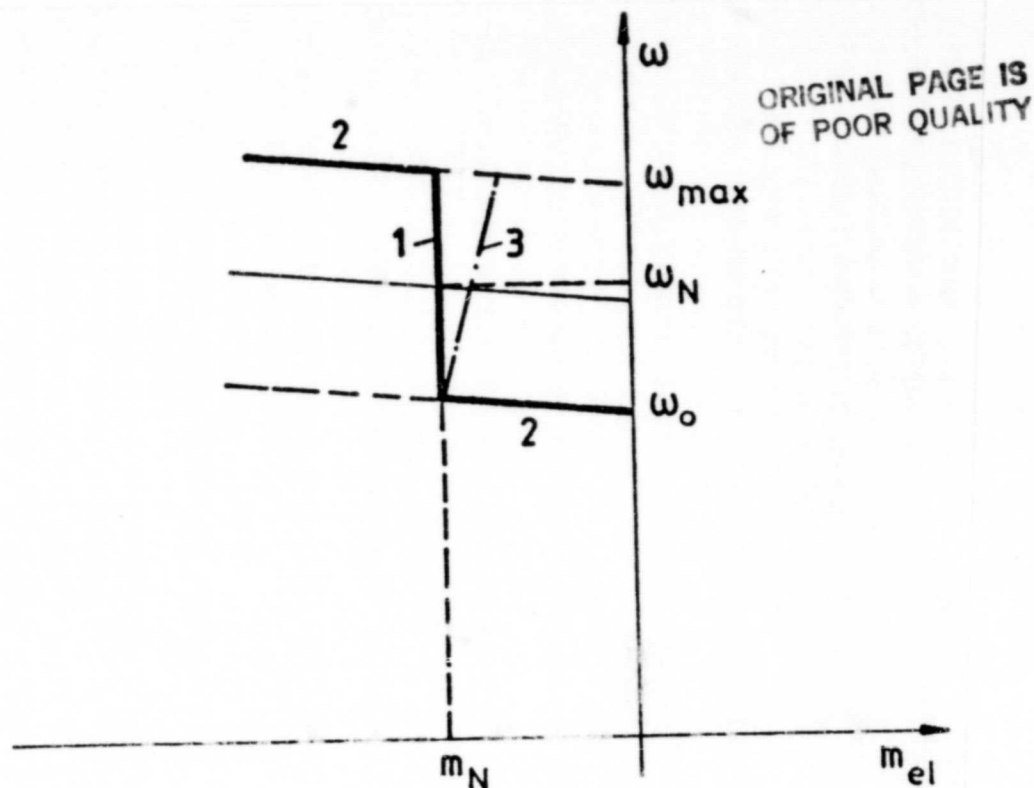


Figure 3.2 Characteristic line field of the over-synchronous current rectifier cascade

the same kinetic energy. For the normal operating range, the facility will, therefore, be along characteristic 1 of Figure 3.2. If the limiting rpm is achieved, then the power delivered to the network has to be changed (characteristics 2 and 2'). For facilities with a larger slip, it may be necessary to hold the entire power ( $P_{\text{stator}} + P_{\text{rotor}}$ ) constant. Then it would be necessary to reduce the moment according to characteristic 3 with increasing rpm. This makes the stability conditions more difficult and this will be tested by means of a digital simulation program.

1276

#### 4. Present status and further procedure

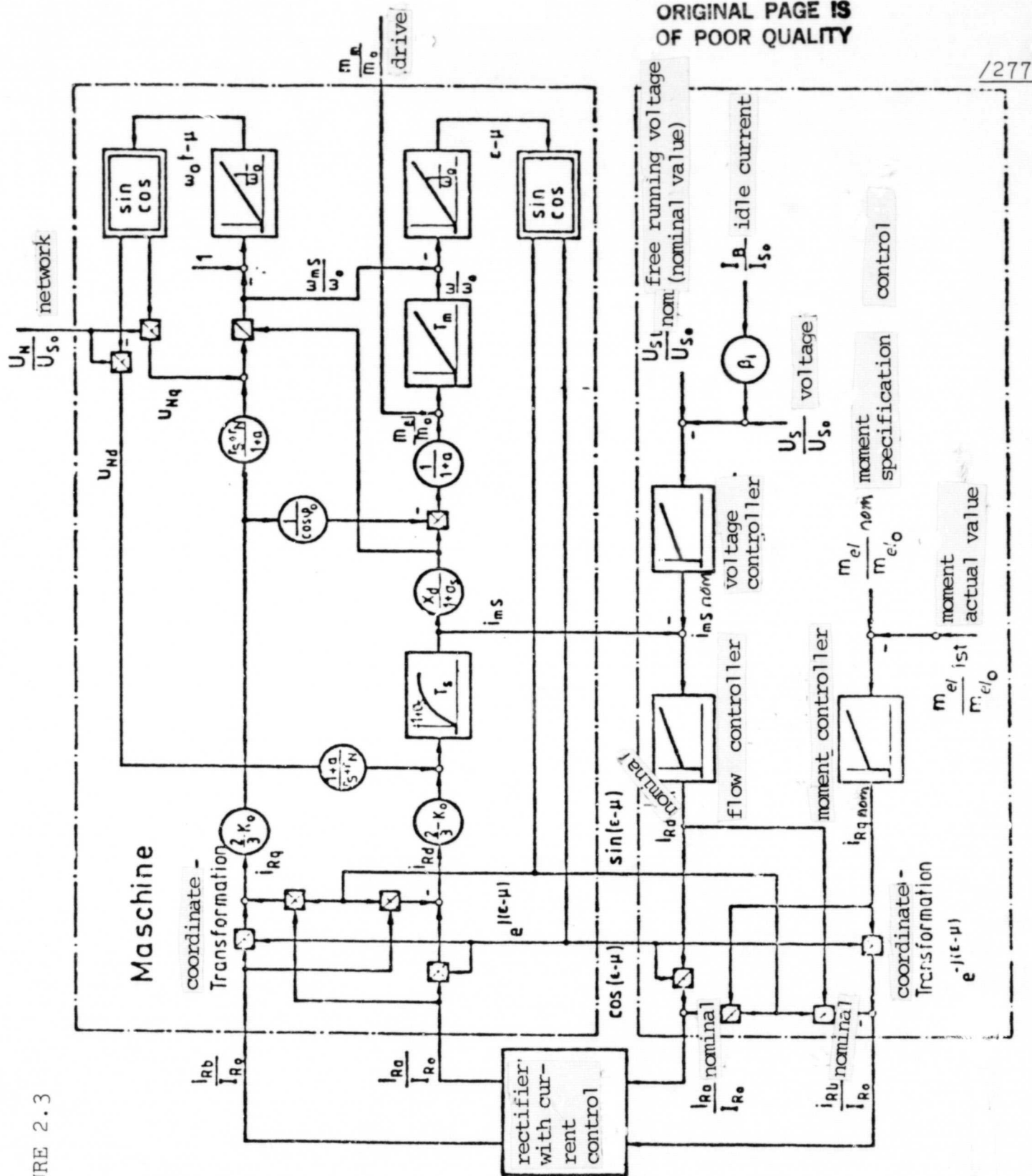
For the double supply asynchronous machine, a computer program has been developed which considers the unsteady operation of the current rectifiers and simulates the dynamic behavior of the control generator. The results will be compared with practical laboratory tests in order to allow generalization. The computer structure shown in Figure 2.7 with peripherals is now finished and at the present time is being tested.

The first testing will be done with a small 1.7 kW-ASM and will be paid for from our own funds and this is supplied with our own transistor rectifier in the rotor circuit. This intermediate stage has been introduced in order to overcome the long delivery times for the direct converter. Therefore, it becomes possible to build up the operating program in the following report year and to test it in steps. We plan to transfer to the larger machine (22 kW) and there will be additional problems because of the direct converter which can be isolated by proceeding in this way.

For oversynchronous current rectifier cascades, at the present time a computer program is being designed which will be used to investigate the dynamic behavior in parallel with the test set up. For the double supply ASM as well as for the current rectifier cascades, this same machine will be used; therefore, we have a direct means of comparing both methods.

Instead of the wind turbine, a direct current machine is used for the drive for which a moment variation will be implemented corresponding to that of the turbine. First test functions (jump, ramps) can be specified. Later on the torque variations determined by GHK will be used as nominal values.

FIGURE 2.3



ORIGINAL PAGE IS  
OF POOR QUALITY

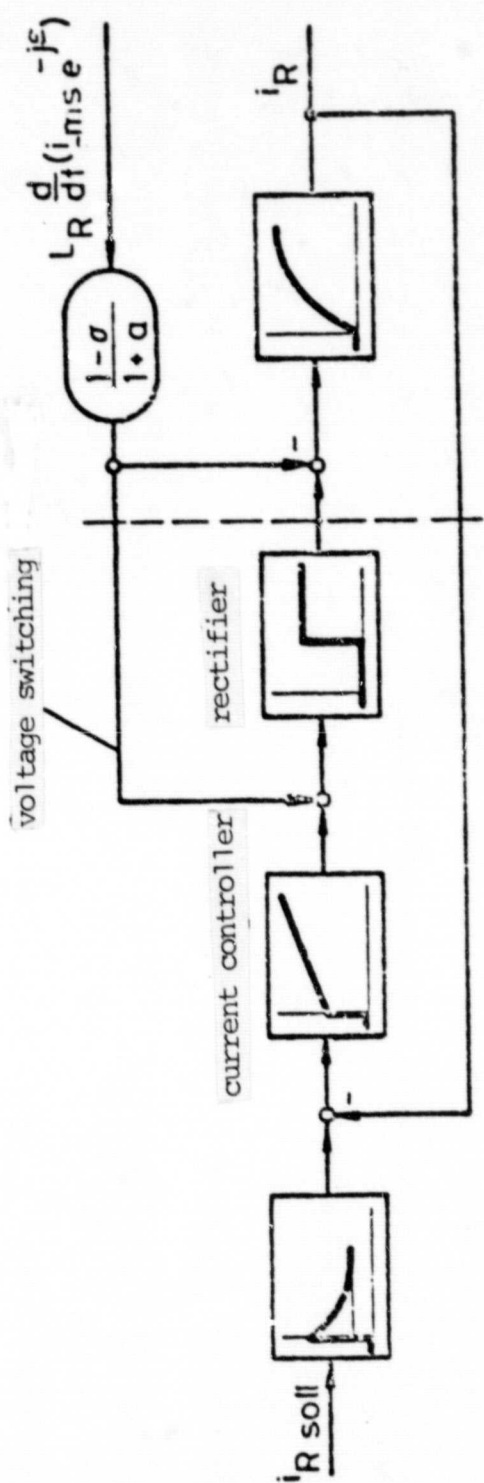


FIGURE 2.4

ORIGINAL PAGE IS  
OF POOR QUALITY

/279

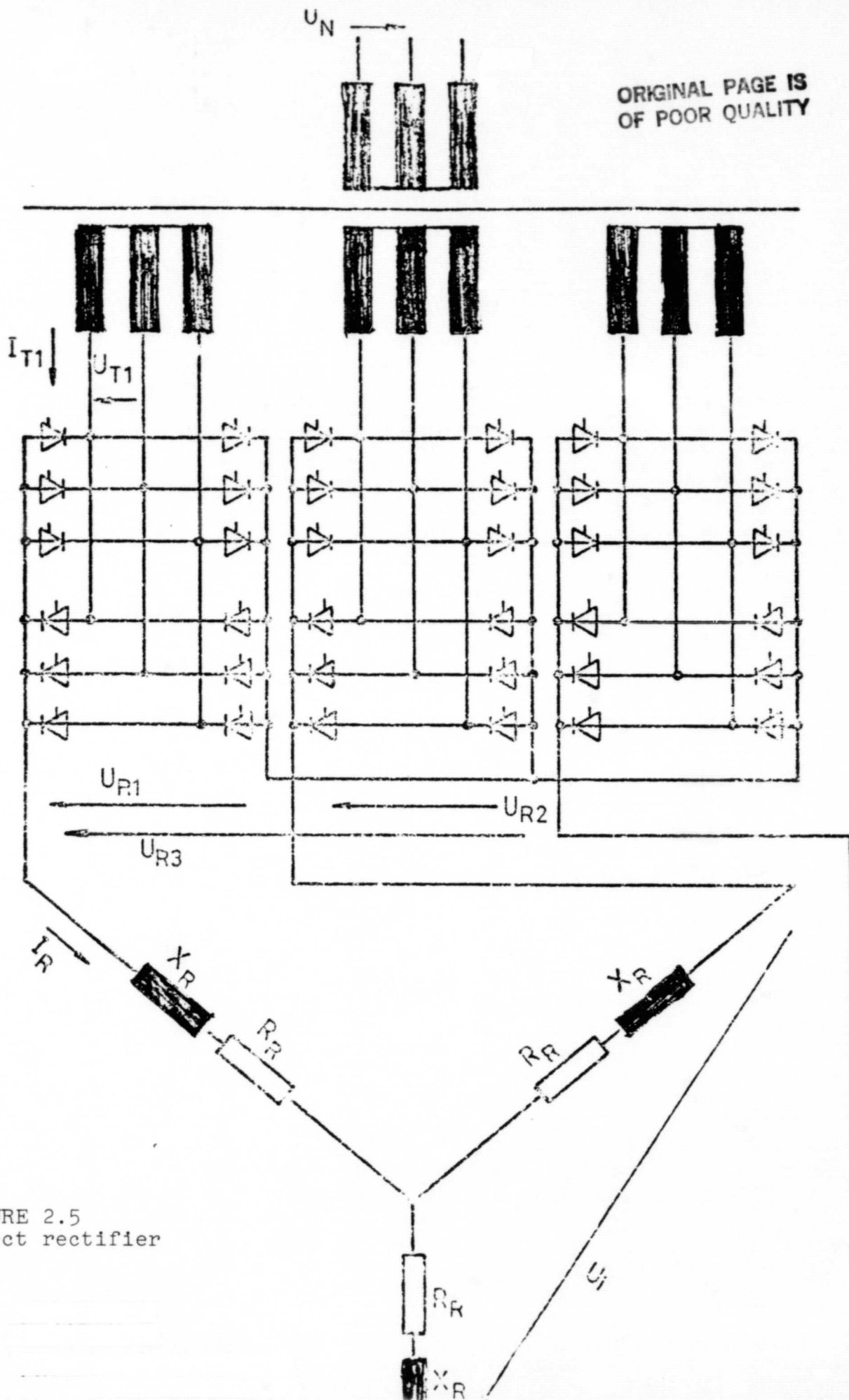


FIGURE 2.5  
direct rectifier



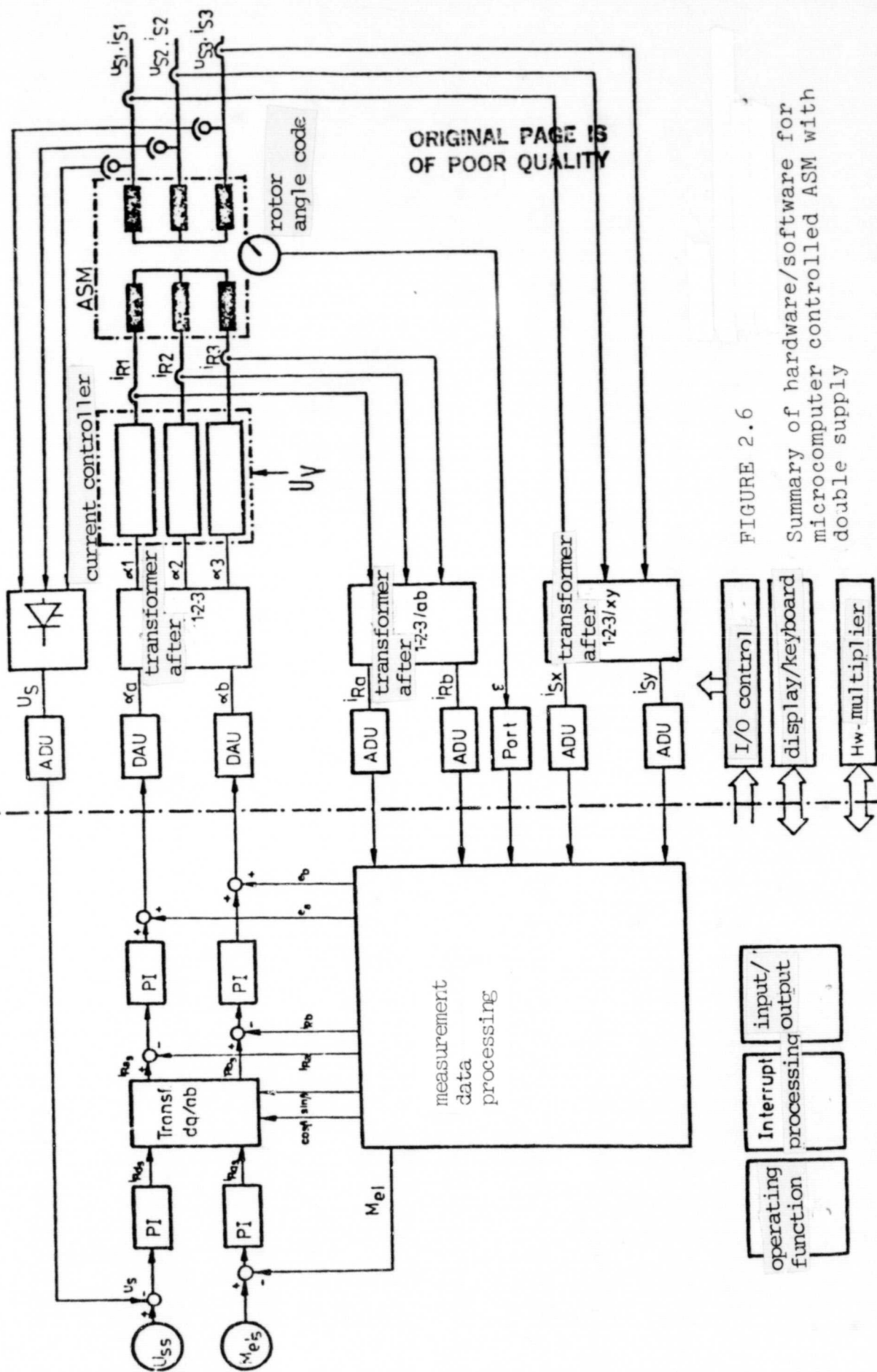


FIGURE 2.6

# Summary of hardware/software for microcomputer controlled ASM with double supply



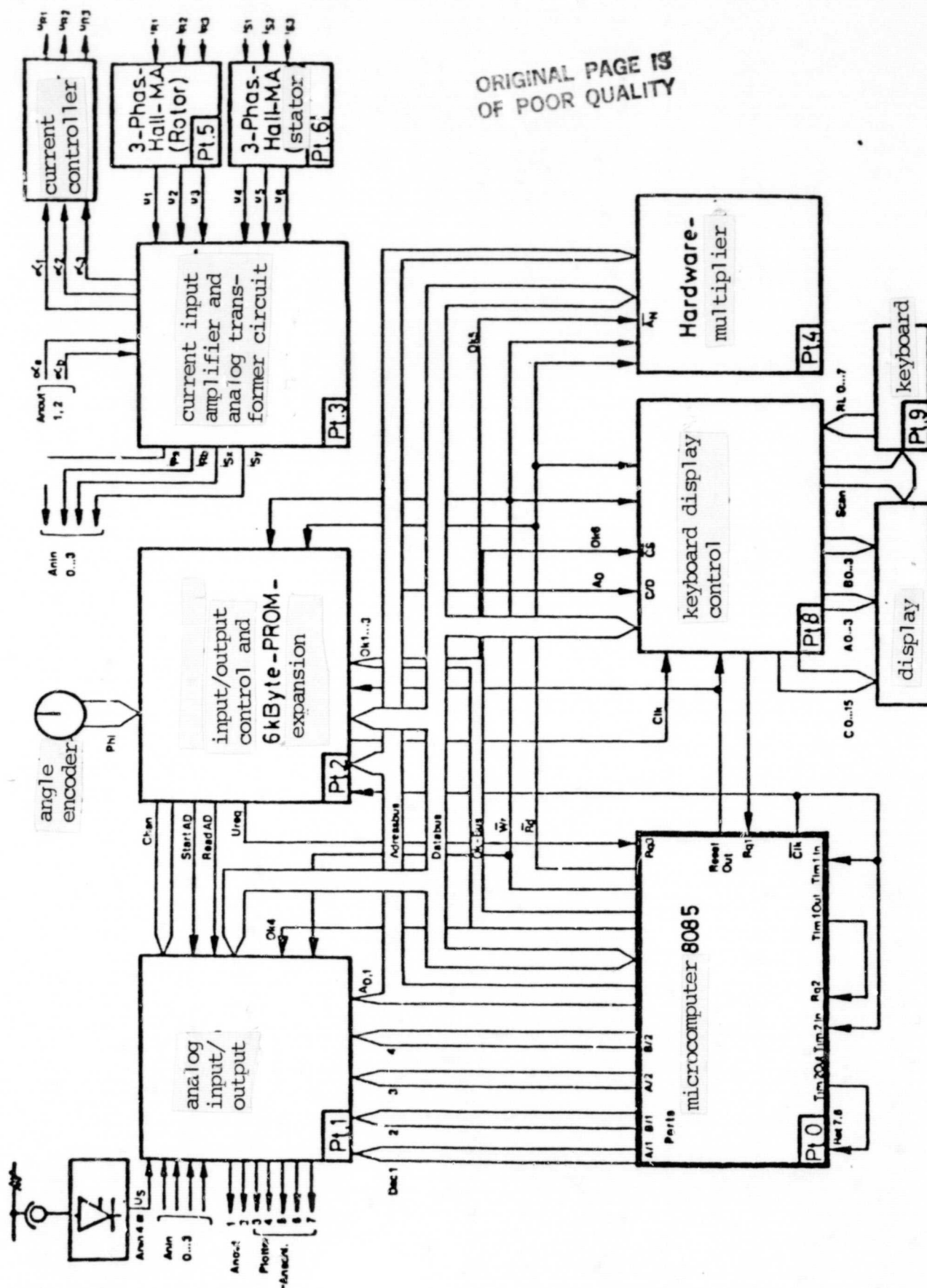


FIGURE 2.7 Hardware summary: Control of a double supply ASM with microcomputer 8085

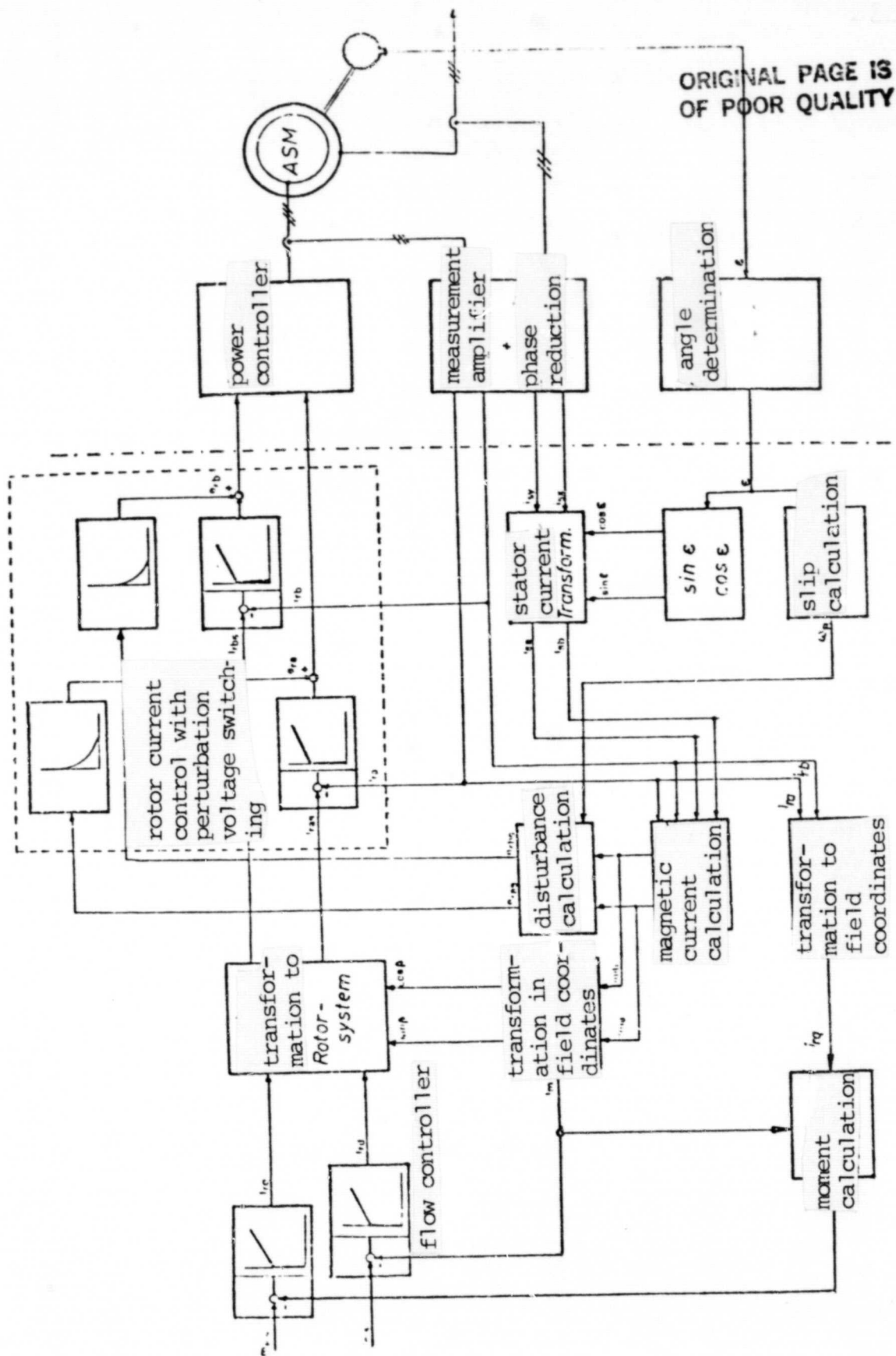


Figure 2.8 Block diagram of a microcomputer generator control system

Table of contents

1. Introduction
2. Simulation of a double supply three phase generator
  - 2.1 Simulation of the closed control circuit
  - 2.2 Simulation of the wind energy supply and the mass inertia of the generator unit
  - 2.3 Design of the controllers
3. Simulation results
  - 3.1 Jump response of the generator for synchronous conditions
  - 3.2 Braking of the generator from synchronous conditions to a minimum rpm
  - 3.3 Nominal value and actual value jump in voltage for asynchronous operation
- 4.1 Present status of test facilities
- 4.2 Measurement results
5. Further procedures
6. Oversynchronous current rectification cascade
  - 6.1 Method of operation
  - 6.2 Calculations for stationary operation
7. Simulation with oversynchronous current rectification cascade
  - 7.1 Differential equations of the direct current intermediate circuit
  - 7.2 Differential equations of the rotor circuit

---

\* TU Braunschweig

- 7.3 Relationships among differential equations of the rotor and those of the intermediate circuit
- 7.4 Stator equation and mechanical motion equations
- 8. Dimensioning of the current controller
- 9. Simulation results
  - 9.1 Operation of the cascade at the nominal point
  - 9.2 Jump response for a change in the nominal current value  $i_{gs}$
  - 9.3 Jump response for a change in the supply mechanical power
- 10. Further procedures

## ANALYSIS OF VARIOUS ENERGY CONVERTERS

### 1. Introduction

In the first report we investigated generators and their controls and compared them. The theory and laboratory setup of the double supply rotary field machine were discussed in detail.

In this report.(II), we first discuss the digital simulation results of the double supply rotary field machine. After this we discuss the measurement protocols obtained with the laboratory setup. In addition, the report has in it extensive description of the theory and the simulation results for oversynchronous current rectification cascades.

### 2. Simulation of a double supply three phase generator

The differential equations of the double supply three phase machine and the block diagram of the entire control concept can be taken from the first intermediate report. Fgiure 2.1 gives a simplified circuit diagram.

#### 2.1 Simulation of the closed control circuit

For the best possible representation of the dynamic properties of the generator, the differential equations of the three phase machine and of the network are related with the properties of the direct rectifier.

In order to limit the calculations, the following simplifications are introduced:

1. The output voltage of the direct rectifier consists of segments of a sinusoidal function, depending on the control angle  $\alpha$ , and the commutation processes are ignored.

2. The blockage time for zero crossing of the current is not considered.



The entire block diagram of the controller concept is shown in Figure 2.3 of the first intermediate report.

## 2.2 Simulation of the wind energy supply and the mass inertia of the generator unit

In order to be able to approximately simulate the operation of a real wind power plant, the dynamics of the wind and the mass inertia of the real wind energy converter have to be simulated for the laboratory machine. This is done by a corresponding control of the direct current motor which drives the three phase machine and in this way gives the fluctuating energy supply of the wind to the generator. Figure 2.1 shows a simplification of the control of the direct current machine. The moments of inertia of the real facility can be simulated by a suitable selection of the integration time constant  $T_m$ . /287

## 2.3 Design of the controller

All of the controllers (see Figure 2.3 of the 1st intermediate report) are determined for the synchronous idle running condition with the assumption of complete uncoupling. Since the paths are of higher order, the theoretical design can only give indications by means of replacement time constants. The final dimensioning is done experimentally during a simulation.

## 3. Simulation results

Figures 3.1a and 3.1b show the simulation results calculated from the test facility and normalized for the nominal quantities and the control circuit was subjected to several disturbances.

### 3.1 Jump response of the generator for synchronous conditions

It is assumed that the generator is in the synchronous idling condition for  $t < 0$ , i.e., the rotor current and the rotor voltages are 0.



At the time  $t = 0$  the nominal quantities of the generator are introduced as nominal quantities instantaneously in the form of a jump to the voltage controller and the moment controller. At the same time, the electrical moment of the generator is specified in the same magnitude. The rpm of the machine remains approximately constant.

Diagrams a, b in Figure 3.1a show the development of the two-phase rotor currents. The real three-phase rotor currents are shown in diagram c. Two of the three-phase rotor voltages are taken from d, e. The electrical moment  $m_{el}$  and voltage  $\Delta U_{act} = U_{nom} - U_{act}$  already have achieved a stationary state after about 100 ms (diagrams f, g). Diagram h shows the slip  $s$  of the machine. The dash and dot line gives the slip of the energy converter. The difference between the electrical moment and the moment of the wind wheel which results during the transient process of the controller circuit is not sufficient to accelerate the machine noticeably. This is not completely achieved with the laboratory facility (see diagram h, curve  $s_{lab}$ ), but the dynamic behavior of the simulated wind energy converter is quite close to the real facility.

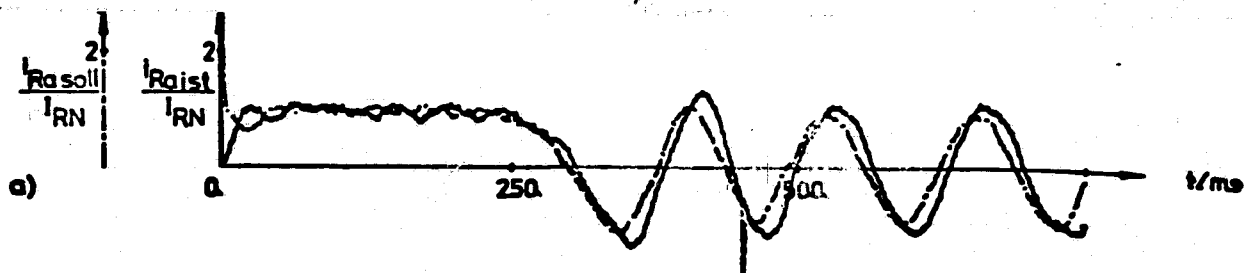
/290

### 3.2 Braking of the generator from the synchronous condition to minimum rpm

The generator is braked with 25 times the nominal moment within 175 ms to its minimum rpm. Diagrams f and g show that these perturbation quantities are quickly controlled by the controllers and that the moment and voltage controls are uncoupled. By means of the control system a slip-frequency sinusoidal rotary current is superimposed on the rotor (c).

### 3.3 Voltage actual value and nominal value jump for asynchronous operation

The generator is in the under synchronous condition ( $s = 15\%$ ). For  $t > 450$  ms the network voltage and the nominal value of the voltage controller are reduced by 10%. Diagram g shows that the stator voltage has reached the new nominal value after about 70 ms. A comparison



/289

ORIGINAL PAGE IS  
OF POOR QUALITY

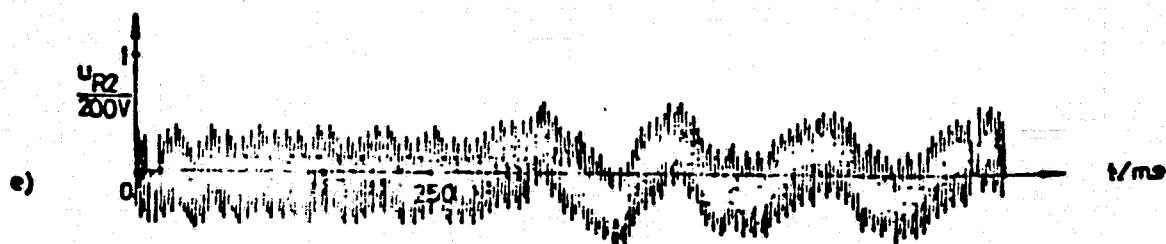
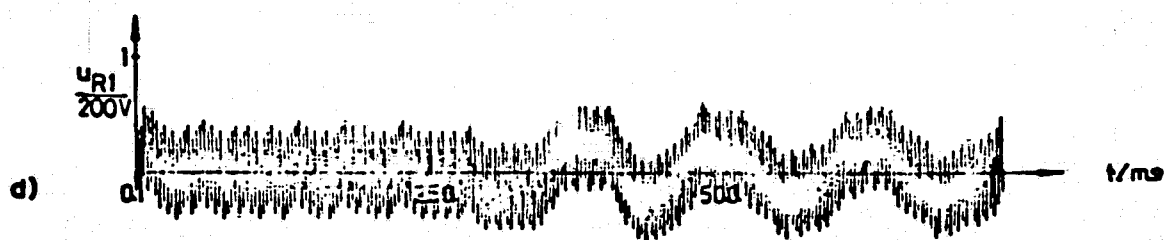
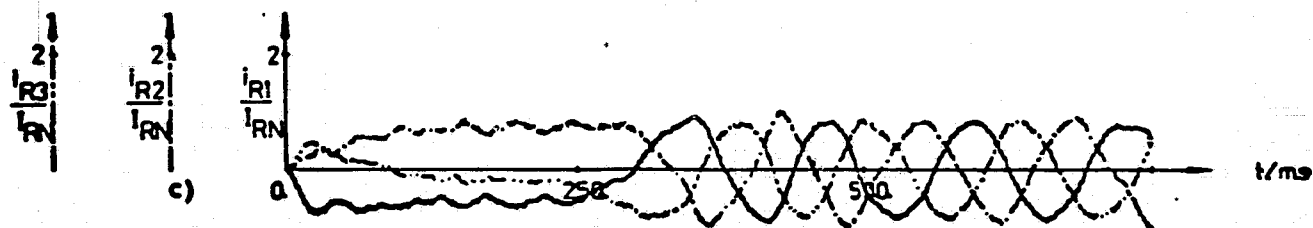
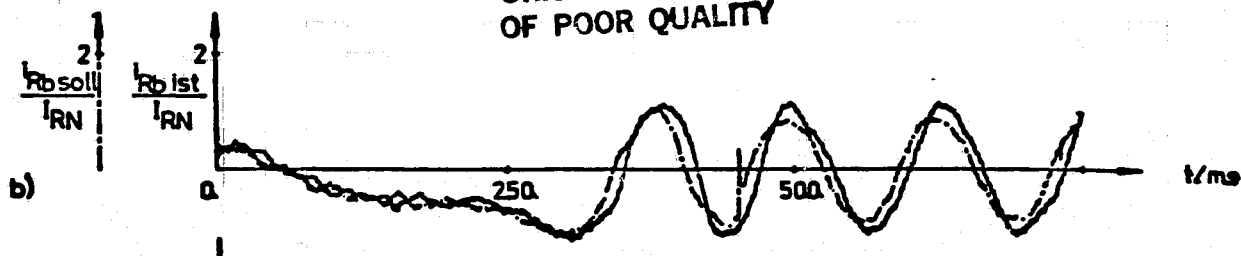


Figure 3.1a: Dynamic behavior of a double supply three-phase machine (simulation)

ORIGINAL PAGE IS  
OF POOR QUALITY

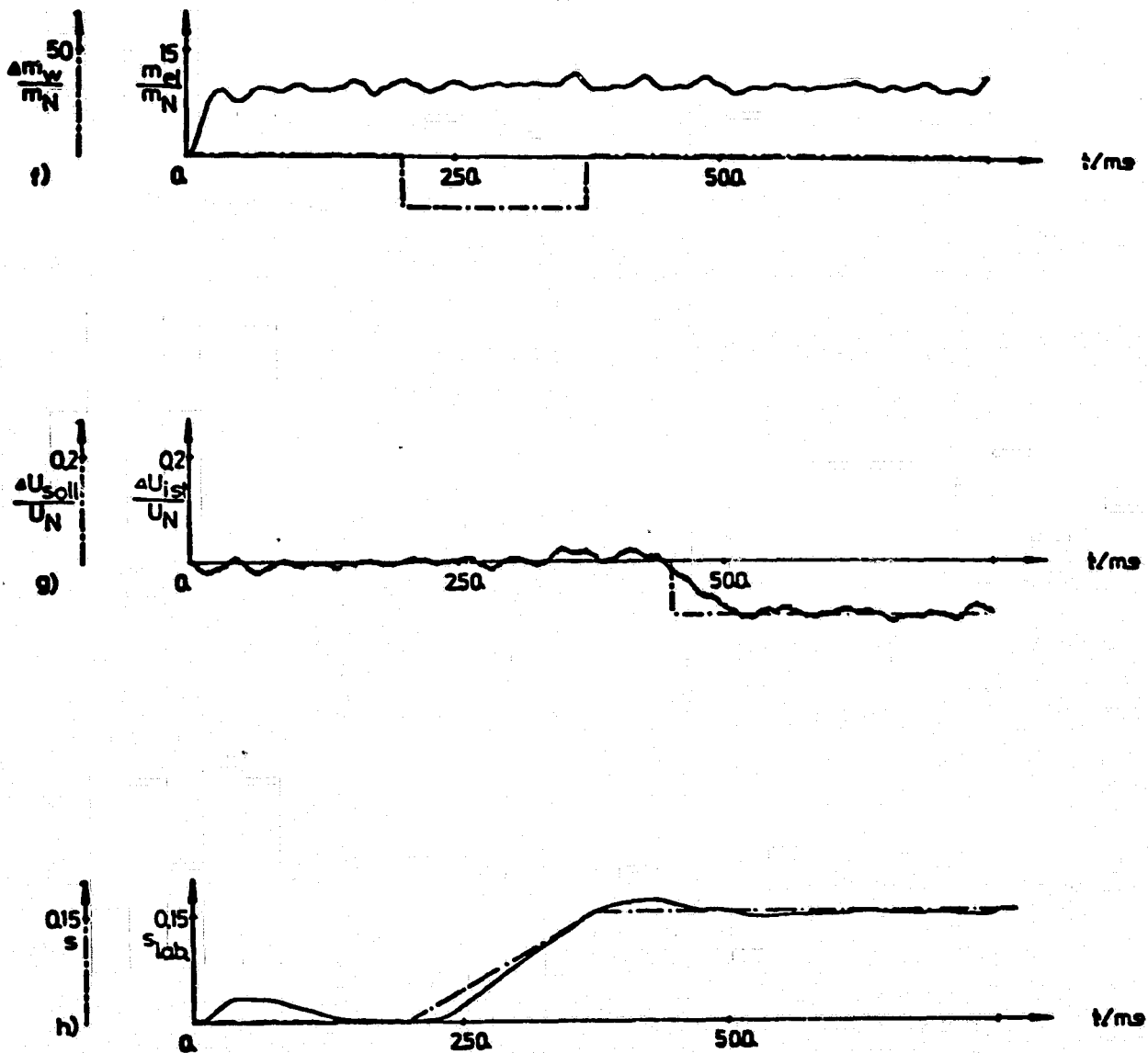


Figure 3.1b: Continuation of Figure 3.1a

between the electrical moment and the stator voltage shows that the two control circuits have the desired uncoupling for this perturbation case.

#### 4.1 Present status of the test setup

A detailed description of the microcomputer system and the power part was given in the first report. In the meantime, the individual components have been operated and have been switched together according to the structure shown in Figure 2.1. The structure and operation of the direct converter resulted in some difficulty because of the fact that the star point was not connected.

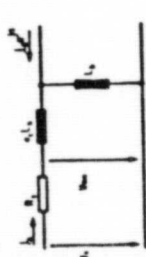
An assembler program was built for controlling the double supply three field machine and was tested with a laboratory setup. A scanning time of 2.5 ms can be achieved for the two current controllers and a scanning time of 5 ms can be achieved for the moment and flow controllers.

The first results with this controlled three phase machine were presented in October at the INTERKAMA 80 fair. Figure 4.1 shows the fair stand of the Institute for Control Techniques during the building phase. The figure shows the 22 kW machine, the controller unit and on the left side there is the rectifier console for the direct current machine. The direct rectifier cannot be seen on the figure. The poster (see Figure 4.2) in the background gives a summary about the purpose, theory and control method. /291

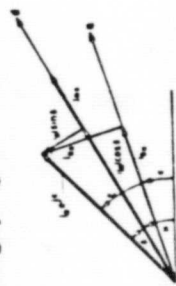
#### 4.2 Measurement results

In the following we will give a brief discussion of measurement protocols of the test set up. Since the facility is not yet optimum, these are only intermediate results. For example, there are still difficulties because of the fact that the star point of the rotor windings is not acceptable and because of the switching delays of the partial bridges of the direct rectifier. In addition, the voltage switching of the induced rotor voltage was not yet operable. However, we already /294 can see that the results obtained with the digital simulation will be confirmed in practice.

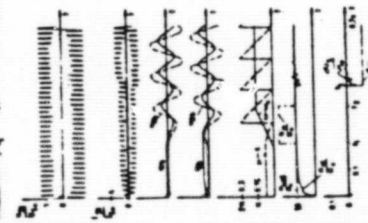
Figure 4.3 shows the variation of the normalized two-phase rotor current of the machine. The controlled direct current machine drives the three phase generator and transfers it from oversynchronous condition to the undersynchronous condition. The phase position of the rotor



1 Ersatzschaltbild für eingepiragten Rotorstrom



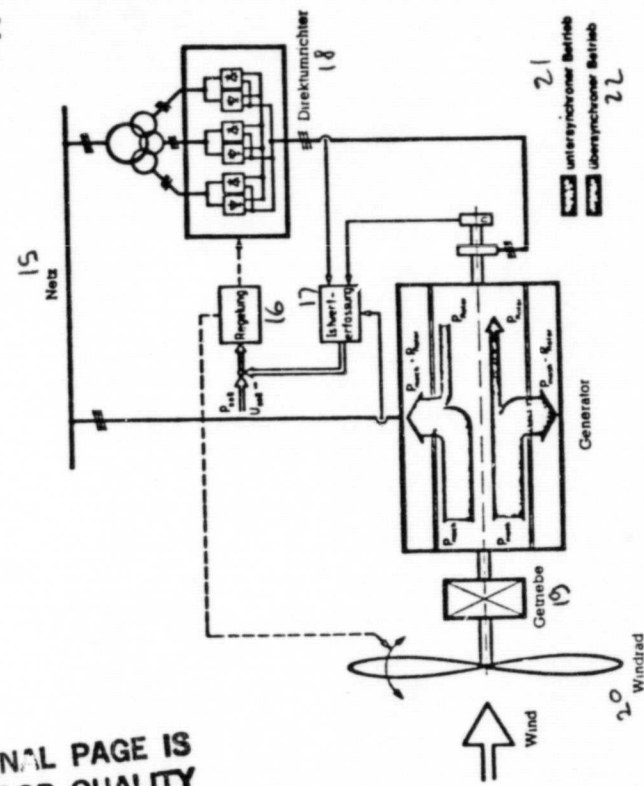
2 Stromvektoren  
 Langstromkomponente des Rotorstromes  $i_{Rd} = i_R \cos \delta$   
 Querkomponente des Rotorstromes  $i_{Rq} = i_R \sin \delta$



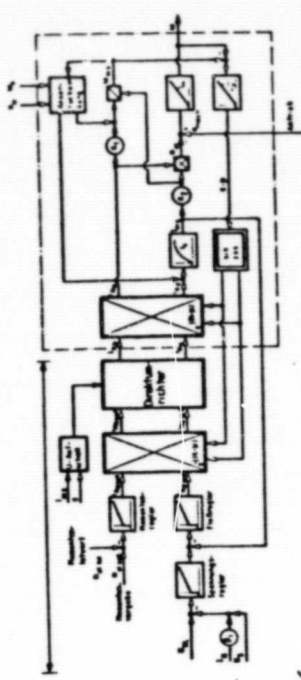
5 Verhalten des Generators bei sprungförmigen Momenten- und Spannungsänderungen (Simulation)

7 Die Leistungsabgabe eines Windkraftwerkes ist stark von der Windgeschwindigkeit abhängig. Kurzzeitige Schwankungen lassen sich durch den Einsatz der rotierenden Massen (Windrad, Getriebe, Rotor) als Schwungrad ausgleichen. Dies setzt voraus, daß der Generator am Netz angeschlossen wird, wenn der Generator in den Netz mit variabler Drehzahl laufen kann. In diesem Projekt wird das Betriebsverhalten verschiedener Generatoren für Windkraftwerke untersucht. Die Bilder beschreiben das für CROWMAN vorgesehene Verhalten der doppelgespeisten Drehstrommaschine.

ORIGINAL PAGE IS OF POOR QUALITY

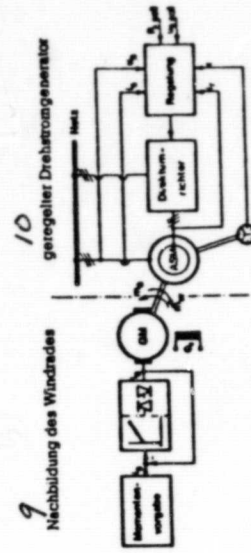


14 Windkraftwerk mit doppelgespeister Drehstrommaschine



6 Entkoppelte Wirk- und Blindleistungsregelung eines doppelgespeisten Drehstromgenerators

8 Eigenschaften des doppelgespeisten Drehstromgenerators  
 • über- und unter-synchroner Betrieb  
 • entkoppelte Wirk- und Blindleistungsregelung  
 • kapazitiver oder induktiver Betrieb



9 Nachbildung des Windrades

10 geregelter Drehstromgenerator  
 13 Laboraufbau  
 Im Labor wird der Generator anstelle eines Windrades durch eine geregelte Gleichstrommaschine angetrieben. Als Führunggröße des Gleichstromantriebes dienen abgespeicherte Momentenverläufe, damit ist auch die Nachbildung von Böen möglich.  
 Förderung durch das BMFT

Figure 4.2: Poster at the Interkama 80 exhibit on applied research

KEY TO FIGURE 4.2 ON PRECEDING PAGE:

1--replacement diagram for superimposed rotor current; 2--current vectors, longitudinal component of rotor current  $i_d = I_m \cos \delta$  flux, transverse component of rotor current  $i_q = I_m \sin \delta$ ; 5--behavior of the generator for jump-like moment and voltage changes (simulation); 7--the power delivery of a wind power plant depends greatly on wind speed. Short time fluctuations can be equalized by using rotating masses (wind wheel, gearing, rotor) as fly wheels. This implies that the generator operating on a fixed network can operate with variable rpm. In this project, the operating behavior of various generators is investigated for wind power plants. The figures show the method adapted for Growian of a double supply 3-phase machine; 6--uncoupled effective and idle power control of a double supply 3-phase generator; 8--properties of a double supply 3-phase generator. -Over and under synchronous operation -Uncoupled effective and idle power control -capacitive or inductive operation; 9--simulation of wind wheel; 10--controlled 3-phase generator; 13--laboratory set up. In the laboratory the generator is driven by a controlled direct current machine instead of the wind wheel. Stored moment variations are used as controlling variables of the direct current drive. This means gusts can be simulated. Supported by BMFT. 14--wind power plant with double supply 3-phase machine; 15--line; 16--control; 17--actual value determination; 18--direct rectifier; 19--gear; 20--wind wheel; 21--subsynchronous operation; 22--over-synchronous operation.

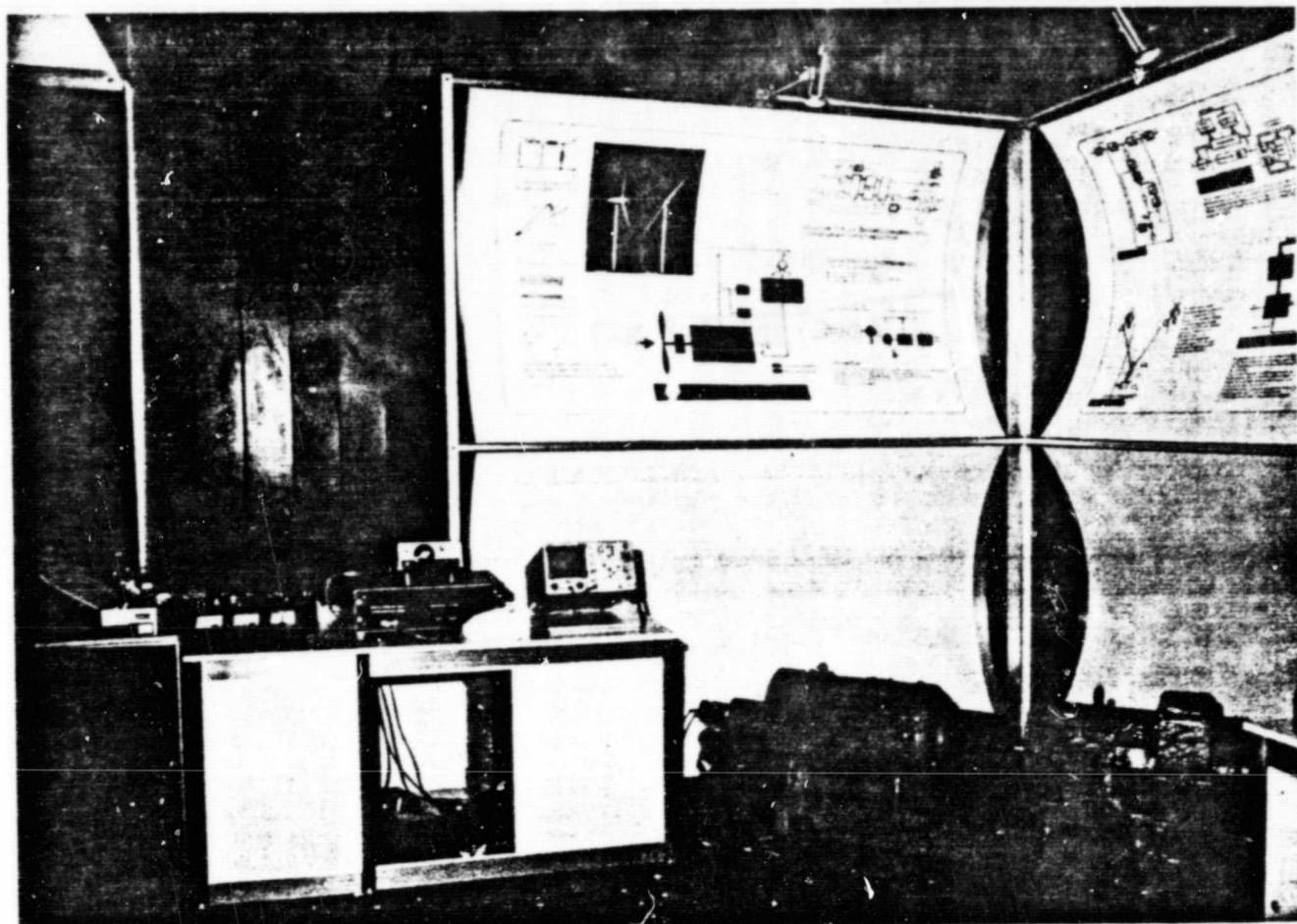


Figure 4.1 Measurement stand of the double supply 3-phase machine Interkama 80

currents changes during transition through the synchronous condition.

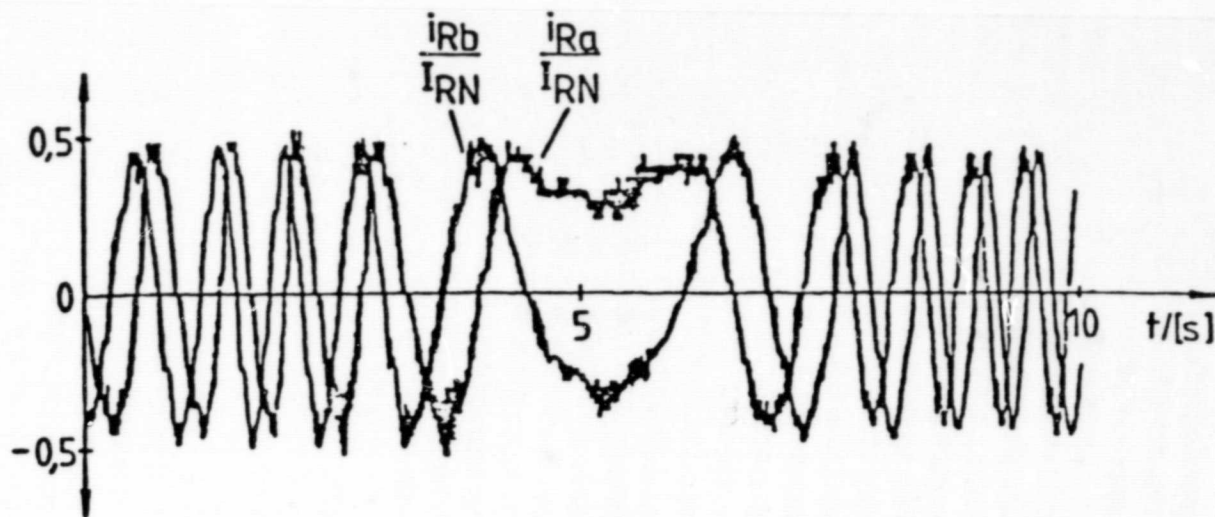
Figure 4.4 shows the variation of the magnitude of the magnetization vector  $\underline{i}_{mS}$  for constant rpm of the generator referred to the magnetization current  $I_\mu$  (for an idling machine). At the time  $t_1$  the nominal value is changed in jump-like fashion for the magnetization current (flow controller). For the maximum voltage of the direct converter selected here, the actual value adjusts to the new nominal value after about 120 ms. The corresponding variation of the a component of the two-phase rotor current is shown in Figure 4.4b.

## 5. Further procedure

ORIGINAL PAGE  
BLACK AND WHITE PHOTOGRAPH

As the protocol shows, the switching of the direct converter and the discrete operation of the microcomputer lead to higher harmonics.





/293

Figure 4.3 Variations of 2-phase rotor currents for transfer from over synchronous to under synchronous operation.

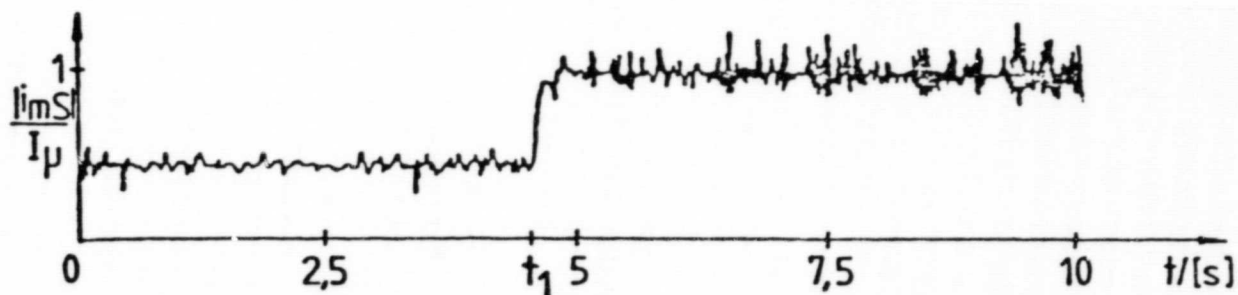


Figure 4.4a. Magnitude of magnetization vector for a jump-like change in the nominal value.

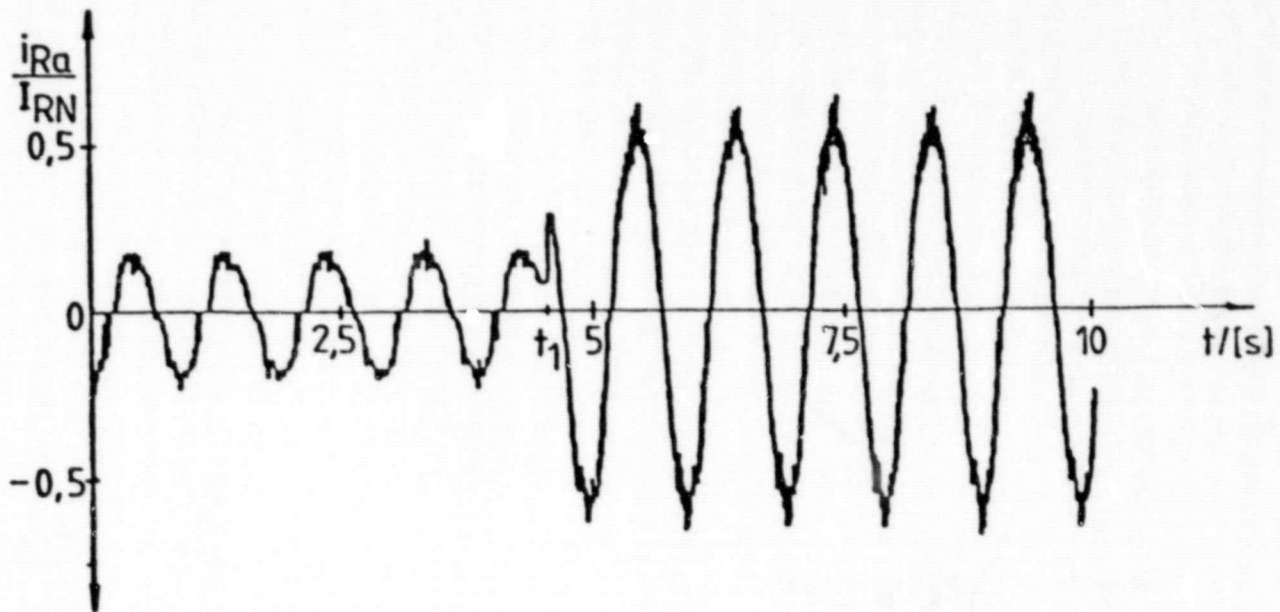


Figure 4.4b. a--component of the 2-phase rotor current

In order to further reduce the influence of the scanning raster of the microcomputer on the higher harmonics, at the present time we are building a new controller unit with a much higher performance 16 bit microcomputer. This means that the phase transformations are also performed digitally. The scanning times expected for the controlled circuit are between 1 ms and 1.5 ms. In addition, we will investigate whether there will be an improved switching and control of the direct converter with regard to the higher harmonics.

## 6. Oversynchronous current rectifier cascade

### 6.1 Method of operation

Figure 6.1 shows the circuit diagram of a current rectifier cascade. The rotor current and, therefore, the rotor power of the slip ring runner machine which is connected to the network can be controlled through the control angle of the rectifier on the network side. Other details about the advantages and disadvantages of this concept are contained in the first report (I).

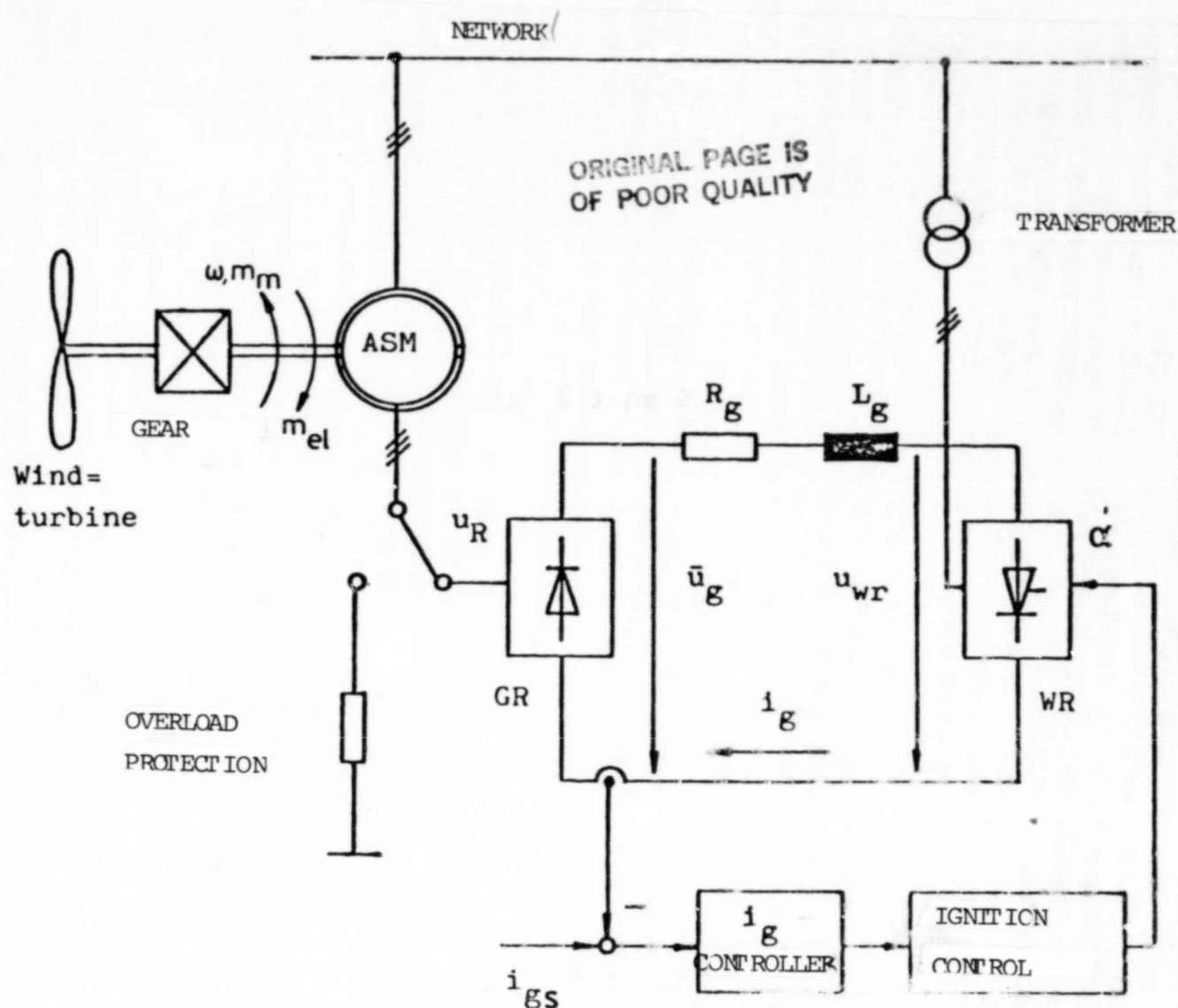


Figure 6.1. Wind energy facility with rectifier cascade

The asynchronous generator for the oversynchronous current rectification cascades circuit is simulated with consideration of the differential equations of the machine and of the current intermediate circuit. The results obtained will be compared in another part of the work with measured results of a test set up and they will be interpreted.

## 6.2 Calculations for stationary operation

The nominal slip of the current rectifier cascade is specified so that the rotating masses are capable for permissible rpm deviations,

to take up or give off the same kinetic energy. For the simulation we set  $s_{\min} = 0$  and  $s_N = 0.15$ . Therefore, we find  $s_{\max} = -0.283$ . Later on we will discuss how the minimum slip cannot exceed a limiting value because of the expected commutation difficulties.

Since we already have simulations of a double supply asynchronous machine, in order to have a simple comparison, these machines data are used for the cascade as well for comparing the systems.

## 7. Simulation of the oversynchronous current rectification cascade

The differential equations of the asynchronous machine have to be related to those of the direct current intermediate circuit for the mathematical description of the oversynchronous current rectification cascade. In the following we will outline the procedure.

### 7.1 Differential equations of the direct current intermediate circuit

If the voltage of the rectifier is assumed as an imposed voltage, then depending on the state of the rectifier, we can write down the following simple differential equations for the direct current intermediate circuit (Figures 7.1 and 7.2).

$$u_g = R_g \cdot i_g + L_g \cdot \frac{di_g}{dt} + u_{WR} \quad (7.1)$$

For the simulation the method of a direct coupling in conjunction with a cyclical exchange is used for the fixed pulse rectifier. The possible 12 states of the rectifier, 6 commutation and 6 noncommutation phases, are related to the equations of the rotor with the correct initial conditions and in the correct sequence. One then obtains a set of 12 differential equation systems.

### 7.2 Differential equations of the rotor circuit

The two phase description of the electrical quantities is selected for describing the asynchronous machine in the a, b system moving with the rotor.

ORIGINAL PAGE IS  
OF POOR QUALITY

/297

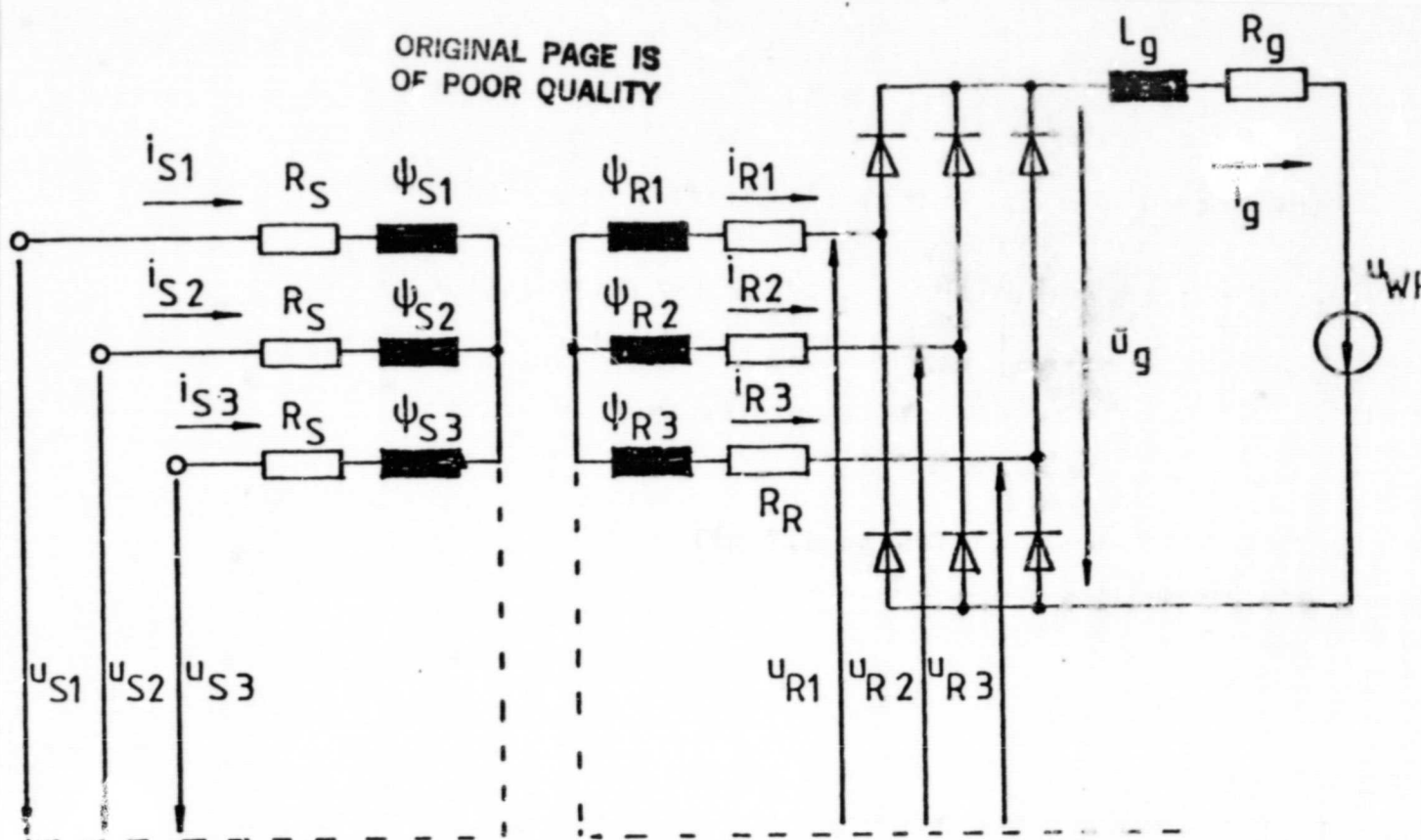


Figure 7.1. Replacement diagram of the current rectifier cascade for establishing the 12 differential equation systems.

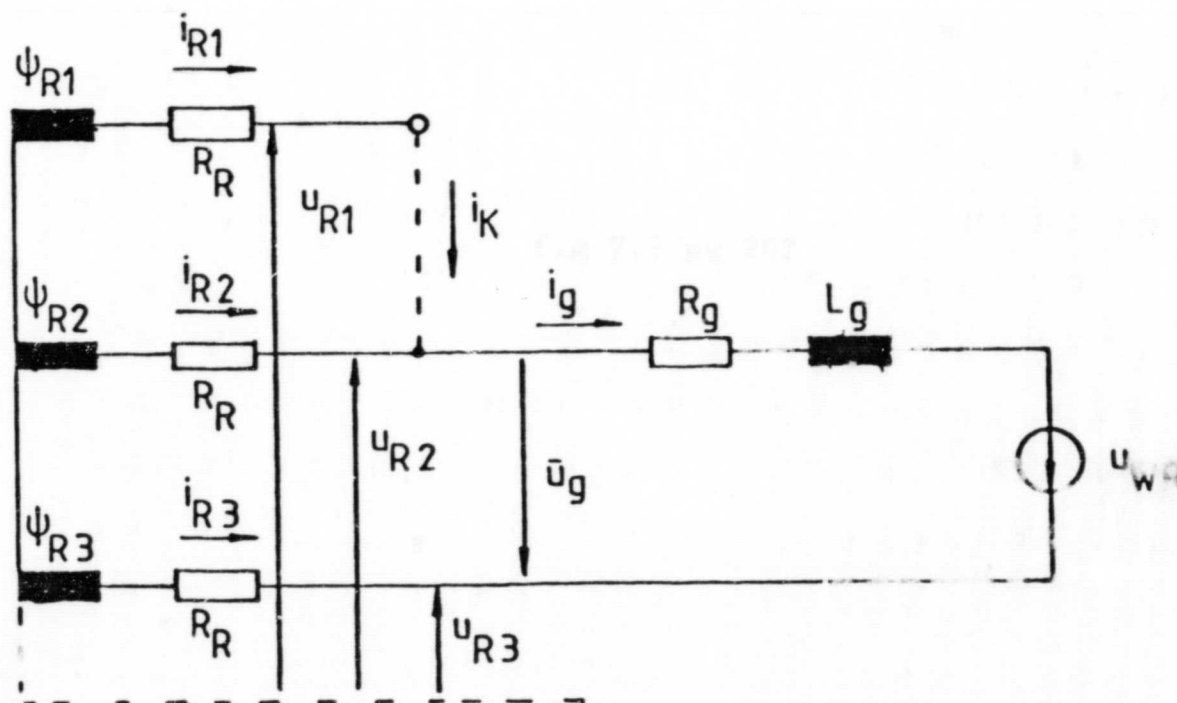


Figure 7.2. Replacement diagram of the current rectifier cascade for setting up a differential equation system.

From Figure 7.1, we can read off the equations of the rotor voltages,

/298

$$\begin{aligned} R_R i_{R1}(t) + \frac{d\psi_{R1}}{dt} &= u_{R1} \\ R_R i_{R2}(t) + \frac{d\psi_{R2}}{dt} &= u_{R2} \\ R_R i_{R3}(t) + \frac{d\psi_{R3}}{dt} &= u_{R3} \end{aligned} \quad (7.2)$$

If the rotor fluxes are expressed by means of the inductivity of the machine and the corresponding transformed electrical quantities, then the rotor voltages can be calculated as follows after a few conversions:

$$\begin{bmatrix} u_{R1} \\ u_{R2} \\ u_{R3} \end{bmatrix} = \underline{A} \begin{bmatrix} i_{Ra} \\ i_{Rb} \end{bmatrix} + \underline{B} \begin{bmatrix} \frac{di_{Ra}}{dt} \\ \frac{di_{Rb}}{dt} \end{bmatrix} + \underline{C} \begin{bmatrix} i_{Sa} \\ i_{Sb} \end{bmatrix} + R_R \begin{bmatrix} i_{R1} \\ i_{R2} \\ i_{R3} \end{bmatrix} + \underline{D} \begin{bmatrix} u_{Sa} \\ u_{Sb} \end{bmatrix} \quad (7.3)$$

The elements of the matrices A, B, C and D consist of the inductions of the machine and the numerical factors resulting from the transformations.

### 7.3 Relationship between the differential equations of the rotor and those of the intermediate circuit

Any state of the direct current bridge can be represented as a combination of the commutation current  $i_k$  and the intermediate circuit  $i_g$ . The following connection relationships can be specified

$$\begin{bmatrix} i_{R1} \\ i_{R2} \\ i_{R3} \end{bmatrix} = \underline{S} \begin{bmatrix} i_g \\ i_k \end{bmatrix} \quad (7.4)$$

$$\begin{bmatrix} u_g \\ 0 \end{bmatrix} = - \underline{S}^T \begin{bmatrix} u_{R1} \\ u_{R2} \\ u_{R3} \end{bmatrix} \quad (7.5)$$

$$\begin{bmatrix} i_{Ra} \\ i_{Rb} \end{bmatrix} = \underline{V} \begin{bmatrix} i_g \\ i_k \end{bmatrix} \quad (7.6)$$

$\underline{S}$ ,  $\underline{S}^T$  and  $\underline{V}$  are switching matrices which depend on the state of the rectifier. By combining equations (7.1) to (7.6), we finally obtain 12 equation systems of the form

$$\begin{bmatrix} R_g i_g + L_g \frac{di_g}{dt} + u_{WR} \\ 0 \end{bmatrix} = - \underline{S}^T \underline{A} \underline{V} \begin{bmatrix} i_g \\ i_k \end{bmatrix} \quad (7.7)$$

$$- \underline{S}^T \underline{B} \underline{V} \begin{bmatrix} \frac{di_g}{dt} \\ \frac{di_k}{dt} \end{bmatrix} - \underline{S}^T \underline{C} \begin{bmatrix} i_{Sa} \\ i_{Sb} \end{bmatrix} - R_R \begin{bmatrix} i_g \\ i_k \end{bmatrix} - \underline{S}^T \underline{D} \begin{bmatrix} u_{Sa} \\ u_{Sb} \end{bmatrix}$$

#### 7.4 Stator equation and mechanical motion equation

The differential equations of the stator currents and of the electrical torque are obtained if one expresses the rotor currents using  $i_g$  and  $i_k$  in the known equations for the asynchronous machine.

#### 8. Dimensioning of the current controller

A simplified block diagram can be designed of the current rectifier cascade for dimensioning the current controller. The following structure can be given for the closed control circuit:



ORIGINAL PAGE IS  
OF POOR QUALITY

/300

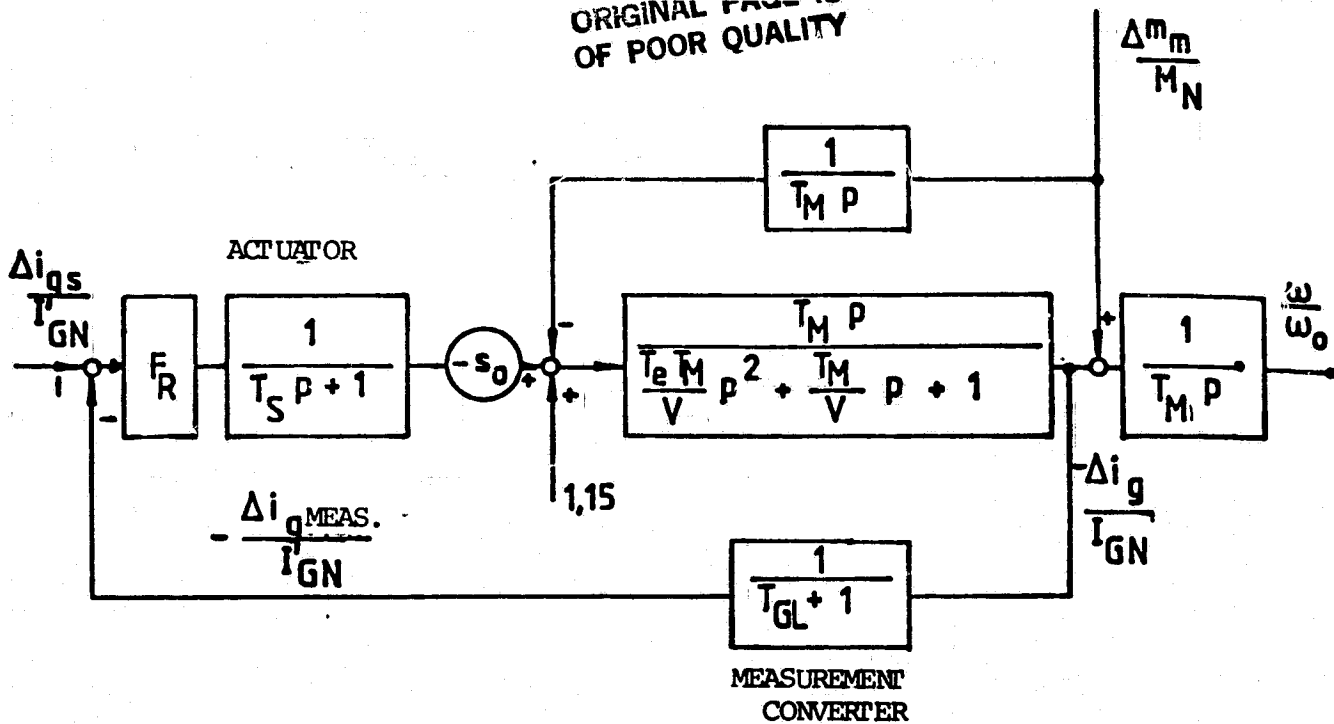


Figure 8.1. Simplified block diagram of the current rectifier cascade.

The  $\Delta$  quantities have the following values:

$$\Delta i_g = i_g - I_{GN}'$$

$$\Delta u_{WR} = u_{WR} - U_{GN}'$$

$$\Delta m_{el} = m_{el} + M_N$$

$$\Delta m_m = m_m - M_N$$

$$T_M = \frac{\omega_0 \cdot \Theta}{M_N}$$

The factors  $T_e$  and  $V$  are determined using the stimulation models. The factor  $-s_0$  considers the fact that for idling the nominal rpm is  $\omega/\omega_0 = 1 - s_0$ .

Using this block diagram the PI controller of the current control circuit can be designed according to the known dimensioning specifications. /301

## 9. Simulation results

The first simulation results are available. The numerical integration of the differential equations is done using the Runge-Kutta method. The rectifier voltage  $u_{WR}$  consists of sections of a sine function, depending on the control angle  $\alpha$ . The controller is dimensioned according to Chapter 8.

### 9.1 Operation of the cascade at the nominal point

Figures 9.1a and 9.1b show the most important electrical and mechanical variables of the cascade at the nominal point. The intermediate circuit current  $i_g$  and the moment  $m$  contain the upper harmonics of the 6 x rotor frequency as well as the higher harmonics of the 6 x network frequency. They are produced by the uncontrolled rectifier and the rectifier in the rotor circuit controlled by the network.

These voltage jumps caused by the rectifier also affect the commutation of the rectifier (see Figures 9.1a, 9.1b). At the time  $t_1$ , the switching condition of the bridge is satisfied but the voltage time area is not sufficient in order to build up a sufficiently large commutation current. The current can only be commutated to the new phase after  $t_2$ .

### 9.2 Jump response for a change in the nominal current value $i_{gs}$

We consider simulating a jump in the nominal current value from  $1.13 I'_{GN}$  to  $0.63 I'_{GN}$ . Figures 9.2a and 9.2b give the result. The actual current value adjusts to the new nominal value with a slight undershot. According to the power division

$$P_{Rotor} = -s P_{Stator} \quad (9.1)$$

the stator power becomes smaller.

### 9.3 Jump response for a change in the supplied mechanical power

Starting at the nominal point, the generator is accelerated up to maximum rpm with an assumed torque within 0.1 sec. Figures 9.3a and

ORIGINAL PAGE IS  
OF POOR QUALITY

/302

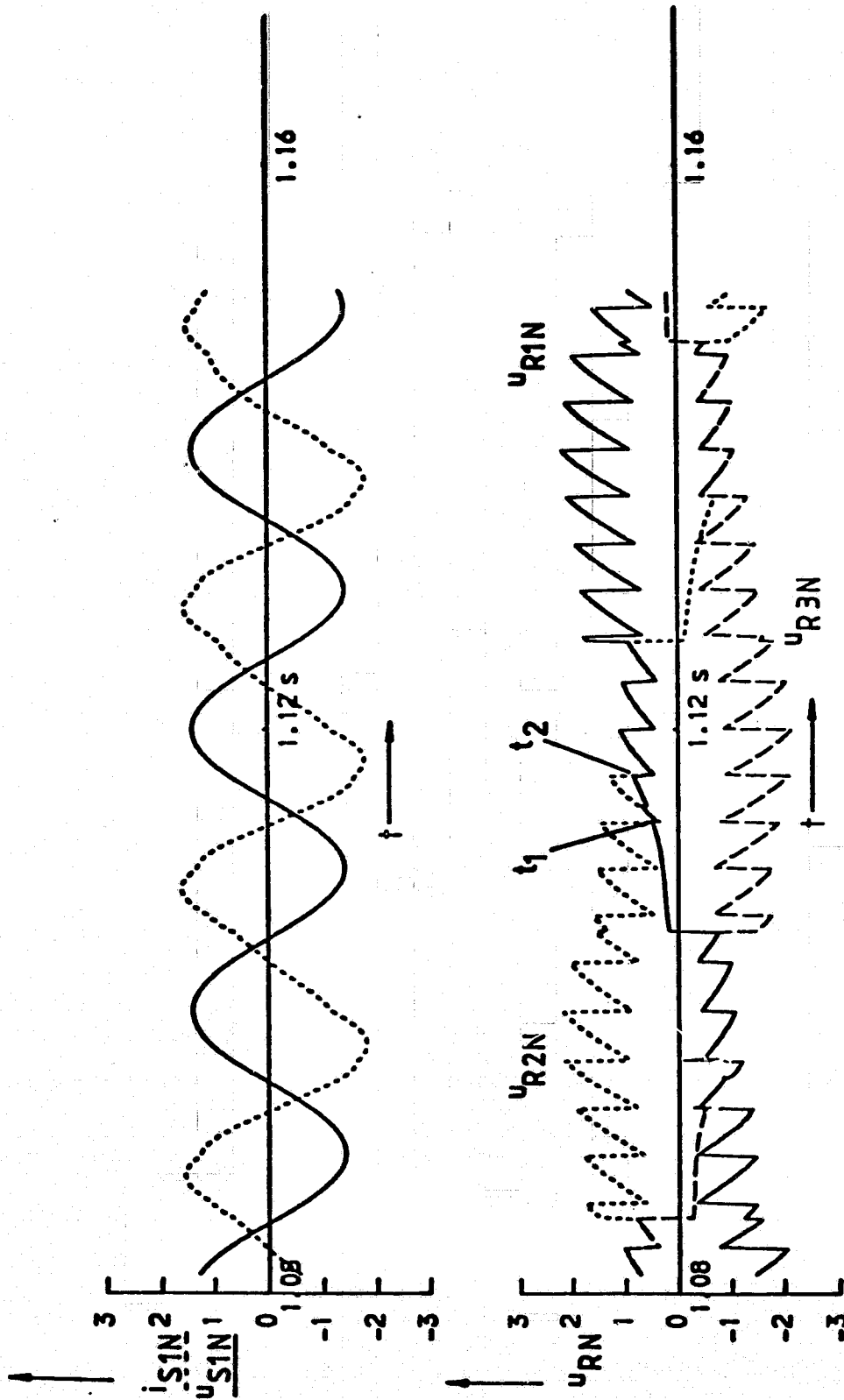


Figure 9.1a. Nominal point of the cascade

ORIGINAL PAGE IS  
OF POOR QUALITY

/303

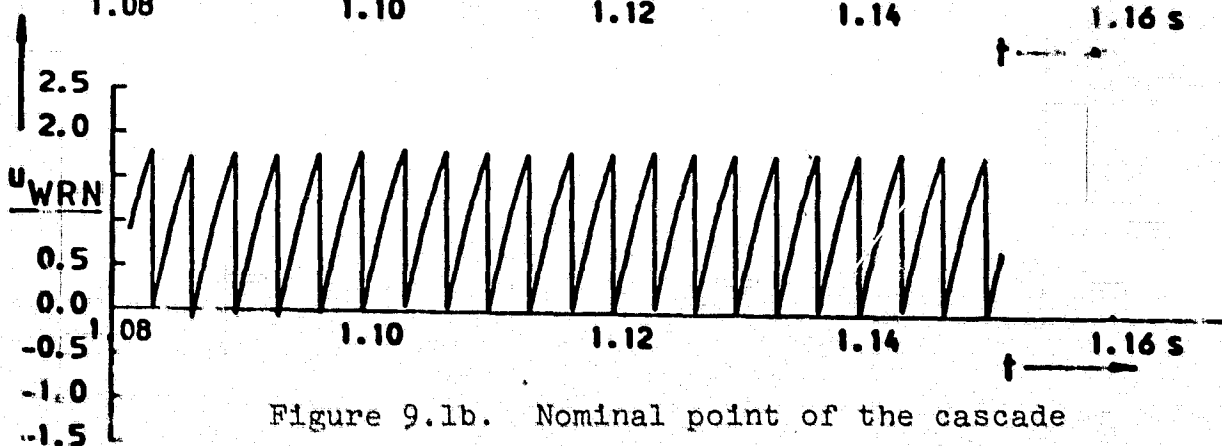
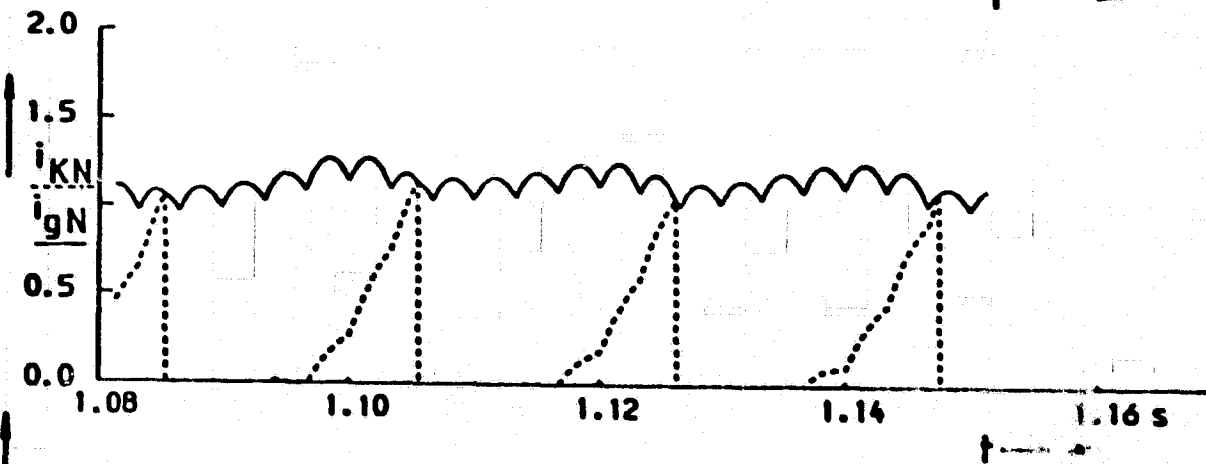
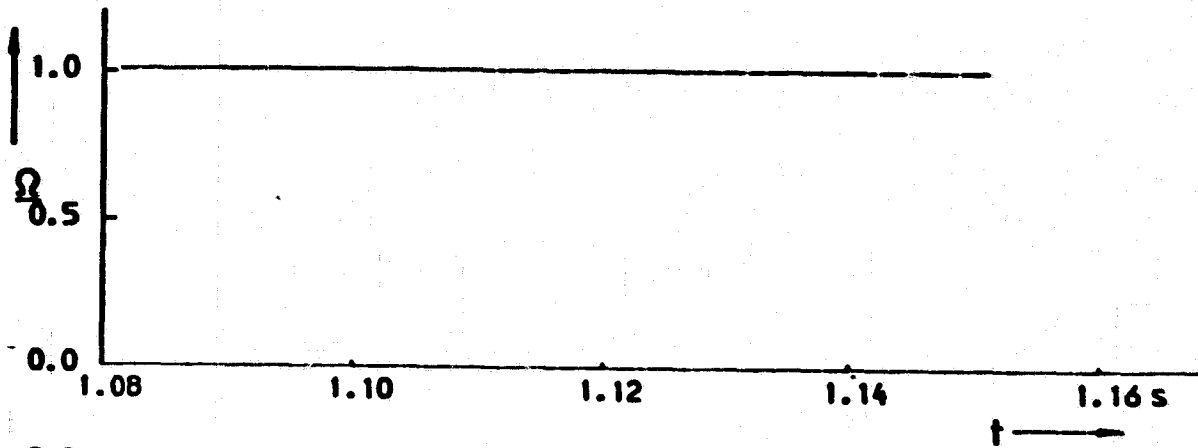
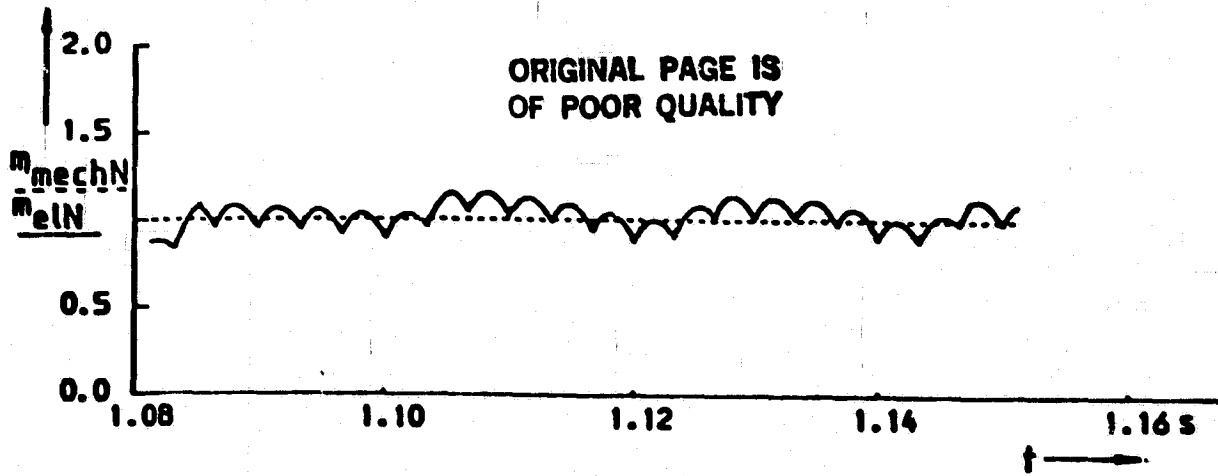


Figure 9.1b. Nominal point of the cascade

ORIGINAL PAGE IS  
OF POOR QUALITY

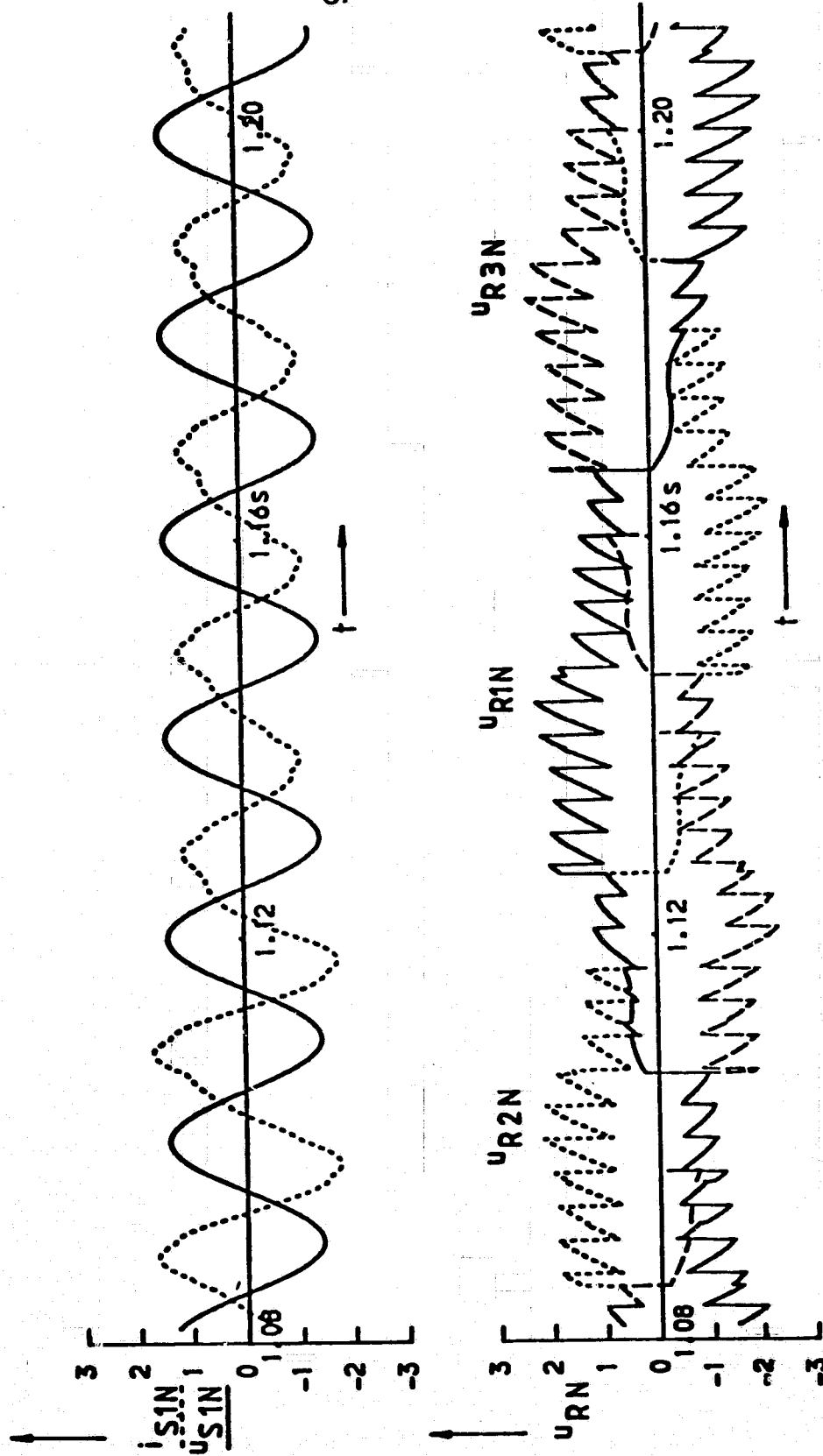


Figure 9.2a. Jump responses of the cascade for changing of the nominal value of  $i_g$   $T_{GL} = 5 \text{ ms}$

/304

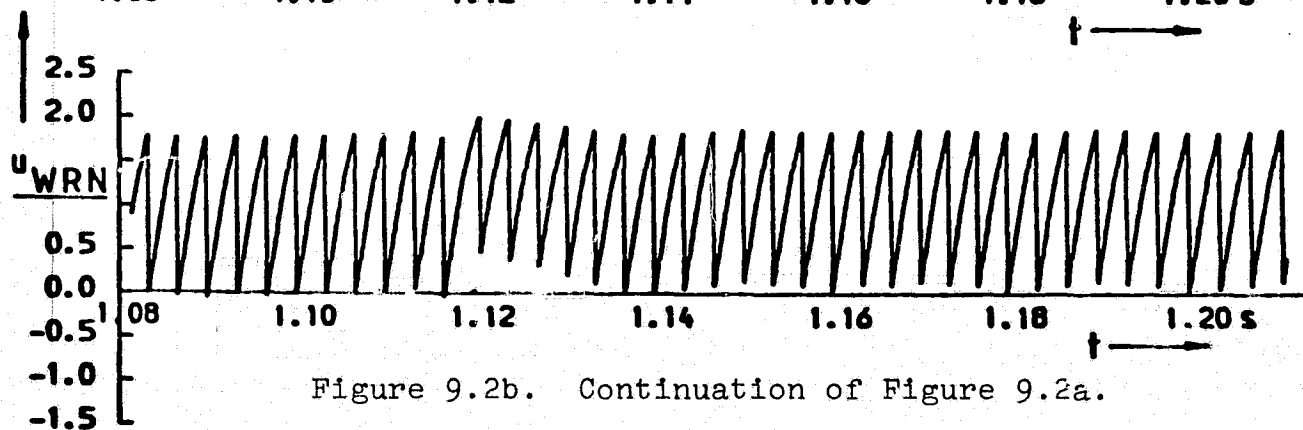
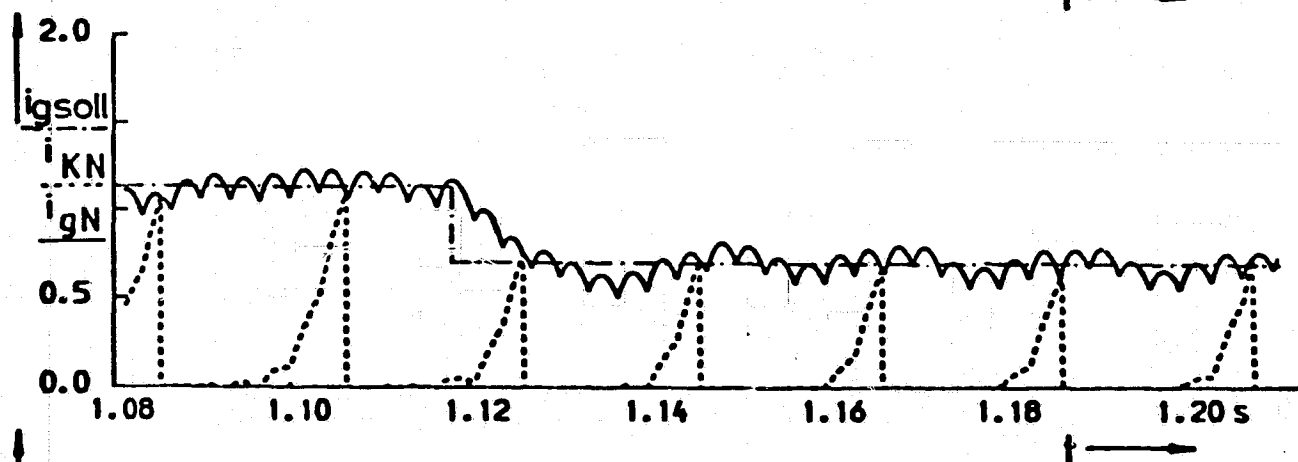
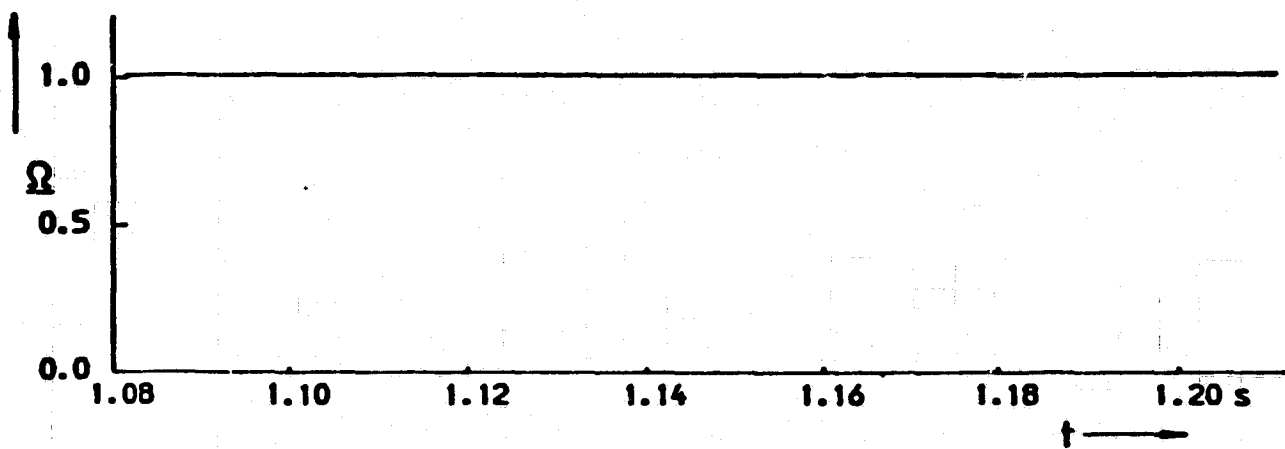
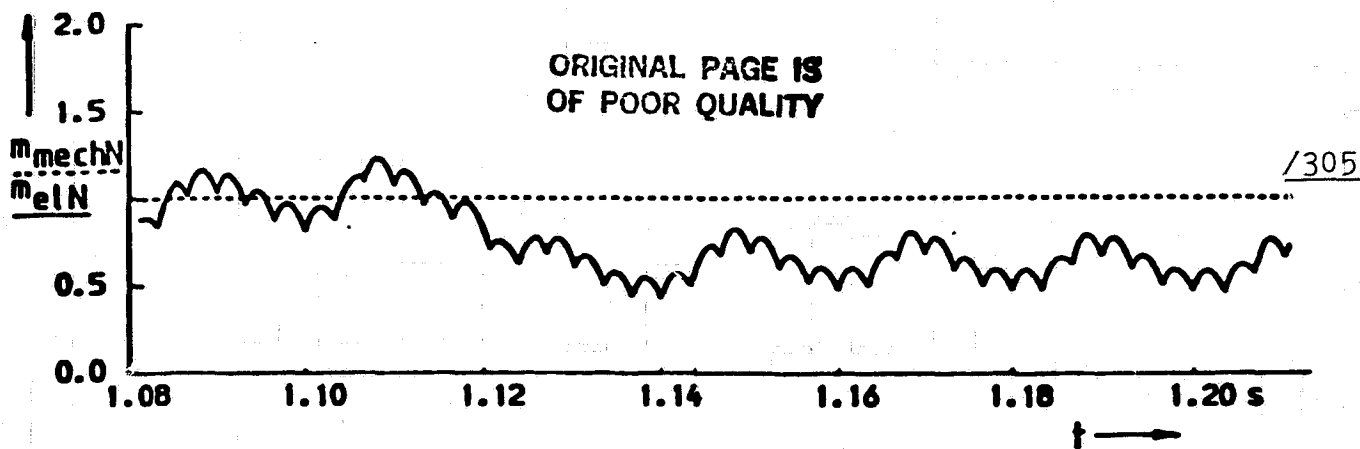
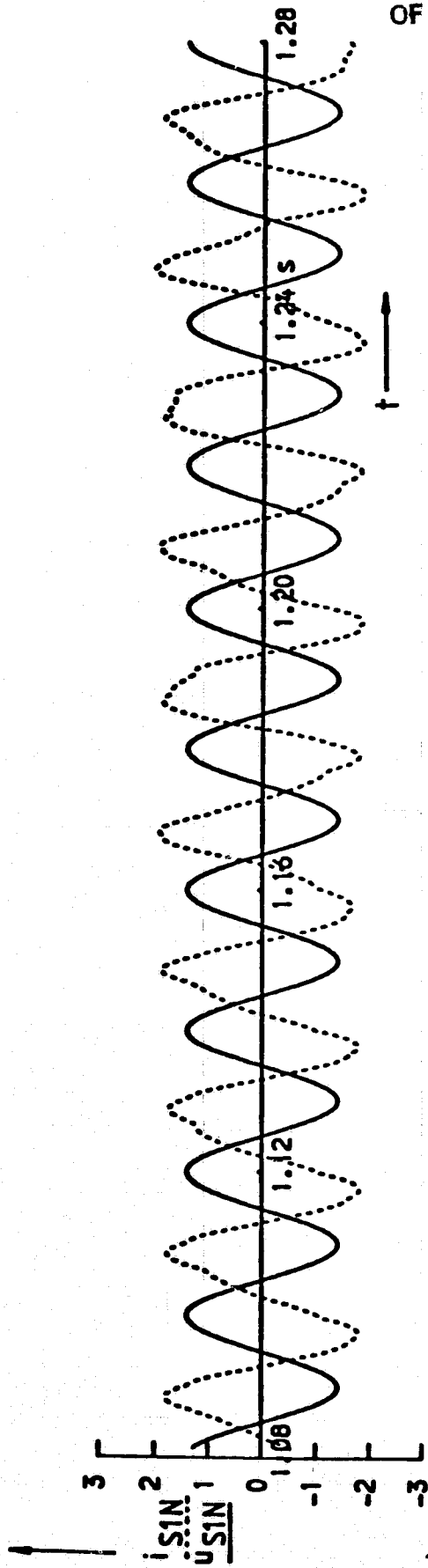


Figure 9.2b. Continuation of Figure 9.2a.



ORIGINAL PAGE IS  
OF POOR QUALITY

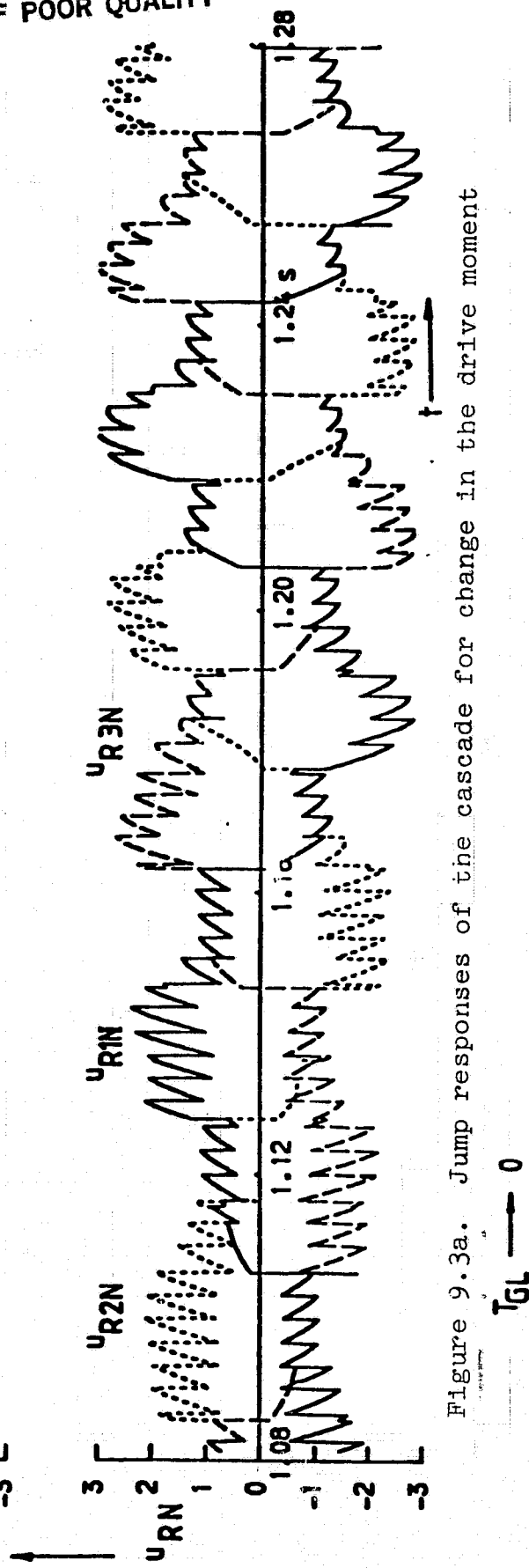


Figure 9.3a. Jump responses of the cascade for change in the drive moment



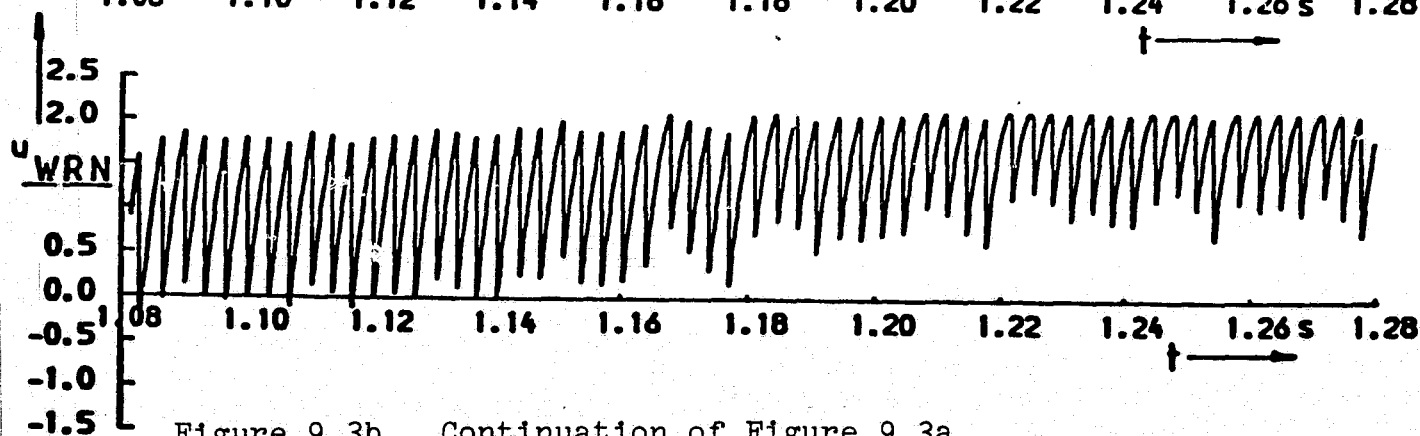
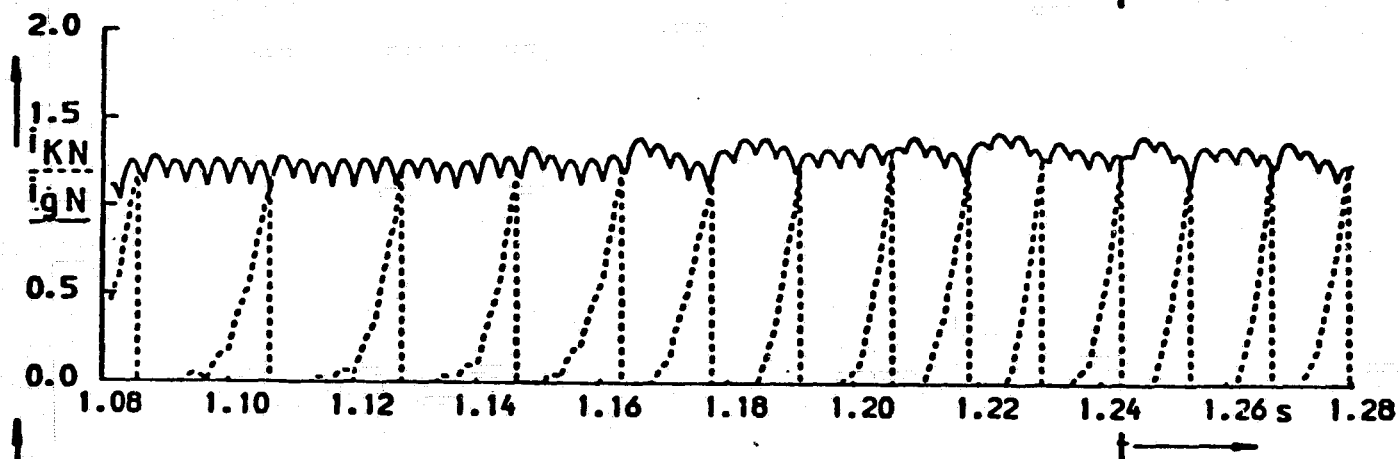
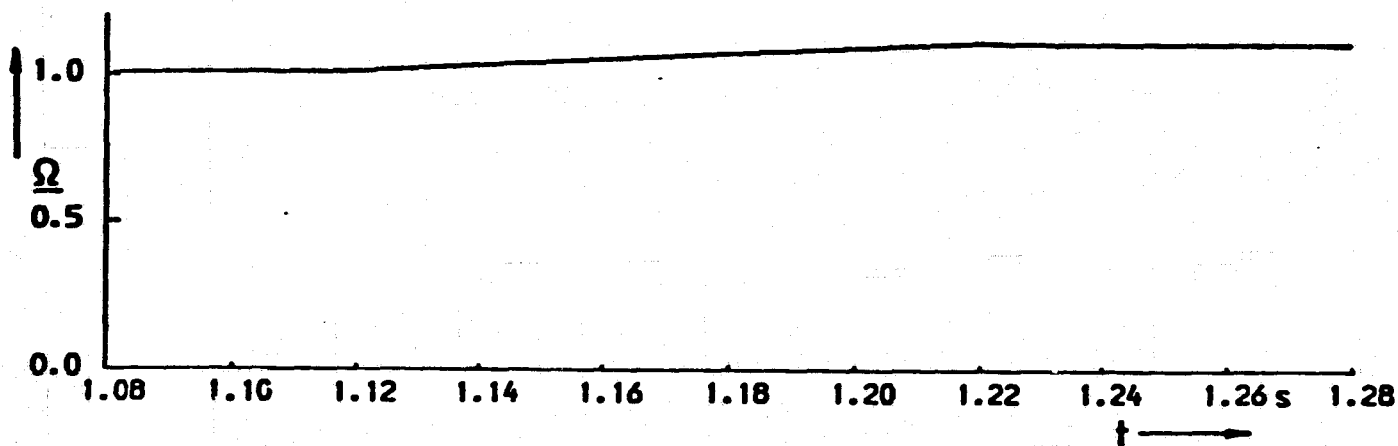
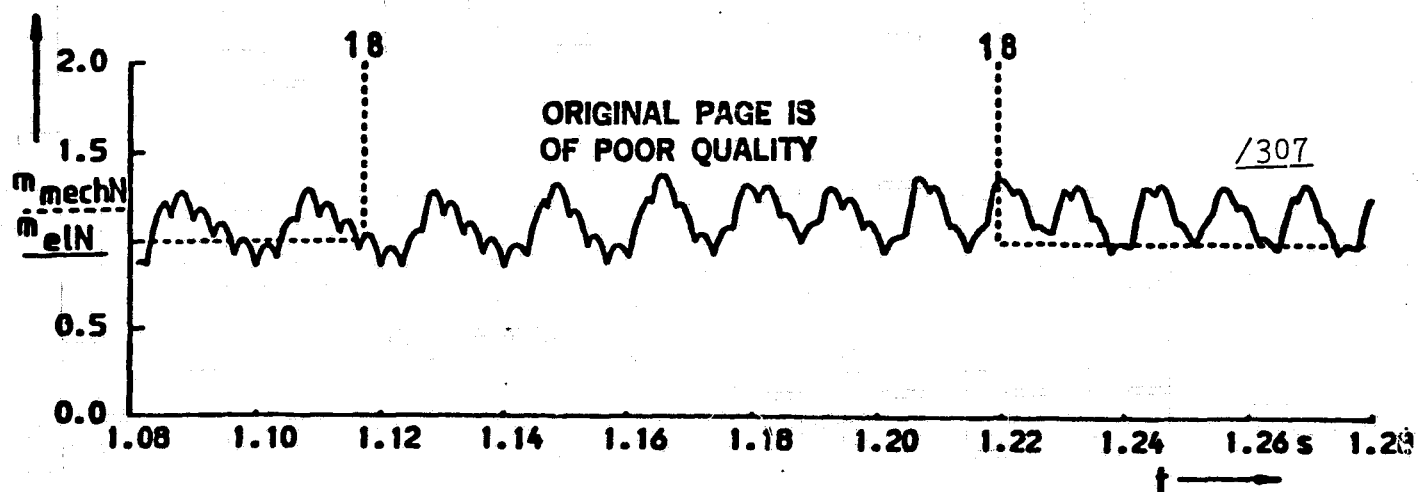


Figure 9.3b. Continuation of Figure 9.3a.

9.3b show that the rotor current and, therefore, the moment of the machine can be maintained constant by control. For uniform power delivery into the network, it is necessary to reduce the nominal value of the electrical moment of the machine according to a function which depends on rpm.

#### 10. Further procedure

The simulation results discussed above allow a first evaluation of the oversynchronous current rectifier cascade. In the second step, the mathematical model will be improved and especially the higher harmonic spectrum and the operating points important for commutation will be investigated. In parallel with the theoretical results, we will build up the test stand and bring about microprocessor control.

#### Abbreviations used

309

$s$	slip
$\epsilon$	mechanical rotation angle
$\omega$	rpm
$m_m$	mechanical moment
$m_{el}$	electrical moment
$R_g$	ohmic resistance of the direct current intermediate circuit
$L_g$	inductivity
$u_g$	intermediate circuit direct voltage
$i_g$	intermediate circuit direct current
$i_R$	rotor current
$i_S$	stator current
$u_R$	rotor voltage
$u_S$	stator voltage
$\Psi_R$	magnetic rotor flux
$P$	electrical power
$i_k$	commutation current
$u_{WR}$	rectifier voltage
$R_R$	rotor resistance
$R_S$	stator resistance

$\theta$  mechanical moment of inertia  
 $T_M$  mechanical time constant  
 $i_{mS}$  magnetization current  
 $I_\mu$  idling magnetization current

CONCENTRATION OF WIND ENERGY IN VORTEX FIELDS AND THEIR  
EXPLOITATION FOR PRODUCING ENERGY (PHASE I)

/311

Project No. ET 4252 A\*

H. Staufenbiel and H. Öry

1. Purpose

/312

Investigation of the physical foundations of wind energy conversion which exploits the concentration of wind energy within vortex fields. According to measurements with wind tunnel and water tunnel models accompanied by theoretical analysis, an economical system is to be defined and the design of an outside model facility is planned.

2. Working program

- Development of the physical foundations of suitable vortices: production, structure and stability for disturbances.
- Estimation of the wave power of various designs for the exploitation of vortex systems as wind energy concentrators.
- Variation of the parameters for the optimization of the aerodynamics with the purpose of producing high energy vortices.
- Critical analysis of concepts with consideration of costs of construction and problems of structural realization.
- Concept selection and definition of wind tunnel models.
- Investigation of selected concepts for wind tunnel testing and calculation methods.
- Economy considerations compared with conventional wind mills.

---

\*The project was introduced to the participants of the Seminar for information purposes because it is not directly related to the Seminar. In this report, therefore, brief summaries are given of the Institutes for Aviation and Space Flight and for Flight Construction as well as two photographs. A more extensive final report will be published in the middle of 1982 (BMFT FB series). During Phase II, a 10 kW-WINK prototype will be tested.

R. Windheim

### 3. Status (end 1980):

The work on the topic wind energy concentration during the report year were designed to investigate the properties of various delta surfaces with realistic installation conditions of the surfaces.

The natural solution for a delta surface on a tower has substantial aerodynamic and structural disadvantages. Support walls below the wing which are more favorable from the structural point of view, could even increase the vortex intensity for some developments. Regarding the use of a concentrator under natural terrain conditions with over speeds, such as would be found over cliffs, for example, seems practical by using a perpendicular half delta surface and seems to be economic.

The power brake was improved in accuracy and the measured power coefficients show an increase by a factor of 10 in the power delivery compared to a rotor with unreinforced incident flow. In addition, the influence of a wind direction change is demonstrated. Up to a slip angle of  $6^\circ$ , no tracking is required. When the azimuth actuator motor has a tracking speed of  $6^\circ/\text{min}$ , then no bursting of the vortices is to be feared.

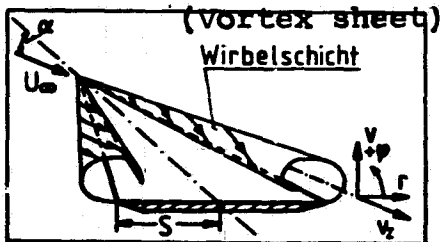
The work on the YEN vortex tower demonstrates the functional capability of the principle. First measurements give a power intensification by a factor of 6. Similar values were also achieved with delta surfaces. The power increase with reduced turbine diameter as given by YEN does not occur and towers with large height--diameter ratios "block" the outlet.

/313

The Institute for Aerodynamics and Space Flight (ILR) and the Institute for Light Construction of the RWTH Aachen since 1978 have been developing concepts for a wind power generation facility using new technology sponsored by BMFT and under the direction of the KFA Juelich. This is a so-called wind energy concentrator (wink).

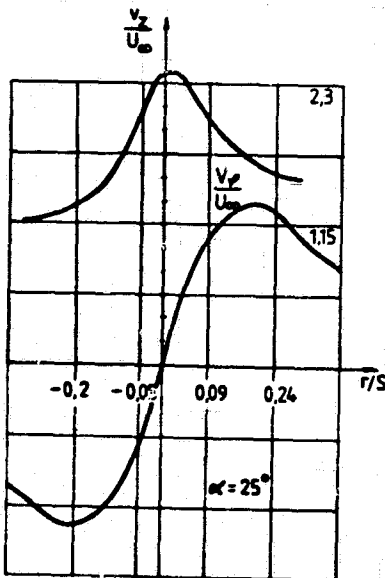
The small density of the natural wind energy makes it natural to consider a concentration for technical and economic reasons. The

concentration can be done using natural terrain forms and suitable wind direction surfaces on designs. One special possibility of concentrating the energy is the production of vortices at suitable, delta--shaped guide surfaces.



A vortex is created at the leading edges of the delta wing.

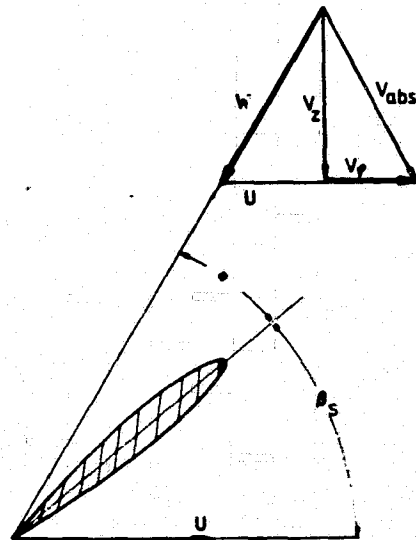
In the vortex the speeds are substantially increased compared with the wind speed  $U_0$ .



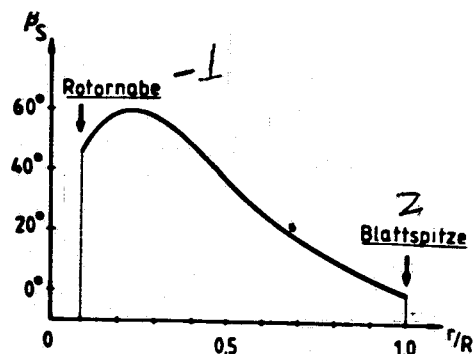
The speeds in the vortex have approximately distribution over the radius.

A substantial throughput increase results in a high rotation energy and a concentration effect.

If we have a rotor with such an angular momentum flow, then each blade element requires substantially greater twists than usual as the velocity triangle shows.



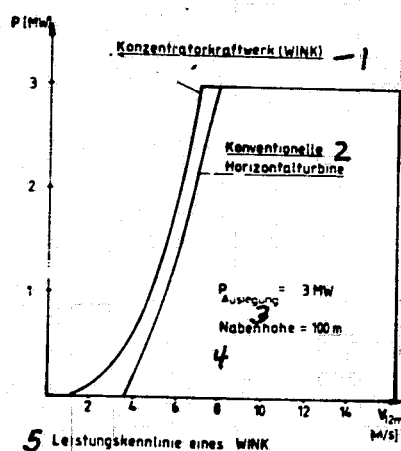
ORIGINAL PAGE IS  
OF POOR QUALITY



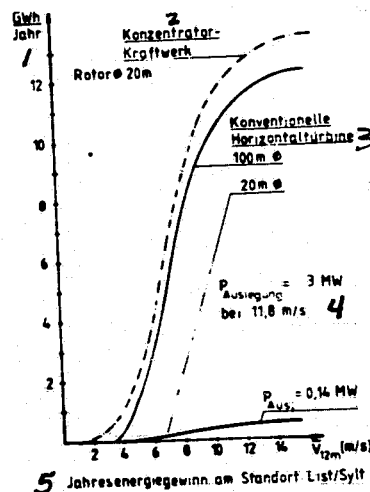
An optimum distribution of the blade adjustment angle is shown above.

1. Rotor hub; 2. Blade tip.

Therefore, the wink results in a greater yearly energy yield. With consideration of the power characteristic line shown below and the frequency distribution of wind speeds prevailing at the location List/Sylt, at a 100 m hub height we find the following sum curve of energy to be gained per year. The reference speed is the measured wind speed at 12 meter height.



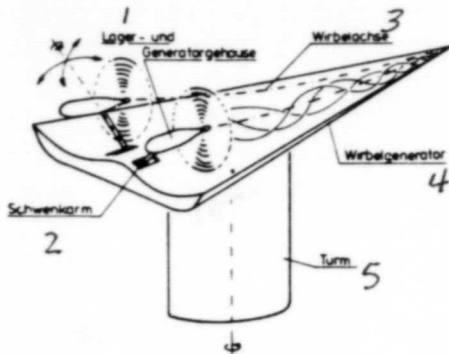
1--concentrator power plant (wink); 2--conventional horizontal turbine; 3--design; 4--hub height; 5--power characteristic of a wink



1--year; 2--concentrator power plant; 3--conventional horizontal turbine; 4--design; 5--yearly energy gain at location list/sylt

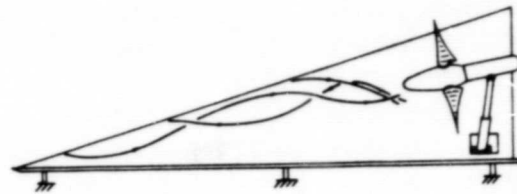


A WINK COULD LOOK LIKE THIS



a high power version (5-10 MW)  
on a stand

- 1--bearing and generator housing;
- 2--deflecting arm; 3--vortex axis;
- 4--vortex generator; 5--tower

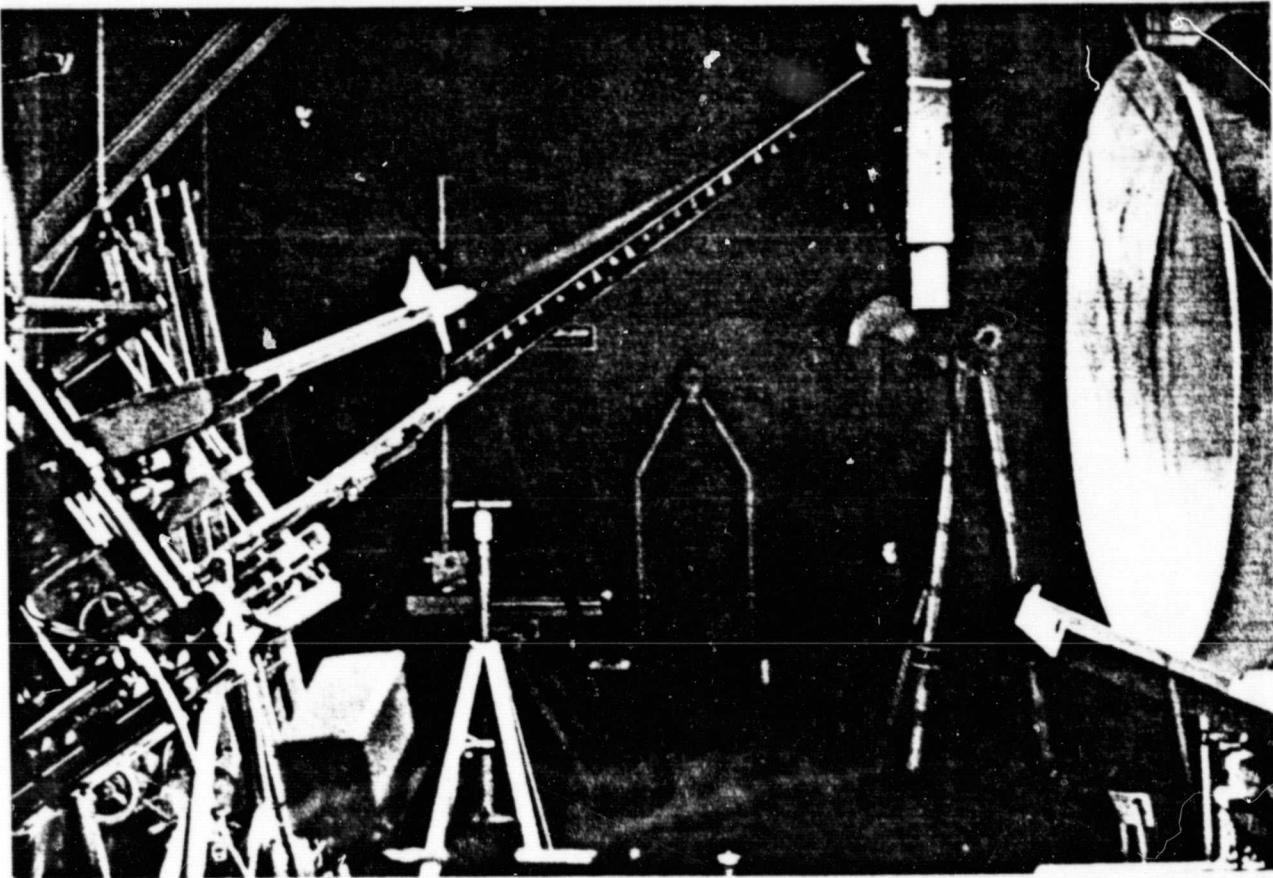


Structurally simpler version with  
half wing, perpendicular near the  
ground (<5MW, see title figure)

/315



Vortex structure of half model-visualization with smoke



Wind energy concentration in the wind tunnel. The stable vortex made visible by condensed air humidity in the center of the picture is produced by the black delta structural part and drives the small white turbine on the left (arrow). A power brake which can be aligned and has  $5^\circ$  of freedom is coupled with the rotor in one unit.

CALCULATION OF LARGE ROTOR BLADES FROM THE CALCULATION  
ENGINEERING POINT OF VIEW

John H. Argyris<sup>\*</sup>, Kurt A. Braun<sup>\*</sup>, Warner Lang<sup>\*\*</sup>

SUMMARY

Extensive calculations are required for designing rotor blades of large wind energy facilities. In the present report we will discuss a part of finite element calculations. We are discussing the cross sectional data for rotor blades which are produced automatically for specified profile contour, spar geometry, materials and wall thickness distribution, and are produced for further processing in an FE system. The input and change of typical parameters can be done interactively by the engineer on a screen. An iterative matching of the structure is, therefore, easily possible and can be done rapidly which saves cost and time for the design of the blades.

/318

SCHEMATIC SEQUENCE OF AN FE-CALCULATION

Before the finite element calculation, there is an aerodynamic design of the rotor blades. With consideration of the wind conditions for a blade of given length, profile type, chord distribution, thickness distribution and twist are specified. This aerodynamically specified wind geometry is available to the engineer in order to house the supporting components in a rotor blade, for example, in a box spar. The geometry of the supporting components and the materials have to be specified. The input of this information is done interactively on the screen for various wing sections. From these spar data, the equivalent beam values are calculated which are required as input for the following FE calculation. This complex and difficult computation step was performed up to the present by the engineer and the beam cross-sections were input for the various blade positions into the FE program.

<sup>\*</sup> University of Stuttgart, Institute for Statics and Dynamics of Aviation and Space Flight Designs

<sup>\*\*</sup> Statics and Dynamics Research Association mbH, Stuttgart

Using static FE analysis of the rotor blade idealized as a beam model, it is possible to determine forces, stresses and displacements due to various design loads (for example, eigen weight). The calculation engineer changes his spar data until the reaction of the structure are satisfactory. As a rule, this makes it necessary to change the spar very frequently and determine the equivalent beam values. The automation of the last step connected with a substantial facilitation of the input and change process of spar data means a substantial savings in time and cost.

If the static design of the blade has been included satisfactorily, then a dynamic investigation is also necessary which gives stability information and time responses of the structure. Here again, as a rule, it will be necessary to change the spar and structural data several times until satisfactory results are achieved.

To interpret the FE results, it is necessary for the beam idealization used to recalculate the generalized beam forces into stresses in the spar. In order to unload the engineer, this is also done automatically. Using clear graphical representations prepared by the computer of the stresses and displacements, a fast interpretation of the results becomes possible. /319

In the following, we will only discuss the input and change of spar data.

#### INPUT OF SPAR DATA

In the idealization of a rotor blade as a beam model using finite elements, for every node point and end point of the individual beam element, one requires the characteristic geometric data. In the previously used investigations we use the beam element BECOS and BETACX of the FE system ASKA / 1 / which are the following:

- transverse area
- moment of inertia

- St. Venant torsion constant
- reciprocal shear surfaces
- coordinates of the thrust center

(see Table 1 and Figures 2 and 3)

In addition, the mass and inertia variables are determined for the dynamic analysis:

- coordinates of the mass c.g.
- mass of the blade cross section
- mass inertia around c.g.

and the latter two quantities are referred to the longitudinal dimension of the blade (for example,  $dm / dr$ ).

The cross section of the rotor blade is idealized as a multicell closed shell. It can have walls, ridges and spars made of different materials so that a composite wing made of many materials can be treated.

The program for the interactive input of spar data requests the following data required on the screen, for example

- number of blade cross sections
- are the cross sections represented graphically?
- number of thrust steps
- number of flanges on the upper and lower spar side
- coordinates of the shell corner points
- configuration of walls, thrust steps and flanges
- material values for individual parts
- wall thicknesses for walls and thrust steps

For simplifying the input, the program asks whether certain special cases prevail, for example

- spar coordinates defined by a known profile?
- perpendicular thrust steps?
- spar walls parallel to x axis?
- constant wall thickness in the cross section"
- constant E modulus over cross section?
- pure flange idealization?

and if a special case occurs, it jumps over the unnecessary questions to the engineer.

#### REPRESENTATION OF THE PROFILE AND THE SPAR GEOMETRY

On request, the profile and/or spar contour can be automatically drawn for the blade sections. The profile geometry can be specified with

- subprogram (up to the present NACA 00 series) with parameters
- data filed with value pairs (previously FX 77-W-153)

therefore, it is very simple to introduce new profiles. In Figure 4, for example, the FX 77-W-153 profile including the spar selected by the engineer is shown. In this case, only the positions of the perpendicular thrust steps are given and determined that the spar corner points lie along the profile contour. In Figure 5 the spar is shown alone. The NACA 0052 was represented in Figure 6 including the fitting spar.

The graphical representation of the spar in the profile contributes substantially to the clarity of the design and clearly shows possible errors before calculations are started.

#### CALCULATION OF THE BEAM CROSS SECTION DATA

The beam cross section data mentioned above are calculated and made available to the FE program (in our case, ASKA).

#### REPRESENTATION OF RESULTS

The stresses calculated from the generalized beam forces as the result of the FE calculation, are automatically plotted in a figure similar to Figure 6 and allow fast evaluation. This part is still being worked on.

#### REFERENCES

- [1] - , ASKA UM 202, ASKA Part I, Linear Static Analysis, User's Reference Manual, ISD-Report No. 73, Stuttgart, 1971, Revision F, 1979.

ORIGINAL PAGE IS  
OF POOR QUALITY

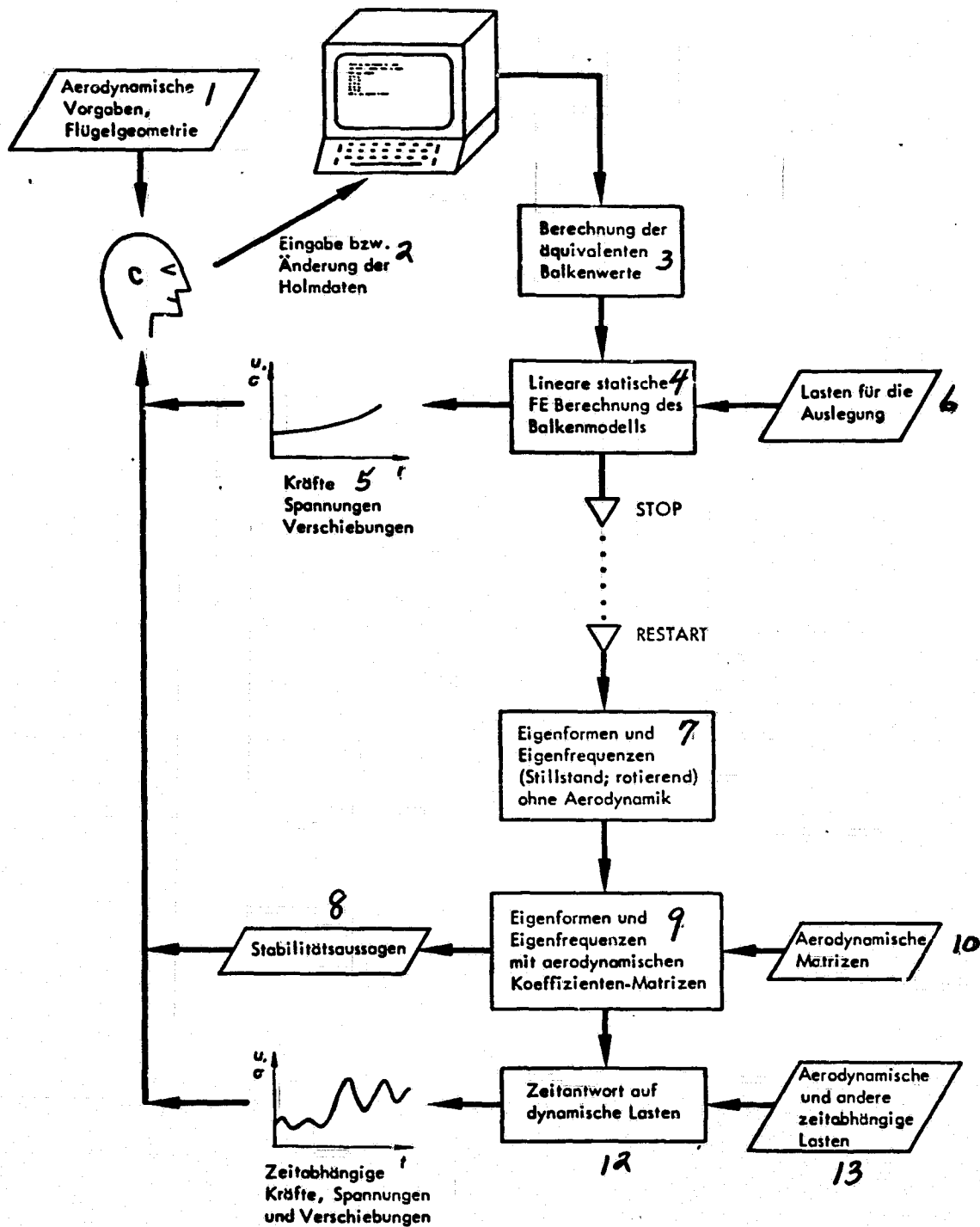


FIGURE 1. Block diagram of the linear rotor blade calculation

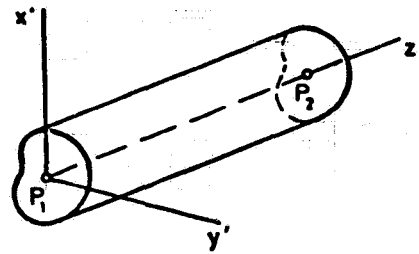


KEY TO FIGURE 1 ON PRECEDING PAGE:

1--aerodynamic specifications wing geometry; 2--input and change of spar data; 3--calculation of equivalent beam values; 4--linear static FE calculation of beam model; 5--forces stresses displacements; 6--load for design; 7--eigen modes and eigen frequencies (standing still, rotating without aerodynamics); 8--stability data; 9--eigen modes and eigen frequencies with aerodynamic coefficient matrices; 10--aerodynamic matrices; 11--time dependent forces, stresses and displacements; 12--time response to dynamic loads; 13--aerodynamic and other time dependent loads

## BECOS

ORIGINAL PAGE IS  
OF POOR QUALITY



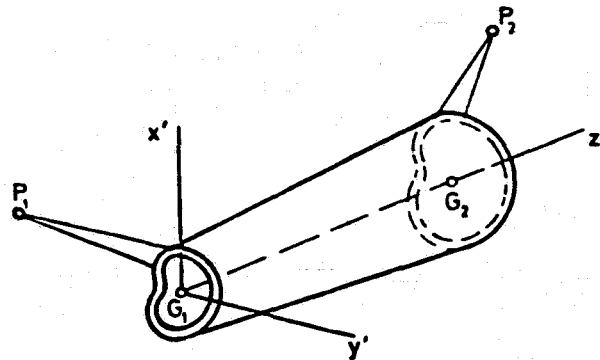
Solid beam of constant cross-section, St. Venant torsion, no shear effects in bending

Number of nodes 2, located on centroid of end cross-sections

Degrees of freedom  $u, v, w, \phi_x, \phi_y, \phi_z$  at each node

Figure 2. The BECOS element

## BETACX



Closed thin-walled tube with linear taper connected to eccentric nodal points,

St. Venant torsion, shear effects in bending

Number of nodes 2

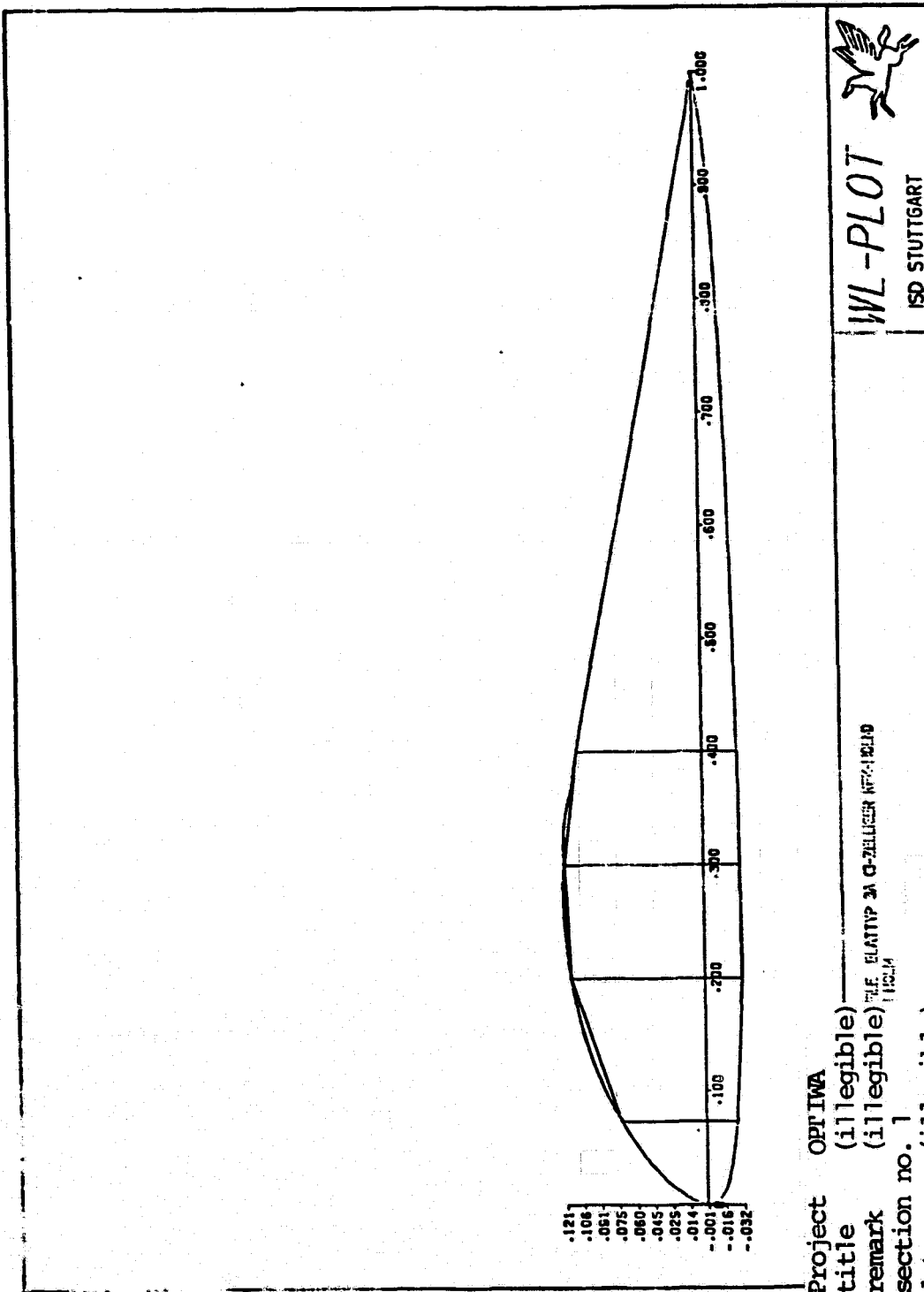
Degrees of freedom  $u, v, w, \phi_x, \phi_y, \phi_z$  at each node

Figure 3. The BETACX element

Element Type	BECOS	BECOC	BECOP	BECOSX	BECOCX	BECOPX	BETAC node 1 node 2	BETACX node 1 node 2
Total number of Input Data	8	13	11	14	19	17	20	26
Area of cross-section A	1	1	1	1	1	1	1 2	1 2
Moments of inertia	2 3 4	2 3 4	2 3 4	2 3 4	2 3 4	2 3 4	3 4 5 6 7 8	3 4 5 6 7 8
St Venant torsion constant J	5	5	5	5	5	5	9 10	9 10
Torsion-bending constant			6			6		
Reciprocal shear areas		6 7 8			6 7 8		11 12 13	11 12 13
Co-ordinates of $P_o$	6 7 8	9 10 11	7 8 9	6 7 8	9 10 11	7 8 9	14 15 16	14 15 16
Co-ordinates of shear center		12 13	10 11		12 13	10 11	17 18 19 20	17 18 19 20
Rigid lever-arm				node 1 node 2 9 10 11 12 13 14 15 16 17 18 19 20 21 22 23 24 25 26				

TABLE 1. Geometric input data for various ASKA beam elements

ORIGINAL PAGE IS  
OF POOR QUALITY



ORIGINAL PAGE IS  
OF POOR QUALITY

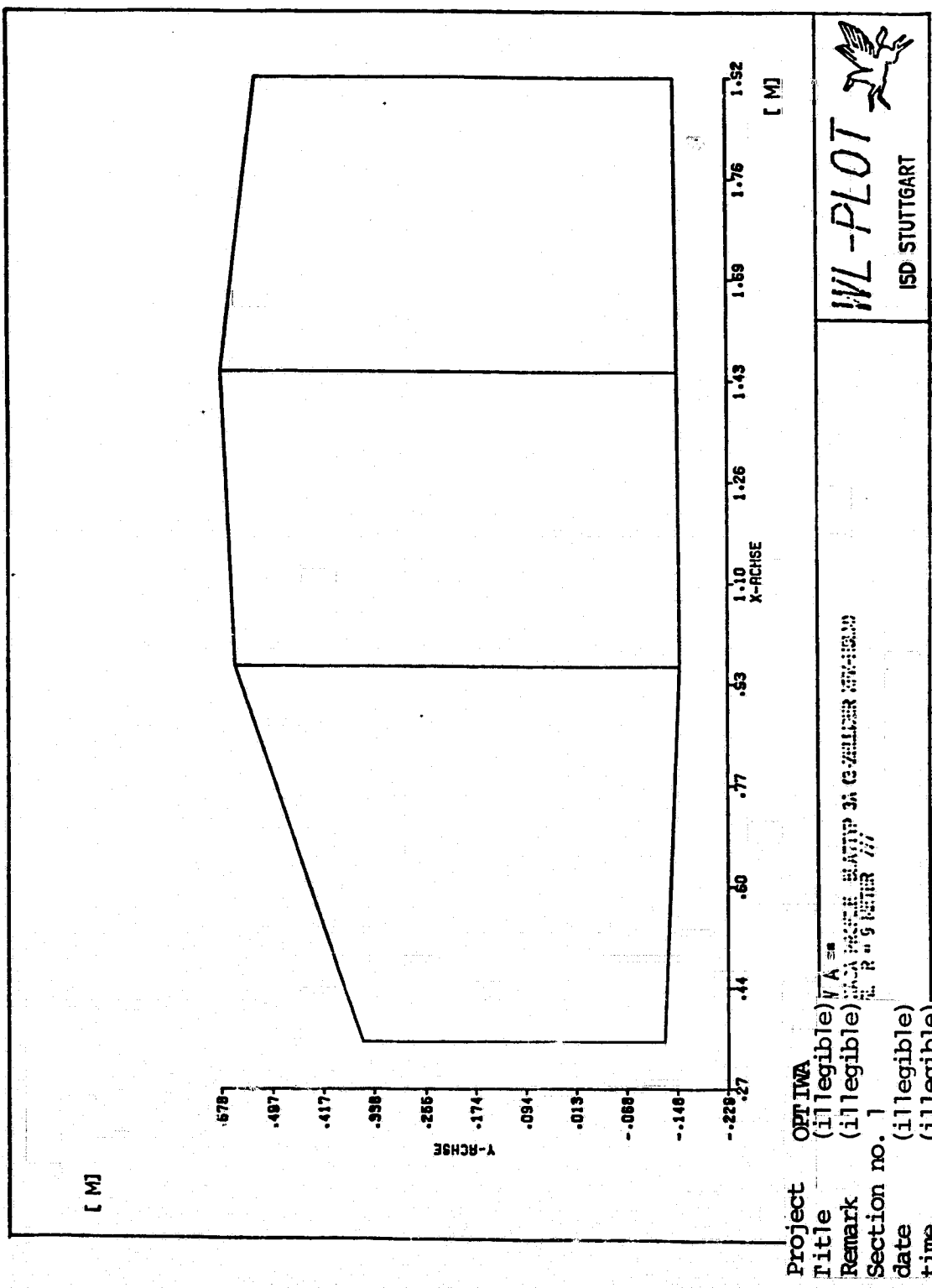


Figure 5. Three cell spar for profile FX-77-W-153

ORIGINAL PAGE IS  
OF POOR QUALITY

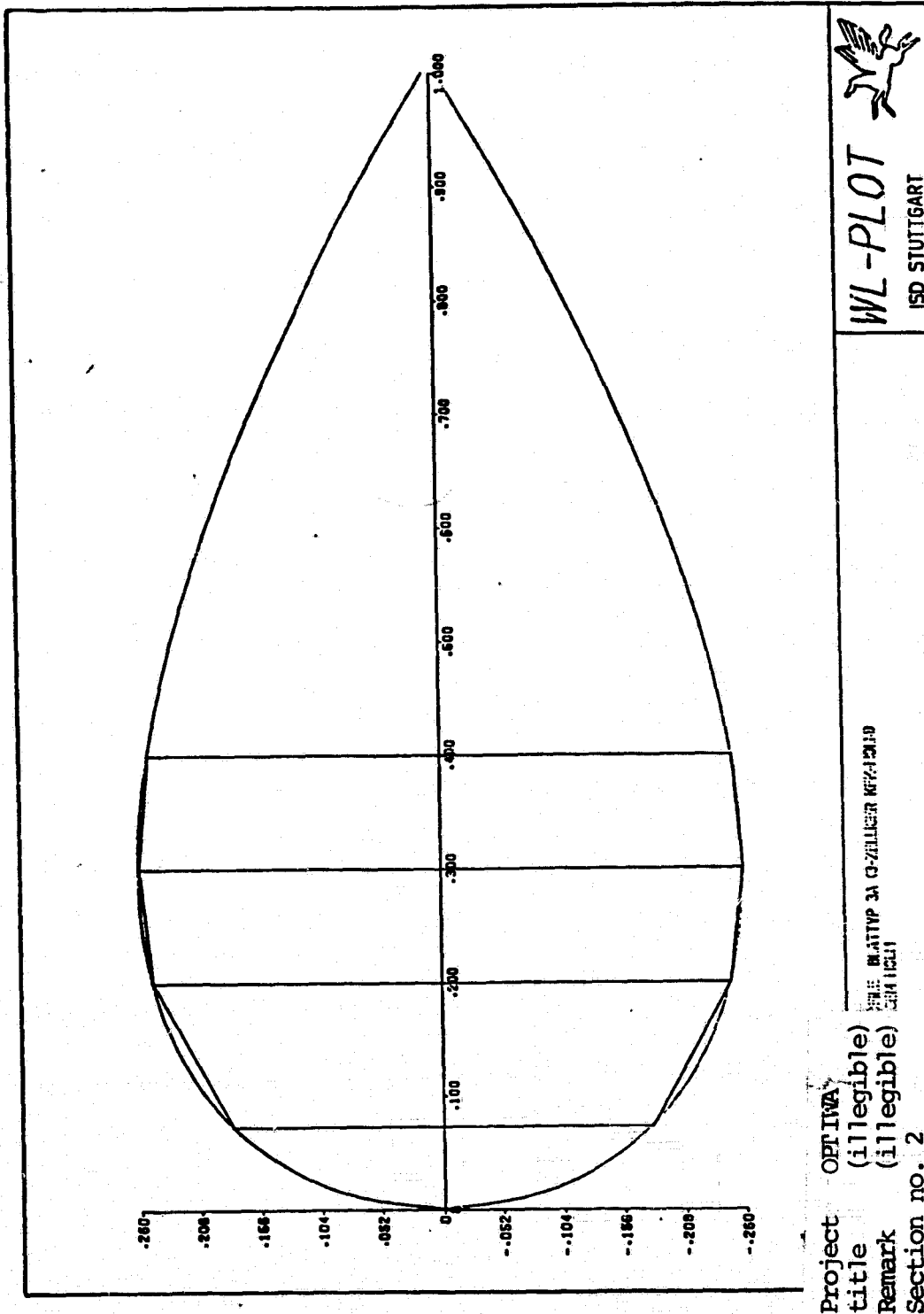


Figure 6. Profile NACA 0052 including spar

WING TECHNOLOGY PROGRAM FOR LARGE  
ENERGY FACILITIES

/329

Project ET 4375 A

D. Muser

In the following we discuss several problems which resulted during the first phase of a wing technology program which obstructed a fast and exact optimization of large rotor blades. The individual problems of various importance have various influence on the rotor blade design.

DEVELOPMENT OF AN OPTIMIZED ROTOR BLADE

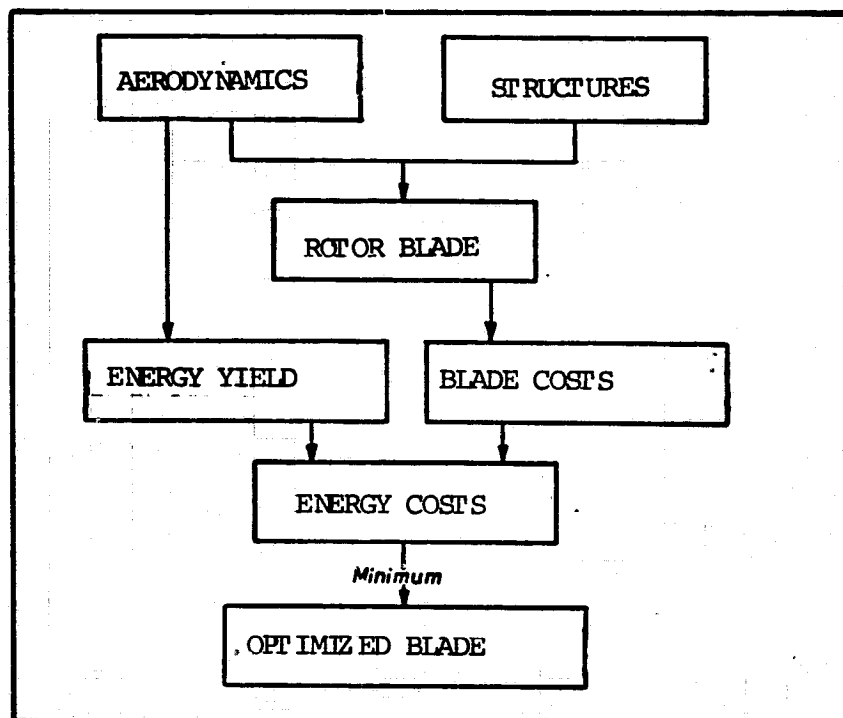
The main purpose of the wing technology program is the development of low cost rotor blades. The rotor blade can only partly be considered as an isolated system because there are substantial feedbacks of the rotor blade on the entire system. Assuming equal total facility concepts and the same rotor concepts, for example, Growian, it is possible to make a simplified analysis for an isolated rotor blade.

The optimization path of the blade leads through aerodynamics and structural designs up to the rotor blade design. The energy yield obtained and the structural costs together give the energy cost. If these reach a minimum, then we have a cost optimized blade.

INFLUENCES ON THE ROTOR BLADE

For the rotor blade, the effects of the profile, geometry and adjustment philosophy as well as the interaction of the supporting and covering structure combined with the materials can be computed separately. Other influences on the energy yield and blade costs are also important for the entire installation.





For a limited wing technology program, only a few combinations can be treated out of the entire matrix of solutions. According to experience with Growian, it is important to investigate new aspects of /331 the profiles and adjustments in conjunction with the structure. However, already during a comparison of calculated data with those of other facilities, the influence of the calculation, the location, the total facility and the number of units will very clearly lead to distortions. At /332 the same time various operating states can only be estimated roughly as to their effects. The influences of contamination (increase of the roughness by a factor of 10 for insects) or the erosion effect on loads, power and lifetime are for the most part unknown.

Also not much information is available about gust distribution and it is difficult to estimate the expected nonrunning times of the facility.

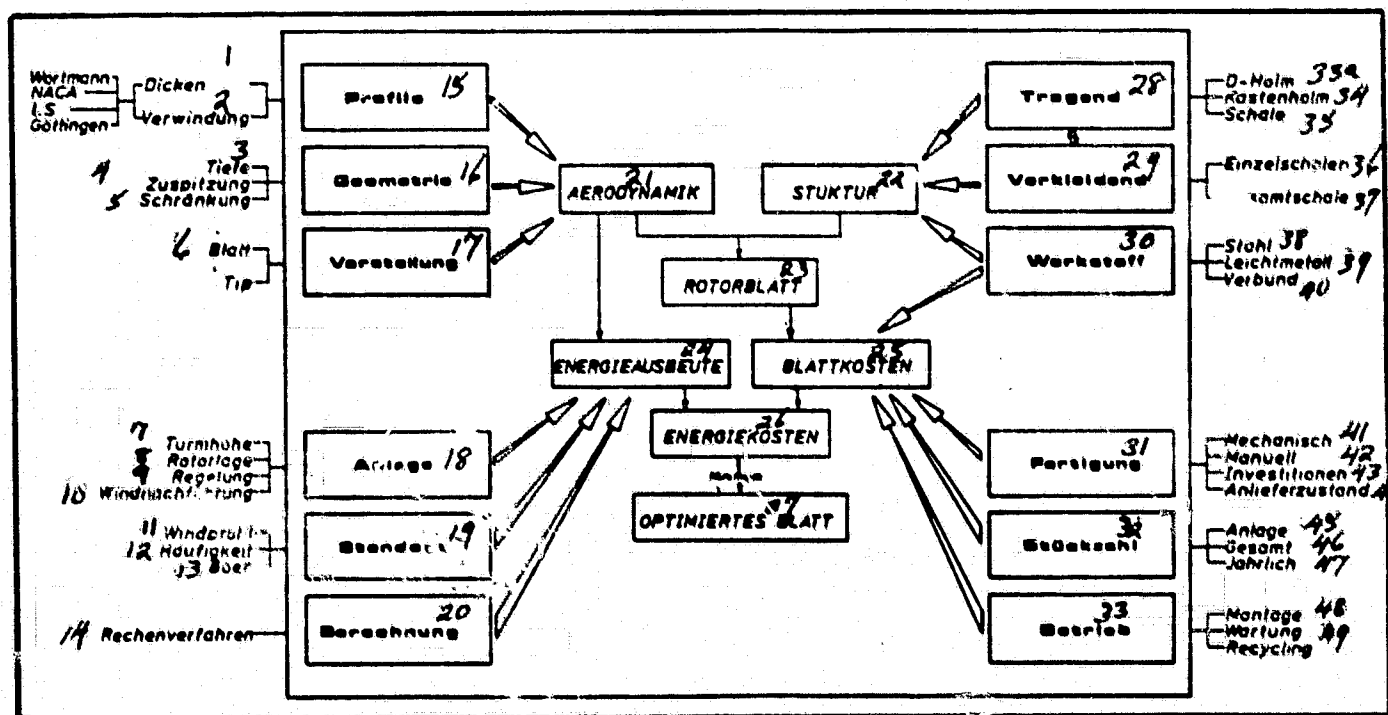
#### POWER COMPARISON

From the cost estimates, one cannot derive certain information about the expected energy costs. At the same time, when comparing

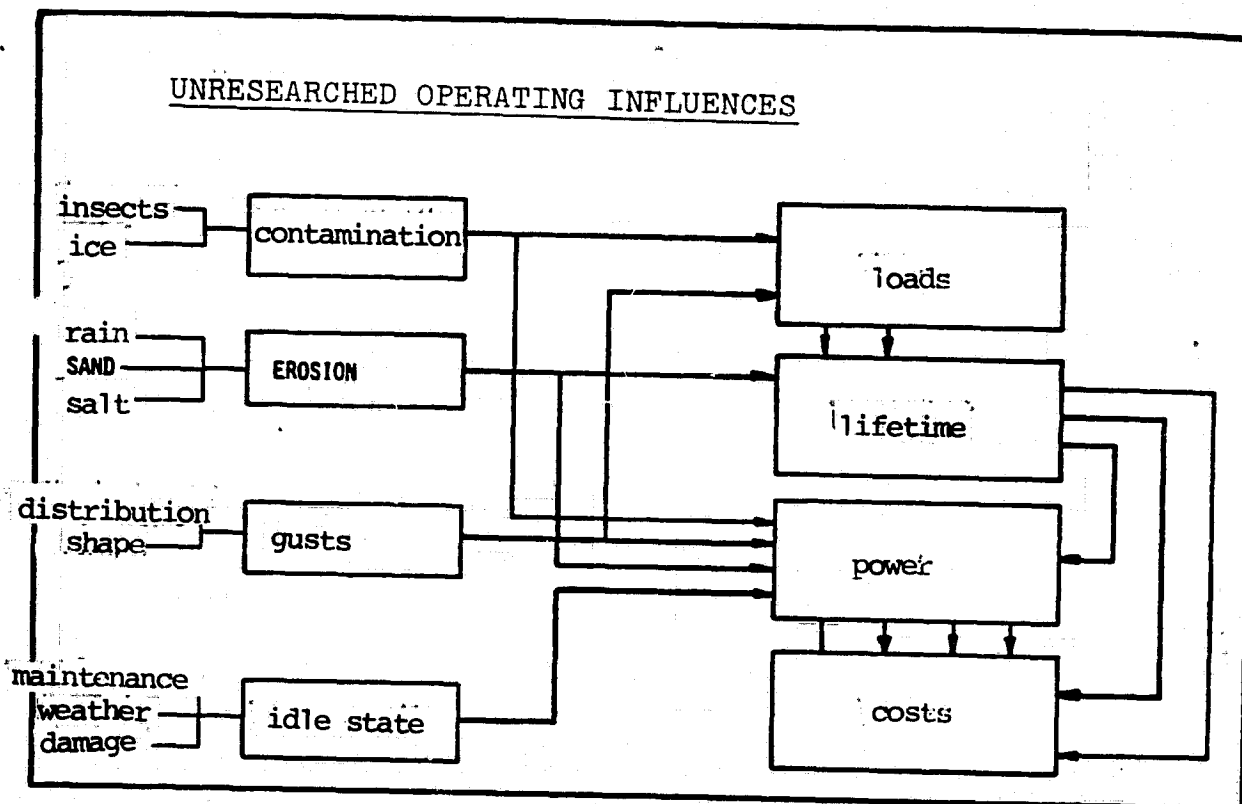
ORIGINAL PAGE IS  
OF POOR QUALITY

KEY TO FIGURE BELOW:

1--thicknesses; 2--twist; 3--chord; 4--tape ring; 5--slenderness;  
6--blade; 7--tower height; 8--rotor position; 9--control; 10--wind  
following; 11--wind profile; 12--frequency; 13--gusts; 14--calcula-  
tion methods; 15--profile; 16--geometry; 17--adjustment; 18--facility;  
19--location; 20--calculation; 21--aerodynamics; 22--structure;  
23--rotor blade; 24--energy yield; 25--blade costs; 26--energy costs;  
27--optimized blade; 28--supported; 29--covered; 30--materials;  
31--manufacturing; 32--number of pieces; 33- operations; 33<sub>a</sub>-D spar;  
34--box spar; 35--shell; 36--individual shells; 37--entire shell;  
38--steel; 39--light metal; 40--composite; 41--mechanical;  
42--manual; 43--investments; 44--delivery state; 45--facility;  
46--total; 47--yearly; 48--assembly; 49--maintenance;



1331



various facility sizes and types, it should be realized that the calculation results are only partly supported by wind distribution, tower shadowing, wind direction fluctuations and wind gradient and the resulting power losses can lead to different results.

/333

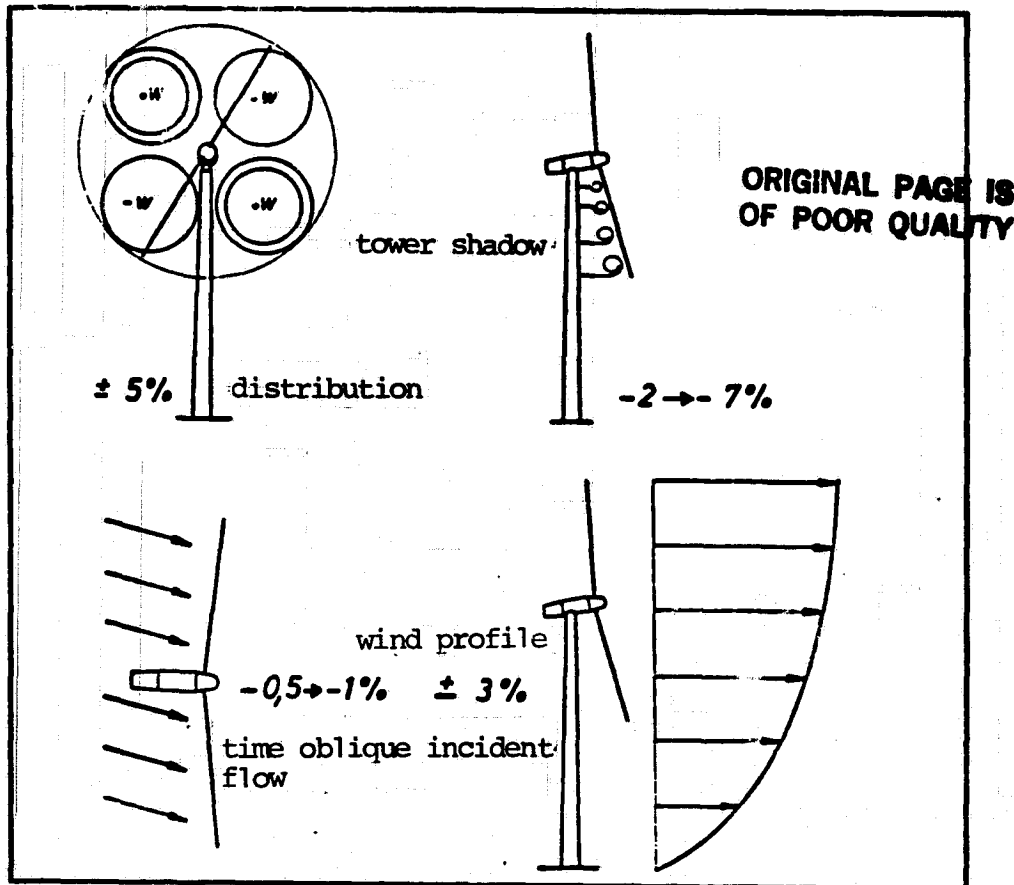
Changes in the power yield can amount to the following:

wind distribution	± 5	percent
tower shadowing	- 2 to -7	"
oblique incident flow	-0.5 to -1	"
and wind gradient	± 3	"

In the superposition case, differences can occur, depending on the assumptions. This can affect the energy yield and the facility cost.

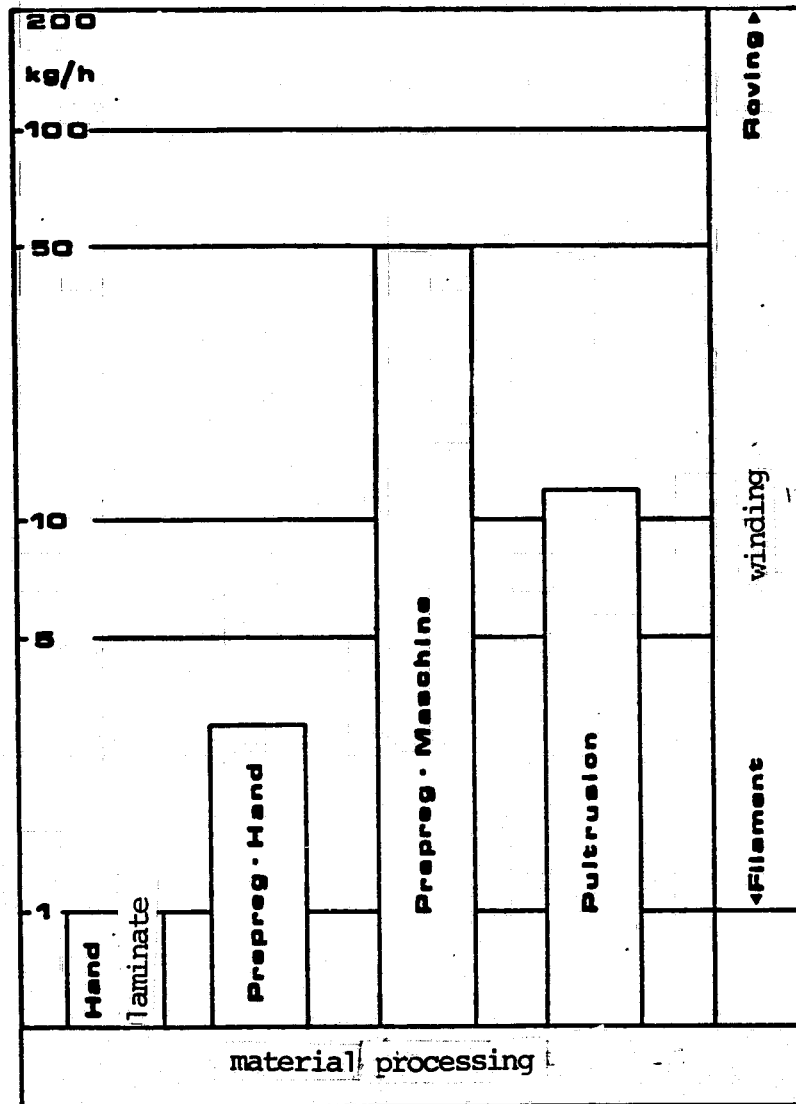
### COST DEVELOPMENT

The prediction of cost development is just as difficult as the prediction of rotor blade manufacturing costs. If one considers the optimized cost estimates of hydrocarbon manufacturers with a minimum



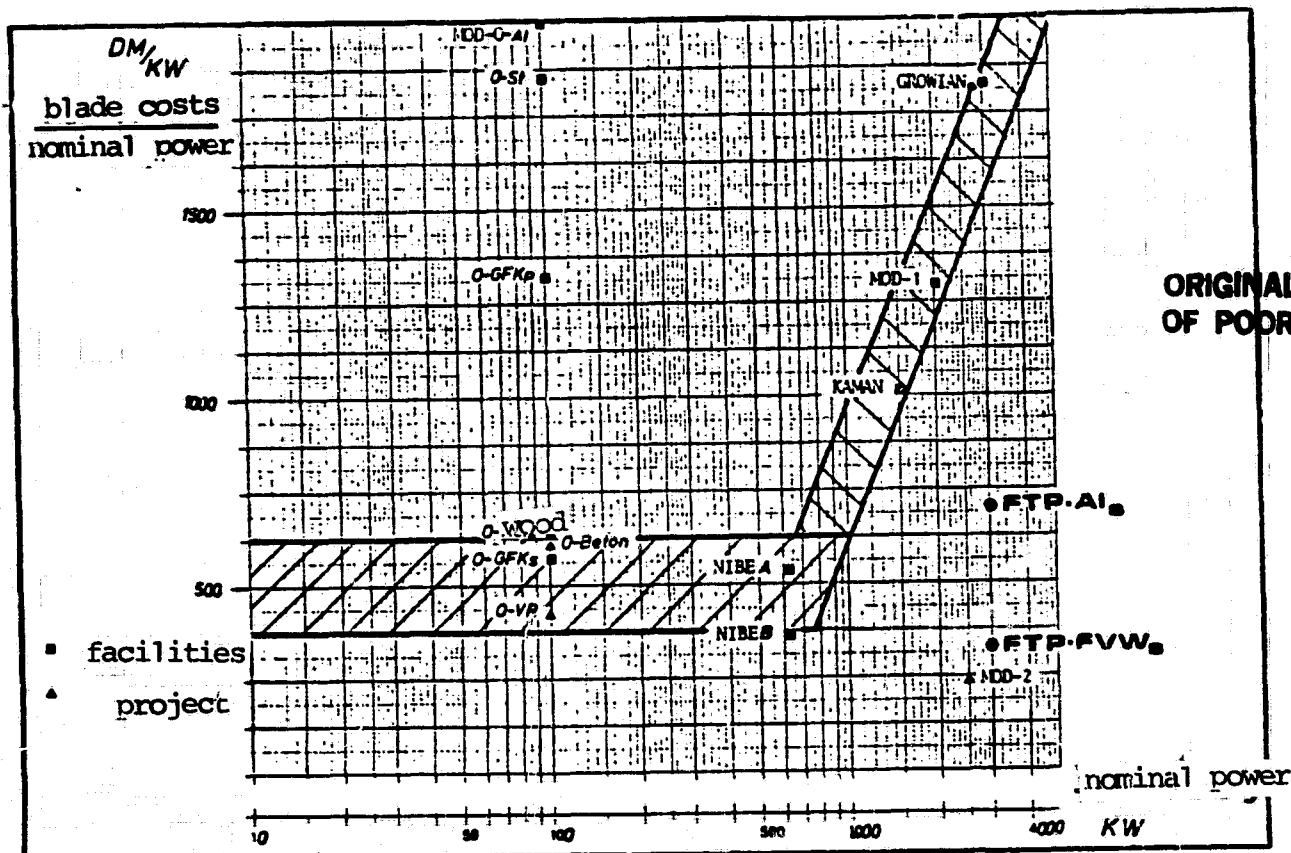
price of 30 DM/kg for the year 1990, then it may be possible to develop a rotor blade whose cost will remain the same up to the year 1990, in spite of increase in resin, glass fiber and labor costs. Under these assumptions, the development of a hydrocarbon blade would have additional advantages.

One condition for this is the development of rational manufacturing techniques and nondestructive testing methods for composite fiber components. The present state of processing speeds of composite fibers varies widely. Per work place or machine, there are values between 1 kg/hrs and 200 kg/hrs. GFK (glass fiber plastic) is assumed and a simple recalculation to other materials can be done using the density of the various fibers. The differences and the difficulty of processing are not important. From this we find that for a suitable blade design, the winding of rovings with a high single thread number seems to be the most favorable manufacturing method at the present time. This is confirmed /335 by the American GFK rotor blades of Kaman and Hamilton Standard. /334



334

The conversion of these possible processing times to mass production of rotor blades becomes problematical. Comparisons with numbers for 1000 rotor blades known from the United States over 10 years could be made. The resulting 100 blades per year, however, would not necessarily have to lead to the lowest price. For large components with high investment costs of the production facilities, the manufacturing costs can again increase with increasing numbers when the facilities are not completely used. At the present state of the optimization work for large wind rotor blades, therefore, one has to design the number of pieces made according to optimum manufacturing methods. At the present time for a light metal blade, we find an optimum piece number of 38 pieces per year. Similar results (32 GFK blades) are known from



Hamilton Standard. Price comparisons with other facilities can be performed but are difficult to evaluate.

/336

The cost of light metal and the composite fiber version for mass production reached the level approximately for the MOD-2 model. This corresponds to the price of about 0.4 pfennig/kilowatt hour. In order to achieve these low costs, which are by a factor of 4 less than the present Growian blade cost, there has to be a substantial manufacturing and material development.

#### MATERIAL AND MANUFACTURING DEVELOPMENT

Material development does not mean a determination of simple characteristics but the development of favorable materials for wind energy applications regarding weathering and loads. Various developments are required for the various materials which increase the manufacturing speed and reduce the manufacturing costs, and are also intended to improve the lifetime of the components. Here especially we are interested in the composite material sector, the most recent group of construction

/337

MATERIAL DEVELOPMENT

ORIGINAL PAGE IS  
OF POOR QUALITY

FIBER COMPOSITE

• PREPEGS

- LOW HARDENING PRESSURE
- LOW HARDENING TEMPERATURE
- LONG STORABILITY
- DIAGONAL FIBER DIRECTION
- HIGH AREA WEIGHT

• TISSUE

SEMI FINISHED GOODS

• METAL

- STRAND PRESSED PROFILES
- GOOD CORROSION RESISTANCE
- HIGH DYNAMIC CHARACTERISTICS
- STRAND DRAWING PROFILES
- SEMIHARD ELEMENTS

• COMPOSITE

materials. It is important to use the possibilities of the material and to reduce overall costs.

The influence of various concepts on the total facility have to be considered. Also there may be required design changes. For two load cases with the example of Growian, one considers the bending moment variations over the blade length. Then for a lifetime calculation of a hub, for steel of LF 1.3 (nominal operation), the hub is not as important as for a composite fiber blade. Using the assumed mass of 16300 kg for a steel blade and 4800 kg for the GFK/CFK blade, LF 1.3 becomes dominating because it is on the same order as 2.5 (negative gust). It is important for the hub design to consider the change load conditions.

/338

For the dimensioning of these components with the load cycle numbers between  $10^8$  and  $10^9$ , there is not much data available. This is also true for the type of lifetime calculation.



MANUFACTURING DEVELOPMENT

METAL	• STEEL	• DEFORMATION TECHNOLOGY
	• LIGHT METAL	• DEFORMATION TECHNIQUE • JOINING TECHNIQUE
FIBER COMPOSITE	• PREPREG	• LAYING DOWN ROBOTS • TEST METHODS
	• WINDING	• IMMERSION METHOD • WINDING SPEED • TEST METHODS
	• GENERAL	• HARDENING CYCLE • JOINING TECHNIQUE

SUMMARY

Considering the various aspects, we can consider the following partial areas for additional wind energy research:

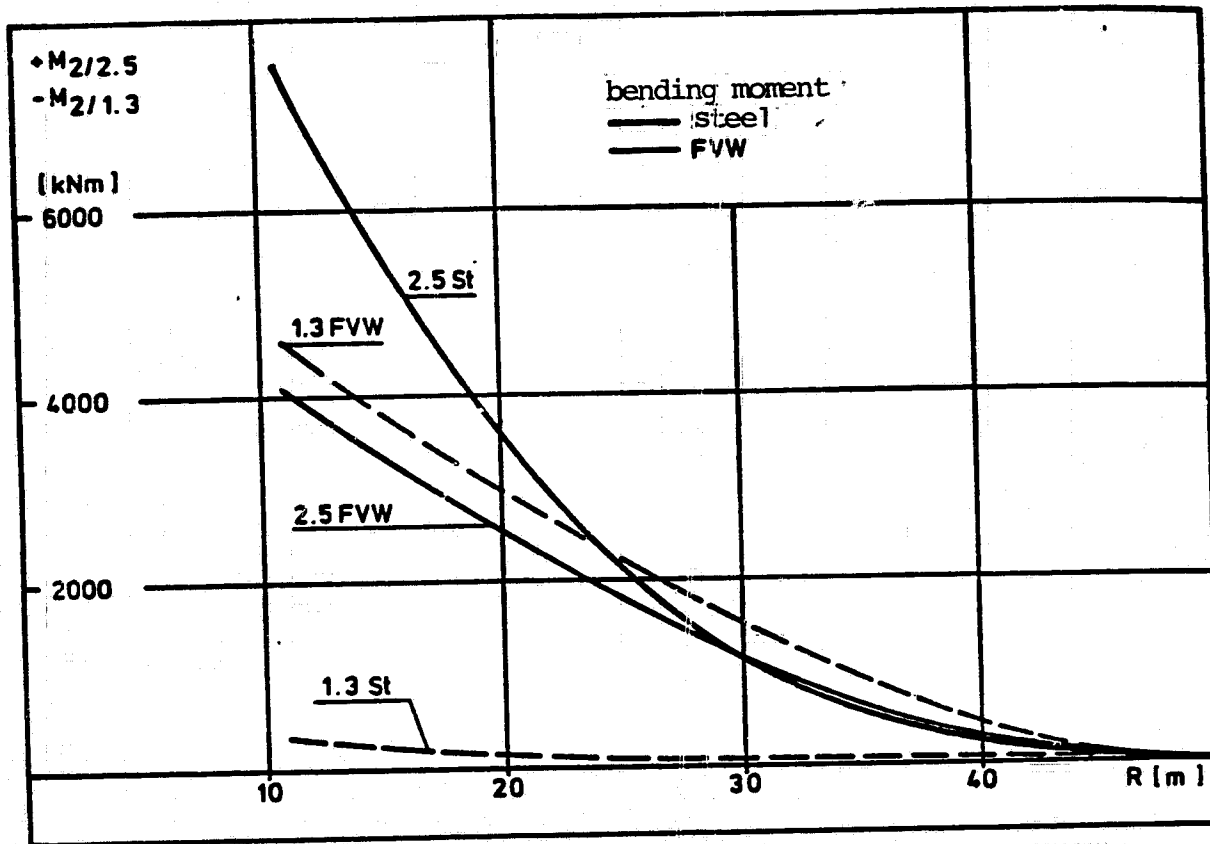
- nominal load list
- performance calculation
- material development
- manufacturing development
- testing

/339

With increasing knowledge of these subjects, the further development of large rotor blades will become easier and will lead to lower energy recovery costs faster.

ORIGINAL PAGE IS  
OF POOR QUALITY

338



341

DEVELOPMENT REGIONS		
SPECIFICATIONS	<ul style="list-style-type: none"> <li>• WIND</li> <li>• GUSTS</li> <li>• ENVIRONMENT</li> </ul>	<ul style="list-style-type: none"> <li>◦ DIRECTION PROFILE</li> <li>◦ VARIATION FREQUENCY</li> </ul>
POWER	<ul style="list-style-type: none"> <li>• CALCULATION</li> <li>• MEASUREMENT</li> </ul>	<ul style="list-style-type: none"> <li>◦ ASSUMPTION METHODS</li> <li>◦ METHODS</li> <li>◦ CALCULATION TESTING</li> </ul>
MATERIAL	<ul style="list-style-type: none"> <li>• SUITABILITY</li> <li>• DEMONSTRATION</li> </ul>	<ul style="list-style-type: none"> <li>◦ MANUFACTURING SPECIFICATIONS</li> <li>◦ DYNAMIC CHARACTERISTICS</li> <li>◦ CALCULATION METHODS</li> </ul>
MANUFACTURING	<ul style="list-style-type: none"> <li>• METHODS</li> <li>• COSTS</li> </ul>	<ul style="list-style-type: none"> <li>◦ FULL SCALE COMPONENTS</li> <li>◦ MASS PRODUCTION</li> <li>◦ DEVELOPMENT</li> <li>◦ MANUFACTURING</li> </ul>
TESTING	<ul style="list-style-type: none"> <li>• POWER</li> <li>• LIFETIME</li> </ul>	

K. Kehl\*

SUMMARY

Computer programs for the analysis of the overall dynamic behavior of Growian I are presented. Problems and solution possibilities in dynamics are discussed with some examples.

/342

1. Introduction

Large wind power facilities with a horizontal rotor axis can perform oscillations when standing still and especially during operation. Because of operation under load, static loads occur which can be amplified by excitations caused by ground tremors, network disturbances, control influences, facility imbalances and wind disturbances. This affects the dimensioning of the facility, both for the extreme low case and for the creep strength. Therefore, certain oscillation deflections and accelerations must not be exceeded.

Large wind power generation facilities have to be dimensioned for operational reasons and cost reasons. In contrast to earlier wind mills, substantial supporting components have to have an almost rigid behavior instead of an elastic behavior. Because of the design yields (for example, tower, rotor blades, drive train, etc.), dynamic instability problems occur, for example, whirl--flutter, bending/torsion and flapping/deflection flutter of the rotor blades. There are also oscillation responses due to system disturbances.

2. Computer programs for the analysis of the overall dynamics

In general, a computer model for determining the overall dynamic behavior of large wind power generation facilities must contain both

---

\* MAN - Neue Technologie

the structural responses as well as the couplings to the control system with the electrical components and also the process control system which is present in many systems. All of the structural parts are modeled with an elastic-yielding method and their relevant eigen frequencies are of comparable magnitude. Such a universal model has the advantage that practically all of the interesting total dynamic problems can be treated in a design. However, one disadvantage of this is that the development times of such an extensive program system are very long and the user costs are very high because of the enormous memory requirement and the long calculation times.

/343

In the case of Growian I, there is a possibility of exploiting certain design properties in order to solve certain individual problems. This has the consequence that some of the problems mentioned above are avoided. Figure 1 shows this. A criterion which justifies an uncoupling of the control system from the structure are the small time constants which have very short control delays as a consequence. This means that the control technology can be considered alone as part of the operational control and the rotor blade is contained as a simple control loop. Using the program SIMBR, simulations of the operating behavior overtime were performed, where the wind is introduced as a stochastic quantity and the blade adjustment angle, rotation rate and power are calculated in real time as responses.

Structural dynamic problems of the coupled rotor/tower system can be simplified if the lowest flapping eigen frequency is much larger than the first tower bending eigen frequency (with the rotor blade as a point mass) with respect to the deformation in the direction of the wind. Symmetric rotor deformations are assumed. If in addition the antimetric rotor loads are uncoupled by a pendulum hub from the tower, then the rotor can be modeled with a simple tower idealization. On the other hand, the elastic tower can be modeled with a rigid rotor performing pendulum motion (program RMOD 1).

To a good degree of approximation, the rotor modeling can be simplified to the problem of single axis bending when the principle axes

of inertia of the rotor blades are untwisted and the external loads during operation primarily act in one of the principal directions of inertia. A model which contains this idealization is the program RBM with which one can calculate dynamic rotor blade interface force magnitudes and deformations due to the various disturbances.

/344

Design reductions in the rotor flapping eigen frequencies have led to the requirement for a refined structural modeling. The rotor is considered to be yielding like the elastically yielding tower and the flapping and deflection bending are considered (program RMOD 2).

A coupling of the structure with the control unit and the electrical network as an additional disturbing quantity allows one to simulate extreme operational situations, such as network collapse for extremely unfavorable wind conditions (program SIM).

### 3. Loads of the rotor due to tower shadow excitation <sup>1)</sup>

The rotor load model designed for the single axis bending (RBM) on the one hand consists of a finite element part with which the eigen oscillation variables of the conservative system are determined and is shown in Figure 2. Using the subsequent modal analysis, all of the eigen oscillation variables of the system damped by aerodynamic forces can be calculated.

The Runge-Kutta method is used to integrate the equations of motion and provide the dynamic responses over time. By direct calculation of the complex frequency changes after corresponding transformation into the frequency range, the dynamic response spectra are determined. As right size for the motion equations (disturbances), one can input constant wind, the linearized boundary layer, symmetric and antisymmetric individual gusts, tower wind shadow or wake systems, eigen weight excitations and centrifugal force excitations due to coning angle and oblique rotational axis. The model also considers the pendulum motion

---

<sup>1)</sup> with the collaboration of Prof. E. Giencke - TU Berlin.

of the rotor which has a blade angle feedback control. As an example, Figure 3 shows the variations of the blade tip deflection and the clamping bending moment due to tower wake disturbances for the stable state. The figure applies for quasistationary aerodynamic forces for a symmetric incident flow constant and time over the rotor area. For the bending moment, we have two main maxima displaced by  $180^\circ$  of about the same magnitude. The first maximum is the direct response of the rotor blade when passing through the tower wake displaced by about  $20^\circ$  in phase. The tip is displaced by  $\pi$  and this is the response of blade A to the tower shadow excitation of blade B. This means that in spite of the antymmetric disturbance of the rotor from the tower shadow, we have essentially symmetric loads on the rotor blade (that is,  $2 \Omega$ ). In the case of the blade tip deflection, this is not so clear which can be explained by the pendulum motion. /345

Figure 4 shows the influence of time dependent aerodynamic forces. Here we show an example of a single gust which has a trapezoidal shape according to the sketch. For the case of quasistationary aerodynamic forces, there are only unessential deviations compared with Figure 3. This shows that the disturbance of the tower wake impulse has already decayed after one revolution and that the rise time of the previous gust is so large that only unessential additional dynamic amplifications occur. It is interesting to consider the unsteady condition for the aerodynamic force trial solution (using the Theodorsen and Schwarz functions). This leads to maximum bending moments which are about 30% smaller which are displaced by about  $15^\circ$  with respect to the stationary case in phase. From this it becomes clear that the unsteady aerodynamic forces have a substantial influence on the dynamic responses because of the high frequency perturbation components.

If the results of the tower shadow calculation with dynamic responses from the stationary flow (static), eigen weight and centrifugal force excitation as well as an idealized boundary layer are superimposed, then for the nominal operating case one finds that the tower shadow is not so important with respect to maximum loads as shown in Figure 5. These loads are much more important, however, for the operating strength



design of the facility.

/346

#### 4. Overall dynamic structural behavior

Calculations were performed with the program RMOD 1 for analyzing the dynamic stability and response behavior of the coupled tower/rotor system. The computer program assumes an elastic tower with a lumped rotor mass which is described by its 5° of freedom.

- $q_1$  = 1st tower bending in wind direction
- $q_2$  = 1st tower bending perpendicular
- $q_3$  = 2nd tower bending in wind direction
- $q_4$  = 2nd tower bending tranverse
- $q_5$  = 1st torsion

as well as an elastically rigid and zero mass 2-blade rotor performing pendulum motions having blade angle feedback control shown in Figure 6. The elastically rigid machine house can be aligned with the wind. The rotor rotation axis is inclined by an input angle with respect to the horizontal.

The computer model I shown in Figure 7 was discussed in [1]. Reference [2] gives detailed results. The modal tower motion equations and the discrete rotor equation motions are coupled to the entire system using a coordinate transformation with the unknown constraint forces. The stability analysis is performed for 2-blade rotors which perform parameter-forced oscillations using the Floquet theory. The state matrix is integrated using a Runge-Kutta method of 4th order with Gill coefficients starting with unit initial conditions over the rotor circulation; the so-called transition matrix is found. The complex eigen values of this matrix are called characteristic multipliers and can be used for the stability analysis. In the program, as a reference point, at the same time the eigen value analysis of the state matrix is performed using coefficients which are averaged over 1 revolution. The eigen value calculation is done using the QR algorithm and the matrix is first transformed to the Hessenberg form.

/347

If the system is dynamically stable, then response calculations of the steady state can be performed for various excitations, such as rotor imbalances, wind gradients, wind direction tracking and oblique flow.

#### 4.1 Dynamic stability calculation

Figure 8 gives the result of a stability analysis. It can be seen that the nominal operational point is in a stable region. A doubling of the nominal speed, which is permissible according to Growian operation, can cross over the instability boundary for excessive rotation rates with zero loads. Operation with power generation is practically always in the stable region. One eigen oscillation mode has been found to be a critical degree of freedom which contains primarily tower torsion and to a great extent, the first tower bending mode in a transverse direction. From the lower half of Table 1, which contains the eigen vectors normalized to 1, we can see that the other tower degrees of freedom are only negligible in the 5th eigen vector. This is different for the calculation with constant coefficients. Here there are substantial couplings with all of the tower degrees of freedom which leads one to the suspicion that the stability property will also be much different.

Figure 9 shows this assumption. The Lehr damping measure is plotted over the nondimensional rpm which is referred to the damping for the nominal operating state. In the representation "without additional system" (lower curve), one can clearly see the dropoff to the unstable region for excessively high rpm. As a reference, we show the input value of the structural damping which here was selected at a value of 0.2% which is low for steel design (corresponding to a logarithmic decrement of about 0.0125). The calculation with constant coefficients gives results which are both quantitatively (more than a power of 10) and qualitatively completely different from the calculation with periodic coefficients. For time variant coefficients, the system damping decreases with rpm; for constant coefficient calculations, it increases practically linearly.

The danger of dynamic instability led to the requirement of damping the critical degree of freedom with additional measures. A dynamic additional system which acts in a transverse direction consisting of an oscillating mass and a spring and damping member was designed for the front machine house shown in Figure 10. With this configuration, on the one hand the critical torsion degree of freedom in the first tower transverse bending mode is improved in terms of damping properties. On the other hand, the dynamic responses in the transverse direction which lead to large oscillation deflections are reduced. Figure 10 gives results from calculations of the optimization of the additional system. From the restrictions above, we made a compromise which, however, is not represented by any local maximum. /348

With a selected additional system, the damping properties of the critical degree of freedom are substantially improved (Figure 9--upper curve), so that we are quite certain that the danger of the instability has now been removed.

#### 4.2 Dynamic response calculation

In addition to the deflections in the transverse direction which are defined for the hub point, there are also pendulum deflections of rotor motion which are substantial dynamic responses of the modeled total system.

Figure 11 shows nondimensional maximum transverse deflections of the hub point plotted against the dimensionless rotation rate for the steady state. Two resonance phenomena can be established. The first peak occurs at about  $0.7 n_n$  and is the result of an excitation of twice the rpm harmonic. Boundary layer influences occur as disturbances here and the oblique attitude of the rotational axis with respect to the horizontal. Oblique flows and wind direction tracking increase these values in some cases. The second resonance peak excited by the first rpm harmonic is the result of rotor imbalances and is about proportional to the amount of imbalance which here is defined as an idealized additional mass at the blade tip. For excessive rpm and incident /349

flow speeds above the nominal speed, the instabilities occur without the additional system which lead to ever increasing deflections for linear systems.

Figure 11 shows the deflections with and without the additional system in the machine house. Comparison of the two curves clearly shows that with the damped additional system the resonance phenomena are reduced by almost an order of magnitude.

Figure 12 in the top part shows the maximum and minimum transverse deflections which are not the same in every operating state. One reason for this is that for the steady case, in general, no harmonic oscillation occurs but instead, there is a superposition of two harmonics at  $\Omega$  and  $2\Omega$  which are weighted differently depending on the load state (small sketches in the top of Figure 12). Especially for power generation (which is not shown here), there are substantial differences between both extreme values in the operating range between  $0.85$  and  $1.3 n_n$ .

In addition to the representation of the transverse deflection of the hub point, Figure 12 also shows the relative motion of the additional system. In the resonance region the magnitudes of the damper deflection are about twice as high as the hub point deflection, whereas in the operating state range they are only about half as large. This means that the additional system during normal operation will practically stand still with consideration of the friction forces ignored here and the designed restrictions of the dampers. This has primarily a positive effect on the creep strength of the additional system.

/350

The lower figure of Figure 12 shows the phase relationships of the extreme deflections of both motion quantities. They are displaced by  $90^\circ$  in the first resonance region and by  $180^\circ$  in the second region. In the transition regions, there are intermediate phase relationships, that is, within the operating rpm range.

The maximum pendulum deflections of the rotor as a function of the

incident flow speed and rpm are shown in Figure 13 without consideration of friction forces. One can see that between the turnon speed ( $V = 6$  m/s) and an extreme speed of 30 m/s which can be withstood for a short time, there are no noticeable differences in the pendulum deflections. This confirms the assumption that in the case of Growian I, the stationary speed which acts in a constant manner only has an indirect influence on the pendulum motion. The reason for this is because a constant speed distribution does not occur over the rotor area. The ground boundary layer leads to a height gradient which is idealized here as a linear speed drop and for the two stationary wind speeds, they are varied in three steps as a quantity to be superimposed. From the computer model I we find that the perturbation speed of the ground boundary layer has a linear influence on the pendulum deflections. The variation of the pendulum amplitudes with rpm has a hyperbolic character which explains that when standing still, there is a neutral equilibrium state. In order to avoid the large pendulum amplitudes which occur for low rpm, additional pendulum dampers were installed in Growian I which allow a free pendulum motion over a defined angular range.

/351

## 5. Summary

The design features (pendulum hub, stiffness relationships, etc.) allow uncoupling of individual problems from the total dynamic analysis so that for their treatment, one can use simplified computer models which, however, do not have a universal character. For calculating the structural dynamic behavior of Growian I, two computer models are presented and results are discussed. As for the rotor blade loads, the excitation by tower shadow which occurs as a perturbation of the incident flow conditions for systems operating leeward is discussed. The dynamics of the coupled tower/rotor system is described in terms of stability and oscillation response for various operational loads. Measures for increasing the modal damping properties and for reducing the transverse oscillations of the machine house are discussed.

eigen vectors		tower degrees of freedom					rotor pendulum motion (blade tip)
additional system	coefficients	1. longitudinal	1. transverse	2. longitudinal	2. transverse	1. Torsion	
with	constant	0,283	0,202	0,248	0,129	1,000	0
	periodic	0,007	1,000	0,025	0,030	0,617	0,023
without	constant	0,174	0,177	0,234	0,130	1,000	0
	periodic	0,042	0,402	0,037	0,024	1,000	0,043

TABLE 1. Eigen vectors of the V total system degree of freedom in the nominal operating state without power production.

ORIGINAL PAGE IS  
OF POOR QUALITY

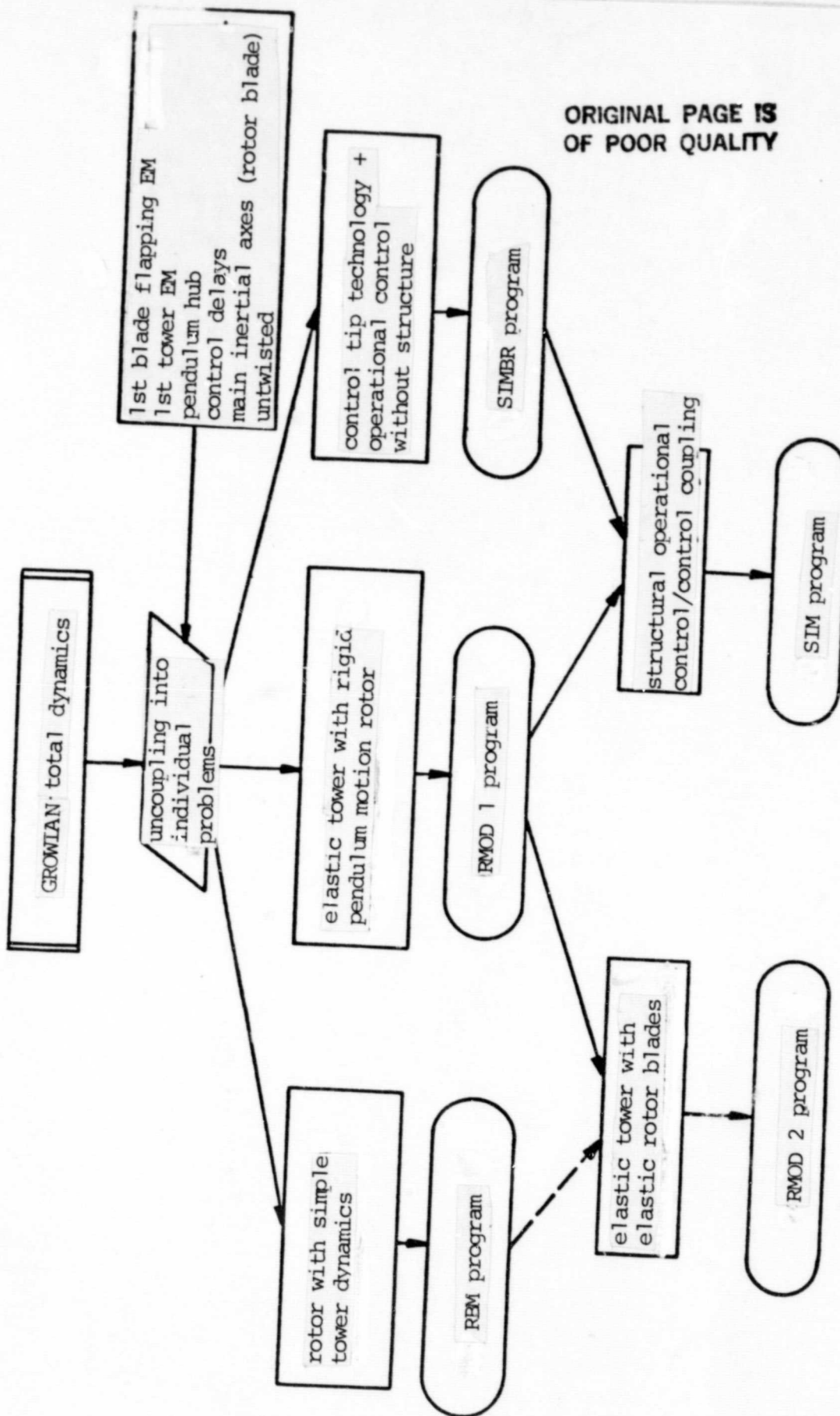


Figure 1. Calculation models of overall dynamics Growian I



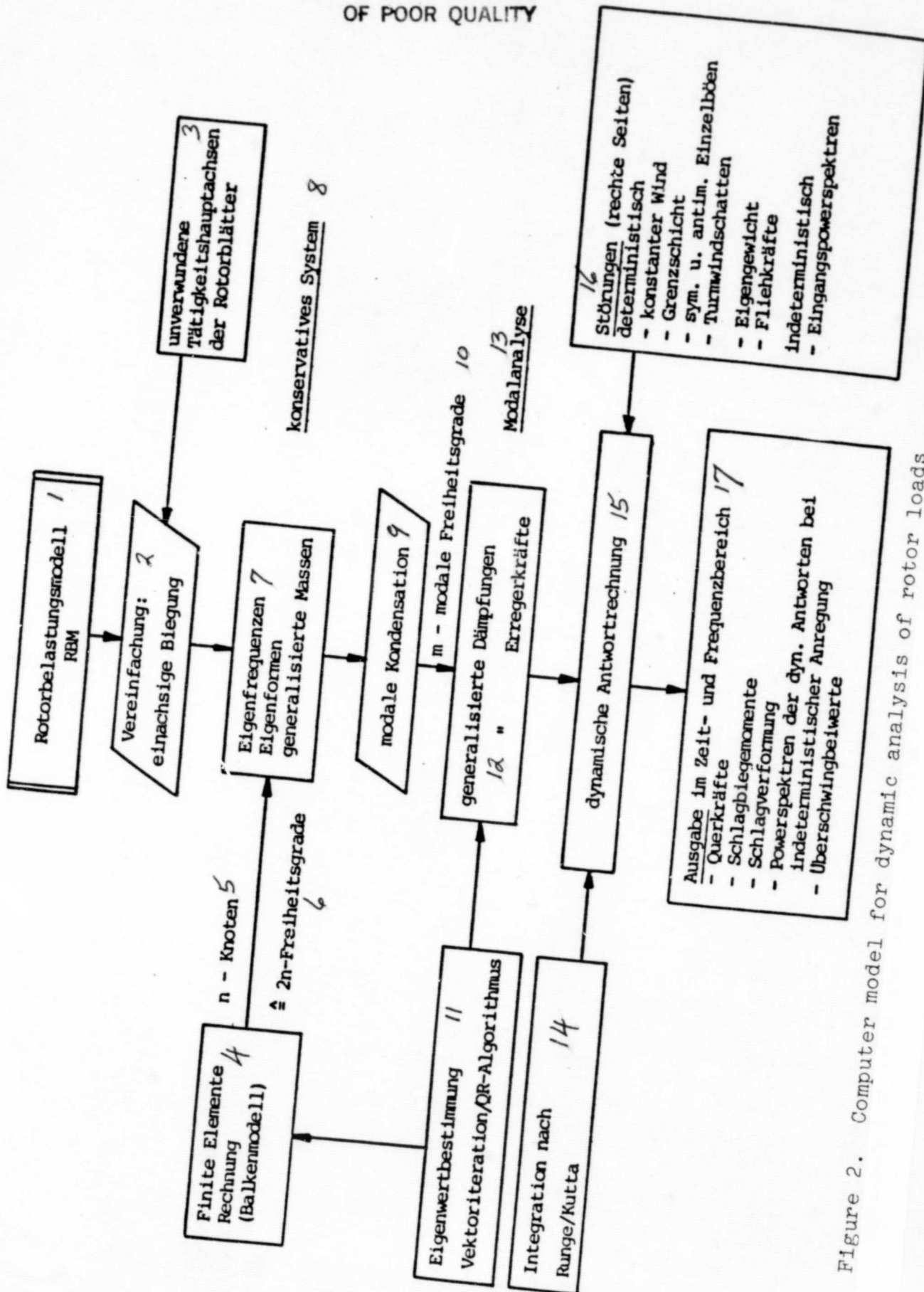
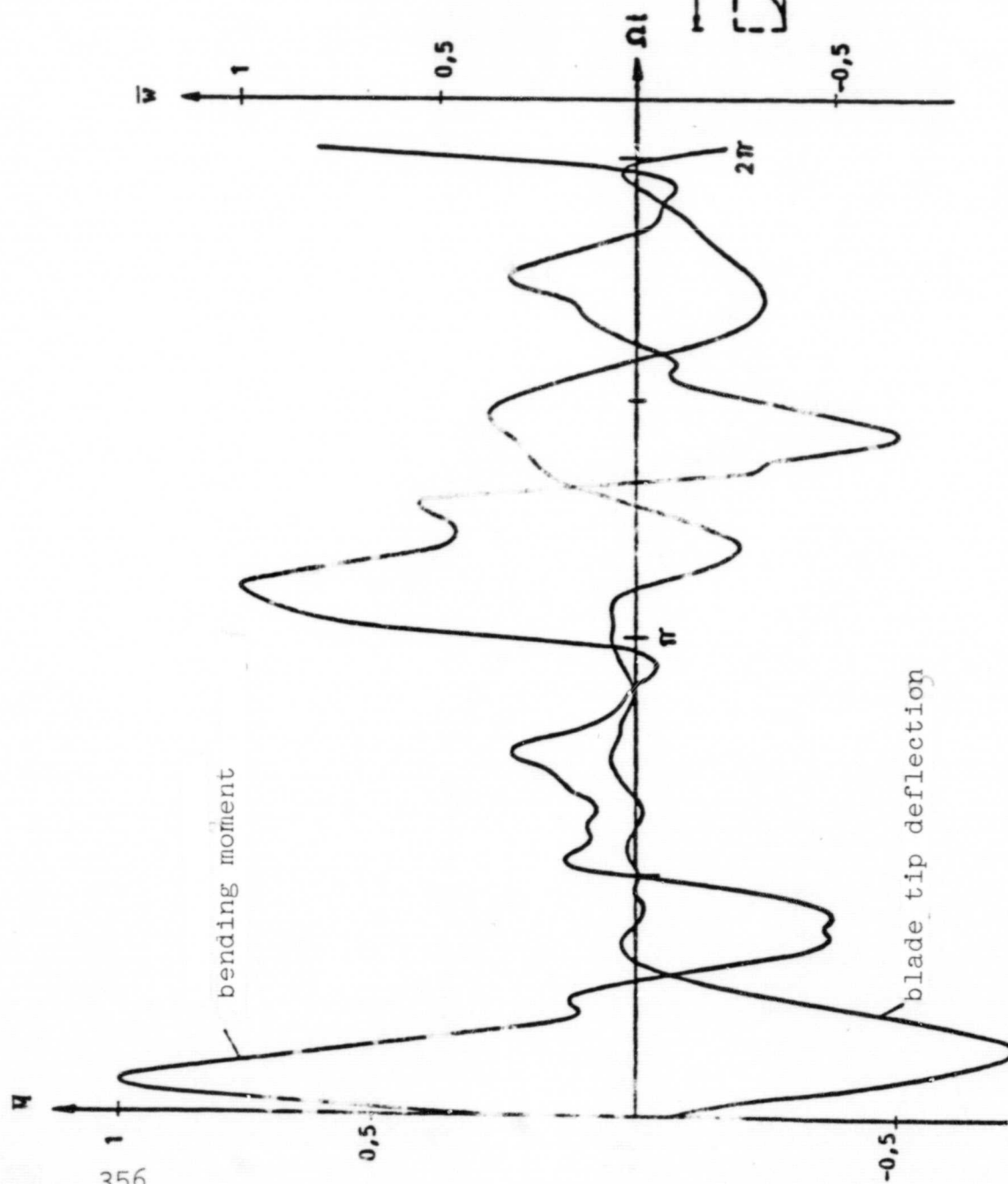


Figure 2. Computer model for dynamic analysis of rotor loads

KEY TO FIGURE 2 ON PRECEDING PAGE:

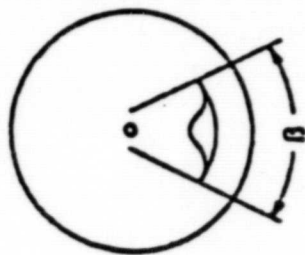
1--rotor load model; 2--simplification: single axis bending;  
3--untwisted inertial principle axes of rotor blades; 4--finite  
elements calculation (beam model); 5--n - nose; 6--2n-degrees of  
freedom; 7--eigen frequencies, eigen nodes, generalized masses;  
8--conservative system; 9--modal condensation; 10--m - modal degrees  
of freedom; 11--eigen value determination vector iteration/QR  
algorithm; 12--generalized damping; generalized excitation forces;  
13--modal analysis; 14--integration according to Runge/Kutta;  
15--dynamic response calculation; 16--disturbances (right sides);  
deterministic--constant wind--boundary layer--symmetric and anti-  
symmetric individual gusts--tower shadow eigen weight centrifugal  
forces. Indeterministic; input power spectra; 17--outputs in the time  
and frequency range--tranverse forces--flapping bending moments--  
flapping deformation--tower spectra of dynamic responses for indeter-  
minate excitation--over oscillation coefficients



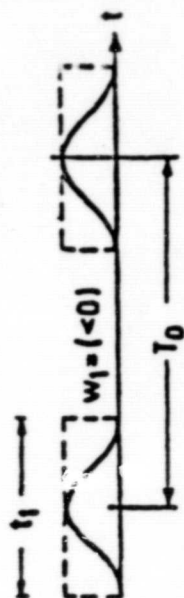
bending moment

blade tip deflection

tower shadow modeling



ORIGINAL PAGE IS  
OF POOR QUALITY



$$t_1 = T_0/20.5$$

Figure 3. Time variation of nondimensional hub moment  $\bar{M}$  at the clamping point and blade tip direction  $\bar{w}$  due to tower wake flow for stationary incoming flow.

ORIGINAL PAGE IS  
OF POOR QUALITY

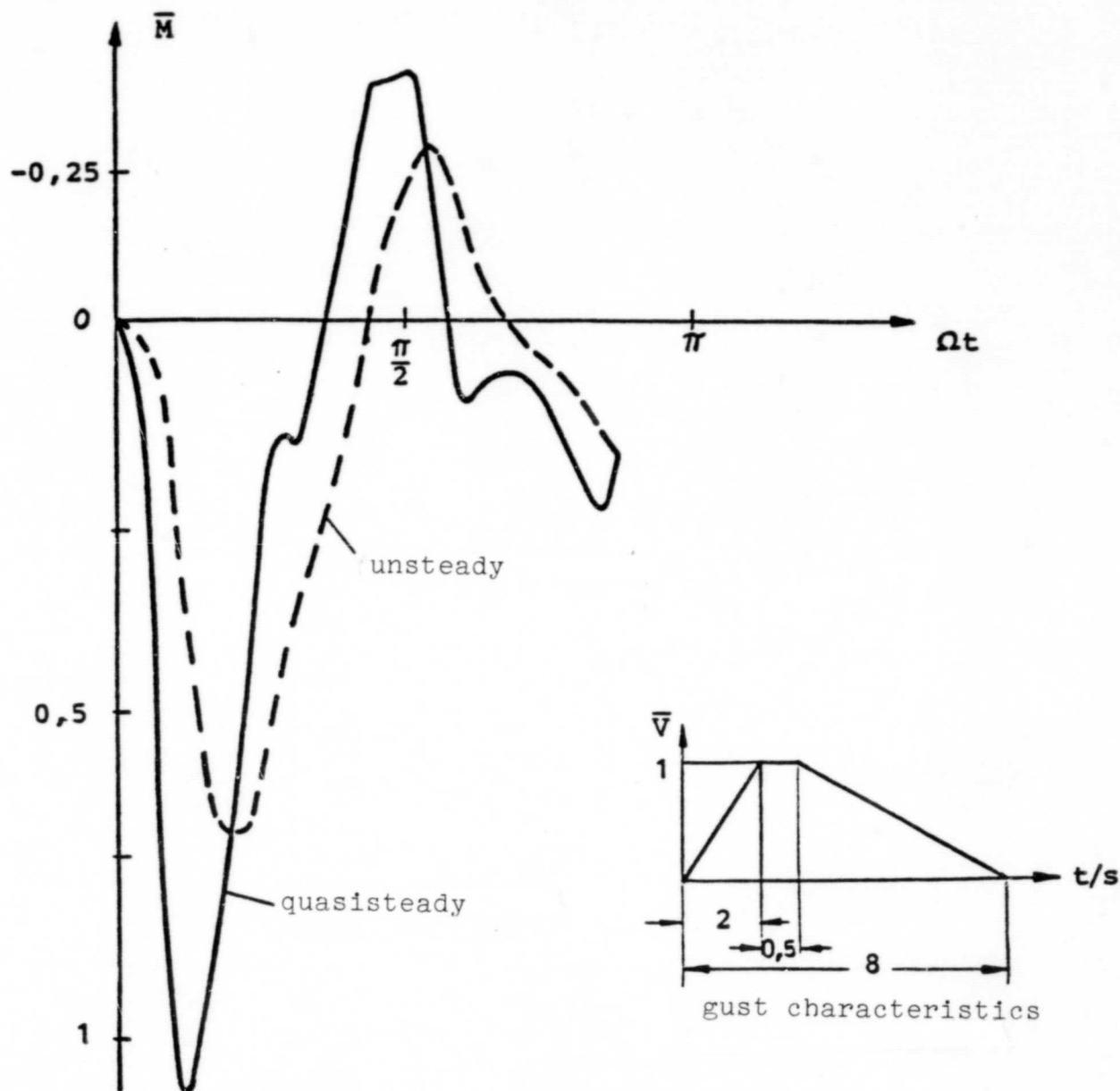
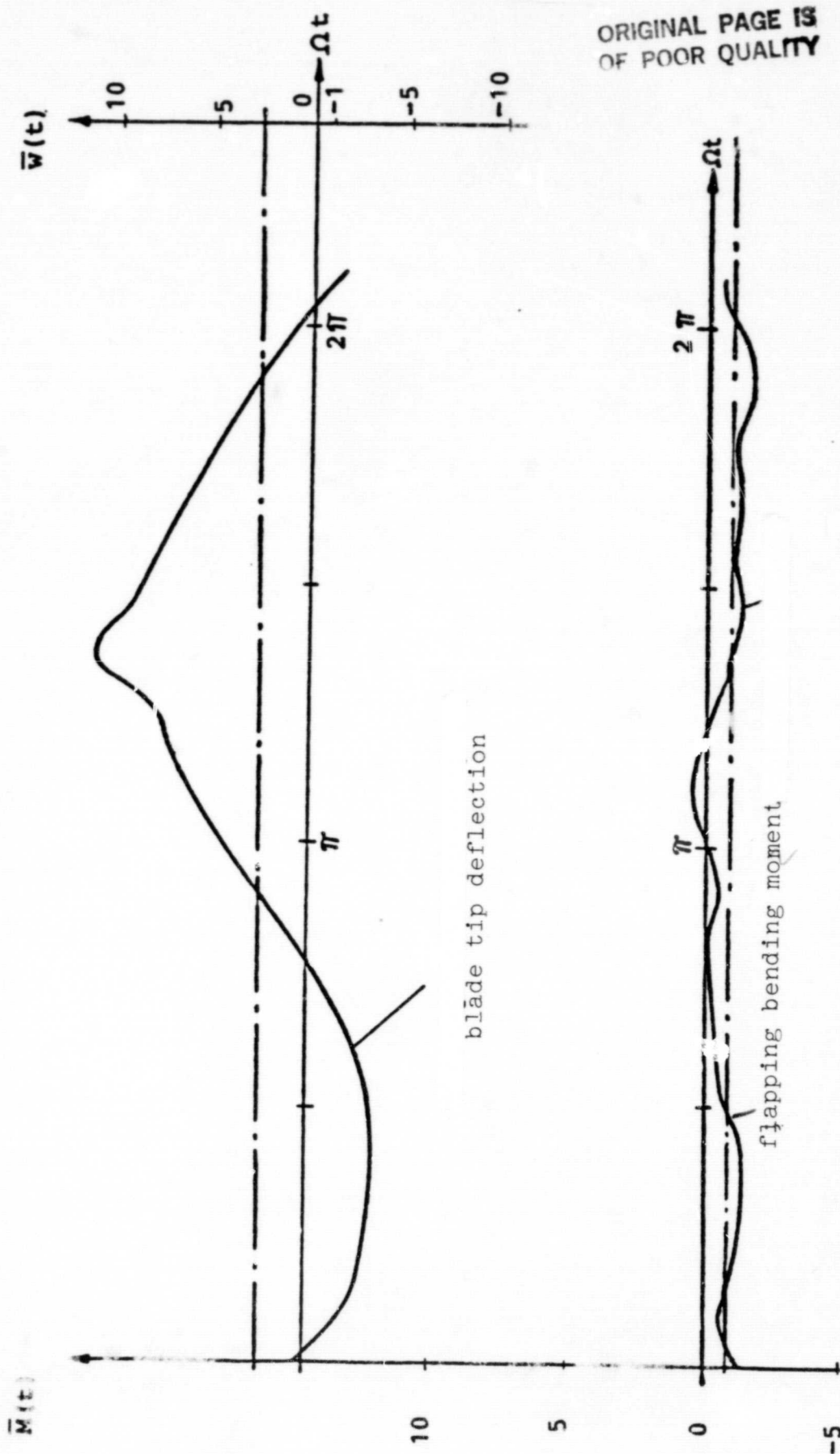


Figure 4. Influence of unsteady aerodynamic forces on the flapping bending moment at the blade clamping point due to the tower wake flow due to a symmetric individual gust. Wake duration  $T_1 = T_0/20.5$



ORIGINAL PAGE IS  
OF POOR QUALITY

horizontal axis wind turbine (HEWT)

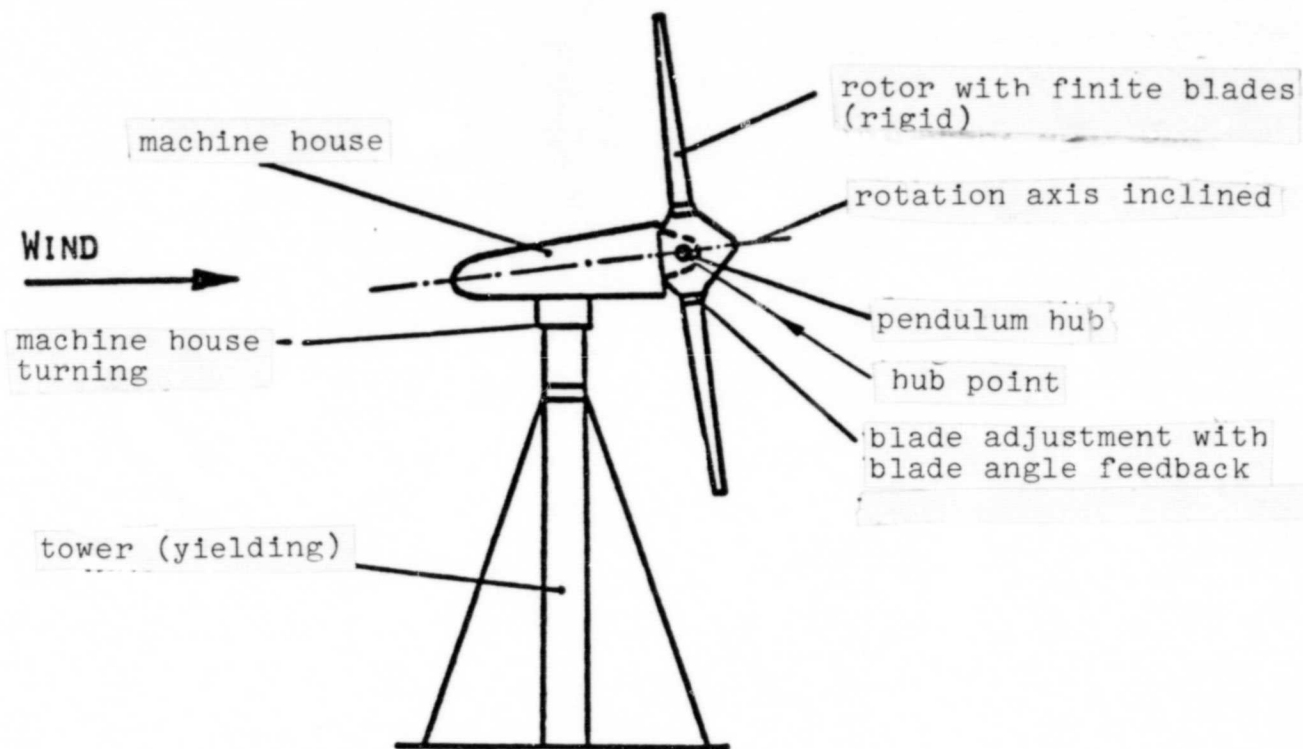


Figure 6. Model assumptions of the overall dynamics calculation of large wind tunnel facilities

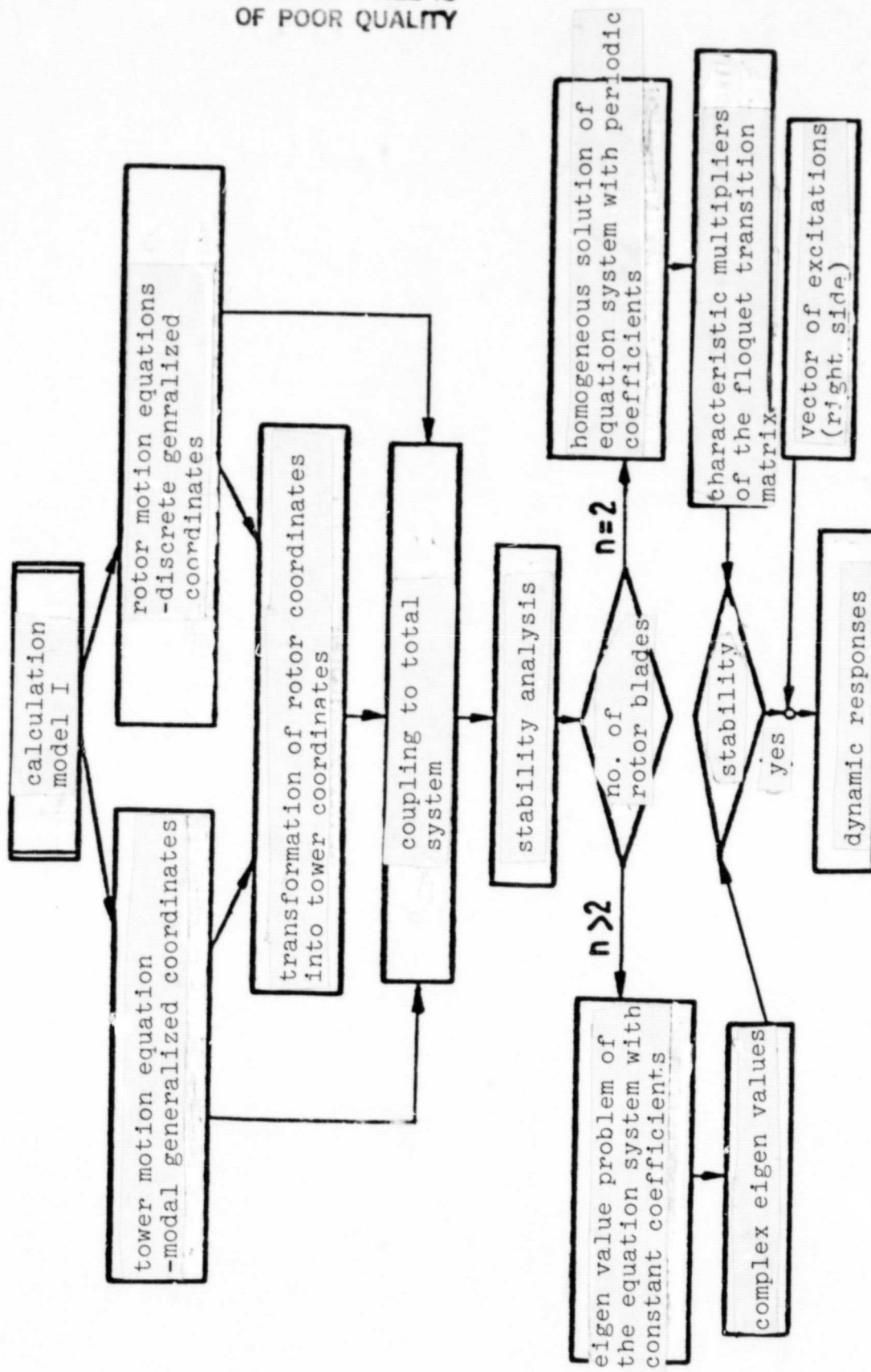


Figure 7. Computer model I (RMODEL)



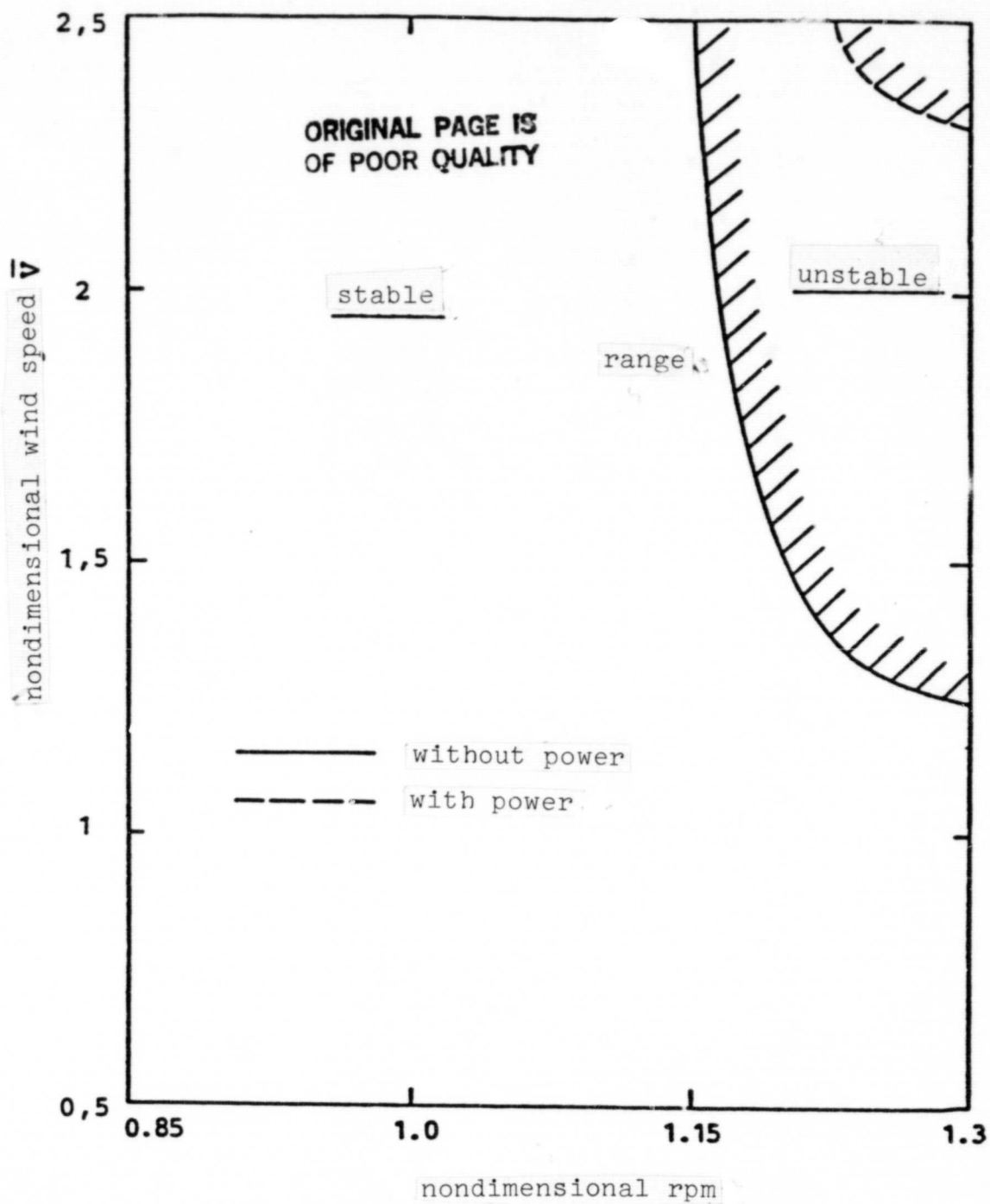


Figure 8. Stability map of Growian--without additional camper--structural damping  $D = 0.2\%$



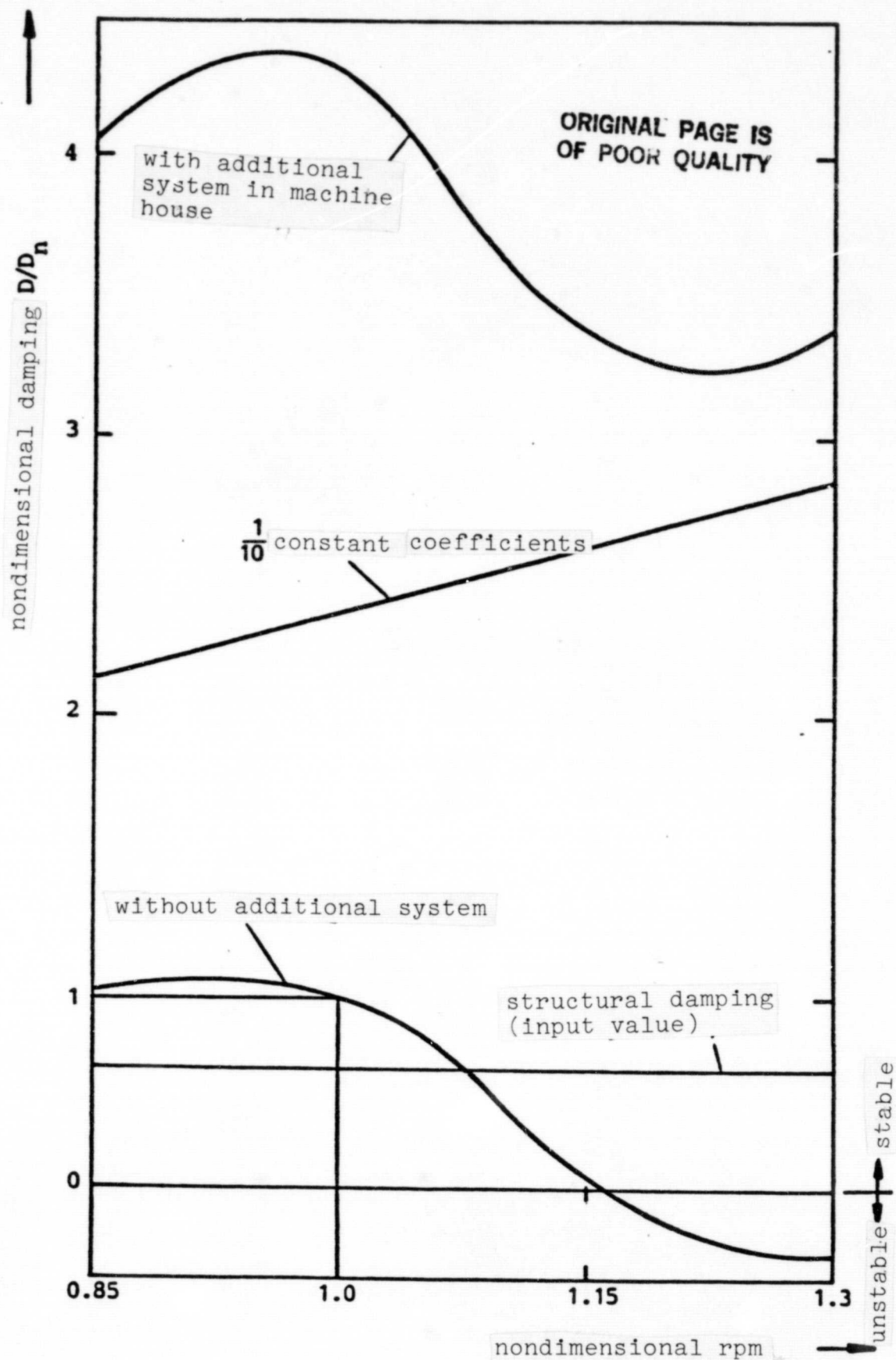
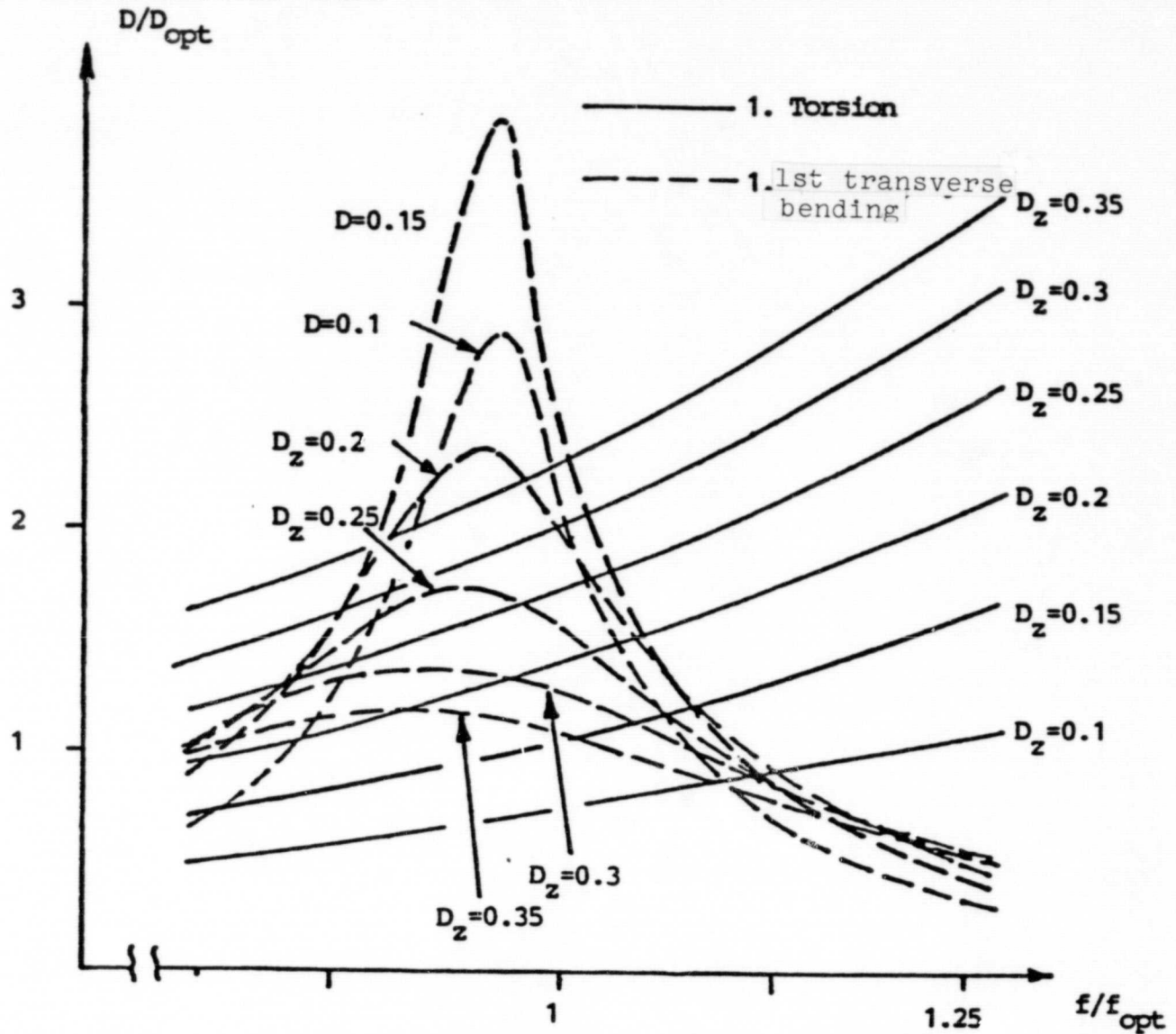


Figure 9. Damping scales of the 5th degree of freedom

Optimization of the damper/reducer additional system in the front machine house



$$f_2 = \frac{1}{2\pi} \sqrt{\frac{C_z}{M_z}}$$

for pendulum suspension

$$C_z = \frac{M_z \cdot g}{I_p} = 9,81 \frac{m}{s^2}$$

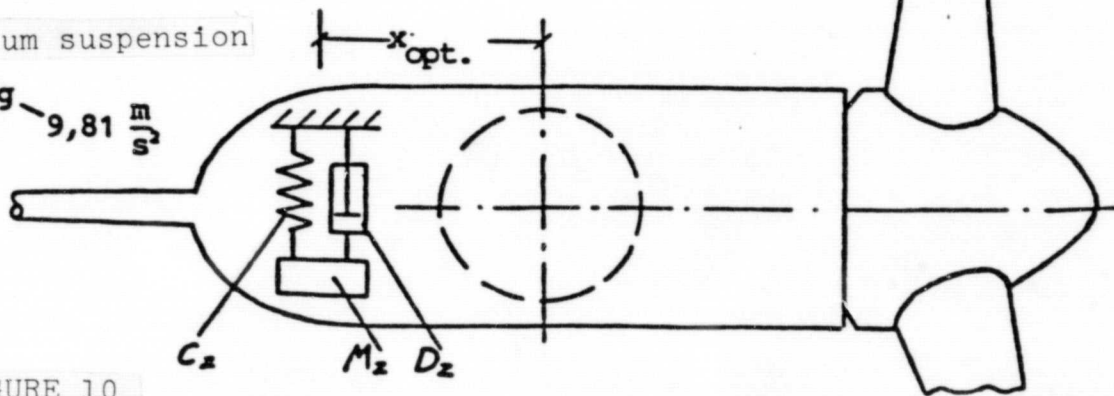


FIGURE 10

ORIGINAL PAGE IS  
OF POOR QUALITY

The first eigen frequency of tower bending in a direction perpendicular to the wind is excited by the:

2nd harmonic

1st harmonic

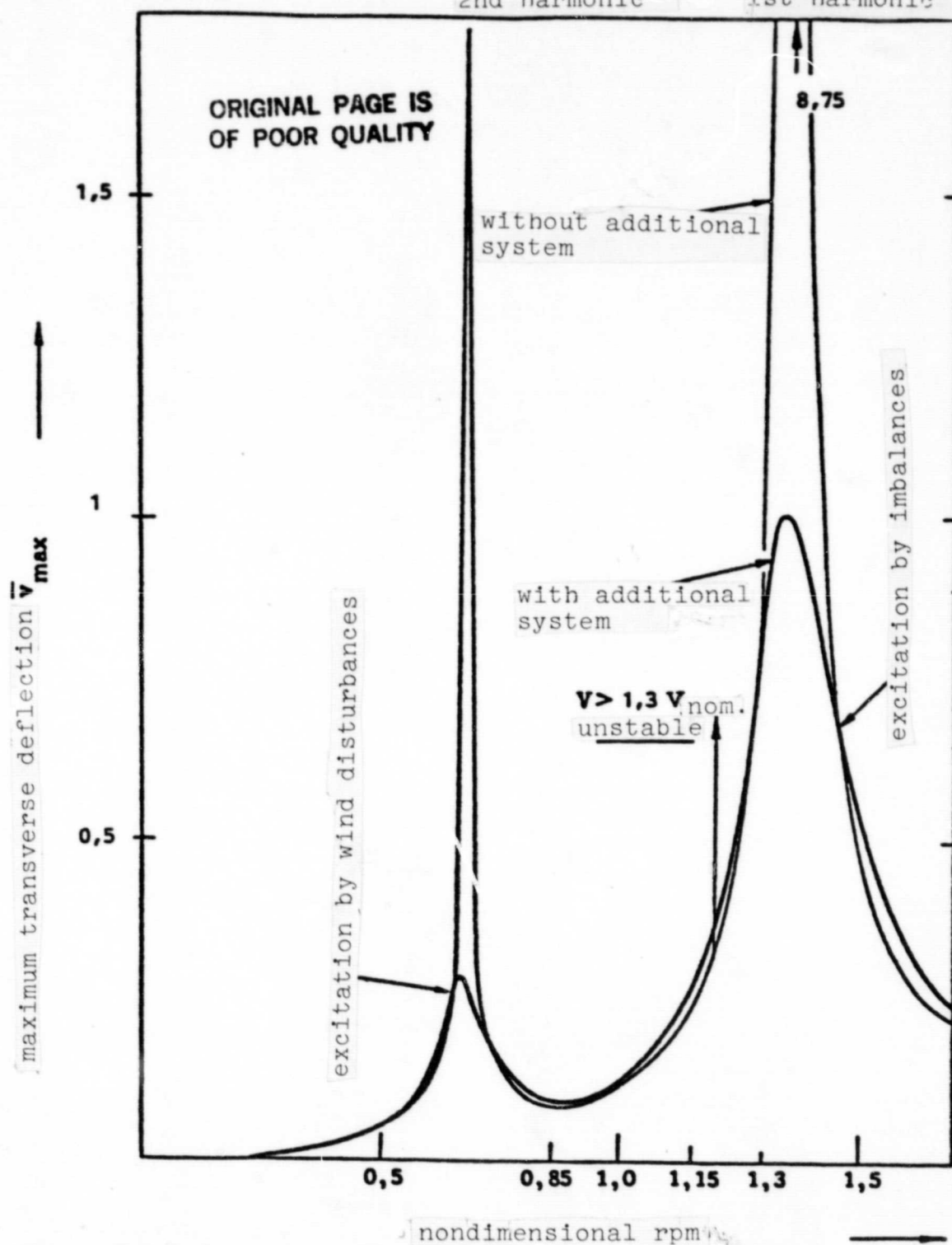


Figure 11. Max. transverse deflections of the hub points for imbalance excitation ( $m_u = 100$  kg) — without power  $V = 24$  m/s wind speed  $\bar{v} = v/v_{max}$

nondimensional maximum deflection

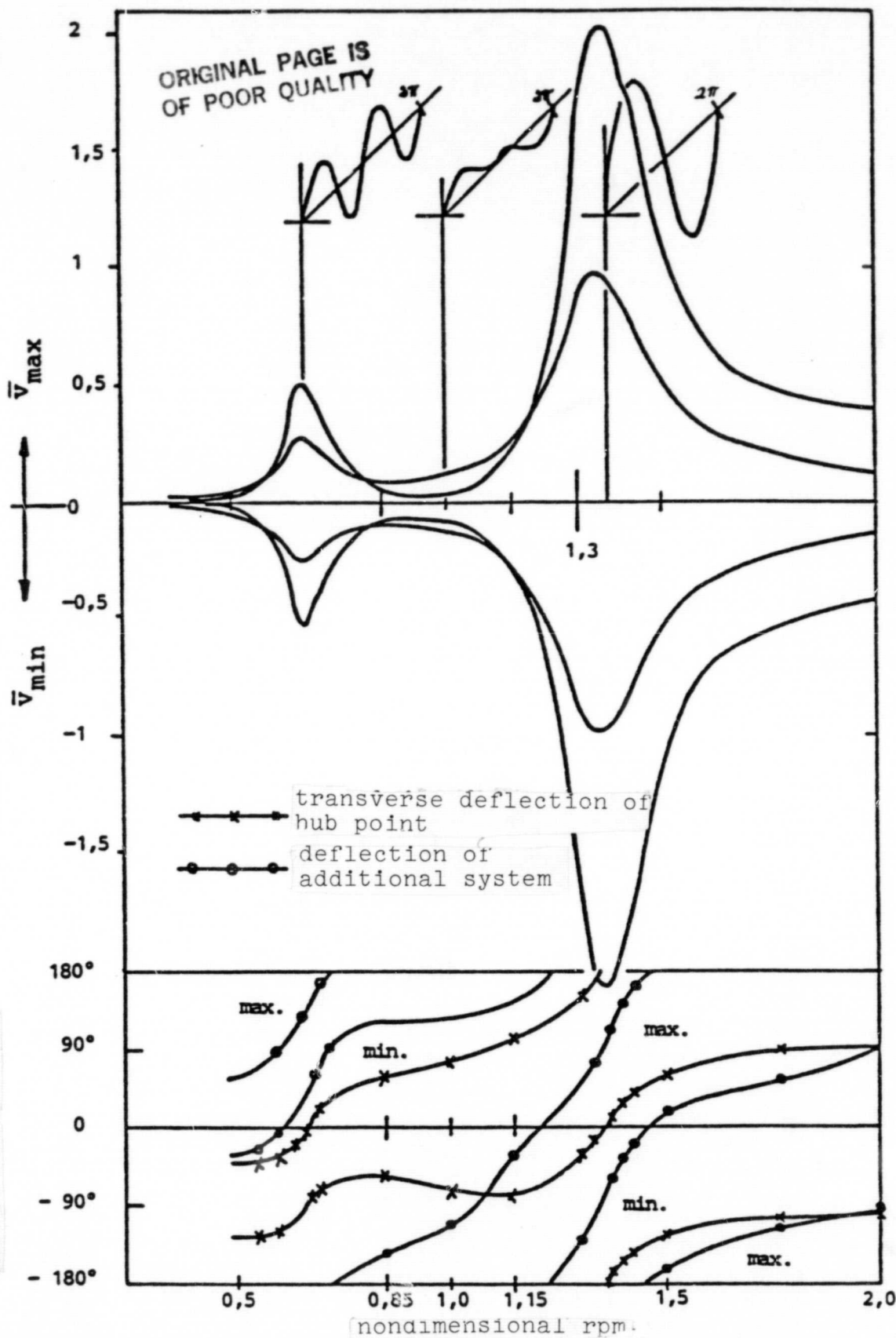


Figure 12. Dynamic response for 100 kg imbalance in a blade tip without power delivery,  $v = 24$  m/s wind speed.

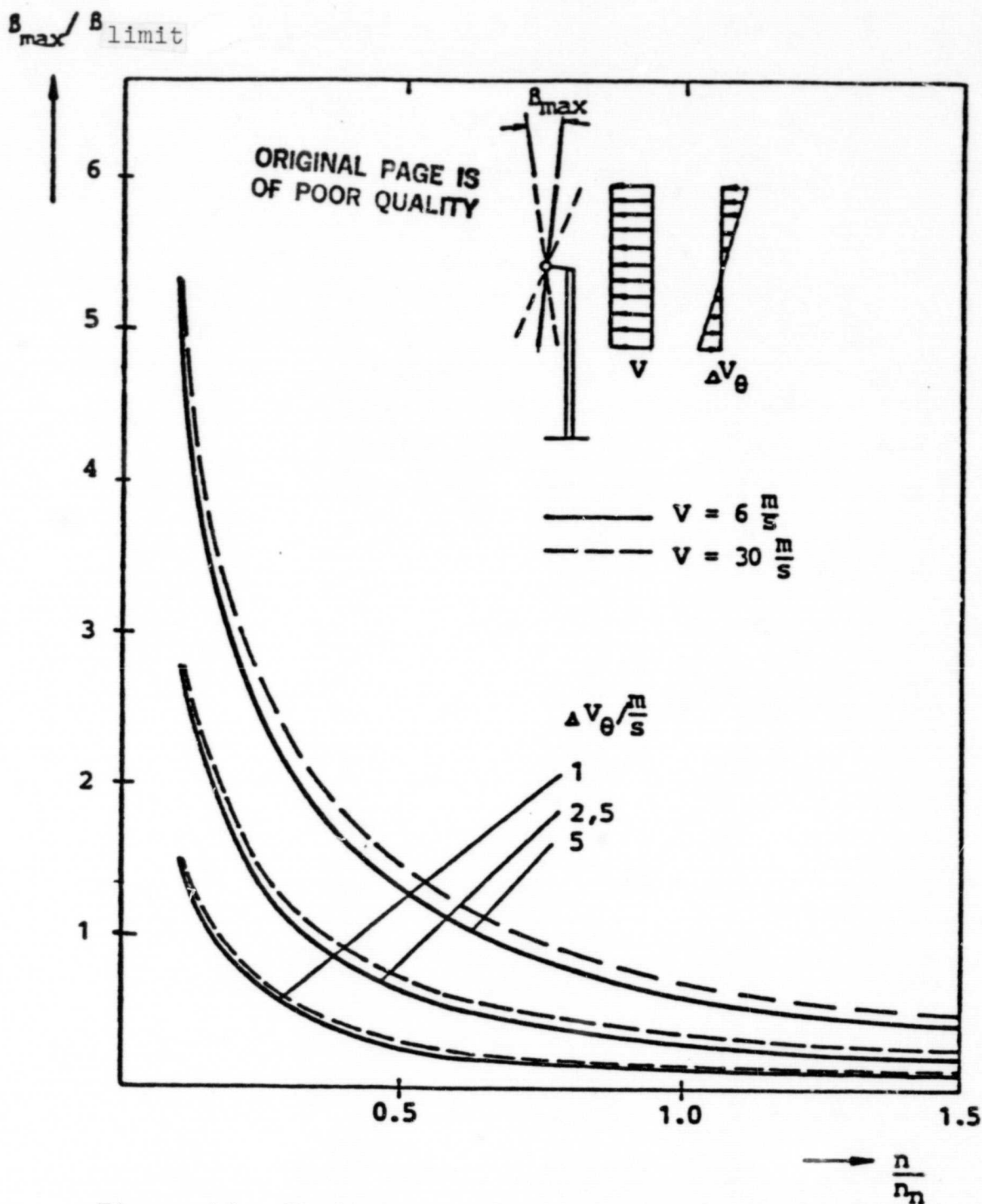


Figure 13. Maximum pendulum deflection as a function of RPM ( $n/n_n$ )--parameter:  
 --parameter: ground boundary-layer ( $\Delta V_\theta$ ) incident flow-speed ( $V$ )  
 --power => thrust = 0

## REFERENCES

- [1] Kehl, K, Keim, W., Kiessling, F., Rippl, A. The dynamics of large wind power facilities, VDI Berichte No. 381, 1980.
- [2] Kiessling, F. Aeroelastic modeling of the coupled wind turbine rotor/tower system, Special reports of the KFA, Juelich, Juel - Spez - 28 (1979).



CONTROL OF OSCILLATIONS OF LARGE FACILITIES

/367

GROWIAN II: Single blade model\*

H. STREHLOW and G. SEITZ

Dynamic Design of the WEA-DEMO Facility

- 1 blade rotor
- drive system
- gondola tower

Oscillation excitation for wind energy facilities with horizon-  
tal rotor axis:

/368

gravity	:	$1\Omega$ -	} main excitation to blade (rotating system)
shear flow	:	$1\Omega, 2\Omega$ -	
tower shadow	:	$(1 \div 12)\Omega$ -	
inclination of rotor axis:		$1\Omega, 2\Omega$ -	
incident oblique flow	:	$1\Omega, 2\Omega$ -	

$\Omega$  : rotor rpm frequency

- measures which contribute to the control of oscillation  
problems of large wind energy facilities with a horizontal rotor axis:

/369

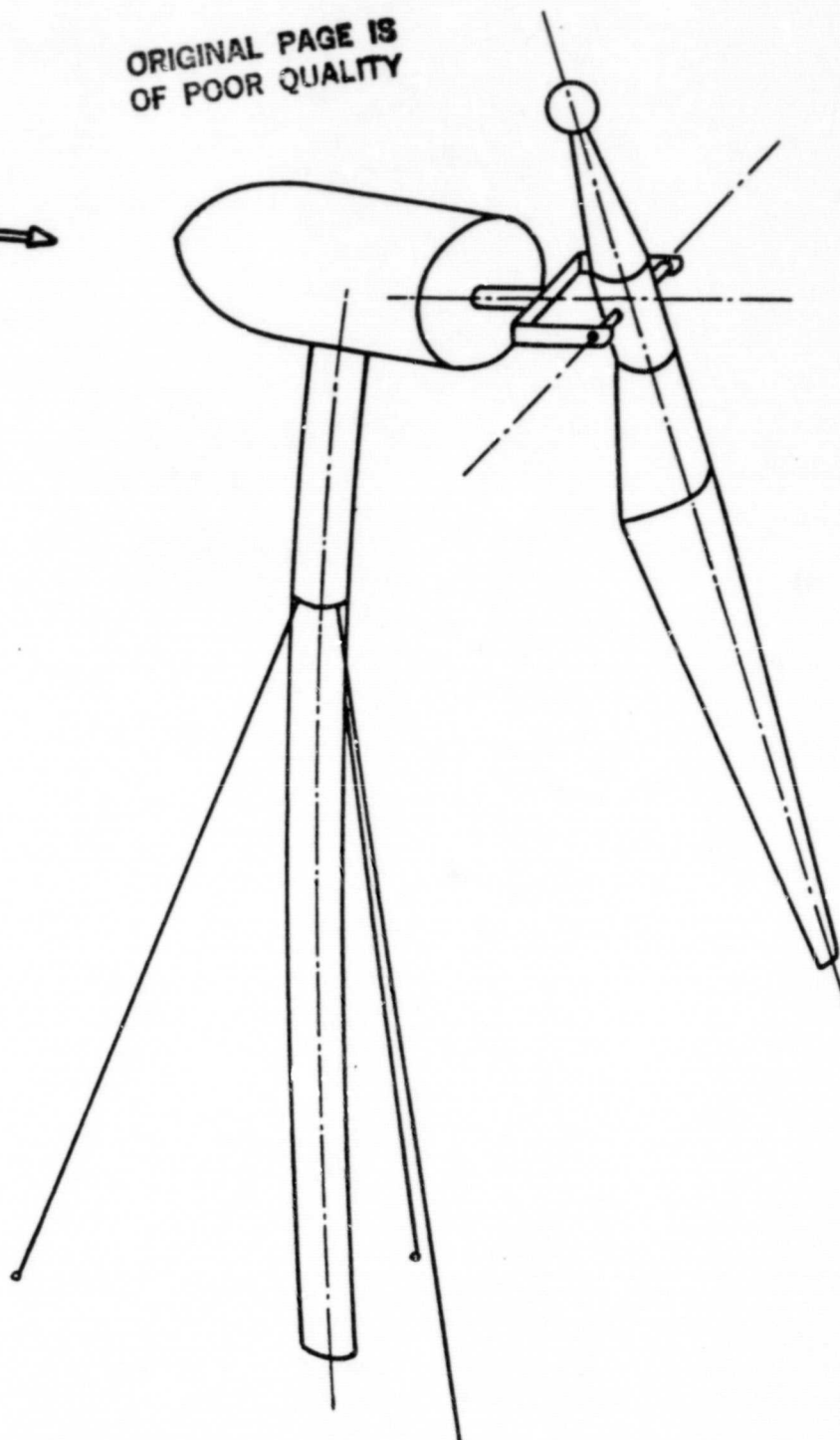
- fast runners with one or two rotor blades of high stiffness
- reduction of dynamic weight loads for stiff deflection blade
- avoidance of aeroelastic rotor stability problems for bending and torsion stiff blades
- rotor with flapping joint and/or pendulum hub
- reduction of flapping bending moments
- free rotor rotation for (doubly supplied) asynchronous generator
- reduction of dynamic deflection bending moments
- tower tuning for overcritical rotor operation

- reduction of tower load for the operating rpm range
- traverse problem
  
- Dynamic features of one and two blade rotors:
  - missing rotor symmetry leads to a system with time dependent (periodic) parameters
  - with a central jointed rotor bearing, the influence of the time bearing parameters on the total system is greatly reduced



ORIGINAL PAGE IS  
OF POOR QUALITY

Wind



Demonstration facility concept:

- levered 1-blade rotor with impact joint
- free rotor rotation (rotating joint) with double supply asynchronous machine
- soft bending tower with rope support for overcritical operation

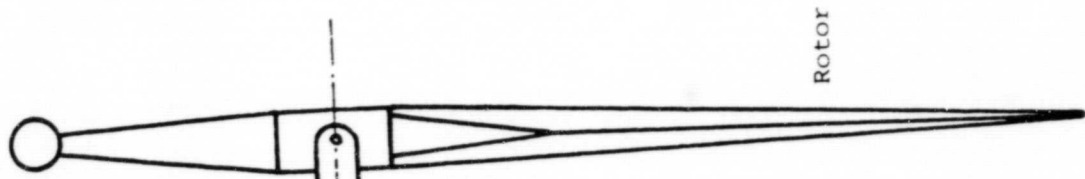
count-erweight for mass  
equilization

ORIGINAL PAGE IS  
OF POOR QUALITY

blade

joint bearing

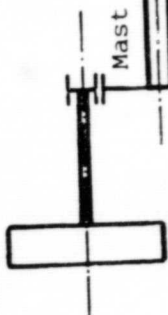
1-blade rotor  
(rotating system)



Rotor

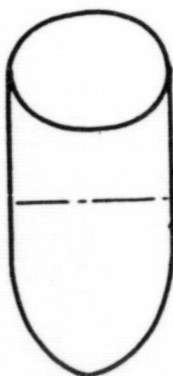
drive system  
(rotating system)

asynchronous  
machine



Mast

gear



gondola

+  
rotor mass  
(concentrated in  
the impact joint)

tower  
(fixed system)

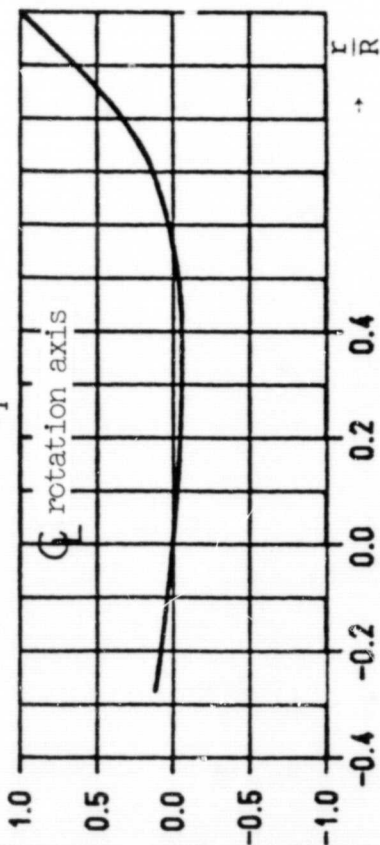
Dynamic main component of the demonstration facility

I. Eigen frequency of the system components of the DEMO wind  
installation

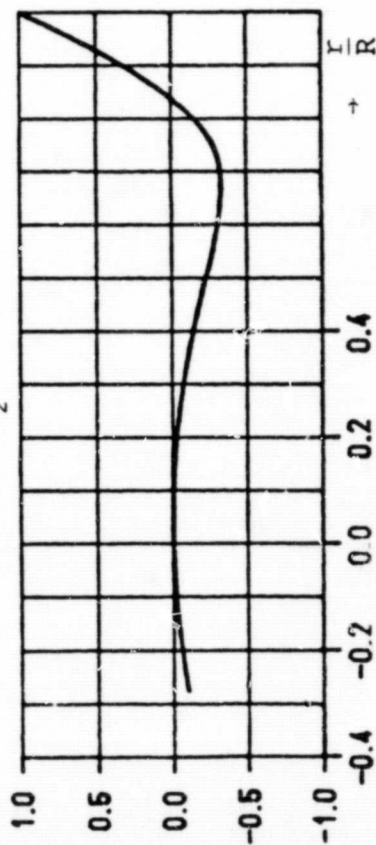
- rotor blade
- tower

/372

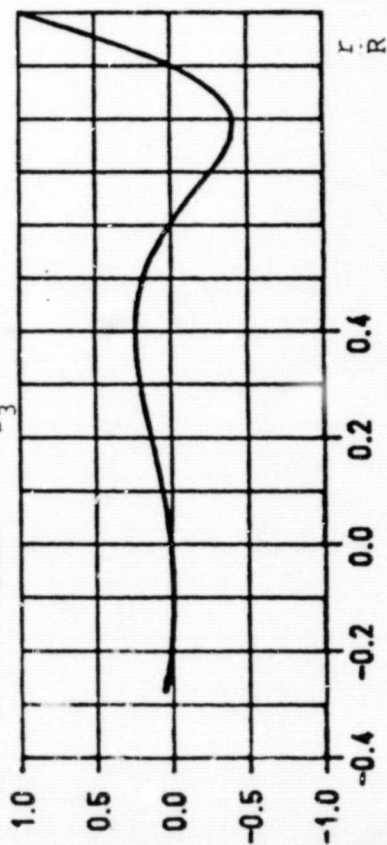
1st flapping bending mode ( $\bar{\omega}_{\beta_1} = 3, 8$ )



2nd flapping bending mode ( $\bar{\omega}_{\beta_2} = 7, 5$ )

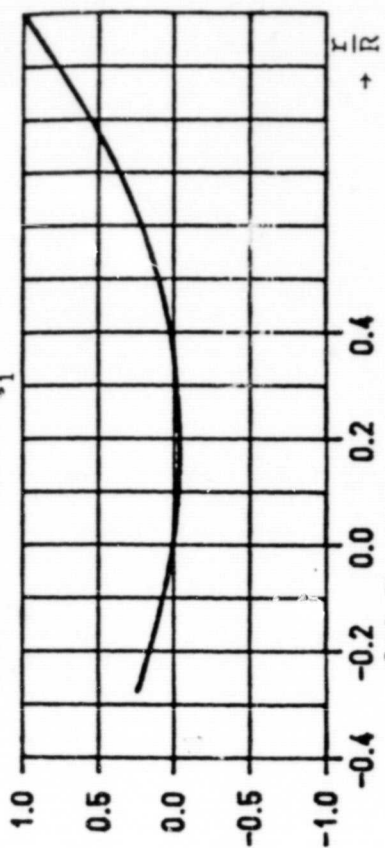


3rd flapping bending mode ( $\bar{\omega}_{\beta_3} = 14, 5$ )

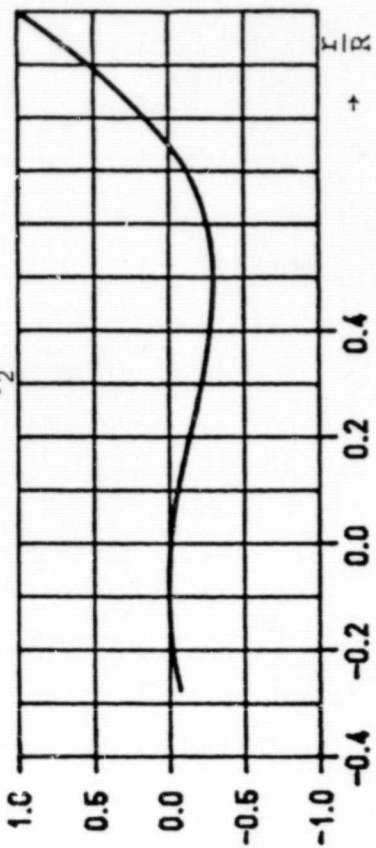


Bending eigen modes of the demonstration rotor (blade counterweight)

1st flapping bending mode ( $\bar{\omega}_{\zeta_1} = 5, 6$ )



2nd flapping bending mode ( $\bar{\omega}_{\zeta_2} = 12, 5$ )



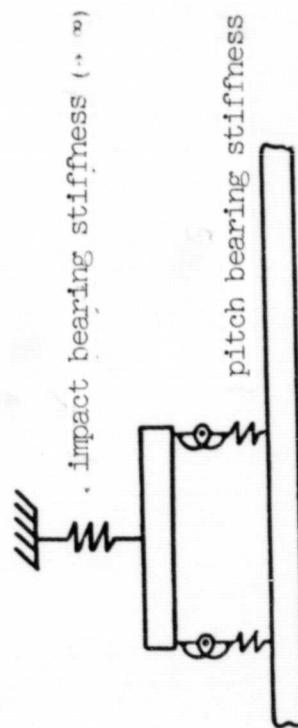
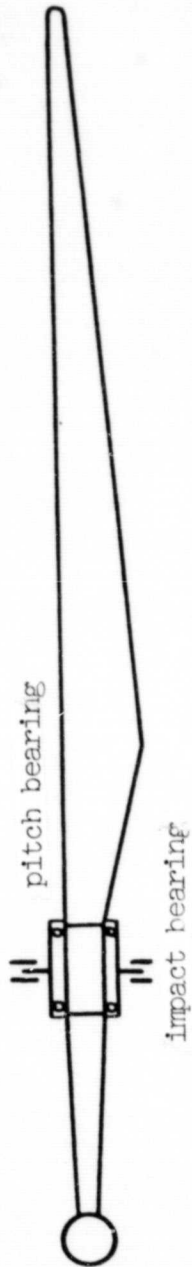
Eigen modes and frequencies for nominal rotational frequency

$$\Omega_N = 4,584 \frac{\text{rad}}{\text{s}}$$

ORIGINAL PAGE IS  
OF POOR QUALITY

ORIGINAL PAGE IS  
OF POOR QUALITY

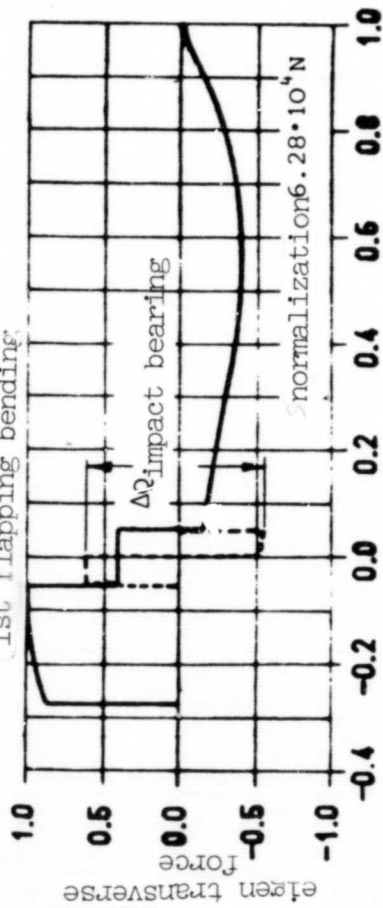
rotor blade demonstration



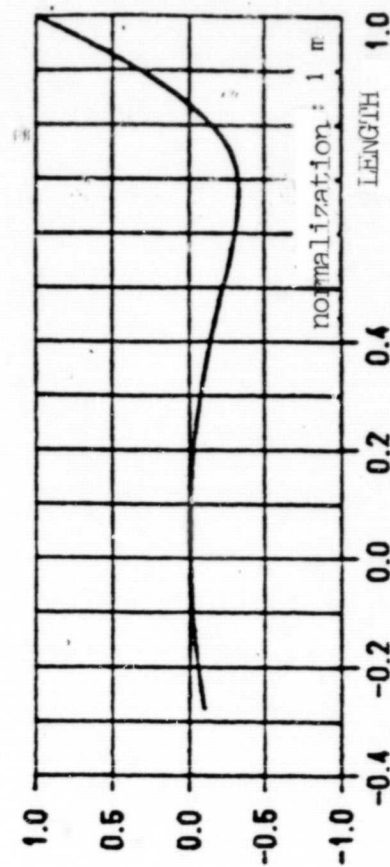
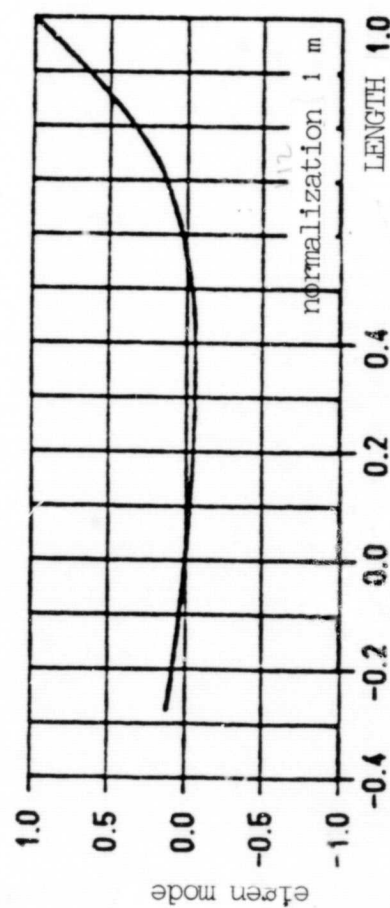
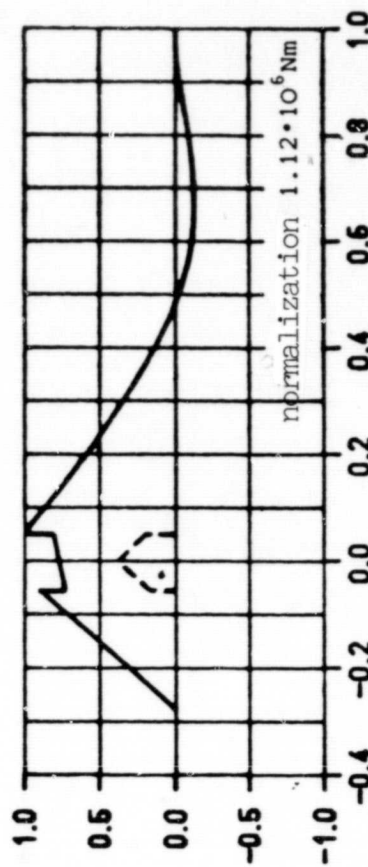
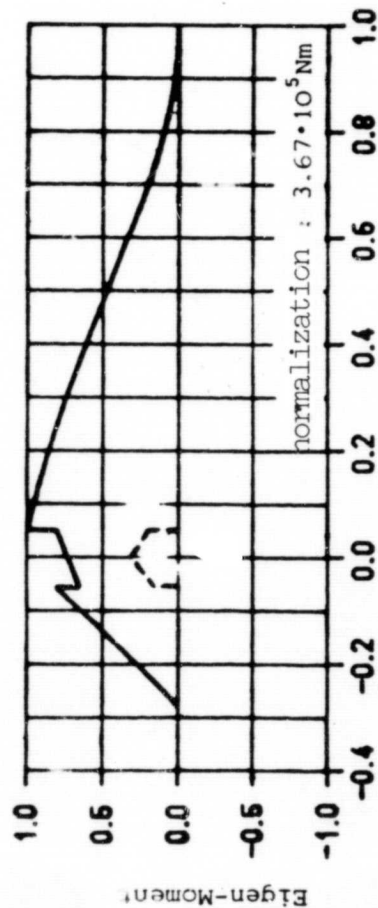
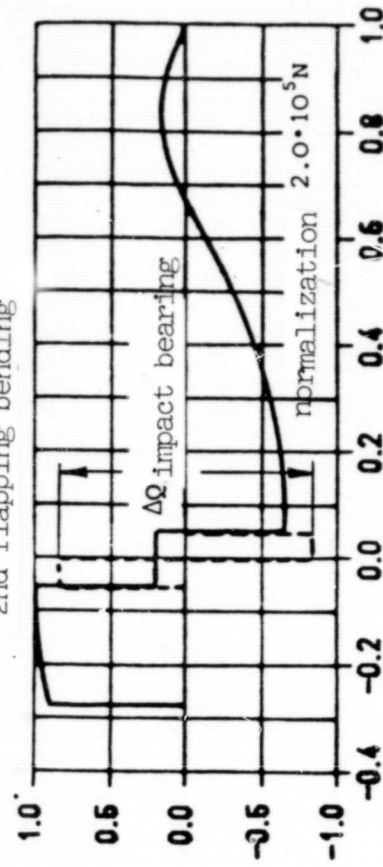
Idealization of the rotor bearing by double beam model



1st flapping bending



2nd flapping bending

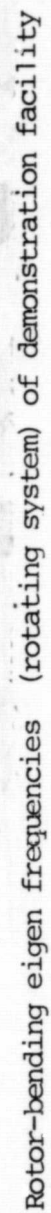


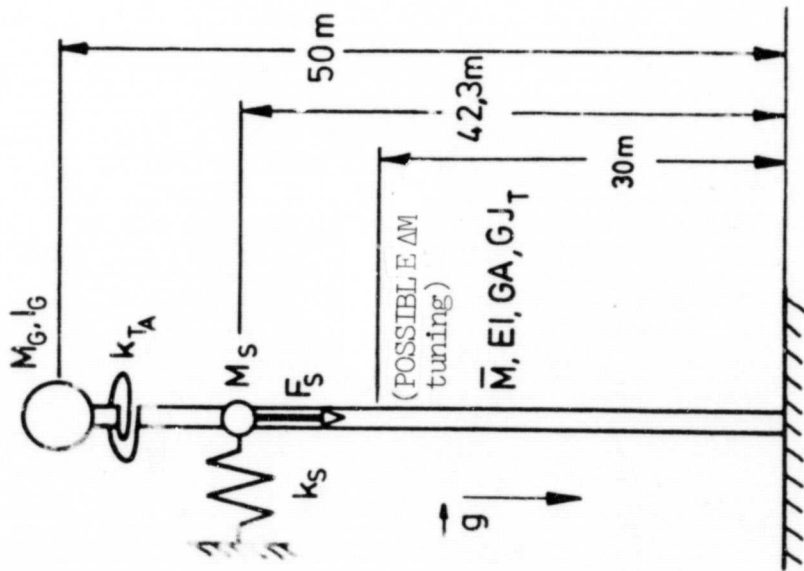
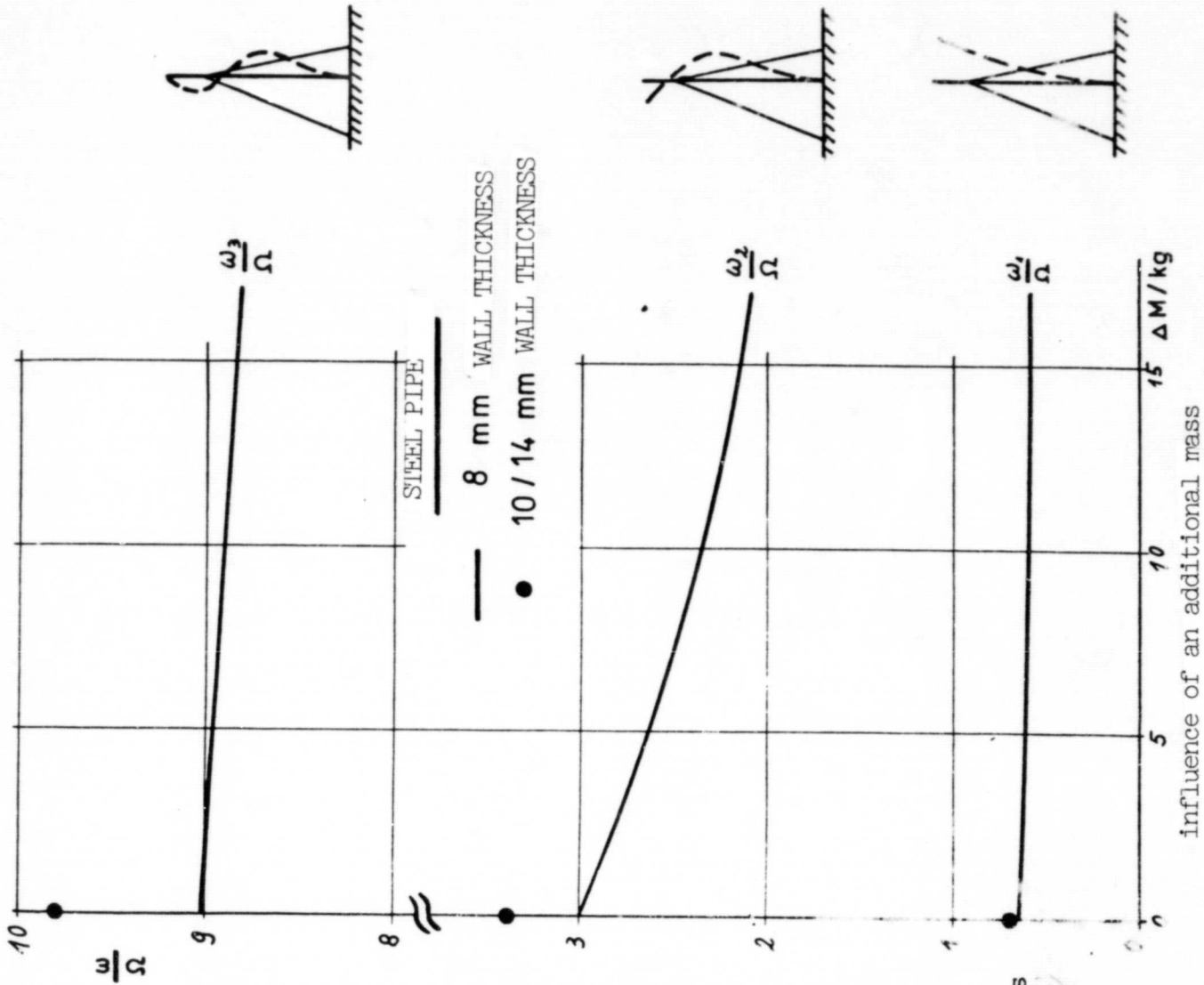
Flapping bending eigen modes and corresponding bending moment and transverse force variation for demonstration facility at  $\Omega_N = 4.584 \text{ rad/s}$

rigid body modes

$$\omega\beta_0 = 1\Omega$$

$$250 = O_{2(m)}$$





Demonstration tower eigen frequencies  
pitch frequency referred to  $\Omega = 4.594 \text{ rad/s}$



II. Specification of the eigen frequencies of the DEMO wind  
facility  
(collection of results)

/378

system component	eigen frequency specifications	
<b>Rotor</b> (blade + counter weight) free-free at $\Omega = 4,584 \frac{1}{s}$  jointed bearing in rotor center	flapping: $\omega_{\beta_1} = 3,8 \Omega = 17,4 \frac{1}{s}$ $\omega_{\beta_2} = 7,5 \Omega = 34,4 \frac{1}{s}$ $\omega_{\beta_3} = 14,5 \Omega = 66,5 \frac{1}{s}$ ----- deflection bending $\omega_{\zeta_1} = 5,6 \Omega = 25,7 \frac{1}{s}$ (edgewise) $\omega_{\zeta_2} = 12,5 \Omega = 57,5 \frac{1}{s}$ ----- blade clamping $\omega_{\theta} \geq 15 \Omega = 68,8 \frac{1}{s}$ torsion (Pitch-control)	rotating system
drive -Torsion (Rotor - gear -Generator)	rotor against $\omega_T = (11,0 \div 12,0) \Omega = (50,4 \div 55,3) \frac{1}{s}$ Generator	rotating system
tower/gondola (rotor mass considered)	transverse bending $\omega_{R1} = 3,68 \Omega = 3,1 \frac{1}{s}$ (rolling) $\omega_{R2} = 3,5 \Omega = 16,04 \frac{1}{s}$ ----- longitudinal $\omega_{N1} = 0,69 \Omega = 3,16 \frac{1}{s}$ bending $\omega_{N2} = 3,4 \Omega = 15,6 \frac{1}{s}$ (pitching) ----- Torsion (yawing) $\omega_{G1} = (2,4 \div 2,6) \Omega = (11,0 \div 11,9) \frac{1}{s}$	nonrotating System

TABLE 1:  
Specification of eigen frequencies for the demonstration wind facility ( $\Omega = 4,584 \frac{1}{s}$ )

For the specification of the eigen frequencies for the main components of the DEMO facility, the following special items should be noted: /380

- The eigen values and the eigen modes which apply for the total WEA system as a rule have multiple frequencies even without the influence of aerodynamic force.

- These multifrequency "eigen oscillations" which are typical for these systems with periodical coefficients in general (without aerodynamic forces) consist of three oscillation components which depend on one another:

$(\omega - \Omega)$  - component

$\omega$  - component

$(\omega + \Omega)$  - component

where  $\Omega$ : rotor rotation rate  
 $\omega$ : system "eigen frequency"

- The WEA system "eigen frequencies" approximately coincide with the component eigen frequencies (rotor, drive, tower) as long as there is no critical resonance case.

The following resonance cases have to be considered: /381

(1) Principal parameter resonance for  $\frac{1}{2} (2\nu - 1)\Omega$   $\nu = 1, 2 \dots$   
important for stability  $\nu = 1 \rightarrow 0,5\Omega$  resonance

(2) Harmonic resonance with  $\nu\Omega$   $\nu = 1, 2 \dots$   
(second parameter resonance)

important for stability:  $\nu = 1 \rightarrow 1\Omega$  resonance

important for response :  $\nu \leq \rightarrow (1-8)\Omega$  resonance

In the evaluation of the resonance points, one has to consider /382  
that for the selected one-blade rotor concept for the tower dynamics,

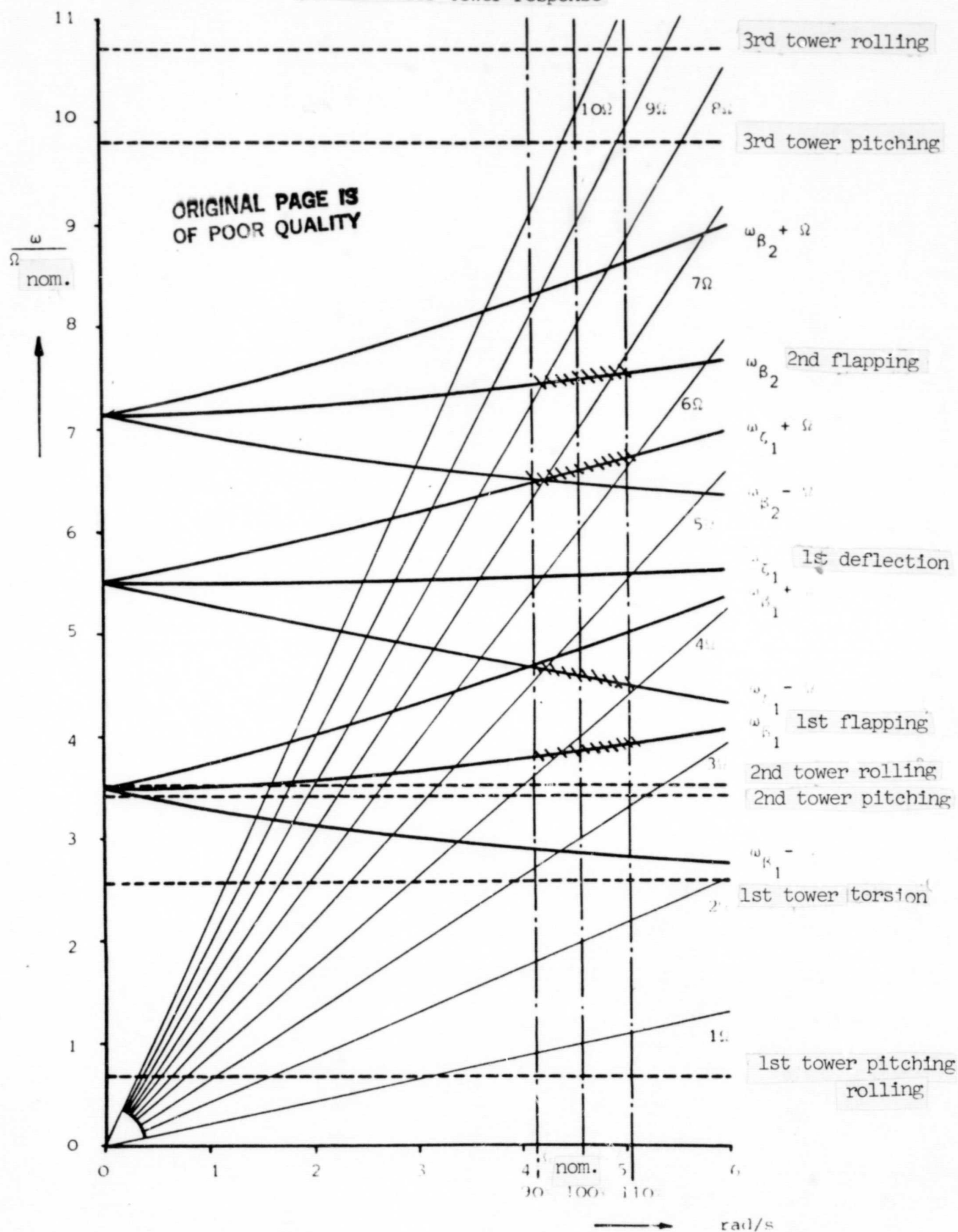
the force transmission from the rotating system to the fixed system is important, whereas for the drive system (drive train), the torque transmission plays a role.

We have flapping bending  $\omega_\beta$  oscillation components important  
for tower (bending)

deflection bending ( $\omega_\zeta$  oscillation components important  
for drive (torsion)

$(\omega_\zeta \pm \Omega)$  oscillation component important for tower  
bending (rolling)

range important for tower response



Eigen frequencies in the fixed system of the demonstration facility

( $\Omega_{\text{Nenn}} = 4,584 \text{ rad/s}$ )

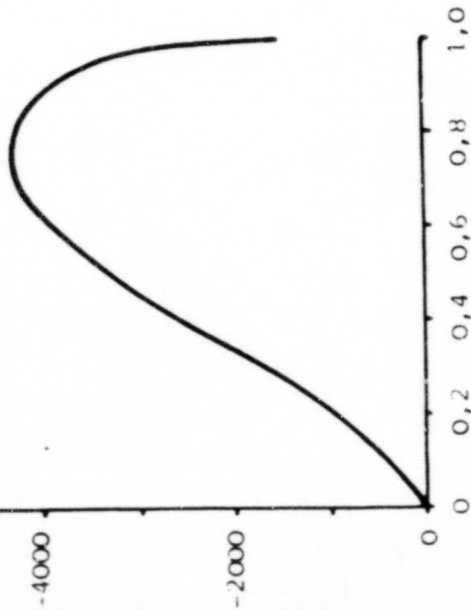
### III. Loads for operation of the DEMO wind facility

/384

$\frac{dS}{dr}$

thrust force distribution

364



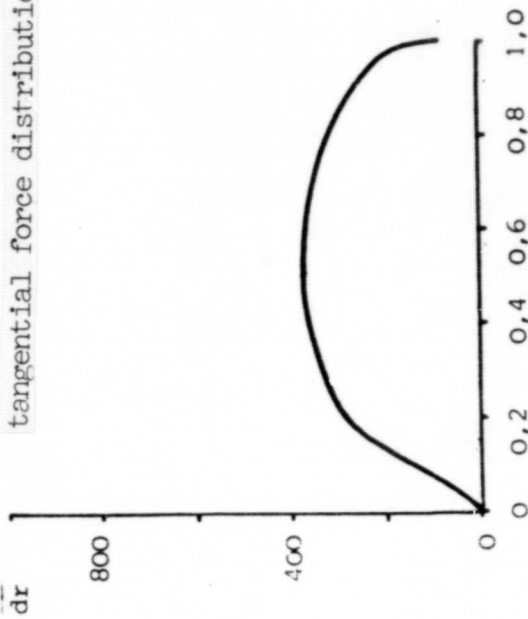
$$V_{\text{Wind}} = 10 \frac{\text{m}}{\text{s}}$$

$$\Omega = 4,953 \frac{1}{\text{s}} \cdot 400$$

$$(\Lambda = 11,97)$$

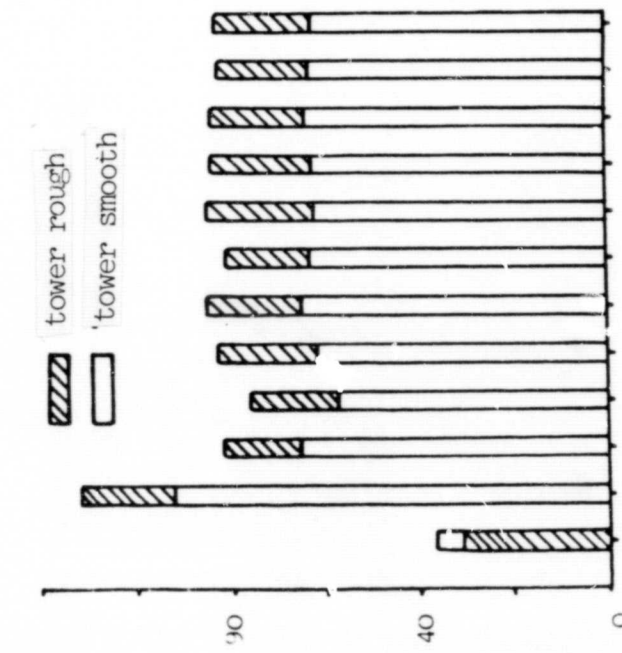
$\frac{dT}{dr}$

tangential force distribution



$\frac{dS}{dr}$

tower rough  
tower smooth

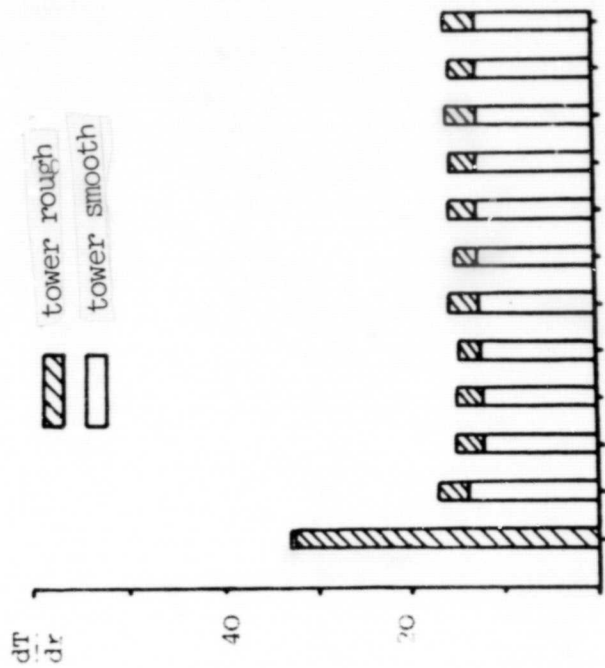


1. 2. 3. 4. 5. 6. 7. 8. 9. 10. 11. 12. harmonic

Aerodynamic loads for demonstration rotor blade

$\frac{dT}{dr}$

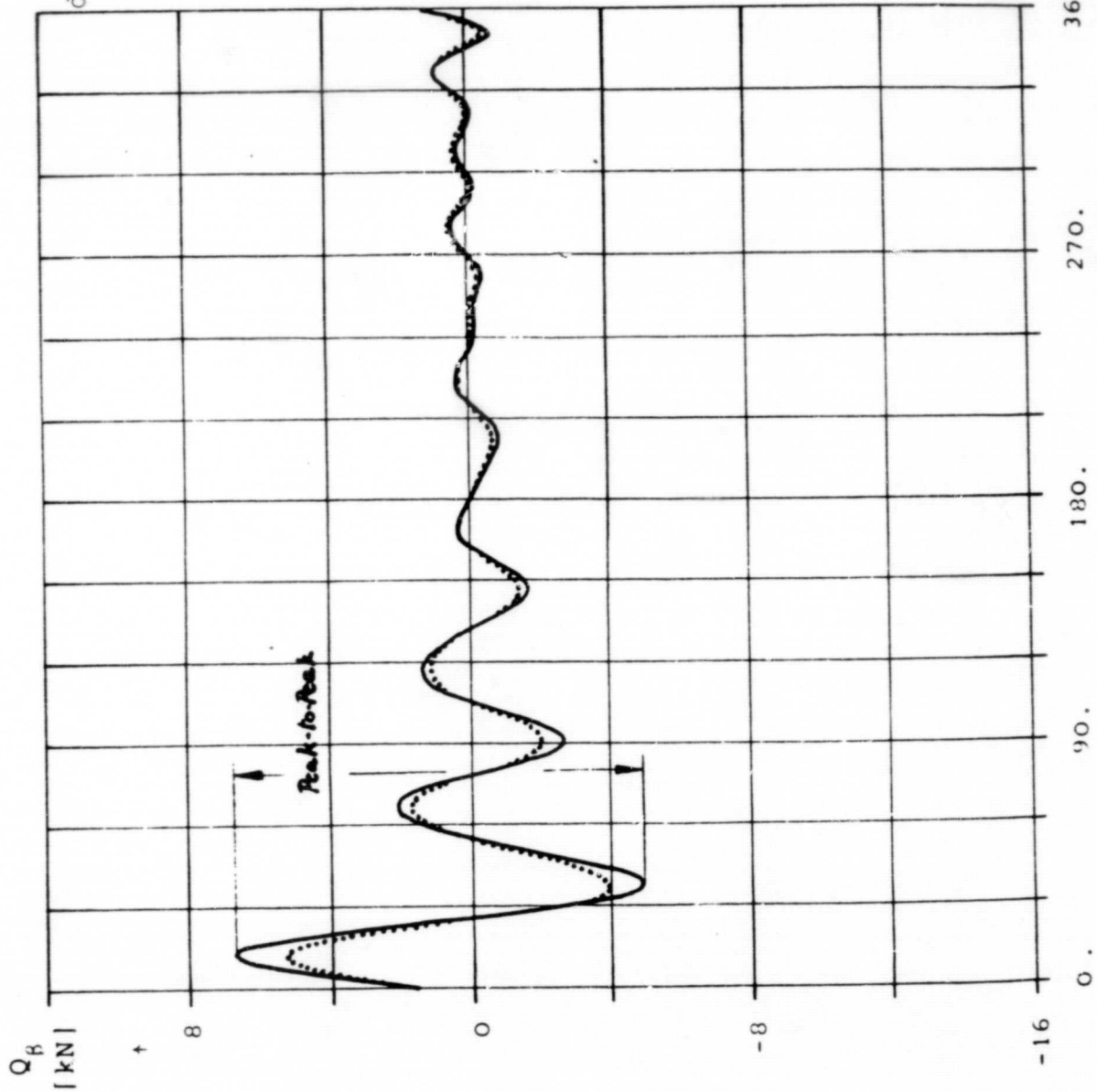
tower rough  
tower smooth



1. 2. 3. 4. 5. 6. 7. 8. 9. 10. 11. 12. harmonic

(Wennekers, MBB-UD-DE123

ORIGINAL PAGE IS  
OF POOR QUALITY



Flapping bending transverse force variation over a rotation in rotor center (blade side)



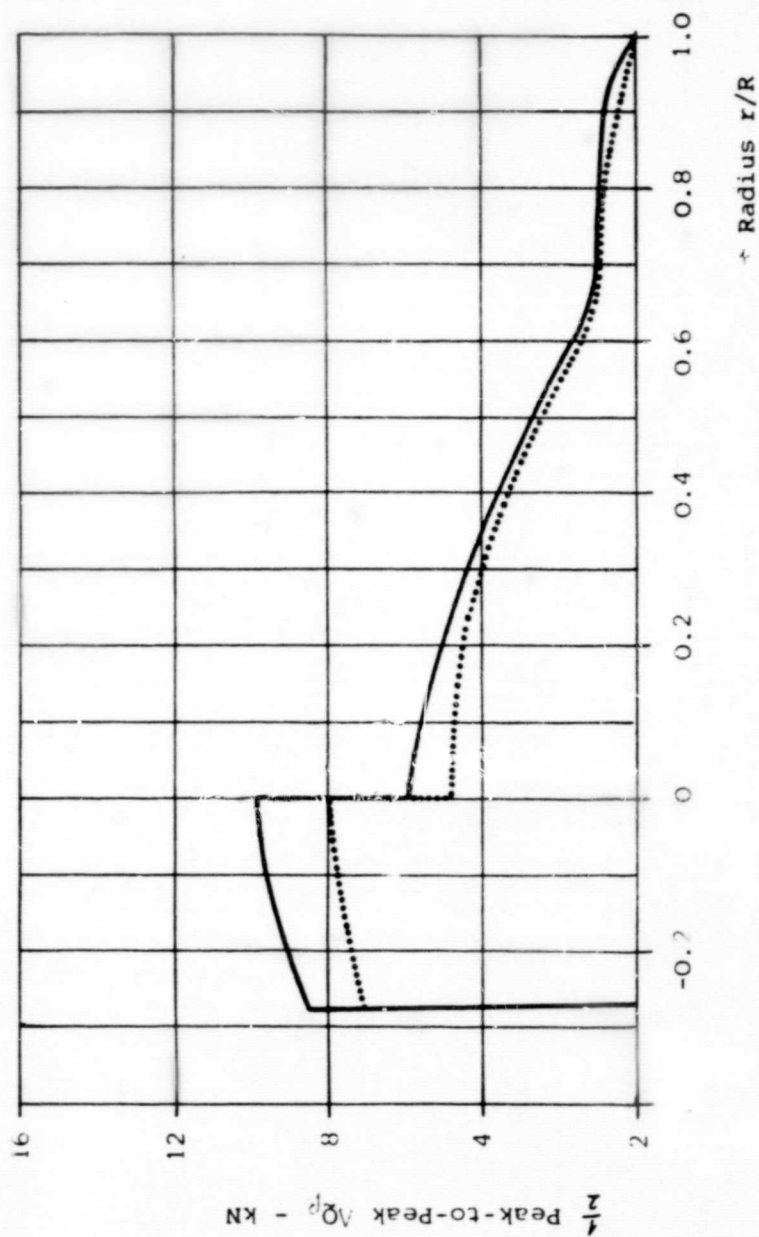
demonstration facility

$$V_{\text{wind}} = 10 \frac{\text{m}}{\text{s}}$$

$$\Omega = 4953 \text{ rad/s}$$

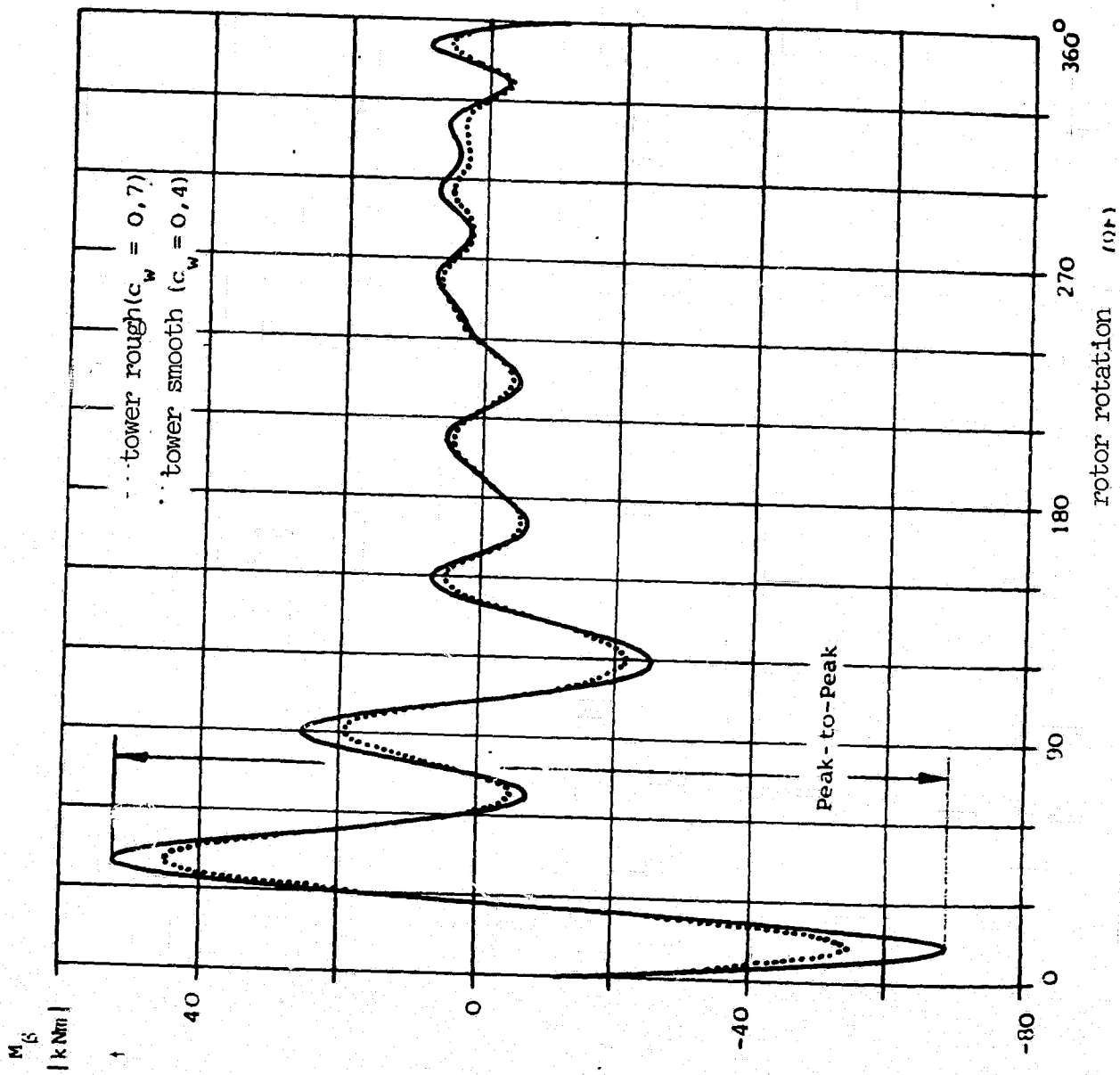
$$(\Lambda = 11.97)$$

ORIGINAL PAGE IS  
OF POOR QUALITY



Maximum alternating flapping bending transverse forces over rotor radius

16.1



demonstration facility

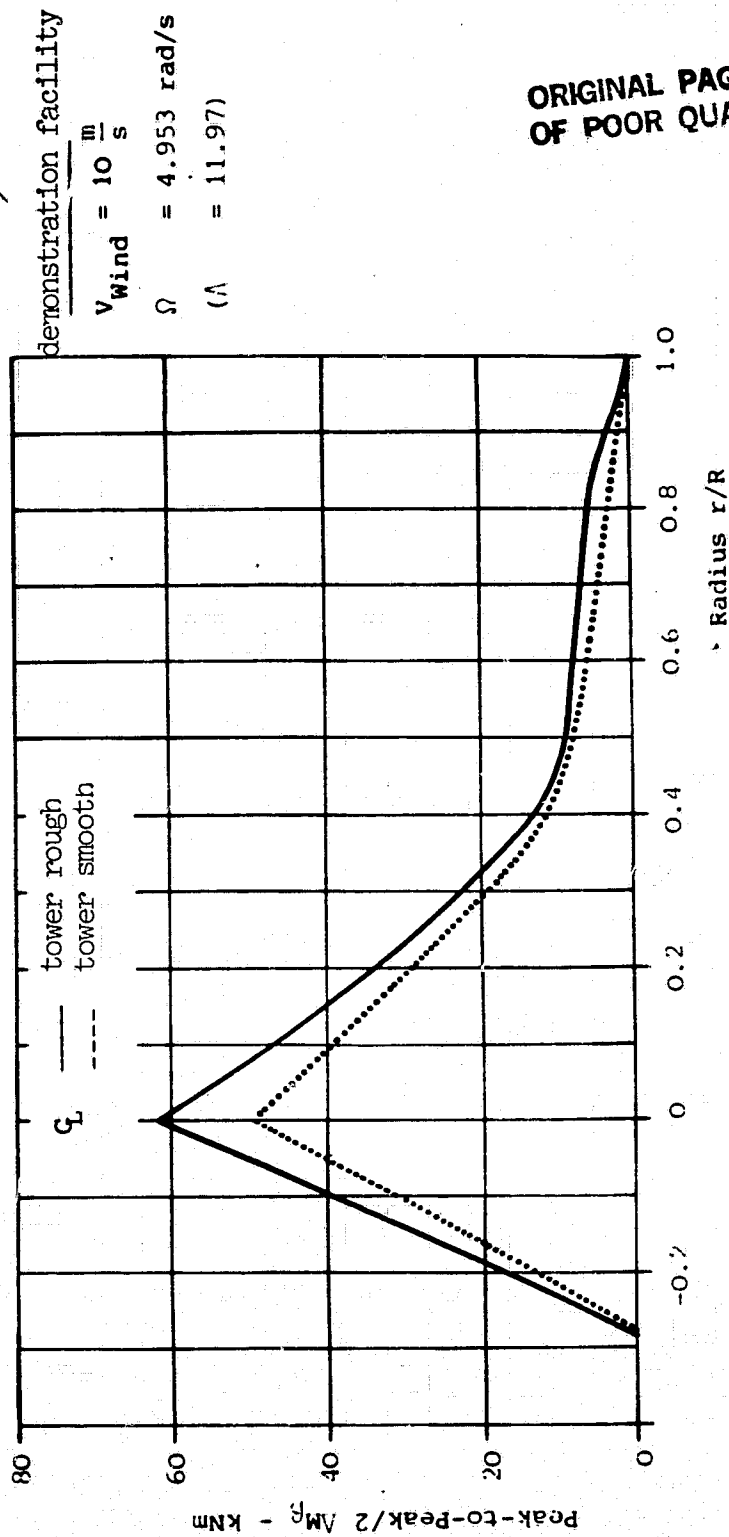
$$V_{\text{Wind}} = 10 \frac{\text{m}}{\text{s}}$$

$$\Omega = 4,953 \text{ rad/s}$$

$$(\lambda = 11,97)$$

ORIGINAL PAGE IS  
OF POOR QUALITY

Flapping bending moment variation over rotation in rotor center



ORIGINAL PAGE IS  
OF POOR QUALITY

Maximum alternating flapping bending moments over rotor radius

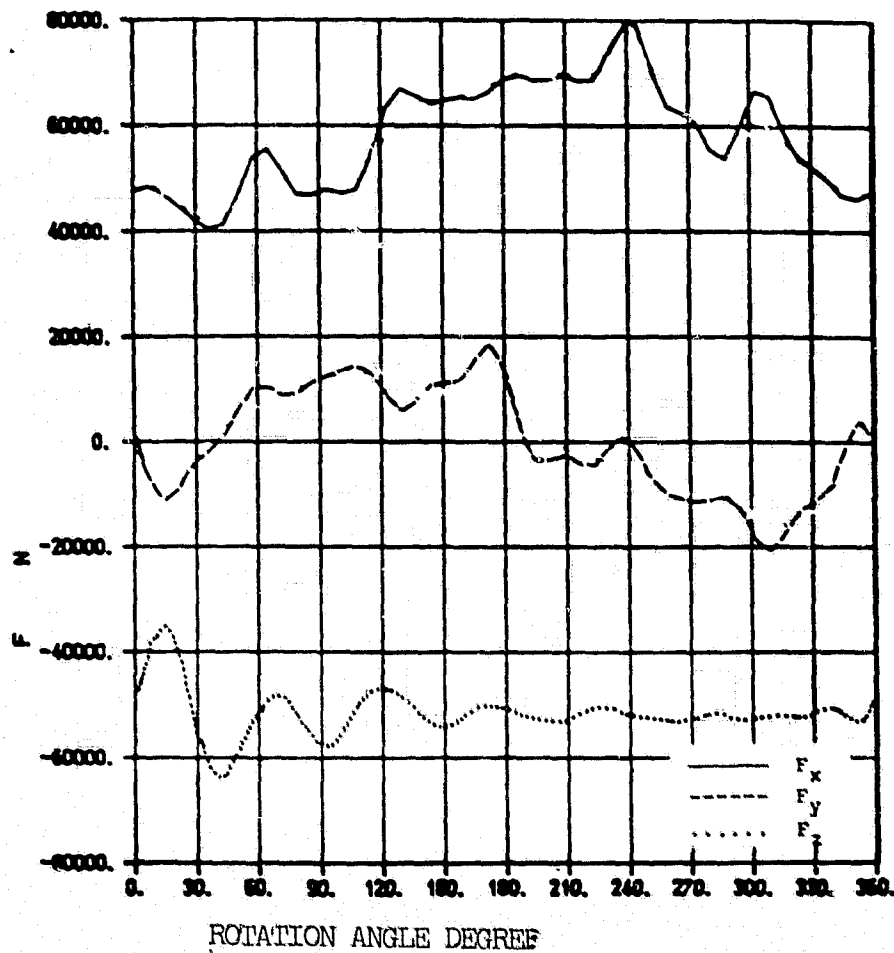
| Calculation case |                  | Flapping direction |                         |                       | Deflection direction |                  |                            |
|------------------|------------------|--------------------|-------------------------|-----------------------|----------------------|------------------|----------------------------|
| no.              | wind speed       | flapping angle     |                         | blade tip deformation |                      | deflection angle | blade tip deformation      |
|                  |                  | $\beta_0$          | $\Delta\beta_{1\Omega}$ | $w_0$                 | $\Delta w_{1\Omega}$ |                  | $u_0$ $\Delta u_{1\Omega}$ |
| 1                | 6 $\frac{m}{s}$  | 6,3°               | <del>±0,8°</del>        | 0,38 m                | ±0,005 m             | ±0,08°           | 0,04 m ±0,06 m             |
| 2                | 10 $\frac{m}{s}$ | 9,7°               | ±1,0°                   | 0,73 m                | ±0,01 m              | ±0,12°           | 0,10 m ±0,06 m             |
| 3                | 16 $\frac{m}{s}$ | 4,0°               | ±0,9°                   | 0,10 m                | ±0,01 m              | ±0,08°           | 0,08 m ±0,06 m             |

Flapping/deflection angle and elastic blade tip deflections of demonstration facility in operation

#### IV. Basic discussion of the passage problem in the DEMO facility

/391

ORIGINAL PAGE IS  
OF POOR QUALITY



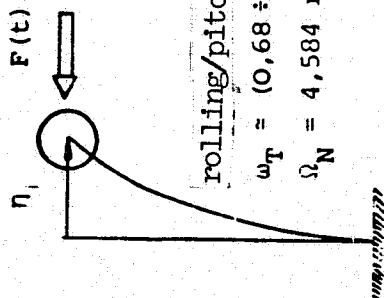
Variation of forces over rotor main bearing for the basic case  
with 10 m/s wind speed for demonstration facility

$F_x$  - vertical force

$F_y$  - horizontal force

$F_z$  - longitudinal force in mast direction

( $F_x$ ,  $F_y$ ,  $F_z$  → tower excitation)



rolling/pitching

$$\omega_T = (0,68 \div 0,69) \text{ N}$$

$$\Omega_N = 4,584 \text{ rad/s}$$

$F$  = gen. force

$m$  = gen. Mass

$\omega_T$  = tower eigen frequency

$D$  = damping

equations of motion

$$m(\ddot{\eta} + 2\omega_T D \dot{\eta} + \omega_T^2 \eta) = F$$

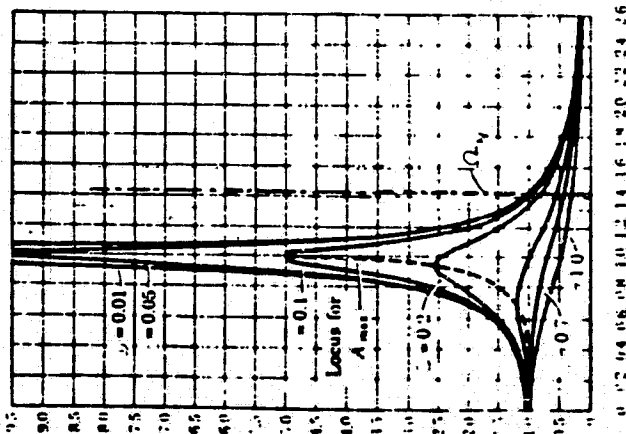
$$F = F_0 \cos \psi$$

$$\eta_0 = \frac{F_0}{\omega_T^2 m}$$

dynamically stable  $\Omega = \text{const.}$

$$F = F_0 \cos \Omega t$$

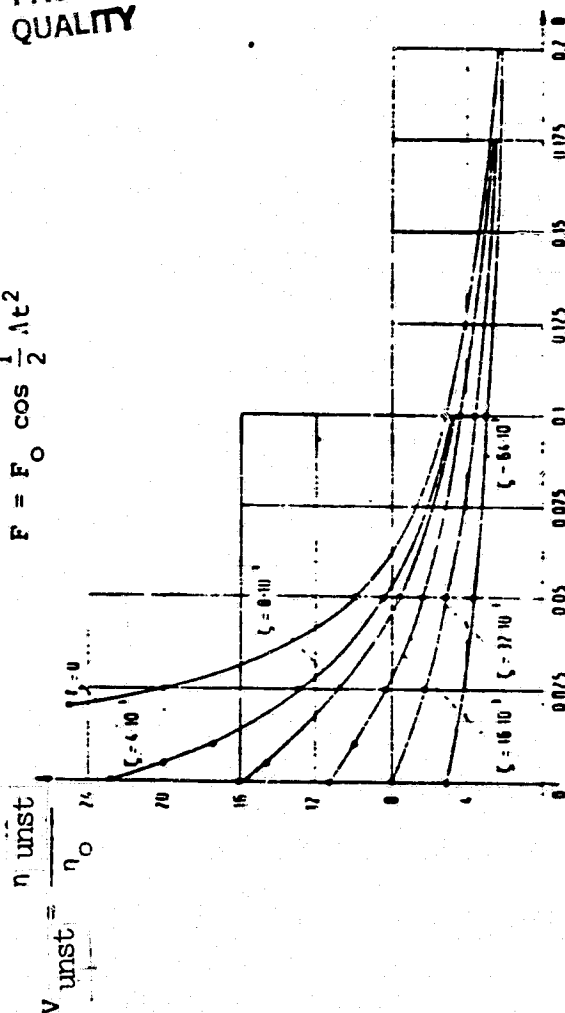
$$\text{stat} = \frac{\eta_{\text{stat}}}{\eta_0}$$



dynamically unstable  $\Omega = \Lambda = \text{const.}$

$$\zeta = \frac{\Lambda}{\omega_T^2}$$

$$F = F_0 \cos \frac{1}{2} \Lambda t^2$$



Passage problem for demonstration tower: Steady and unsteady amplification functions



John H. Argyris<sup>\*</sup>  
Bertold Kirchgassner

### SUMMARY

Selected results of dynamic analysis are presented for a special rotor blade design with flapping joint, deflection joint and a coupling between angle of attack and the flapping angle. This includes the stability of the rotor blade for nominal conditions and the displacements and stresses for stationary operation, for a gust condition and in the tower wake. In addition, continuing work in the area of the dynamics of the total facility are presented.

/396

### INTRODUCTION

The dynamic investigation of wind energy converters includes two different problems; on the one hand, self-excited oscillations, dynamic instabilities and on the other hand, foreign excited oscillations, the dynamic response of the system to external excitation forces. Dynamic instabilities, for example, flutter and ground resonance, have to be avoided at all costs because, due to the rapidly increasing amplitudes, the support structure is destroyed in a short time if large amplitudes are not damped by nonlinear effects. Using a stability investigation, we therefore have to prevent the occurrence of self-excited oscillations.

Far and excited oscillations cannot be avoided for wind energy converters because even in the ideal case of constant incident flow, there will be at least cyclical weight forces over the rotor plane for horizontal axis machines. For vertical axis machines there will be at least cyclical aerodynamic forces. Using a favorable relationship between the eigen frequencies and the excitation frequencies, resonances have to be avoided in order to make the deformation amplitude and

---

<sup>\*</sup>University of Stuttgart, Institute for Statics and Dynamics of Aviation and Space Flight Design

therefore the alternating loads on the structure small.

/397

#### ROTOR BLADE DESIGN WITH FLAPPING AND DEFLECTION JOINT

If one considers rigid body motions in a dynamic system whose stiffness is only the result of external forces, for example, centrifugal forces, then the alternating loads which occur in the structure can be reduced among other things by allowing the periodic or stochastic excitation forces to produce substantial oscillations. However, they are allowed only to contain small elastic components and therefore only load the structure slightly.

During the research project entitled "Investigation of rotor stressing and smoothness of operation of large-scale wind energy conversion systems", which was supported by IEA with the participation of BMFT, a rotor blade design with flapping joint and deflection joint [1] -[4] was investigated in which the stationary and unsteady loads are to be absorbed for the most part by the centrifugal stiffness. In addition, the rotor blade had a flapping joint on the rotation axis, a deflection joint at about 10% of the blade length and a coupling between the blade adjustment angle and the flapping angle for stabilization of the cone angle, the so-called blade angle feedback control. Figure 1 shows the blade model and the FE idealization.

In addition, a mass distribution was selected for the rotor blade for which the flapping bending moments for the most part vanish for nominal operation because the resultant of the corresponding centrifugal force and aerodynamic force components points in the direction of the blade longitudinal axis. For operating points outside of the nominal state, of course, changed cone angles occur.

When a horizontal axis machine rotates, a cyclical gravity force applies to the rotor blade and its importance increases with increasing facility size. For the rotor concept considered here, in this way a deflection oscillation is excited which runs in a counterphase to the gravity force moment because the lowest deflection eigen frequency is

far below the excitation frequency. For the most part, this is a rigid body motion.

#### DYNAMIC ANALYSIS OF THE BLADE MODEL

/398

For the linear investigation of the blade design a number of assumptions are made:

- rotation axis clamped
- rotation rate constant
- quasistationary, linearized aerodynamics

This resulted in a system of linear differential equations of motion with constant coefficients which was set up using the FE system ASKA and was condensed using the eigen modes of the system without aerodynamic and Coriolis forces [3]. Figure 2 shows these eigen modes for the blade model with free flapping motion or free deflection motion and blade angle feedback control. In the condensed system, the stability of the system was determined by calculating the complex eigen frequencies and the motion of the system by direct integration. The important data of the blade model is given in Table 1.

A stability analysis of the corresponding rigid body system with flapping, deflection and blade angle feedback control [4] gave an instability for the rigid body deflection eigen frequency. In addition, estimates for the gravity--excited deflection motion led to the prediction of excessively high deflection amplitudes and, therefore, the principle of free deflection was given up and a deflection joint was planned with a viscous damping and a spring stiffness. The lowest deflection eigen frequency also remained under the rotation frequency.

/399

#### STABILITY OF THE ROTOR BLADE FOR NOMINAL OPERATION

For the blade model modified in this way, the stability for nominal operation was investigated as a function of the blade feedback control factor and the ratio of angle of attack change and flapping angle change [3]. Figure 3 shows the frequencies and Figure 4 the damping values as

a function of blade feedback control factor. The first deflection eigen frequency is very slightly damped in this case as well. For a continuing investigation of these oscillation modes, probably non-linear aerodynamics would be necessary in order to determine the aerodynamic damping more accurately. The second eigen frequency belongs to the lowest flapping eigen mode which for  $n = 0$  essentially represents a rigid body motion. For increasing  $n$  the oscillation mode has increasing parts of higher flapping eigen modes. At the same time, the damping of this flapping motion rapidly decreases above  $n = 4$ ; the motion remains stable in the investigated range up to  $n = 7$ .

#### DYNAMIC RESPONSE OF THE BLADE MODEL

Also the response of the blade model was investigated for nominal operation with cyclical gravity force excitation for which there was a global gust from 10 to 20 m/s within one second and with a simulated tower wake with a wind speed reduction of 45% [3]. The results for nominal operation and tower wake are acceptable within the framework of the linear theory. The results for gust excitation have a more qualitative character, first of all, because of the large displacements in the deflection direction and also because of the nonlinearities of the aerodynamics which occur for the substantial displacements which are ignored in the linearized model discussed here.

Figure 5 shows the displacements of the blade model for gust loads.  $\phi$  is the deflection angle,  $\psi$  is the flapping angle,  $u_8$  and  $u_{14}$  are the displacements in the flapping direction at the node 8 in the center of the blade or at node 14 at the blade tip.  $w_8$  and  $w_{14}$  are the corresponding displacements in the deflection direction. The gust only starts after one rotation so that up to  $t = 3.77$  s, we only see the gravity-excited oscillation of nominal operation. The response after the beginning of the gust consists of the gravity-excited oscillation with rotation frequency and the superimposed gust response whose most important component is a deflection oscillation of high amplitude with a slightly damped first deflection eigen frequency. Figure 6 shows the corresponding stresses at various points of the blade. Here the

gravity-excited oscillation with rotational frequency dominates, whereas in the outer ranges of the blade, higher frequency components also can be found after the gust starts.

Figure 7 shows the displacements of the rotor blade for nominal operation with the tower wake and Figure 8 shows the corresponding stresses. There is an additional load on the outer wing because of the excited higher eigen modes.

In Figures 9 and 10, we finally show the flapping and deflection angles as a function of blade angle feedback control factor  $n$ . There is hardly any dependence in the deflection direction, but the flapping angle amplitude is drastically reduced for increase in  $n$ .

/401

#### PROGRAM SYSTEM FOR THE STABILITY ANALYSIS OF THE TOTAL SYSTEM

One of the most complicated problems in the dynamic investigation of the wind energy converter is the stability analysis of the overall system. During the project ET 4406 A "OPTIWA", at the present time a program system is being developed toward this. The displacements of the partial systems tower and rotor are described by the eigen modes of the partial systems, the kinetic and potential energies of the entire system are set up and then the linearized equations of motion are derived using the Lagrange equation. In the general case, the motion equations contain cyclical coefficients and the stability analysis is done using the Floquet theory. The number of generalized degrees of freedom of the entire system is first restricted to about 30.

#### NONLINEAR INVESTIGATION OF THE "STUTTGART TOWER"

In [1] a new tower design was suggested through which the dynamic behavior of the entire system can be substantially improved so that in this way a soft and overcritical support of the rotor shaft can be brought about. The tower has a joint bearing at the lower end and the tower head is guided along approximately a circular trajectory using a corresponding rope support. The frequency of the yaw oscillation of the tower head is, therefore, proportional to the square root of the

rotor thrust and for nominal operation is far below the rotational frequency.

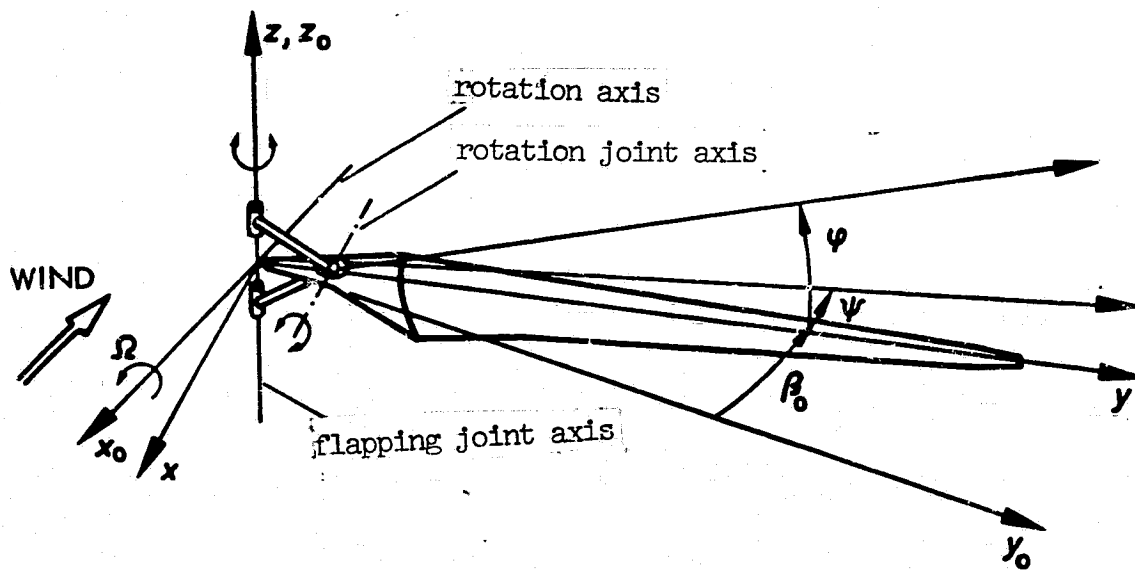
Investigations on the kinematics of this tower concept started in [5] were continued during the project ET 4406 A "OPTIWA". Also there is a nonlinear static and dynamic analysis using a nonlinear FE program system LARSTRAN.

/402

#### REFERENCES

- [1] F. X. Wortmann: Description of the concept of the oscillating wind turbine. Report of the Institute for Aerodynamics and Gas Dynamics, Stuttgart 1977.
- [2] J. H. Argyris, K. A. Braun, B. Kirchgassner: Static investigation of rotor blades under their eigen weight and for stationary operation. ISD report no. 243, Stuttgart 1979.
- [3] J. H. Argyris, K. A. Braun, B. Kirchgassner: Dynamic analysis of the rotor blade with free flapping capability, free deflection capability and blade angle feedback control. ISD report no. 258, Stuttgart 1979.
- [4] J. H. Argyris, B. Kirchgassner: Stability and gravity response of the flapping deflection motion of a rigid rotor blade with blade angle feedback control. ISD report no. 244, Stuttgart 1979.
- [5] J. H. Argyris, K. A. Braun: Static and dynamic investigation of various towers for wind turbines. ISD report no. 261, Stuttgart, 1979.

ORIGINAL PAGE 13  
OF POOR QUALITY



without representation of blade angle feedback

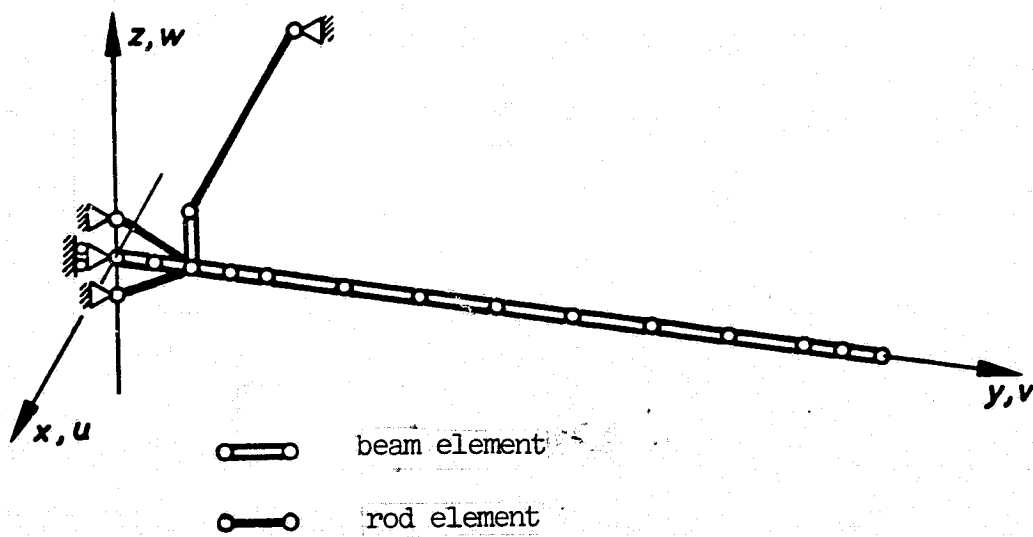


Figure 1. Rotor blade and finite element idealization



ORIGINAL PAGE IS  
OF POOR QUALITY

|  |               |          |
|--|---------------|----------|
| blade length                                     | 60,0          | m        |
| position of turning joint at r =                 | 6.0           | m        |
| position of CG at r =                            | 30,657        | m        |
| blade mast                                       | $12,989^{+3}$ | kg       |
| moment of inertia around turning joint           | $1,0991^{+7}$ | $m^2 kg$ |
| moment of inertia around blade longitudinal axis | $1,2580^{+4}$ | $m^2 kg$ |
| maximum wing chord                               | 6,0           | m        |
| rpm  | 1,667         | rad/s    |
| cone angle for nominal operation                 | 12            | o        |

Table 1. The most important data of blade model

ORIGINAL PAGE IS  
OF POOR QUALITY

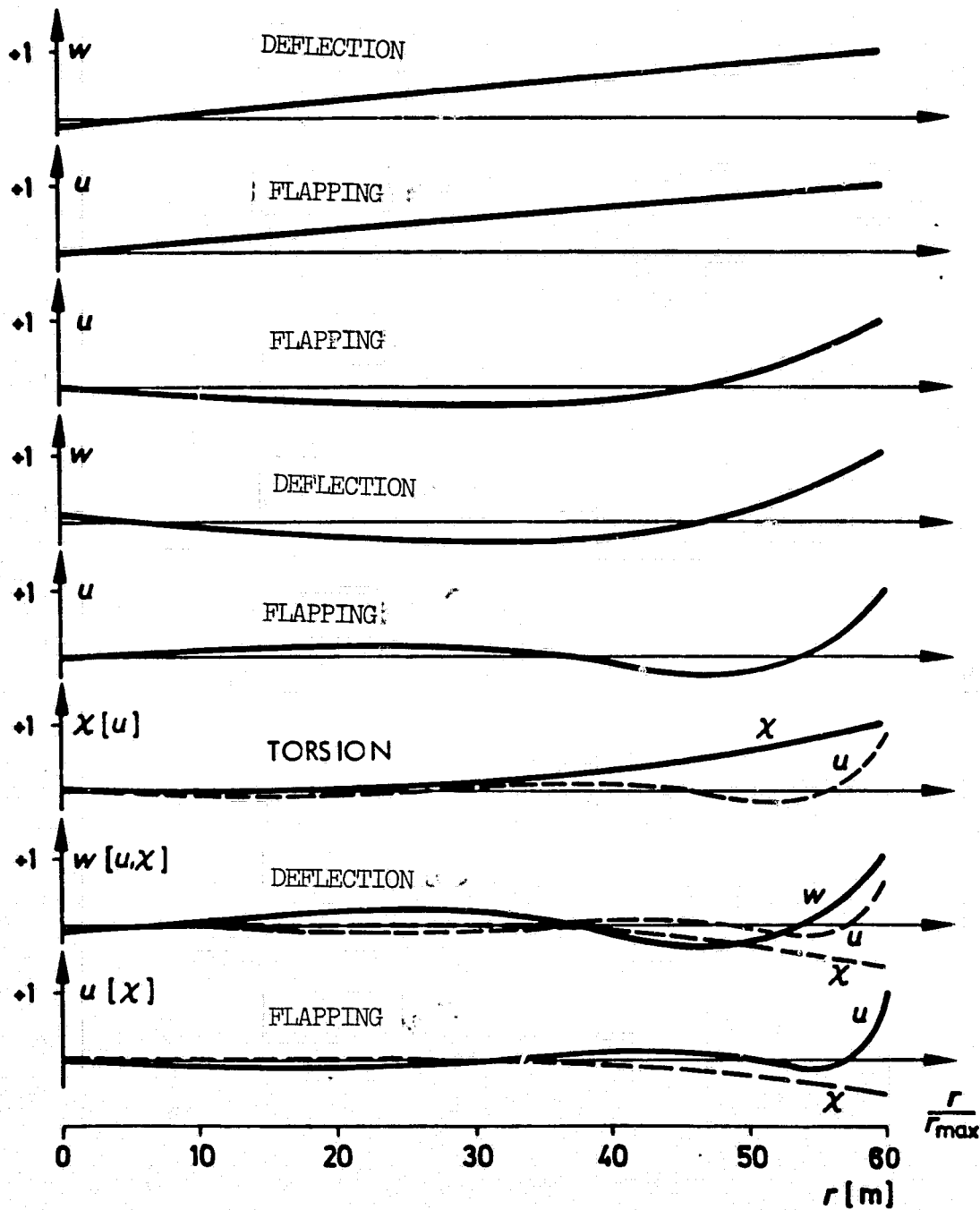


Figure 2. Eigen oscillation modes of the conservative system without Coriolis forces for a blade model with no flapping, no deflection and a blade angle feedback factor of  $n = 5$   $\Omega = 1.667$  rad/s

ORIGINAL PAGE IS  
OF POOR QUALITY

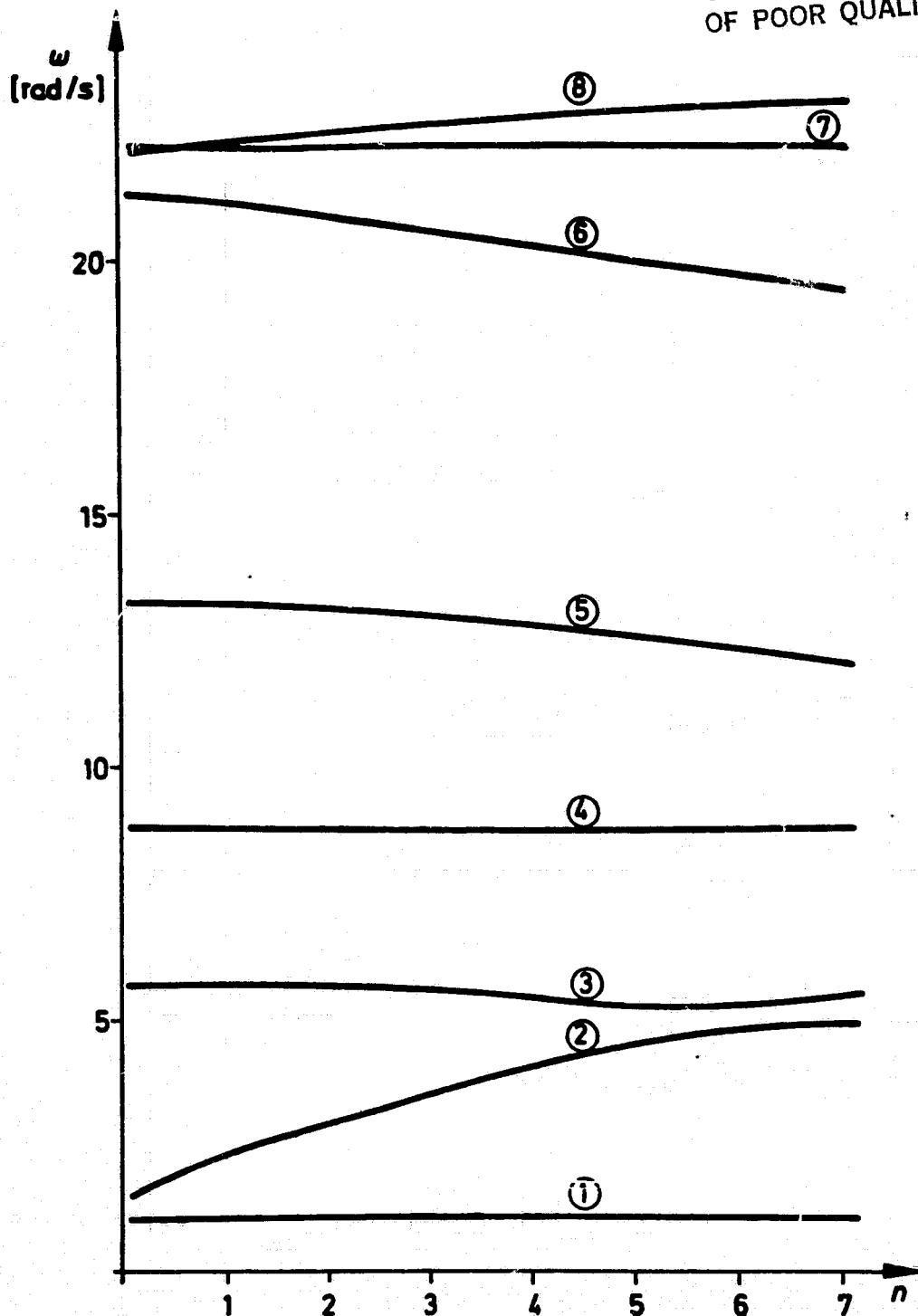


Figure 3. Imaginary part of the complex eigen frequencies as a function of blade angle feedback factor and  $\Omega = 1.667$  rad/s

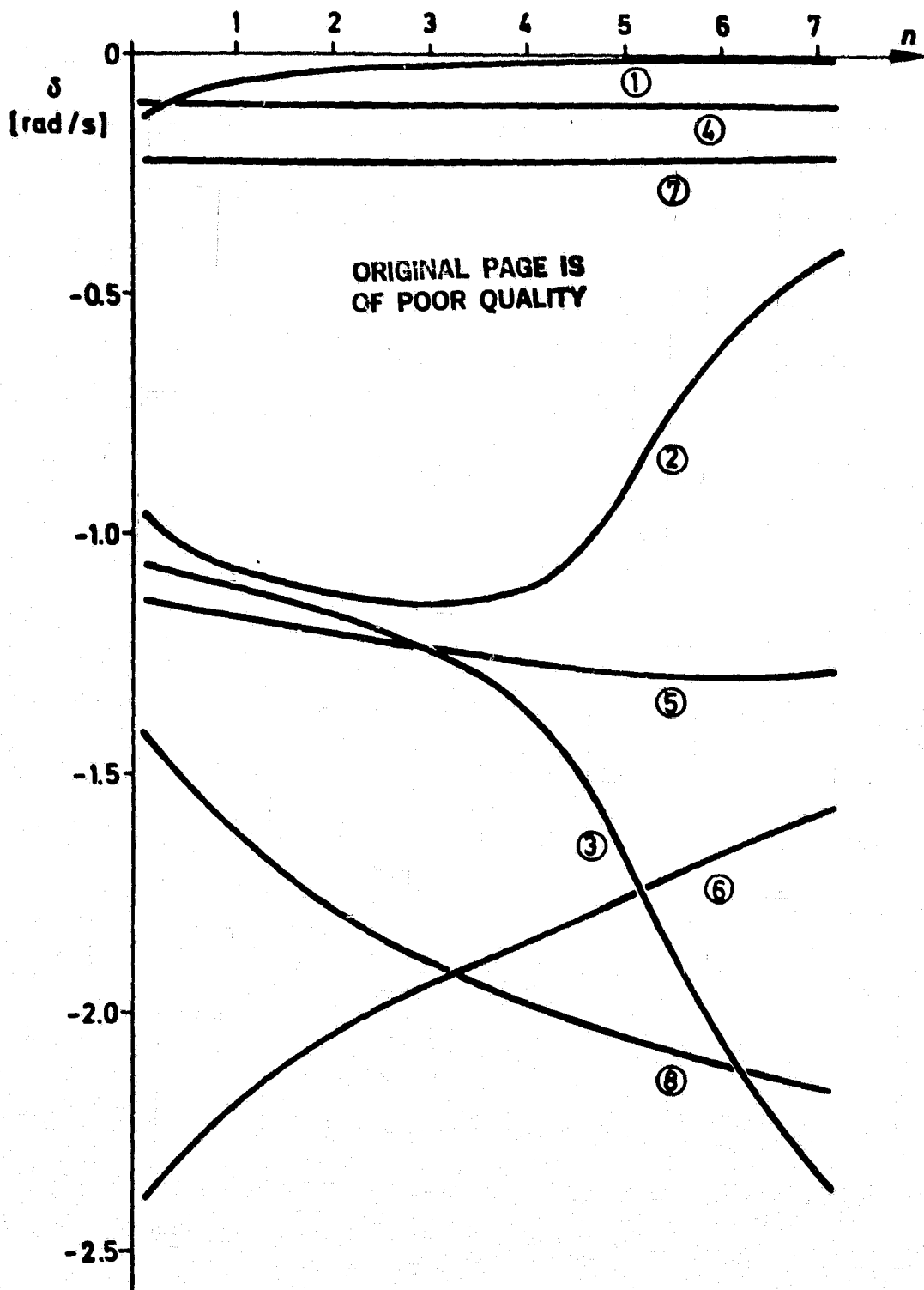


Figure 4. Real part of complex eigen frequencies as a function of blade angle feedback factor and  $\Omega = 1.667$  rad/s

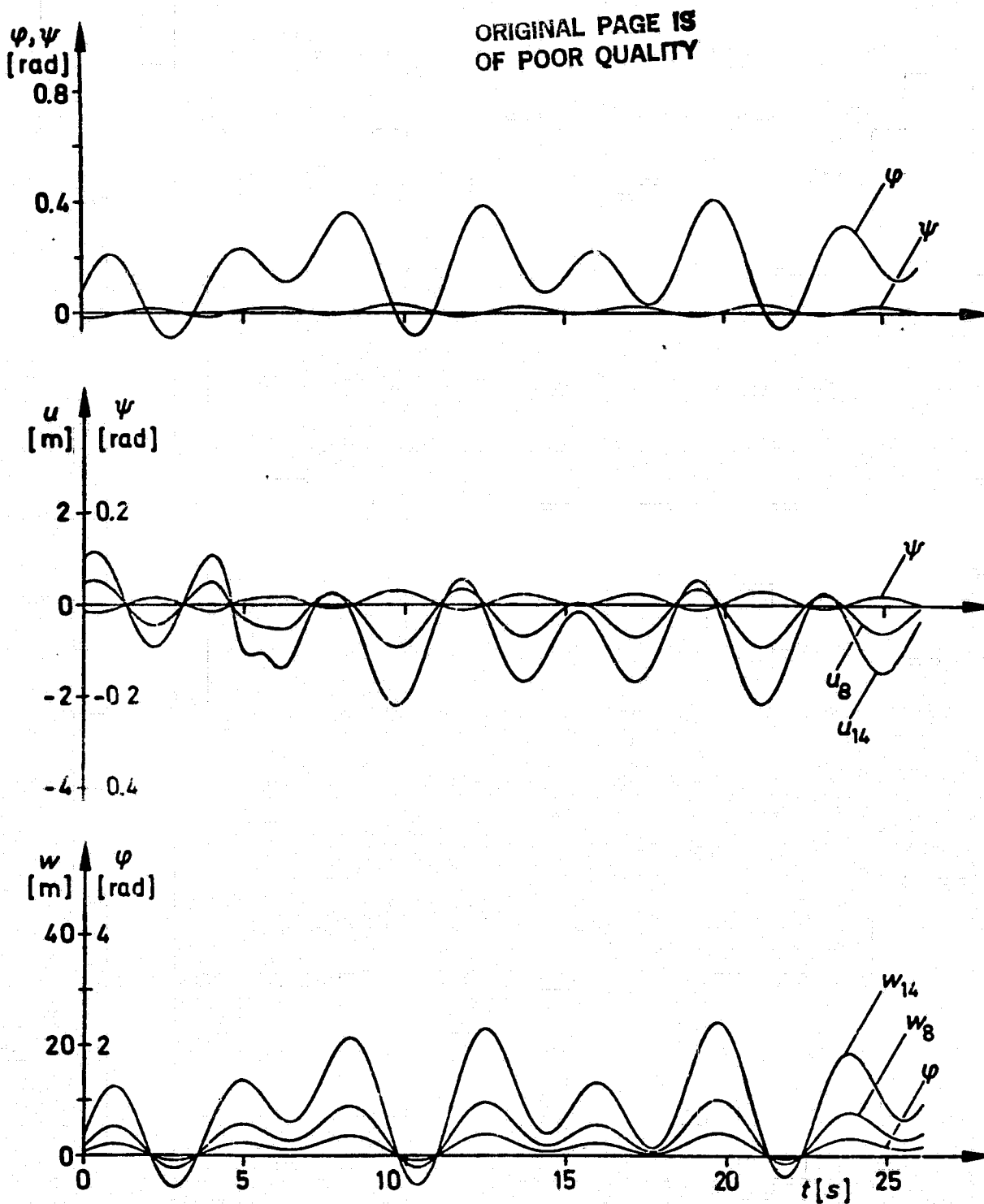


Figure 5. Flapping and deflection motion of a rotor blade with  $n = 5$  with a gust beginning of the gust at  $t = 3.77$  s

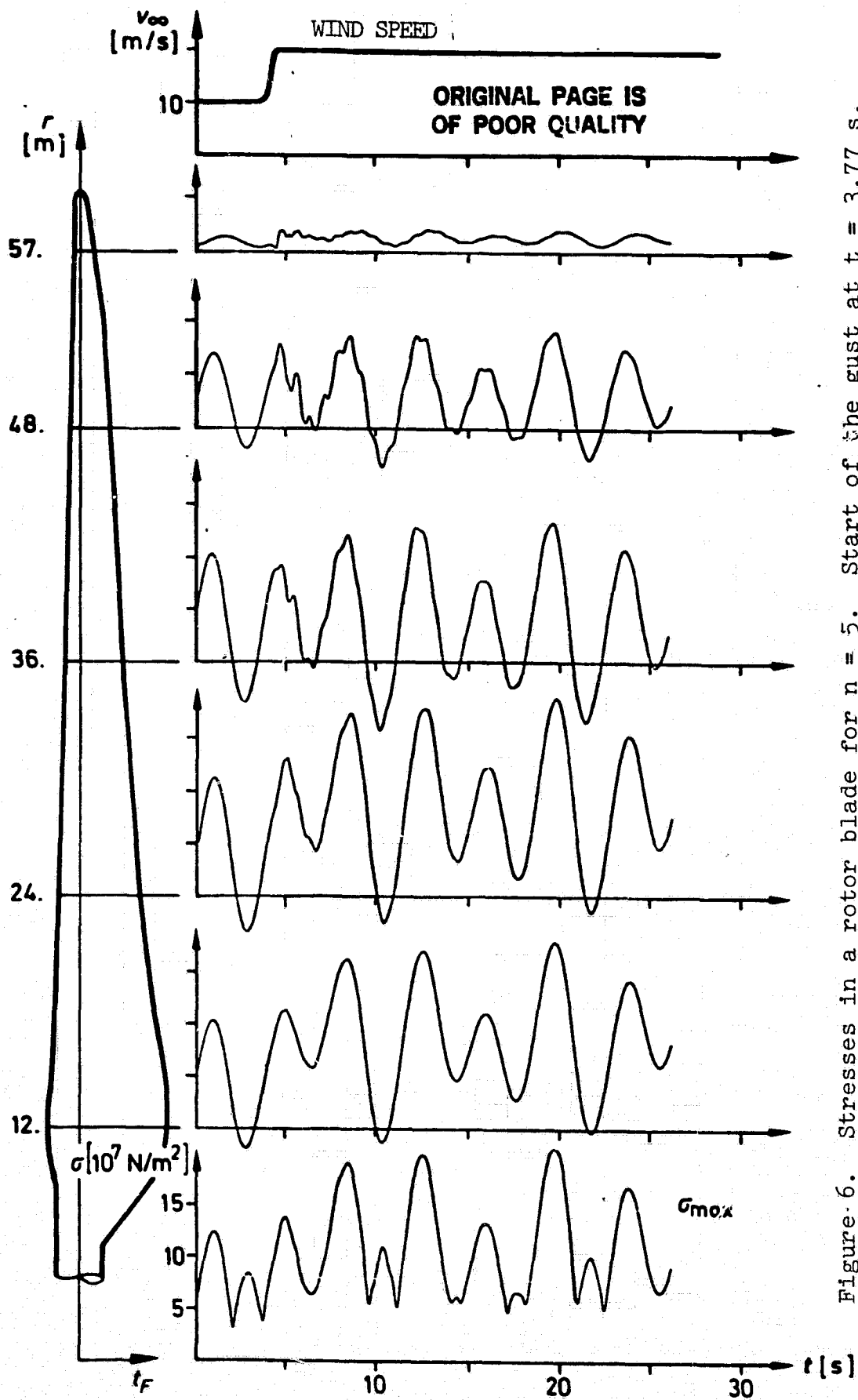


Figure 6. Stresses in a rotor blade for  $n = 5$ . Start of the gust at  $t = 3.77$  s.

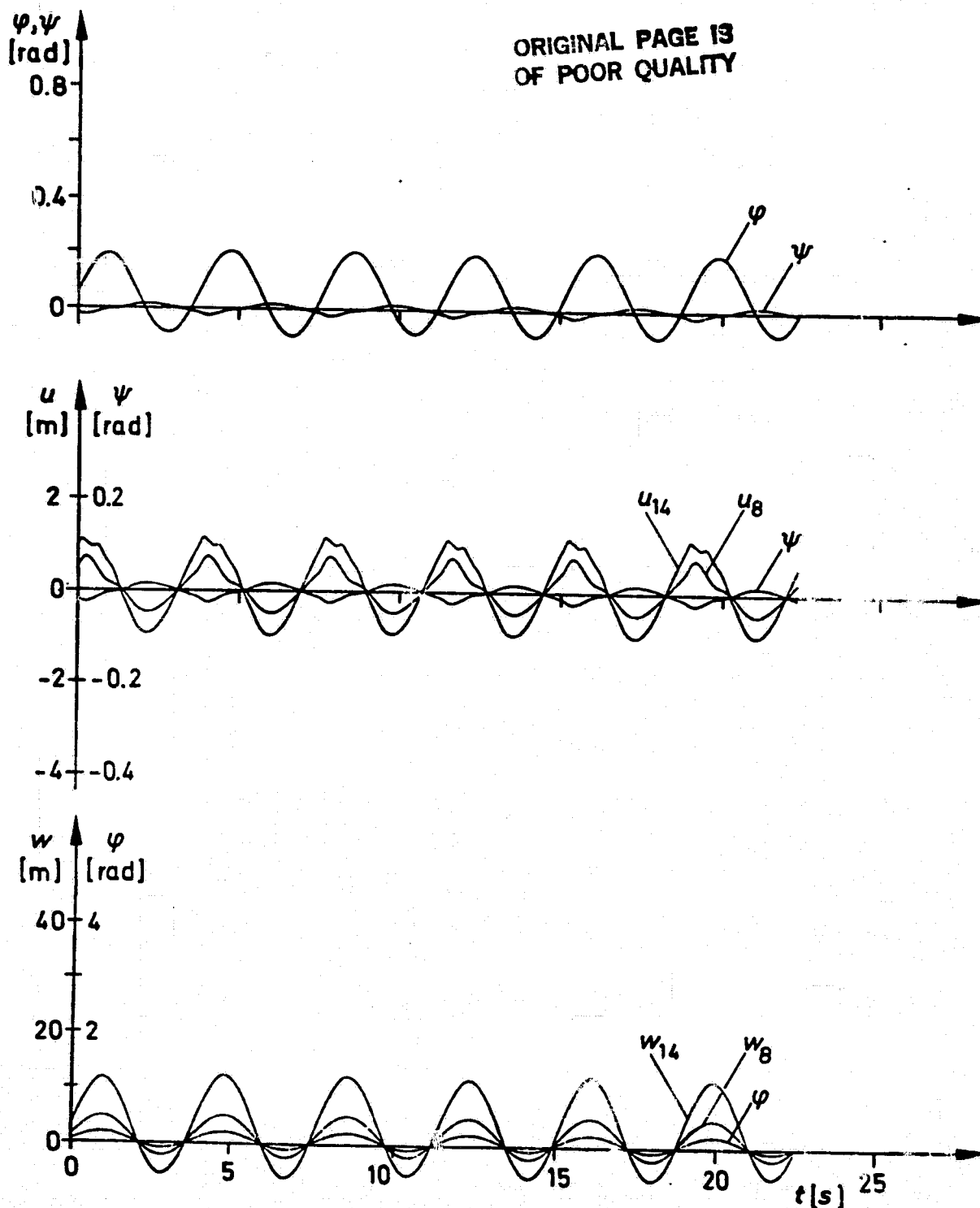


Figure 7. Flapping and deflection motion of the rotor blade for  $n = 5$  in the tower wake

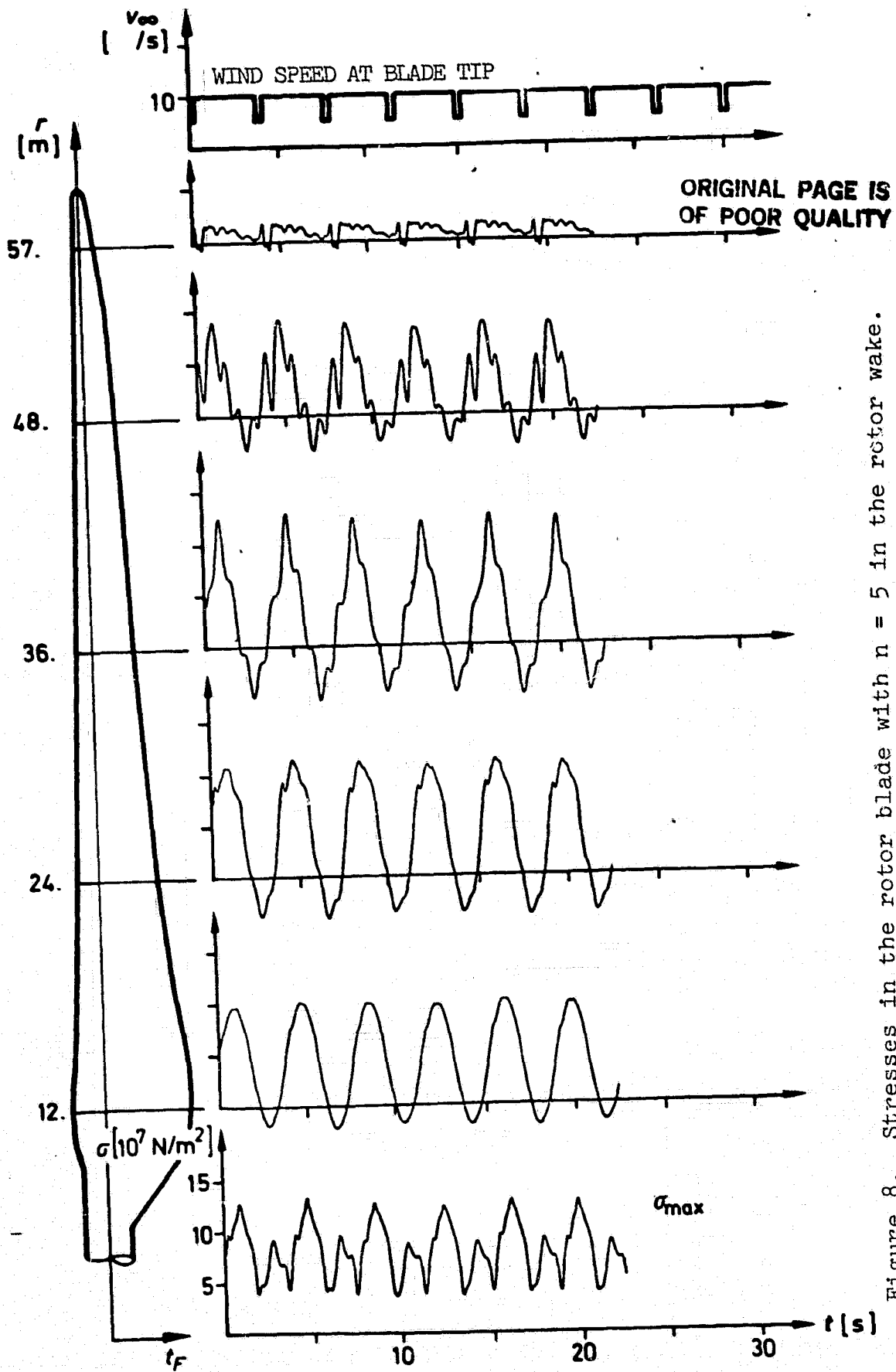


Figure 8. Stresses in the rotor blade with  $n = 5$  in the rotor wake.



ORIGINAL PAGE IS  
OF POOR QUALITY

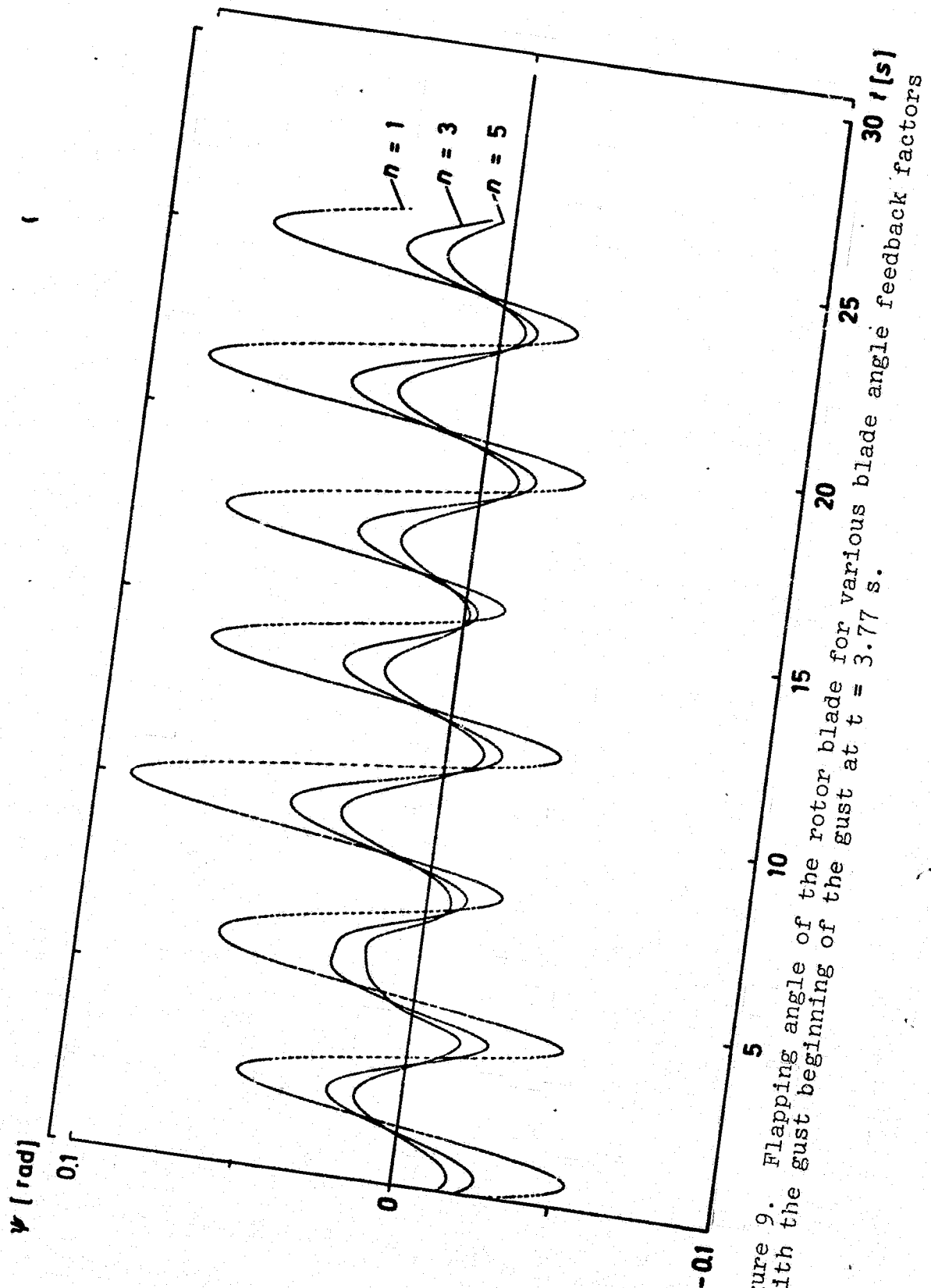


Figure 9. Flapping angle of the rotor blade for various blade angle feedback factors  $n$  with the gust beginning of the gust at  $t = 3.77$  s.

ORIGINAL PAGE IS  
OF POOR QUALITY

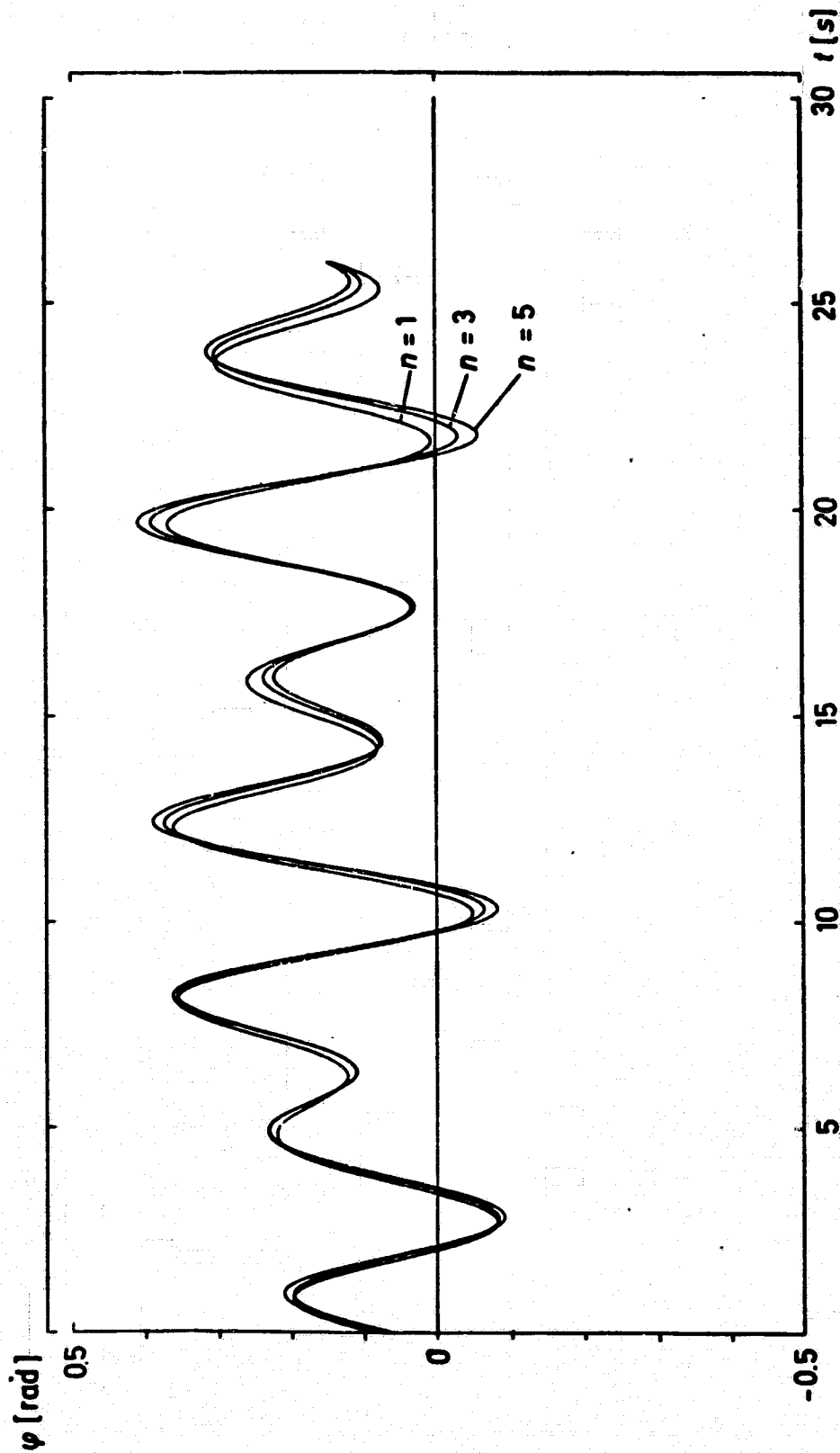


Figure 10. Deflection angle of the rotor blade for various blade angle feedback factors and for gust. Starting of the gust for  $t = 3.77$  s

|                       |   |
|-----------------------|---|
| Hr. Banzhaff          | Voith Getriebe KG, Heidenheim                   |
| Hr. Bergermann        | Schlaich + Partner, Stuttgart                   |
| Hr. Blattmann         | MAN-Neue Technologie, München                   |
| Hr. Dr. Braun         | Univ. Stuttgart, Inst. f. Statik und<br>Dynamik |
| Hr. Dr. Cuntze        | MAN-Neue Technologie, München                   |
| Hr. Prof. Fahlbusch   | Hochschule der Bundeswehr, München              |
| Hr. Hau               | MAN-Neue Technologie, München                   |
| Hr. Helm              | MAN-Neue Technologie, München                   |
| Hr. Hofmann           | Voith Getriebe KG, Heidenheim                   |
| Hr. Dr. Hollighaus    | KFA-PLE, Jülich                                 |
| Hr. Dr. Kehl          | MAN-Neue Technologie, München                   |
| Hr. Kirchgäßner       | Univ. Stuttgart, Inst. f. Statik und<br>Dynamik |
| Hr. Prof. Kleinkauf   | Ges.hochschule Kassel                           |
| Hr. Dr. Körber        | MAN-Neue Technologie, München                   |
| Hr. Lehmhus           | Germ. Lloyd                                     |
| Hr. Prof. Leonhard    | TU-Braunschweig                                 |
| Hr. Dr. Matthes       | BMFT  |
| Hr. Dr. Meggle        | MBB-UD, München                                 |
| Hr. Dr. Mickeler      | Univ. Stuttgart, Inst. f. Aerodynamik           |
| Hr. Möller            | KFA-PLE, Jülich                                 |
| Hr. Muser             | MAN-Neue Technologie, München                   |
| Hr. Prof. Öry         | RWTH Aachen                                     |
| Hr. Prof. Roth        | Univ. Hannover                                  |
| Hr. Schierning        | MAN-Nürnberg                                    |
| Hr. Schlusnus         | Elektromark, Hagen                              |
| Hr. Spittler          | Voith Getriebe KG, Heidenheim                   |
| Hr. Prof. Staufenbiel | RWTH Aachen                                     |
| Hr. Thiele            | MAN-Neue Technologie, München                   |
| Hr. Wackerle          | MBB-UD, München                                 |
| Hr. Dr. Windheim      | KFA-PLE, Jülich                                 |
| Hr. Witt              | HEW BHK, Hamburg                                |
| Hr. Prof. Wortmann    | Univ. Stuttgart, Inst. f. Aerodynamik           |